ISSN: 2153-1196 Volume 11, Number 10, October 2020

Scientific Research Publishing

Journal of Modern Physics

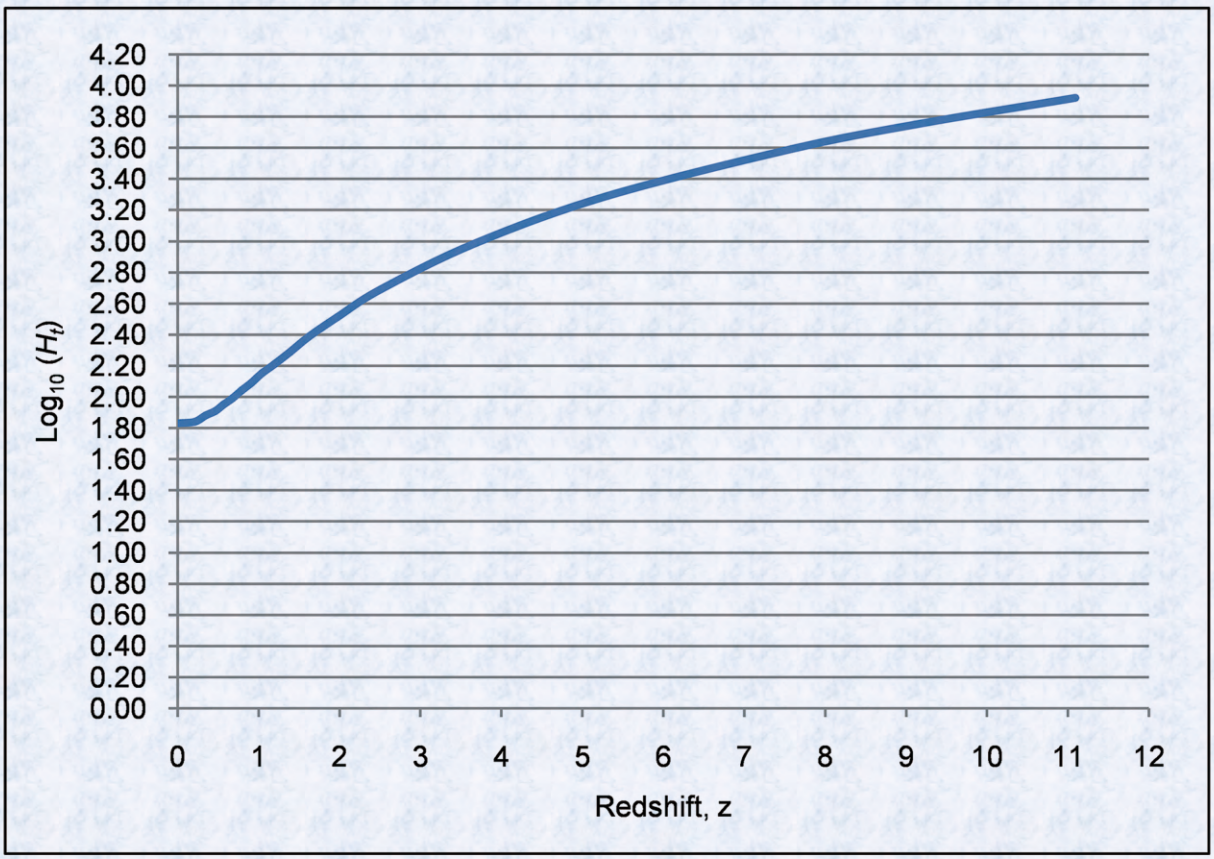

ISSN: 2153-1196
9 772153 119007 10

https://www.scirp.org/journal/jmp

Journal Editorial Board

ISSN: 2153-1196 (Print) ISSN: 2153-120X (Online)
https://www.scirp.org/journal/jmp

Editor-in-Chief

Editorial Board

Journal of Modern Physics, 2020, 11, 1493-1742
https://www.scirp.org/journal/jmp
ISSN Online: 2153-120X
ISSN Print: 2153-1196

Table of Contents

Volume 11 Number 10 October 2020

How Flat Space Cosmology Models Dark Energy

E. T. Tatum, U. V. S. Seshavatharam.....1493

Energy Spectrum of Turbulent Velocity Pulsations at Arbitrary Values of Fluid Viscosity

E. V. Teodorovich.....1502

Generation of Multipartite Entangled States Using Switchable Coupling of Cooper-Pair-Boxes

S. J. Rinner, T. Pittorino.....1514

Multiple Emulsions Able to Be Used for Oral Administration of Active Pharmaceutical Ingredients: Physico-Chemical Parameters Study of Different Phases

L. A. D. Diouf, A. R. Djiboune, M. Soumboundou, S. M. Dieng, P. M. Sy, G. Mbaye, M. Diarra.....1528

Circular Scale of Time and Its Use in Calculating the Schrödinger Perturbation Energy of a Non-Degenerate Quantum State

S. Olszewski.....1536

Erratum to "Empirical Equation for the Gravitational Constant with a Reasonable Temperature" [Journal of Modern Physics 11 (2020) 1180-1192]

T. Miyashita.....1559

A Mechanism for How a Particle Detects and Moves in a Field Gradient

D. J. Pons.....1560

New Method Proving Clausius Inequality

C. S. Jin.....1576

Dark Future for Dark Matter

D. H. Eckhardt, J. L. Garrido Pestaña.....1589

Towards Unification of Fundamental Interactions Using Non-Local Hidden-Variable Theory

D. J. Pons.....1598

Link between Allais Effect and General Relativity's Residual Arc during Solar Eclipse

R. Bagdoo.....1620

The Dirac Propagator for One-Dimensional Finite Square Well

P. Kongkhuntod, N. Yongram.....1639

Journal of Modern Physics, 2020, 11, 1493-1742
https://www.scirp.org/journal/jmp
ISSN Online: 2153-120X
ISSN Print: 2153-1196

Property of Tensor Satisfying Binary Law 2

K. Ichidayama.....1649

A Mathematical Comparison of the Schwarzschild and Kerr Metrics

J.-F. Pommaret.....1672

On the Dynamical 4D BTZ Black Hole Solution in Conformally Invariant Gravity

R. J. Slagter.....1711

Charged Particle in a Flat Box with Static Electromagnetic Field and Landau's Levels

G. V. López, J. A. Lizarraga.....1731

The figure on the front cover is from the article published in Journal of Modern Physics, 2020, Vol. 11, No. 10, pp. 1493-1501 by Eugene Terry Tatum, and U. V. S. Seshavatharam.

Journal of Modern Physics (JMP)
Journal Information

SUBSCRIPTIONS

The *Journal of Modern Physics* (Online at Scientific Research Publishing, https://www.scirp.org/) is published monthly by Scientific Research Publishing, Inc., USA.

Subscription rates:
Print: $89 per issue.
To subscribe, please contact Journals Subscriptions Department, E-mail: sub@scirp.org

SERVICES

Advertisements
Advertisement Sales Department, E-mail: service@scirp.org

Reprints (minimum quantity 100 copies)
Reprints Co-ordinator, Scientific Research Publishing, Inc., USA.
E-mail: sub@scirp.org

COPYRIGHT

PRODUCTION INFORMATION

For manuscripts that have been accepted for publication, please contact:
E-mail: jmp@scirp.org

Journal of Modern Physics, 2020, 11, 1493-1501
https://www.scirp.org/journal/jmp
ISSN Online: 2153-120X
ISSN Print: 2153-1196

How Flat Space Cosmology Models Dark Energy

Eugene Terry Tatum[1], U. V. S. Seshavatharam[2]

[1]Independent Researcher, Bowling Green, KY, USA
[2]Honorary Faculty, I-SERVE, S. No-42, Hitech City, Hyderabad, India
Email: ett@twc.com, seshavatharam.uvs@gmail.com

How to cite this paper: Tatum, E.T. and Seshavatharam, U.V.S. (2020) How Flat Space Cosmology Models Dark Energy. *Journal of Modern Physics*, **11**, 1493-1501.
https://doi.org/10.4236/jmp.2020.1110091

Received: September 3, 2020
Accepted: October 10, 2020
Published: October 13, 2020

Abstract

Equations of Flat Space Cosmology (FSC) are utilized to characterize the model's scalar temporal behavior of dark energy. A table relating cosmic age, cosmological redshift, and the temporal FSC Hubble parameter value is created. The resulting graph of the log of the Hubble parameter as a function of cosmological (or galactic) redshift has a particularly interesting sinuous shape. This graph greatly resembles what ΛCDM proponents have been expecting for a scalar temporal behavior of dark energy. And yet, the FSC $R_h = ct$ model expansion, by definition, neither decelerates nor accelerates. It may well be that apparent early cosmic deceleration and late cosmic acceleration both ultimately prove to be illusions produced by a constant-velocity, linearly-expanding, FSC universe. Furthermore, as discussed herein, the FSC model would appear to strongly support Freedman *et al.* in the current Hubble tension debate, if approximately 14 Gyrs can be assumed to be the current cosmic age.

Keywords

Flat Space Cosmology, Dark Energy, Hubble Parameter, Galactic Redshift, $R_h = ct$ Model

1. Introduction and Background

We are currently in a "golden age" of astronomy and cosmology. Astrophysical observations in the coming decade are expected to bring much greater resolution concerning the behavior and fundamental nature of dark matter and dark energy. These are two of the remaining great mysteries of the universe.

With respect to the behavior of dark energy, the expansion history of our universe, going back to the earliest galaxies, should come into greater focus. If all goes well with these observations, we should be able to fill in many details with respect to the velocities of galactic separation going all the way back to the first

few hundred million years of cosmic expansion. We should then have a remarkably accurate "moving picture" computer simulation of the history of that portion of the universe we can now observe.

When astrophysicists concern themselves with the velocities of galactic separation on scales greater than those of the local clusters held together by gravity and dark matter, they are studying the Hubble parameter and its tight correlation with cosmological redshift. When the Hubble parameter is characterized as a "snapshot" of the universe at a particular point in cosmic time (at the present time, for instance), it can be referred to as the Hubble *constant*. On a *global* scale, making use of cosmic microwave background (CMB) observations, the 2018 Planck Collaboration has arrived at a *current* Hubble constant H_0 value of 67.36 +/− 0.54 km·s^{-1}·Mpc^{-1} [1].

The ongoing temporal (*i.e.*, "moving picture") studies of the universe are expected to show that, over the great span of cosmic time, the Hubble parameter is, in fact, *scalar* in some way. The first evidence of this became apparent in 1998, with studies of Type Ia supernovae [2], which revealed the presence of dark energy. Thus, it became apparent that there is an unseen energy, presumably within the cosmic vacuum, which prevents gravitational deceleration of the expanding universe. We now know that universal expansion, at present, is either occurring at constant velocity (as treated by $R_h = ct$ cosmological models) or *very slightly* accelerating (as claimed by ΛCDM concordance model cosmologists). Both types of cosmological models are still viable at the present time [3]-[8]. Observations in the coming decade may well identify which model is superior.

Flat Space Cosmology (FSC) is perhaps the most successful $R_h = ct$ model to date [9]. It *predicts* a current Hubble parameter H_0 value of 66.893 km·s^{-1}·Mpc^{-1}, fitting with the 2018 Planck Collaboration consensus. It also predicts the COBE CMB dT/T anisotropy ratio of 0.66×10^{-5}. A book chapter summary of FSC is now freely available online [10]. In contrast to ΛCDM cosmology (which incorporates observations *ad hoc* but makes relatively few falsifiable predictions), the FSC equations provide for very specific predictions, which can falsify the model if proven wrong. Remarkably, to date, the FSC model has not been falsified.

The purpose of the current report is to show how FSC models the temporal dark energy expansion of the universe. We show in great detail the scalar nature of the FSC Hubble parameter, so that it can be compared to the observations to be made in the coming decade.

2. Methods

Previously-published equations of FSC, relating cosmological (or galactic) redshift z, temporal cosmic temperature T_p, temporal cosmic radius R_p, the associated temporal Hubble parameter H_p, the currently-observed Hubble parameter H_o, the currently-observed cosmic temperature T_o, and cosmic age t, are brought together in the Results section in order to derive the parameter values given in Table 1 and Figure 1.

3. Results

The following two FSC equations are useful for deriving the model relationships between a given cosmological (or galactic) redshift z and the associated temporal Hubble parameter H_t:

$$z \cong \left(\frac{T_t^2}{T_o^2} - 1 \right)^{1/2} \tag{1}$$

and

$$T_t^2 R_t \cong 1.027246639815497 \times 10^{27}\ \mathrm{K}^2 \cdot \mathrm{m} \tag{2}$$

The first equation relates the redshift to the temporal cosmic temperature T_t and the currently-observed cosmic temperature T_o [11]. The second equation relates the temporal cosmic temperature T_t to the temporal cosmic radius R_t [12].

Recalling the FSC Hubble parameter definition ($H_t = c/R_t$), rearrangement and substitution gives:

$$T_0^2 \left(z^2 + 1 \right) \cong H_t \left[\frac{1.027246639815497 \times 10^{27}\ \mathrm{K}^2 \cdot \mathrm{m}}{c} \right] \tag{3}$$

To convert the H_t term from reciprocal seconds (s^{-1}) to the conventional Hubble parameter units of $\mathrm{km \cdot s^{-1} \cdot Mpc^{-1}}$, the left-hand term is multiplied by $3.08567758 \times 10^{19}\ \mathrm{km \cdot Mpc^{-1}}$:

$$\begin{aligned} & T_0^2 \left(z^2 + 1 \right) \left(3.08567758 \times 10^{19}\ \mathrm{km \cdot Mpc^{-1}} \right) \\ & \cong H_t \left[\frac{1.027246639815497 \times 10^{27}\ \mathrm{K}^2 \cdot \mathrm{m}}{c} \right] \end{aligned} \tag{4}$$

Rearrangement of terms gives:

$$\left(z^2 + 1 \right) \cong H_t \left[\frac{1.027246639815497 \times 10^{27}\ \mathrm{K}^2 \cdot \mathrm{m}}{T_0^2 c \left(3.08567758 \times 10^{19}\ \mathrm{km \cdot Mpc^{-1}} \right)} \right] \tag{5}$$

Using $T_0 = 2.72548$ K, this simplifies to:

$$H_t \cong \frac{\left(z^2 + 1 \right)}{0.014949183831548} \tag{6}$$

The final useful equation relates cosmic time t (in Gyrs after the Planck epoch) to the current Hubble parameter H_0 value of 66.893 $\mathrm{km \cdot s^{-1} \cdot Mpc^{-1}}$, the temporal Hubble parameter H_t value, and the current FSC cosmic age of 14.617 Gyrs:

$$H_t \cong H_0 \left(\frac{14.617}{t} \right) \tag{7}$$

Equations (5), (6) and (7) can then be used to create **Table 1** and **Figure 1**. The last two z values given in **Table 1** are two of the highest galactic redshifts observed to date.

Table 1. Cosmic age, Redshift z, Hubble parameter, Log_{10} Hubble parameter.

Cosmic Age (Gyrs)	Redshift z	H_t (km·s^{-1}·Mpc^{-1})	Log_{10} (H_t)
14.617	0.00	66.893	1.83
14	0.21	69.84	1.84
13.8	0.24	70.85	1.85
13	0.35	75.21	1.88
12	0.47	81.48	1.91
11	0.57	88.89	1.95
10	0.68	97.78	1.99
9	0.79	108.64	2.04
8	0.91	122.22	2.09
7	1.04	139.68	2.15
6	1.20	162.96	2.21
5	1.39	195.55	2.29
4	1.63	244.44	2.39
3	1.97	325.92	2.51
2	2.51	488.89	2.69
1	3.69	977.77	2.99
0.5	5.31	1955.55	3.29
0.25	7.58	3911.1	3.59
0.174	9.11	5618.51	3.75
0.1179	11.09	8293.97	3.92

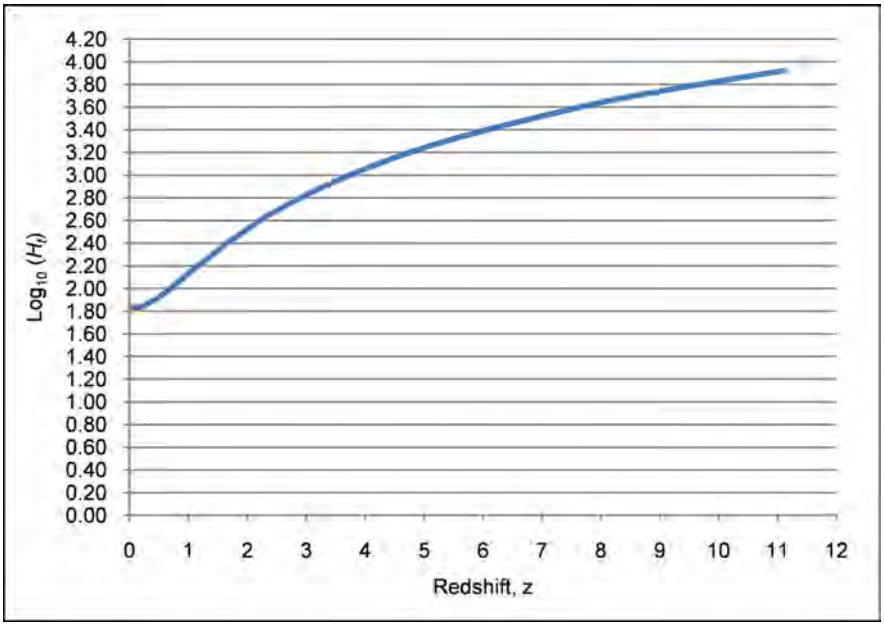

Figure 1. Log_{10} (H_t) as a function of cosmological (or galactic) redshift z.

Notice the *sinuous* appearance of this graph. Its overall shape greatly resembles what cosmologists have been expecting for a scalar temporal behavior of dark energy!

4. Discussion

Proponents of the ΛCDM concordance model of cosmology, and $R_h = ct$ model cosmologists, are currently in a pitched battle to establish which model is more accurate with respect to observations and predictions. As documented in recent publications [13] [14], FSC is a realistic linear light-speed cosmic expansion model which can also be considered a modified Milne "empty universe" model. Following a sign convention which treats gravitationally-attracting matter energy density as positive and "repulsive gravity" vacuum energy density as negative, the FSC *net* global energy density is perpetually zero. Thus, the FSC cosmic model follows the "empty" line exactly between deceleration and acceleration in this **Figure 2** open source graph [15] from the Supernova Cosmology Project. *One can readily see that the observational error bars allow for BOTH models* [*i.e., the blue line of ΛCDM accelerating expansion, as well as the "empty" pink line corresponding to constant velocity expansion of the FSC* $R_h = ct$ *model*].

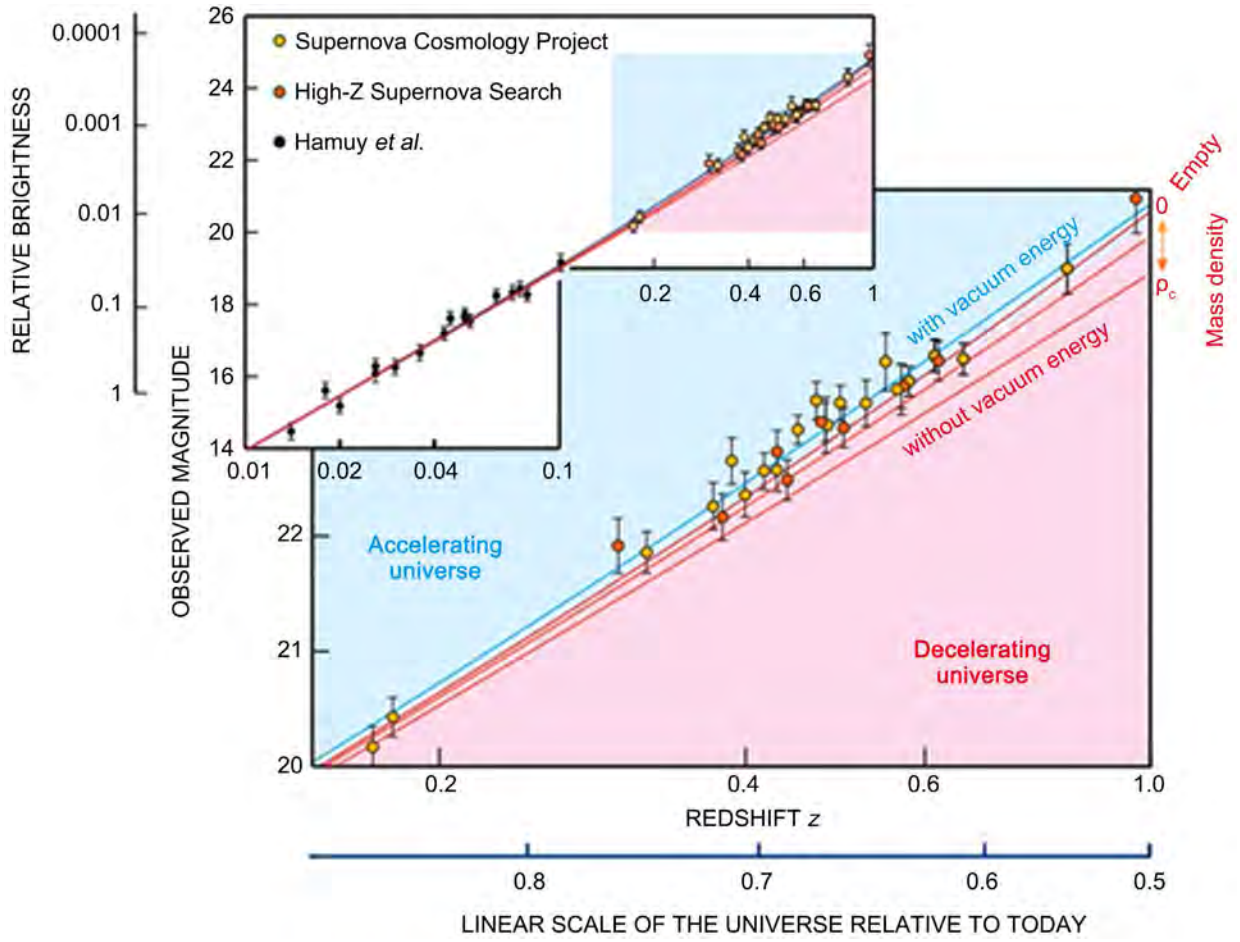

Figure 2. Observed magnitudes of type Ia supernovae vs redshift *z*.

Notice also that this graph correlates a redshift z value of 1.0 with a cosmic scale of 0.5 times the current scale. This is true for FSC as well as ΛCDM, although the two models differ slightly with respect to the current cosmic age.

In ΛCDM cosmology, the post-inflationary cosmological vacuum energy density is assumed to be a constant. This is not an absolute requirement of general relativity, so long as the vacuum energy density is scalar according to $\Lambda = 3H_t^2/c^2$. In the FSC quintessence model, this scalar relationship holds true and is equivalent to $\Lambda = 3/R_t^2$ [16]. In FSC, the vacuum energy density declines in the forward time direction approximately 121 logs of 10 from the Planck scale epoch to the present. Thus, in contrast to ΛCDM cosmology, there is no "cosmological constant problem" in the FSC model.

As speculated in the FSC book chapter summary, ongoing cosmological matter creation may be paired with a continual decline in the cosmological vacuum energy density, as a requirement for conservation of energy in such a finite isolated expanding system. It should be remembered that the details of matter creation in *all* cosmological models are a mystery. In FSC, matter creation is an ongoing process, whereas ΛCDM cosmologists generally assume that all matter was created nearly instantaneously. However, as a result, a major difference between the two models is that *only ΛCDM cosmology has a cosmological constant problem, based upon its embedded constant post-inflationary vacuum energy density assumption.*

As a consequence of the dark energy observations, in addition to their cosmological constant and instantaneous matter creation assumptions, ΛCDM cosmologists must now also assume certain features of the universal expansion. These features had not been required when it was once thought (*i.e.*, before 1998) that the cosmological vacuum energy density might actually be perpetually zero. They now require that universal expansion decelerated during the first half of the cosmic time span since the Big Bang, and then, almost imperceptibly, began to accelerate approximately 6 billion years ago. This becomes absolutely necessary if one requires a post-inflationary cosmological *constant* at the currently observed value of about 10^{-9} J·m^{-3}. Nevertheless, this deceleration-followed-by-acceleration scenario of universal expansion is clearly debatable, especially when one considers the observational statistical error bars in **Figure 2**.

When one compares the relative luminosity and angular diameter distances between the two competing models, in the form of a ratio, it has recently been shown that the ΛCDM model contention of late cosmic acceleration could be an illusion produced by a $R_h = ct$ universe [17].

Further support that cosmic acceleration could be an illusion is clearly evident in **Figure 1** of the current report. It is readily apparent that the FSC graph of the log of the Hubble parameter as a function of redshift z is *sinuous* in appearance. We see the following: an upward flexion curve out to a z value of about 1.0 (corresponding to the last 7.3 billion years of the FSC cosmic expansion); a roughly straight line segment for $1.0 < z < 1.7$ (corresponding to 3.76 to 7.3 billion years

of cosmic age); and an opposite flexion curve for z values greater than about 1.7 (corresponding to the first 3.76 billion years of the FSC cosmic expansion). The overall shape of the graph greatly resembles what ΛCDM proponents have been expecting for a scalar temporal behavior of dark energy. And yet, the FSC $R_h = ct$ model expansion, by definition, neither decelerates nor accelerates!

The upward curving portion of our **Figure 1** graph out to a z value of about 1.5, is already largely filled in by the accumulated Type Ia supernovae data [18]. Not yet known are the *exact* Hubble parameter values at the cosmic times when these supernovae exploded. Fortunately, the coming decade of observational studies should give us a better idea of the precise scalar nature of the Hubble parameter.

Regardless, given the overall shape of our **Figure 1** graph, it may well be that *apparent* early cosmic deceleration and late cosmic acceleration *both* ultimately prove to be illusions produced by a constant-velocity, linearly-expanding, FSC universe.

Given the ongoing tension between different research teams considering what *current* near and deep space observations might be telling us about the H_0 value as a snapshot in time, it is worth noting the following:

The 2018 Planck Collaboration analysis of the CMB looked at 99.998 percent of the current radius of the universe. Their consensus H_0 estimate of 67.36 $km \cdot s^{-1} \cdot Mpc^{-1}$ appears, in FSC, to fit with a 14.6 Gyr old universe. According to **Table 1**, the Freedman, *et al.* H_0 observation of 69.6 $km \cdot s^{-1} \cdot Mpc^{-1}$ [19] appears to be fitted nicely to a 14 Gyr estimated cosmic age. Whereas, the SHoES project H_0 observations of 74 - 77 $km \cdot s^{-1} \cdot Mpc^{-1}$ [20] appear to be ideally fitted to a 13 Gyr (or less) cosmic age. One need only consider the current 14.27 +/− 0.38 Gyr best age estimate of the HD 140283 "Methuselah star" [21] to judge which current H_0 estimate is the most likely outlier.

5. Summary and Conclusion

Equations of FSC have been utilized to characterize the model's temporal behavior of dark energy. A table relating cosmic age, cosmological redshift, and the temporal FSC Hubble parameter value has been created. The resulting graph of the log of the Hubble parameter as a function of cosmological (or galactic) redshift has a particularly interesting sinuous shape: an upward flexion curve out to a z value of about 1.0 (corresponding to the last 7.3 billion years of the FSC cosmic expansion); a roughly straight line segment for $1.0 < z < 1.7$ (corresponding to 3.76 to 7.3 billion years of cosmic age); and an opposite flexion curve for z values greater than about 1.7 (corresponding to the first 3.76 billion years of the FSC cosmic expansion). The overall shape of the graph greatly resembles what ΛCDM proponents have been expecting for a scalar temporal behavior of dark energy. And yet, the FSC $R_h = ct$ model expansion, by definition, neither decelerates nor accelerates. It may well be that apparent early cosmic deceleration and late cosmic acceleration both ultimately prove to be illusions produced by a con-

stant-velocity, linearly-expanding, FSC universe.

Dedications and Acknowledgements

This paper is dedicated to Dr. Stephen Hawking and Dr. Roger Penrose for their groundbreaking work on black holes and their possible application to cosmology. Dr. Tatum also thanks Dr. Rudolph Schild of the Harvard-Smithsonian Center for Astrophysics for his past support and encouragement. Author Seshavatharam UVS is indebted to professors Brahmashri M. NagaphaniSarma, Chairman, Shri K.V. Krishna Murthy, founding Chairman, Institute of Scientific Research in Vedas (I-SERVE), Hyderabad, India, and to Shri K.V.R.S. Murthy, former scientist IICT (CSIR), Govt. of India, Director, Research and Development, I-SERVE, for their valuable guidance and great support in developing this subject.

Conflicts of Interest

The authors declare no conflicts of interest regarding the publication of this paper.

References

[1] Aghanim, N., *et al.* (2018) Planck 2018 Results VI. Cosmological Parameters.

[2] Perlmutter, S., *et al.* (1999) *Astrophysical Journal*, **517**, 565-586.

[3] Melia, F. (2012) *Astronomical Journal*, **144**, 110. https://doi.org/10.1088/0004-6256/144/4/110

[4] Nielsen, J.T., *et al.* (2015) *Scientific Reports*, **6**, Article No. 35596. https://doi.org/10.1038/srep35596

[5] Wei, J.-J., *et al.* (2015) *Astronomical Journal*, **149**, 102. https://doi.org/10.1088/0004-6256/149/3/102

[6] Tutusaus, I., *et al.* (2017) *Astronomy & Astrophysics*, **602**, A73. https://doi.org/10.1051/0004-6361/201630289

[7] Dam, L.H., *et al.* (2017) *Monthly Notices of the Royal Astronomical Society*, **472**, 835-851. https://doi.org/10.1093/mnras/stx1858

[8] Melia, F. (2019) *Modern Physics Letters A*, **33**, Article No. 1930004. https://arxiv.org/abs/1904.11365 https://doi.org/10.1142/S0217732319300040

[9] Tatum, E.T. (2018) *Journal of Modern Physics*, **9**, 1867-1882. https://doi.org/10.4236/jmp.2018.910118

[10] Tatum, E.T. (2019) A Heuristic Model of the Evolving Universe Inspired by Hawking and Penrose. In: Tatum, E., Ed., *New Ideas Concerning Black Holes and the Universe*, IntechOpen, London, 5-21. https://doi.org/10.5772/intechopen.75238

[11] Tatum, E.T. and Seshavatharam, U.V.S. (2015) *International Journal of Astronomy and Astrophysics*, **5**, 133-140. https://doi.org/10.4236/ijaa.2015.53017

[12] Tatum, E.T. and Seshavatharam, U.V.S. (2018) *Journal of Modern Physics*, **9**, 1404-1414. https://doi.org/10.4236/jmp.2018.97085

[13] Tatum, E.T. (2019) *Journal of Modern Physics*, **10**, 974-979. https://doi.org/10.4236/jmp.2019.108064

[14] Tatum, E.T. and Seshavatharam, U.V.S. (2018) *Journal of Modern Physics*, **9**, 2008-2020. https://doi.org/10.4236/jmp.2018.910126

[15] Perlmutter, S. (2016) Supernova Cosmology Project. Lawrence Berkeley National Laboratory, Berkeley. http://www.supernova.lbl.gov

[16] Tatum, E.T. and Seshavatharam, U.V.S. (2018) *Journal of Modern Physics*, **9**, 1469-1483. https://doi.org/10.4236/jmp.2018.98091

[17] Tatum, E.T. and Seshavatharam, U.V.S. (2018) *Journal of Modern Physics*, **9**, 1397-1403. https://doi.org/10.4236/jmp.2018.97084

[18] Betoule, M., *et al.* (2014) *A & A*, **568**, A22.

[19] Freedman, W.L., *et al.* (2020) *Astrophysical Journal*, **891**, 57-75. https://doi.org/10.3847/1538-4357/ab7339

[20] Reiss, A.G., *et al.* (2016) A 2.4% Determination of the Local Value of the Hubble Constant.

[21] Vandenberg, D.A., *et al.* (2014) *Astrophysical Journal*, **792**, Art. No. 110. https://doi.org/10.1088/0004-637X/792/2/110

Journal of Modern Physics, 2020, 11, 1502-1513
https://www.scirp.org/journal/jmp
ISSN Online: 2153-120X
ISSN Print: 2153-1196

Energy Spectrum of Turbulent Velocity Pulsations at Arbitrary Values of Fluid Viscosity

Edward V. Teodorovich

Ishlinsky Institute for Problems in Mechanics, Russian Academy of Sciences, Moscow, Russia
Email: teodor@ipmnet.ru

How to cite this paper: Teodorovich, E.V. (2020) Energy Spectrum of Turbulent Velocity Pulsations at Arbitrary Values of Fluid Viscosity. *Journal of Modern Physics*, **11**, 1502-1513.
https://doi.org/10.4236/jmp.2020.1110092

Received: August 7, 2020
Accepted: October 10, 2020
Published: October 13, 2020

Abstract

The problem of calculating the energy spectrum of turbulent velocity pulsations in the case of homogeneous isotropic and stationary turbulence is considered. The domain of turbulent energy production is treated as "a black box" on which boundary the spectral energy flux is given. It is assumed that the spectrum is formatted due to intermodal interactions being local in the wave-number space that leads to a cascade mechanism of energy transfer along the wave-number spectrum and the possibility of using the renormalization-group method related to the Markovian features of the process under consideration. The obtained formula for energy spectrum is valid in a wide wave-number range and at arbitrary values of fluid viscosity. It is shown that in functional formulation of the statistical theory of turbulence, the procedure of separating local intermodal interactions, which govern energy transfer (straining effect), and filtering out nonlocal interactions, which have no influence on energy transfer (sweeping effect), is directly described without providing additional arguments or conjectures commonly used in the renormalization-group analysis of turbulent spectra.

Keywords

Spectral Flux, Spectral Energy Density, Local and Nonlocal Interactions, Inertial Term, Renormalization-Group Invariance, Epsilon-Expansion Procedure

1. Introduction

The problem of calculating the energy distribution over wave-numbers of turbulent fluid (spectral energy density) is a subject of numerous investigations.

Even within the framework of the simplest model of homogeneous isotropic and stationary turbulence, solving this problem is complicated by the fact that the Navier-Stokes equations, which describe a turbulent fluid, are nonlinear and for obtaining a closed set of equations for energy one needs to express the quantity of third-order statistical moment in terms of the second-order statistical moment with the help of one or other hypotheses of closing (as a survey see [1]) or to construct a solution in the form of perturbation theory series with subsequent term-by-term averaging the series obtained [2]. In the last case, the technique of Feynman diagrams is commonly applied. The specific feature of the system under consideration consists in the fact that in a fully developed turbulence, a large number of various mode scales are excited and the effect of modes of all scales appears to be essential and has to be accounted for since a single act of intermodal interactions is only a link in a long cascade chain via the mechanism of energy transfer from the range of large-scale modes, where the turbulent energy of stochastic fluid velocity pulsations due to a development of instability of large-scale flows is produced, into the range of small-scale modes where the energy dissipates due to fluid viscosity.

Somewhat different approach to finding the spectral energy density beyond the scope of explicit applying the Navier-Stokes equations was proposed by A. N. Kolmogorov [3] who postulated that the energy transfer along the wave-number spectrum goes due to nonlinear intermodal interactions between the modes of close scales, whereas the interaction between the modes of essentially distinguished scales is realized through the cascade sequence of acts relevant to intermodal interactions between modes of intermediate scales (the Richardson-Kolmogorov cascade); in other words, it has a place "a locality in the wave-number space" of intermodal interactions that form a cascade process of energy transfer over wave-number spectrum. The question of a locality nature was discussed in detail in the surveys devoted to application of the renormalization-group method in turbulence theory [4] [5]. The locality relates to the fact that intermodal interaction between the modes with essentially different scales reduces to a primitive transfer of small-scale modes by large-scale ones without energy redistribution between modes (sweeping effect) [6]. In connection with this, when studying the spectrum form it arises the problem of selecting weak local interactions (dynamic interactions) forming the energy spectrum and acting against the ground of strong nonlocal (kinematic) interactions [7]. In the author's paper [8] it was claimed and argued the statement that in the turbulence theory with applying the RG-method [4] [5] use of the ε-expansion procedure, well-known in the theory of critical phenomena, is a way to select the local intermodal interactions and filtering out the effects of non-local (distant) interactions.

Kolmogorov proposed to divide the wave-number spectrum into three parts.

1) The range of turbulent energy production in the domain of small wave numbers $k < k_g$ where the energy of turbulent pulsations is generated due to

development of instability of large-scale flows. The energy production is simulated by the action of an external random force that is similar to the Langevin force used in the theory of random processes. The energy production range lies beyond the scope of our analyses and in our model it will be treated as "a black box" when one knows nothing concerning the processes in the box and only knows conditions on its boundary (spherical surface of radius k_g in the wave-number space). As a boundary condition it is taken the spectral flux through the boundary surface $W\left(k_g\right)$, which is equal to the rate of energy pumping $\mathcal{E}$ received from the range $k < k_g$.

2) The inertial range is a domain of wave numbers where there is no energy production and the dissipation effects are negligible. In this range the spectral flux remains constant, and it goes the process of energy transfer from the range of small wave numbers into the range of large wave numbers via the cascade sequence of local intermodal interaction acts. In the case of high Reynolds numbers (very small fluid viscosity) the inertial range has a sufficiently long length. In the inertial range it takes a place the Kolmogorov formula for spectral energy density

$$E\left(k\right) = C_K \mathcal{E}^{2/3} k^{-5/3}, \tag{1.1}$$

where C_K is the Kolmogorov constant. This formula has been obtained only on the basis of dimensionality arguments without reference to the Navier-Stokes equations.

3) The dissipation range relates to the case when the Reynolds number is not high and dissipation effects are not neglectable. As the Reynolds number decreases (the fluid viscosity grows) the domain of inertial range existence tends to zero and the Kolmogorov formula appears to be inapplicable. Below we consider the problem of building the model that is true beyond the inertial range and obtain the formula for spectral energy distribution $E\left(k\right)$ with account for viscosity that is valid for all wave-numbers with the exception of ones from the energy production range.

2. The Problem of Calculating Energy Spectrum

If the fluid viscosity is accounted for, the spectral flux will depend on wave number and due to the locality of intermodal interactions the spectral energy density $E\left(k\right)$ will be determined by the value of spectral flux at given wave-number $W\left(k\right)$. This fact has to be accounted for when applying the dimensionality arguments. As the result, the formula for $E\left(k\right)$ may be written in the form of "generalized Kolmogorov formula"

$$E\left(k\right) = C\left(k\right) W\left(k\right)^{2/3} k^{-5/3} \tag{2.1}$$

Here $C\left(k\right)$ is a dimensionless function of dimensionless variables $W\left(k\right)/W\left(k_g\right)$, $C\left(k_g\right)$, k/k_g and $H\left(k\right) = W\left(k\right)/\nu^3 k^4$; ν is the fluid viscosity and k_g is the upper boundary of energy production range.

Beyond the energy production range $k > k_d$ the equation of energy balance

has the form

$$\frac{\mathrm{d}W(k)}{\mathrm{d}k} = -2\nu k^2 E(k) \tag{2.2}$$

that relates two unknown quantities $W(k)$ and $E(k)$. For solving the problem one may use the energy balance Equation (2.2) in combination with the "generalized Kolmogorov formula" (2.1), but in this case it remains one more unknown function $C(k)$, which is a functional analog of the Kolmogorov constant. Thus it arises the need to have one more equation followed from some additional considerations or hypotheses. One of them was proposed by Kovazhny [9], whose conjecture appears to be equivalent to the statement $C(k) = \text{const}$. In this approximation Equation (2.2) gives

$$W(k) = \mathcal{E}\left[1 + \frac{\nu C(k_g)}{2\mathcal{E}^{1/3}}\left(k^{4/3} - k_g^{4/3}\right)\right]^3, \quad \mathcal{E} = W(k_g)$$

$$E(k) = C(k_g)\mathcal{E}^{2/3}\left[1 + \frac{\nu C(k_g)}{2\mathcal{E}^{1/3}}\left(k^{4/3} - k_g^{4/3}\right)\right]^2 k^{-5/3} \tag{2.3}$$

According to Equation (2.3) the spectral flux $W(k)$ decreases as the wave-number grows, however, at a certain value of wave-number

$$k_d = k_g\left[1 + \frac{2\mathcal{E}^{1/3}}{\nu C(k_g)k_g^{4/3}}\right]^{3/4}$$

the flux becomes zero and at $k > k_d$ it becomes negative whereas the spectral energy grows that corresponds to the transport of the energy produced by a certain fictitious source from small-scale flows to large-scale ones. This "nonphysical result" points out to the fact that the approximation $C(k) = \text{const} = C(k_g)$ is unsatisfactory and needs for a refinement. In particular, in author's paper [10] it was proposed to treat the result (2.3) as two first terms of the series expansion in fluid viscosity powers of exponent that reproduces the results obtained by Pao [11] (see also [12]). Below it will be shown that this proposal appears to be true.

3. Cascade Mechanism of Turbulent Energy Transfer and Renormalization-Group Method

The required additional equation, which allows one to find $C(k)$, may be obtained by taking into account the cascade mechanism of energy transfer by local in the wave-number space intermodal interactions.

The locality of intermodal interaction acts, which are treated as links of cascade chain, manifest itself in the fact that there is no a certain scale which stands out of another scales (the equal role in cascade chain of all links with given scale). In this case the characteristics of all links in cascade chain $W(k)$ and $C(k)$ are defined only by the characteristics $W_0 = W(k_0)$, $C_0 = C(k_0)$ of the link with $k = k_0$ selected as initial one and are independent of how this link was formatted (the independence of a previous history). This means that the process

of energy transfer over wave-number spectrum is a Markovian process. If the energy transfer be a Markovian process, we will have

$$W(k)=W(k;W_0,C_0,k_0),\quad C(k)=C(k;W_0,C_0,k_0)$$

And the dimensionality arguments enable one to represent the functions desired in the form of dimensionless functions of dimensionless variables

$$W(k)=W_0\varphi_1(k/k_0,H(k_0),C_0),\quad C(k)=C_0\varphi_2(k/k_0,H(k_0),C_0),$$
$$H(k)=W(k)/\nu^3k^4 \tag{3.1}$$

From Equation (3.1) it follows that the dimensionless functions $\varphi_{1,2}(x,h,c)$ of dimensionless variables $x=k/k_0$, $h=H(k_0)$ and $c=C_0$ obey the normalization conditions

$$\varphi_{1,2}(1,h,c)=1 \tag{3.2}$$

The functions $\varphi_{1,2}(x,h,c)$ possess a certain additional symmetry related to an ambiguity in a way of setting the boundary conditions that are reduced to a choice of a certain link with wave-number k_0 as an initial link in cascade chain and specifying the characteristics of this link, namely, W_0 and C_0; in what follows the value k_0 will be referred to as the normalization point.

If another link with the wave-number $k=k_1$ be taken as initial one and the values of parameters of this link $W(k_1)=W_1$ and $C(k_1)=c_1$ be given, the form of functions $\varphi_{1,2}$ remains unchanged; this means that the following relationships have to be satisfied

$$W(k)=W_0\varphi_1\left(\frac{k}{k_0},h,c\right)=W_1\varphi_1\left(\frac{k}{k_1},h_1,c_1\right)$$
$$C(k)=c\varphi_2\left(\frac{k}{k_0},h,c\right)=c_1\varphi_2\left(\frac{k}{k_1},h_1,c_1\right) \tag{3.3}$$

Due to the presence of ambiguity in a choice of the value k_0 (unit of scale) it follows that the functions $\varphi_{1,2}(x,h,c)$ are invariant with respect to the operation of scale transformation $k_0\to k_1$ and relevant change (renormalization) of the parameters $W_0\to W_1=W(k_1)$ and $c\to c_1=C(k_1)$.

The totality of above pointed operators of scale transformations in combination with renormalization of governing parameters obeys the group composition law, contains the operators of identical and inverse transformations, i.e. it made up a group called the renormalization group (RG-group), and the invariance of the function forms under RG-transformations referred to as RG-invariance. In a special case when RG-transformations and RG-invariance are related to change in putting initial or boundary conditions (our case) the term "functional self-similarity" is used [13].

Putting $k=k_1$ in Equation (3.3) and using the normalization condition (3.2)

$$W_1=W_0\varphi_1(\alpha,h,c),\quad c_1=c\varphi_2(\alpha,h,c),\quad \alpha=k_1/k_0 \tag{3.4}$$

we arrive at the functional RG equations

$$\varphi_{1,2}(x,h,c)=\varphi_{1,2}(\alpha,h,c)\varphi_{1,2}(x,h,c)\left(\frac{x}{\alpha},\frac{h\varphi_1(\alpha,h,c)}{\alpha^4},c\varphi_2(\alpha,h,c)\right) \tag{3.5}$$

here α is an arbitrary dimensionless parameter.

These equations are similar to the Kolmogorov-Chapman semi-group equations in the theory of Markovian random processes (the Einstein-Smolukhovsky equations in physics of Brownian motion).

By differentiating the functional RG-equations with respect to α and next putting $\alpha=1$ we obtain the RG-differential equations

$$r_{1,2}(h,c)\varphi_{1,2}(x,h,c)+\left\{-x\frac{\partial}{\partial x}+\left[r_1(h,c)-4\right]h\frac{\partial}{\partial h}+r_2(h,c)c\frac{\partial}{\partial c}\right\}\varphi_{1,2}(x,h,c)=0 \tag{3.6}$$

here

$$r_{1,2}(h,c)=\left.\frac{\partial\varphi_{1,2}(x,h,c)}{\partial x}\right|_{x=1} \tag{3.7}$$

The functions $r_{1,2}$ are similar to the operators of infinitesimal transformations in the Lie theory of continuous groups.

In terms of the functions $\varphi_{1,2}$ the balance energy Equation (2.2) takes the form

$$\frac{\partial\varphi_1(x,h,c)}{\partial x}=-2ch^{-1/3}x^{1/3}\varphi_1^{2/3}(x,h,c)\varphi_2(x,h,c) \tag{3.8}$$

from which it follows

$$r_1(h,c)=-2ch^{-1/3} \tag{3.9}$$

However, the differential RG Equations (3.6) contain a new unknown quantity $r_2(h,c)$ determined by the function $C(k)$ in the generalized Kolmogorov Equation (2.10). Knowledge of this function is necessary for solving the RG differential equation. However, in our analyses it is enough to know this quantity in the lowest perturbation theory approximation, namely, the first-order term of a series expansion in the fluid viscosity. This is in agreement with the procedure of improving the perturbation theory by applying the RG method proposed by Bogoyubov and Shirkov in the quantum field theory [14].

To the zero-order approximation of perturbation theory it is assigned the case when $C(k)=\text{const}$, *i.e.* $\varphi_2=1$ and $r_2=0$, that reproduce the Kovazhny theory containing "nonphysical singularity". The first-order approximation contains a term being proportional to fluid viscosity of first degree. An account for dimensionality arguments gives the following representation for the function $\varphi_2(x,h,c)$

$$\varphi_2(x,h,c)=1+\mu ch^{-1/3}\left(x^{4/3}-1\right)$$

where μ is a certain dimensionless parameter calculated by using statistical solving the Navier-Stokes equations within the framework of perturbation theory [2] at given external random force. This lies beyond the scope of the

model under consideration. From that it follows $r_2(h,c)=\mu r_1(h,c)$ and we will analyze the relevant solution

$$\varphi_1(x,h,c)=\left\{1-\frac{1-3\mu}{2}ch^{-1/3}\left(x^{4/3}-1\right)\right\}^{3/(1-3\mu)},$$

$$\varphi_2(x,h,c)=\varphi_1^{\mu}(x,h,c) \tag{3.10}$$

From Equation (3.10) one can see that in the range $0<\mu<1/3$ the solution contains "nonphysical" singularity and the position of a singular point goes from k_d to infinity as μ goes from zero to 1/3. Since the transition to $\mu\to 1/3$ is weakly defined, we consider this case separately by direct solving the differential RG Equation (3.6).

The equation for $\ln\varphi_1(x,h,c)$ can be written in the form

$$\left\{-x\frac{\partial}{\partial x}-4h\frac{\partial}{\partial h}+\left[r_1(h,c)h\frac{\partial}{\partial h}+r_2(h,c)c\frac{\partial}{\partial c}\right]\right\}\ln\varphi_1(x,h,c)=-r_1(h,c) \tag{3.11}$$

From the easily verified identity

$$\left[r_1(h,c)h\frac{\partial}{\partial h}+r_2(h,c)c\frac{\partial}{\partial c}\right]r_1(h,c)=\left[-r_1(h,c)/3+r_2(h,c)\right]r_1(h,c)$$

it follows that the expression in square brackets is zero when $r_2=r_1/3$. Thus one can seek for the solution to Equation (3.10) in the form

$$\ln\varphi_1(x,h,c)=r_1(h,c)F(x)$$

where the function $F(x)$ obeys the equation

$$1+\left[-x\frac{\mathrm{d}}{\mathrm{d}x}+\frac{4}{3}\right]F(x)=0,\quad F(1)=0,\quad \left.\frac{\mathrm{d}F(x)}{\mathrm{d}x}\right|_{x=1}=1$$

that gives

$$F(x)=\frac{3}{4}\left(x^{4/3}-1\right)$$

As the result the formulas for spectral flux and spectral energy density take the forms

$$W(k)=\mathcal{E}\exp\left\{-\frac{3}{2}\frac{c\nu}{\mathcal{E}^{1/3}}\left(k^{4/3}-k_g^{4/3}\right)\right\} \tag{3.12}$$

$$E(k)=c\mathcal{E}^{2/3}k^{-5/3}\exp\left\{-\frac{3}{2}\frac{c\nu}{\mathcal{E}^{1/3}}\left(k^{4/3}-k_g^{4/3}\right)\right\} \tag{3.13}$$

Here we choose the wave-number k_g, corresponding to the upper boundary of turbulent energy production range, as a normalization point, and use the notation $\mathcal{E}=W(k_g)$ and $c=C(k_g)$. In particular case when $k_g=0$ the results (3.12)-(3.13) appear to be identical to formulas proposed by Pao [11] [12], who put forward the hypothesis on proportionality of energy density $E(k)$ to spectral flux $W(k)$ without any argumentation.

If the parameter μ exceeds one third the spectral characteristics monotonically decrease as k tends to infinity and no singularities arise. In this case the

formulas for energy flux and spectral energy density take the forms

$$W(k)=\varepsilon\left\{-\frac{3}{2}\frac{c\nu}{\varepsilon^{1/3}}\left(k^{4/3}-k_g^{4/3}\right)\right\}^{-3/(3\mu-1)} \tag{3.14}$$

$$E(k)=c\varepsilon^{2/3}k^{-5/3}\left\{-\frac{3}{2}\frac{c\nu}{\varepsilon^{1/3}}\left(k^{4/3}-k_g^{4/3}\right)\right\}^{-(3\mu+2)/(3\mu-1)} \tag{3.15}$$

4. Local and Nonlocal Interactions

Our analysis is based on the statement that the energy spectrum is formed due to intermodal interactions being local in the wave-number space, and this enables one to tell about a cascade mechanism of energy transfer over wave-number spectrum and a Markovian character of the process. Precisely this property of the process gives a possibility to assume that the solution describing the cascade chain depends uniquely on numerical parameters of the link in the chain treated as initial one and is independent of the fact how this link was formatted (independence on previous history). The property of independence on previous history of formatting the initial and boundary conditions (functional self-similarity) is an inherent one for differential equations that do not contain integral terms. Solutions to such equations possess the property of invariance with respect to the way of setting additional (initial and boundary) conditions. Namely, under the shift of the hyper-surface on which additional conditions are given and relevant changing (renormalization) numerical parameters specifying additional conditions the solution remains to be unchanged. The balance energy Equation (2.2) relates to the class of such equations.

However, in the statistical theory of turbulence, the chain of equations that relates statistical moments of various orders arises due to nonlinearity of the Navier-Stokes equation, and this relation necessary contains integral terms. In particular, the equation for the Fourier-transform of the second-order statistic moment of velocity field $B(k,\omega)$ has the form

$$L^{(0)}(k,\omega)B(k,\omega)+T(k,\omega)=D^{(0)}(k,\omega)G(k,\omega) \tag{4.1}$$

where the second-rank tensor $T(k,\omega)$, also referred to as the inertial term, is expressed via the integral of the third-order statistical moment of turbulent velocity pulsations (Equation (A.4) in Appendix). The inertial term describes the processes of momentum and energy redistribution due to mixing induced by velocity pulsations. The relevant intermodal interactions are obviously nonlocal, and the question of validity the form of balance energy Equation (2.2) and an ability to use various symmetry properties like the RG-invariance arises. Thus we arrive at the problem of filtering out these interactions. In the Yakhot-Orszag renormalization-group theory of turbulence [15], this problem is solved by using the ε-expansion procedure when one first calculates the quantity desired in the low-order approximation in ε near the point $\varepsilon=0$ and next extends the result obtained into the point $\varepsilon=4$. This procedure is similar to the t'Hooft-Veltman dimensional regularization method in quantum field theory.

An account for the effect of turbulent velocity pulsations leads to a correction to fluid viscosity (a turbulent viscosity), and as a result the representation for the Fourier-transform of reverse Green's function takes the form

$$G^{-1}(k,\omega)=\left[G^{(0)}(k,\omega)\right]^{-1}-\Sigma(k,\omega) \tag{4.2}$$

$\left[G^{(0)}(k,\omega)\right]^{-1}=L^{(0)}(k,\omega)=-i\omega+\nu k^2$ is the reverse Green function of the linear problem. (This equation can be rewritten in the form of Dyson's equation well-known in quantum-field-theory

$$G(k,\omega)=G^{(0)}(k,\omega)+G^{(0)}(k,\omega)\Sigma(k,\omega)G(k,\omega)$$

where $\Sigma(k,\omega)$ is referred to as the self-energy operator.)

Another result of account for a mixing by turbulent velocity pulsations consists in appearance of effective random force which variance is written as

$$D(k,\omega)=D^{(0)}(k,\omega)+D^{(1)}(k,\omega) \tag{4.3}$$

Here $D^{(0)}(k,\omega)$ is the variance of external random forces that simulate the emergence of stochasticity due to development of instability of large-scale flows and is similar to Langevin forces in the theory of random processes; the second summand $D^{(1)}(k,\omega)$ arises due to account for transport phenomena produced by mixing processes.

The quantity $D(k,\omega)$ enters into the equation for the second-order statistic moment of velocity field $B(k,\omega)$

$$B(k,\omega)=G(k,\omega)D(k,\omega)G(-k,-\omega) \tag{4.4}$$

first obtained by Schwinger [16] when building the theory of quantized fields beyond the scope of perturbation methods. The Schwinger approach is based on statistical description of quantized fields in terms of characteristic (generating) functional. In the statistical theory of turbulence this equation was obtained by Wyld [2] with the help of summing up the perturbation theory series and applying the technique of Feynman diagrams.

In the space-time variables the inertial term $T(1,2)$ contains the third-order statistical moment of velocity field (see Appendix, Equation (A4)) and the question arises whether the Fourier-transform of inertial term will contain integral terms and how to close the set of equations by excluding the third-order statistical moment.

Within the framework of statistical description of turbulence in terms of characteristic (generating) functional it can be obtained the formula for inertial term

$$T(k,\omega)=-\Sigma(k,\omega)B(k,\omega)-G(k,\omega)D^{(1)}(k,\omega) \tag{4.5}$$

firstly pointed out in author's paper [17]. It should be noted that this formula is an exact one since no approximations or additional conjectures were used in its derivation.

The quantities Σ and $D^{(1)}$ are defined by solving the Navier-Stokes equations, but these quantities can be excluded by using Equation (4.2) and Equation

(4.4) that gives

$$T(k,\omega) = -L^{(0)}(k,\omega)B(k,\omega) + G(k,\omega)D^{(0)}(k,\omega) \tag{4.6}$$

For the quantity $T(k) = \int T(k,\omega)\mathrm{d}\omega/2\pi$ we obtain

$$T(k) = -\nu k^2 B(k) + G(k)D^{(0)}(k)$$

If to put $T(k) = \mathrm{d}W(k)/\mathrm{d}k$, we arrive at the balance energy equation that coincides with Equation (2.2) beyond the energy production range. The above presented procedure is another way of excluding nonlocal intermodal interactions when building the theory of turbulent spectra.

5. Conclusion

The theory of spectral energy distribution is based on the Kolmogorov conjecture that the energy spectrum is formatted by intermodal interactions being local in wave-number space. From this, it follows a cascade mechanism of energy transfer along the wave-number space, the Markovian properties of the process, as well as an ability to apply various similarity arguments such as the property of renormalization-group invariance (functional self-similarity). In this case, the problem of separating local intermodal interactions (straining effects) and filtering out nonlocal ones (sweeping effects) arises. An account for mixing processes by turbulent velocity pulsations (swimming effects) reveals in the form of an addition $D^{(1)}$ to a variance of external random forces (turbulent random force) and addition Σ to viscous term in the Navier-Stokes equations (turbulent viscosity). In Section 4 it was shown that in the functional formulation of statistical description of turbulence, these quantities prove to be excluded from the balance energy equation. As the result, the problem of selecting local intermodal interactions and filtering out nonlocal ones appears to be solved exactly without applying other methods such as the ε-RG (see more recent survey [18]).

Acknowledgements

The work was carried out within the framework of the State Task (project No AAAA-A17-117021310375-7).

Conflicts of Interest

The author declares no conflicts of interest regarding the publication of this paper.

References

[1] Monin, A.S. and Yaglom, A.M. (1975) Statistical Fluid Mechanics, Vol. 2. MIT Press, Cambridge.

[2] Wyld, H.W. (1961) *Annals of Physics*, **14**, 143-165. https://doi.org/10.1016/0003-4916(61)90056-2

[3] Kolmogorov, A.N. (1941) *Doklady Akademii Nauk SSSR*, **30**, 299-303.

[4] Teodorovich, E.V. (1993) *Izvestiya, Russian Academy of Sciences: Atmospheric and*

Oceanic Physics, **29**, 149-163.

[5] Zhou, Y. and Vahala, G. (1992) *Physical Review A*, **46**, 1136-1139. https://doi.org/10.1103/PhysRevA.46.1136

[6] Kadomtsev, B.B. (1964) Plasma Turbulence. In: *Problems in Theory of Plasmas*, Vol. 4, Atomizdat, Moscow, 188. (In Russian)

[7] Teodorovich, E.V. (1990) *Fluid Dynamics*, **25**, 522-527. https://doi.org/10.1007/BF01049856

[8] Zakharov, V.E. and L'vov, V.S. (1975) *Izvestiya Vuzov. Radiofizika*, **28**, 1470-1487. https://doi.org/10.1007/BF01040337

[9] Kovasznay, L.S.G. (1948) *Journal of the Aeronautical Sciences*, **15**, 745-753. https://doi.org/10.2514/8.11707

[10] Teodorovich, E.V. (2017) *Applied Mathematics and Mechanics*, **81**, 450-454. https://doi.org/10.1016/j.jappmathmech.2018.03.013

[11] Pao, Y.-H. (1965) *Physics of Fluids*, **8**, 1063-1075. https://doi.org/10.1063/1.1761356

[12] Leslie, D.C. (1973) Developments in the Theory of Turbulence. Clarendon Press, Oxford.

[13] Shirkov, D.V. (1982) *Soviet Physics—Doklady*, **27**, 197-199.

[14] Bogolyubov, N.N. and Shirkov, D.V. (1984) Introduction to the Theory of Quantized Fields. Nauka, Moscow. (In Russian)

[15] Yakhot, V. and Orszag, S.A. (1986) *Journal of Scientific Computing*, **1**, 3-51. https://doi.org/10.1007/BF01061452

[16] Schwinger, J. (1949) *Physical Review*, **75**, 651-679. https://doi.org/10.1103/PhysRev.75.651

[17] Teodorovich, E.V. (2013) *Journal of Modern Physics*, **4**, 56-63. https://doi.org/10.4236/jmp.2013.41010

[18] Zhou, Y. (2010) *Physics Reports*, **488**, 1-49. https://doi.org/10.1016/j.physrep.2009.04.004

Appendix. Basic Equations in Space-Time Variables

To simplify the writing in formulas we will use digital notation for space-time variables and the index of vector components $\{r_1, t_1, \alpha_1\} \equiv 1$ according to which $u_{\alpha_1}(r_1, t_1) \equiv u(1)$. Also it will be implied the integration over space-time coordinates and the summing over component indexes for coinciding digital numbers (the Einstein rule), *i.e.*

$$u(1)v(1) \equiv \int u(r_1, t_1) \cdot v(r_1, t_1) \mathrm{d}r_1 \mathrm{d}t_1$$

The Navier-Stokes equations (NSE) with the presence of the external random force $X(1)$ and the external regular force $f(1)$

$$L^{(0)}(1,2)u(2) + \frac{1}{2}V(1|2,3)u(2)u(3) = X(1) + f(1) \tag{A.1}$$

(for more details related to notation see [16]).

Variance of external random force

$$D^{(0)}(1,2) = \langle X(1)X(2) \rangle \tag{A.2}$$

The equation for $B(1,2) = \langle u(1)u(2) \rangle$

$$L^{(0)}(1,1')B(1',2) + T(1,2) = G(1,1')D^{(9)}(1',2) \tag{A.3}$$

Inertial term

$$T(1,2) = \frac{1}{2}V(1|3,4)B(3,4,2), \quad B(1,2,3) = \langle u(1)u(2)u(3) \rangle \tag{A.4}$$

Exact representation for inertial term

$$T(1,2) = -B(1,1')\Sigma(1',2) - G(1,1')D^{(1)}(1',2) \tag{A.5}$$

The Schwinger-Wyld formula

$$B(1,2) = G(1,1')G(2,2')D(1',2') \tag{A.6}$$

$D(1,2)$ is the variance of effective random forces.

Another form of Equation (A.6)

$$B(1,1')G^{-1}(1',2) = G(1,1')D(1',2) \tag{A.7}$$

Journal of Modern Physics, 2020, 11, 1514-1527
https://www.scirp.org/journal/jmp
ISSN Online: 2153-120X
ISSN Print: 2153-1196

Generation of Multipartite Entangled States Using Switchable Coupling of Cooper-Pair-Boxes

Stefan J. Rinner, Tindaro Pittorino

Interstate University of Applied Science NTB, Buchs, Switzerland
Email: stefan.rinner@ost.ch

How to cite this paper: Rinner, S.J. and Pittorino, T. (2020) Generation of Multipartite Entangled States Using Switchable Coupling of Cooper-Pair-Boxes. *Journal of Modern Physics*, **11**, 1514-1527.
https://doi.org/10.4236/jmp.2020.1110093

Received: August 5, 2020
Accepted: October 11, 2020
Published: October 14, 2020

Abstract

We propose a scheme for a switchable coupling between several Cooper-pair boxes in the charge regime. The switch is embodied in a SQUID element contained in the center conductor of a transmission-line resonator. Altering the flux bias through the SQUID allows for changing the effective resonator length. Thus the position of the nodes and anti-nodes of the relevant eigenmodes changes and leads to a variable interaction strength between qubit and cavity vacuum field. For the coupled qubits the interaction is dispersive. An example for the application of this switch is the generation of multipartite entangled states for three and four charge qubits. Although used as a discrete switch in the present proposal, the combined system of SQUID module integrated into the transmission line may be operated continuously as well.

Keywords

Switchable, Variable Interaction

1. Introduction

Quantum Optics on a chip represents an intriguing and promising pace on the way to a scalable Quantum Computer. In [1] and [2] the strong coupling of a single photon to a superconducting qubit using circuit quantum electrodynamics has been demonstrated and their work was followed by other investigations in this field [3] [4] [5]. Some years ago, the construction of a reconfigurable quantum optical circuit on a chip and the control of entangled states with up to four photons were reported [6]. At the heart of this device is a simple heating element that changes the phase in one arm of an interferometer. In addition, there exist proposals for the design and fabrication of photonic quantum circuits

[7] as well as their characterization [8]. In [9] researchers report that on a single chip, sources of entangled photons are combined with optical elements that can perform complex manipulations of quantum signals. Other groups have realised quantum circuits using quantum dots and superconducting devices [10]. In this context, mesoscopic devices, such as the Cooper-pair box (CPB), appear to be promising candidates for building blocks in the hardware of a quantum computer. The logic states of the qubit are formed by a large number of Cooper pairs and are distinguished by the number of excess Cooper pairs on the superconducting island which is connected to a superconducting reservoir by a Josephson junction.

Exemplarily, more recent publications [11]-[16] demonstrate that the interest in superconducting qubits for quantum computation still remains a vivid area of research.

Probably the most prominent advantage of mesoscopic systems, like the CPB or quantum dots, compared to atomic systems or photons is the fact that they can be fabricated and operated with standard present-day technology, and that their designs are scalable. In the fabrication process their properties can be customized, and no extra effort has to be taken to keep their number and location fixed. On the other hand, due to their size they are more strongly exposed to noise and decoherence effects than their atomic or photonic counterparts. The time window available for preparation and coherent manipulation of states in the so-called circuit-QED setup was reported by Wallraff *et al.* [1] who measured a coherence time as long as 500 ns for a single CPB inside a cavity. Placing the CPB in a resonator is believed to screen part of the environmental effects. Therefore, this design is—apart from its importance due to the analogy with cavity QED—a prime candidate for the investigation of multi-qubit systems.

In order to work with multi-qubit devices, e.g. for the realization of quantum-information processing tasks, a tunable coupling is desirable. Lately, a high-fidelity quantum processor was built in the form of a two-dimensional array of 54 transmon qubits [17]. In their experiment, each of these qubits is tunably coupled to four nearest neighbours, in a rectangular lattice. The authors claim to have demonstrated quantum supremacy experimentally. For CPBs, a variety of coupling ideas have been proposed (e.g., [18] [19] [20] [21] [22]). Circuit-QED offers an alternative possibility to couple the CPB via the cavity [1] [23]. In this article we propose a scheme for dispersive CPB coupling. The most important feature of our proposal is the fully controllable switch for inter-qubit coupling where no internal manipulations on the qubits themselves (such as changing the gate voltages on each of them simultaneously and synchronically) are needed to start and stop their interaction. This is achieved by controlling only one external parameter (the magnetic flux through the SQUID loop), increasing the experimental feasibility and reducing possible sources for decoherence. Our proposal is based on the setup of the Yale group [1]. The action of the switch makes use of vacuum modes only.

With the tunable coupling at hand, one may look for applications based on the manipulation of the interaction between the CPBs inside the cavity. A particularly interesting application is the preparation of multipartite entangled states. For example, one may seek to prepare multipartite states representing locally inequivalent classes of entanglement such as the *GHZ* and the *W* state [24]. In cavity QED with atoms there are several theoretical proposals for the generation of such states [25] [26], as well as for trapped ions [27]. In Ref. [28], *GHZ* states with up to six ions could be generated, while in Ref. [29], *W* states with up to eight ions have been created. There are other proposals for the generation of such states [30] [31] [32] [33] [34] as well as experimental realisations [35]-[42]. One aim of this work is to present a method of preparing similar states in circuit QED with Cooper pair boxes [43].

A similar proposal was made by Wallquist *et al.* [44], yet in our approach the bus is used indirectly to obtain effective qubit-qubit coupling, rather than directly with the bus.

In order to support the experimental feasibility of our proposal, we exemplarily mention the work of Palacios *et al.* [45] and Sandberg *et al.* [46].

The outline of this paper is as follows. In Section 2 we explain the operation of the switch for turning on and off the interaction between the qubits. We then present a way to use this switch for the controlled generation of multipartite entangled states of the qubits (Section 3). We conclude with a discussion of our results and possibilities to extend them in Section 4.

2. Switchable Resonator

2.1. Concept

In our proposal, the resonator acts as the coupling device between the qubits. It can be used to control the coupling between an *on* position and an *off* position (discrete coupling switch). To this end the center conductor of the resonator contains a SQUID loop. The switch is realized by changing the effective length of the center conductor of the transmission line resonator (**Figure 1**) via changing the flux through the SQUID loop between integer and half integer number of flux quanta.

The *on* position of the switch corresponds to the full length $L^{(0)}$ of the center conductor (cf. **Figure 1**). The CPBs are located where the electric field strength has a node (vanishing coupling between CPB and cavity mode, see **Figure 1(a)**). Note that we refer to the second eigenmode of the cavity

$$\omega_2^{(0)} = 2\left(v\pi/L^{(0)}\right) \tag{1}$$

with the phase velocity $v = 1/\sqrt{lc}$, in close analogy with Ref. [1], with capacitance per length c and inductance per length l. As the total current through a SQUID depends on the external flux Φ applied to the ring, $J_{\text{total}} \propto \cos\left(\frac{e}{\hbar}\Phi\right)$, for the *on* position of the switch the flux in the loop needs to be equal to an in-

teger number of the flux quantum $\Phi_0 = \frac{h}{e}$. It has been shown that in superconducting rings the magnetic flux is quantised in the following manner $\Phi_n = n \cdot \frac{h}{2e}$. The Josephson energy of the junctions in the SQUID device should be chosen large enough in order not to interrupt the resonator.

If the switch is "off" (*i.e.*, if the flux through the SQUID loop equals a half integer number of flux quanta) the resonator is cut into left and right parts of length $L^{(1)}$ and $L^{(2)}$ respectively: charge cannot flow from the left to the right resonator (see **Figure 1(b)**). Note however that the electromagnetic field in the left resonator is still coupled capacitively to the rest of the transmission line (through the junction capacitances of the SQUID loop). The CPBs now couple to the second eigenmode of the left resonator as their position is chosen such that the electric field strength is large. In contrast to the setup in Ref. [1] the level splitting of the CPBs is *not* in resonance with the new eigenfrequency of the left resonator, rather we choose it to be slightly detuned. This causes the qubits to interact with the left cavity mode dispersively without exchanging excitations.

Assuming dimensions in the cm range for the resonator length and ~2 μm for each CPB, an inter-CPB distance of ~100 μm should be sufficient to exclude direct coupling between the CPBs and, on the other hand, facilitate equal coupling constants of the CPBs with the cavity mode [47].

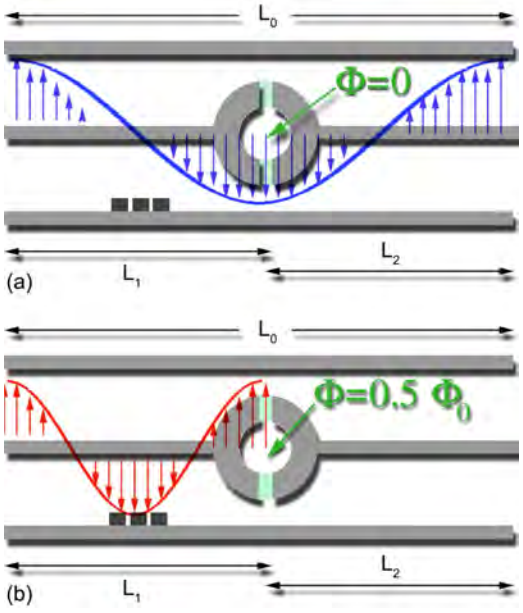

Figure 1. Schematic layout showing three cooper pair boxes (black squares) in the transmission line resonator and the corresponding field modes. (a) Switch in the *on* position, with SQUID loop closed. The effective resonator length equals the total length $L^{(0)}$ of the center conductor. The CPB are located at a node position of the $\omega_2^{(0)}$ mode; (b) Switch in the *off* position. The Josephson coupling between left and right part of the center conductor is zero. The new effective resonator length is close to $L^{(0)}/2$ (see text) and the resonance frequency is detuned from the CPBs' level splitting.

Let us now consider the effect of the SQUID loop on the transmission line. In general, an infinitesimally short transmission line of length dx can be approximated using the lumped component model depicted in Figure 2.

In this model, the current I and the voltage U are generally functions of the time t and of the position x. The values l, c, r and g represent respectively the inductance, the capacitance, the resistance and the conductance per unit of length for the transmission line. Using Kirchoff's voltage and current laws on the lumped model and assuming $dx \to 0$ the following equations can be derived:

$$\begin{cases} \dfrac{\partial I}{\partial x} = gU + c\dfrac{\partial U}{\partial t} \\ \dfrac{\partial U}{\partial x} = rI + l\dfrac{\partial I}{\partial t} \end{cases} \tag{2}$$

By calculating the derivative with respect to x of the first equation and the time derivative of the second equation, the current flowing in the transmission line can be expressed by the following expression:

$$\frac{\partial^2 I}{\partial x^2} = grI + (gl + rc)\frac{\partial I}{\partial t} + lc\frac{\partial^2 I}{\partial t^2} \tag{3}$$

In the specific case of a SQUID, the system will only work at very low temperature. Under this condition, it is not false to consider the transmission line as lossless ($r = 0$ and $g = 0$). Equation (3) can be hence approximated as:

$$\frac{\partial^2 i}{\partial x^2} = lc\frac{\partial^2 i}{\partial t^2} \tag{4}$$

Let us consider the effect of the SQUID loop for the resonance frequencies of the transmission line more quantitatively. In an infinitesimal lumped-element circuit model for a transmission line (without SQUID element) the current I obeys the wave equation

$$\frac{1}{c}\frac{\partial^2 I}{\partial x^2} - l\frac{\partial^2 I}{\partial t^2} = 0 \tag{5}$$

with boundary conditions $I(x=0) = I\left(x = L^{(0)}\right) = 0$. We assume that this wave equation is satisfied also with the switch in the *on* position.

For the *off* position of the switch this equation is modified. While in the left and the right part of the transmission line Equation (5) remains unchanged, at

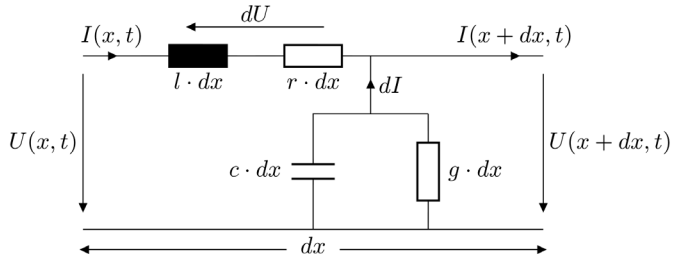

Figure 2. Transmission line lumped model for an infinitesimally short line.

$x = x_0$ the total capacitance C_0 of the junctions in the loop (which can be assumed to be point-like at the position x_0) contributes another term that couples left and right resonator part:

$$\frac{1}{c}\frac{\partial^2 I}{\partial x^2} - l\frac{\partial^2 I}{\partial t^2} - \frac{1}{C_0} I\delta\left(x - x_0\right) = 0. \tag{6}$$

The resulting problem for the eigenmodes of this resonator is analogous to a quantum-mechanical particle of mass $c/2$ in a double-well potential (of lengths $L^{(1)}$ and $L^{(2)}$) separated by a δ-barrier of strength $1/C_0$ at $x = x_0$. We choose $L^{(1)}$, $L^{(2)}$ to differ by a few per cent in order to avoid the symmetry point $L^{(1)} = L^{(2)}$ for which the solutions have peculiar properties. Moreover, this allows us to arrange for the proper detunings of the various modes. We are interested in the case of weak coupling between the "potential wells", that is, weak capacitive coupling $C_0 \ll cL^{(0)}$ between the parts of the center conductor. In this case the new eigenmodes differ only little from the modes of the unperturbed problem (that is, no coupling at all, $C_0 \to 0$). To first order we obtain, e.g., for the second mode of the left resonator (cf. also Ref. [1])

$$\omega_2^{(1)} \approx 2\frac{\nu\pi}{L^{(1)}}\left(1 - \frac{C_0}{cL^{(1)}}\right). \tag{7}$$

The first term in this expression represents the resonant solution (cf. Equation (1)), the second one accounts for the effect of detuning. Given the typical capacitance of a transmission line, the capacitance C_0 may be on the order of several 10^{-14} F to satisfy the weak-coupling condition.

2.2. Quantitative Considerations

In this section we briefly discuss the relevant modes for the two regimes of the switch and estimate possible errors. When the cavity mode is in resonance with the qubit frequency there is coupling between cavity and CPBs with coupling strength g which is proportional to the strength of the local electric field, i.e. the coupling with resonant modes vanishes at their nodes and is maximal at their antinodes. This coupling strength is modified in the case of detuning and results in an effective coupling strength $\lambda_i^k = g^2/\Delta_i^{(k)}$ as will be shown in the following paragraph.

In the *off* regime for modes $\omega_i^{(1)}$ in the left resonator $\Delta_i^{(1)}$ is large (on the order of the cavity eigenfrequency) only except for the slightly detuned $\omega_2^{(1)}$. The mode $\omega_2^{(2)}$ (eigenmode of the right resonator) might leak into the left part if the disconnection is not perfect. However, not only is it also detuned (given $L_1 \neq L_2$) but also decays its amplitude rapidly at the left side rendering the coupling to this mode a negligible quantity at the site of the CPBs.

In the *on* regime the CPBs are sited at a node of the (also detuned) mode $\omega_2^{(0)}$, so that the coupling vanishes. The mode with the smallest detuning with respect to the CPB eigenfrequency in this regime is $\omega_4^{(0)}$. Its impact on the CPB may still be ignored as discussed in further detail below.

In order to realize a dispersive interaction of the CPBs with cavity mode $\omega_2^{(1)}$, we require a detuning of, say $\delta\omega_2^{(1)}/\omega_2^{(1)} \sim 10^{-2}$. The other resonator modes need to have much stronger detuning in order to reduce their coupling to the qubit, in particular for the *on* position of the switch. For example, we may choose $L^{(1)} \simeq 0.54L^{(0)}$ and $C_0/cL^{(1)} \simeq 0.05$ which yields ~10% red shift of the resonance frequency $\omega_2^{(0)}$ from the closest mode of the *off* switch and ~12% detuning from the 4th mode of the full-length resonator. For coupling strengths in the MHz regime and frequencies on the order of 10^{10} Hz this detuning leads to an effective coupling strength $\lambda \simeq 10^{-3} g$ with respect to the coupling strength g in the resonant case.

A CPB spacing of $\Delta x = 100\,\mu\text{m}$ corresponds to one per cent of the cm dimensions of the resonator. Consequently, the amplitude of the mode $\omega_2^{(1)}$ differs from its maximal value at position $x_{\max}$ by a factor of around 10^{-4} at positions $x = x_{\max} \pm 100\,\mu\text{m}$ and by a factor of 10^{-3} for $\Delta x = 300\,\mu\text{m}$ for a resonator length of 3 cm.

In the following section we will show how to use this digital switch in order to generate multipartite entanglement between the qubits via the dispersive interaction with the cavity mode.

3. Generation of Multipartite Entangled States

The starting configuration of the system cavity plus CPBs is the following: the flux through the ring configuration is $\Phi = 0$. The state of the cavity field is assumed to be the vacuum state $|0_f\rangle_0$ where the first subscript stands for "field" and the second denotes the cavity eigenmode of the resonator with length $L^{(0)}$.

In the interaction picture the system is described by the Tavis-Cummings Hamiltonian [48], the N-atom generalized Jaynes-Cummings Hamiltonian [49]:

$$H_0 = \hbar g_0 \sum_{j=1,2,3} \left(\mathrm{e}^{-i\delta t} a^\dagger \sigma_j^- + \mathrm{e}^{i\delta t} a \sigma_j^+ \right) \tag{8}$$

containing the bosonic creation (annihilation) operators $a^\dagger$ (a) for a photon in the cavity mode, the creation (annihilation) operators $\sigma_j^\dagger$ (σ_j) for an excitation of the jth Cooper pair box, the detuning δ and the coupling strength g_0 between the dipole moment of each CPB and the electric field. In the interest of legibility we use g_0 instead of $g_2^{(0)}$. The three CPBs are assembled at a position where the electric field strength of the relevant cavity eigenmode vanishes. Consequently, there is (approximately) no interaction beyond the free evolution ($g_0 \simeq 0$). Due to this condition a well-defined initial state can be prepared that does not exchange excitations with the cavity field.

Suppose now the flux through the SQUID is suddenly changed by half a flux quantum. The effective resonator length changes to the smaller $L^{(1)}$ with the new eigenmode in its vacuum state $|0_f\rangle_L$. The new resonator frequency $\omega_2^{(1)}$ is detuned from the CPB resonance and the coupling strength g_L (again instead of $g_2^{(1)}$) still being near its maximal value. Denoting the detuning between cavity mode and each CPB by Δ and the creation (annihilation) operators for

the cavity mode b by $b^\dagger$ (b), the new Tavis-Cummings Hamiltonian can be written in the interaction picture as

$$H = \hbar g_L \sum_{j=1,2,3} \left(\mathrm{e}^{-i\Delta t} b^\dagger \sigma_j^- + \mathrm{e}^{i\Delta t} b \sigma_j^+ \right). \tag{9}$$

The corresponding time-evolution operator $U(t) = U(t, t_0 = 0)$ is given up to second order by

$$U(t) \approx 1 - \frac{i}{\hbar} \int_0^t \mathrm{d}t' H(t') - \frac{1}{\hbar^2} \int_0^t \mathrm{d}t' H(t') \int_0^{t'} \mathrm{d}t'' H(t''). \tag{10}$$

We use this expansion to derive the effective Hamiltonian for large detuning, *i.e.*, $\Delta \gg g_L$, where no energy exchange between the CPB system and the cavity is possible. The first-order term gives

$$\begin{aligned} U^{(1)}(t) &= -\frac{i}{\hbar} \int_0^t \mathrm{d}t' H(t') \\ &= \frac{g_L}{\Delta} \sum_{j=1,2,3} \left[\left(\mathrm{e}^{-i\Delta t} - 1 \right) b^\dagger \sigma_j^- - \left(\mathrm{e}^{i\Delta t} - 1 \right) b \sigma_j^+ \right], \end{aligned}$$

and the second-order term

$$\begin{aligned} U^{(2)}(t) &= -\frac{1}{\hbar^2} \int_0^t \mathrm{d}t' H(t') \int_0^{t'} \mathrm{d}t'' H(t'') \\ &= -\frac{i g_L^2}{\Delta} \int_0^t \mathrm{d}t' \sum_{j=1}^3 \left(\mathrm{e}^{-i\Delta t'} b^\dagger \sigma_j^- + \mathrm{e}^{i\Delta t'} b \sigma_j^+ \right) \sum_{k=1}^3 \left(\left(\mathrm{e}^{-i\Delta t'} - 1 \right) b^\dagger \sigma_j^- - \left(\mathrm{e}^{i\Delta t'} - 1 \right) b \sigma_j^+ \right). \end{aligned}$$

Note that after carrying out the above product of sums the subsequent integration will yield additional prefactors of order $1/\Delta$ for all terms except for those which involve the product of complex conjugate exponentials. With this in mind it is easy to see that

$$\begin{aligned} U^{(2)}(t) = -\frac{i g_L^2}{\Delta} \sum_{j=1}^3 \Big(& -b^\dagger b \sigma_j^- \sigma_j^+ + b b^\dagger \sigma_j^+ \sigma_j^- \Big) t \\ & - \frac{i g_L^2}{\Delta} \underbrace{\left(-b^\dagger b + b b^\dagger \right)}_{= \left[b, b^\dagger \right] = 1} \Big(\sigma_1^- \sigma_2^+ + \sigma_1^- \sigma_3^+ + \sigma_2^- \sigma_1^+ \\ & + \sigma_2^- \sigma_3^+ + \sigma_1^+ \sigma_3^- + \sigma_2^+ \sigma_3^- \Big) t + \mathcal{O}\left(\frac{1}{\Delta^2} \right). \end{aligned}$$

Here and in the following $\sigma_1^- \sigma_3^+$, e.g., is shorthand for $\sigma_1^- \otimes 1_2 \otimes \sigma_3^+$. Keeping only terms linear in time we arrive at

$$\begin{aligned} U(t,0) &\approx 1 - \frac{i}{\hbar} \left(\frac{\hbar g_L^2}{\Delta} \right) \Bigg[\sum_{j=1}^3 \left(b b^\dagger \sigma_j^+ \sigma_j^- - b^\dagger b \sigma_j^- \sigma_j^+ \right) \\ &\quad + \left(\sigma_2^- \sigma_3^+ + \sigma_1^- \sigma_3^+ + \sigma_1^+ \sigma_2^- + \sigma_1^+ \sigma_3^- + \sigma_2^+ \sigma_3^- + \sigma_2^+ \sigma_1^- \right) \Bigg] t \\ &\approx \exp\left[-\frac{i}{\hbar} H_{\mathrm{eff}} t \right]. \end{aligned}$$

with the effective Hamiltonian in the interaction picture

$$H_{\text{eff}} = \hbar \underbrace{\left(\frac{g_L^2}{\Delta}\right)}_{=:\lambda} \Bigg[\sum_{j=1,2,3} \left(bb^\dagger \sigma_j^+ \sigma_j^- - b^\dagger b \sigma_j^- \sigma_j^+ \right) + \left(\sigma_2^- \sigma_3^+ + \sigma_1^- \sigma_3^+ + \sigma_1^+ \sigma_2^- + \sigma_1^+ \sigma_3^- + \sigma_2^+ \sigma_3^- + \sigma_2^+ \sigma_1^- \right) \Bigg].$$

Consider now the case when the cavity is in its vacuum state. Then the above Hamiltonian reduces to

$$H_{\text{eff}} = \hbar\lambda \left[\sum_{j=1,2,3} \left| e_j \right\rangle \left\langle e_j \right| + \left(\sigma_2^- \sigma_3^+ + \sigma_1^- \sigma_3^+ + \sigma_1^+ \sigma_2^- + \sigma_1^+ \sigma_3^- + \sigma_2^+ \sigma_3^- + \sigma_2^+ \sigma_1^- \right) \right],$$

since $bb^\dagger \left| 0_f \right\rangle_L = \left| 0_f \right\rangle_L, b^\dagger b \left| 0_f \right\rangle_L = 0$.

This shows that there is an effective interaction between the qubits even though no excitation is transferred from the qubits to the cavity mode. Next we want to show how to use such interactions in order to generate three-qubit and four-qubit entangled states. To this end, one has to solve the Schrödinger equation for this Hamiltonian. In the following, applying the conventional nomenclature for qubits let $\left| 1_j \right\rangle$ denote the excited state of the jth CPB $\left| e_j \right\rangle$ since no field Fock states are needed anymore and confusion is thus avoided. States which initially are computational basis states can be divided into three classes with the corresponding time evolution:

1) only one CPB is in state $\left| 1 \right\rangle$, e.g., $\left| \psi(0) \right\rangle = \left| 100 \right\rangle$:

$$\left| \psi_1(t) \right\rangle = \frac{\mathrm{e}^{-3i\lambda t} + 2}{3} \left| 100 \right\rangle + \frac{\mathrm{e}^{-3i\lambda t} - 1}{3} \left(\left| 010 \right\rangle + \left| 001 \right\rangle \right).$$

2) only one CPB is in state $\left| 0 \right\rangle$, e.g. $\left| \psi(0) \right\rangle = \left| 110 \right\rangle$:

$$\left| \psi_2(t) \right\rangle = \frac{1}{3} \mathrm{e}^{-i\lambda t} \left[\left(\mathrm{e}^{-3i\lambda t} + 2 \right) \left| 110 \right\rangle + \left(\mathrm{e}^{-3i\lambda t} - 1 \right) \left(\left| 011 \right\rangle + \left| 101 \right\rangle \right) \right].$$

3) all CPBs are in the same state, *i.e.* $\left| \psi_3(t) \right\rangle = \left| 000 \right\rangle$ or $\left| \psi_3(t) \right\rangle = \left| 111 \right\rangle$.

With the coupling switched off, the state of the CPB system only acquires a phase factor (we assume that, in principle, such states can be prepared). Now the dispersive coupling is switched on suddenly. By starting from the state of the first type and adjusting the interaction time such that $\tau = \frac{2\pi}{9\lambda}$ the state of the CPB system evolves into a W state of the form

$$\begin{aligned} \left| \psi_1(\tau) \right\rangle &= \frac{\mathrm{e}^{-i2\pi/3} + 2}{3} \left| 100 \right\rangle + \frac{\mathrm{e}^{-i2\pi/3} - 1}{3} \left(\left| 010 \right\rangle + \left| 001 \right\rangle \right) \\ &= \frac{1}{\sqrt{3}} \left[\mathrm{e}^{-i\pi/6} \left| 100 \right\rangle + \mathrm{e}^{-i5\pi/6} \left(\left| 010 \right\rangle + \left| 001 \right\rangle \right) \right] \\ &= \mathrm{e}^{-i5\pi/6} \frac{1}{\sqrt{3}} \left[\mathrm{e}^{i2\pi/3} \left| 100 \right\rangle + \left(\left| 010 \right\rangle + \left| 001 \right\rangle \right) \right]. \end{aligned}$$

For a detuning $\Delta \sim 100$ MHz and a coupling strength $g_L \sim 15$ MHz, the time required to generate this W state is $\tau \sim 300$ ns.

This is an example of the general N-qubit W state with arbitrary phases:

$$|W_N\rangle = \frac{1}{\sqrt{N}}\left(e^{i\theta_1}|1000\cdots0\rangle + e^{i\theta_2}|0100\cdots0\rangle + e^{i\theta_3}|0010\cdots0\rangle + \cdots + e^{i\theta_N}|0000\cdots1\rangle\right).$$

The concurrences between any two qubits of the above state are all equal to $2/N$ and do not depend on the phases [50].

By extending this method to four qubits it is also possible to generate a three-CPB W state with equal phases: Starting from one CPB in the excited state and the remaining three CPBs in the ground state $|\psi_4(t=0)\rangle = |1000\rangle$ the dispersive interaction leads to a state

$$|\psi_4(t)\rangle = c_1(t)|1000\rangle + c_2(t)\left[|0100\rangle + |0010\rangle + |0001\rangle\right] \tag{11}$$

with the probability amplitudes

$$c_1(t) = \frac{\sqrt{3}+1}{2\sqrt{3}}e^{i(\sqrt{3}-2)\lambda t} + \frac{\sqrt{3}-1}{2\sqrt{3}}e^{-i(\sqrt{3}+2)\lambda t}$$

$$c_2(t) = \frac{1}{2\sqrt{3}}\left(e^{-i(\sqrt{3}+2)\lambda t} - e^{i(\sqrt{3}-2)\lambda t}\right).$$

Detection of the first qubit in the state $|0\rangle$ then gives the desired W state for the remaining three CPBs:

$$|W(t)\rangle = \frac{1}{\sqrt{3}}|0\rangle \otimes \left[|100\rangle + |010\rangle + |001\rangle\right] \tag{12}$$

where the common phase factor has been discarded.

We emphasize that there is no need for a specific interaction time in order to create this superposition state. The trade-off, however, is in the necessity to perform a read-out on the first qubit and the probabilistic nature of the preparation procedure.

As a final example we mention the generation of *GHZ*-like states for four qubits. By choosing the initial state $|\psi_5(t=0)\rangle = |1100\rangle$ the time evolution with the interaction switched on results in

$$|\psi_5(t)\rangle = C_1(t)|1100\rangle + C_2(t)|0011\rangle + C_3(t)\left[|1010\rangle + |1001\rangle + |0110\rangle + |0101\rangle\right]$$

with probability amplitudes

$$C_1(t) = \frac{1}{6}e^{-4i\lambda t} + \frac{1}{3}e^{2i\lambda t} + \frac{1}{2}$$

$$C_2(t) = \frac{1}{6}e^{-4i\lambda t} + \frac{1}{3}e^{2i\lambda t} - \frac{1}{2}$$

$$C_3(t) = \frac{1}{6}e^{-4i\lambda t} - \frac{1}{6}e^{2i\lambda t}$$

Noting that $C_3(\tau) = 0$ for the choice $\tau = \pi/3\lambda$ one can prepare a state belonging to the *GHZ*-class [24] [26] [51] of the form

$$|\psi_5(\tau)\rangle = \frac{1}{4}\left[\left(i\sqrt{3}+1\right)|1100\rangle + \left(i\sqrt{3}-3\right)|0011\rangle\right] \tag{13}$$

as desired.

4. Conclusions

We have presented a theoretical proposal to implement a switch for controlled dispersive coupling of several Cooper pair boxes in a transmission line resonator. The coupling can be turned on and off by changing the flux through a SQUID loop integrated into the center conductor of the resonator. Here a few additional remarks are due regarding the practical realization of this idea.

First, we have discussed the switch as a digital device between an "on" and an "off" position. The latter position is, strictly speaking, only an "almost off" position with a much smaller coupling $g_0 \ll g_L$ compared to the "on" case. This is due to the structure of the effective coupling constant g_L^2/Δ: due to the presence of the other modes (far off resonance) there is always a residual coupling. As we have mentioned in Section 2, a difference of at least one order of magnitude is realistic. This sets a limit for the idle periods of the setup: if this limit is exceeded, the time evolution of the (almost) uncoupled CPB system is not proportional to the identity (apart from a phase factor), but a more general uncontrolled many-qubit gate.

Secondly, the switching operation is not limited to the digital mode. In principle, the resonator modes constitute continuous functions of the flux Φ through the SQUID loop. As the discussion in Section 2 shows, one may view the action of the loop also as a control of the boundary conditions for the electromagnetic field in the transmission line (see also a related proposal [52]). A detailed analysis needs to take into account Josephson inductance L_J of the SQUID loop that depends on the (flux-dependent) Josephson energy $E_J(\Phi)$ as $L_J \propto 1/E_J(\Phi)$ in parallel to the capacitance C_0, and will be carried out elsewhere.

Apart from the advantages of the switch (e.g., no simultaneous switching of CPB controls) that contribute to reducing noise, the presence of the SQUID loop introduces also new decoherence sources: the Josephson junctions of the loop (which are subject to dielectric losses [53]) and flux noise.

Finally, we have discussed the application of this coupling scheme for the generation of multi-qubit entanglement between the CPBs. We have emphasized the principle of the idea, and we have not considered a detailed setup which should include also the methods for state preparation and measurements. In particular, we have shown how *W* states for three qubits and *GHZ* states for four qubits can be obtained. The protocols are surprisingly simple and, apart from state preparation and measurements, do not require complicated sequences of operations and can be realized in a single shot. Thus one may conclude that the setup provides an interesting starting point for various multi-qubit applications based on circuit-QED.

Acknowledgements

We would like to thank G. Falci and E. Werner for illuminating discussions and comments.

Conflicts of Interest

The authors declare no conflicts of interest regarding the publication of this paper.

References

[1] Blais, A., Huang, R.-S., Wallraff, A., Girvin, S.M. and Schoelkopf, R.J. (2004) *Physical Review A*, **69**, Article ID: 062320. https://doi.org/10.1103/PhysRevA.69.062320

[2] Wallraff, A., Schuster, D.I., Blais, A., Franzio, L., Huang, R.-S., Majer, J., Kumar, S., Girvin, A.M. and Schoelkopf, R.J. (2004) *Nature*, **431**, 162-167. https://doi.org/10.1038/nature02851

[3] Irish, E.K., Gea-Banaloche, J., Martin, I. and Schwab, K.C. (2005) *Physical Review B*, **72**, Article ID: 195410. https://doi.org/10.1103/PhysRevB.72.195410

[4] Devoret, M.H., Girvin, S. and Schoelkopf, R. (2007) *Annals of Physics*, **16**, 767. https://doi.org/10.1002/andp.200710261

[5] You, J.Q., Liu, Y.X., Sun, C.P. and Nori, F. (2007) *Physical Review B*, **75**, Article ID: 104516. https://doi.org/10.1103/PhysRevB.75.104516

[6] Berr, D.W. and Wiseman, H.M. (2009) *Nature Photonics*, **3**, 317-319. https://doi.org/10.1038/nphoton.2009.84

[7] Poot, M., Schuck, C., Ma, X.-S., Guo, X. and Tang, H.X. (2016) *Optics Express*, **24**, 6843-6860. https://doi.org/10.1364/OE.24.006843

[8] Poot, M. and Tang, H.X. (2016) *Applied Physics Letters*, **109**, Article ID: 131106. https://doi.org/10.1063/1.4962902

[9] Jin, H., Liu, F.M., Xu, P., Xia, J.L., Zhong, M.L., Yuan, Y., Zhou, J.W., Gong, Y.X., Wang, W. and Zhu, S.N. (2014) *Physical Review Letters*, **113**, Article ID: 103601. https://doi.org/10.1103/PhysRevLett.113.103601

[10] Deng, G.-W., Guo, G.-P. and Guo, G.-C. (2016) On-Chip Quantum Optics with Quantum Dots and Superconducting Resonators. *Proc. SPIEE* 10029, *Quantum and Nonlinear Optics*, Vol. 4, Article ID: 1002909.

[11] Liu, Y.-X., Xu, X.-W., Miranowicz, A. and Nori, F. (2014) *Physical Review A*, **89**, Article ID: 043818. https://doi.org/10.1103/PhysRevA.89.043818

[12] Mirza, I.M. and Schotland, J.C. (2016) *Physical Review A*, **94**, Article ID: 012309. https://doi.org/10.1103/PhysRevA.94.012302

[13] Armata, F., Calajo, G., Jaako, T., Kim, M.-S. and Rabl, P. (2017) *Physical Review Letters*, **119**, Article ID: 183602. https://doi.org/10.1103/PhysRevLett.119.183602

[14] Blais, A., Girvin, S.M. and Oliver, W.D. (2020) *Nature Physics*, **16**, 247-256. https://doi.org/10.1038/s41567-020-0806-z

[15] Mirza, I.M. and Schotland, J.C. (2016) *Physical Review A*, **94**, Article ID: 012302. https://doi.org/10.1103/PhysRevA.94.012302

[16] Ciccarello, F., Paternostro, M., Palma, G.M. and Zarcone, M. (2009) *New Journal of Physics*, **11**, Article ID: 073040. https://doi.org/10.1088/1367-2630/11/11/113053

[17] Arute, F., *et al.* (2019) *Nature*, **574**, 505-510.

[18] Makhlin, Yu., Shnirman, S. and Schön, G. (1999) *Nature*, **398**, 305-307.

[19] Siewert, J., Fazio, R., Palma, G.M. and Sciacca, E. (2000) *Journal of Low Temperature Physics*, **18**, 795. https://doi.org/10.1023/A:1004612016347

[20] You, J.Q., Tsai, J.S. and Nori, F. (2002) *Physical Review Letters*, **89**, Article ID: 197902. https://doi.org/10.1103/PhysRevLett.89.197902

[21] Averin, D.V. and Bruder, C. (2003) *Physical Review Letters*, **91**, Article ID: 057003. https://doi.org/10.1103/PhysRevLett.91.057003

[22] Lantz, J., Wallquist, M., Shumeiko, V.S. and Wendin, G. (2004) *Physical Review B*, **70**, Article ID: 140507(R). https://doi.org/10.1103/PhysRevB.70.140507

[23] Plastina, F. and Falci, G. (2003) *Physical Review B*, **67**, Article ID: 224514. https://doi.org/10.1103/PhysRevB.67.224514

[24] Dür, W., Vidal, G. and Cirac, J.I. (2000) *Physical Review A*, **62**, Article ID: 062314. https://doi.org/10.1103/PhysRevA.62.062314

[25] Zeilinger, A., Horne, M.A. and Greenberger, D.M. (1997) NASA Conference Publication No. 3135. National Aeronautics and Space Administration, Code NTT, Washington DC.
Guo, G.-C. and Zhang, Y.-S. (2002) *Physical Review A*, **65**, Article ID: 054302.

[26] Guo, G.-P., Li, C.-F., Li, J. and Guo, G.-C. (2002) *Physical Review A*, **65**, Article ID: 042102. https://doi.org/10.1103/PhysRevA.65.042102

[27] Roos, C.F., Riebe, M., Häffner, H., Hänsel, W., Benhelm, J., Lancaster, G.P.T., Becher, C., Schmidt-Kaler, F. and Blatt, R. (2004) *Science*, **304**, 1478.

[28] Leibfried, D., Knill, E., Seidelin, S., Britton, J., Blakestad, R.B., Chiaverini, J., Hume, D.B., Itano, W.M., Jost, J.D., Langer, C., Ozeri, R., Reichle, R. and Wineland, D.J. (2005) *Nature*, **438**, 639. https://doi.org/10.1038/nature04251

[29] Häffner, H., Hänsel, W., Roos, C.F., Benhelm, J., Chek-al-kar, D., Chwalla, M., Körber, T., Rapol, U.D., Riebe, M., Schmidt, P.O., Becher, C., Gühne, O., Dür, W. and Blatt, R. (2005) *Nature*, **438**, 643. https://doi.org/10.1038/nature04279

[30] Peng, Z.H., Liu, Y.-X., Nakamura, Y. and Tsai, J.S. (2012) *Physical Review B*, **85**, Article ID: 024537. https://doi.org/10.1103/PhysRevB.85.024537

[31] Yang, C.-P. (2011) *Physical Review A*, **83**, Article ID: 062302. https://doi.org/10.1103/PhysRevA.83.042112

[32] Wang, Y.-D., Chesi, S., Loss, D. and Bruder, C. (2010) *Physical Review B*, **81**, Article ID: 104524. https://doi.org/10.1103/PhysRevB.81.104524

[33] Aldana, S., Wang, Y.-D. and Bruder, C. (2011) *Physical Review B*, **84**, Article ID: 134519. https://doi.org/10.1103/PhysRevB.84.134519

[34] Bishop, L.S., *et al.* (2009) *New Journal of Physics*, **11**, Article ID: 073040.

[35] Song, C., Xu, K., Liu, W.X., Yang, C.-P., Zheng, S.-B., Deng, H., Xie, Q.W., Huang, K.Q., Guo, Q.J., Zhang, L.B., Zhang, P.F., Xu, D., Zheng, D.N., Zhu, X.B., Wang, H., Chen, Y.-A., Lu, C.-Y., Han, S.Y. and Pan, J.-W. (2017) *Physical Review Letters*, **119**, Article ID: 180511. https://doi.org/10.1103/PhysRevLett.119.180511

[36] Barends, R., Kelly, J., Megrant, A., *et al.* (2014) *Nature*, **508**, 500-503. https://doi.org/10.1038/nature13171

[37] Huang, S.-Y., Goan, H.-S., Li, X.-Q. and Milburn, G.J. (2013) *Physical Review A*, **88**, Article ID: 062311. https://doi.org/10.1103/PhysRevA.88.062311

[38] Feng, W., Wang, P.Y., Ding, X.M., Xu, L.T. and Li, X.-Q. (2011) *Physical Review A*, **83**, Article ID: 042313.

[39] Di Carlo, L., Reed, M., Sun, L., *et al.* (2010) *Nature*, **467**, 574-578. https://doi.org/10.1038/nature09416

[40] Neeley, M., Bialczak, R., Lenander, M., *et al.* (2010) *Nature*, **467**, 570-573. https://doi.org/10.1038/nature09418

[41] Chow, J.M., DiCarlo, L., Gambetta, J.M., Nunnenkamp, A., Bishop, L.S., Frunzio, L., Devoret, M.H., Girvin, S.M. and Schoelkopf, R.J. (2010) *Physical Review A*, **81**, Ar-

ticle ID: 062325. https://doi.org/10.1103/PhysRevA.81.062325

[42] Majer, J., Chow, J., Gambetta, J., *et al.* (2007) *Nature*, **449**, 443-447. https://doi.org/10.1038/nature06184

[43] Guillaume, A. and Dowling, J.P. (2006) *Physical Review A*, **73**, Article ID: 040304(R).

[44] Wallquist, M., Shumeiko, V.S. and Wendin, G. (2006) *Physical Review B*, **74**, Article ID: 224506. https://doi.org/10.1103/PhysRevB.74.224506

[45] Palacios-Laloy, A., Nguyen, F., Mallet, F., *et al.* (2008) *Journal of Low Temperature Physics*, **151**, 1034-1042. https://doi.org/10.1007/s10909-008-9774-x

[46] Sandberg, M., *et al.* (2008) *Applied Physics Letters*, **92**, Article ID: 203501. https://doi.org/10.1063/1.2929367

[47] Wallraff, A. (2005) Private Communication.

[48] Tavis, M. and Cummings, F.W. (1968) *Physical Review*, **170**, 379. https://doi.org/10.1103/PhysRev.170.379

[49] Jaynes, E.T. and Cummings, F.W. (1963) *Proceedings of the IEEE*, **51**, 89. https://doi.org/10.1109/PROC.1963.1664

[50] Wang, X. (2001) *Physical Review A*, **64**, Article ID: 012313. https://doi.org/10.1103/PhysRevA.64.012313

[51] Greenberger, D.M., Horne, M. and Zeilinger, A. (1980) Going beyond Bell's Theorem. In: Kafatos, M., Ed., *Bell's Theorem, Quantum Theory and Conceptions of the Universe*, Kluwer, Dordrecht, 69.

[52] Wallquist, M., Shumeiko, V.S. and Wendin, G. (2006) *Physical Review B*, **74**, Article ID: 224506.

[53] Martinis, J.M., Cooper, K.B., McDermott, R., Steffen, M., Ansmann, M., Osborn, K.D., Cicak, K., Oh, S., Pappas, D.P., Simmonds, R.W. and Yu, C.C. (2005) *Physical Review Letters*, **95**, Article ID: 210503. https://doi.org/10.1103/PhysRevLett.95.210503

Journal of Modern Physics, 2020, 11, 1528-1535
https://www.scirp.org/journal/jmp
ISSN Online: 2153-120X
ISSN Print: 2153-1196

Multiple Emulsions Able to Be Used for Oral Administration of Active Pharmaceutical Ingredients: Physico-Chemical Parameters Study of Different Phases

Louis Augustin Diaga Diouf[1], Alphonse Rodrigue Djiboune[1], Mamadou Soumboundou[2], Sidy Mouhamed Dieng[3], Papa Mady Sy[1], Gora Mbaye[1], Mounibé Diarra[1]

[1]Pharmaceutical Physics and Biophysics Laboratory, Faculty of Medicine, Pharmacy and Odontology, Cheikh Anta Diop University of Dakar, Dakar, Senegal
[2]Pharmaceutical Physics and Biophysics Laboratory, Healthy UFR of Thies, University of Thies, Thies, Senegal
[3]Galenic and Industrial Pharmacy Laboratory, Healthy UFR of Thies, University of Thies, Thies, Senegal
Email: louyoguiste@yahoo.fr, alphonserodrigue.djiboune@ucad.edu.sn, mamadou.soumboundou@univ-thies.sn, sidym.dieng@univ-thies.sn, papamady.sy@ucad.edu.sn, Gora.mbaye@ucad.edu.sn, mounibe.diarra@ucad.edu.sn

How to cite this paper: Diouf, L.A.D., Djiboune, A.R., Soumboundou, M., Dieng, S.M., Sy, P.M., Mbaye, G. and Diarra, M. (2020) Multiple Emulsions Able to Be Used for Oral Administration of Active Pharmaceutical Ingredients: Physico-Chemical Parameters Study of Different Phases. *Journal of Modern Physics*, **11**, 1528-1535.
https://doi.org/10.4236/jmp.2020.1110094

Received: July 15, 2020
Accepted: October 11, 2020
Published: October 14, 2020

Abstract

Multiple emulsions are of great therapeutic interest especially in the administration of medicines which can be inactivated by digestive enzymes; moreover the researches of formulation not being often easy, a control of the different phases physicochemical parameters would be of great interest in rapid formulations and at low cost. When formulating emulsions, the preliminary tests, also known as formulation tests, constitute a step which can be long and expensive because of the quantity of reagents that can be used. A rigorous methodology could thus be of great interest, which is at the aim of our study which consists of evaluating the physico-chemical parameters of different phases used to make thus multiple emulsions. In our study, physico-chemical parameters such as conductivity, pH, density, viscosity, and surface tension have been studied by direct measurement using equipment and also by means of suitable mounting. The results showed that the pH and the surface tension have an important role in the prediction of the stability of emulsions, these latter must be of the same order of magnitude. For all phases conductivity does not have too much interest apart from helping to determine the type of the emulsion.

Keywords

Active Pharmaceutical Ingredients, Multiple Emulsions, Stability,

Physico-Chemical Parameters

1. Introduction

Emulsions are thermodynamically unstable systems; they are mixtures of two immiscible phases to be dispersed one within the other. The main goal is to keep this dispersion stable for a long time. In practice, according to Salager, "formulators of emulsions have experienced the unpleasant occurrence of the lack of reproduction of the physical properties (type, stability, viscosity) of an emulsion formulated with identical raw materials following the same rigorously definitive experimental protocol" [1] [2] [3]. Based on this assertion, we have studied the physical parameters which allow us to find information that is relevant for obtaining emulsions with good stability and which would be carried out within a rational time.

With regard to emulsions in general, many studies have been carried out on the various techniques which improve their quality and stability. These techniques are based on compositional, formulation and process variables [4] [5] [6] [7]. Concerning the formulation and composition variables, the type of surfactant, the HLB, and also the proportions of the various constituents were studied.

2. Material

2.1. Reagents

For the formulation of multiple emulsion, a mixture of Span® 80/Tween® 80 which HLB can vary from 4.3 to 15 is used as surfactant for oil in water emulsion, the surfactant used for water in oil emulsion is Montane® 481 VG (M481VG) (HLB 4.5).

The oily or lipophilic phase used was peanut oil and the hydrophilic one consisted of Phosphate buffer Saline (PBS) pH 7.2; mixed with Carboxymethylcellulose (CMC).

2.2. Equipment

Equipment used consisted of:

- pH meter Schott Geräte CG820
- Conductimeter Schott Geräte CG820
- Magnetic stirrer fisher scientific
- Precision balance Ohaus explorer
- Surface tension meter Dognon-Abribat model PROLABO

3. Methods

For both the lipophilic and the hydrophilic phase, the physico-chemical parameters as pH, conductivity, surface tension and viscosity are studied through the above cited apparatus. To measure the viscosity, the method used consisted to

form a drop of dispersed phase in the dispersing phase and in measuring the speed of migration of the drop thus formed, the device is shown in Figure 1.

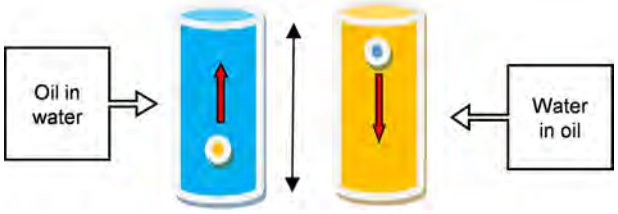

Figure 1. Viscosity measuring device [6].

The following Equation (1), determines the viscosity obtained using the limiting velocity reached by a moving particle in a viscous medium:

$$\eta = \frac{2\left(\rho_{\text{drop}} - \rho_{\text{medium}}\right)}{9 \cdot v_{\text{limit}}} \cdot g \cdot r_{\text{drop}}^2 \tag{1}$$

η = viscosity, ρ = density, v = velocity of the formed drop, r = radius of the formed drop, g = gravity acceleration.

It was also studied the changes of the contact angles by observing the behavior of two superposed and not mixed phases [8].

The hydrophilic phase was mixed with 1% of CMC and with the emulsifiers constituted by the span 80/tween 80 pair at 10%. The proportion of the mixture of Span® 80/Tween® 80 which gave different HLB is indicated in Table 1.

Table 1. Proportions of span 80/tween 80 emulsion for HLB ranging from 7 to 14.

Span 80	Tween 80	HLB
74.77%	25.23%	7
65.42%	34.58%	8
46.73%	53.27%	10
28.04%	71.96%	12
9.35%	90.65%	14

The HLBs vary from 7 to 14 and are intended for the production of O/W emulsions.

Concerning the surfactant Montane® 481 VG (M481VG) used to prepare W/O emulsion his HLB is fixe (4.5) and the proportion used is noted in Table 2.

Table 2. Proportions of M481VG used for W/O emulsion.

Sample	Composition (%)
M1	5
M2	6
M3	7
M4	8
M5	10

4. Results

4.1. Hydrophilic Phase

The hydrophilic phase consists essentially of 1% CMC solution for which the pH measurement gave a value of 6.8, therefore slightly acidic. For the conductivity, its measurement gave a value of 17 mS/cm for the 1% CMC solution and 18 mS/cm for the 2% solution.

The surface tension determined by the immersion blade method gave a value of 38.50 mN/m.

For the hydrophilic phase with 1% CMC mixed with the emulsifiers constituted of the span 80/tween 80 pair at 10%, the results of the measurements of the pH, conductivity and surface tension are listed in Table 3.

Table 3. Physico-chemical parameters of the CMC solution containing 10% span 80/tween 80 mixture.

HLB	pH	Conductivity (mS/cm)	Surf. Tens. (mN/m)
7	5.25	0.91	30.656
8	5.13	0.96	31.392
10	4.9	1.01	29.675
12	4.81	1.02	30.961
14	4.66	1.15	31.147

It is noted a decrease in pH corresponding to an increase in the degree of acidity, a slight increase in conductivity and small fluctuations in the surface tension between 29 and 31 mN/m.

4.2. Lipophilic Phase

The results of pH measurements of the lipophilic phase, in which the proportions of emulsifying agent vary from 0% to 8%, are shown in Table 4.

Table 4. pH measurements of the lipophilic phase.

Proportions	pH
0%	2.78
2%	3.8
4%	3.5
6%	4.3
8%	4.5

An acidic pH is observed for all lipophilic phases, we noted an increase with the proportions of surface-active agent constituted by M481VG.

For different concentrations of montane 481 VG we also measured the surface tension which results are shown in Figure 2.

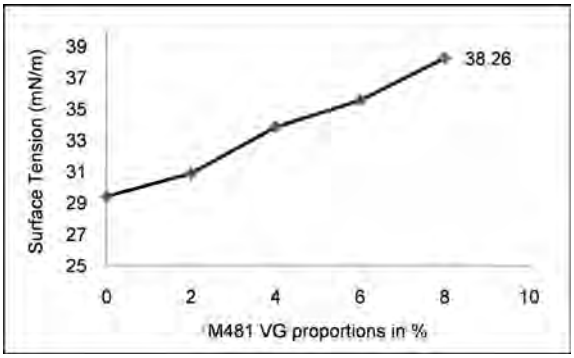

Figure 2. The surface tension variation curve of lipophilic phase as a function of montane 481 VG concentration.

These results show that montane 481 VG increases surface tension instead of decreasing it, this is justified in so far as we have emulsions in which it is the most dense phase that must be introduced in the least dense phase, this explains the need to increase the density of the latter to avoid the sedimentation of the internal phase due to the action of gravity [8] [9].

These changes in interfacial tension are also visible when the two solutions are superposed. A decrease in the contact angle of the oil phase with the wall of the beaker is thus observed as shown in **Figure 3** following the Equation (2)

$$F = 2\pi Rs \cdot \cos\theta \tag{2}$$

s = surface tension coefficient, R = droplet radius, q = contact angle.

There is also a beginning of penetration of the oil phase into the aqueous one, which indicates a decrease in the interfacial tension.

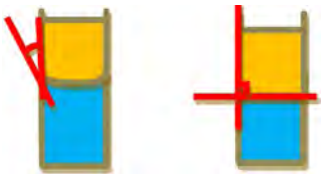

Figure 3. Variation of the contact angle of the lipophilic phase before (16˚) and after (90˚) addition of the surfactant [8].

For the measurement of the density, the results are given in **Figure 4**.

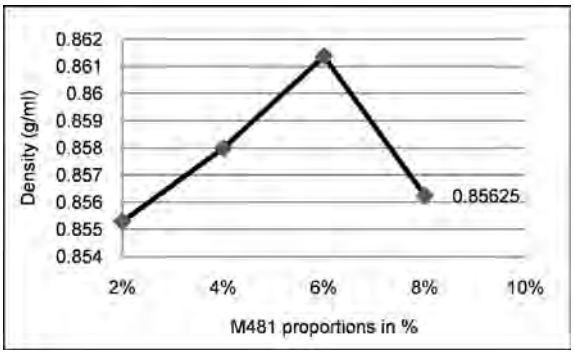

Figure 4. Variation of the density as function of concentration of montane 481VG.

A maximal density is noted at the concentration of 6% of M481VG in the lipophilic phase.

The results of the viscosity measurements, obtained by the immersion drop method identical to the ball drop method, are shown in Figure 5.

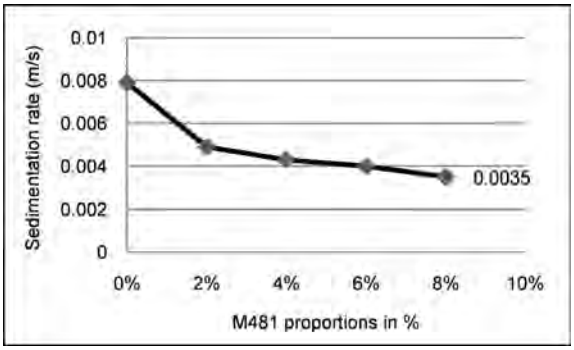

Figure 5. Variation of the sedimentation rate as a function of montane 481VG concentration.

5. Discussion

The emulsions intended to do are W/O/W emulsions type [8] [9]. For the realization we used three types of surfactants that allowed varying the hydrophilic/lipophilic balance. These surfactants are, tween 80 and span 80, but also montane 481VG.

Data from the literature have shown that emulsifiers for water-in-oil emulsions must have an HLB between 1 and 6, hence the use of the montane 481VG which has HLB equal to 4.5, and for oil-in-water emulsions the HLB must be between 7 and 14 hence the use of span 80 tween 80 couple [3] [10].

The study of the physico-chemical parameters such as pH, conductivity and surface tension allowed seeing the variations of these properties as function of HLB especially with regard to the external hydrophilic phase. Since the goal was the formulation of multiple emulsions, the stability of the latter depends more on the external aqueous phase. For the latter, composition was of the utmost importance. Thus, as for the internal aqueous phase for which the pH is slightly acid in order of 6.8, the acidic pH is also observed for the external aqueous phase, which decreases as the HLB increases. The pH of the external hydrophilic phase to which we obtained a stable emulsion (HLB 8) of the order of 5.13 is quite close to that of the lipophilic phase with 6% emulsifier having a pH of 4.3. This acidity of the pH of the two phases is a stability indicator because an identical zeta potential can be observed around the droplets, which may be at the origin of a force of electrostatic repulsions between the droplets [11] [12] [13].

We also noted that the HLB of span/tween 80 torque giving stable emulsions are the same as those found by ANKURMAN [14].

The most interesting parameter we have studied is the surface tension at the interface of two liquids. Indeed, the main objective in the formulation of the emulsions is to reduce the interfacial tension. Therefore, if the surface tension of

the aqueous phase oscillates between 29 and 30 mN/m, that of the oily phase increases in proportion to the M481VG concentration and varies from 29 to 38 mN/m. Thus, superficial tensions observed are practically the same order of magnitude. It is also noted that the surface tension of the aqueous phase has decreased by almost half. We have tried to materialize that drop in the interfacial tension by measuring the contact angle of the aqueous phase. This shows an increase of the contact angle which has passed from 16˚ before addition of the surfactant to 90˚ after addition of 6% of surfactant. This makes the analysis of the evolution of the surface tension of two liquids a good indicator in the prediction of stability [15]. Besides pH and interfacial tension, the viscosity measurement can also give information about the feasibility of the emulsions. Indeed, by observing the curve of variation of the viscosity by means of the sedimentation rate of a drop of dispersed phase, it is observed that this velocity decreases and tends to stabilize around a value which, in regard to our emulsions, is 6%.

6. Conclusions

The study of the physico-chemical parameters such as pH, conductivity, surface tension… allowed seeing the variations of these properties as function of HLB especially with regard to the external hydrophilic phase. Since the goal was the formulation of multiple emulsions, the stability of the latter depends more on the external aqueous phase. For the latter, composition was of the utmost importance.

When making emulsions, the preliminary tests, also known as formulation tests, constitute a step which can be long and expensive because of the quantity of reagents that can be used. A good methodology could therefore be of great interest. Thus the results of the study showed that the pH and the interfacial tension have an important role in the prediction of stability of emulsion; the interfacial tension of the two phases must be of the same order of magnitude. The measurement of the conductivity does not have too much interest apart from helping to determine the type of the emulsion.

Author Contributions

All authors have contributed to the research and design of this item.

Conflicts of Interest

The authors declare no conflicts of interest regarding the publication of this paper.

References

[1] Salager, J.L., Anton, R. and Aubry, J.M. (2006) Formulation des émulsions par la méthode HLD. In Techniques de l'ingénieur, vol génie des procédés J2, Chapter 158, 1-16.

[2] Becher, P. (1983-96) Encyclopedia of Emulsion Technology. Vol. 4, M. Dekker, New York.

[3] Griffin, C. (1949) *Journal of Cosmetic Science*, **1**, 311-326.

[4] ICI Americas Inc. Wilmington (1984) The HLB System, a Time Saving Guide to Emulsifier Selection.

[5] Silva Cunha, A., Grossiord, J.L., Puissieux, F. and Seiller, M. (1997) *International Journal of Pharmaceutics*, **158**, 79-89. https://doi.org/10.1016/S0378-5173(97)00249-4

[6] Kaci, M., Meziani, S., Arab-Tehrany, E., Gillet, G., Desjardins-Lavisse, I. and Desobry, S. (2014) *Ultrasonics Sonochemistry*, **21**, 1010-1017. https://doi.org/10.1016/j.ultsonch.2013.11.006

[7] Li, J., Su, L., Li, J., Liu, M.-F., Chen, S.-F., Li, B., Zhang, Z.-W. and Liu, Y.-Y. (2015) *RSC Advances*, **5**, 83089-83095. https://doi.org/10.1039/C5RA11155B

[8] Diouf, L.A.D. (2017) Elaboration et évaluation d'émulsions multiples pour l'administration de l'insuline par voie orale. Thèse de doctorat de Physique—Biophysique 2017 Université Cheikh Anta DIOP Dakar (Sénégal).

[9] Diouf, L.A.D., Mbaye, G., Ndiaye, A., Sy, P.M., Djiboune, A.R., *et al.* (2015) *International Journal of Current Research*, **7**, 22420-22423.

[10] Lange, N.A. and Dean, J.A. (1967) Lange's Handbook of Chemistry. 10th Edition, McGraw Hill, New York, 1661-1665.

[11] Gadhave, A. (2014) *International Journal of Science and Research*, **3**, 573-575.

[12] Emeche, A.K., Okujagu, D.C. and Okwu, E. (2017) *International Journal of Research and Development*, **2**, 1-8.

[13] Strassner, J.E. (1968) *Journal of Petroleum Technology*, **20**, 303-312. https://doi.org/10.2118/1939-PA

[14] Shrestha, A. (2011) Effect of Span 80-Tween 80 Mixture Compositions on the Stability of Sunflower Oil-Based Emulsions Bachelor of Technology in Biotechnology Rourkela India.

[15] Kanouni, M., Rosano, H.L. and Naouli, N. (2002) *Advances in Colloid and Interface Science*, **99**, 229-254. https://doi.org/10.1016/S0001-8686(02)00079-9

Journal of Modern Physics, 2020, 11, 1536-1558
https://www.scirp.org/journal/jmp
ISSN Online: 2153-120X
ISSN Print: 2153-1196

Circular Scale of Time and Its Use in Calculating the Schrödinger Perturbation Energy of a Non-Degenerate Quantum State

Stanisław Olszewski

Institute of Physical Chemistry, Polish Academy of Sciences, Warsaw, Poland
Email: solszewski@ichf.edu.plolsz@ichf.edu.pl

How to cite this paper: Olszewski, S. (2020) Circular Scale of Time and Its Use in Calculating the Schrödinger Perturbation Energy of a Non-Degenerate Quantum State. *Journal of Modern Physics*, **11**, 1536-1558.
https://doi.org/10.4236/jmp.2020.1110095

Received: July 20, 2020
Accepted: October 13, 2020
Published: October 16, 2020

Abstract

The paper presents a circular scale of time—and its diagrams—which can be successfully applied in calculating the Schrödinger perturbation energy of a non-degenerate quantum state. This seems to be done in a more simple way than with the aid of any other of the perturbation approaches of a similar kind. As an example of the theory suitable to comparison is considered the Feynman diagrammatic method based on a straight-linear scale of time which represents a much more complicated formalism than the present one. All diagrams of the approach outlined in the paper can obtain as their counterparts the algebraic formulae which can be easily extended to an arbitrary Schrödinger perturbation order. The calculations and results descending from the perturbation orders N between $N = 1$ and $N = 7$ are reported in detail.

Keywords

Circular Scale of Time, Schrödinger Perturbation Energy in Non-Relativistic Quantum Mechanics, Non-Degenerate Quantum States

1. Introduction

What is time? My answer is that it is a parameter which allows us to distinguish a later event from an earlier one; this distinction seems to be a fundamental property of time. On the other hand, according to Springer's "Physikalisches Handwörterbuch" [1], time is defined as an independent variable of classical mechanics. One is suggested to add here the adjective "non-relativistic" to the notion of mechanics, because the relativity—in its special picture—makes any time interval dependent on such parameters as the body velocity and light velocity. Evidently in the general relativity the dependence of time is still more ex-

tended, for example due to the presence of the mass of the body [2].

In science an important problem of time became to couple its behaviour with some other physical properties than those given by classical mechanics. Perhaps the best known example is here the entropy and its connections with time. In brief we need the parameters, or effects, which can be examined parallelly with time, though they do not necessarily represent an explicit dependence on the time variable.

In the present case such example of the time connected with physics is given by a quantum perturbation effect. We assume that at some time moment—more or less accurately known—some time-independent perturbation to a quantum system is applied. For a ground state in the absence of the perturbation effect the notion of a stationary state implies an infinite duration of that state. Usually we are unable to follow in detail the history of a system changed by the perturbation, but—according to Schrödinger—we know the end of the state history equivalent to the end of the perturbation process: this is a new stationary state having a new eigenenergy, different than possessed by the system state before the perturbation was applied.

Our aim is to present the time dependence of the perturbation history—and its results—in a possibly transparent way.

2. Quantum-Mechanical Characteristics of the Schrödinger Perturbation Process

In fact the original characteristics of the perturbation process done by Schrödinger [3] did not involve the idea, or a variable, of time. Also in more modern treatments of the Schrödinger perturbation theory—see e.g. [4]—the time does not enter the calculations.

In fact when the Hamiltonian operator $\hat{H}_0$ of an unperturbed quantum problem is given, the main idea is to calculate the eigenenergies $E^{(0)}$ and eigenfunctions $\psi^{(0)}$ satisfying the eigenequation

$$\hat{H}^{(0)}\psi^{(0)}(\boldsymbol{r}) = E^{(0)}\psi^{(0)}(\boldsymbol{r}). \tag{1}$$

The $E^{(0)}$ are constant energy terms and $\psi^{(0)}(\boldsymbol{r})$ are eigenfunctions dependent solely on the position vector parameter $\boldsymbol{r}$. In principle there can exist an infinite set of $\psi^{(0)}(\boldsymbol{r})$ and $E^{(0)}$.

Let the perturbed problem be due to introduction of the so-called small perturbation potential

$$V^{\text{per}} = V^{\text{per}}(\boldsymbol{r}) \tag{2}$$

which is dependent only on the position variable $\boldsymbol{r}$. By assuming—for the sake of simplicity—that the unperturbed problem is a non-degenerate one, we look now for the solution of the perturbed eigenequation

$$\hat{H}^{\text{per}}\psi^{\text{per}}(\boldsymbol{r}) = \left[\hat{H}^{(0)} + V^{\text{per}}(\boldsymbol{r})\right]\psi^{\text{per}}(\boldsymbol{r}) = E^{\text{per}}\psi^{\text{per}}(\boldsymbol{r}) \tag{3}$$

where

$$E^{\mathrm{per}} \quad \text{and} \quad \psi^{\mathrm{per}}\left(\boldsymbol{r}\right) \tag{4}$$

are the sets of the energy eigenvalues and eigenfunctions calculated respectively to some chosen perturbation potential (2).

The idea of Schrödinger and his followers became—instead of solving (3)—to calculate the perturbed quantities (4) in terms of the sets of unperturbed $E_n^{(0)}$ and $\psi_n^{(0)}\left(\boldsymbol{r}\right)$ belonging to various solutions *n*. If we limit the calculations to the energy problem alone, the perturbed term for energy can be represented by a series of terms belonging to different perturbation orders *N*, where *N* varies according to the sequence of the integer numbers

$$N = 1, 2, 3, 4, \cdots, N_{\max}. \tag{5}$$

The order *N* can be referred to the perturbation energy E^{per} and perturbation wave function $\psi^{\mathrm{per}}\left(\boldsymbol{r}\right)$ of a non-degenerate quantum state by the formulae (see e.g. [4]):

$$E^{\mathrm{per}} = E^{(0)} + \lambda\Delta E_1 + \lambda^2\Delta E_2 + \lambda^3\Delta E_3 + \cdots + \lambda^{N_{\max}}\Delta E_{N_{\max}} \tag{5a}$$

whereas

$$\psi^{\mathrm{per}} = \psi^{(0)} + \lambda\Delta\psi^{(1)} + \lambda^2\Delta\psi^{(2)} + \lambda^3\Delta\psi^{(3)} + \cdots + \lambda^{N_{\max}}\Delta\psi^{(N_{\max})}. \tag{5b}$$

The both series, (5a) and (5b), are expressed in terms of the powers of a parameter λ. These powers of λ represent in (5a) the order given in (5) of the energy correction ΔE_N and in (5b) the order of the wave function correction $\Delta\psi^{(N)}$, respectively.

The number $N_{\max}$ denotes a maximal value of *N* applied in some practical calculation. In effect, for a convergent perturbation method and $N_{\max}$ sufficiently large, the accuracy of results for the perturbed energy is expected to increase with the increase of a chosen $N_{\max}$. In many occasions—in order to get a good approximation of the perturbed energy E^{per}—there is necessary to calculate a series of terms due to a large $N_{\max}$:

$$E^{\mathrm{per}} = E^{(0)} + \Delta E^{(1)} + \Delta E^{(2)} + \Delta E^{(3)} + \cdots. \tag{6}$$

Here we have put $\lambda = 1$ in (5a) and the term $E^{(0)}$—entering also (5a)—labels the energy of an unperturbed state. The superscript entering ΔE represents the energy contribution due to the energy contribution to (6) due to the perturbation order *N*.

The subscript *n* which labels the index of the quantum state submitted to perturbation has been omitted in (5a), (5b) and (6) for the sake of brevity. Also, for the same reason, $N_{\max}$ entering further calculations will be replaced simply by *N*.

The main—and a rather fundamental problem of the Schrödinger theory—is that the number and complication of the perturbation terms which are necessary for calculating any

$$\Delta E^{(N)} \tag{7}$$

entering (6) increases rapidly with *N*; an increase of the number of terms neces-

sary to obtain (7) is represented by the formula [5] [6]

$$S_N = \frac{(2N-2)!}{N!(N-1)!} \tag{8}$$

and detailed values of S_N are given in Table 1. But simultaneously—to the best of my knowledge—no systematic rule was provided to build up the set of individual terms entering (8), and this task becomes a much complicated one for large N.

In effect the calculation of terms (7) suitable for large N becomes a difficult task already at the stage of their construction. But a removal of this complication provides us not only with a simplicity necessary to solve the calculational problem. In fact, the importance of the perturbation methods in general can be considered as a decreasing obstacle in view of the development of the computational machinery and its technique applied to solve the physical problems. The point of importance is that an essential simplification can be attained due to the introduction of the time parameter into the perturbation theory. This introduction provides us with a suitable arrangement of the time points on the scale labelling the contact events of the perturbation potential with an originally unperturbed quantum system. The details of this idea and its use in the Schrödinger method are presented below.

3. Perturbation Order and a Suitable Scale of Time

Not only in the everyday life, but in physics too, we are accustomed to applying a straight-linear scale of time according to which each of the later events does happen after an earlier one. Topologically the scale does assume the shape of an infinite straight line on which a distance of some chosen earlier point to an actual point of time increases systematically with the time variable; see Figure 1. This

Table 1. The S_N numbers from formula (8) and Feynman's $P(N)$ numbers of formula (9) (see [8]) calculated for different N.

Perturbation order N	$S(N)$	$P(N)$
1	1	1
2	1	1
3	2	2
4	5	6
5	14	24
6	42	120
7	132	720
8	429	5040
9	1430	40,320
10	4862	362,880
11	16,796	3,628,800
12	58,786	39,916,800

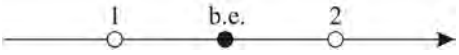

Figure 1. The straight-linear (progressive) scale of time. The point b.e. represents the present situation: *b* is the beginning point of the future (on the right), the point *e* is the end point of the past (on the left). An access is solely from point 1 to 2; no access is from 2 to 1.

situation does not change also in the case when—according to the Feynman's idea—the terms of the Schrodinger perturbation theory are sought to be plotted along the scale with the aim to calculate the necessary diagrams of energy [7] [8]. These diagrams can be classified also according to the perturbation order N, however, in order to get a contribution of energy $\Delta E^{(N)}$ given in (7) the number of diagrams should be not that presented in (8) but becomes

$$P(N)=(N-1)! \tag{9}$$

Only for very small N we have

$$P(N)=S(N), \tag{10}$$

but for $N \gg 1$ the inequality

$$P(N) \gg S(N) \tag{11}$$

evidently does exist giving for example for $N=20$ the ratio

$$P(20):S(20) \cong 0.7\times 10^{8}, \tag{12}$$

The formulae (11) and (12) imply that in order to get—in average—a single Schrödinger component term for the perturbation energy of a non-degenerate quantum state—a large, or even very large, number of results due to the Feynman energy diagrams should be first calculated, next suitably combined. Such a difficulty does not apply to the calculations based on a circular scale developed in the present paper.

4. Perturbation Process along a Circular Scale of Time and Its Energy Terms

We assume that the perturbation process is a set of successive collisions of the perturbation potential (2) with an unperturbed quantum system. The collision events are extended along a topological circle characteristic for a given order N of the perturbation potential; in the next step the collisions are labelled by separate time points whose number is equal to N. Therefore the number of the time points on the scale increases gradually with the increase of N; see **Figure 2** and **Figure 3**.

A characteristic feature is that the set of the time points present on the scale characteristic for a given N is sufficient to represent all S_N perturbation terms given in (8); moreover we obtain a one-to-one correspondence between the individual diagrams obtained with the aid of the scale and the Schrödinger energy terms entering the perturbation order N; see [9] [10] [11]. This goal can be attained on condition the following rules concerning formation of supplementary diagrams characteristic for any N are satisfied:

Figure 2. Time scale for the perturbation order $N = 1$. Only one time point (beginning-end = b.e.) is present on the scale.

Figure 3. Time scale for the perturbation order $N = 2$. Beyond the beginning-end (b.e.) point there is only one other point 1 on the scale.

1) one of the time points on each scale is considered as the beginning-end point of that scale and this point cannot be submitted to contractions with the other time points present on that scale;

2) the lines created in result of contractions of the time points on the scale should not cross;

3) any other contraction of the time points than that satisfying the rules 1) and 2) should not be taken into account.

In effect, beyond the time loops indicated in **Figure 1** and **Figure 3** also other loops of time can be created; they correspond to $N > 2$ and are discussed below. In the terminology applied henceforth the time loop having the beginning-end point on it is called the main loop of time; it is a single loop on any diagram. The other loops of time, called the side loops, are due to contraction, or contractions, of the time points; see Section 6.

A general look on the time-point contractions and their applications is given in Section 10.

5. Energy Terms Belonging to $N = 1$ and $N = 2$

Evidently—according to the rules 1) and 2) given above—no contraction as well as no side loop can be created for $N = 1$ and $N = 2$. The first contraction of the time points is possible for $N = 3$ between the points 1 and 2 represented by the formula

$$t_1 : t_2 = 1 : 2. \tag{13}$$

In this case, beyond a non-contracted diagram for $N = 3$ presented in **Figure 4**, we obtain a new diagram connected with (13); see **Figure 5**. In effect we obtain for $N = 3$ the number of two diagrams: that of **Figure 4** and that of **Figure 5**. This is in accordance with the formula (8) from which we have

$$S_3 = 2. \tag{14}$$

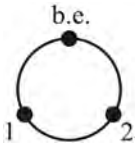

Figure 4. Time scale for the perturbation order $N = 3$. Beyond the beginning-end (b.e.) point, there are two other points, 1 and 2, on the scale.

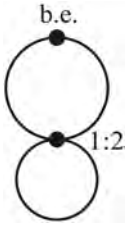

Figure 5. Contraction of the time points 1 and 2 present on the scale representing the perturbation order $N = 3$ creates a side loop of time on the scale similar to the time loop characteristic for $N = 1$; see **Figure 2**.

It is easy to check that

$$S_1 = S_2 = 1 \tag{15}$$

which imply only single diagrams present for $N = 1$ and $N = 2$ in **Figure 1** and **Figure 3** respectively. Let us consider now the energy terms associated with the obtained diagrams.

The perturbation energy connected with $N = 1$ is represented by

$$\Delta E_1 = \langle V \rangle = \langle n | V^{\text{per}} | n \rangle \tag{16}$$

which is a single matrix element.

On the other hand, for $N = 2$ a summation process over the running states p different than n is involved:

$$\Delta E_2 = \langle VPV \rangle = \sum_{p \neq n} \frac{\langle n | V^{\text{per}} | p \rangle \langle p | V^{\text{per}} | n \rangle}{E_n^{(0)} - E_p^{(0)}}. \tag{17}$$

The symbols V are connected with the matrix elements in the numerator, symbol P refers to a single energy difference in the denominator.

6. Contractions of the Time Points on the Scale Provide us with the Side Loops of Time; Perturbation Orders $N = 3$ and $N = 4$

For $N = 3$ we have three time points on the scale: 1, 2, and 3. Let 3 be the beginning-end point, so the points 1 and 2 can be submitted to contraction:

$$t_1 : t_2 = 1 : 2; \tag{18}$$

no contraction with point 3 can be applied. Since $S_3 = 2$ we have two Schrödinger terms for $N = 3$. The first one corresponds to the lack of contractions on the

scale; see Figure 4. This gives the energy term

$$\langle VPVPV\rangle = \sum_p \sum_q \frac{\langle n|V^{\text{per}}|p\rangle\langle p|V^{\text{per}}|q\rangle\langle q|V^{\text{per}}|n\rangle}{\left(E_n^{(0)} - E_p^{(0)}\right)\left(E_n^{(0)} - E_q^{(0)}\right)} \tag{19}$$

where $p \neq n$ and $q \neq n$. On the other side, the contraction (18) (see Figure 5) gives the energy term

$$-\langle VP^2V\rangle\langle V\rangle \tag{20}$$

which is a product of

$$\langle VP^2V\rangle = \sum_{p\neq n} \frac{\langle n|V^{\text{per}}|p\rangle\langle p|V^{\text{per}}|n\rangle}{\left(E_n^{(0)} - E_p^{(0)}\right)^2} \tag{21}$$

and $\langle V\rangle$ which is the term given in (16). The product (20) is taken with a minus sign.

It has to be noted that the power of the energy term in the denominator in (21) is equal to the power of P on the left of (21). The minus sign in (20) is dictated by the even number of the bracket terms present in the product in (20); an odd number of the bracket terms presenting an energy term leads to a plus sign for that term; see (16), (17) and (19).

The term $\langle V\rangle$ in (20) represents a contribution due to a side loop of time created by contraction (18); see Figure 5. Because of a difference of the time point indices 2 and 1 entering (18) which is equal to

$$2-1=1, \tag{22}$$

the side loop created by contraction (18) contributes the term

$$\langle V\rangle = \Delta E_1 \tag{23}$$

entering as a multiplier in (20). In effect the total perturbation energy of $N=3$ is equal to a sum:

$$\Delta E_3 = \langle VPVPV\rangle - \langle VP^2V\rangle \Delta E_1 \tag{24}$$

because of (23) taken into account in (20).

The energy belonging to the order $N=4$ (see Figure 6) can be considered in a similar way. If the beginning-end point on the scale is labelled by 4, we have three time points

$$t_1 = 1,\ t_2 = 2,\ t_3 = 3, \tag{25}$$

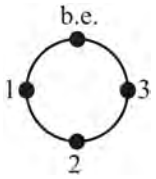

Figure 6. Time scale for the perturbation order $N=4$. Beyond the beginning-end (b.e.) point, three other points (1, 2 and 3) are present on the scale.

which are suitable to contractions. Without any time contraction the contribution to energy is represented by the term

$$\langle VPVPVPV\rangle = \sum_p \sum_q \sum_r \frac{\langle n|V^{\text{per}}|p\rangle\langle p|V^{\text{per}}|q\rangle\langle q|V^{\text{per}}|r\rangle\langle r|V^{\text{per}}|n\rangle}{\left(E_n^{(0)}-E_p^{(0)}\right)\left(E_n^{(0)}-E_q^{(0)}\right)\left(E_n^{(0)}-E_r^{(0)}\right)} \tag{26}$$

where $p,q,r \neq n$. Next come contractions of the points in (25):

$$t_1 : t_2 = 1:2, \tag{27}$$

$$t_1 : t_3 = 1:3, \tag{28}$$

$$t_2 : t_3 = 2:3, \tag{29}$$

$$t_1 : t_2 : t_3 = 1:2:3. \tag{30}$$

The contractions presented in (27)-(30) give respectively the energy terms:

$$-\langle VP^2VPV\rangle\langle V\rangle = -\sum_p \sum_q \frac{\langle n|V^{\text{per}}|p\rangle\langle p|V^{\text{per}}|q\rangle\langle q|V^{\text{per}}|n\rangle}{\left(E_n^{(0)}-E_p^{(0)}\right)^2\left(E_n^{(0)}-E_q^{(0)}\right)}\langle V\rangle \tag{31}$$

where $p,q \neq n$ and $\langle V\rangle = \Delta E_1$ [contraction 1:2],

$$-\langle VP^2V\rangle\langle VPV\rangle = -\sum_p \frac{\langle n|V^{\text{per}}|p\rangle\langle p|V^{\text{per}}|n\rangle}{\left(E_n^{(0)}-E_p^{(0)}\right)^2}\sum_q \frac{\langle n|V^{\text{per}}|q\rangle\langle q|V^{\text{per}}|n\rangle}{E_n^{(0)}-E_q^{(0)}} \tag{32}$$

where $p,q \neq n$ and $\langle VPV\rangle = \Delta E_2$ because of (17) [contraction 1:3],

$$-\langle VPVP^2V\rangle\langle V\rangle = -\sum_p \sum_q \frac{\langle n|V^{\text{per}}|p\rangle\langle p|V^{\text{per}}|q\rangle\langle q|V^{\text{per}}|n\rangle}{\left(E_n^{(0)}-E_p^{(0)}\right)\left(E_n^{(0)}-E_q^{(0)}\right)^2}\langle V\rangle \tag{33}$$

where $p,q \neq n$ and $\langle V\rangle = \Delta E_1$ [contraction 2:3],

$$\langle VP^3V\rangle\left(\langle V\rangle\right)^2 = \sum_p \frac{\langle n|V^{\text{per}}|p\rangle\langle p|V^{\text{per}}|n\rangle}{\left(E_n^{(0)}-E_p^{(0)}\right)^3}\left(\langle V\rangle\right)^2 \tag{34}$$

where $p \neq n$ and $\left(\langle V\rangle\right)^2 = \left(\Delta E_1\right)^2$ [contraction 1:2:3]. Let us note that the sum of powers of P in any energy term is equal to $N-1=3$, and the sum of powers of V within the brackets of each energy term is $N=4$.

Together with the energy term (26) we obtain from (31)-(34)

$$S_4 = \frac{(2\times 4-2)!}{3!4!} = \frac{6!}{3!4!} = 5 \tag{35}$$

energy terms for $N=4$. The perturbation energy belonging to $N=4$ is equal to a sum of five terms given in (26) and (31)-(34):

$$\begin{aligned}\Delta E_4 = {} & \langle VPVPVPV\rangle - \langle VP^2VPV\rangle\Delta E_1 - \langle VP^2V\rangle\Delta E_2 \\ & - \langle VPVP^2V\rangle\Delta E_1 + \langle VP^3V\rangle\left(\Delta E_1\right)^2.\end{aligned} \tag{36}$$

Evidently the fourth term on the right of (36) is equal to the second term because of symmetry.

The rule defining the sign of the perturbation terms is very simple: for an odd number of terms entering the product giving a perturbation term the sign of

product is positive; an even number of terms entering a similar product giving a perturbation term makes this term to have a negative sign.

7. Energy of the Perturbation Orders $N = 5$ and $N = 6$

The time scales corresponding to above N are presented in Figure 7 and Figure 8.

Here the recurrence procedure can be useful to apply, so for $N = 5$ we take first into account the perturbation terms of the order N lower than 5, and for $N = 6$ the terms of the order lower than 6, respectively.

In this way the first five terms belonging to the order $N = 5$ can be obtained from $S_4 = 5$ terms of Section 6 by introducing the time point 4 as a free point different than the beginning-end point of time. This makes any bracket contribution due to the main loop of time entering ΔE_4 [see (36)] changed by an increase equal to PV put at the end of the bracket term. The first 5 energy terms belonging to ΔE_5 are:

$$\begin{aligned}&\langle VPVPVPVPV\rangle - \langle VP^2VPVPV\rangle \Delta E_1 - \langle VP^2VPV\rangle \Delta E_2 \\ &- \langle VPVP^2VPV\rangle \Delta E_1 + \langle VP^3VPV\rangle (\Delta E_1)^2 .\end{aligned} \tag{37}$$

The first term in (37) is a modification of the term (26), the remaining four energy terms in (37) are due to suitable modifications of the terms entering (36).

Further contributions to ΔE_5 are due to the fact that in the case of $N = 5$ the new time point 4 can be submitted also to contractions. They begin with point 1 and the other points between 1 and 4:

$$1{:}4,\ 1{:}2{:}4,\ 1{:}3{:}4,\ 1{:}2{:}3{:}4. \tag{38}$$

The contractions in (38) together with the side loops created by them give the following energy terms:

$$-\langle VP^2V\rangle \Delta E_3, \langle VP^3V\rangle \Delta E_1 \Delta E_2, \langle VP^3V\rangle \Delta E_2 \Delta E_1, -\langle VP^4V\rangle (\Delta E_1)^3 . \tag{39}$$

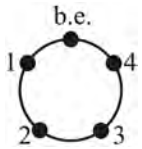

Figure 7. Time scale for the perturbation order $N = 5$. Beyond the beginning-end (b.e.) point, four other points (1, 2, 3 and 4) are present on the scale.

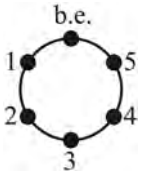

Figure 8. Time scale for the perturbation order $N = 6$. Beyond the beginning-end (b.e.) point, five other points (1, 2, 3, 4 and 5) are present on the scale.

Since ΔE_3 present in the first term in (39) gives two Schrödinger perturbation terms, the set of terms in (39) represents the next $S_4 = 5$ perturbation terms of energy belonging to $N = 5$. The index 4 of S_4 refers to a maximal number 4 of the time points entering contractions (38).

In a further step contraction of the time points 2 and 3 with point 4 have to be considered. They are

$$2:4,\ \ 2:3:4, \tag{40}$$

which give respectively two perturbation energy terms:

$$-\left\langle VPVP^2V\right\rangle \Delta E_2,\ \ \left\langle VPVP^3V\right\rangle \left(\Delta E_1\right)^2. \tag{41}$$

The last set of the energy perturbation terms belonging to $N = 5$ is given by a single contraction

$$3:4. \tag{42}$$

In this case the time points 1 and 2 present before point 3 can be either free, or contracted together. For 1 and 2 free the contraction in (42) gives the perturbation term

$$-\left\langle VPVPVP^2V\right\rangle \Delta E_1. \tag{43}$$

On the other hand, the contraction 1:2 combined with that in (42) gives the perturbation term

$$1:2\bigcap 3:4\to \left\langle VP^2VP^2V\right\rangle \left(\Delta E_1\right)^2. \tag{44}$$

In effect we obtain from (37), (39), (41), (43) and (44) a sum of

$$S_5 = \frac{(2\times 5-2)!}{4!5!} = \frac{8!}{4!5!} = 14 \tag{45}$$

perturbation terms belonging to $N = 5$, if we note that ΔE_3 in (39) combines two Schrödinger perturbation terms.

A full perturbation energy of the order $N = 5$ becomes a sum of S_5 terms entering the formulae quoted before (45):

$$\begin{aligned}\Delta E_5 = {} & \left\langle VPVPVPVPV\right\rangle - \left\langle VP^2VPVPV\right\rangle \Delta E_1 - \left\langle VP^2VPV\right\rangle \Delta E_2 \\ & - \left\langle VPVP^2VPV\right\rangle \Delta E_1 + \left\langle VP^3VPV\right\rangle \left(\Delta E_1\right)^2 - \left\langle VP^2V\right\rangle \Delta E_3 \\ & + \left\langle VP^3V\right\rangle \Delta E_1\Delta E_2 + \left\langle VP^3V\right\rangle \Delta E_2\Delta E_1 - \left\langle VP^4V\right\rangle \left(\Delta E_1\right)^3 \\ & - \left\langle VPVP^2V\right\rangle \Delta E_2 + \left\langle VPVP^3V\right\rangle \left(\Delta E_1\right)^2 \\ & - \left\langle VPVPVP^2V\right\rangle \Delta E_1 + \left\langle VP^2VP^2V\right\rangle \left(\Delta E_1\right)^2.\end{aligned} \tag{46}$$

Again, because of the presence of ΔE_3, the sixth term on the right of (46) represents two Schrödinger perturbation terms. Evidently—because of symmetry—some terms entering (46), for example the second term and one-by-last term on the right, become equal.

The calculation of ΔE_6 being the energy of the perturbation order $N = 6$ is much similar. The first 14 terms are obtainable from the energy expression (46)

representing ΔE_5 due to the fact of supplying the time point 5 as a free point for the case of $N = 6$. The corresponding part of the perturbation energy ΔE_6 comes by adding the PV term at the end of any bracket term in ΔE_5 which is due to the main loop of time. On the basis of (46) we obtain the following contribution of $S_5 = 14$ energy terms entering ΔE_6:

$$\begin{aligned}
&\langle VPVPVPVPVPV\rangle - \langle VP^2VPVPVPV\rangle \Delta E_1 - \langle VP^2VPVPV\rangle \Delta E_2 \\
&- \langle VPVP^2VPVPV\rangle \Delta E_1 + \langle VP^3VPVPV\rangle (\Delta E_1)^2 - \langle VP^2VPV\rangle \Delta E_3 \\
&+ \langle VP^3VPV\rangle \Delta E_1 \Delta E_2 + \langle VP^3VPV\rangle \Delta E_2 \Delta E_1 - \langle VP^4VPV\rangle (\Delta E_1)^3 \\
&- \langle VPVP^2VPV\rangle \Delta E_2 + \langle VPVP^3VPV\rangle (\Delta E_1)^2 - \langle VPVPVP^2VPV\rangle \Delta E_1 \\
&+ \langle VP^2VP^2VPV\rangle (\Delta E_1)^2 .
\end{aligned} \tag{47}$$

In the next step we take into account that the time point 5 for $N = 6$ can contract with point 1 and all points between 1 and 5. This gives the following contractions and the energy terms corresponding to them:

$$1:5 \to -\langle VP^2V\rangle \Delta E_4 \qquad (5) \tag{48}$$

$$1:2:5 \to \langle VP^3V\rangle \Delta E_1 \Delta E_3 \qquad (2) \tag{49}$$

$$1:3:5 \to \langle VP^3V\rangle (\Delta E_2)^2 \qquad (1) \tag{50}$$

$$1:4:5 \to \langle VP^3V\rangle \Delta E_3 \Delta E_1 \qquad (2) \tag{51}$$

$$1:2:3:5 \to -\langle VP^4V\rangle (\Delta E_1)^2 \Delta E_2 \qquad (1) \tag{52}$$

$$1:2:4:5 \to -\langle VP^4V\rangle \Delta E_1 \Delta E_2 \Delta E_1 \qquad (1) \tag{53}$$

$$1:3:4:5 \to -\langle VP^4V\rangle \Delta E_2 (\Delta E_1)^2 \qquad (1) \tag{54}$$

$$1:2:3:4:5 \to \langle VP^5V\rangle (\Delta E_1)^4 \qquad (1) \tag{55}$$

In the brackets at the end of each row is given the number of Schrödinger energy terms connected with the considered row. This means that (48)-(55) give next $S_5 = 14$ Schrödinger perturbation terms. Here 5 is a maximal number of points entering contractions listed in the above formulas. The other time contractions are:

$$2:5 \to -\langle VPVP^2V\rangle \Delta E_3 \qquad (2) \tag{56}$$

$$2:3:5 \to \langle VPVP^3V\rangle \Delta E_1 \Delta E_2 \qquad (1) \tag{57}$$

$$2:4:5 \to \langle VPVP^3V\rangle \Delta E_2 \Delta E_1 \qquad (1) \tag{58}$$

$$2:3:4:5 \to -\langle VPVP^4V\rangle (\Delta E_1)^3 \qquad (1) \tag{59}$$

with the time point 1 left free giving 5 perturbation terms because the index 4 due to presence of contraction points gives $S_4 = 5$.

But both points 1 and 2 can be left free combining with contractions

$$3:5 \to -\left\langle VPVPVPVP^2V \right\rangle \Delta E_2, \tag{60}$$

$$3:4:5 \to \left\langle VPVPVPVP^3V \right\rangle \left(\Delta E_1\right)^2. \tag{61}$$

Another situation is obtained when 1 and 2 contract together, in this case we obtain in place of (60) and (61) the energy terms combined with 1:2, so

$$1:2 \bigcap 3:5 \to \left\langle VP^2VP^2V \right\rangle \Delta E_1 \Delta E_2, \tag{60a}$$

$$1:2 \bigcap 3:4:5 \to -\left\langle VP^2VP^3V \right\rangle \left(\Delta E_1\right)^3. \tag{61a}$$

In effect from the formulae (60) to (61a) we obtain next 4 perturbation terms belonging to ΔE_6.

Finally a single contraction

$$4:5 \tag{62}$$

can combine either with the free points

$$1, 2, 3 \tag{63}$$

giving one energy term

$$-\left\langle VPVPVPVP^2V \right\rangle \Delta E_1, \tag{64}$$

or with contractions of 1, 2, and 3, *viz.*

$$1:2 \bigcap 4:5 \to \left\langle VP^2VPVP^2V \right\rangle \left(\Delta E_1\right)^2, \tag{65}$$

$$1:3 \bigcap 4:5 \to \left\langle VP^2VP^2V \right\rangle \Delta E_2 \Delta E_1, \tag{66}$$

$$1:2:3 \bigcap 4:5 \to -\left\langle VP^3VP^2V \right\rangle \left(\Delta E_1\right)^3, \tag{67}$$

$$2:3 \bigcap 4:5 \to \left\langle VPVP^2VP^2V \right\rangle \left(\Delta E_1\right)^2, \tag{68}$$

which give together four energy terms presented in the second step of (65)-(68).

In effect the number of the perturbation terms belonging to $N = 6$ obtained from (47), (48)-(55), (56)-(59), (60)-(61a), and (62)-(68) becomes:

$$14+14+5+4+1+4 = 42 = S_6 \tag{69}$$

which is the expected result; see Table 1. A full perturbation energy of the order $N = 6$ is equal to a sum of the terms belonging to expressions listed above equation (69); see (47)-(61a) and (64)-(68).

8. Perturbation Energy Belonging to $N = 7$

This is the most complicated case considered in the present paper. The first $S_6 = 42$ terms are those connected with $N = 6$ because the time point 6 is now a free point of time on the scale; see Figure 9 and a list of terms below (69). The energy terms can be constructed by substituting the product

$$PV$$

at the end of any main bracket expression entering the energy term belonging to $N = 6$ obtained in Section 6:

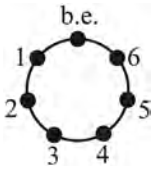

Figure 9. Time scale for the perturbation order $N = 7$. Beyond the beginning-end (b.e.) point, six other points (1, 2, 3, 4, 5 and 6) are present on the scale.

$$\begin{aligned}
&\langle VPVPVPVPVPVPV\rangle - \langle VP^2VPVPVPVPV\rangle \Delta E_1 - \langle VP^2VPVPVPV\rangle \Delta E_2 \\
&- \langle VP^2VPVPVPV\rangle \Delta E_1 + \langle VP^3VPVPVPV\rangle (\Delta E_1)^2 - \langle VP^2VPVPV\rangle \Delta E_3 \\
&+ \langle VP^3VPVPV\rangle \Delta E_1 \Delta E_2 + \langle VP^3VPVPV\rangle \Delta E_2 \Delta E_1 - \langle VP^4VPVPV\rangle (\Delta E_1)^3 \\
&- \langle VPVP^2VPVPV\rangle \Delta E_2 + \langle VPVP^3VPVPV\rangle (\Delta E_1)^2 - \langle VPVPVP^2VPVPV\rangle \Delta E_1 \\
&+ \langle VP^2VP^2VPVPV\rangle (\Delta E_1)^2 - \langle VP^2VPV\rangle \Delta E_4 + \langle VP^3VPV\rangle \Delta E_1 \Delta E_3 \\
&+ \langle VP^3VPV\rangle (\Delta E_2)^2 + \langle VP^3VPV\rangle \Delta E_3 \Delta E_1 - \langle VP^4VPV\rangle (\Delta E_1)^2 \Delta E_2 \\
&- \langle VP^4VPV\rangle \Delta E_1 \Delta E_2 \Delta E_1 - \langle VP^4VPV\rangle \Delta E_2 (\Delta E_1)^2 + \langle VP^5VPV\rangle (\Delta E_1)^4 \\
&- \langle VPVP^2VPV\rangle \Delta E_3 + \langle VPVP^3VPV\rangle \Delta E_1 \Delta E_2 + \langle VPVP^3VPV\rangle \Delta E_2 \Delta E_1 \\
&- \langle VPVP^4VPV\rangle (\Delta E_1)^3 - \langle VPVPVP^2VPV\rangle \Delta E_2 + \langle VPVPVP^3VPV\rangle (\Delta E_1)^2 \\
&+ \langle VP^2VP^2VPV\rangle \Delta E_1 \Delta E_2 - \langle VP^2VP^3VPV\rangle (\Delta E_1)^3 - \langle VPVPVPVP^2VPV\rangle \Delta E_1 \\
&+ \langle VP^2VPVP^2VPV\rangle (\Delta E_1)^2 + \langle VP^2VP^2VPV\rangle \Delta E_2 \Delta E_1 - \langle VP^3VP^2VPV\rangle (\Delta E_1)^3 \\
&+ \langle VPVP^2VP^2VPV\rangle (\Delta E_1)^2 .
\end{aligned} \tag{70}$$

The next $S_6 = 42$ energy terms come from contractions of point 6 with point 1 and the points between 1 and 6:

$$1:6 \to -\langle VP^2V\rangle \Delta E_5 \quad (14) \tag{71}$$

$$1:2:6 \to \langle VP^3V\rangle \Delta E_1 \Delta E_4 \quad (5) \tag{72}$$

$$1:3:6 \to \langle VP^3V\rangle \Delta E_2 \Delta E_3 \quad (2) \tag{73}$$

$$1:4:6 \to \langle VP^3V\rangle \Delta E_3 \Delta E_2 \quad (2) \tag{74}$$

$$1:5:6 \to \langle VP^3V\rangle \Delta E_4 \Delta E_1 \quad (5) \tag{75}$$

$$1:2:3:6 \to -\langle VP^4V\rangle (\Delta E_1)^2 \Delta E_3 \quad (2) \tag{76}$$

$$1:2:4:6 \to -\langle VP^4V\rangle \Delta E_1 (\Delta E_2)^2 \quad (1) \tag{77}$$

$$1:2:5:6 \to -\langle VP^4V\rangle \Delta E_1 \Delta E_3 \Delta E_1 \quad (2) \tag{78}$$

$$1:3:4:6 \to -\langle VP^4V\rangle \Delta E_2 \Delta E_1 \Delta E_2 \quad (1) \tag{79}$$

$$1:3:5:6 \to -\langle VP^4V\rangle (\Delta E_2)^2 \Delta E_1 \quad (1) \tag{80}$$

$$1:4:5:6 \to -\langle VP^4V\rangle \Delta E_3 (\Delta E_1)^2 \quad (2) \tag{81}$$

$$1:2:3:4:6 \to \left\langle VP^5V \right\rangle \left(\Delta E_1\right)^3 \Delta E_2 \quad (1) \quad (82)$$

$$1:2:3:5:6 \to \left\langle VP^5V \right\rangle \left(\Delta E_1\right)^2 \Delta E_2 \Delta E_1 \quad (1) \quad (83)$$

$$1:2:4:5:6 \to \left\langle VP^5V \right\rangle \Delta E_1 \Delta E_2 \left(\Delta E_1\right)^2 \quad (1) \quad (84)$$

$$1:3:4:5:6 \to \left\langle VP^5V \right\rangle \Delta E_2 \left(\Delta E_1\right)^3 \quad (1) \quad (85)$$

$$1:2:3:4:5:6 \to -\left\langle VP^6V \right\rangle \left(\Delta E_1\right)^5 \quad (1) \quad (86)$$

which give also a set of $S_6 = 42$ perturbation terms:

$$14+5+2+2+5+2+1+2+1+1+2+1+1+1+1+1=42 \quad (87)$$

because a maximum of 6 points coupled together. Here (87) is a sum of the number of the perturbation terms indicated in brackets at the end of each row in (71)-(86).

The next contractions of the time points give $S_5 = 14$ terms because of a maximal number of 5 points entering contractions:

$$2:6 \to -\left\langle VPVP^2V \right\rangle \Delta E_4 \quad (5) \quad (88)$$

$$2:3:6 \to \left\langle VPVP^3V \right\rangle \Delta E_1 \Delta E_3 \quad (2) \quad (89)$$

$$2:4:6 \to \left\langle VPVP^3V \right\rangle \left(\Delta E_2\right)^2 \quad (1) \quad (90)$$

$$2:5:6 \to \left\langle VPVP^3V \right\rangle \Delta E_3 \Delta E_1 \quad (2) \quad (91)$$

$$2:3:4:6 \to -\left\langle VPVP^4V \right\rangle \left(\Delta E_1\right)^2 \Delta E_2 \quad (1) \quad (92)$$

$$2:3:5:6 \to -\left\langle VPVP^4V \right\rangle \Delta E_1 \Delta E_2 \Delta E_1 \quad (1) \quad (93)$$

$$2:4:5:6 \to -\left\langle VPVP^4V \right\rangle \Delta E_2 \left(\Delta E_1\right)^2 \quad (1) \quad (94)$$

$$2:3:4:5:6 \to \left\langle VPVP^5V \right\rangle \left(\Delta E_1\right)^4 \quad (1) \quad (95)$$

Next come $S_4 = 5$ energy terms due to contractions

$$3:6 \to -\left\langle VPVPVP^2V \right\rangle \Delta E_3 \quad (2) \quad (96)$$

$$3:4:6 \to \left\langle VPVPVP^3V \right\rangle \Delta E_1 \Delta E_2 \quad (1) \quad (97)$$

$$3:5:6 \to \left\langle VPVPVP^3V \right\rangle \Delta E_2 \Delta E_1 \quad (1) \quad (98)$$

$$3:4:5:6 \to -\left\langle VPVPVP^4V \right\rangle \left(\Delta E_1\right)^3 \quad (1) \quad (99)$$

which do exist with free time points 1 and 2 on the scale giving the energy terms presented above. But also we can have contractions combined with 1:2 giving other $S_4 = 5$ energy terms:

$$1:2 \cap 3:6 \to \left\langle VP^2VP^2V \right\rangle \Delta E_1 \Delta E_3 \quad (2) \quad (100)$$

$$1:2 \cap 3:4:6 \to -\left\langle VP^2VP^3V \right\rangle \left(\Delta E_1\right)^2 \Delta E_2 \quad (1) \quad (101)$$

$$1:2 \cap 3:5:6 \to -\left\langle VP^2VP^3V \right\rangle \Delta E_1 \Delta E_2 \Delta E_1 \quad (1) \quad (102)$$

$$1:2\bigcap 3:4:5:6\to \left\langle VP^2VP^4V\right\rangle \left(\Delta E_1\right)^4 \qquad (1) \qquad (103)$$

Let us note that each ΔE_3 in (96) and (100) gives $S_3 = 2$ terms.

Another set of contractions involving point 6 represents

$$4:6\to -\left\langle VPVPVPVP^2V\right\rangle \Delta E_2 \qquad (104)$$

$$4:5:6\to \left\langle VPVPVPVP^3V\right\rangle \left(\Delta E_1\right)^2 \qquad (105)$$

on condition the time points 1, 2, and 3 are left free. But (104) and (105) can be combined also with contractions of the points 1, 2, and 3 giving

$$1:2\bigcap 4:6\to \left\langle VP^2VPVP^2V\right\rangle \Delta E_1\Delta E_2, \qquad (106)$$

$$1:2\bigcap 4:5:6\to -\left\langle VP^2VPVP^3V\right\rangle \left(\Delta E_1\right)^3, \qquad (107)$$

$$1:3\bigcap 4:6\to \left\langle VP^2VP^2V\right\rangle \left(\Delta E_2\right)^2, \qquad (108)$$

$$1:3\bigcap 4:5:6\to -\left\langle VP^2VP^3V\right\rangle \Delta E_2\left(\Delta E_1\right)^2, \qquad (109)$$

$$1:2:3\bigcap 4:6\to -\left\langle VP^3VP^2V\right\rangle \left(\Delta E_1\right)^2\Delta E_2, \qquad (110)$$

$$1:2:3\bigcap 4:5:6\to \left\langle VP^3VP^3V\right\rangle \left(\Delta E_1\right)^4, \qquad (111)$$

$$2:3\bigcap 4:6\to \left\langle VPVP^2VP^2V\right\rangle \Delta E_1\Delta E_2, \qquad (112)$$

$$2:3\bigcap 4:5:6\to -\left\langle VPVP^2VP^3V\right\rangle \left(\Delta E_1\right)^3. \qquad (113)$$

In effect the number of terms due to (104)-(113) is equal to $2S_4 = 10$ because the points 1, 2 and 3 can combine in $S_4 = 5$ ways.

The last set of contractions containing point 6 is represented by 5:6. When a combination of 5:6 with the set of free time points 1, 2, 3, and 4 is considered we obtain

$$5:6\to -\left\langle VPVPVPVPVP^2V\right\rangle \Delta E_1 \qquad (1) \qquad (114)$$

The remaining combinations with 5:6 are due to contractions between points 1, 2, 3 and 4:

$$1:2\bigcap 5:6\to \left\langle VP^2VPVPVP^2V\right\rangle \left(\Delta E_1\right)^2 \qquad (1) \qquad (115)$$

$$1:3\bigcap 5:6\to \left\langle VP^2VPVP^2V\right\rangle \Delta E_2\Delta E_1 \qquad (1) \qquad (116)$$

$$1:4\bigcap 5:6\to \left\langle VP^2VP^2V\right\rangle \Delta E_3\Delta E_1 \qquad (2) \qquad (117)$$

$$1:2:3\bigcap 5:6\to -\left\langle VP^3VPVP^2V\right\rangle \left(\Delta E_1\right)^3 \qquad (1) \qquad (118)$$

$$1:2:4\bigcap 5:6\to -\left\langle VP^3VP^2V\right\rangle \Delta E_1\Delta E_2\Delta E_1 \qquad (1) \qquad (119)$$

$$1:3:4\bigcap 5:6\to -\left\langle VP^3VP^2V\right\rangle \Delta E_2\left(\Delta E_1\right)^2 \qquad (1) \qquad (120)$$

$$1:2:3:4\bigcap 5:6\to \left\langle VP^4VP^2V\right\rangle \left(\Delta E_1\right)^4 \qquad (1) \qquad (121)$$

$$1:2\bigcap 3:4\bigcap 5:6\to -\left\langle VP^2VP^2VP^2V\right\rangle \left(\Delta E_1\right)^3 \qquad (1) \qquad (122)$$

$$2:3\cap 5:6\to \left\langle VPVP^2VPVP^2V\right\rangle \left(\Delta E_1\right)^2 \quad (1) \quad (123)$$

$$2:4\cap 5:6\to \left\langle VPVP^2VP^2V\right\rangle \Delta E_2\Delta E_1 \quad (1) \quad (124)$$

$$2:3:4\cap 5:6\to -\left\langle VPVP^3VP^2V\right\rangle \left(\Delta E_1\right)^3 \quad (1) \quad (125)$$

$$3:4\cap 5:6\to \left\langle VPVPVP^2VP^2V\right\rangle \left(\Delta E_1\right)^2 \quad (1) \quad (126)$$

The total number of energy terms due to (114)-(126) is $S_5 = 14$ which is the number of combinations due to presence of the 4 free time points, see (8) and Table 1.

In total we obtain for $N = 7$ the $S_6 = 42$ energy terms collected in (70), next also $S_6 = 42$ energy terms collected in (87). Another set of terms is given in the formulae from (88) to (95) which provide us with

$$5+2+1+2+1+1+1+1=14 \quad (127)$$

terms. The next $2S_8 = 10$ perturbation terms are given by the formulae (96)-(99) and (100)-(103), but also 10 terms are provided by (104)-(113). Finally contraction 5:6 gives from (114) to (126) the energy terms whose number is

$$1+1+1+2+1+1+1+1+1+1+1+1+1+1=14=S_5. \quad (128)$$

This makes a total number of kinds of the energy perturbation terms belonging to $N = 7$ equal to:

$$42+42+14+10+10+14=132=S_7 \quad (129)$$

which is not only in accordance with the formula (8), but satisfies also the formula:

$$S_1S_6+S_2S_5+S_3S_4+S_4S_3+S_5S_2+S_6S_1=S_7. \quad (130)$$

The result in (130) is a special case of a general formula which holds for calculating S_N:

$$S_N=S_1S_{N-1}+S_2S_{N-2}+S_3S_{N-3}+\cdots+S_{N-3}S_3+S_{N-2}S_2+S_{N-1}S_1. \quad (131)$$

9. General Characteristics of the Energy Perturbation Terms

In general the terms of the Schrödinger perturbation energy which originate from a non-degenerate quantum state are represented by the products of the contribution due to the main loop of time and contributions due to the side loops. This second kind of contributions is equal to definite perturbation energies

$$\Delta E^{(N')} \quad (132)$$

of the order N' smaller than the examined order N. The formulae of the kind of (132) which are due to the side loops of time provide an important simplification of the perturbed energy calculations.

The side loops originate from contractions of the time points on the main loop characteristic for a given perturbation order N. In effect the order N' characteristic for any expression (132) is equal to a difference of the indices representing the time points entering contraction. There can exist also multiple

contractions giving products

$$\Delta E^{(N')}\Delta E^{(N'')}\Delta E^{(N''')}\cdots \tag{133}$$

where $N', N'', N''', \cdots$ are defined by the difference between the time point indices participating successively in a multiple contraction.

One point on the main loop, which is the beginning-end point of the scale, is excluded from contractions. Respectively, for each N does exist only one energy term which is given solely by the main loop of time; this loop of time has no contractions and the corresponding energy term does not involve the contributions of the side loops.

The kind of energy contributions due to the main loop is in general different than that given in (132) or (133). In the absence of contractions the main loop gives a single energy term equal to

$$\langle VPVPVP\cdots PVPV\rangle \tag{134}$$

in which the number of V is equal to the perturbation order N and number of P amounts $N-1$. In effect any time point on the scale—excepting the beginning-end point—has its own P, and the number of terms V is equal to the number of distances separating the neighbouring time points on the scale.

The contractions change the power exponents of P entering (134) which are all equal to 1 in (134) into the exponents

$$\tau > 1. \tag{135}$$

The number τ is equal to the number of the time points participating in contraction, therefore τ becomes equal to the number of the side loops created by contraction increased by one. So for one side loop present in a given time point

$$\tau = 1+1, \tag{135a}$$

for two side loops present in the same point

$$\tau = 1+2, \tag{135b}$$

etc. In effect the number of P terms which remain on the main loop of time and have the exponents represented by (135) is equal to the number of the time contractions present on the scale.

An important feature is that some P entering (134) can be shifted to the side loops. This situation holds in case when the differences between the time-point indices entering contraction are larger than 1. For example the contraction between the points 1 and 3 shifts the point 2—and its P term—to a side loop. This is an expected result if we note that $N', N'', N''', \cdots$ in (132) or (133) can be larger than unity.

Nevertheless the sum of the power exponents of P present along the scale—those which remain on the main loop as well as those which are shifted to the side loop or loops—should remain unchanged. In effect any perturbation term belonging to a given N has the same number $N-1$ of the P terms and number N of the V terms, because the total number of V terms in the main loop and side loops remains constant. All S_N terms give different diagrams along the

time scale plotted for a given N, but the computational results due to several diagrams can be equal which is the effect of the diagram symmetry.

10. General View on Contractions of the Time Points on the Time Scales and Their Application

The way of calculating the Schrödinger perturbation energy—called sometimes also the Rayleigh-Schrödinger perturbation series—presented in the paper is rather different than procedures applied in the former approaches; see e.g. [12]. In fact the terms entering the series can be obtained mainly from an analysis of the geometry of the time-point patterns present on the scale, and by applying the rules connecting that geometry with the time-independent matrix elements entering the Schrödinger wave mechanics, than by proceeding according to any of the developed wave-mechanical perturbation formalisms.

A basic property concerns the importance of contraction points of time entering the applied time scale and their origin. At the first step—*i.e.* in the absence of contractions—the scale giving the perturbation energy of order N is assumed to have N separate time points on it, and one of these points is the beginning-end point of the scale. Evidently for $N = 1$ there is present only the beginning-end point. We assume that this point cannot be submitted to contractions in case of any N. Therefore an increase of the perturbation order to $N = 2$ gives the scale which has two points on it: one is the beginning-end point and the second point is allowed which remains free.

A substantial difference in the calculation scheme begins with $N = 3$. In this case there exist outside the beginning-end point two other points which (a) can be left separated each from other, but also (b) can be contracted together. What does it mean from the point of view of the scale geometry and the calculations? The case (a) represents two separate points of time any of which gives its own contribution to the perturbation energy term belonging to $N = 3$. According to Section 6 the energy term supplied by these both points together becomes

$$\langle VPVPV \rangle. \tag{136}$$

So what is the effect of contraction of two points on the scale upon the perturbation energy? Geometrically it means that contraction of point 1 with point 2 labelled by the symbol

$$1:2 \tag{137}$$

produces *two* different scales of time. The first one is the scale containing the beginning-end point of the original loop of time. The time parameters t_1 and t_2 labelling the perturbation events on that loop become equal, so an alternative formula to (137) is

$$t_1 = t_2. \tag{137a}$$

This means that there is no possibility to have a time point between t_1 and t_2 on the main loop of time. But contraction represented by (137a) implies creation of a supplementary loop of time for which the situation given in (137a) represents the beginning-end point of time. This supplementary loop, called also a side

loop, is independent of the original (main) loop of time. The side loop has no time points on it excepting the beginning-end point (137a). Such loop is identical with the main loop of time for $N=1$; see Figure 2.

In effect of creation of the new loop of time, a new—*i.e.* the second—perturbation term of energy is obtained for the perturbation order $N=3$ beyond the term given in (136). This is a product of two bracket terms, *viz.*

$$-\langle VP^2V\rangle\langle V\rangle=-\langle VP^2V\rangle\Delta E_1. \tag{138}$$

The first bracket term is given in (21), the second term is simply the perturbation energy of order one ($N=1$); see (16).

For $N>3$, say for $N=4$, the free time points on the main loop can be t_1, t_2 and t_3, whereas the point t_4 is assumed to represent the beginning-end point on the loop; see Figure 6. In this case—beyond contractions between the neighbouring time points like (137) and (137a)—the contraction between the non-neighbouring time points

$$t_1=t_3 \tag{139}$$

or

$$1:3 \tag{139a}$$

is also possible. This contraction implies that the point t_2 which originally is placed between t_1 and t_3 should be shifted to a side loop. This side loop has its beginning-end point given by contraction (139) or (139a), but one free time point, namely t_2, does remain on the loop. In effect the side loop becomes identical to that for $N=2$; see Figure 3. The perturbation energy due to contraction (139) is therefore equal to product

$$-\langle VP^2V\rangle\langle VPV\rangle=-\langle VP^2V\rangle\Delta E_2. \tag{140}$$

For the first bracket term in (140) see (21), for the second bracket term—see (17). The minus sign in (138) and (140) is dictated by the even number of the bracket terms entering product.

In Table 2 we summarize the data on the time points and their contractions which give the energy terms belonging to the perturbation orders from $N=1$ to $N=6$.

11. Conclusions

The history of investigations on time is probably as old as the history of science. In the Newtonian formulation of mechanics, the time interval is independent of any other physical parameter; in the theory of relativity, the dependence of the time interval is mainly due to the speed of the observed change.

But in many cases, including the problem considered in the present paper, the influence of the speed effect—or other physical parameters—on the time intervals can be neglected. The kind of approach proposed here is different than the Newtonian-like, namely an insight into time given by Leibniz [13] [14] [15] seems to be here of importance.

Table 2. Number of the time points on the main loop of time and symbols of contraction points giving the side loops for the perturbation orders from $N = 1$ to $N = 6$. The second component entering the last column is equal to the contractions number of the time points (see the 3rd column).

N	Number of the time points on the main loop of time	Contractions of the time points	Total number of the perturbation terms S_N (see Table 1)
1	1 + 0	no contractions	1
2	1 + 1	no contractions	1
3	1 + 2	1:2	1+1=2
4	1 + 3	1:2, 1:3, 2:3, 1:2:3	1+4=5
5	1 + 4	1:2, 1:3, 1:4, 2:3, 2:4, 3:4, 1:2⋂3:4, 1:2:3, 1:2:4, 1:3:4, 1:4⋂2:3, 1:2:3:4, 2:3:4	1+13=14
6	1 + 5	1:2, 1:3, 1:4, 1:5, 2:3, 2:4, 2:5, 3:4, 3:5, 4:5, 1:2:3, 1:2:4, 1:2:5, 1:3:4, 1:3:5, 1:4:5, 2:3:4, 2:3:5, 2:4:5, 3:4:5, 1:2:3:4, 1:2:3:5, 1:2:4:5, 1:3:4:5, 2:3:4:5, 1:2:3:4:5, 1:2:3⋂4:5, 1:2⋂3:5, 1:2⋂4:5, 1:2⋂3:4:5, 1:2⋂3:4, 1:3⋂4:5, 2:3⋂4:5, 1:4⋂2:3, 1:5⋂2:4, 1:4:5⋂2:3, 1:5⋂2:3, 1:5⋂3:4, 1:5⋂2:3:4, 1:2:5⋂3:4, 2:5⋂3:4	1+41=42

Leibniz idea was that time is represented by a sequence of events which appear successively in a definite order. A knowledge of the sizes of time intervals between the separate events become then of not much use, since the main point concerns an arrangement of the events along a proper scale of time.

In the present paper the problem of the shape of the time scale and its physical verification has been attached to the Schrödinger perturbation theory. Physically this means that the history of a perturbed quantum state—done by a potential independent of time—becomes of importance. This history has a non-relativistic background, for it refers to a general applicability of the non-relativistic Schrödinger equation in the quantum physics.

In principle the perturbation theory—linked also with the Schrödinger's authorship [3]—provides us with a method how solutions known for a simple problem can provide us with an approximate knowledge of more complicated Schrödinger's solutions. A difficulty was that a tedious procedure had to be applied in order to extract to calculations the separate kinds of energy terms belonging to a large perturbation order N. This difficulty could be much reduced when the time scale of a circular character composed of the N collision time points of a quantum system with the perturbation potential V^{per} is assumed for each N.

The number of the allowed time-point arrangements on the scale provides us precisely with the S_N perturbation energy terms characteristic for a given N. In effect the perturbation terms should not be derived with the aid of a usually tedious iterative procedure connected with solving the perturbed Schrödinger equation, but can be readily obtained by analyzing the contractions to which the time points are submitted along the scale.

It should be noted that agreement of the results for S_N, as well as the energy perturbation terms for a given N, obtained in the present theory with those calculated by the Schrödinger formalism is not proved in general but has been demonstrated in the paper for the perturbation orders beginning from $N = 1$ to $N = 7$.

No time intervals or continuous time variables are considered in the paper. The calculations are based on definite sets of the discrete time points representing the collisions of an unperturbed non-degenerate quantum system with a time-independent perturbation potential.

Conflicts of Interest

The author declares no conflicts of interest regarding the publication of this paper.

References

[1] Berliner, A. and Scheel, K. (1932) Physikalisches Handwörterbuch. Springer, Berlin. https://doi.org/10.1007/978-3-642-99643-6

[2] Landau, L.D. and Lifshitz, E.M. (1948) Field Theory. 2nd Edition, OGIZ, Moscow. (In Russian)

[3] Schrödinger, E. (1926) *Annalen der Physik*, **80**, 437.

[4] Schiff, L.I. (1968) Quantum Mechanics. 3rd Edition, McGraw-Hill, New York.

[5] Huby, R. (1961) *Proceedings of the Physical Society* (*London*), **78**, 529. https://doi.org/10.1088/0370-1328/78/4/306

[6] Tong, B.Y. (1962) *Proceedings of the Physical Society* (*London*), **80**, 1101. https://doi.org/10.1088/0370-1328/80/5/308

[7] Feynman, R.P. (1966) *Science*, **153**, 699-708. https://doi.org/10.1126/science.153.3737.699

[8] Mattuck, R.D. (1976) A Guide to Feynman Diagrams of the Many-Body Problem. 2nd Edition, McGraw-Hill, New York.

[9] Olszewski, S. (1991) *Zeitschrift fuer Naturforschung*, **46A**, 313-320. https://doi.org/10.1515/zna-1991-0404

[10] Olszewski, S. (2004) *Studia Philosophiae Christianae*, **40**, 57.

[11] Olszewski, S. (2018) *Journal of Modern Physics*, **9**, 1491-1521. https://doi.org/10.4236/jmp.2018.98093

[12] Ziman, J.M. (1969) Elements of Advanced Quantum Theory. Cambridge University Press, Cambridge.

[13] Leibniz, G.W. (1924) Hauptschriften zur Grundlagen der Philosophie. Vol. 1, Leipzig.

[14] Rescher, N. (2013) On Leibniz. University of Pittsburgh Press, Pittsburgh. https://doi.org/10.2307/j.ctt7zw8g2

[15] Szumilewicz, I. (1964) On the Direction of the Time Flow. Państwowe Wydawnictwo Naukowe, Warszawa. (In Polish)

Journal of Modern Physics, 2020, 11, 1559
https://www.scirp.org/journal/jmp
ISSN Online: 2153-120X
ISSN Print: 2153-1196

Erratum to "Empirical Equation for the Gravitational Constant with a Reasonable Temperature" [Journal of Modern Physics 11 (2020) 1180-1192]

Tomofumi Miyashita

Miyashita Clinic, Osaka, Japan
Email: tom_miya@plala.or.jp

Received: September 27, 2020
Accepted: October 13, 2020
Published: October 16, 2020

The original online version of this article (Miyashita, T. (2020) Empirical Equation for the Gravitational Constant with a Reasonable Temperature. *Journal of Modern Physics*, **11**, 1180-1192. https://dx.doi.org/10.4236/jmp.2020.118074) unfortunately contains the very important mistakes. The calculated temperature was 2.7195 K, which is similar to the temperature of the cosmic microwave background 2.7254 K.

2.1. Our Empirical Equation

Our empirical equation is quoted from Wikipedia.
https://en.wikipedia.org/wiki/Proton

$$\frac{Gm_p}{\frac{\lambda_p}{2}} \times 1\text{kg} = \frac{9}{2}kT \tag{1}$$

G: gravitational constant, 6.6743×10^{-11} ($m^3 \cdot kg^{-1} \cdot s^{-2}$)
m_p: the rest mass of a proton, 1.6726×10^{-27} (kg)
r_p: charge radius, 8.41×10^{-16} (m) (We must not use this value.)
lp: Compton wavelength 1.321409×10^{-16} (m)
k: Boltzmann constant, 1.380649×10^{-23} (J/K)
T: temperature (K)
1 kg: the standard mass (kg)

The temperature calculated using this formula was 2.71953 K, which is similar to the temperature of the cosmic microwave background of 2.72548 K. We must use the half of Compton wavelength. The proton consists of three quarks. Then, we must consider 9/2 kT and not 3 kT. But the main theory can be unchanged.

Journal of Modern Physics, 2020, 11, 1560-1575
https://www.scirp.org/journal/jmp
ISSN Online: 2153-120X
ISSN Print: 2153-1196

A Mechanism for How a Particle Detects and Moves in a Field Gradient

Dirk J. Pons

Department of Mechanical Engineering, University of Canterbury, Christchurch, New Zealand
Email: dirk.pons@canterbury.ac.nz

How to cite this paper: Pons, D.J. (2020) A Mechanism for How a Particle Detects and Moves in a Field Gradient. *Journal of Modern Physics*, **11**, 1560-1575.
https://doi.org/10.4236/jmp.2020.1110097

Received: September 1, 2020
Accepted: October 13, 2020
Published: October 16, 2020

Abstract

Problem: The mechanisms whereby force operates are poorly understood at the fundamental level. **Purpose:** This paper proposes a mechanism for how a particle detects the field gradient, and how it moves therein. **Approach:** A non-local hidden-variable (NLHV) theory is used, specifically the Cordus NLHV theory. **Findings:** The operation of force is proposed to occur from the interaction between the energisation sequence of the particle, with the field gradient, resulting in discrete displacement motions of the particle. Specifically the particle sub-structures sweep through a volume of space during their energisation cycle. This locus is warped by the incoming field, hence preferentially displacing the particle along the gradient. **Originality:** The novel contribution of this work is providing a candidate mechanism for how a particle detects and moves in a field gradient.

Keywords

Field, Interaction, Fundamental, Quantum

1. Introduction

The operation of force is something taken for granted. It is intuitively accepted that a particle moves in the gradient of a field. However given that a particle is also assumed to be a zero-dimensional (0-D) point, it is unclear how such a particle would detect the direction or gradient of the field.

A common, though simplistic, explanation is by analogy to a small sphere (e.g. a marble) on an inclined plane in a gravitational situation: it will naturally roll downhill. However this analogy does not extend to a 0-D point. For the marble, the line of action of the centre of mass is offset from the contact point with the surface, so a moment arises to roll the ball downwards. For a 0-D point there cannot be a moment arm, hence the analogy fails. If a particle did have

volume, either by a volumetrically dispersed aggregation of other 0-D particles (the quantum mechanics premise), or because fundamental particles had volume (the premise of hidden variable theories), it is unclear how that volume might help the particle detect the field direction in real situations outside of the analogy.

The slope analogy represents the field as continuous. Another explanation might be attempted by assuming it is discrete, *i.e.* mediated by the exchange of gauge bosons. In that case it is easier to understand that there may be more incoming gauge bosons on one side of a test particle than on the other, and that this underlies the field gradient. However what such theories fail to explain is the direction of force. What is the mechanism that causes opposite electrical charges to attract, and similar to repel? How does an incoming gauge boson cause movement of the 0-D test particle?

Hence there is an underlying ontological problem with describing how field force interactions occur at the level of fundamental particles. This paper proposes a mechanism for how a particle detects the field gradient, and how it moves therein.

2. Context

The explanation was developed from a non-local hidden-variable (NLHV) theory, specifically the Cordus theory. All NLHV theories propose that fundamental particles have sub-structure, though differ greatly in what they propose for those structures. In the case of the Cordus theory the proposal is for an open string-like structure. The structure was inferred by applying design principles to the photon behaviour of the double-slit device, and thereby determining what set of physical features would be sufficient to explain the observations [1]. The outcome was a particle with two reactive ends connected by a fibril. The fibril is inert relative to other particles and provides the coordination between the two ends. This design intrinsically accommodates non-local behaviour. The reactive ends are periodically energized at the de Broglie frequency, during which they emit discrete forces into space in three orthogonal emission directions, see **Figure 1**. These directions are denoted r, a, and t in the figure [2] [3]. The particle interacts with other particles only at its reactive ends. The discrete forces are joined into flux tubes. Since these propagate out into space, the space between particles therefore comprises a fabric of discrete forces [4].

The key conceptual point of departure is the proposal that a particle has two separate ends. In contrast, conventional theories have the particle being a zero dimensional point, or a distribution of substance around a central point. In the Cordus theory, there is nothing at the nominal central location of the particle. The idea of two reactive ends is conceptually close to a string theory interpretation, and the dipole concept of classical electromagnetism. Indeed the number of parameters required to define the Cordus particle structure is similar to the number of dimensions in some string theories [6]. The theory describes multiple physical phenomena, see **Table 1**.

Table 1. Phenomena for which the Cordus theory has an explanation. Adapted from [7].

Phenomenon explained	Key concept	Reference
Wave-particle duality in the double slit device	One reactive end passes through each slit.	[1]
Derivation of optical laws from a particle perspective	Includes derivation of reflection and refraction laws, and Brewster's Angle from particle basis.	[1]
Prediction of particle structures	Electron, proton, neutron, neutrino species, photon.	[5] [8] [9] [10] [11]
Explanation of the decay processes and prediction of a deeper decay model	Dependency identified on neutrino species loading.	[9] [10]
Explanation for the selective spin characteristics of neutrinos whereby the direction of spin is correlated with the matter-antimatter species	Spin direction arises from reaction between incomplete discrete force emissions from the particle, and the background fabric.	[10]
Explanation for particle spin and derivation of the electron g factor g = 2	Cordus particle structure naturally causes g = 2.	[7]
Explanation for the annihilation process	Description of the discrete force changes involved in remanufacture of these particle identities. Includes a conceptual explanation of the difference between otho- and para-positronium decay rates (ortho and para refer to spin combinations of the bound electron and anti-electron/positron).	[12]
Provision of a mechanics for pair production	Rearrangement of discrete forces changes the particle identity.	[13]
Explanation of process of photon emission	Excess energy in the electron changes it span, which is opposed by bonding constraints.	[3] [14]
Synchronous interaction	Synchronous interaction between discrete forces of different matter particles causes the strong nuclear force.	[2]
Predicted structure of atomic nuclei and explanation of stability for nuclides H to Ne	Protons and neutrons are arranged in a nuclear polymer. The rules for this arrangement, and for the bridge neutrons, are inferred and are qualitatively consistent with observed stability/instability/non-existence of all nuclides in this range.	[15] [16]
Prediction of a mechanism for asymmetrical baryogenesis	Predicts a decay path for remanufacture of the antielectron to the proton. This also solves the asymmetrical leptogenesis problem.	[8]
Origin of entropy	Fabric increases the Irreversibility of geometric position of particle.	[17]
A theory for time as an emergent property of matter rather than a universal attribute	Time arises from the interaction between the frequency of a particle and the local density of the fabric.	[4]
Nature of the vacuum and the cosmological horizon	Vacuum comprises fabric of discrete forces from massy particles.	[18]
Origin of the finite speed of light	Determined by fabric density, hence variable with epoch of universe and local distribution of mass.	[19]
Quantitative derivation of the relativistic Doppler and the Lorentz factor	Derivation accomplished from a particle perspective. Identifies fabric density as a covert variable.	[20]

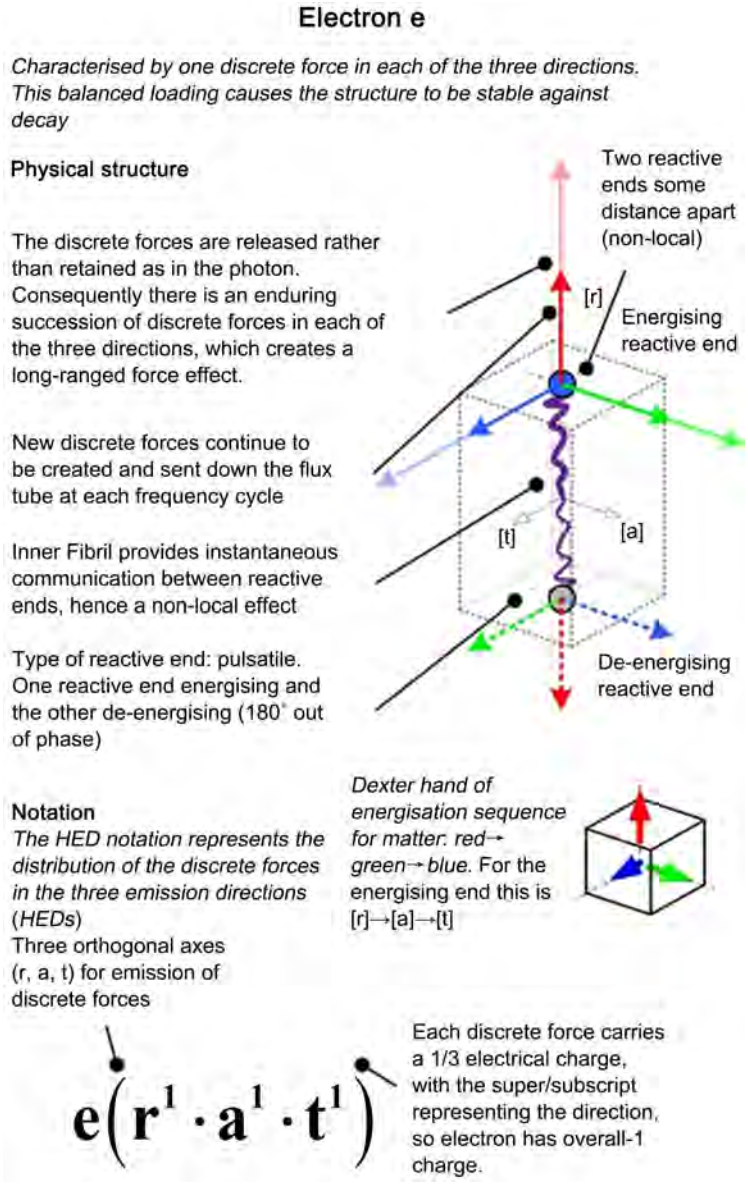

Figure 1. The representation of the electron's internal and external structures. It is proposed that the particle has three orthogonal discrete forces, energised in turn at each reactive end. Adapted from [5].

3. Approach

Prior work showed that the Lorentz, relativistic Doppler, and time dilation could be derived from first principles using the Cordus theory [20], but required the flux tube to be stretchable. This imposes a conceptual conundrum. How could discrete forces, which are required in the context of synchronous bonding [2] to be in a binary state of energisation, also be continuous as required in the general relativity context? The existence of this duality implies the potential existence of a deeper mechanics, once that could give either outcome depending on the perspective taken. The specific situation under examination was how the electro-magneto-gravitational fields operated, *i.e.* the long ranged interactions (ex-

cluding the strong and weak).

The approach used abductive reasoning. It started with the high-level behaviour, and applied inference to determine the possible deeper mechanics. Conceptual propositions, or lemmas, were identified. These are indicated§.

4. Results

4.1. A Proposed General Mechanism for Force

Consider test particle B, say an electron, in an electrostatic field set up by particle A. Each particle has two reactive ends, and for B these are denoted B_1 and B_2. See Figure 2. The location of interest is reactive end B_1 which receives forces from A, and emits its own discrete forces.

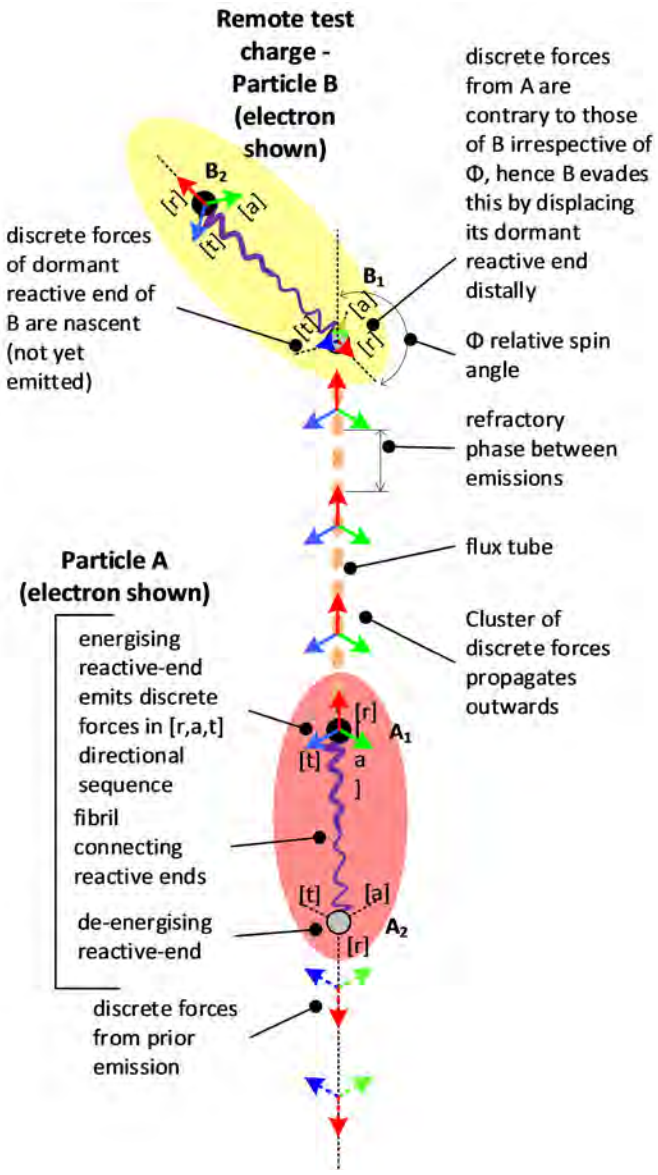

Figure 2. Discrete forces emitted by basal particle A, and intercepted by remote test particle B. Each particle has two reactive ends.

Emission of discrete forces occurs at the energisation frequency of the particle (§1)

It is proposed that discrete forces are emitted from massy particles, and at each cycle of energisation a fresh discrete force is created and emitted. It follows that higher frequency particles, *i.e.* those that are in more energetic states, emit discrete forces more frequently. The corollary is that the magnitude of the force effect is proposed to be determined by the number of discrete forces received.

Similar-charged particles interact via the transphasic synchronous interaction, while opposite-charged particles interact via the cisphasic interaction (§2)

The theory predicts that bonds between *proximal* particles arise from synchronisation of their discrete force emissions. This is called the synchronous interaction [2] and has been applied to predict the structure of the atomic nucleus for multiple nuclides [15] [16], and also explains Pauli pair structures [7]. Favourable emission states have already been defined for this theory, see [2], and include assembly of opposite charge discrete forces and complete sets of discrete forces. There are two subtypes to the synchronous interaction, which are transphasic and cisphasic. These are when reactive ends from different particles energise out- and in-phase respectively.

This lemma extends the synchronous principle to *ranged* particles: it is proposed that the same mechanism applies even if the particles are some distance apart, e.g. in the electrostatic force and ranged forces generally. If the emission of discrete forces of one particle favours the emissions of the other, then the particles move closer together. The direction of motion is along the gradient in a direction that favours increased compatibility or evades incompatibility (as the case may be).

Force is caused by coercive displacement of reactive ends (§3)

Under these assumptions, force at the deeper level is a process of discrete displacements of reactive ends, under the coercive effect of incoming discrete forces. More specifically, force on test particle B is caused by incoming discrete forces interacting with the emission sequence of B's discrete forces. This coerces the reactive end to re-energise in a different location. Those incoming discrete forces may be from other particle A or the fabric (many other particles) generally.

The nature of the interference for B is the phase difference between its intended emissions vs. the incoming emissions. This prescription causes the reactive end of B to move its location in space, such that it more nearly synchronises its emissions in or out of phase (cis- or transphasic respectively) with the external discrete forces. The process is one of the reactive end of B being drawn to, or evading, the discrete forces produced by distant particles.

Such a motion is a finite displacement and occurs during the energisation cycle of the particle, hence we refer to it as a coerced discrete displacement. It is the particle's response to the external discrete force. This has the effect that the reactive end energises at a *different location* to its natural preference, hence

causing the position of the particle as a whole to change, and this effect is perceived as force.

The response depends on the bound state of B. For free particle B the free reactive end may move in response to the external discrete forces. For a partially bonded particle B, one reactive end is co-located with the reactive end of other particles, and hence B is constrained in span and frequency and this limits the available locations into which it can move. For particle B bonded at both reactive ends, there is no ability to move. If there is sufficient reaction force applied to the test particle, then it can be prevented from making this discrete displacement. Instead the body as a whole responds to the external discrete forces. Hence a larger body is subject to the same effect of prescribed displacement, but in an aggregate manner. Thus the effect of prescribed displacement scales from the small to the macroscopic discoherent state. If the external discrete forces are sufficiently compelling, even full bonded particle A may be broken free from its assembly. This is consistent with the effect of ionising radiation.

The displacement is not uniform or fixed, being instead determined by the relative strengths of the native vs. incoming discrete force emissions (hence also type and mass of test particle), and the degree of freedom or constraint on the test particle. The test particle makes a small displacement each time it de-energises, and hence the underlying response to the field is a series of discrete motions. As particles have high frequencies (de Broglie frequency), this process is apparently continuous at the macroscopic scale. Hence the explanation does not undermine classical continuous mechanics, but rather offers a deeper explanation. Likewise the force bosons of quantum mechanics are re-explained as discrete forces. Quantum mechanics requires different bosons for each interaction, whereas the Cordus theory proposes that different attributes of the discrete forces result in the different interactions.

A field comprises sequential discrete forces (§4)

A field is interpreted to comprise discrete forces, the action of which causes a particle to move in a rapid series of finite displacements in space. The perturbing external discrete force is of finite duration, hence the displacement per energisation cycle is also finite. For a particle B in a steady field, the next discrete force it encounters causes a displacement consistent with the previous one. Hence the particle in this situation shows a consistent direction of discrete displacements, hence a motion of increasing velocity, *i.e.* acceleration in response to the force field. Thus the effect of the force appears smooth and continuous at the macroscopic level of examination, even though it is fundamentally discrete.

Discrete forces are connected in flux tubes (§5)

The sequence of discrete forces emitted by any one particle is proposed to be connected in a *flux tube*, this being a curvilinear assembly of discrete forces. The discrete force in the flux tube is a persistent structure even when not energised [20]. As a particle moves, so the next discrete force is emitted from a different position of the reactive end. Hence the direction of action of the following dis-

crete force will be slightly different to that before it. Thus the flux tube is expected to have bends, for a moving emitter.

The discrete force interactions are fundamentally unidirectional (§6)

It is proposed that the displacement effect of a received discrete force, and hence the force interaction, is fundamentally unidirectional: when test particle B *receives* a discrete force, it reacts to it via the displacement effect. The *emitting* particle A is unaffected, unless it also receives a discrete force from B. This means that the process whereby A emits a discrete force does not commit A to a future interaction dependent on whether or not that discrete force is intercepted by B.

This is an unorthodox premise since force is generally held to be reciprocal in action. Indeed in the type of *situation* in which the Earth is positioned, similar particles affect each other equally, and hence the bi-directional nature of force is recovered. Nonetheless in general the theory predicts unidirectional effects: discrete forces from A unidirectionally affect B, and those from B affect A, but there is no fixed reciprocity or an exchange per se.

Discrete forces are not consumed in the interactions (§7)

Discrete forces are not consumed by interactions but continue to propagate outward to affect yet other particles. In specific cases, the discrete force may be consumed, such as annihilation of matter-antimatter particles [12], and pair-production [13].

The capability to make discrete displacement of a reactive end is affected by its energisation state (§8)

The discrete displacement of a reactive end is affected by its energisation state. A reactive end that is fully energised in one of its emission directions (r, a, t) is momentarily stationary in that direction, or would prefer to be so. At times of incomplete energisation the reactive end is mobile and most susceptible to being displaced by an incoming discrete force.

The reactive end samples the discrete forces around it (§9)

A reactive end experiences all the discrete forces passing through that region of space which it occupies in its migrations. The reactive end is transparent in that the external discrete forces intrude into the reactive end temporarily as they propagate. A particle is not solely affected by the fields (or in this case the discrete forces) passing through its centre (or in this case its two reactive ends). Instead it is affected by discrete forces in the nearby locality of the reactive end. The incoming discrete forces occupy a volume of space during their transit. Consequently the reactive end has the ability to sense what is happening in the volume of space immediately around it, with an interaction between the external environment, discrete forces, and reactive end. This is non-local behaviour.

Sampling of the environment provides the mechanism for the reactive end to determine the field gradient (§10)

At intermediate stages of energisation the reactive end moves a small distance in reaction as it undertakes its own emissions. This results in a small-scale repe-

titive displacement motion of the reactive end at the de Broglie frequency. This motion is in all three directions of space, which allows the reactive end to sweep through-and sample-a small volume of space. This is proposed as the mechanism whereby it senses the gradient of the external field.

The mechanism whereby the reaction end moves under the influence of an external field arises because the RE spends longer time in those regions of space where the density (or strength) of external discrete forces is more favourable (higher or lower depending on relative attributes of particles A and B). It preferentially energises there. Since energisation also means the RE is stationary, it dwells there longer, hence the mean position of the RE is changed.

4.2. Mechanism for Force & Discrete Movement in an Imposed Field

Above it was stated that force is caused by coercive displacement of reactive ends (§3), that the reactive end samples the discrete forces around it (§9), and that this provides the mechanism for the reactive end to determine the field gradient (§10). These conceptual propositions are now represented in a quantitative formulation.

Discrete force emissions take the form $\sin^2(\theta/2)$ (§11)

Previous diagrams have shown the reactive ends as either energised or not, but this is simplistic. The strength of energisation, hence also of the emitted discrete forces, evolves over time. The question is what the shape of this energisation function might be. We are required, for reasons of logical consistency with the Lorentz work [20], to see the reactive ends as producing a continuous flux tube, without breaks, so abrupt step-like functions are excluded. It is logical to assume it takes a sinusoidal function, and ranges between 1 and 0 over a cycle (discrete forces of massy particles do not change sign, though photons do). We also need to consider the second reactive end B_2 and that the energy oscillates between the two—this is an established principle of the theory. This requires that the total energy is conserved at any one moment. A relationship that fits these criteria is $\sin^2(\theta/2)$ where θ is the phase angle of energisation, and this is marked as a lemma.

Thus the potential energy U of a discrete force in a particular direction (say r) at reactive ends B_1 and B_2 is:

$$U_{B_1} = \sin^2 \frac{\theta_B}{2} \tag{1a}$$

$$U_{B_2} = \cos^2 \frac{\theta_B}{2} \tag{1b}$$

Given also that there are three orthogonal discrete force emissions (r, a, t) and that the energisation sequence of these determines the matter-antimatter species [12], then the potential energy is partitioned into three components offset at thirds of the phase cycle:

$$U_{B_1}(r) = \sin^2 \frac{\theta_B}{2} \tag{2a}$$

$$U_{B_1}(a) = \sin^2\left(\frac{\theta_B}{2} - 120^\circ\right) \quad (2b)$$

$$U_{B_1}(t) = \sin^2\left(\frac{\theta_B}{2} - 240^\circ\right) \quad (2c)$$

See Figure 3 for a representation of these three phases. The discrete force emissions do not subtract energy from the particle.

Thus the reactive end is never fully de-energised (except momentarily in one axis), and this is consistent with the expectations from the Lorentz derivation for a stretchable flux tube. This also means that the energy at the basal generator, *i.e.* the reactive end B_1 has a circular function, see Figure 4.

Thus the phased emission of discrete forces corresponds to a torsional energisation that is carried out into space by the discrete forces. The remote particle B receives this torsional package of discrete forces, and assuming both A and B are matter particles, finds this conducive to its own emissions and moves closer along the field gradient.

The process of emitting discrete forces causes the reactive end to move cyclically in the (r, a, t) directions (§12)

It is proposed that the sinusoidal potential energy function of the discrete forces corresponds to a movement of the reactive end itself. The nature of the motion is inferred as follows. The discrete forces themselves are a type of potential displacement. Hence the displacement that underpins them is the square root of their potential energy function, hence a $\sin(\theta/2)$ dependency. However the motion must be cyclical, *i.e.* the reactive end must return to its original

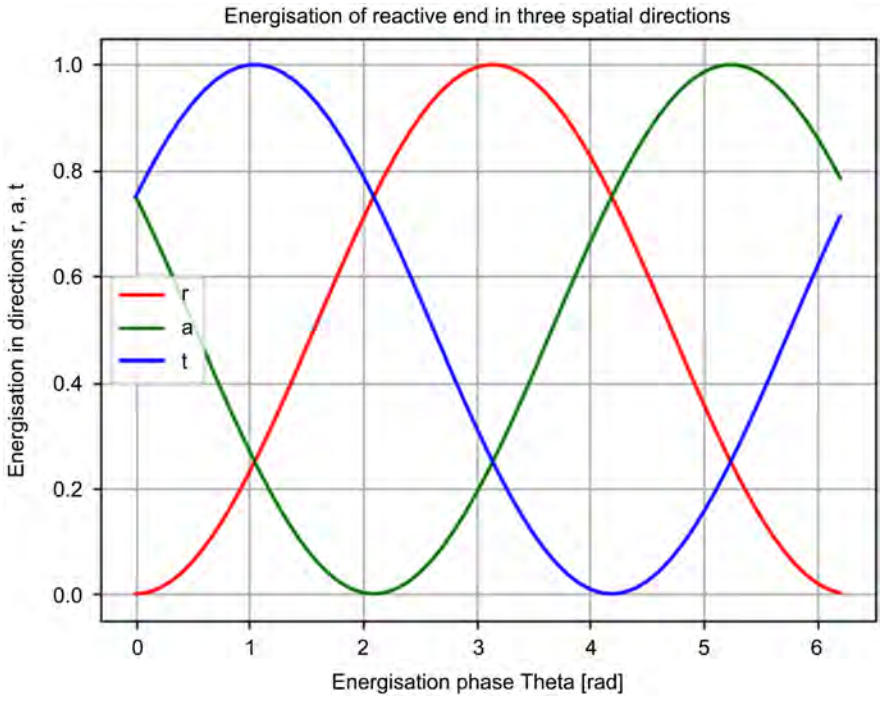

Figure 3. Energisation phases in the three orthogonal emission directions (r, a, t) follow a $\sin^2(\theta/2)$ relation.

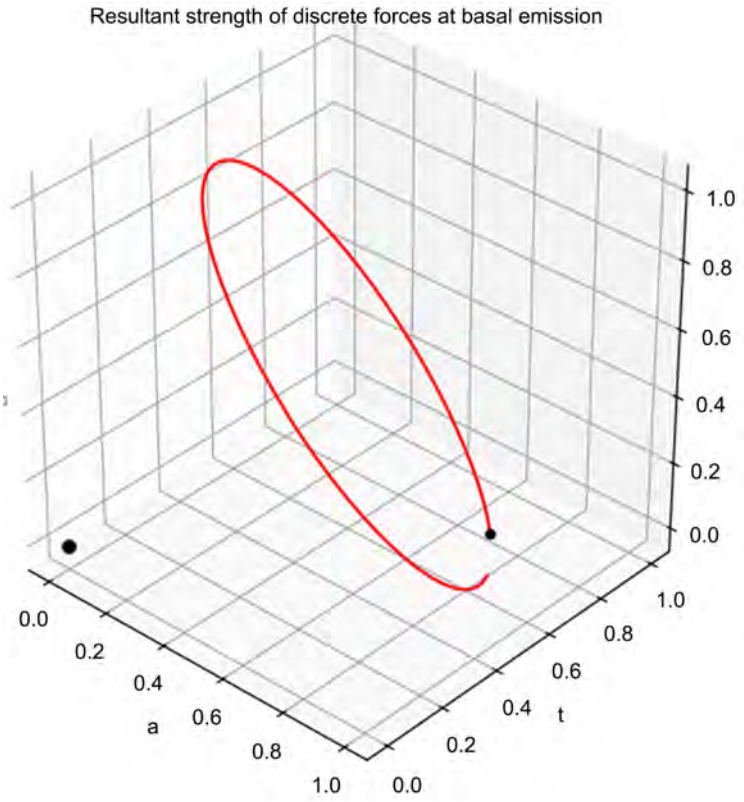

Figure 4. Resultant energy at the basal generator B_1 due to a matter negative charge. The axes are (r, a, t). The larger black marker indicates the nominal origin (0, 0, 0), and the smaller black marker indicates the location for $\theta = 0$. The chart is deliberately shown incomplete to indicate the direction of rotation.

position, and this requires positive and negative components to its motion, hence a $\sin(\theta)$ function. Finally, the motion of the reactive end is inversely related to its energisation, being motionless when fully energised, hence a $\cos(\theta)$ relationship. This is shown for a single axis in **Figure 5**, and for all three axes in **Figure 6**. Thus the displacement of the reactive end may be inferred to be a circular locus around the nominal location of the reactive end.

While the positional locus is circular in the absence of an imposed field, the reactive end expands its excursion when in a field. Assuming a field gradient applies and consider only the r direction. The amount of displacement from the locus is presumed to be determined by two factors. The first is the strength of the field, which for simplicity is assumed to be linear (which is approximately true far from the field origin) with gradient P_{grad} and strength P_{centre} at the nominal centre point of the reactive end. Thus one side of the positional locus experiences the field as slightly stronger than the other. The second factor is the mobility of the reactive end, which is inversely related to its energisation, hence to $\cos^2\theta/2$. The result is a non-linear distortion of the positional locus of the form:

$$r_{moved}(\theta) = r(\theta) + \left(P_{grad} r(\theta) + P_{centre}\right)\cos^2\frac{\theta}{2} \tag{3}$$

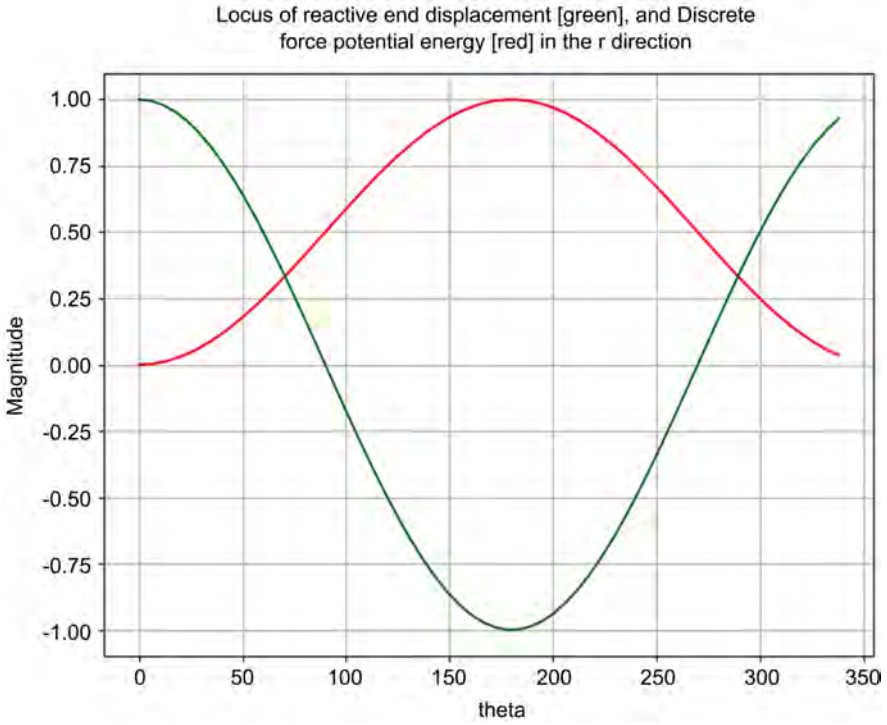

Figure 5. The locus of motion of the reactive end follows a cos (θ) dependency for each axis, whereas the potential energy follows $\sin^2(\theta/2)$.

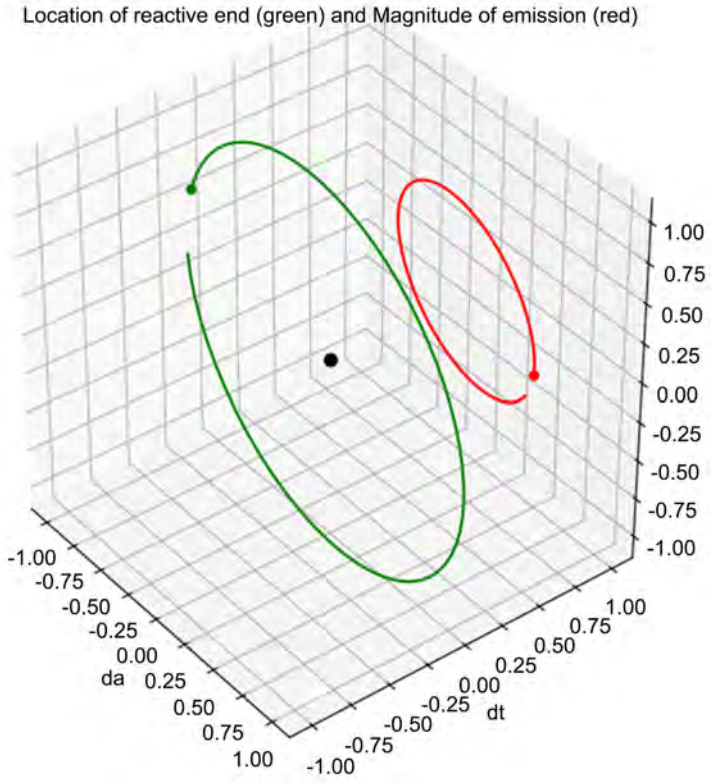

Figure 6. Circular locus of positon of the reactive end over a complete cycle of emission from both reactive ends, for an electron. Green shows the location locus, and red the energy. The vertical axis is the r direction.

An example of a distorted positional locus is shown in Figure 7(a). Even with a linear field the new locus is a non-linear distortion of the original circular track, *i.e.* the reactive end is sensitive to the spatial change in field strength. The progressive accumulation of displacement results in a distorted spiral locus with dwell regions of low progression, see Figure 7(b).

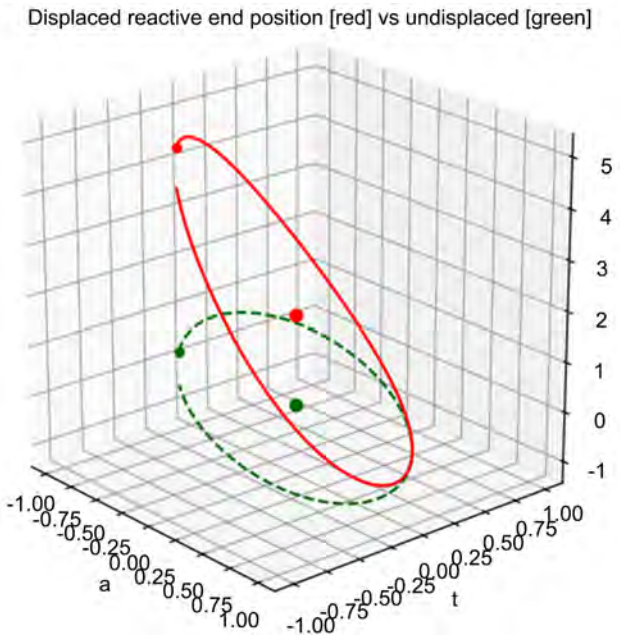

(a)

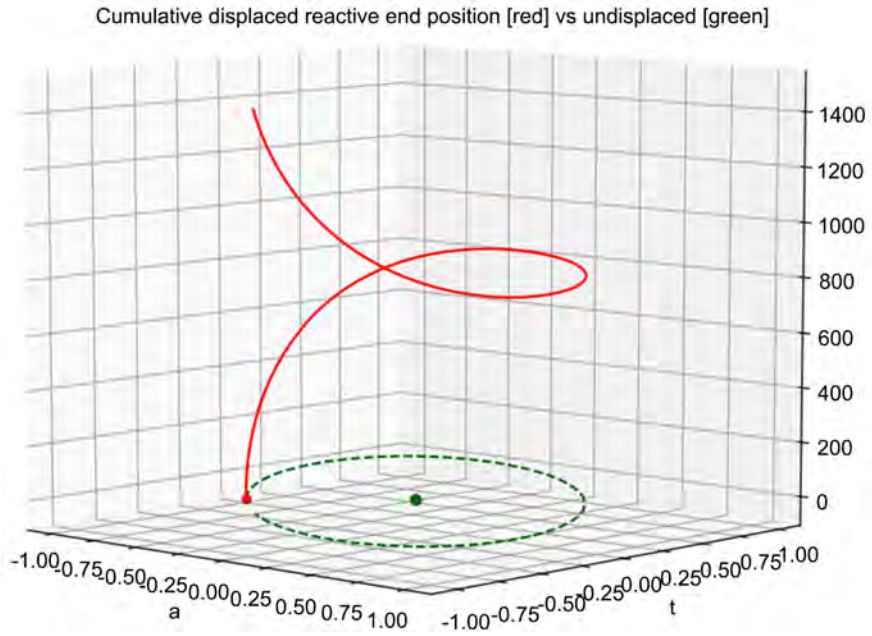

(b)

Figure 7. (a) Distorted positional locus for a reactive end under the effect of a linear field in the r direction. The larger round symbols show the centre point of the locus, *i.e.* the nominal position of the reactive end. Values in the r direction are nominal; (b) Cumulative locus of the reactive end. Values are nominal.

The significance is that the mean location of the reactive end changes under the effect of the field. This adjustment occurs in discrete intervals at each frequency cycle while the reactive end is exposed to the field. Thus the following lemma is noted.

The positional locus of a reactive end is distorted by the effect of field gradient (§13)

While the above example is based on an electrostatic interaction, there does not appear to be impediment to generalise the principles to any of the ranged fields.

5. Discussion

5.1. Findings

The novel contribution of this work is providing a candidate mechanism for how a particle detects and moves in a field gradient. The explanation accommodates the continuous vs. discrete duality of forces, as evidenced in the general relativity vs. quantum perspectives. Emitted discrete forces have a sinusoidal strength function. At the receiving particle, the mobility of the reactive end is inversely related to its energisation, so the interaction has dwell periods. The emitted field is continuous but the effect is discrete.

It also answers another duality question: how can a flux tube be continuous if the forces it contains are discrete [20]? The answer is that the reactive end binary states of energised vs. de-energised are an approximation of a sinusoidal strength relationship for energisation. Furthermore, with emissions in three orthogonal directions, there is no point in time when the flux tube is completely de-energised, hence its continuity is preserved.

5.2. Limitations and Future Research Opportunities

The present work has elucidated a mechanism for force generally. This has been formulated in a discrete force function. It could be interesting to develop specific formulations for each of the three ranged interactions: electrostatic, magnetic, and gravitational. There may different formulations for the discrete force function that could also be acceptable.

6. Conclusions

Per this theory, the operation of force at a more fundamental level is proposed to occur via the following mechanisms.

1) The reactive end moves in a cyclic locus in reaction to its own emission of discrete forces, hence sweeps through a volume of space during its energisation cycle.

2) This motion provides a mechanism for the reactive end to sample the field gradient around it.

3) The locus is warped by the discrete forces of the incoming field, hence preferentially displacing the reactive end along the gradient. The mechanism is that

the reactive end spends longer time in those regions of space where the density (or strength) of external discrete forces is more favourable, and this changes its mean position in space. This adjustment occurs in discrete intervals at each frequency cycle while the reactive end is exposed to the field.

4) The resulting direction of motion is along the gradient in a direction that favours increased compatibility or evades incompatibility between the discrete forces from the two particles.

The underlying mechanism for force is therefore proposed to be a process of discrete displacements of reactive ends, under the coercive effect of incoming discrete forces from the field.

Conflict of Interest Statement

The author declares that there are no financial conflicts of interest regarding this work.

References

[1] Pons, D.J., *et al*. (2012) *Physics Essays*, **25**, 132-140. https://doi.org/10.4006/0836-1398-25.1.132

[2] Pons, D.J., Pons, A.D. and Pons, A.J. (2013) *Applied Physics Research*, **5**, 107-126. https://doi.org/10.5539/apr.v5n5p107

[3] Pons, D.J., Pons, A.D. and Pons, A.J. (2016) *Journal of Modern Physics*, **7**, 1049-1067. https://doi.org/10.4236/jmp.2016.710094

[4] Pons, D.J., Pons, A.D. and Pons, A.J. (2013) *Applied Physics Research*, **5**, 23-47. https://doi.org/10.5539/apr.v5n6p23

[5] Pons, D.J. (2015) Internal Structure of the Electron (Image Licence Creative Commons Attribution 4.0). Wikimedia Commons, (Creative Commons Attribution 4.0 International License).

[6] Pons, D.J. (2012) A Physical Interpretation of String Theory? http://vixra.org/abs/1204.0047

[7] Pons, D.J., Pons, A.D. and Pons, A.J. (2019) *Journal of Modern Physics*, **10**, 835-860. https://doi.org/10.4236/jmp.2019.107056

[8] Pons, D.J., Pons, A.D. and Pons, A.J. (2014) *Journal of Modern Physics*, **5**, 1980-1994. https://doi.org/10.4236/jmp.2014.517193

[9] Pons, D.J., Pons, A.D. and Pons, A.J. (2015) *Applied Physics Research*, **7**, 1-11. https://doi.org/10.5539/apr.v7n1p1

[10] Pons, D.J., Pons, A.D. and Pons, A.J. (2014) *Applied Physics Research*, **6**, 50-63. https://doi.org/10.5539/apr.v6n3p50

[11] Pons, D.J. (2015) Internal Structure of the Photon (Image Licence Creative Commons Attribution 4.0). Wikimedia Commons, (Creative Commons Attribution 4.0 International License).

[12] Pons, D.J., Pons, A.D. and Pons, A.J. (2014) *Applied Physics Research*, **6**, 28-46. https://doi.org/10.5539/apr.v6n2p28

[13] Pons, D.J., Pons, A.D. and Pons, A.J. (2015) *Journal of Nuclear and Particle Physics*, **5**, 58-69.

[14] Pons, D.J. (2015) *Applied Physics Research*, **7**, 14-26.

https://doi.org/10.5539/apr.v7n4p24

[15] Pons, D.J., Pons, A.D. and Pons, A.J. (2015) *Physics Research International*, **2015**, Article ID: 651361. https://doi.org/10.1155/2015/651361

[16] Pons, D.J., Pons, A.D. and Pons, A.J. (2013) *Applied Physics Research*, **5**, 145-174. https://doi.org/10.5539/apr.v5n6p145

[17] Pons, D.J., Pons, A.D. and Pons, A.J. (2016) *Journal of Modern Physics*, **7**, 1277-1295. https://doi.org/10.4236/jmp.2016.710113

[18] Pons, D.J. and Pons, A.D. (2013) *The Open Astronomy Journal*, **6**, 77-89. https://doi.org/10.2174/1874381101306010077

[19] Pons, D.J., Pons, A.D. and Pons, A.J. (2016) *Applied Physics Research*, **8**, 111-121. https://doi.org/10.5539/apr.v8n3p111

[20] Pons, D.J., Pons, A.D. and Pons, A.J. (2018) *Journal of Modern Physics*, **9**, 500-523. https://doi.org/10.4236/jmp.2018.93035

Journal of Modern Physics, 2020, 11, 1576-1588
https://www.scirp.org/journal/jmp
ISSN Online: 2153-120X
ISSN Print: 2153-1196

New Method Proving Clausius Inequality*

Chengshu Jin

School of Food and Pharmaceutical Engineering, Suihua College, Suihua, China
Email: jinchengshu_1@163.com, 2569740682@qq.com

How to cite this paper: Jin, C.S. (2020) New Method Proving Clausius Inequality. *Journal of Modern Physics*, **11**, 1576-1588.
https://doi.org/10.4236/jmp.2020.1110098

Received: September 3, 2020
Accepted: October 17, 2020
Published: October 20, 2020

Abstract

It is impossible that proving the internal energy change has the relations with volume and pressure. About the second law of thermodynamics, many mistakes of formulations need to be put right and modified, and many new concepts are surveyed too. The equality and inequality on the ratios of internal energy change to temperature and work to temperature are discussed. The relation between the reversible paths and their realistic paths is also researched. In an isothermal process, the internal energy change for the gases is equal to zero, but the internal energy change is not equal to zero for the phase transition or chemical reaction. The Clausius inequality can be derived from the equation calculating the internal energy change in mathematics; it is the new method proving the Clausius inequality. These change laws of thermodynamics could be applied to the gravitational field and mechanical motion and so on.

Keywords

First Law of Thermodynamics, Clausius Inequality, Internal Energy Change, Chemical Reaction, Gravitational Field

1. Introduction

In text, the heat and work are taken as positive if the energy is supplied to the system and negative if the energy is lost out of the system. W_{other} expresses the other work (also called the non-expansion work), and $-p\mathrm{d}V$ indicates the pressure-volume work (namely the expansion work).

According to the first law of thermodynamics [1] [2] [3], if the expansion work doesn't exist, the internal energy change is equal to the non-expansion work in the adiabatic process. If any work doesn't exist, the internal energy change is equal to the heat in a constant volume process (namely that $\mathrm{d}U = C_V \mathrm{d}T$, where, C_V is

*New Method proving Clausius Inequality.

the heat capacity at the constant volume). If the other work doesn't exist in a constant pressure process, the internal energy change is equal to $\Delta U = \Delta H - p\Delta V$ (where, $\Delta H = C_p \Delta T$, C_p is the heat capacity at the constant pressure, ΔH is the enthalpy change at the constant pressure). In a process, the heat, work, and internal energy change can transfer each other, but the relation of heat, work, and internal energy change has to obey the energy conservation law namely the first law of thermodynamics.

The difference on the ratios of work to temperature between a reversible process and its realistic process is no more than zero; simultaneously, the difference on the ratios of internal energy change to temperature between a reversible process and its realistic process is no less than zero. If the latent heat and chemical reactions do not exist, the internal energy change in an isothermal process will be zero [4]. In this paper, the new method proving the Clausius inequality will be investigated.

Attentively, "d" and "δ" are total differential symbols to the state function and path function, respectively. "Δ" expresses the change of quantity value. "∫" is integral symbol. "∂" is partial differential symbol. The internal energy change is the state function. The heat and work are the path functions in many processes. The enthalpy change at the constant pressure is the state function too.

2. New Concepts about the Ratios of Internal Energy Change to Temperature and Work to Temperature

In a spontaneous or realistic process, according to the first law of thermodynamics, we can obtain [4] [5]

$$\begin{aligned} &\int_i^f \frac{\mathrm{d}U_r(A)}{T} - \int_i^f \frac{\mathrm{d}U_{real}(B)}{T_{res}} \\ &= \int_i^f \frac{\delta Q_r(A)}{T} - \int_i^f \frac{\delta Q_{real}(B)}{T_{res}} + \int_i^f \frac{\delta W_r(A)}{T} - \int_i^f \frac{\delta W_{real}(B)}{T_{res}} \end{aligned} \tag{1}$$

The criterion equation for a process is obeyed as the follows

$$\int_i^f \frac{\delta Q_r(A)}{T} - \int_i^f \frac{\delta Q_{real}(B)}{T_{res}} \geq 0. \tag{2}$$

In a spontaneous or realistic process, the following equations must be also obeyed

$$\int_i^f \frac{\delta W_r(A)}{T} - \int_i^f \frac{\delta W_{real}(B)}{T_{res}} \leq 0, \tag{3}$$

$$\int_i^f \frac{\mathrm{d}U_r(A)}{T} - \int_i^f \frac{\mathrm{d}U_{real}(B)}{T_{res}} \geq 0. \tag{4}$$

where, the equality is usually for a reversible process, the inequality is for an irreversible process. (B) and (A) express the realistic path and reversible path, respectively. The realistic paths may include the reversible or irreversible paths. The friction does not exist in any reversible process. ΔS and $\int_i^f \frac{\delta Q_r(A)}{T}$ all

express the entropy change, that is, $\Delta S = \int_i^f \frac{\delta Q_r(A)}{T}$. $\int_i^f \frac{\delta W_r(A)}{T}$ is indicated with ΔS_W, namely that $\Delta S_W = \int_i^f \frac{\delta W_r(A)}{T}$. $\int_i^f \frac{dU_r(A)}{T}$ is expressed with ΔS_U, namely that $\Delta S_U = \int_i^f \frac{dU_r(A)}{T}$. In a process, T_i and T_f are the thermodynamics temperature of system in the initial state and final state, respectively. T expresses the thermodynamics temperature of system transforms from T_i to T_f. T_{res} is the thermodynamics temperature of surroundings or reservoirs, and T_{res} can vary or influence the thermodynamics temperature of system except the adiabatic system. Of course, T_{res} is the same as T in any reversible process or constant temperature process. T_{res} is not always considered as a constant in a realistic process. Any spontaneous or realistic process has to obey the Clausius inequality [6] [7] [8].

$\Delta S_g = \int_i^f \frac{\delta Q_r(A)}{T} - \int_i^f \frac{\delta Q_{real}(B)}{T_{res}}$, where, ΔS_g is called the entropy generation [9] [10] [11]. In a spontaneous or realistic process, we can gain $\Delta S_g \geq 0$. In the adiabatic process, ΔS_g is not equal to zero for an irreversible process.

$(\Delta S_W)_g = \int_i^f \frac{\delta W_r(A)}{T} - \int_i^f \frac{\delta W_{real}(B)}{T_{res}}$, where, $(\Delta S_W)_g$ is defined as the ratio of work to temperature generation. In a spontaneous or realistic process, we have $(\Delta S_W)_g \leq 0$. If any work doesn't exist, $(\Delta S_W)_g$ is equal to zero.

$(\Delta S_U)_g = \int_i^f \frac{dU_r(A)}{T} - \int_i^f \frac{dU_{real}(B)}{T_{res}}$, where, $(\Delta S_U)_g$ is defined as the ratio of internal energy change to temperature generation. In a spontaneous or realistic process, we shall obtain $(\Delta S_U)_g \geq 0$. In the isothermal process, $(\Delta S_U)_g$ is equal to zero. Equation (1) can be rewritten as $(\Delta S_U)_g = \Delta S_g + (\Delta S_W)_a$.

Certainly, the values of ΔS_g, $(\Delta S_W)_g$, and $(\Delta S_U)_g$ all will change into zero in the reversible process or equilibrium changeless state for the spontaneous or realistic processes. The ΔS_g, $(\Delta S_W)_g$, and $(\Delta S_U)_g$ are the path functions, not the state functions. According to Equations (1), (3), we know $\Delta S_g \geq (\Delta S_U)_g$.

$\int_i^f \frac{\delta Q_{real}(B)}{T_{res}}$ is the path functions called the entropy flow [12]. When the solids and liquids are cooled, it will release the heat and its temperature will fall, the entropy change is negative value which conforms to the Clausius inequality, it is very reasonable nature results, but the entropy generation is no less than zero in the processes, that is, $\Delta S_g \geq 0$. In a process, ΔS is unable to be varied by the entropy flow or path or energy like work and heat, since it is the state functions. The entropy generation could be changed from negative to positive by the entropy flow or path or energy. In the living things, the entropy generation in the glucose synthesized reaction will be changed from negative to positive. If there is not any energy supplied to system, the damage cells in the living things could not be repaired, and the life will end and die.

3. New Method Proving the Clausius Inequality

The internal energy change has to be equal to zero for the ideal and real gases in any isothermal process, namely that, $\left(\frac{\partial U}{\partial V}\right)_T = 0$ and $\left(\frac{\partial U}{\partial p}\right)_T = 0$ (where, the subscript T indicates constant temperature). In the Rossini and Frandsen experiment [4] [13], the high pressure gas slowly expands and enters the air through the valve and pipeline, the water heated by heater in trough will keep constant temperature, but the expansion gas is open will still do work to air, so the heat is unable to be accurately determined. Therefore, it is regretful that the Rossini and Frandsen experiment could not prove the internal energy change having a relation with the pressure and volume for the gas. In the Rossini and Frandsen experiment, the pressure-volume work is equal to $-\int_i^f p\mathrm{d}V$, which is approximately equal to $-p\Delta V$ (where, p is the constant pressure).

If the latent heat and chemical reactions do not exist, we can obtain [4]

$$\mathrm{d}U = C_V \mathrm{d}T . \tag{5}$$

The gases, solids and liquids all obey Equation (5). If the phase transition or chemical reactions exist in the constant temperature and constant pressure, the internal energy change will be given by

$$\Delta U = Q_V ,$$

$$\Delta U = \Delta H - p\Delta V .$$

where, the enthalpy change is the latent heat or chemical reaction heat in the constant temperature and constant pressure. Therefore, the internal energy change is the state functions for the phase transition or chemical reactions.

If the phase transition or chemical reactions does not exist for the closed system, we can obtain $\mathrm{d}U = \delta Q + \delta W_{other} - p\mathrm{d}V$ and $C_V \mathrm{d}T = T\mathrm{d}S + \delta W_{other} - p\mathrm{d}V$. Where, $\delta W_{real}(B) = \delta W_{other}(B) - p\mathrm{d}V(B)$, $\delta Q_{real}(B) = T\mathrm{d}S(B)$ (it is dependable, since $\mathrm{d}S(B) = \frac{\delta Q_{real}(B)}{T}$, $\int_i^f \frac{\delta Q_r(A)}{T} = \int_i^f \frac{\delta Q_{real}(B)}{T} = \Delta S$), $\delta Q_r(A) = T\mathrm{d}S(A)$, $\delta W_r(A) = \delta W_{other}(A) - p\mathrm{d}V(A)$, $p\mathrm{d}V(A) \neq p\mathrm{d}V(B)$. Attentively, T is often not the constant in the isothermal irreversible path (B), but $T_i = T_f = T_{res}$. T is the constant in the isothermal reversible path (A).

Thereinafter, using Equation (4) will prove the Clausius inequality is absolutely correct.

According to Equation (5), we can prove Equation (4) is absolutely right in mathematics. When $\mathrm{d}T \geq 0$, we find $T \leq T_{res}$ and $\frac{\mathrm{d}T}{T} \geq \frac{\mathrm{d}T}{T_{res}}$. If $\mathrm{d}T \leq 0$, we find $T \geq T_{res}$ and $\frac{-\mathrm{d}T}{T} \leq \frac{-\mathrm{d}T}{T_{res}}$, further, $\frac{\mathrm{d}T}{T} \geq \frac{\mathrm{d}T}{T_{res}}$. Hence, $\int_i^f \frac{\mathrm{d}T}{T} \geq \int_i^f \frac{\mathrm{d}T}{T_{res}}$. Thus, $\int_i^f \frac{\mathrm{d}U_r(A)}{T} \geq \int_i^f \frac{\mathrm{d}U_{real}(B)}{T_{res}}$.

If $\Delta S_g \geq 0$, that is, $\int_i^f \frac{\delta Q_r(A)}{T} - \int_i^f \frac{\delta Q_{real}(B)}{T_{res}} \geq 0$, on the basis of Equation (1),

we can obtain

$$\int_i^f \frac{\mathrm{d}U_r(A)}{T} - \int_i^f \frac{\mathrm{d}U_{real}(B)}{T_{res}} \geq \int_i^f \frac{\delta W_r(A)}{T} - \int_i^f \frac{\delta W_{real}(B)}{T_{res}}.$$

In order to guarantee that above-mentioned inequality is absolutely right, according to Equation (4), the value of $\int_i^f \frac{\delta W_r(A)}{T} - \int_i^f \frac{\delta W_{real}(B)}{T_{res}}$ must be no more than zero (namely that $\int_i^f \frac{\delta W_r(A)}{T} - \int_i^f \frac{\delta W_{real}(B)}{T_{res}} \leq 0$). If $\int_i^f \frac{\delta Q_r(A)}{T} - \int_i^f \frac{\delta Q_{real}(B)}{T_{res}} < 0$, we can obtain

$$\int_i^f \frac{\mathrm{d}U_r(A)}{T} - \int_i^f \frac{\mathrm{d}U_{real}(B)}{T_{res}} < \int_i^f \frac{\delta W_r(A)}{T} - \int_i^f \frac{\delta W_{real}(B)}{T_{res}}.$$

On the basis of Equation (4), we have $\int_i^f \frac{\delta W_r(A)}{T} - \int_i^f \frac{\delta W_{real}(B)}{T_{res}} > 0$.

If $\int_i^f \frac{\delta W_r(A)}{T} - \int_i^f \frac{\delta W_{real}(B)}{T_{res}} > 0$, according to Equation (1), we can obtain

$$\int_i^f \frac{\mathrm{d}U_r(A)}{T} - \int_i^f \frac{\mathrm{d}U_{real}(B)}{T_{res}} > \int_i^f \frac{\delta Q_r(A)}{T} - \int_i^f \frac{\delta Q_{real}(B)}{T_{res}}.$$

In order to guarantee that aforesaid inequality is absolutely right, according to Equation (4), the value of $\int_i^f \frac{\delta Q_r(A)}{T} - \int_i^f \frac{\delta Q_{real}(B)}{T_{res}}$ must be no more than zero (that is, $\int_i^f \frac{\delta Q_r(A)}{T} - \int_i^f \frac{\delta Q_{real}(B)}{T_{res}} < 0$). If $\int_i^f \frac{\delta W_r(A)}{T} - \int_i^f \frac{\delta W_{real}(B)}{T_{res}} \leq 0$, we have

$$\int_i^f \frac{\mathrm{d}U_r(A)}{T} - \int_i^f \frac{\mathrm{d}U_{real}(B)}{T_{res}} \leq \int_i^f \frac{\delta Q_r(A)}{T} - \int_i^f \frac{\delta Q_{real}(B)}{T_{res}}.$$

Consequently, according to Equation (4), we can find

$$\int_i^f \frac{\delta Q_r(A)}{T} - \int_i^f \frac{\delta Q_{real}(B)}{T_{res}} \geq 0.$$

There are two results generated by Equation (4), but their conclusions are contrary. Which result should be selected? We need to eliminate a wrong answer from the next procedures.

When any work doesn't exist, we can gain $\int_i^f \frac{\delta W_r(A)}{T} - \int_i^f \frac{\delta W_{real}(B)}{T_{res}} = 0$. According to Equation (1), we have

$$\int_i^f \frac{\mathrm{d}U_r(A)}{T} - \int_i^f \frac{\mathrm{d}U_{real}(B)}{T_{res}} = \int_i^f \frac{\delta Q_r(A)}{T} - \int_i^f \frac{\delta Q_{real}(B)}{T_{res}}.$$

Therefore, on the basis of Equation (4), we can get

$$\int_i^f \frac{\delta Q_r(A)}{T} - \int_i^f \frac{\delta Q_{real}(B)}{T_{res}} \geq 0.$$

Furthermore,

$$\left|\int_i^f \frac{\delta Q_r(A)}{T} - \int_i^f \frac{\delta Q_{real}(B)}{T_{res}}\right| \geq \left|\int_i^f \frac{\delta W_r(A)}{T} - \int_i^f \frac{\delta W_{real}(B)}{T_{res}}\right|. \quad (6)$$

where, $|\ |$ expresses absolute value symbol of quantity. In the isothermal process, $\int_i^f \frac{\mathrm{d}U_r(A)}{T} - \int_i^f \frac{\mathrm{d}U_{real}(B)}{T_{res}} = 0$, we can gain

$$\int_i^f \frac{\delta Q_r(A)}{T} - \int_i^f \frac{\delta Q_{real}(B)}{T_{res}} + \int_i^f \frac{\delta W_r(A)}{T} - \int_i^f \frac{\delta W_{real}(B)}{T_{res}} = 0.$$

Accordingly, we can confirm $\int_i^f \frac{\delta W_r(A)}{T} - \int_i^f \frac{\delta W_{real}(B)}{T_{res}} \leq 0$.

The aforementioned results prove the Clausius inequality is right. These Equations (2)-(6) are all the results of nature option. The other methods proving the Clausius inequality see the references [14] [15].

4. Results and Discussion

4.1. Relation between the Reversible Paths and Its Realistic Paths in the Gases and Chemical Reactions

In a spontaneous or realistic process, we would assume [4]

$$Q_{real}(B) = Q_r(A) + Q_{pf}(B), \quad (7)$$

$$W_{real}(B) = W_r(A) + W_{pf}(B). \quad (8)$$

where, $Q_r(A)$ and $W_r(A)$ do not contain $Q_{pf}(B)$ and $W_{pf}(B)$. Here, $W_{pf}(B)$ can cause the temperature change.

According to the first law of thermodynamics, in a process, the following equations are given by $\Delta U_r(A) = Q_r(A) + W_r(A)$, $\Delta U_{real}(B) = Q_{real}(B) + W_{real}(B)$, and $\Delta U_r(A) = \Delta U_{real}(B)$. Where, $\Delta U_r(A)$ and $\Delta U_{real}(B)$ are the internal energy change in a reversible path (A) and its realistic path (B), respectively. Because $\Delta U_r(A) = \Delta U_{real}(B)$, we can get

$$Q_{pf}(B) = -W_{pf}(B) \quad (9)$$

Attentively, $W_r(A)$ and $W_{real}(B)$ can be calculated from p-V diagram for the gases (employing the gas equation of state or the state experiment datums). A reversible path and its irreversible path are distinction for the gases, otherwise, $W_{pf}(B)$ will be equal to zero.

In a reversible path (A) and its realistic path (B), the following equations have to be obeyed [5] [16], such as

$$Q_r(A) \geq Q_{real}(B), \quad (10)$$

$$W_r(A) \leq W_{real}(B), \quad (11)$$

$$Q_{pf}(B) = -W_{pf}(B) \leq 0. \quad (12)$$

where, the equality is for the identical reversible paths (if any work doesn't exist, the equality is also for the irreversible paths), the inequality is for other irrevers-

ible paths. So that, the reversible path (A) and its realistic path (B) are not arbitrary.

If the other work doesn't exist for a chemical reaction, in an isothermal and constant volume process, we have $\Delta U_{TV} = Q_V$. Where, ΔU_{TV} is the internal energy change, Q_V is the chemical reaction heat at the constant volume, they are all the state function. In an isothermal and constant pressure process, we have $\Delta U_{Tp} = \Delta H - p\Delta V$. Where, ΔU_{Tp} is the internal energy change, and ΔH is the chemical reaction heat at the constant pressure, they are all the state function. In the same temperature for a chemical reaction, we can find $\Delta U_{TV} = \Delta U_{Tp}$, so that, we have $Q_V = \Delta H - p\Delta V$, where, p is the constant pressure.

When the chemical reaction and other work all do not exist at the non-constant pressure, on the basis of Equations (3), (11), the gases in the closed system obey $-\int_i^f p\mathrm{d}V(A) \le -\int_i^f p\mathrm{d}V(B)$. Where, $W_r(A) = -\int_i^f p\mathrm{d}V(A)$, and $W_{real}(B) = -\int_i^f p\mathrm{d}V(B)$.

If the chemical reactions exist and any work does not exist in the constant pressure and isothermal process, according to Equations (2), (10), we have $\int_i^f T\mathrm{d}S(A) \ge \int_i^f T\mathrm{d}S(B)$. At the moment, even if any work does not exist, we still find $Q_{pf}(B) = -W_{pf}(B) \ne 0$. This result indicates us the internal friction resistance is existence namely that $W_{pf}(B) \ne 0$ for the chemical reactions in the irreversible path (B).

In the constant pressure and isothermal process for the unclosed system, if the chemical reaction exists and the other work does not exist, according to Equations (2), (10), we still obtain $\int_i^f T\mathrm{d}S(A) \ge \int_i^f T\mathrm{d}S(B)$. We know $-p\Delta V(A) = -p\Delta V(B)$, $W_r(A) = -p\Delta V(A)$, and $W_{real}(B) = -p\Delta V(A) + W_{pf}(B)$. On the basis of Equation (11), we have $W_{pf}(B) \ge 0$. According to Equations (2), (10), we can get

$$\begin{aligned} T\Delta S_g &= Q_r(A) - Q_{real}(B) = -Q_{pf}(B) = T\Delta S(A) - \Delta U + W_{real}(B) \\ &= T\Delta S(A) - \Delta U - p\Delta V(B) = T\Delta S(A) - \Delta H = -\Delta G \ge 0 \end{aligned}$$

thus, $T\Delta S_g \ge 0$ (where, T is the constant) or $\Delta G = Q_{pf}(B) \le 0$, which are criterions without the other work in the constant pressure and isothermal chemical reactions.

If the chemical reaction and other work all exist in the constant pressure and isothermal process, we have

$W_r(A) = \Delta U - Q_r(A) = \Delta U - T\Delta S(A) = W_{other}(A) - p\Delta V(A)$, where,

$W_r(A) = W_{other}(A) - p\Delta V(A)$. Because $\Delta H = \Delta U + p\Delta V$ and $\Delta G = \Delta H - T\Delta S$ (where, ΔG is free energy change. In the constant pressure and isothermal process, ΔG is the state function), the result is $W_{other}(A) = \Delta G$. In the realistic process, we can find $W_{real}(B) = W_{other}(B) - p\Delta V(B)$, therefore,

$W_{real}(B) = \Delta U - Q_{real}(B) = W_{other}(B) - p\Delta V(B)$, further,

$Q_{real}(B) = \Delta H - W_{other}(B)$. On the basis of Equations (2), (10), we can gain $T\Delta S_g = Q_r(A) - Q_{real}(B) = T\Delta S(A) - \Delta H + W_{other}(B) = W_{other}(B) - \Delta G \ge 0$, that is, $T\Delta S_g \ge 0$ (here, T is the constant), or $W_{other}(B) \ge \Delta G$ and

$W_{other}(B) \geq W_{other}(A)$, which are criteria when the other work exists in the constant pressure and isothermal chemical reactions (see Figure 1).

4.2. Maxwell Relations and Joule-Thomson Throttling Experiment

Maxwell [17] thought the thermodynamics functions obey the following relations, namely that

$$\left(\frac{\partial T}{\partial V}\right)_S = -\left(\frac{\partial p}{\partial S}\right)_V,$$

$$\left(\frac{\partial T}{\partial p}\right)_S = \left(\frac{\partial V}{\partial S}\right)_p,$$

$$\left(\frac{\partial S}{\partial V}\right)_T = \left(\frac{\partial p}{\partial T}\right)_V,$$

$$\left(\frac{\partial S}{\partial p}\right)_T = -\left(\frac{\partial V}{\partial T}\right)_p.$$

They are all obtained by commutation relations, but these commutation relations are not always correct. Moreover, the both sides (namely that, the left side and right side) per Maxwell equality correspond to the different processes, their results for the gases are no-confidence. Simultaneously, the Maxwell relations are also not right for the unclosed system. Therefore, the Maxwell relations are not right and disobey the Clausius inequality.

The formula $\mathrm{d}U = C_V \mathrm{d}T + \left[T\left(\frac{\partial p}{\partial T}\right)_V - p\right]\mathrm{d}V$ [1] is error, and it disobeys the Clausius inequality. The van der Waals gas equation of state does not obey the thereinbefore conclusions, furthermore, it is an approximate equation, but its availability values could not be denied.

The Joule-Thomson throttling experiment (the sketch sees Figure 2) [17] is an adiabatic process, so that, $Q = 0$, $\Delta U = W$. Thereby

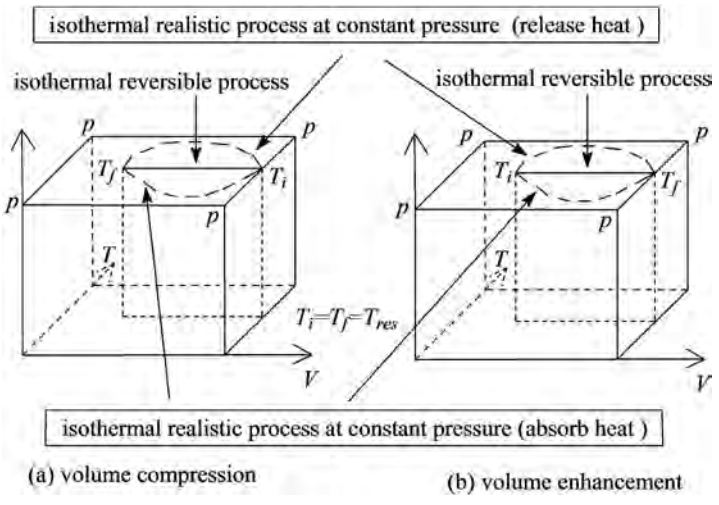

Figure 1. The unclosed system paths of chemical reactions in the constant pressure and isothermal process.

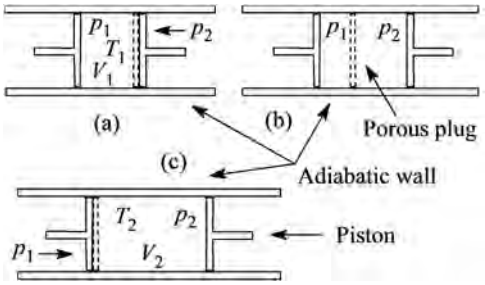

Figure 2. The Joule-Thomson throttling experiment. (a) is the initial state; (b) is the transition state; (c) is the final state.

$$W = -\sum\left(p_2 \mathrm{d}V_2 + p_1 \mathrm{d}V_1\right) = -p_2\left(V_2 - 0\right) - p_1\left(0 - V_1\right) = -p_2V_2 + p_1V_1 .$$

Because the other work does not exist, hence, $\Delta H = 0$ (where, ΔH is the enthalpy change). We know $\Delta U = C_V \Delta T$, thus, the temperature change is given by

$$\Delta T = \frac{-p_2V_2 + p_1V_1}{C_V} . \tag{13}$$

So that, the average value of Joule-Thomson coefficient μ_{JT} is approximately equal to

$$\mu_{JT} = \left(\frac{\partial T}{\partial p}\right)_H \approx \frac{\Delta T}{\Delta p} = \frac{-p_2V_2 + p_1V_1}{C_V\left(p_2 - p_1\right)} .$$

The Joule-Thomson throttling experiment is an irreversible process, thereof, μ_{JT} is not the state function. The temperature in the chamber 1 will raise since the work is done by surroundings. The temperature in the chamber 2 will fall since the gas does work to surroundings. Therefore, the formula (13) calculating the temperature change in the Joule-Thomson throttling experiment is an approximate equation.

4.3. Applying to the Earth Gravitational Field and Motional Body

In the gravitational field, $mg\Delta h$ is the gravitational potential energy change, m is the mass, g is the acceleration of gravity, Δh is the elevation change. In a process, the relations among the gravitational potential energy change, kinetic energy change, and internal energy change had been investigated [18] [19] [20]. Attentively, the motion path in the reversible process is the same as the realistic process. According to the conservation law of energy, we can get

$$\Delta U - Q - W = 0 , \tag{14}$$

$$\Delta U_r - Q_r + mg\Delta h + \Delta E_{kin} + \Delta E_{ele} + \int_i^f p\mathrm{d}V - W_b = 0 , \tag{15}$$

$$\Delta U_{real} - Q_{real} + mg\Delta h + \Delta E'_{kin} + \Delta E'_{ele} + \int_i^f p\mathrm{d}V - W_b = 0 . \tag{16}$$

where, p is the pressure between system and surroundings (it isn't internal pressure [21]). ΔE_{ele} and $\Delta E'_{ele}$ are the electrical energy change in a reversible and realistic process, respectively. ΔE_{kin} and $\Delta E'_{kin}$ are the kinetic energy change

in a reversible and realistic process respectively. Attentively, the positive or negative sign for the electrical energy, kinetic energy, and gravitational potential energy are all against the corresponding work. The kinetic energy and gravitational potential energy are called mechanical energy. For the motional body, W_b expresses the work done by the buoyancy or non-friction resistance. W_b does not belong to the mechanical work, electrical work, or friction work. It is obvious that the air buoyancy exists for the gravitational field in the irreversible process. W_b cannot cause the heat change directly, but it can influence the kinetic energy change. In a process, the absorbed heat is positive, the released heat is negative.

If the obtained energy including heat and work with the mechanical work could not be repeatedly calculated for the motional body, but they should be able to transform into the kinetic energy. For the closed gas, the mechanical work with the pressure-volume work is unable to be repeatedly calculated. For instance, the bullet and rocket could obtain the heat energy from the burned ammunition and fuel, but the obtained heat need to avoid repeating calculation with the mechanical work in Equations (15), (16) (see Figure 3). In the parachute, W_b has to be considered. In the pipeline system of fluid, the mechanical work and pressure-volume work have to be all considered.

Because $mg\Delta h$, ΔE_{kin}, ΔE_{ele}, and W_b all do not belong to the heat, therefore, they all belong to the work, we can gain

$$W_r = -mg\Delta h - \Delta E_{kin} - \Delta E_{ele} - \int_i^f p\mathrm{d}V + W_b, \tag{17}$$

$$W_{real} = -mg\Delta h - \Delta E'_{kin} - \Delta E'_{ele} - \int_i^f p\mathrm{d}V + W_b. \tag{18}$$

where, in a reversible process, $W_{other}(A) = -mg\Delta h - \Delta E_{kin} - \Delta E_{ele} + W_b$. In a realistic process, $W_{other}(B) = -mg\Delta h - \Delta E'_{kin} - \Delta E'_{ele} + W_b$.

The conservation law of mechanical energy disobeys on the earth system except the vacuum state. The equation of conservation law of mechanical energy is given by $mg\Delta h + \Delta E_{kin} = 0$. For a bulk condensed matter in the gravitational

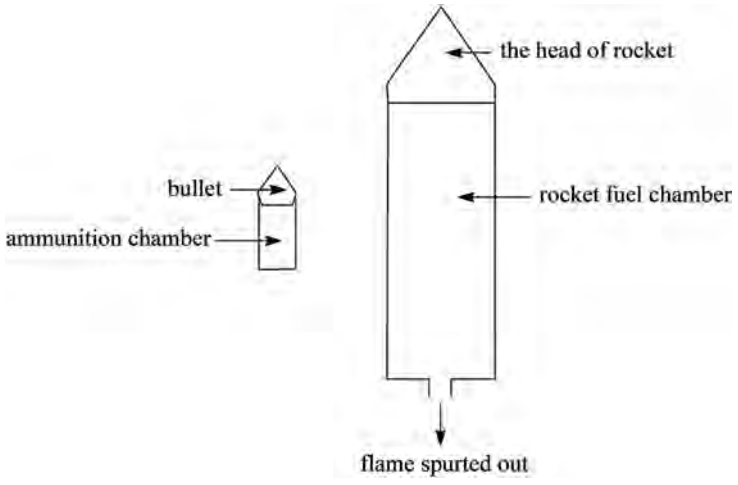

Figure 3. The processes of heat energy obtained from the burned ammunition and fuel in the bullet and rocket.

field of earth, if the influence of heat, internal energy change, pressure-volume work, electrical energy change, and W_b can be neglected, on the basis of Equation (11), we have $mg\Delta h + \Delta E_{kin} \approx 0$, W_{real} will be no less than zero, that is, $W_{real} = -mg\Delta h - \Delta E'_{kin} \geq 0$ or $mg\Delta h + \Delta E'_{kin} \leq 0$. If the bulk condensed matters are still namely that $\Delta E'_{kin} = 0$, we can obtain $\Delta h \leq 0$, namely that the bulk condensed matters such as the solid ball and rain will fall on earth's surface. The process obeys Equation (3) too.

For the particles and gases, the pressure-volume work, electrical energy change, and W_b can be all neglected in the unclosed earth atmosphere system. In altitudes, the temperature is low and the internal energy change will decrease. If the heat effect is not considered, or the process absorbs the heat, W_r and W_{real} will become negative, so that, $W_{real} = -mg\Delta h - \Delta E'_{kin} \leq 0$ or $mg\Delta h + \Delta E'_{kin} \geq 0$. If the particles are motionless namely that $\Delta E'_{kin} = 0$, we find $\Delta h \geq 0$ (namely that, the particles will raise on the open earth system), but the raising height will be limited according to Equation (3), where, T_{res} is less than T in the process.

In the wind, the friction resistance is generally small, therefore, W_r is approximately equal to W_{real}. According to Equation (3), if W_r and W_{real} are negative, the wind can easily spontaneously blow from low temperature to high temperature on the same altitude (if $\Delta h = 0$, $\Delta E'_{kin} \geq 0$). In this process, if the internal energy change keeps constant, the absorbed heat mostly converts into the work. In the heat wave, if W_r and W_{real} will easily become into positive, the heat wave will blow from high temperature to low temperature on the same altitude (but $\Delta E'_{kin} \leq 0$), the motional distances will be finite.

If the temperature varies little for the heated He(II) superfluid, the internal energy change will be very small. Because W_r and W_{real} are easily affected by the heat, W_r and W_{real} will all be negative value. Consequently, on the basis of Equation (3), it is easily the He(II) superfluid spontaneously flow from low temperature to high temperature, then, the heat will mostly convert into the kinetic energy change.

If the body could raise, the following equation will be obeyed besides Equation (3), and it is given by

$$mg\Delta h = Q_{real} - \Delta U_{real} - \Delta E'_{kin} - \Delta E'_{ele} - \int_i^f p\mathrm{d}V + W_b \geq 0.$$

5. Conclusions

The Clausius inequality should be derived from Equation (4), the Carnot theorem can be proven by Kelvin and Clausius formulations of the second law of thermodynamics which are inconvenient compared with Equations (2)-(6). The Carnot theorem can be proven by the Clausius inequality.

In the equilibrium and changeless state, ΔU, Q, W, ΔS, ΔS_W, ΔS_U, ΔS_g, $(\Delta S_W)_g$, and $(\Delta S_U)_g$ are all equal to zero. In a reversible process, ΔS_g, $(\Delta S_W)_g$, and $(\Delta S_U)_g$ are all equal to zero, but ΔU, Q_r, W_r, ΔS, ΔS_W, and ΔS_U could not be all equal to zero simultaneously. Obviously, the change of $(\Delta S_U)_g$ will cause the temperature change.

In the isothermal process, Equation (4) is not the criterion. If any work doesn't exist, Equation (3) is not the criterion. It is not surprising the He(II) superfluid, particles, and gases disobey the conservation law of mechanical energy. The conservation law of mechanical energy is a bad conservation law. Equations (1)-(5), (10), (11) should be able to apply to a single particle or big object. The pressure-volume work of gases could be generated easily. In any case for a particle or big object, the friction work is all positive value, and the friction heat will be negative. The afore-mentioned function such as ΔS_W and ΔS_U are all the state function for the ideal gas in a reversible process. For the vacuum state, any irreversible process does not exist for the motional body.

For the whole unclosed system, the expansion work for the chemical reactions in the constant pressure and isothermal process is not equal to $-\int_i^f p\mathrm{d}V$, but it is equal to $-p\Delta V$ in fact. The application scope of thermodynamics could not refuse the gravitational field and mechanical motion.

Altogether, for the organisms, all the processes including the biological chemical reactions obey the Clausius inequality. It is above comprehension that the organisms disobey the second law of thermodynamics. The sign of surroundings entropy is opposite to the system entropy, and the surroundings entropy is equal to negative value of the entropy flow ($\int_i^f \frac{\delta Q_{real}(B)}{T_{res}}$). Therefore, the system entropy may be less than zero sometime in the isolated system, but the entropy generation has to be no less than zero in the isolated system. The principle of entropy increase is not always right in the isolated system and non-isolated system.

The organisms are a type of heat engine, but they are controlled by the biological chemical reactions, DNA, and RNA etc. (not mechanism).

If assuming that the surroundings entropy or entropy flow are equal to zero, the entropy generation has to be equal to the entropy change. For the isolated system in a realistic path (B), the entropy change will become the entropy generation which is the non-state function except when $Q_{real}(B)=0$. So that, the principle of entropy increase is an error for many cases. A reversible path (A) may contain a few processes in its realistic path (B), and a realistic path (B) may contain a few processes in its reversible path (A) too.

Conflicts of Interest

The author declares no conflicts of interest regarding the publication of this paper.

References

[1] Borgnakke, C. and Sonntag, R.E. (2014) Fundamentals of Thermodynamics. 8th Edition, John Wiley & Sons Singapore Pte Ltd., Singapore.

[2] Callen, H.B. (1985) Thermodynamics and an Introduction to Thermostatics. 2nd Edition, John Wiley, New York.

[3] Jacobs, P. (2013) Thermodynamics. Imperial College Press, London.

[4] Jin, C. (2019) *Theoretical Physics*, **4**, 117-130. https://doi.org/10.22606/tp.2019.43001

[5] Jin, C. (2017) *International Journal of Physical Sciences*, **12**, 205-210. https://doi.org/10.5897/IJPS2017.4624

[6] Atkins, P. and Paula, J. (2014) Atkins' Physical Chemistry. 10th Edition, Oxford University Press, Oxford.

[7] Muschik, W. (2014) *Journal of Non-Equilibrium Thermodynamics*, **39**, 113-121. https://doi.org/10.1515/jnet-2014-0016

[8] Sandler, S.I. and Woodcock, L.V. (2010) *Journal of Chemical & Engineering Data*, **55**, 4485-4490. https://doi.org/10.1021/je1006828

[9] Zhang, Z., Drapaca, C., Zhang, Z., Zhang, S., Sun, S. and Liu, H. (2018) *Entropy*, **20**, 14. https://doi.org/10.3390/e20010014

[10] Dincer, I. and Cengel, Y.A. (2001) *Entropy*, **3**, 116-149. https://doi.org/10.3390/e3030116

[11] Lucia, U. (2015) *Physica A*: *Statistical Mechanics and Its Applications*, **419**, 115-121. https://doi.org/10.1016/j.physa.2014.10.040

[12] Grazzini, G., Borchiellini, R. and Lucia, U. (2013) *Journal of Non-Equilibrium Thermodynamics*, **38**, 259-271. https://doi.org/10.1515/jnetdy-2013-0008

[13] Rossini, F.D. and Frandsen, M. (1932) *Bureau of Standards Journal of Research*, **9**, 733-747. https://doi.org/10.6028/jres.009.053

[14] Lee, S., Lee, K. and Lee, J. (2015) *Journal of Chemical Education*, **9**, 771-773. https://doi.org/10.1021/ed5007822

[15] Nieto, R., González, C., Jiménez, Á., López, I. and Rodríguez, J. (2011) *Journal of Chemical Education*, **88**, 597-601. https://doi.org/10.1021/ed100798p

[16] Jin, C. (2016) The Inequality of Work Derived from Clausius Inequality and Carnot Theorem. 2016 *International Conference on Energy, Power and Electrical Engineering*, Shenzhen, 30-31 October 2016, 315-317. https://doi.org/10.2991/epee-16.2016.71

[17] Levine, I.N. (2012) Physical Chemistry. 6th Edition, McGraw-Hill Education (Asia) and Tsinghua University Press Limited, Beijing.

[18] Gislason, E.A. and Craig, N.C. (2013) *Journal of Chemical Education*, **90**, 584-590. https://doi.org/10.1021/ed300570u

[19] DeVoe, H. (2013) *Journal of Chemical Education*, **90**, 591-597. https://doi.org/10.1021/ed300797j

[20] Abreu, R. and Guerra, V. (2012) *American Journal of Physics*, **80**, 627-637. https://doi.org/10.1119/1.3698160

[21] Marcus, Y. (2013) *Chemical Reviews*, **113**, 6536-6551. https://doi.org/10.1021/cr3004423

Scientific Research Publishing

Journal of Modern Physics, 2020, 11, 1589-1597
https://www.scirp.org/journal/jmp
ISSN Online: 2153-120X
ISSN Print: 2153-1196

Dark Future for Dark Matter

Donald H. Eckhardt[1], José Luis Garrido Pestaña[2*]

[1]Canterbury, NH, USA
[2]Departamento de Física, Universidad de Jaén, Campus Las Lagunillas, Jaén, España
Email: *jlg@ujaen.es

How to cite this paper: Eckhardt, D.H. and Garrido Pestaña, J.L. (2020) Dark Future for Dark Matter. *Journal of Modern Physics*, **11**, 1589-1597.
https://doi.org/10.4236/jmp.2020.1110099

Received: September 2, 2020
Accepted: October 17, 2020
Published: October 20, 2020

Abstract

The prevailing cosmological constant and cold dark matter (ΛCDM) cosmic concordance model accounts for the radial expansion of the universe after the Big Bang. The model appears to be authoritative because it is based on the Einstein gravitational field equation. However, a thorough scrutiny of the underlying theory calls into question the suitability of the field equation, which states that the Einstein tensor $\boldsymbol{G}_{\mu\nu}$ is a constant multiple of the stress-energy tensor $\boldsymbol{T}_{\mu\nu}$ when they both are evaluated at the same 4D space-time point: $\boldsymbol{G}_{\mu\nu} = 8\pi k\boldsymbol{T}_{\mu\nu}$, where k is the gravitational constant. Notwithstanding its venerable provenance, this equation is incorrect unless the cosmic pressure is $p = 0$; but then all that remains of the Einstein equation is the Poisson equation which models the Newtonian gravity field. This shortcoming is not resolved by adding the cosmological constant term to the field equation, $\boldsymbol{G}_{\mu\nu} + \Lambda\boldsymbol{g}_{\mu\nu} = 8\pi k\boldsymbol{T}_{\mu\nu}$, as in the ΛCDM model, because then $p = \Lambda$, so the pressure is a universal constant, not a variable. Numerous studies support the concept of a linearly expanding universe in which gravitational forces and accelerations are negligible because the baryonic mass density of the universe is far below its critical density. We show that such a coasting universe model agrees with SNe Ia luminosity vs. redshift distances just as well or even better than the ΛCDM model, and that it does so without having to invoke dark matter or dark energy. Occam's razor favors a coasting universe over the ΛCDM model.

Keywords

Classical General Relativity, General Relativity and Gravitation: Fundamental Problems and General Formalism, Fundamental Aspects of Astrophysics, Relativity and Gravitation, Dark Energy, Mathematical and Relativistic Aspects of Cosmology

1. Introduction

The ΛCDM model is used to represent the expanding universe for the interpretation 1) of type Ia supernovae (SNe Ia) brightness and redshift data, and 2), of measurements of anisotropies in the cosmic microwave background (CMB) spectrum of the early universe. The model conjectures the existence of dark matter and dark energy—a lot of both. With a felicitous balance of the two, an ostensibly credible model is derived. However, a ΛCDM model has drawbacks. Firstly, the existence of dark matter is an unverified hypothesis.[1] There have been numerous experiments dedicated to finding dark matter here on Earth, in underground experiments [2] [3] and satellite detectors [4], as well as in the Large Hadron Collider [5]. Yet, there has been no unambiguous dark matter detection [6], which, by induction [7], is evidence of absence. Moreover, aside from the ΛCDM model, there is no theoretical call for dark energy; nor has there even been an observational hint of its existence. Kang *et al.* [8] have recently challenged a key premise in the derivation of the ΛCDM model, and by addressing the problem with a different approach, we show that the model is utterly untenable. We expand, revise and interpret the Einstein field equation to find a simple viable alternative to the ΛCDM model.

2. Einstein Field Equation

We use the standard nomenclature of GR (e.g., see Kenyon [9]), except k is the Newtonian gravitational constant and $c=1$ is the speed of light. The Einstein field equation is

$$\boldsymbol{G}_{\mu\nu} = 8\pi k \boldsymbol{T}_{\mu\nu}, \tag{1}$$

where $\boldsymbol{G}_{\mu\nu}$ is the Einstein tensor and $\boldsymbol{T}_{\mu\nu}$ is the stress-energy tensor of a perfect fluid,

$$\boldsymbol{T}_{\mu\nu} = \{\{\rho, p, p, p\}\}, \tag{2}$$

where $\{\{\cdots\}\} \equiv \mathrm{diag}[\cdots]$, ρ is the mass density, and p is the pressure (energy density).

The line element, $\mathrm{d}s^2 = \boldsymbol{g}_{\mu\nu}\mathrm{d}x^{\mu}\mathrm{d}x^{\nu}$, reduces for the weak isotropic cosmic field, to ([10], Eq. 10.84)

$$\mathrm{d}s^2 = (1+2\phi)\mathrm{d}t^2 - (1-2\phi)\delta_{ij}\mathrm{d}x^i\mathrm{d}x^j, \tag{3}$$

According to Einstein ([11], p. 84), $\boldsymbol{G}_{\mu\nu}$ "must be a differential tensor in the $\boldsymbol{g}_{\mu\nu}$ that is completely determined by the following three conditions:

1) It may contain no differential coefficients of the $\boldsymbol{g}_{\mu\nu}$ higher than the second.

[1]Dark matter had a sullied reputation from the nineteenth century, when astronomers searched fruitlessly for another sort of invisible matter—an intramercurial planet, Vulcan [1], that was thought to be responsible for otherwise unexplainable orbital perturbations of Mercury. As it turned out, what had been missing was not matter, but an authoritative theory: GR. So, is it now missing matter, or missing theory?

2) It must be linear in these second differential coefficients.

3) Its divergence must vanish identically."

For the nonce, let ∂ represent any partial derivative operator ∂_{x^i}, and let g represent any component of $\boldsymbol{g}_{\mu\nu}$. According to the first two conditions, each component of $\boldsymbol{G}_{\mu\nu}$ has the form $\partial g \partial g \sim \partial\phi\partial\phi$ or $g\partial^2 g \sim (1-2\phi)\partial^2\phi$ (… or zero). Then, to the first power in ϕ, the only non-zero form of a $\boldsymbol{G}_{\mu\nu}$ component is $\partial^2\phi$.

With $G_{00} = 2\partial^2\phi$ and $T_{00} = \rho$, Equation (1) yields the Poisson equation. If any other $\boldsymbol{G}_{\mu\nu}$ component, say G_{11}, is non-zero, then $G_{11} \sim \partial^2\phi = G_{00}/2$; therefore $T_{11} \sim \rho$, and $G_{11} \neq 0$ implies that $p \sim \rho$. With such an equation of state, the fluid is relativistic, which is to say that the characteristic thermal speed of the fluid is close to c, which it generally is not. The only viable alternative is to set G_{11} and all other terms of $\boldsymbol{G}_{\mu\nu}$ except G_{00} equal to zero. But this requires that $p = 0$, which is not generally true. We overcome this dilemma by adding $8\pi k\boldsymbol{g}_{\mu\nu}p$ to the RHS of Equation (1). Then both sides of

$$\boldsymbol{G}_{\mu\nu} = 8\pi k\left[\boldsymbol{T}_{\mu\nu} + \boldsymbol{g}_{\mu\nu}p\right] \tag{4}$$

remain generally covariant and, with this essential correction, Equation (4) becomes

$$\boldsymbol{G}_{\mu\nu} = \left\{\left\{2\partial^2\phi, 0, 0, 0\right\}\right\} = 8\pi k\left\{\left\{\varrho, 0, 0, 0\right\}\right\}, \tag{5}$$

where $\varrho = \rho + p$. This is the full Poisson equation,

$$\partial^2\phi = 4\pi k\varrho, \tag{6}$$

which applies in all coordinate systems. It notably takes into account the gravitational charge equivalence of mass density ρ and energy density p [12];[2] adapted to this nicety, ϕ is the Newtonian potential.

In general, the density does not need to be uniform. We can approximate the mass of the universe with an assemblage of point masses and consider just one point mass at a time. Then the Poisson equation for the potential due to one point mass M is $\partial^2\phi = kM$, and the Einstein field equation is a linear superposiition of Poisson equations.

3. The Expanding Universe

For a universe with vanishingly small ϱ, the line element 3 reduces to

$$\mathrm{d}s^2 = \mathrm{d}t^2 - \delta_{ij}\mathrm{d}x^i\mathrm{d}x^j. \tag{7}$$

Then $\boldsymbol{G}_{\mu\nu} = 0$ because this metric is independent of ϕ; GR obviously does not apply. But what if this nearly empty universe expands according to Hubble's law? Then

$$\mathrm{d}s^2 = \mathrm{d}t^2 - \mathrm{e}^{2H_0 t}\delta_{ij}\mathrm{d}x^i\mathrm{d}x^j, \tag{8}$$

[2]Using an arbitrary equation of state for a perfect fluid, Peebles ([11], Eq. 4.21) generalizes the RHS of Equation (6) to $4\pi k\varrho \to 4\pi k(\rho + 3p)$ instead of $4\pi k\varrho \to 4\pi k(\rho + p)$.

so that $\boldsymbol{G}_{\mu\nu} = 3H_0^2 \boldsymbol{g}_{\mu\nu}$, assuming that GR does apply.[3] The Einstein field equation is $3H_0^2 \boldsymbol{g}_{\mu\nu} = 0$, so $H_0 = 0$. Clearly GR does not apply in this case either. However, we can force GR to apply by replacing the Einstein tensor $\boldsymbol{G}_{\mu\nu}$ with its Lovelock [15] form $\boldsymbol{G}_{\mu\nu} \to \boldsymbol{G}_{\mu\nu} + b\boldsymbol{g}_{\mu\nu}$. Then the field equation is

$$\left(3H_0^2 + b\right)\boldsymbol{g}_{\mu\nu} = 0. \tag{9}$$

But b is merely an invention that allows us to broaden the scope of the field equation by allowing for Hubble expansion; it has no significance of its own. In fact, the Hubble expansion is real, but it is independent of GR.

Refashioned to try to accommodate Hubble expansion, Equation (5) becomes

$$\boldsymbol{G}_{\mu\nu} + b\boldsymbol{g}_{\mu\nu} = \left\{\left\{2\partial^2\phi, 0, 0, 0\right\}\right\} + \Lambda\boldsymbol{g}_{\mu\nu} = 8\pi k\left\{\left\{\varrho, 0, 0, 0\right\}\right\}, \tag{10}$$

where $\Lambda = 3H_0^2 + b$, which is zero according to Equation (9). There is no real change from Equation (5), but we use this form of the equation in Section 5, where Λ—there designated as the cosmological constant—is regarded as a proxy for dark energy.

4. The Coasting Universe

Evidence for the existence of dark matter is not at all conclusive. It is not needed to explain the flat rotation curves of spiral galaxies nor the CMB simulations. Concerning the rotation curves, alternate explanations have been published by Milgrom [16] [17], Brownstein and Moffat [18], Mannheim and O'Brien [19], Verlinde [20], ourselves [21], and others. As far as the CMB data are concerned, they show a compatibility with the ΛCDM model, but not that an equivalent compatibility is impossible for other models [22] [23] [24] [25]. Therefore if there is no dark matter $\varrho \approx \rho_b$, the density of baryonic matter, whose value [26], $\rho_b \approx 3.6\times10^{-28}\,\mathrm{kg\cdot m^{-3}}$, is two orders of magnitude smaller than the critical density, $\rho_c = 3H_0^2/8\pi k$, so the gravitational forces and accelerations are negligible. Kolb [27] proposed such a linearly coasting universe, which Sethi *et al.* [28] found to agree "surprisingly" well with SNe Ia observations. Subsequently many others [29]-[58] have confirmed the validity of a coasting fit, which we now corroborate. The coasting universe expands without acceleration,

$$a(t) = 1 + H_0 t. \tag{11}$$

For redshift z, the distance between a source (then) and observer at $t = 0$ (now) is

$$r = \left(c/H_0\right)\ln\left(1+z\right). \tag{12}$$

The distance modulus depends on the area, $4\pi f^2$, of the wavefront at $t = 0$. For an open universe [59],

[3]We derive this expression using L. Parker's Mathematica [13] notebook, *Curvature and the Einstein Equation* [14], with only the following principal modifications:

```
coord ={t, x, y, z};
g11 = −Exp [2 H0 t];
metric = {{1, 0, 0, 0}, {0, g11, 0, 0}, {0, 0, g11, 0}, {0, 0, 0, g11}}
```

$$f = \frac{c}{H_0}\sinh\left[\ln(1+z)\right] = \frac{c}{2H_0}\left[1+z-\frac{1}{1+z}\right] \tag{13}$$

is the luminosity distance.

In Figure 1, we plot a set of high-confidence Union 2.1 data [60]. We used these data to estimate $H_0 = 68.22 \pm 1.00\ \text{km·s}^{-1}\text{·Mpc}^{-1}$ ($\chi^2 = 576.45$). It is the only parameter needed for calculating the superposed coasting curve. Because the number of degrees of freedom $\nu = 579$ is large, the variable $\xi = \left(\chi^2 - \nu\right)/\sqrt{2\nu}$ is approximately normally distributed with unit variance. For our solution, $\xi = -0.075$ which, being a small value, substantiates the Union 2.1 observational error estimates as well as the coasting fit to the data.[4] According to our H_0, the age of the coasting universe is the Hubble time, $H_0^{-1} = 14.33 \pm 0.21\ \text{Gyr}$. This is gratifyingly close to the 14.46 ± 0.31 Gyr age of HD 140283, the oldest star for which a reliable age has been determined [62].

5. The ΛCDM Model

Equating the $\mu\nu = 00$ element pairs on both sides of Equation (10) gives

$$2\partial^2\phi + \Lambda = 8\pi k\varrho, \tag{14}$$

whereas equating any of the $\mu\nu = 11, 22$ or 33 element pairs gives

$$\Lambda = 0. \tag{15}$$

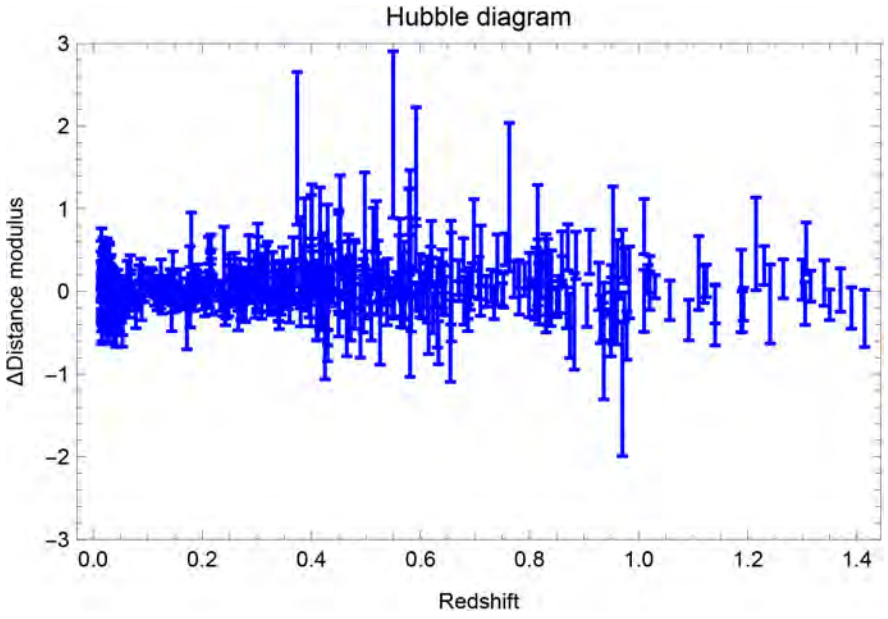

Figure 1. Hubble diagram residuals for the linearly coasting model that best fits the Union 2.1 compilation set of 580 SNe Ia data points.

[4]With a three parameter (H_0, ρ, Λ) ΛCDM fit to the same Union 2.1 data, the Planck team [61] estimates $H_0 = 70\ \text{km·s}^{-1}\text{·Mpc}^{-1}$, $\chi^2 = 545.11$, and $\xi = -0.939$, which we view *per se* as reasonable because the magnitude of ξ, although larger than ours, is less than one standard deviation. (A smaller χ^2 is not necessarily better in a χ^2 test: the best fit occurs when $\chi^2 = \nu$.) The qualities of the SNe Ia fits (ours and the Planck team's) are commensurate, but the team's ΛCDM model depends on the existence of an untenable fiction: dark energy.

The ΛCDM model is based on Equation (14) (but while also implicitly ignoring Equation (15)). The first integral of Equation (14) is

$$2\frac{\mathrm{d}\phi}{\mathrm{d}r}=\frac{\left(8\pi k\varrho-\Lambda\right)r}{3}, \tag{16}$$

which, by Newton's second law of motion, is

$$\frac{\mathrm{d}^2r}{\mathrm{d}t^2}=\frac{r}{6}\left(\Lambda-8\pi k\varrho\right). \tag{17}$$

With this choice, the ΛCDM scale factor for an expanding universe decelerates at first when $8\pi k\varrho>\Lambda$, then later accelerates after $\Lambda>8\pi k\varrho$; the orthodox ΛCDM model does not expand at the same rate as the well substantiated linearly coasting universe that are discussed in Section 4. There is no way of formulating a linearly coasting universe with the ΛCDM model, so purported ΛCDM scale accelerations [60] [63]-[68] are then merely expected artifacts of the Equation (17) procrustean template. Anyway, according to Equation (9) of Section 3, and to the conventionally ignored Equation (15), the cosmological constant must be zero: the ΛCDM model should be rejected because it does not expand at all.

6. Conclusions

GR can be reconciled with a static universe by starting with the Einstein field equation (Equation (1)) if $p=0$, or with the modified field equation (Equation (4)) if $p\geq 0$. GR can also be reconciled with a uniformly expanding universe by replacing the Einstein tensor with its Lovelock form $\boldsymbol{G}_{\mu\nu}\to\boldsymbol{G}_{\mu\nu}+b\boldsymbol{g}_{\mu\nu}$. GR then turns out to be in full accord with the linear coasting universe determined from the collation of type Ia supernovae (SNe Ia) brightness and redshift data—without recourse to the existence of dark matter or dark energy.

The ΛCDM model requires the existence of vast quantities of (attractive) dark matter and (repulsive) dark energy. They are the sources of fanciful opposing forces that mostly cancel each other out. We have shown why this model must be wrong: according to Equation (15), $\Lambda=0$. There can be no dark energy in the context of the ΛCDM approach, so this broadly accepted model is incorrect. Whereas dark energy is implausible and unnecessary, dark matter is not implausible and its need is unresolved. We recommend a linearly coasting universe—one that is consistent both with GR and with SNe Ia observations—as a viable ΛCDM alternative.

Conflicts of Interest

The authors declare no conflicts of interest regarding the publication of this paper.

References

[1] Baum, R. and Sheehan, W. (1997) Search of Planet Vulcan. Plenum Press, New York. https://doi.org/10.1007/978-1-4899-6100-6

[2] Aprile, R., *et al.* (2018) *Physical Review Letters*, **121**, Article ID: 111302.

https://doi.org/10.1103/PhysRevLett.121.111302

[3] Agnes, P., *et al.* (2018) *Physical Review Letters*, **121**, Article ID: 081307. https://doi.org/10.1103/PhysRevLett.121.081307

[4] Albert, A., *et al.* (2017) *The Astrophysical Journal*, **834**, 110. https://doi.org/10.3847/1538-4357/834/2/110

[5] Kahlhoefer, F. (2017) *International Journal of Modern Physics A*, **32**, Article ID: 1730006. https://doi.org/10.1142/S0217751X1730006X

[6] Hoof, S., Geringer-Sameth, A. and Trotta, R. (2020) *Journal of Cosmology and Astroparticle Physics*, No. 2, 012. https://doi.org/10.1088/1475-7516/2020/02/012

[7] Hales, S.D. (2005) *Think*, **4**, 109. https://doi.org/10.1017/S1477175600001287

[8] Kang, Y., Lee, Y.-W., Kim, Y.-L., Chung, C. and Ree, C.H. (2020) *The Astrophysical Journal*, **889**, 8. https://doi.org/10.3847/1538-4357/ab5afc

[9] Kenyon, I.R. (1990) General Relativity. Oxford University Press, Oxford.

[10] Peebles, P.J.E. (1993) Principles of Physical Cosmology. Princeton University Press, Princeton.

[11] Einstein, A. (1923) The Meaning of Relativity. Princeton University Press, Princeton.

[12] Genova, A., *et al.* (2018) *Nature Communications*, **9**, 289. https://doi.org/10.1038/s41467-017-02558-1

[13] Wolfram, S. (1999) The Mathematica Book. Cambridge University Press, Cambridge.

[14] Hartle, J.B. (2002) Gravity: An Introduction to Einstein's General Relativity. Addison-Wesley Pub. Co., Boston.

[15] Lovelock, D.J. (1971) *Journal of Mathematical Physics*, **12**, 498. https://doi.org/10.1063/1.1665613

[16] Milgrom, M. (1983) *The Astrophysical Journal*, **270**, 365. https://doi.org/10.1086/161130

[17] Milgrom, M. (1983) *The Astrophysical Journal*, **270**, 371. https://doi.org/10.1086/161131

[18] Brownstein, J.R. and Moffat, J.W. (2006) *The Astrophysical Journal*, **636**, 721. https://doi.org/10.1086/498208

[19] Mannheim, P.D. and O'Brien, J.G. (2011) *Physical Review Letters*, **106**, Article ID: 121101. https://doi.org/10.1103/PhysRevLett.106.121101

[20] Verlinde, E.P. (2017) *SciPost Physics*, **2**, 016. https://doi.org/10.21468/SciPostPhys.2.3.016

[21] Pestaña, J.L.G. and Eckhardt, D.H. (2011) *The Astrophysical Journal Letters*, **741**, L31. https://doi.org/10.1088/2041-8205/741/2/L31

[22] McGaugh, S. (1999) *The Astrophysical Journal Letters*, **523**, L99. https://doi.org/10.1086/312274

[23] McGaugh, S. (2000) *The Astrophysical Journal Letters*, **541**, L33. https://doi.org/10.1086/312902

[24] McGaugh, S. (2004) *The Astrophysical Journal*, **611**, 26. https://doi.org/10.1086/421895

[25] Angus, G. and Diaferio, A. (2011) *MNRAS*, **417**, 941. https://doi.org/10.1111/j.1365-2966.2011.19321.x

[26] Bahcall, N., Ostriker, J.P., Perlmutter, S. and Steinhardt, P.J. (1999) *Science*, **284**,

1481. https://doi.org/10.1126/science.284.5419.1481

[27] Kolb, E.W. (1989) *The Astrophysical Journal*, **344**, 543. https://doi.org/10.1086/167825

[28] Sethi, G., Dev, A. and Jain, D. (2005) *Physics Letters B*, **624**, 135. https://doi.org/10.1016/j.physletb.2005.08.005

[29] John, M.V. and Narlikar, J.V. (2002) *Physical Review D*, **65**, Article ID: 043506. https://doi.org/10.1103/PhysRevD.65.043506

[30] Dev, A., *et al.* (2002) *Physics Letters B*, **548**, 12. https://doi.org/10.1016/S0370-2693(02)02814-9

[31] John, M.V. (2005) *The Astrophysical Journal*, **630**, 667. https://doi.org/10.1086/432111

[32] Zhu, Z.-H., *et al.* (2008) *Astronomy & Astrophysics*, **483**, 15. https://doi.org/10.1051/0004-6361:20077797

[33] Eckhardt, D.H., Pestaña, J.L.G. and Fischbach, E. (2010) *New Astronomy*, **15**, 175. https://doi.org/10.1016/j.newast.2009.07.005

[34] Bilicki, M. and Seikel, M. (2012) *Monthly Notices of the Royal Astronomical Society*, **425**, 1664. https://doi.org/10.1111/j.1365-2966.2012.21575.x

[35] Melia, F. and Shevchuk, A.S.H. (2012) *Monthly Notices of the Royal Astronomical Society*, **419**, 2579. https://doi.org/10.1111/j.1365-2966.2011.19906.x

[36] Mitra, M. (2014) *Monthly Notices of the Royal Astronomical Society*, **442**, 382. https://doi.org/10.1093/mnras/stu859

[37] López-Corredoira, M. (2014) *The Astrophysical Journal*, **781**, 96. https://doi.org/10.1088/0004-637X/781/2/96

[38] Melia, F. (2014) *Astronomy & Astrophysics*, **561**, A80. https://doi.org/10.1051/0004-6361/201322285

[39] Melia, F. and McClintock, T.M. (2015) *The Astronomical Journal*, **150**, 119. https://doi.org/10.1088/0004-6256/150/4/119

[40] Shafer, D.L. (2015) *Physical Review D*, **91**, Article ID: 103516. https://doi.org/10.1103/PhysRevD.91.103516

[41] Singh, P. and Lohiya, D. (2015) *Journal of Cosmology and Astroparticle Physics*, **5**, 061. https://doi.org/10.1088/1475-7516/2015/05/061

[42] Wei, J.-J., Wu, X.F. and Melia, F. (2015) *The Astronomical Journal*, **149**, 165. https://doi.org/10.1088/0004-6256/149/5/165

[43] Lopez-Corredoira, M., *et al.* (2016) *International Journal of Modern Physics D*, **25**, Article ID: 1650060. https://doi.org/10.1142/S0218271816500607

[44] Melia, F. (2016) *Proceedings of the Royal Society A*, **472**, Article ID: 20150765. https://doi.org/10.1098/rspa.2015.0765

[45] Melia, F. (2016) *Monthly Notices of the Royal Astronomical Society*, **463**, L61. https://doi.org/10.1093/mnrasl/slw157

[46] Nielsen, J.T., Guffanti, A. and Sarkar, S. (2016) *Scientific Reports*, **6**, Article No. 35596. https://doi.org/10.1038/srep35596

[47] Tutusaus, I., *et al.* (2016) *Physical Review D*, **94**, Article ID: 103511. https://doi.org/10.1103/PhysRevD.94.103511

[48] Wei, J.-J., Wu, X.F. and Melia, F. (2016) *Monthly Notices of the Royal Astronomical Society*, **463**, 1144. https://doi.org/10.1093/mnras/stw2057

[49] Zeng, H., Melia, F. and Zhang, L. (2016) *Monthly Notices of the Royal Astronomi-*

cal Society, **462**, 3094. https://doi.org/10.1093/mnras/stw1817

[50] Tutusaus, I., *et al.* (2017) *Astronomy & Astrophysics*, **602**, A73. https://doi.org/10.1051/0004-6361/201630289

[51] Melia, F. (2017) *Monthly Notices of the Royal Astronomical Society*, **464**, 1966. https://doi.org/10.1093/mnras/stw2493

[52] Melia, F. and López-Corredoira, M. (2017) *International Journal of Modern Physics D*, **26**, Article ID: 1750055. https://doi.org/10.1142/S0218271817500559

[53] Wei, J.-J., Melia, F. and Wu, X. (2017) *The Astrophysical Journal*, **835**, 270. https://doi.org/10.3847/1538-4357/835/2/270

[54] Leaf, K. and Melia, F. (2018) *Monthly Notices of the Royal Astronomical Society*, **474**, 4507. https://doi.org/10.1093/mnras/stx3109

[55] Yennapureddy, M.K. and Melia, F. (2018) *Physics of the Dark Universe*, **20**, 65. https://doi.org/10.1016/j.dark.2018.03.003

[56] Melia, F., *et al.* (2018) *Europhysics Letters*, **123**, 59002. https://doi.org/10.1209/0295-5075/123/59002

[57] Melia, F. (2019) *Monthly Notices of the Royal Astronomical Society*, **489**, 517. https://doi.org/10.1093/mnras/stz2120

[58] John, M.V. (2019) *Monthly Notices of the Royal Astronomical Society*, **484**, L35. https://doi.org/10.1093/mnrasl/sly243

[59] Dolgov, A.D., Sazhin, M.V. and Zeldovich, Y.B. (1990) Basics of Modern Cosmology. Editions Frontières, Gif-sur-Yvette, France.

[60] Suzuki, N., *et al.* (2012) *The Astrophysical Journal*, **746**, 85. https://doi.org/10.1088/0004-637X/746/1/85

[61] Ade, P.A.R., *et al.* (2014) *Astronomy & Astrophysics*, **571**, A16. https://doi.org/10.1051/0004-6361/201321591

[62] Bond, H.E., *et al.* (2013) *The Astrophysical Journal Letters*, **765**, L12. https://doi.org/10.1088/2041-8205/765/1/L12

[63] Riess, A.G., *et al.* (1998) *The Astronomical Journal*, **116**, 1009. https://doi.org/10.1086/300499

[64] Perlmutter, S., *et al.* (1999) *The Astrophysical Journal*, **517**, 565. https://doi.org/10.1086/307221

[65] Riess, A.G., *et al.* (2004) *The Astrophysical Journal*, **607**, 665. https://doi.org/10.1086/383612

[66] Riess, A.G., *et al.* (2007) *The Astrophysical Journal*, **659**, 98. https://doi.org/10.1086/510378

[67] Frieman, J.A., Turner, M.S. and Huterer, D. (2010) *Annual Review of Astronomy and Astrophysics*, **46**, 385. https://doi.org/10.1146/annurev.astro.46.060407.145243

[68] Amanullah, R., *et al.* (2010) *The Astrophysical Journal*, **716**, 712. https://doi.org/10.1088/0004-637X/716/1/712

Journal of Modern Physics, 2020, 11, 1598-1619
https://www.scirp.org/journal/jmp
ISSN Online: 2153-120X
ISSN Print: 2153-1196

Towards Unification of Fundamental Interactions Using Non-Local Hidden-Variable Theory

Dirk J. Pons

Department of Mechanical Engineering, University of Canterbury, Christchurch, New Zealand
Email: dirk.pons@canterbury.ac.nz

How to cite this paper: Pons, D.J. (2020) Towards Unification of Fundamental Interactions Using Non-Local Hidden-Variable Theory. *Journal of Modern Physics*, **11**, 1598-1619.
https://doi.org/10.4236/jmp.2020.1110100

Received: September 2, 2020
Accepted: October 19, 2020
Published: October 22, 2020

Abstract

Problem: In principle there might be a single deeper mechanism underlying the fundamental interactions at both the extremely small scale of particles, and the large scale of gravitation. However it is unclear what form such a theory might take, as the obvious candidates have not yet been successful. **Purpose:** This work constructs a conceptual framework for the interactions from a non-local hidden-variable (NLHV) perspective, specifically the Cordus NLHV theory. **Findings:** All the interactions can be attributed to the discrete force emissions from the particle, more specifically from the different attributes thereof. Thus the electrostatic appears to arise from the direct linear effect of the discrete forces; magnetic from bending of the flux tube; gravitation from handed energisation sequence; strong from the synchronisation of emissions; and weak from rearrangement of discrete force emissions hence remanufacturing of particle identity. **Originality:** An explanation is provided for all the interactions based on non-local hidden-variable theory. Apart from the concept of the discrete force, and its multiple attributes, no new particles or bosons are required.

Keywords

Field, Interaction, Fundamental, Quantum

1. Introduction

The concept of force is well established in mechanics and the resulting principles of statics and dynamics extensively applied in science and engineering with great success. However, despite the precision and familiarity with force at the macroscopic level, the fundamental physics of force are incompletely understood.

Furthermore there is no single coherent theory for all the fundamental interactions. This paper proposes mechanisms for the deeper common causality between interactions. It approaches this from the perspective of a non-local hidden-variable (NLHV) theory [1] [2].

2. Existing Approaches

The first problem is explaining how force arises. The effects of electrostatic, magnetic, and gravitational (EMG) forces are well represented by Newtonian and classical continuum mechanics. However these mechanics do not describe the underlying mechanisms of how force arises or operates. The same limitation applies for general relativity (GR). In quantum mechanics (QM) force is conceptualised as occurring by the exchange of smaller particles, the gauge bosons. However there are many unexplained processes, such as how intrinsic properties are transferred between particles. Furthermore the bosons can only be detected as forces not individual particles.

The second problem is the lack of a single coherent theory for explaining all the fundamental force interactions. The interactions—excluding hypothetical dark energy mechanisms—are the electrostatic, magnetic, gravitational, weak, and strong. The standard model of QM proposes that electromagnetism is carried by virtual photons, the strong interaction between quarks by the gluon, and the weak interaction (e.g. quark flavour-changing between left-handed fermions) by W and Z bosons. The strong nuclear force has a partial explanation in quantum chromodynamics (QCD), but the theory is limited to quarks. It also has no explanation of nuclear structures at the level of nucleons and atomic nuclei. A coherent explanation of gravitation is especially problematic from a particle perspective. In GR, gravity arises from the warping of space time, *i.e.* the effect is a geometric one [3]. Holographic theory provides an explanation for gravitation as an entropic force [4], but not for the deeper mechanisms or the other forces. It seems that any theory that explains gravitation does not explain all the other interactions. QM has attempted to explain gravitation by loop quantum gravity, but a solution is elusive. Alternatively, gravitons may be the boson for gravity, though this is speculative. Thus there is no accepted explanation within QM for gravitation.

Existing efforts at unification have primarily attempted to extend quantum mechanics, on the expectation that a continuum physics like general relativity is unsuited to representing particle interactions. A second premise that has historically shaped the research is the belief that there ought to exist an undiscovered single progenitor force that, at sufficiently high energy density, forms the basis for all the other interactions. Unification is indeed available for the electrostatic and magnetic forces into the electromagnetic with the photon as the boson, and decay interactions (weak nuclear force) via electroweak unification. Models exist providing grand unified theories whereby the electromagnetic, weak, and strong forces might unite into an electronuclear force. However the predicted new particles have not been observed. Furthermore QCD is not integrated with electroweak theory, and gravitation has been especially problematic.

The elusiveness of solutions may indicate that the necessary physics is not accessible with the premises that underpin quantum mechanics. QM is premised on particles—and bosons being zero-dimensional (0-D) points with stochastic and intrinsic properties. If the interactions were to actually have a spatial component, then 0-D points might be inherently unable to represent the mechanisms. Hence alternative theories of physics are also candidates, with their greater number of dimensions for their particles. These other theories may be broadly categorised into string theories, and hidden variable theories. Neither has been especially effective.

String theory has been attempted as a route to a theory of all the interactions. However its lack of specificity has frustrated progress. Hidden variable theories take the premise of physical realism, that manifest attributes are carried by physical substructures to the particle, but they too have been mostly unsuccessful. Of the NLHV theories, historically the de Broglie-Bohm has been the best known [5] [6], but has made no contribution to a holistic explanation of force interactions. Hence a unified theory of all interactions remains elusive, despite considerable effort.

3. Method

The purpose of this paper was to seek explanations for each of the interactions under the Cordus NLHV theory [1]. The earlier work of [7] and [8] provided the initial conceptual basis.

The approach used abductive reasoning, which starts with the known observations and seeks to find the simplest mechanisms that will account for the phenomena consistent the existing premises. "Simple" in this context was interpreted as parsimonious and sufficient, while "Consistent" refers to system integration.

- Parsimoniousness—New particle sub-structures should not be created for each new phenomenon (function) being included. This is conceptually similar to the need to avoid over-parameterisation and model degeneracy in quantitative modelling.
- Sufficiency—The solution needs to be a sufficient match to the empirical phenomena. This corresponds to the function needs in the language of design, see also [9].
- System integration—Any newly proposed particle substructures or concepts must be integrated into the rest of the theory. This is necessary for conceptual coherence. Where appropriate this is expected to result in reconsideration of parts of the theory that show conceptual discoherence.

This approach was applied iteratively. The results present the final theory that emerged, not the intermediate work. The theory is constructed of lemmas, indicated §, which are conceptual propositions that are valid within the wider Cordus theory, even if unable to be immediately verified. The abductive reasoning process is represented diagrammatically in **Figure 1**.

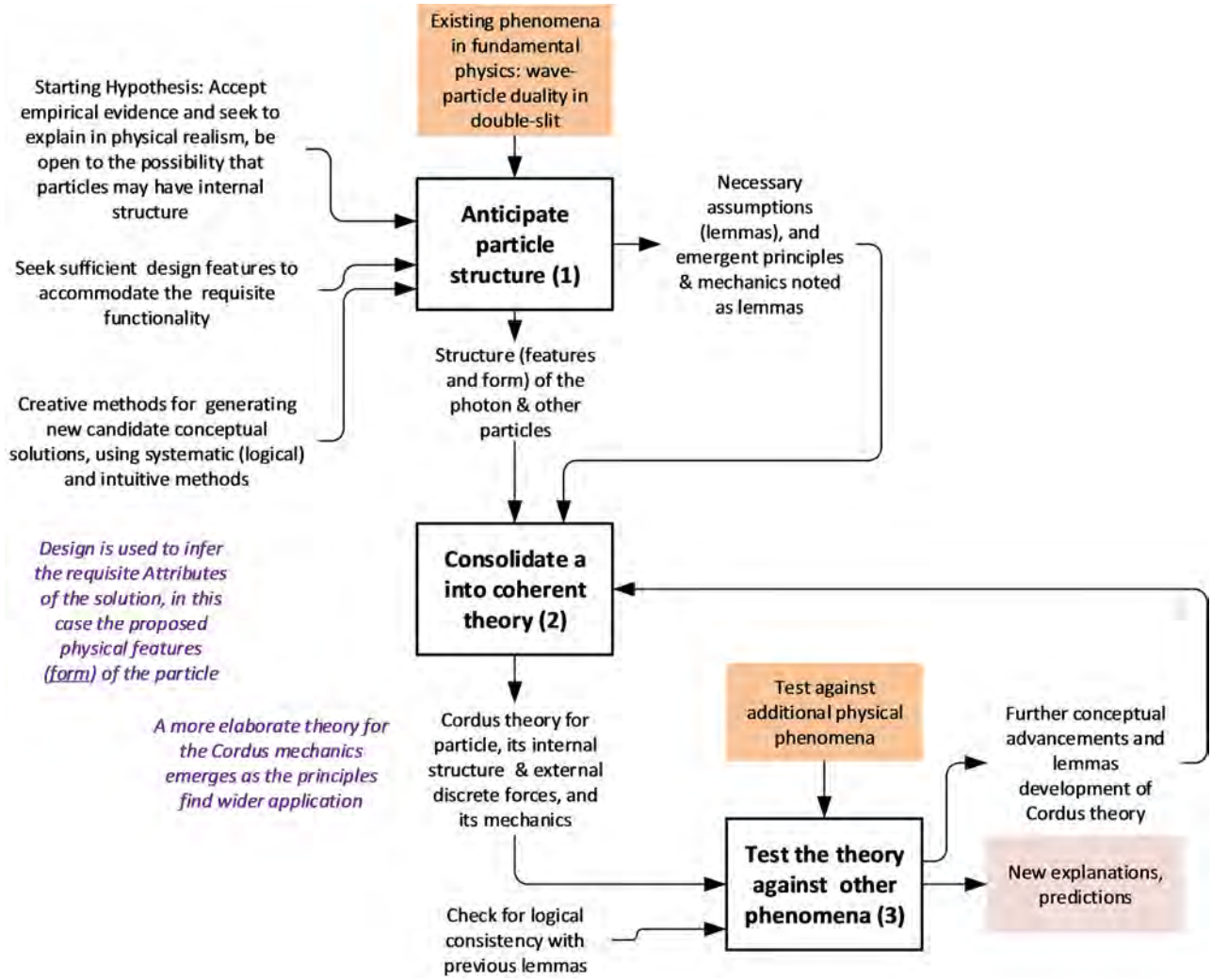

Figure 1. Flowchart representing the abductive reasoning method as applied to this theory.

We first present general principles for interactions, and then elaborate on the different sub-types of interaction.

4. Results

4.1. Context

4.1.1. Structure of the Cordus Particle

Like any NLHV theory, the Cordus theory proposes that particles are not zero dimensional points but instead have internal structures that provide the observed functionality (charge, mass, spin, etc.). It makes specific predictions about the identity of these structures at the sub-particle level [1]. The key difference compared to other theories is that the particle is proposed to comprise two reactive ends some short distance apart, connected by a fibril, see **Figure 2**. The fibril does not interact with other particles, instead the interaction occurs at the reactive ends. The reactive ends are energised at the de Broglie frequency, at which time they emit discrete forces into space in each of three spatial directions (r, a,

and t, see Figure 2) [10] [11]. For massy particles the discrete forces are encapsulated into extended fibril structures that propagate into space—these are called flux tubes. The aggregation of these in space makes up a fabric of discrete forces [12].

4.1.2. A Proposed General Mechanism for Force

A general mechanism for force has been proposed within this theory [13]. The reactive end moves as it goes through its energisation cycle, and traces out a cyclic locus in space. This locus is then distorted by the incoming discrete forces of the external field. As a consequence the mean position of the reactive end changes. This provides a mechanism whereby the reactive end is able to sample the spatial distribution of field around it, *i.e.* the gradient of the field, and move accordingly. The direction of motion adjustment is along the gradient in the direction of greater compatibility of discrete force emissions. Generally this means

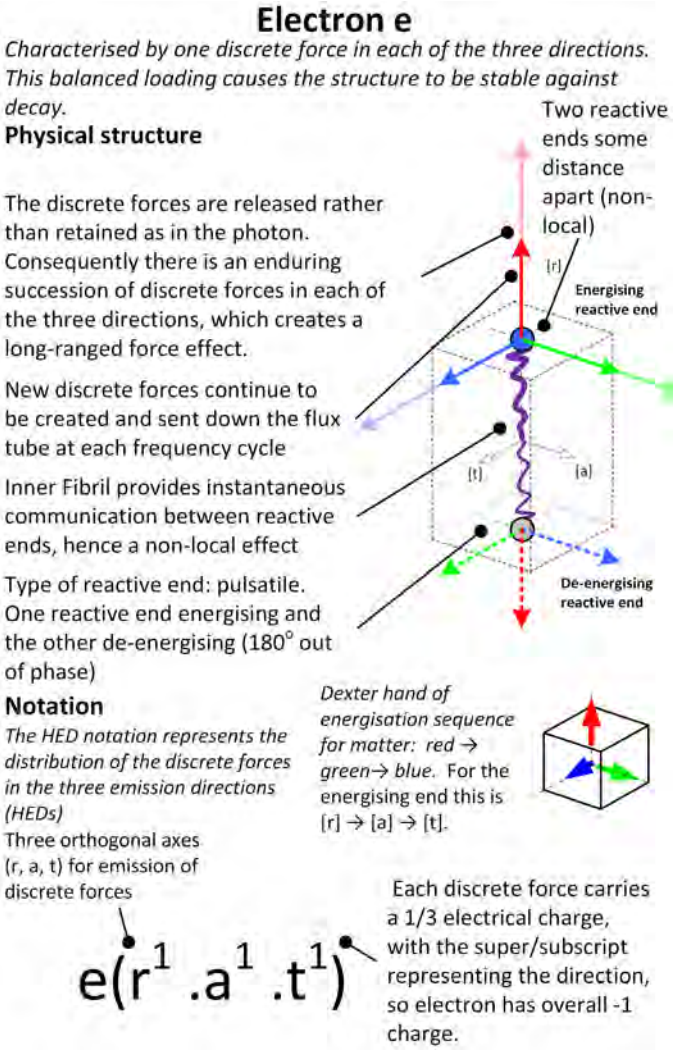

Figure 2. The representation of the electron's internal and external structures. It is proposed that the particle has three orthogonal discrete forces, energised in turn at each reactive end. Reproduced from [13], being an adaption of [14] with permission.

the *type* of emissions, e.g. the phase energisation sequence (matter-antimatter), and *direction* of emission (charge). Hence force arises as "coerced displacement of the reactive end" [13].

4.1.3. Geometric Properties of Flux Tubes Correspond to Interactions

The flux tube has three geometric properties of linear strength (radial emissions), curvature (bending), and twist (torsion). It is proposed that these geometric properties provide the mechanisms for the electrostatic, magnetic, and gravitational (EMG) force interactions respectively. This concept arises from [7] and [8], and is further elaborated below. A fourth attribute of the discrete forces (not so much of the flux tube) is the synchronisation of emission between two particles [10], and this is proposed as the mechanism for the strong interaction (see below). The weak (decay) interaction is proposed to have an altogether different cause (see below).

The above are the general principles for how force operates within the Cordus theory. Next these principles are applied to offer explanations for the different interactions.

4.2. Electrostatic Interaction

Consider test particle B, say an electron, in an electrostatic field set up by basal particle A. Each particle has two reactive ends, and for B these are denoted B_1 and B_2. See **Figure 3**. The location of interest is reactive end B_1 which receives forces from A, and emits its own discrete forces.

4.2.1. The Electrostatic Interaction arises from the Linear (Radial) Component of Discrete Forces (§1)

The theory proposes that the electrostatic interaction arises from the direct linear action of the incoming discrete force on a remote particle. It applies in a direction along the line of the flux tube, and the effect is to move the remote particle B closer or further from the emitting particle A depending on the relative charge.

The underling mechanism is proposed to be that the recipient reactive end attempts to emit its own discrete forces, but is affected by the incoming discrete force. It may be enhanced or inhibited depending on the compatibility between the native and external discrete forces. This changes the position of the reactive end, with the displacement being along the axis of the fibril. A similar mechanism for the spatial readjustment of the reactive end has been proposed for photon absorption and emission [15]. The direction of the discrete force is the basis for the sign of the electric charge. This is presumed to be the direction of action of the discrete forces within an outward travelling flux tube. Negative charge is assumed outwards—this is merely a sign convention.

4.2.2. Explanation for Like-Charge Interaction

Consider the interaction between two electrons, being a typical like-charge case. Electron A is the basal one and is nominally assumed to be fixed, while B is the remote test charge that reacts to A. Each electron has two reactive ends (1 and 2)

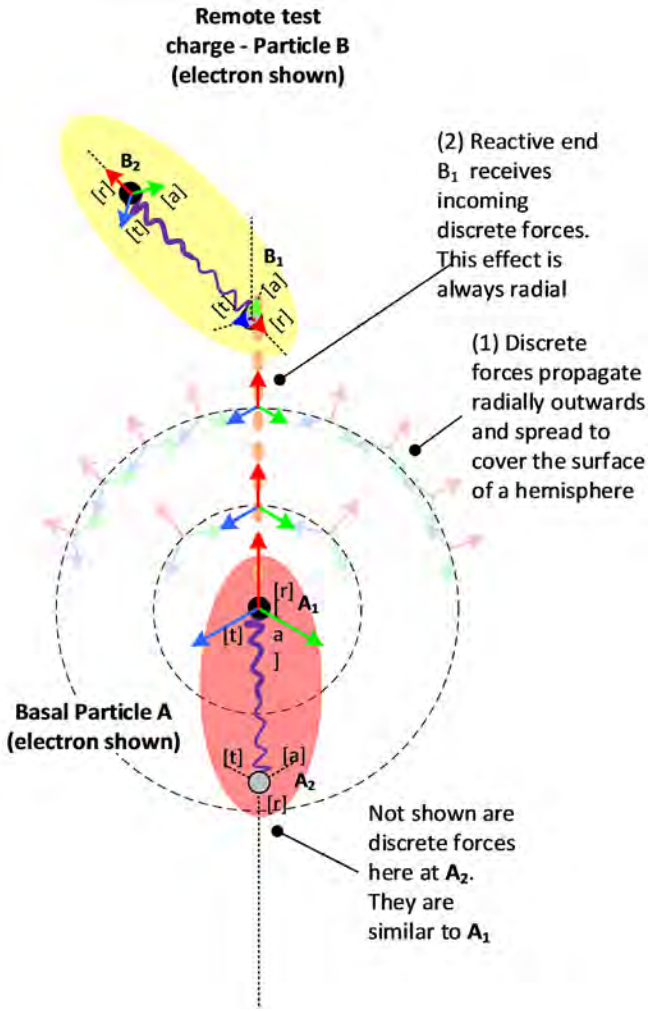

Figure 3. The electrostatic interaction arises from the direct linear action of discrete forces emitted by basal particle A.

per this theory. The reactive end A_1 of electron A emits discrete forces packages in a flux tube, which propagate out into space at the local speed of light and impinge on reactive end B_1 of remote test electron B.

Consider now the energisation of dormant reactive end B_1. As B_1 begins to energise it encounters incoming discrete forces from A_1 that are incompatible with its own emissions. Per lemma 1, this ranged interaction is transphasic, since the particles have like charge, and the synchronous interaction therefore operates to put the emissions $\pi/2$ out of phase. However B_1 cannot delay its energisation indefinitely. This is because energisation state and frequency are determinants of particle identity and energy respectively [16] [17]. Consequently B_1 has to adjust its location to move with those imposed forces, in the repulsive direction.

If the remote charged body has physical depth, *i.e.* comprises many particles, then the incoming discrete forces apply displacements to the foremost parts of the body, then pass through and apply displacements to the deeper layers. Hence a charged macroscopic object feels the electrostatic effect and moves holistically.

4.2.3. Electric Field

At the macroscopic scale of a negatively charged sphere, each of many electrons generates its own discrete forces and flux tubes. Macroscopic bodies tend not to exhibit quantum behaviours. The Cordus theory interprets such bodies as discoherent assemblies of matter, wherein the particle spans are not aligned [2]. Hence a discoherent sea of electrons can be expected to generate flux tubes pointing in random directions. This is consistent with the observation of an electrostatic field that is smooth, continuous, and uniform in all directions. The theory predicts that the field will however be granular at the frequency of the charge emitters.

The electrical force $\boldsymbol{F}_{eB}$ between two particles of charge q_A and q_B is:

$$\boldsymbol{F}_{eB} = -K\frac{q_A q_B}{r^2}\hat{r} \tag{1}$$

where r is the radial separation, $\hat{r}$ is the radial direction and K is a constant. A qualitative explanation for the form of this relationship follows. The reason for the product of charge ($q_A q_B$) is that charge determines the number of discrete forces involved: the amount of displacement coercion (hence force) experienced by particle B is determined by the strength q_A of the incoming discrete forces, and the strength of its own response q_B, hence a multiplicative relationship. The inverse square relationship $1/r^2$ arises from the expansion of the discrete forces on a spherical front. This expansion occurs because the discrete forces are emitted in three orthogonal directions in surface shells at each energisation cycle.

Irrespective of the relative orientation (spin) of A and B, there is always a component of B's emissions that is radial to A, *i.e.* in the direction $\hat{r}$. The electrostatic interaction may be simplified to only this component.

Dissimilar charges attract even across the matter-antimatter species. This implies that the energisation sequence—which differentiates the species—is immaterial for the electrostatic interaction.

4.2.4. Electrostatic Shielding

An electric field is known to be shieldable by a Faraday cage, whereas gravitation is not. The present theory predicts that discrete forces penetrate all matter, but in a Faraday cage the electric field only appears to be shielded, because electrons in the conductive cage material have sufficient mobility to move in response to the external field and set up a countering field.

In contrast the photon can be shielded: it can be absorbed, by mechanisms identified in [15]. Applying this to interaction of electromagnetic radiation *photons* from an antenna or reflector, the present theory explains that the frequency and span of the photons is inversely related [1], which is consistent with the observation that the conducting elements of the antenna need to be closer spaced for higher frequency radiation. As the photon frequency rises still further, the required conductive loops are of the order of atomic spacing, *i.e.* the shield must be of a continuous material. For even greater frequencies the electrons cannot

encounter all the discrete forces in which case the photons pass straight through.

4.3. Magnetic Interaction

A test charge q moving with velocity V in a magnetic field Bm experiences a sideways force F_m that is perpendicular to both its direction of travel and the *external* magnetic field, *i.e.* excludes the magnetic field of the test charge itself):

$$F_m = qV \times Bm \tag{2}$$

This is explained as follows.

4.3.1. Movement of the Basal Charge Bends the Flux Tube (§2)

A flux tube is a directional propagation of discrete forces. It is proposed that this may be bent by movement of the basal emitting reactive end. Per Lemma 8, motion of a reactive end occurs in discrete displacements during its de-energised state. This results in emissions expanding from each progressive location of energisation. Consequently the flux tube, which is continuous, has kinks. The new curvature moves outward with the discrete forces at the local speed of light. If the speed of light was infinite, *i.e.* disturbances propagated instantly, then there would be no magnetic effect.

4.3.2. The Magnetic Interaction Arises from Curvature of the Flux Tube (§3)

Under these premises the magnetic interaction arises interpreted as the action of the incoming discrete forces in a recurved flux tube, causing a yaw adjustment in the velocity of a remote moving charged particle [7]. A remote test particle B moving with velocity V_B receives at reactive end B_1 the discrete forces and the re-curved flux tube emitted by A. This causes a coerced displacement of B_1, which provides a yaw moment that changes the direction of motion of B to be more parallel or antiparallel (depending on the charge) to the velocity of A. See **Figure 4**.

4.3.3. Coerced Displacement of a Remote Moving Charge

How does a curved flux tube create the magnetic force on the moving remote test charge? If the remote test charge is stationary, then any curvature of the incoming discrete forces in their flux tube only re-orients the *direction* of the electrostatic force, *i.e.* momentarily changes spin. Since the flux tube is recurved, this imposes a transient change in orientation that integrates to zero. However, if the test charge is also moving, and encounters a curved flux tube, then the magnetic interaction attempts to realign the *locus* of the moving test charge to the same handed direction of motion as the basal charge.

When the discrete force in its flux tube reaches the remote moving test charge B, it upsets the geometric location for the reactive end B_1 of the moving test charge. Whether it delays or advances that reactive end depends on the sign of the magnetic field, *i.e.* the relative direction of the velocity of B, and the relative charges. The discrete force pulse prevents B_1 from advancing forward as far as it usually might during a frequency cycle, or it pushes it forward.

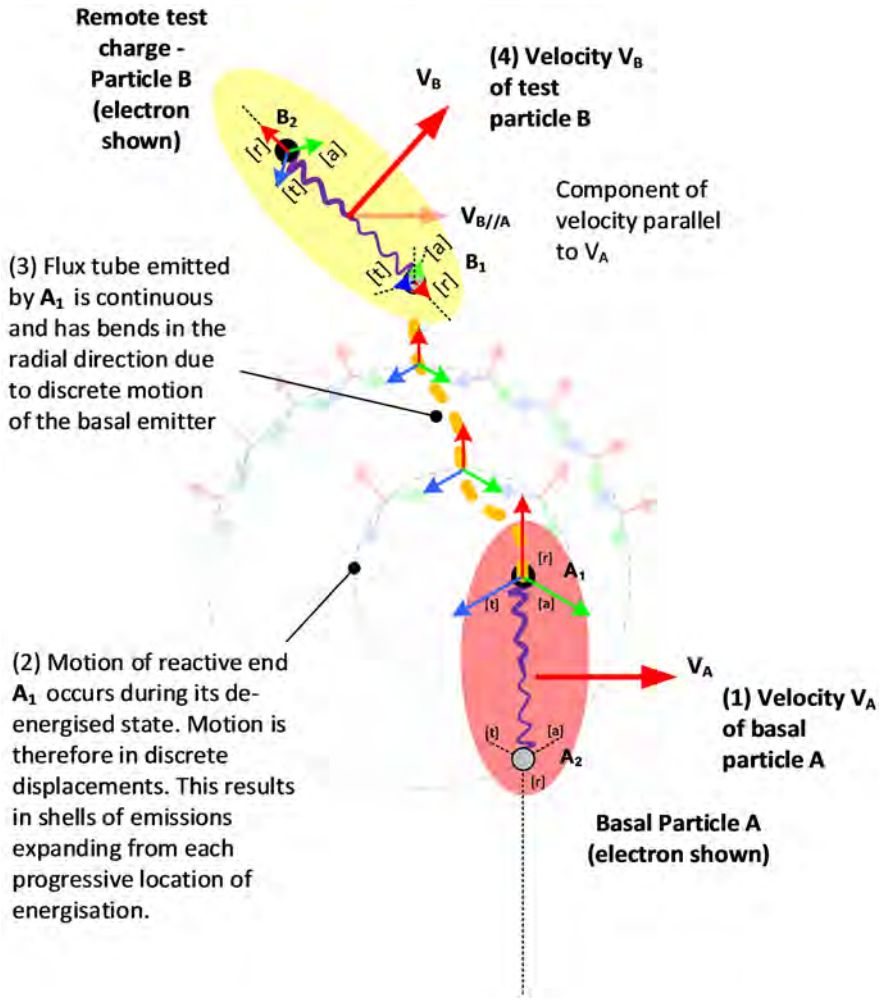

Figure 4. The magnetic interaction arises from the rotational action of the incoming discrete forces in a recurved flux tube.

The incoming discrete forces are not consumed but pass on outward to the other reactive end of the remote particle. The effect on B as a whole is additive rather than being negated, since the direction of the flux tube is reversed when it reaches its other reactive end. This sets up a yaw moment across the fibril of the remote particle, thereby adjusting the direction in which the remote charge is moving.

4.3.4. Magnetic Fields

Magnetic fields represent the motion of the charge (basal generator) that is emitting the discrete forces. A remote moving charge changes direction to be more closely parallel (or antiparallel depending on charge sign) to the locus of the basal charge [18]. The magnetic force $\boldsymbol{F}_{mB}$ in the radial direction $\hat{r}$, experienced by particle B of charge q_B and velocity $\boldsymbol{v}_B$ in a magnetic field created by particle A with q_A and $\boldsymbol{v}_A$ is:

$$\boldsymbol{F}_{mB} = \frac{\mu_0}{4\pi}\frac{q_A q_B}{r^2}\boldsymbol{v}_A \times \boldsymbol{v}_B \tag{3}$$

where r is the radial separation, and μ_0 is a constant. A qualitative explanation for the form of this relationship follows. The reasons for the product of charge ($q_A q_B$) and the inverse square relationship $1/r^2$ are as before. Having more charges q moving in the same direction does not increase the curvature but simply means that there are more discrete forces reaching the remote test charge, *i.e.* the effect simply scales for increase in either of the charges. The direction of the magnetic field is perpendicular to the plane in which the curvature of flux tube occurs. The velocity dependency arises because the faster the basal charge moves $\boldsymbol{v}_A$ the greater the curvature of the flux tube. The greater the velocity $\boldsymbol{v}_B$ the greater the rate at which the kinks are encountered, hence a multiplicative relationship. The magnetism effect depends not simply on the speed of the charges, but also their relative directions. The effect depends on the component of curvature that is apparent to B in its direction of motion, hence the cross product. Thus magnetism only works in remote particles that already have some degree of alignment of their locus with the velocity of the basal charge.

It is proposed that the reason for the effect being right-handed is due to the way that reactive ends emit discrete forces in an energisation sequence (see **Figure 2**), and the dominance of the matter species. Each package of discrete forces has three orthogonal sub-forces and these are energised in a sequence. This sequence has been proposed as the distinguishing structural feature of the matter-antimatter species [19], the anti-electron structure [20], and the basis for annihilation [21].

A common illustration of magnetism depicts a moving charge being forced into a circular trajectory in the presence of a uniform magnetic field. Our explanation is that when the magnetic field is large and uniform, then the transecting moving test charge is forced into a circular path which is the same motion as the large basal current required to make that magnetic field. In this case the magnetic field dominates the interaction, and the moving test charge tends to move into a circular or helical trajectory (its own back-reaction is miniscule). However the case of the uniform field obscures the important fact that creation of that uniform field requires charges to be moving in a circular path too. Uniform magnetic fields are therefore a special case. It is the interaction of two moving charged particles where the more interesting mechanics occurs. The geometrically simplest form of magnetism, two particles affecting each other, is surprisingly complex. The moving test charge is not simply a passive participant, but also radiates its own discrete forces in their flux tube. If the basal charge is of similar size, it will be affected in turn by the magnetism of the test charge. For this and relativistic considerations see [22] and earlier work by [18]. We propose it can be qualitatively interpreted as one moving charge attempting to force another to conform to the same direction of motion: it is a type of alignment effect.

If the test charge is not moving, then the effect of incoming magnetism is to align the remote test charge, which means interfering with its orientation (spin).

This is consistent with behaviour of permanent magnets and magnetic resonance imaging. In both cases the spins of all the electrons in the macroscopic body tend towards alignment. Again this shows that magnetism is primarily an alignment effect.

4.3.5. Permanent Magnets

A permanent ferromagnet has a magnetic field, but no apparent electric field. The usual explanation is that that the electron and nucleon spins are aligned across a domain (region of atoms). The present theory explains this based on the orientation of the particle. It is proposed that the alignment of the span of electrons and nucleons, *i.e.* spin, results in the discrete forces in their flux tubes pointing in the same direction along the axis of the magnetic poles, but randomly orientated in the transverse directions. Hence the effect is summated along the axis, and neutralised laterally. The magnet does not appear to be charged or to emit an electric field because of the equal contribution of positive and negative charges. Nonetheless it emits discrete forces in their flux tube. The magnetic domains are proposed to be formed in the first instance because electron discrete forces extend to neighbouring atoms and encourage alignment of other electrons. We suggest that within the magnetic material the electrons themselves move, either through their unfilled orbitals, or as current flow within the sub-lattices of the material, and this generates curvature of the discrete forces in their flux tubes and thus magnetic fields.

4.4. Gravitation

4.4.1. The Gravitational Interaction Arises from Torsion of the Flux Tube, Which Arises from the Handedness of the Emission of Discrete Forces (§4)

Up to here the discrete forces have been implied to be discrete, and represented diagrammatically as arrows. However this is a simplification of a deeper mechanics. They are instead believed to take the form $\sin^2(\theta/2)$ and to comprise emissions in three orthogonal directions (r, a, t) [13], see Equation (4). Thus the potential energy U_{B_1} in the flux tube has three components offset at thirds of the phase angle θ_B:

$$U_{B_1}(r) = \sin^2 \frac{\theta_B}{2} \tag{4a}$$

$$U_{B_1}(a) = \sin^2\left(\frac{\theta_B}{2} - 120^\circ\right) \tag{4b}$$

$$U_{B_1}(t) = \sin^2\left(\frac{\theta_B}{2} - 240^\circ\right) \tag{4c}$$

See **Figure 5** for a representation of these three phases for a matter species (electron). This energisation sequence results in a torsional effect on remote particle B, which moves closer or further along the field gradient depending on the mutual compatibility.

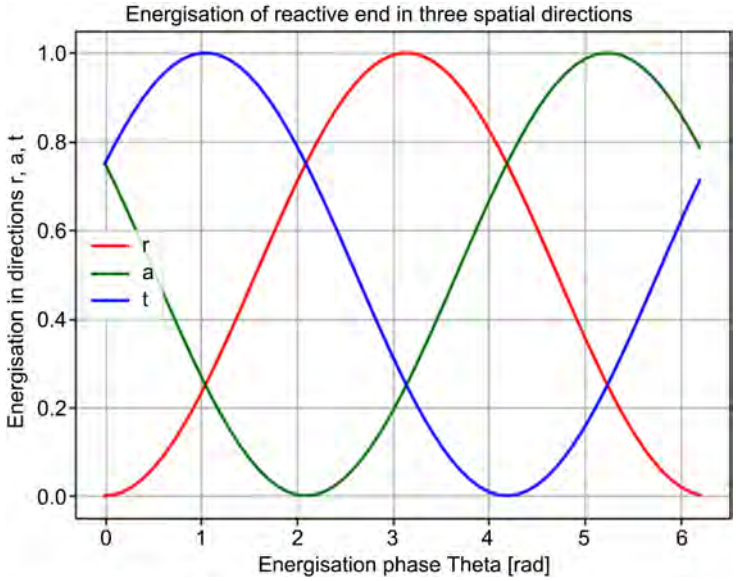

Figure 5. Energisation phases in the three orthogonal emission directions (r, a, t) follow a $\sin^2(\theta/2)$ relation. This is for a matter particle (electron). Image from [13] with permission.

4.4.2. Further Implications

There are several implications. The first is that the reactive end is never fully de-energised. While any one discrete force does momentarily go to zero in strength, the reactive end as a whole maintains its energisation. This satisfies another part of the theory which showed that the Lorentz and relativistic Doppler could be derived on the premise of a stretchable flux tube [23].

A second implication is that the potential energy function for reactive end B_1 has a circular function, and the reactive end moves in reaction to trace a small cyclic locus in space [13]. The locus is circular with normal [1, 1, 1] in the [r, a, t] directions. However when an external field is imposed, then the reactive end expands its excursion asymmetrically, and this moves its mean location.

A third implication concerns the question of why the gravitational interaction between matter and matter is attractive when the electrostatic interaction repels like charges. The answer is that for the electrostatic the opportunity for greater coordination between particles arises if their directions of emissions (charge) are opposite, irrespective of the energisation sequence (species). In contrast for gravitation the opportunity arises if the emissions have the same hand: receiving particle B is attracted to the transphasic interaction [13] whereby it energises within the null points in the incoming (r, a, t) emission. This it can only do if the energisation sequence is the same, which always arises for when both particles are matter species.

4.4.3. Matter-Antimatter Gravitation

In this theory the energisation sequence (r, a, t) vs. (a, r, t) determines the matter-antimatter species [19] [24]. Thus we predict that antimatter-antimatter gravitation is attractive, and matter-antimatter repulsive. The reasoning follows. For the case of an anti-electron the energisation sequence is (a, r, t) and the charge is

inverted. The corresponding energy locus for the reactive end is shown in Figure 6 for the electron and antielectron. This shows that the rotation is opposite in direction for antimatter. It logically follows that the gravitational interaction between two antimatter particles would be attractive, and repulsive between matter and antimatter.

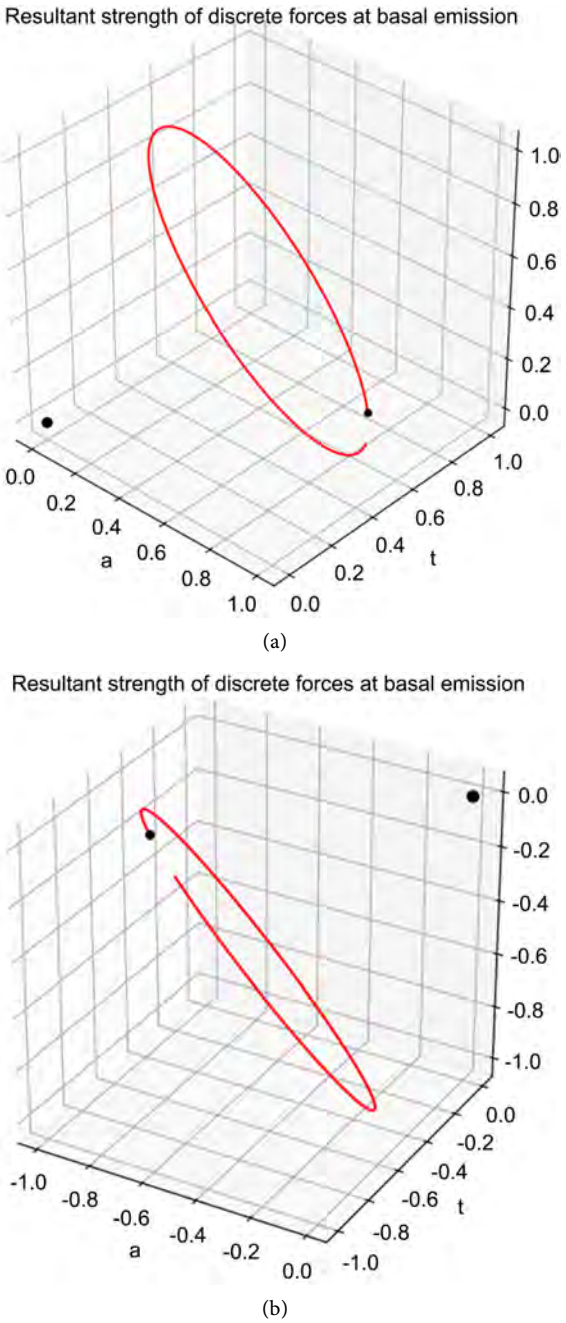

Figure 6. Resultant energy at the basal generator B_1 due to (a) matter negative charge (electron) from [13], and (b) antimatter positive charge (antielectron). The axes are (r, a, t). The larger black marker indicates the nominal origin (0, 0, 0), and the smaller black marker indicates the location for $\theta = 0$. The locus is deliberately shown incomplete to indicate the direction of rotation.

4.4.4. Gravitational Force

The gravitational force $\boldsymbol{F}_{gB}$ in the radial direction $\hat{r}$, experienced by particle B of mass m_B in a gravitational field created by particle A with m_A is conventionally:

$$\boldsymbol{F}_{gB} = G\frac{m_A m_b}{r^2} \tag{5}$$

The reason for the product of charge ($m_A m_b$) is that that the effect is enhanced by more incoming discrete forces (m_A) per lemma 1, and a greater frequency of response (m_b) per lemma 8. The inverse square relationship $1/r^2$ is because of the dilution of discrete forces across an expanding spherical shell, as before.

4.5. Synchronous Interaction (Strong Nuclear Force)

The equivalent of the strong nuclear force in the Cordus theory is the synchronous interaction [10]. This interaction is between reactive ends from different particles, that are co-located. If their discrete force emissions are compatible, then this locks the reactive ends together. As identified in Lemma 2 [13], the synchronous interaction has two subtypes, which are transphasic and cisphasic. The terms refer to the phase difference at synchronisation.

The strongest form of compatibility is where the assembly provides a balanced and complete set of discrete force emissions in all three directions [25]. In this case the reactive ends energise simultaneously, and this is the cis-phasic subtype of the synchronous force. An example of the cis-phasic interaction is proposed in the bond between the proton and neutron in the atomic nucleus, see **Figure 7**.

The other subtype of synchronous interaction is trans-phasic, where the reactive ends from two separate particles energise out of phase. The type example of this is the Pauli electron pair [2], see **Figure 8**.

Application of the synchronous principle is able to explain the structure of the atomic nucleus as a polymer of neutrons and protons. Rules for these bonds have been deduced, and these are sufficient to economically explain why any nuclide is stable, unstable, or non-existent. This has been demonstrated for H to Ne [25] [26] and the trends appear to hold up to at least Ar.

Thus the nuclear force may be explained as a synchronisation of emissions between different reactive ends. The theory proposes that the strong force at the deeper quark level is likewise a synchronous interaction, though the internal structure of the proton and neutron have yet to be fully elucidated within this theory.

4.6. Remanufacturing (Weak) Interaction

Per QM the weak interaction mediates the nucleon beta decay and electron capture processes via exchange of W and Z bosons. From the Cordus theory the interpretation is somewhat different, as the analysis [16] suggests the weak interactions are part of a more general family of processes that change particle identity. From this perspective the weak bosons are merely transitional assemblies, rather

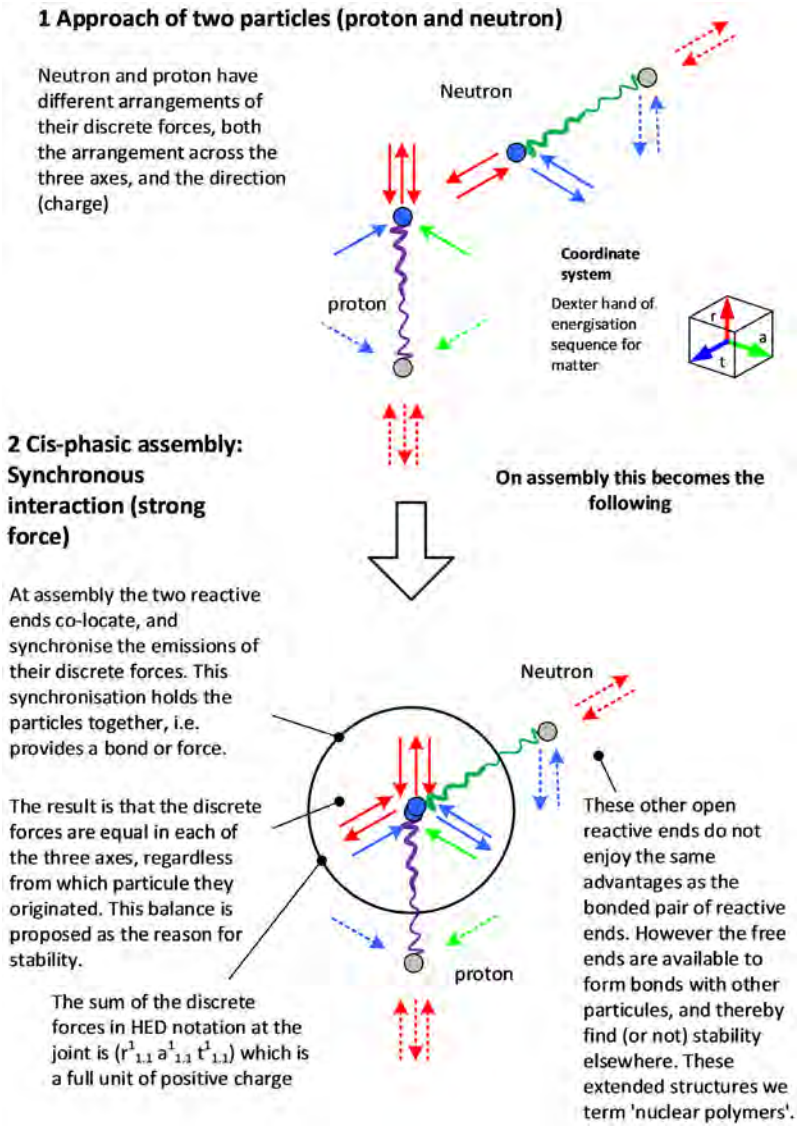

Figure 7. Key features of cis-phasic synchronous interaction as illustrated in the proton-neutron bond. Adapted from [10].

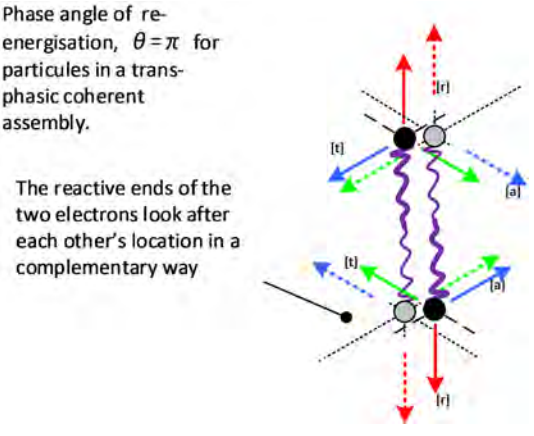

Figure 8. The Pauli pair of electrons uses the trans-phasic interaction to provide a degree of bonding. Adapted from [2].

than particles that cause change in quarks. Hence they do not deserve to be called bosons or their process singled out as a fundamental interaction. Instead we propose a set of principles of discrete force manipulation for the remanufacturing processes generally.

Particle identity, in the Cordus theory, arises from the characteristic pattern of discrete force emissions. Change these, and the particle identity is also changed. This process is called "remanufacturing" because the discrete forces are conserved. The conventional term "decay" implies a degenerative, disorderly, or destructive process, which from the Cordus theory is quite the wrong way to think about these transformations. Consideration of the discrete forces and the rules for their transformation [16] shows that it is necessary for many processes to change the *order* of energisation sequence. The theory shows that the neutrino species achieve this by removing unwanted handedness from the assembly [17]. Note that in this theory the handedness is also proposed as the matter-antimatter species differentiator [17] [21]. This is a further reason to use "remanufacture" (*manus* = hand). All the remanufacturing processes use the synchronous interaction.

The Cordus theory provides a unified equation for nucleon remanufacture:

$$\boldsymbol{p}+2\boldsymbol{y}+\boldsymbol{iz}=\boldsymbol{n}+\underline{\boldsymbol{e}}+\boldsymbol{v} \tag{6}$$

with particle identities and discrete force structures as follows:

n	neutron	$n\left(r_1^1\cdot a_1^1\cdot t\right)$	Shown for overt part. There is also a large covert component
p	proton	$p\left(r_{1.1}^1\cdot a_1\cdot t_1\right)$	ibid
e	electron	$e\left(r^1\cdot a^1\cdot t^1\right)$	
$\underline{e}$	antielectron	$\underline{e}\left(r_{\perp}\cdot a_{\perp}\cdot t_{\perp}\right)$	positron
v	neutrino	$v\left(r_1^1\cdot a\cdot t_1^1\right)$	
$\underline{v}$	antineutrino	$\underline{v}\left(r_{\perp}^{\perp}\cdot a\cdot t_{\perp}^{\perp}\right)$	
y	photon	$y\left(r^{\updownarrow}\cdot a\cdot t\right)$	$^{\updownarrow}$denotes oscillating discrete force, extended and withdrawn
z	discrete force complex	$x_{1.1}^{1.1}$	x is one of the emission directions [r. a. t]
$2y$	a pair of photons	$\left[r_{\perp}^1\cdot a_{\perp}^1\cdot t_{\perp}^1\right]$	With sufficient energy can also correspond to an electron-antielectron pair
i	quantity, e.g. of photons		

Note that antimatter is shown with underscore in this notation.

The equation works in both directions. Transfers of a particle across the equality result in inversion of the matter-antimatter species (hand). Rearrangement of the equation gives β–, β+, and EC in the conventional forward directions, and predicts induced decays too [27].

From this perspective the emission/absorption of a photon is also a remanu-

facturing process [15], as is pair production [28], and annihilation [21]. Furthermore the asymmetrical baryogenesis and leptogensis problems have solutions with the Cordus theory [24], with the genesis remanufacturing process involving electron-antielectron pair production, with the antielectron remanufactured (with the additional of further photon discrete force structures) into the proton:

$$\mathbf{8}\boldsymbol{y} + \boldsymbol{z} \Rightarrow e + p + 2\underline{\boldsymbol{\nu}} \tag{7}$$

with particle identities as above. This manufacturing process was derived from consideration of the discrete force structures. It simultaneously addresses baryo- and leptogenesis. Diagrammatically it is represented in Figure 9.

In summary, the weak force is reconceptualised as a remanufacturing process. The W and Z bosons are denied causal identity as vectors of change, but instead proposed to be merely transitional assembly structures. This is consistent with their short lives and ranges. Consequently we propose that the weak is not a force interaction. Nonetheless it is a powerful mechanism because it gives rise to all observed matter. Furthermore, like all the other interactions, it is based on attributes of the discrete forces, though the aggregate thereof rather than individual attributes.

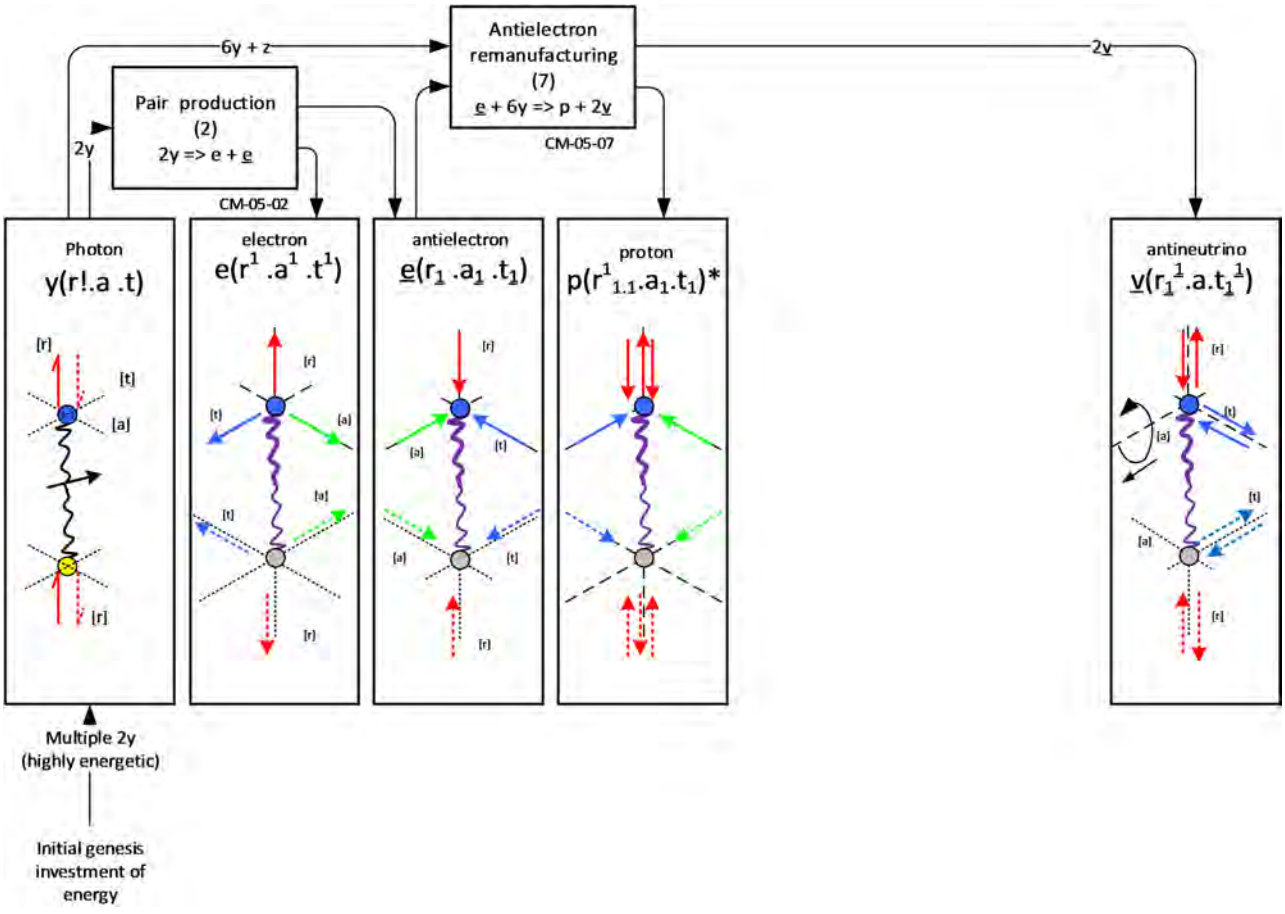

Figure 9. Asymmetrical genesis production stream. The discrete force rules predict a process whereby the antielectron from pair production is remanufactured into a proton, with two antineutrinos ejected in the waste stream. From [24].

5. Discussion

5.1. Findings

The results offer a new way of categorising the interactions. Thus the synchronous interaction becomes the mechanism for bonding coherent assemblies of matter, whereas the electro-magneto-gravitational interactions operate on discoherent matter. These interactions are not continuous but in discrete force increments. The remanufacturing interaction is somewhat different to the others, being less a force and more a large family of processes that change the internal assembly of multiple discrete forces and thereby change particle identity, though it too is synchronous in nature.

We find against the conventional idea that unification might be found at higher energy levels. Instead energy is only a proxy variable. The energy in an interaction between particles depends on the number of discrete force involved (hence also mass), and the type of synchronisation of emissions (discoherent or synchronous). Thus there is an approximate increase of energy involved with the progression from the electro-magneto-gravitational forces, to the synchronous, and to the remanufacturing processes with the many discrete forces involved. However we propose it is not energy per se that provides the explanation for unification.

Furthermore the theory offers an information interpretation. The emitted discrete forces communicate to other particles in the universe at large, by broadcasting the identity and attributes of the emitting particle. These attributes include position, orientation, velocity, cis/trans-phasic partnership opportunities, etc. They are a type of information broadcast that consumes no energy, yet allows other remote particles to change their behaviour.

5.2. Contrasts

QM attributes the electrostatic interaction to the virtual photon gauge boson. The Cordus theory instead proposes that the interaction occurs via discrete forces. In the Cordus theory there is an important difference between the single pair of discrete forces emitted by a photon, and the three orthogonal ones emitted by a massy particle [15]. The former continue to propagate outwards whereas the latter are extended and then withdrawn. Hence we disfavour identifying the interaction with a virtual photon like structure.

QM proposes that the strong force between quarks arises from the exchange of gluons, and the nuclear force arises from the residual force thereof. The QM concept of three colour charges has parallels with the three orthogonal charge emission directions of the Cordus theory, and the gluons with the discrete forces. However a key difference is that QM has different bosons for each interaction, whereas the Cordus theory attributes the interactions to different functional attributes of the same discrete forces throughout.

The Cordus perspective of gravitation emerges as being similar to but also different from General relativity (GR). In GR, gravitation arises from the curva-

ture of spacetime, and is not so much a force as a geometric interaction of the moving body with that curvature. GR does not explain what makes up spacetime. By comparison the Cordustheory proposes the vacuum is filled with a tangle of discrete forces in their flux tube, which is called the *fabric* [29] [30]. Both perspectives agree that gravitation is an effect that a mass does to the whole universe. The relativistic Doppler and time dilation have also been derived from first principles using the Cordus theory [23], so there are areas of substantive alignment between the theories.

Both QM and the Cordus theory agree that gravitation is quantised. The Cordus theory offers a specific mechanism, via the discrete forces and their effect on the position of the reactive end. QM is unable to explain gravitation, and its closest approach is loop quantum gravity that proposes that the fabric consists of spin networks. A region of Cordus fabric contains multiple discrete forces in their flux tube, and conceptually these momentarily define small dynamic domains: perhaps these correspond to spin networks. However from the Cordus perspective the underlying mechanism is force lines and force pulses. Loops in the fabric are not precluded, but are interpreted as secondary phenomena rather than the mechanism itself.

5.3. Implications

Of the main theoretical approaches to developing a new physics to unite the interactions, quantum mechanics has been the dominant area of endeavour. While string theory is still an active area of research, it has seen less attention and been less successful in this area. The third branch, the NLHV sector, has been conceptually unproductive and become obscure. Specific solutions for the hidden structure have seemed intractable or ridiculous. Nonetheless the NLHV approach has many positive attributes, as shown here, once the question of substructure can be resolved. Demonstrating conceptually that the interactions may be unified in an NLHV theory opens up new lines of thinking.

6. Conclusions

The originality in this work is providing an explanation for all the interactions based on non-local hidden-variable theory. Under the assumptions of this theory, the interactions arise from different aspects of a single underlying mechanism, of the discrete force emissions.

1) The electrostatic interaction results from the direct *linear* operation of the discrete forces.

2) The magnetic interaction results from the *bending* of the flux tube containing the discrete forces.

3) Gravitation results from the *handed sequence* of the discrete force emission, a type of torsional effect.

4) The strong interaction (and nuclear force) arises from the *synchronisation* of timing of discrete force emissions between reactive ends on different particles.

5) The weak (decay) interactions arise from the *rearrangement* of discrete force emissions, which results in *remanufacturing* of particle identity.

Apart from the concept of the discrete force, and its multiple attributes, no new particles or bosons are required.

Acknowledgements

This work builds on earlier conceptual papers [7] and [8]. The contribution made by those authors is acknowledged with gratitude.

Conflict of Interest Statement

The author declares that there are no financial conflicts of interest regarding this work.

References

[1] Pons, D.J., Pons, A.D., Pons, A.M. and Pons, A.J. (2012) *Physics Essays*, **25**, 132-140. https://doi.org/10.4006/0836-1398-25.1.132

[2] Pons, D.J., Pons, A.D. and Pons, A.J. (2019) *Journal of Modern Physics*, **10**, 835-860. https://doi.org/10.4236/jmp.2019.107056

[3] Smolin, L. (2015) Lessons from Einstein's 1915 Discovery of General Relativity. 1-14.

[4] Verlinde, E. (2011) *Journal of High Energy Physics*, **2011**, 29. https://doi.org/10.1007/JHEP04(2011)029

[5] de Broglie, L. (1929) The Wave Nature of the Electron, in Nobel Lecture. Nobel Prize in Physics.

[6] Bohm, D. and Bub, J. (1966) *Reviews of Modern Physics*, **38**, 453-469. https://doi.org/10.1103/RevModPhys.38.453

[7] Pons, D.J., Pons, A.D., Pons, A.M. and Pons, A.J. (2011) Electromagnetism. 1-17. http://vixra.org/abs/1104.0027

[8] Pons, D.J., Pons, A.D., Pons, A.M. and Pons, A.J. (2011) Gravitation, Mass and Time. 1-14. http://vixra.org/abs/1104.0029

[9] Ackoff, R.L. (1962) Scientific Method Optimising Applied Research Decisions. John Wiley & Sons, New York.

[10] Pons, D.J., Pons, A.D. and Pons, A.J. (2013) *Applied Physics Research*, **5**, 107-126. https://doi.org/10.5539/apr.v5n5p107

[11] Pons, D.J., Pons, A.D. and Pons, A.J. (2016) *Journal of Modern Physics*, **7**, 1049-1067. https://doi.org/10.4236/jmp.2016.710094

[12] Pons, D.J., Pons, A.D. and Pons, A.J. (2013) *Applied Physics Research*, **5**, 23-47. https://doi.org/10.5539/apr.v5n6p23

[13] Pons, D.J. (2020) *Journal of Modern Physics*, **11**, 1560-1575. http://dx.doi.org/10.4236/jmp.2020.1110097

[14] Pons, D.J. (2015) Internal Structure of the Electron (Image Licence Creative Commons Attribution 4.0). Wikimedia Commons, (Creative Commons Attribution 4.0 International license). https://commons.wikimedia.org/wiki/File:Internal_structure_of_the_electron.jpg

[15] Pons, D.J. (2015) *Applied Physics Research*, **7**, 14-26.

https://doi.org/10.5539/apr.v7n4p24

[16] Pons, D.J., Pons, A.D. and Pons, A.J. (2014) *Applied Physics Research*, **6**, 50-63. https://doi.org/10.5539/apr.v6n3p50

[17] Pons, D.J., Pons, A.D. and Pons, A.J. (2015) *Applied Physics Research*, **7**, 1-11. https://doi.org/10.5539/apr.v7n1p1

[18] Sard, R.D. (1947) *Electrical Engineering*, **66**, 61-65. https://doi.org/10.1109/EE.1947.6443336

[19] Pons, D.J., Pons, A.D. and Pons, A.J. (2014) *Physics Essays*, **27**, 26-35. https://doi.org/10.4006/0836-1398-27.1.26

[20] Pons, D.J. (2015) Internal Structure of the Anti-Electron (Positron) (Image Licence Creative Commons Attribution 4.0). Wikimedia Commons, (Creative Commons Attribution 4.0 International License). https://commons.wikimedia.org/wiki/File:Internal_structure_of_the_anti-electron_(positron).jpg

[21] Pons, D.J., Pons, A.D. and Pons, A.J. (2014) *Applied Physics Research*, **6**, 28-46. https://doi.org/10.5539/apr.v6n2p28

[22] Minkin, L. and Shapovalov, A.S. (2018) *Physics Education*, **53**, Article ID: 035014. https://doi.org/10.1088/1361-6552/aaab88

[23] Pons, D.J., Pons, A.D. and Pons, A.J. (2018) *Journal of Modern Physics*, **9**, 500-523. https://doi.org/10.4236/jmp.2018.93035

[24] Pons, D.J., Pons, A.D. and Pons, A.J. (2014) *Journal of Modern Physics*, **5**, 1980-1994. https://doi.org/10.4236/jmp.2014.517193

[25] Pons, D.J., Pons, A.D. and Pons, A.J. (2015) *Physics Research International*, **2015**, Article ID: 651361. https://doi.org/10.1155/2015/651361

[26] Pons, D.J., Pons, A.D. and Pons, A.J. (2013) *Applied Physics Research*, **5**, 145-174. https://doi.org/10.5539/apr.v5n6p145

[27] Pons, D.J., Pons, A.D. and Pons, A.J. (2015) *Applied Physics Research*, **7**, 1-13. http://vixra.org/abs/1412.0279 https://doi.org/10.5539/apr.v7n2p1

[28] Pons, D.J., Pons, A.D. and Pons, A.J. (2015) *Journal of Nuclear and Particle Physics*, **5**, 58-69.

[29] Pons, D.J. and Pons, A.D. (2013) *The Open Astronomy Journal*, **6**, 77-89. https://doi.org/10.2174/1874381101306010077

[30] Pons, D.J., Pons, A.D. and Pons, A.J. (2016) *Applied Physics Research*, **8**, 111-121. https://doi.org/10.5539/apr.v8n3p111

Journal of Modern Physics, 2020, 11, 1620-1638
https://www.scirp.org/journal/jmp
ISSN Online: 2153-120X
ISSN Print: 2153-1196

Link between Allais Effect and General Relativity's Residual Arc during Solar Eclipse

Russell Bagdoo

Saint-Bruno-de-Montarville, Quebec, Canada
Email: rbagdoo@yahoo.ca, rbagdoo@gmail.com

How to cite this paper: Bagdoo, R. (2020) Link between Allais Effect and General Relativity's Residual Arc during Solar Eclipse. *Journal of Modern Physics*, **11**, 1620-1638.
https://doi.org/10.4236/jmp.2020.1110101

Received: September 4, 2020
Accepted: October 23, 2020
Published: October 26, 2020

Abstract

The purpose of this article is to establish a relation between two gravitational anomalies: one that has attracted part of the scientific community, the Allais effect that occurs during solar eclipse; the other, noticed but forgotten by the whole scientific community, the General Relativity's residual arc of the curvature of rays of light in the solar gravitational field during the same eclipse. There is a systematically observed deflection about 10% larger than the theoretical value of General Relativity, which coincides with the "eclipse effect" found by Maurice Allais, thrown aside because it upsets the established truths. These corresponding anomalies were never explained by any theories and turn out to be new gravitational physics.

Keywords

Allais Effect, Paraconical Pendulum, General Relativity, Eclipse Experience, Parallax, Arc Residue, Interferometry

1. Introduction

1.1. Preliminaries

Based on the equivalence principle, Einstein revealed a deep relation of gravity to the geometry of spacetime. General Relativity (GR) has undergone an impressive series of confirmations mostly regarding "strong" fields. But in "weak" fields where GR does not distinguish from the Newtonian limit, there are unexplained phenomena like galaxy rotation curves, the Pioneer anomaly. There is little direct evidence that conventional theories of gravity are correct on large scales. Despite all the success of Newtonian gravity and GR on the scale of the solar system, data of unique precision collected for the last two decades by satellite-based telescopes covering all frequencies and digital image processing gave a

number of results where these theories run into problems, such as the unexpected secular increase of the Astronomical Unit or the abnormal change in acceleration for flybys of spacecraft. We emphasize the scientific aspect of peculiar movements exhibited by an anisotropic paraconical pendulum at the time of a solar eclipse in 1954.

The aim of this article is to establish a relation between the abnormal deviation of the pendulum (Allais effect) during this solar eclipse and the observed residual arc of the curvature of the rays of light in the solar gravitational field (GR) during the same eclipse. Both gravitational anomalies were never explained by GR or by any other theories and it raises question about their nature. Our approach is as follows. In Section 1, we describe the gravitational deflection of light by the Sun during solar eclipses insisting on the fact that many observations gave a deflection 10% larger than the theoretical value during eclipse experience. We present from the outset the Allais effect, first reported in 1954 by Maurice Allais, which is an anomalous precession of the plane of oscillation of a paraconical pendulum during a solar eclipse. In Section 2, we make a mathematical link between the unexpected turn that the pendulum took during the eclipse, changing its angle of rotation by 13.5˚, and the about 10% arc's deviation observed during the same eclipse experience. Although it is not the task of this paper, we also speculate on modification of Einsteinian gravitational mechanics and a discussion mentions briefly that these anomalies turn out to be new gravitational physics including "antigravity". In Section 3, the fact that an exact agreement between theory and measurements has been obtained by radio interferometry, but has never been obtained by eclipse technique, indicating a genuine insufficiency of Einstein's theory during eclipse. In Section 4, we discuss two manners to experiment the behaviour of the gravity: measure the angle of deflection of light and measure the delay time of signals. In Section 5, we show three possible cosmological consequences of the Allais effect linked to GR's residual arc during total solar eclipse. Conclusion in Section 6: during the eclipse, the unexplained excess of arc of general relativity would be consistent with the abrupt deviation of the oscillation plane of the Allais pendulum; for these two phenomena, the currently accepted physical theories offer no explanation for this slight deviation from gravitational laws, which suggest a new physics.

1.2. Many Observations Gave a Deflection 10% Larger Than the Theoretical Value of General Relativity during Eclipse Experience

The first test of Einstein's prediction was the apparent bending of light as it passes near a massive body [1]. This effect was conclusively observed during the solar eclipse of May 29, 1919, when the Sun was silhouetted against the Hyades star cluster, for which the positions were well known. It was mainly made through the initiative of the British astronomer Eddington. He was stationed on an island off the western coast of Africa and sent another group of British scientists to Brazil. Their measurements of several of the stars in the cluster showed

that the light from these stars was indeed bent as it grazed the Sun. The result obtained by measuring the plates (1.98" ± 0.12" and 1.61" ± 0.31") confirmed almost the exact displacement of Einstein's predictions [2].

GR predicts that locally straight lines that pass near the Sun are bent relatively to the straight lines that pass far from the Sun in completely empty space by an additional 0.875 arcsecond. Thus, the total deflection must be ~1.75 arcseconds. The apparent displacement of light results from the warping of space in the vicinity of the massive object through which light travels. The light never changes course, but merely follows the curvature of space. Astronomers now refer to this displacement of light as gravitational lensing. But the Sun's gravity is relatively weak compared with what's out there in the depths of space. As a dramatic example of gravitational lensing, the light from a quasar (a young, distant galaxy that emits prodigious amounts of radio energy) 8 billion light years away is bent round by the gravity of a closer galaxy that's "only" 400 million light years distant from Earth.

Although the eclipse results distinguished clearly among the possibilities of no deflection, the Newtonian deflection, and the Einsteinian deflection, their relatively large experimental errors made it important to repeat the measurements. Since that time, measurements of the deflection of the light by the Sun, although they are difficult, have been made at a number of around 400 total eclipses with only modest improvement over previous eclipse measurements. The values were anywhere between three-quarters and one and one-half times the general relativistic prediction: many observations gave a deflection 10% larger than the theoretical value. The deviation between theory and measurements is too high to be only due to errors of observation [2] [3].

Even if there is no doubt that GR is nearer the truth than the value obtained from Newtonian mechanics or any other theory so far proposed, even if radio interferometry now replaced the eclipse technique bringing an almost exact agreement between theory and measurements (which has never been obtained by eclipse technique), this deviation during eclipse indicates a genuine insufficiency of Einstein's theory.

1.3. Allais Effect; An Experience of Great Precision

Professor Maurice Allais is a French physicist, winner of the 1988 Nobel Prize in Economics, winner of the 1959 Galabert Prize of the French Astronautical Society, and also a laureate of the United States Gravity Research Foundation due to his gravitational experiments. In the 1950s he undertook several experimental series in Paris which involved repeated determinations of the rate of precession of a paraconical pendulum which he had invented. Suspended via a small steel ball bearing, this pendulum with anisotropic support has this peculiarity to be able to raise abruptly the oscillation plane when there is a sudden disturbance. 7 series of experiments succeeded one another: 32 days in June and July 1954; 9 in September 1954; 37 in November and December 1954; and in 1955, 7, 15, 30 and

17 days. He released his pendulum every 20 minutes—for more security, the pendulum was stopped vertically, then re-tautened—and recorded the azimuth every minute for 14 minutes. There were thus 72 series of experiments by 24 hours without missing a data point. He detected various periodic anomalies in the motion of this pendulum by using elaborate statistical analysis. One of these experimental series happened to overlap with the eclipse of Sun of June 30th, 1954 [4] [5] [6].

During the eclipse, M. Allais put in evidence an unexpected disturbance of the effect of Foucault. At the exact onset of the eclipse, the plane of the oscillation got up abruptly of 4.5˚.

Twenty minutes before the maximum of the eclipse, it reached 13.5˚ to decline slowly until an abnormality of 1˚ at the end of the phenomenon. This unexpected large scale excursion in the angular plane persisted throughout the length of the eclipse, a total of 2.5 hours of observations from eclipse start on Earth's west limb to end on the east limb. Both before and after the eclipse, the pendulum experienced normal rotation, the Foucault effect, of 0.19˚/minute. M. Allais was not looking for any effect here [6].

He got similar results when he later repeated the experiment to a much lesser degree during a solar eclipse on October 2, 1959 (the amount of the solar surface eclipsed in Paris was only 36.8% of the surface eclipsed in 1954). Like in the first case a well-defined anomaly was detected in the motion of the paraconical pendulum: its plane of oscillation shifted abruptly. Both were partial eclipses in Paris, the point of observations. Currently accepted physical theory offers no explanation whatsoever for this phenomenon. His finding raises new questions about the nature of such phenomena.

Attempts to confirm Allais's observations upon the behavior of a pendulum during a solar eclipse have met with varied results: some experiments have confirmed the presence of anomalies, while some yielded ambiguous results, and others detected nothing unusual. However none of these trials used a paraconical pendulum according to Allais's design (hangs from a special joint that permits free rotation around the vertical and it can track the Earth's rotation); nor did the experimenters follow Allais's operational procedures or ask his advice on design of the experiments.

Most of this kind of experiments had been performed using other sorts of pendulums or with Foucault's pendulum which gives spectacular effects. Even if they are close, there are essential differences between the Foucault pendulum and the paraconical pendulum with anisotropic support. The paraconical pendulum is short, can turn on itself (capable of rolling in all directions upon a plane horizontal surface), was observed without discontinuity while Foucault pendulum is long, connected to the thread which supports it and has never been observed without discontinuity for the previous experiments. Although difficulties are inherent to a short Allais pendulum, and its movement is a complex phenomenon, difficult to analyze, as long as the pendulum oscillation remains flat, the movement in azimuth of the pendulum oscillation plane is reduced to

the Foucault effect. The experiments of the paraconical pendulum with anisotropic support include totally the Foucault effect.

The deviation of the plane with regard to the plane corresponding to the Foucault effect, at most twenty minutes before the maximum of the eclipse, entailed increases of angular speeds corresponding to the fast variations of azimuth observed. In his book *Anisotropie de l'Espace* [7], who is dedicated to the analysis of the eclipse effect in a more general context, M Allais quotes: "*we can finally notice that the fast variations of azimuth observed from* 11:20 *am to* 12 *am and from* 12:20 *am to* 1 *pm correspond to angular speeds of the order of* 6.2×10^{-5} *and* 7.9×10^{-5} *radian per second which are respectively* 1.13 *and* 1.43 *times the Foucault effect* (*that is* 5.5×10^{-5} *radian per second in the latitude of Saint-Germain's laboratory*). *The strengths involved in the noticed disturbances are thus of the order of magnitude of those who intervene in the Foucault effect*".

This deviation due to the eclipse is interpreted as a kind of antigravitation. While for other pendulums (without free support) the antigravity will manifest itself by a change in the direction of rotation of the plane of oscillation and a lower angular speed of rotation (such as the torsion pendulum of Saxl and Allen in 1970 [8] which leads to the same conclusions as M. Allais), it will manifest itself in the case of the paraconical pendulum by a greater angular speed within the framework of a deviated plane.

The eclipse effect was again observed during the eclipse of the Sun on October 2, 1959. Later, at the University of Jassy (Romania), during the eclipse of the Sun on February 15, 1961, a sudden deviation from the oscillation plane of a Foucault pendulum was observed. The pendulum had oscillated in the same plane until the moment of the deflection. An experiment carried out in China during the 1973 eclipse seemed to confirm an Allais effect, but the experiment was not very conclusive because the protocol did not exclude many biases. Another experiment concerning the eclipse effect was carried out in Mexico City during the eclipse of July 11, 1991. After the maximum of the eclipse, a decrease in the rotational speed of the plane of oscillation was observed. During the total solar eclipse of August 11, 1999, the Allais effect was studied in Bucharest, using two Foucault pendulums. On the occasion of the eclipse, NASA (National Aeronautics and Space Administration) proposed a program to observe the effect. Several universities and laboratories around the world have participated in this program, coordinated by Dr. David Noever, but no in-depth analysis of the results was published. At the same time the phenomenon received the denomination of "Allais effect". Observations in Zambia and Australia between 2001 and 2002 also show anomalies. Eight gravimeters and two pendulums were deployed across six monitoring sites in China for the solar eclipse of July 22, 2009. Although one of the scientists involved described in an interview having observed the Allais effect, no result has been published in any academic journal [5] [6].

Observations of the Allais effect are rare and rather contradictory, not only because of the rarity of such eclipses, but also because no rigorous experimental protocol has been followed. The sometimes ambiguous experimental results

mean that the veracity of the Allais effect remains controversial within the scientific community.

Regarding the experimental results for the eclipse experiment, let's say that since the total solar eclipse of May 29, 1919, proclaimed as the triumph of Einstein's theory, measurements of the deviation of light by the Sun were performed at a number of total eclipses. Although the measurements were difficult, the effect was very close to the predicted magnitude which is double the value obtained from Newtonian mechanics. But exact agreement between theory and measurement has never been achieved. The average of the observations made during eight eclipses between 1919 and 1960 gives a figure of 1.97 for the deviation. This figure, although considered to be one of the proofs of relativity, is higher than the number predicted by the calculation and in a proportion greater than the experimental errors. Several physicists seem to estimate that a deflection 10% greater than the theoretical value is due to observation errors. Rather, we think that this is a real insufficiency of Einstein's theory, and the connection we have made between the Allais effect and the arc residue only strengthens our understanding.

To establish a link between the Allais effect and the anomaly of the arc residues of General Relativity during total solar eclipses, we will not take into account the unexplained regularities of lunisolar periodicity discovered by M. Allais to examine only the sudden and unpredictable disturbance that occurred during the solar eclipse of June 30, 1954, when the Moon interposing itself between the Earth and the Sun acted as a screen against gravity. We will perform the unorthodox calculation which follows by treating the paraconical pendulum as if it were a simple pendulum.

2. Mathematical Treatment

2.1. Gravitational Acceleration during the Disturbance Due to the Eclipse

Let us take a simple pendulum in Paris (49˚N), which can be considered to be a point mass suspended from a string or rod of negligible mass, and suppose this resonant system with a single resonant frequency is with a free anisotropic support. For small amplitudes, the period of such a pendulum can be approximated by

$$T = 2\pi\left(l/g\right)^{1/2} \tag{1}$$

(l: length; gravitational acceleration g in Paris is 9.8094 m/s^2) [9]. The time of a complete revolution of the oscillation plane around the vertical is

$$T = 2\pi/\left(w\sin\theta\right) = 24h/\left(w\sin 49^\circ\right) = 31.8h. \tag{2}$$

As the oscillation plane got up of 13.5˚ (360˚ + 13.5˚ = 373.5˚) with the eclipse, we apply the rule of three to find the time which would take the pendulum in Paris to make the complete rotation of the oscillation plane around the vertical line. If 360˚ = 31.8 hours, 373.5˚ = 32.9925 h. The time would be prolonged of

32.9925 − 31.8 = 1.1925 *h*, or 71.55 mn. It would mean that with the anomaly due to the eclipse (increase of 13.5˚), the time in Paris would be 1.0375 times longer (32.9935/31.8).

Considering that the length *l* of the formula (1) remains the same, the gravitational acceleration due to the eclipse will be

$$\frac{4\pi^2 l}{T^2_{\text{Paris with anomaly}}} = \frac{4\pi^2 T^2_{\text{Paris}} g_{\text{Paris}}}{4\pi^2 1.0375 T^2_{\text{Paris}}} = \frac{g_{\text{Paris}}}{1.0375} = \frac{9.8094}{1.0375} = 9.4548 \text{ m/s}^2 . \quad (3)$$

We notice a decline of the gravitational acceleration: 9.4548 m/s^2 instead of 9.8094 m/s^2 [9].

A decrease of the gravitational acceleration is equivalent to a longer range of the radius. We know that 9.8094 m/s^2 apply to the Earth's radius 6.3776×10^6 m

$$R_E = \left(GM_E/g\right)^{1/2} = \left(G5.98\times10^{24}\text{kg}/9.8094 \text{ m/s}^2\right)^{1/2} . \quad (4)$$

Let us find the terrestrial radius equivalent to a gravitational acceleration of 9.4548 m/s^2:

$$R_E = \left(GM_E/g\right)^{1/2} = \left(G5.98\times10^{24}\text{kg}/9.4548\text{m/s}^2\right)^{1/2} = 6.49608\times10^6\text{m} . \quad (5)$$

The radius is 118,481 m (6.49608×10^6 m − 6.3776×10^6 m). This implies, during the disturbance due to the eclipse, an addition of 118.481 km to the Earth's radius, which gives a gravitational acceleration of 9.4548 m/s^2 in Paris.

2.2. Parallax

The solar parallax in general is the difference in the apparent position of the Sun as seen from the Earth's centre and a point one Earth radius away, *i.e.*, the angle subtended at the Sun by the Earth's mean radius. If the Sun is at the zenith (directly overhead) its parallax is 0. The parallax is at maximum when the Sun is seen on the horizon and it is called the horizontal parallax. Solar parallax is very important since it indicates the Sun's distance from Earth. Foucault, after making a more accurate measurement of the velocity of light, determined from the aberration of star light that the solar parallax must be about 8.80". Michelson and Newcomb, using Foucault's method, found a more accurate velocity of light, which when combined with a better aberration value, gave a solar parallax of 8.80" ± 0.01". The value of 8.80" for the average equatorial horizontal parallax was adopted in Paris in 1896 by the "*Conférence internationale des étoiles fondamentales*". Simply put, the parallax of Sun is the angle ASE under which an observer at the centre of Sun would see the terrestrial radius (**Figure 1**) [10].

We will suppose that during the eclipse the centre of the Sun is the theoretical apparent position of the star. We already know the distance Sun-Earth which is 1.495×10^{11} m. S is the centre of Sun and the angle ASE is the horizontal solar parallax. Because this angle is so short, we can confuse, without sensible error, the Earth radius *r* with the arc AE of 8.80 arcseconds (or 8.80"), which is part of a circumference with centre the centre S of Sun and for radius the length *d*, average distance between the two centres.

The length of arc AE, compared with the entire circumference, is given by the

proportion:

$$\frac{\text{Arc AE}}{2\pi d}=\frac{8.80''}{360^{\circ}}=\frac{r}{2\pi R_{S-E}}=\frac{6.3776\times10^{6}\,\text{m}}{2\pi 1.495\times10^{11}\,\text{m}}=6.789\times10^{-6} \quad (6)$$

The arc AE, or the parallax angle 8.80", is equivalent to the Earth radius 6.3376×10^6 m, and to a gravitational acceleration of 9.8094 m/s^2 $\left[g=GM/R_T^2\right]$. For the gravitational acceleration of 9.4548 m/s^2 at most of the disturbance of the eclipse, corresponding to a radius being 6.49608×10^6 m, we shall obtain the parallax angle 8.9634" (if 6.3776×10^6 m = 8.80" and 6.49608×10^6 m = x; x = 8.9634"). The angle would vary of 0.1634" (8.9634" − 8.80").

If we reverse the parallax as if the Earth was the centre, and as if the radius of the Sun formed an arc length on the circumference having the distance Earth-Sun for radius, we find the same circumference with a tiny increase of the arc length (Figure 2). If we place 0.1634 arcsecond at the point p of minimum approach of the Sun, the minimal distance of approach d, slightly superior to the radius of the Sun, would be exceeded. The point p would pass at p', pushing away the straight line constituting the deviated trajectory of photons, so widening the angle which it makes with the not deviated trajectory of photons emitted by the distant star.

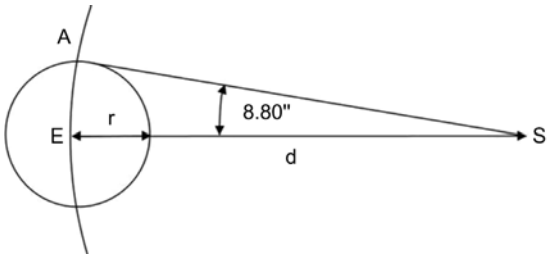

Figure 1. Parallax of the Sun. (E: Earth; S: Sun; r: radius of the Earth; d: the distance of the centers of the two stars; angle ESA: parallax, *i.e.*, the angle under which an observer, placed in the center of the Sun, would see the terrestrial radius. According to the value adopted by the International Conference of Fundamental Stars held in Paris in 1896, the average equatorial horizontal parallax of the Sun is 8".80).

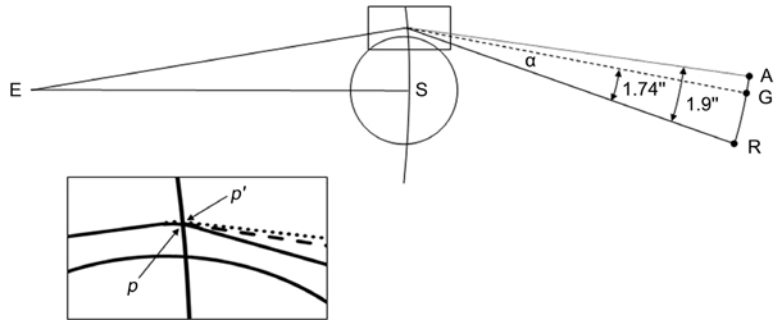

Figure 2. Parallax of the Earth during the solar eclipse where the Allais effect corresponds to the arc residue of General relativity. (E: Earth; S: Sun; R: real star with ray light; G: apparent star in accordance with GR with 1.74 arcseconds for the calculated angle RpG of deviation of rays of light; A: real observations of apparent star during total solar eclipses with ~1.9" for the observed angle Rp'A. The angular difference Gp'A coincides strangely with the brutal disturbance on the Allais pendulum during the total solar eclipse).

This tiny increase of the arc length from p to p', *i.e.* the angle $Gp'A$, constitutes a deviation about 10% of the theoretical value of the Relativity (if 1.7424" = 100%; 0.1634" = 9.37%). We regard this as in satisfactory correspondence with the so-called residual arc, which have been tested by observations made at time of total eclipse on the apparent positions of stars whose light has passed close to the limb of the Sun [11].

2.3. Value Calculated by General Relativity

The value calculated by the theory of relativity of the angle of deviation of light by the Sun is

$$\Delta = 2\alpha = 4GM_S / c^2 R_S \tag{7}$$

(*G is the universal constant of gravitation*; *c is the speed of light*; *M_S is the solar mass and R_S is the Sun's radius* [12]).

$$\begin{aligned} 4GM_S / c^2 R_S &= 4G1.98\times10^{30}\,\text{kg} / \left(c^2 \sim 6.9535\times10^{8}\,\text{m}\right) \\ &= \left(8.4475\times10^{-6}\,rad\right)\times 57^{\circ}295\times 3600" = \sim 1.7424" \end{aligned} \tag{8}$$

2α indicates a deflection of light in the field of an attracting mass which is twice as great as would be calculated from the Newtonian theory for a particle travelling with the velocity of light, which is a huge progress. The factor 2 finds its origin in the existence of a temporal and "spatial" curvature in the metrics of Schwarzschild which represents the spacetime around the Sun. It allows verifying the existence of a deflection of light in passing through the gravitational field in the neighbourhood of the Sun, and to decide between Newtonian or Einsteinian theory [11].

2.4. Value Calculated by the Theory of Relativity by Considering the Allais Effect

The value calculated by the theory of relativity does not foresee nor explain the supplementary residual hundredth of arcsecond which were part of several measurements during eclipse of the bending of starlight by the Sun. No more than it foresees and explains the Allais effect during the total solar eclipse of 1954 when the Moon between Earth and Sun decreased the solar attraction.

The reckoning (6) giving 0.1634 arcsecond starts from a sudden disturbance on the Allais pendulum due to the total eclipse which reveals a decline of gravitational acceleration and consequently a length more remote from the terrestrial attractive centre. This added length, projected by means of the calculation of parallaxes on the circumference having for diameter the centres of the Sun and the Earth, is equivalent to the residual arc observed during experiments on the bending of light by gravity. Both observed phenomena, which arrive simultaneously only in eclipse time and are of the same magnitude, would be owed to the same cause: the antigravity provoked by the eclipse.

If we take into account the Allais disturbance and the residual arc observed during a total eclipse of the Sun, it will be necessary from the theory of relativity

to consider that the point p of minimum approach of the Sun is widened towards the outside and to add $\Delta\alpha$, the residual arc ensuing from the antigravity, to the angle of deviation 2α. From an *ad hoc* point of view, purely observational, and only during eclipses, the Einsteinian formula could be:

$$2\alpha + \Delta\alpha = \left[4GM_S/c^2R_S\right] + \Delta\alpha = 1.7424'' + 0.1634'' = \sim 1.90588''. \quad (9)$$

The angle does not correspond any more to the value calculated by the General theory of Relativity but rather to the average of the observations which gives a 10% deviation wider than the theoretical value (1.74" + (1.74" × 10%) = ~1.916") [13].

Let us underline that most of the experiments of eclipse collected results falling between 1.6" and 2.2". Experimenters found results below 1.74" (between 1.74" and 1.6"), as if there was a kind of overgravity similar to the Pioneer effect. In that case the equation would become

$$2\alpha - \Delta\alpha = \left[4GM_S/c^2R_S\right] - \Delta\alpha = 1.7424'' - \Delta\alpha \quad (10)$$

$\Delta\alpha$ being a fragment of arc going from p towards the centre of the Sun, and which expresses a supplementary gravity due to the eclipse.

The formula of the General Relativity during total eclipse could thus be:

$$2\alpha \pm \Delta\alpha = \left[4GM_S/c^2R_S\right] \pm \Delta\alpha\,. \quad (11)$$

The three *ad hoc* formulae (9) (10) (11), although in compliance with the observations, remain nevertheless profoundly deficient not to say erroneous.

2.5. Discussion

According to General Relativity, a light ray passing in the vicinity of a celestial body undergoes a deflection in the direction of the decreasing gravitational potential, that is turned towards the celestial body itself, deflection of size $2\alpha = 4GM_S/c^2R_S$. We suppose that the speed of light, given by

$$ds^2 = g_{uv}dx_u dx_v = 0\,, \quad (12)$$

equals 0, and that $g_{44}/2$, who plays the gravitational potential role determining the movement of the material point in a gravitational field stipulated almost static, does not vary [14]. At ordinary times, without eclipse, the interferometric experiments practically validated this formula in which α and d are inversely proportional inside the point p (**Figure 2** & **Figure 3**). With a more stressed curvature of light, the deflection angle α becomes wider as much as d, the minimal distance of approach of the centre of the Sun, gets closer to the length of the solar radius. It is the inverse for a lesser curvature.

During a total eclipse, our reckoning from the gravitational disturbance pin down by the pendulum gives a distance d stretched out as well as a widened angle 2α. They are proportional, what seems incomprehensible. By locating 0.1634 arcsecond at p, the minimal distance of approach of the centre of the Sun d, slightly superior to the Sun radius R_S, is surpassed. Point p placed at p', pushes

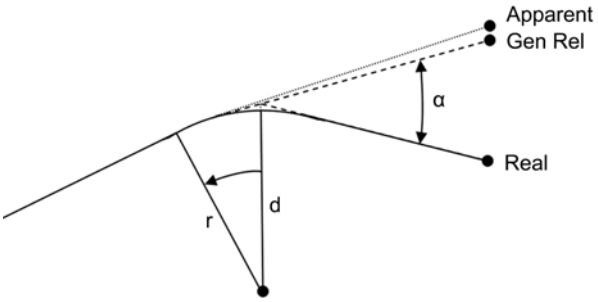

Figure 3. Deflection of a light ray in the vicinity of the Sun. (d is the minimum distance between the trajectory of the light ray and the centre of the Sun and is at a lightly upper distance than the Sun's radius R_S)

away towards the outside the straight line forming the "deviated" trajectory of photons, so widening the angle which it makes with the "not deviated" trajectory of photons emitted by the distant star. This makes the formula inexplicable but the antigravity is implicit [13] [15].

Supposing that the pendulum got an excess of gravity, the calculation would have given a shorter distance d corresponding to a smaller angle 2α, that is going towards 1.6 arcseconds already observed during experiment of eclipse. Here also the distance d would be proportional to the angle 2α.

It is clear that the size d observed during an eclipse is not the same as the theoretical value in normal time and is on average larger. We can suppose that the speed of light would *not equal* any more 0 (12) and that the gravitational potential can vary [15]. With the Allais effect of the 1954 eclipse, a ray of light passing along a celestial body would suffer a deflection on the side of the increasing gravitational potential, which is on the side opposed to the celestial body. The g_{uv} would have varied in an unexpected way. There would have been, in addition to a concavity turned toward the Sun, which means that light rays curve with regard to the system of coordinates, a tiny concavity turned toward the outside, what indicates that starlight rays "straighten" [16]. It seems that from p pointing toward p' the curvature of the space around a big mass such the Sun decreases and that a particle (planet or photon) is solicited according to the Newtonian laws. As if the gravitational potential $GM_S/R_S = c^2$ acquired higher potential during eclipse. As if c^2 becoming v^2 indicated an antigravity, meaning a lighter mass M_S and an increasing "decurve" beyond the point p.

Certainly there is anomaly. The sudden proportionality between the angle α and the distance d during the eclipse means a fundamental change in the interpretation of the expression GM_S/c^2. The factor $(2\alpha + \Delta\alpha)$ plays a role as essential as 2α in the tests of the General Relativity and can only emerge on a new conception of the gravity.

2.6. Formula of GR Altered during Solar Eclipses with Antigravitational Potential

According to General Relativity, light emitted from a source far away from the

Sun and passing near the Sun should be deflected by a theoretical ~1.74 arcseconds (7, 8), and the angle α is inversely proportional to d the minimal distance of approach of the centre of the Sun.

Nevertheless, during total solar eclipse the observational angle is higher than the theoretical one and d should be longer if there a real link between the eclipse and the lower gravity detected on Earth by the pendulum. So, if α and d are higher, and the speed of lightstays the same, the solar mass should be higher. It seems impossible, unless there is an addition of a negative mass ($-\Delta M_S$) which would act apparently as a positive mass. With d higher, the trajectory of the ray of light is divergent outwards. Then the formula should be

$$2\alpha_{obs} = \left[4GM_S\left(1+v^2/c^2\right)^{1/2}\right] \Big/ \left[c^2 R_S\right] \tag{13}$$

$$2\alpha_{obs} = 1.902'' = \left[4G1.98\times10^{30}\,\mathrm{kg}\left(1+v^2/c^2\right)^{1/2}\left(57^{\circ}.29578\times60'\times60''\right)\right] \div \left[c^2\left(6.9535\times10^{8}\,\mathrm{m}\right)\right]$$

$$1.90588''/1.7424'' = 1.09382461 = \left(1+v^2/c^2\right)^{1/2}$$

$$v = \sim 1.33\times10^{8}\,\mathrm{m/s}\,.$$

The Moon plays the role of a negative mass inducing an antigravity. And v^2 of $\left(1+v^2/c^2\right)^{1/2}$ could be considered as an antigravitational potential.

3. Eclipse and Radio Interferometry Measurements

We see that the numbers show that the Allais anomaly is in connection with the observed additional residual arcseconds and that both anomalies arise during a total solar eclipse.

Let us note on one hand that today the measure of these deflections is made by radio interferometry [1] [13] [16]. One of the advantages of this technique is that it can be made every year, by opposition to the measures of eclipse, which are sporadically taken and in inhospitable places.

The development of the interferometric methods in radio astronomy allowed verifying in a very precise way the predictions of Einstein and to impose strong limits on the possible anomalies of the General Relativity. On the other hand, it is strange that since 1919, while the best observations made by Eddington in favour of the value predicted by the General Relativity agreed in approximately 20% near, the measure of about four hundred stars during various eclipses did not allow to improve the precision of this method. The fact is that an exact agreement between theory and measurements has been obtained by radio interferometry but has never been obtained by eclipse technique [2]. The more effective measure with a precision of 0.05 of the bending of light made by radio interferometry inclines scientists to conclude that the General Relativity's value is confirmed, allows to release from eclipse experiences and end of story.

We conclude, on the contrary, that it rather confirms that there is an essential and intrinsic difference between the measures observed during eclipse and those

without eclipse [13] [17] [18]. Our interpretation is that both anomalies result from the same phenomenon revealing an antigravity. The paraconical pendulum, of which the oscillation plane is free to turn all sides at the same time, seems to indicate that the more the anomaly increases the degree of oscillating plane (with regard to the plane corresponding to the Foucault effect), the more the deviated plane escapes the gravitation. The pendulum, and thus the Earth, is "lightened". Within the framework of the General Relativity, the excess of arcsecond would mean that there is "flatness", or a geodesic more remote from the Sun than the theoretical geodesic.

4. Two Manners to Experiment

Others could attribute it to an excess of gravity similar to the Pioneer effect [19]. Although the observational experiments are difficult it is important to compare experiments with total eclipse with other without eclipse for consistency. Fortunately, modern technology is available for such a comparison. The time delay can be measured as well as the arcseconds angles since the delay experienced by light passing a massive object is closely related to the deflection of starlight. Two manners thus offer to experiment to know if there is less or more gravity.

4.1. Measure the Angle of Deflection of Light

We could take the measure of light deflection near the Sun by using the radio interferometry on quasars. For some decades, the effect of deflection of the electromagnetic trajectories by a field of gravitation is determined by radio astronomers by using quasars 3C273 and 3C279. Quasars are, by definition, the best sources of radio energy. The positions of these two very close radio sources are exactly known and well placed to verify the deflection of radio energy by the Sun. On October 8th every year the movement of the Earth in orbit brings the Sun in the line with 3C279, darkening it. According to the prediction of Einstein, 3C279 disappears slightly later and reappears slightly earlier on the remote side from the Sun. The convenient position of 3C373 gives to radio astronomers a reference point to see how the apparent position of 3C279 is changed when it is on the edge of the Sun. Radio astronomers can see the separation angle with time, determine the deflection of light as a function of distance from the Sun and translate that into a deflection of a grazing ray. One can imagine that if ever such a heavenly coincidence could also coincide with a total solar eclipse, the photos taken by radio astronomers could be compared with those without eclipse. By careful analysis of the eclipses measurements they could see if there is in the sky an essential difference of the bending of light [1] [3] [17] [18].

4.2. Measure Signal Delay

Currently the deflection of "light" is best measured using radio astronomy, since radio waves can be measured during the day without waiting for an eclipse of the Sun. Einstein predicts that light will be delayed instead of accelerated when

passing close to the Sun. By using the very precise radar techniques, we could measure the delay of the signals passing near the Sun during a total eclipse and to compare it with the delay obtained without eclipse. A radar impulse is sent from the Earth on a target of the solar system (a planet for example) which reflects this radio signal and sends it back on Earth. The measured round trip travel time of the radio wave has a slightly bigger value according to the General Relativity than according to Newton's theory. The difference is so much greater as the signal passes closer of the Sun. The first experiments used radar echo on planets Venus or Mercury in superior conjunction with the Sun: the wave radio cross, in that case, the field of solar gravitation on the way out and on the way back. It was matching the predicted amount of relativist time delay. The experiments have been repeated many times since, with increasing accuracy. This effect is now given by using a spacecraft behind the Sun instead of a star. Radar echo on space probes Mariner VI and VII who were placed on solar orbits after their observations of Mars, in 1969, gave delay observations which agree with Einstein within ~0.9 standard deviations. This was first done by Irwin Shapiro between 1966 and 1970 [19] [20] [21]. The duration of a radar signal during the eclipse should have shorter value than a delay observation without eclipse, and this shorter delay would go to the sense of an "antigravity". An additional delay during eclipse would mean "overgravity" similar to the Pioneer effect.

5. Possible Cosmological Consequences

We assume that there is a relation between the Allais effect and the not resolute anomaly of residual arc during total solar eclipse. It is evident at this stage that it needs further investigations in order to dissipate the confusion between significant gravitational anomaly and errors of observation, and determine if our calculation is indeed genuine or facility artefact. It must be taken into consideration that if the effects of these anomalies are real and in coincident evidence [22] [23], it gives a new aspect of the Allais effect which could lead at least to three possible cosmological consequences:

5.1. If the Allais Effect Is Real, Gravity Would Be Attractive and Repulsive

GR, based on the equivalence principle, is in an extension of special relativity and Newtonian gravity, but even if it is full of elegance and simplicity it doesn't mean that the theory is in agreement with recent observations (pioneer anomaly, anomaly of the astronomical unit, galaxy rotation curves, etc.) [24] [25]. If the Allais effect is real, gravitation could not be considered any more like a space-time curvature or as only an attractive force. The element "antigravity" would put it to the rank of the other forces which have all an attractive and repulsive aspect. It would be then possible to describe gravity in the framework of quantum field theory like the other fundamental forces.

5.2. The Allais Effect on Cosmological Scales Would Apply to the Gravitational Lenses and to the Distribution of Matter

It is easy to imagine that if the Allais effect is applied to the light-bending effect measured during a total eclipse of the Sun, then there is overwhelming evidence that this effect exists on various scales where eclipses are associated with light following curved paths through space distorted by the presence of matter.

According to GR, mass "warps" space-time to create gravitational fields and therefore bend light as a result. After this theory was confirmed in 1919 during a solar eclipse, Einstein realized that it was also possible for astronomical objects to bend light, and that under the correct conditions, one would observe multiple images of a single source, called a "gravitational lens" or sometimes a "gravitational mirage". It was not until 1979 that the first gravitational lens would be discovered. It became known as the "Twin Quasar" since it initially looked like two identical quasars. In the 1980s, astronomers realized that the combination of CCD imagers and computers would allow the brightness of millions of stars to be measured each night. Gravitational microlensing can provide information on comparatively small astronomical objects, such as Machos within our own galaxy, or extrasolar planets. Strong and weak gravitational lensing of distant galaxies by foreground clusters can probe the amount and distribution of mass, which is dominated by invisible dark matter. Aside from determining how much dark matter they contain, gravitational lensing can also be used to measure the expansion history of the Universe (its size as a function of time since the big bang), which is encoded in Hubble's law [1] [26] [27].

Einstein's GR demonstrates that a large mass can deform spacetime and bend the path of light. So, a very massive object, such as a cluster of galaxies can act as a gravitational lens (deflector). When light passes through the cluster from an object lying behind it, the light is bent and focused to produce an image or images of the source. Viewed from the observer (the Earth), the image may be magnified, distorted, or multiplied by the lens, depending upon the position of the source with respect to the lensing mass. So, let us suppose that a sufficiently visible or invisible massive object is moving between Earth and the deflector, or between the deflector and the source, would not there be an Allais effect?

If the data could be compared, before, during and after, that the massive object travels between us, the gravitational lens and the source, there could be an excessive residual arc of the optic angle due to the antigravity, a divergent angle showing itself by a little less brilliance than foreseen by the Relativity, different images. The Einstein effect, in times of eclipse, should have a slightly lower shift of the spectral lines towards the red (*blueshift*) than in times without eclipse. In case it would be an effect similar to the Pioneer effect (over gravity) we should have a slightly superior movement of the spectral lines towards the red than in a frame without eclipse.

Because on the surface of celestial bodies reigns a field of very intense gravitation and the movements of the lines are considerable, gravitational lensing for

the generalized Relativity is a powerful tool to estimate mass distribution on cosmological scales. But if the additional Allais effect is true, the mass distribution and the interpretation of gravity could be different.

5.3. Eclipse Perturbation Instead of Tidal Friction; Main Witness Becomes Main Culprit

Universal time and the length of day would be subject to variations not only because of the tides, atmospheric circulation, internal effects, but also because of the Allais eclipse effect. Modern research shows that the Earth's rotation has slowed down by a fractional amount over the past 4000 years. The acceleration of the Moon's orbit would be associated with the deceleration of the Earth's rotation.

It is assumed that the Moon in its orbit experiences an outward accelerating effect caused by the friction of lunar and solar tides which slow the Earth's rotation. As the Earth rotates on its axis, it experiences the friction of the tides imposed by the gravitational pull of the Moon and, to a lesser extent, the Sun. This secular acceleration gradually transfers the angular momentum from the Earth to the Moon. As the Earth loses energy and slows down, the Moon gains this energy and its orbital period, as well as its distance from Earth, increases. Measurements over the past 40 years indicate that the Moon's orbit is receding from Earth at a rate of 4 cm per year.

It was on the basis of the Moon-Earth alignments at the time of the ancient eclipses that it was possible to conclude that—as a trend—the Earth's rotation is slowing down. Because a number of ancient eclipses have been collected, contemporary researchers have been able to determine that the daylength in the past was somewhat shorter than the current daylength (86,400 seconds). It seems that during the previous 4000 years the length of the day has gradually grown longer, and it is inferred that the ever increasing length of the day could be attributed to the decelerated rotation of the Earth. The observed lengthening of daylight, a change in the rate of rotation of −0.0018 seconds/century, across four millennia is found to have accumulated in the end a total increase of +0.07 seconds. This increase in the current day length of +0.07 seconds over the ancient days of 4000 years ago means that the rate of Earth's rotation has slowed down by −0.0018 seconds per century. While the indication that daylength has increased by a total of only 0.07 seconds over the past 4000 years may appear minimal, it is nonetheless significant; the accumulation of longer days, produced by a diminishing rotation, causes, after millennia, a noticeable change [28] [29].

It is thus assumed that the Moon in its orbit experiences an acceleration effect due to lunar and solar tides friction slowing down Earth's spin. The wave of tide lifting waters of oceans, moves the other way around of the rotation of the Earth; so it produces a friction which slows down the rotation. At the same time, the Moon undergoes a counteraction to that of the tide and goes away constantly from the Earth. However things seem more complicated than supposed. The

vertical constituent of the force of Newton's static theory produces only an insignificant disturbance. The horizontal constituent of the force of the dynamic theory produces more impressive effects on the liquid masses but the influence of the oceanic friction can only be considered in the regions of weak depth and strong tides, what is the exception rather than the rule. Furthermore the atmospheric tides in resonance with the present period of rotation tend to accelerate the rotation and to compensate for the braking due to the oceanic tides. Thus no absolute conclusion can be formulated and it would be possible that this theory contributes only very partially to the slowing down of the Earth [14] [30] [31].

Our suggestion is that the slowing rotation of the Earth, the increasing length of the day associated to the wider lunar orbit, are above all caused by eclipses instead of tidal friction. In this respect we suggest to examine in depth the Allais eclipse effect [32]. It could reveal that mechanisms of "antigravity" could produce "cosmological leaps" and "cosmological leap seconds" (different from "leap seconds" filling the split between the Earth's rotation second and the atomic clock second) and be so the main cause of the deceleration in the Earth's spin rate and, simultaneously, of the receding of the Moon. The listed total solar eclipses were always the only historic *witnesses* of the non-uniform change of rate of the rotation of Earth and of the day length. More than witness of the changes in Earth's dynamical behaviour, we think that eclipse could be also considered as *perpetrator* if the eclipse records and the Allais effect were scientifically investigated. Eclipse would have acted like a pyromaniac who, having lit a long series of fires, hurries to indicate every fire to the authorities who, in turn, use him as unique witness for the prosecution against possible suspects.

6. Conclusions

Does the relationship between the Allais effect and the higher displacement than predicted by GR of the positions of star images during solar eclipse a simple hypothesis, or is it a consequence of the observation at the time of the total eclipse? We think that it is a consequence of the observational results at the time of the total eclipse and the measurements suggest that both anomalous phenomena have a common origin. Our approach to relating the two anomalies was first to calculate the gravitational acceleration in Paris during the disturbance caused by the total solar eclipse of June 30, 1954, starting from the plane of oscillation of the paraconical pendulum of M. Allais which rose 13.5 degrees. Then find the Earth's radius equivalent to this abnormal gravitational acceleration. Using the average horizontal parallax of the Sun which is 8.80" of arc, we find that the abnormal addition to the Earth's radius during the eclipse is equivalent to a parallax angle that would vary by 0.1634". By reversing the parallax, we find the same circumference for the Sun with an excess of arc. It just so happens that 0.1634" corresponds to the deviation of about 10%, that is to say to the arc residue verified during total eclipse experiments and which is beyond the experimental errors.

Scientific history seems to want to repeat itself. When the GR predicted for the deflection of starlight just grazing the edge of the Sun an angular distance of 1.74", or two times the Newtonian prediction, the question of the precise value of the deviation became a matter of principle which had to allow choosing between both theories. The Relativity took it. Today, the Allais effect and the anomaly of residual arc during total solar eclipse persuade us that it is not the complete story. The observed 1.97" for the deviation is higher than the number predicted by the calculation and in a proportion superior to the experimental errors. And, as we tried to demonstrate, the unexplained arcseconds excess of these experiments would be in concomitance and accordance with the abrupt deviation of the plane of oscillation of the Allais pendulum with regard to the plane corresponding to the Foucault effect. GR does not explain the anomaly of the arc residue during total eclipses, which suggests that it is conceptually incomplete and that some substantive work needs to be done. We do not hesitate to assert that these confirmed experiences and these collected figures call into question the interpretation of GR and once again question our conception of the Universe.

Conflicts of Interest

The author declares no conflicts of interest regarding the publication of this paper.

References

[1] Bouquet, A. (1998) L'Univers de la Gravitation. Science & Vie, No. 205, Hors-Série, 86-89.

[2] Born, M. (1962) Einstein's Theory of Relativity. Dover Publications Inc., Mineola, 358-359.

[3] Will, C.M. (1986) Was Einstein Right? Basic Books Inc., New York, 72-80, 82-86.

[4] Science@ NASA (1999) Decrypting the Eclipse. http://science.nasa.gov/newhome/headlines/ast06aug99_1

[5] Wikipedia, Allais Effect. http://en.wikipedia.org/wiki/Allais_effect

[6] Science du Monde (1969) La Gravité. Librairie Jules Tallandier et Nelson Doubleday Inc., 36-37.

[7] Allais, M. (1997) L'Anisotropie de l'Espace. Edition Clément Juglar, 91, 162-164, 171-175.

[8] Saxl, E.J. and Allen, M. (1971) *Physical Review D*, **3**, 823. https://doi.org/10.1103/PhysRevD.3.823

[9] Resnick-Halliday (1979) Mécanique. Édition du renouveau pédagogique, 308, 309, 315, 362, 16-3 No. 6.

[10] Simard, H. (1916) Cours élémentaire de Cosmographie. Laflamme et Proulx, Quebec, 114-119.

[11] Tolman, R.C. (1987) Relativity Thermodynamics and Cosmology. Dover Publications, Inc., Mineola, 209-211.

[12] Rocard, J.-M. (1986) Newton et la Relativité, Que sais-je? Presse universitaire de

France, Paris, 105-106.

[13] Pascoli, G. (1986) La Gravitation, Que sais-je? Presse universitaire de France, Paris, 43-45.

[14] Öpik, E.J. (1960) Initiation à l'astronomie, Petite Bibliothèque Payot. 66-67, 25-29, 39-40, 43-44.

[15] Balabar, F. (2002) Albert Einstein, Physique, Philosophie, Politique. Édition du Seuil, 326-327, 356-359, 363-365.

[16] Einstein, A. (1952) The Principle of Relativity. Dover Publications Inc., Mineola, 107-108.

[17] Mavridès, S. (1988) La Relativité, Que sais-je? Presse universitaire de France, Paris, 118-120.

[18] Nottale, L. (1994) L'Univers et la Lumière, Champs Flammarion. 188-190.

[19] Shapiro, I.I., *et al.* (1977) *Journal of Geophysical Research*, **82**, 4329-4334. https://doi.org/10.1029/JS082i028p04329

[20] Calder, N. (1980) Einstein's Universe. Penguin Books, New York, 105-107.

[21] Wright, E.L. (2004) Deflection and Delay of Light. http://Astro.ucla.edu/~wright/deflection-delay.html

[22] Aujard, H. (2001) 21*st Century Science & Technology*, **14**, 70. http://www.21stcenturysciencetech.com

[23] Duif, C.P. (2004) A Review of Conventional Explanations of Anomalous Observations during Solar Eclipses.

[24] Unzicker, A. (2008) Why Do We Still Believe in Newton's Law? Facts, Myths and Methods in Gravitational Physics.

[25] Amador, X.E. (2006) Review on Possible Gravitational Anomalies.

[26] Wikipedia, Gravitational Lenses. http://en.wikipedia.org/wiki/gravitational_lens

[27] Gribbin, J. and Rees, M. (1989) Cosmic Coincidences. Bantam Books, New York, 212-213.

[28] Steel, D. (1999) Eclipse. Headline Book Publishing, London, 141-152.

[29] Espenak, F. and Meeus, J. (2006) Five Millennium Canon of Solar Eclipses: −1999 to +3000. NASA Technical Publication TP-2006-214141. http://Eclipse.gsfc.NASA.gov/eclipse

[30] Bouteloup, J. (1968) Vagues, marées, courants marins, Que sais-je? Presses universitaires de France, Paris, 61-64.

[31] Rouch, J. (1961) Les Marées, Payot, Paris, Bibliothèque Scientifique, 70, 214-216.

[32] Oberg, E. (2007) Location of the Allais Effect on the Earth's Surface: A Hypothetical Field Model, Note 2.

Journal of Modern Physics, 2020, 11, 1639-1648
https://www.scirp.org/journal/jmp
ISSN Online: 2153-120X
ISSN Print: 2153-1196

The Dirac Propagator for One-Dimensional Finite Square Well

P. Kongkhuntod, N. Yongram

Department of Physics, Faculty of Science, Naresuan University, Phitsanulok, Thailand
Email: phonphimonk61@nu.ac.th, nattapongy@nu.ac.th

How to cite this paper: Kongkhuntod, P. and Yongram, N. (2020) The Dirac Propagator for One-Dimensional Finite Square Well. *Journal of Modern Physics*, **11**, 1639-1648.

https://doi.org/10.4236/jmp.2020.1110102

Received: August 28, 2020
Accepted: October 23, 2020
Published: October 26, 2020

Abstract

The solution of Dirac particles confined in a one-dimensional finite square well potential is solved by using the path-integral formalism for Dirac equation. The propagator of the Dirac equation in case of the bounded Dirac particles is obtained by evaluating an appropriate path integral, directly constructed from the Dirac equation. The limit of integration techniques for evaluating path integral is only valid for the piecewise constant potential. Finally, the Dirac propagator is expressed in terms of standard special functions.

Keywords

Path-Integral, Dirac Equation, Dirac Propagator, Finite Square Well

1. Introduction

The solution of quantum mechanical problems in non-relativistic Schrödinger and relativistic Dirac equation with a finite square well potential which were conceptually very relevant for our understanding about 80 years ago seem to be no longer of primary importance. Occasionally, however, there is a new line of inquiry into this problem typically by applying new mathematical technique [1–5]. Moreover the finite square well potential is of great practical importance since it forms the basis for understanding low-dimensional structures such as quantum well devices.

For relativistic quantum mechanics, the problem of a Dirac particle confined in a finite square well potential is a useful tool to discuss, in advanced quantum mechanics courses. The issues arise when one extends quantum mechanics to incorporate special relativity. In a series of papers [6, 7] titled "The Relativistic One-Dimensional Square Potential" and the textbooks of Relativistic Quantum Mechanics [8] the problem of relativistic spin-$\frac{1}{2}$ particle (or Dirac particle) confined in a finite square well potential is studied by solving the one-dimensional Dirac equation. It is surprising that this problem has not been solved

using path integral approach despite the fact that one can do so for the non-relativistic counterpart, for example Nevels *et al.* [9] evaluated the path integral when a spinless particle encounters an infinite potential barrier, Janke and Kleinert [10] exhibited the path integral for particle in a box (infinite square well), Goodman [11] solved the problem of the infinite squarewell potential in one dimension using the path integral, and Barut and Duru [12] evaluated the exact path integral for the propagator for square potential barriers in one dimension and for the radial square-well potential in two dimensions. Here we will solve the problem of Dirac particle confined in a finite square well potential via the path integral for Dirac equation.

It is fair to say that the Dirac equation and its propagator are more fundamental concepts than the Schrödinger equation and its propagator. There have been attempts to write down a path integral expression for the Dirac propagator similar to the Feynman path integral expression for the Schrödinger propagator. For example Riazanov [13] showed that the Feynman path integral is identical to the propagation function of the Dirac equation. Papadopoulos and J. T. Devreese [14] obtained the Dirac propagator through the Feynman path integral [15–18], directly constructed from the Dirac equation. Gaveau and Schulman [19] constructed path integral formula for the Dirac propagator in three spatial dimensions, called the "projector path" summation, which is one of a generalization of the Feynman "checkerboard" propagator [18]. Rosen [20] discovered that the Feynman path summation for the one-dimensional Dirac equation can be projected into three spatial dimensions to yield a path-summation formula for physical spin-$\frac{1}{2}$ particles of nonzero 2 mass. Since the three-space projection matrix is independent of time and does not involve the particle's mass, relativistic motion governed by the Dirac equation has an underlying one-dimensional aspect.

The purpose of the present paper is to write down the Dirac propagator for Dirac particles confined in a one-dimensional square well potential of depth $V_0 \leq 0$ and width a. The organization of the rest of the paper is as follows: In Section 2 we evaluate the propagator of the Dirac particle in a square well. Finally, we summarize our results in Section 3.

2. Dirac Propagator for a One-Dimensional Square Well

This section deals with the construction and the evaluation of the propagator of Dirac particles confined in an one-dimensional finite square well potential of depth $V_0 \leq 0$ and width a. The one-dimensional Dirac Hamiltonian for the motion in one dimension under the influence of square well potential is

$$H = H_0 + V(x) \tag{1}$$

where

$$H_0 = -\mathrm{i}c\hbar\alpha_x \frac{\partial}{\partial x} + m_0c^2\beta \tag{2}$$

is the free particle Hamiltonian, the matrix α_x is

$$\alpha_x = \begin{pmatrix} 0 & \sigma_x \\ \sigma_x & 0 \end{pmatrix} \tag{3}$$

where the Pauli matrix $\sigma_x = \begin{pmatrix} 0 & 1 \\ 1 & 0 \end{pmatrix}$, the matrix β is

$$\beta = \begin{pmatrix} \mathbf{1} & 0 \\ 0 & -\mathbf{1} \end{pmatrix} \tag{4}$$

where $\mathbf{1} = \begin{pmatrix} 1 & 0 \\ 0 & 1 \end{pmatrix}$ is identity 2×2 matrix, and $V(x)$ denotes square well potential

$$V(x) = \begin{cases} -V_0, & \text{for } -a/2 < x < a/2 \\ 0 & \text{for } x \leq -a/2, x \geq a/2 \end{cases} \tag{5}$$

The propagator $K(x_b, t_b; x_a, t_a)$ satisfies the Dirac equation

$$\left(\mathrm{i}\hbar \frac{\partial}{\partial t} - H \right) K = 0 \tag{6}$$

The short-time propagator of the above equation is given by

$$K(x_j, t_{j-1} + \varepsilon; x_{j-1}, t_{j-1}) = \exp\left(-\frac{\mathrm{i}}{\hbar} H\varepsilon \right) I_4 \delta(x_j - x_{j-1}) \tag{7}$$

where I_4 is the 4×4 identity matrix.

The finite-time propagator can be constructed via the composition law

$$\begin{aligned} K(x_b, t_b; x_a, t_a) = \lim_{\varepsilon \to 0} \Bigg[& \int_{-a/2}^{a/2} \prod_{j=1}^{N-1} \mathrm{d}x_j \prod_{j=1}^{N} K(x_j, t_{j-1} + \varepsilon; x_{j-1}, t_{j-1}) \\ & + \int_{-\infty}^{-a/2} \prod_{j=1}^{N-1} \mathrm{d}x_j \prod_{j=1}^{N} K_0(x_j, t_{j-1} + \varepsilon; x_{j-1}, t_{j-1}) \\ & + \int_{a/2}^{\infty} \prod_{j=1}^{N-1} \mathrm{d}x_j \prod_{j=1}^{N} K_0(x_j, t_{j-1} + \varepsilon; x_{j-1}, t_{j-1}) \Bigg] \end{aligned} \tag{8}$$

This is the propagator for Dirac particles confined in an one-dimensional finite square well, then, each integral is limited to the domain $-a/2 < x < a/2$, otherwise the propagators for free Dirac particles are taken into account, and allows all imaginable paths, including those with velocities greater than that of light. It seems like the principles of relativistic mechanics is being violated. However, the situation is similar to that of nonrelativistic quantum mechanics in which the non-classical paths are allowed.

The first term on right-hand side (RHS) of (8) depends only on the short-time propagator

$$\begin{aligned} K(x_j, t_{j-1} + \varepsilon; x_{j-1}, t_{j-1}) &= x_j | \exp\left(-\frac{\mathrm{i}}{\hbar} \varepsilon H \right) | x_{j-1} \\ &= x_j | \exp\left(-\frac{\mathrm{i}}{\hbar} \varepsilon H_0 - \frac{\mathrm{i}}{\hbar} \varepsilon V(x_j) \right) | x_{j-1} \end{aligned} \tag{9}$$

It can be approximate up to the order of $O(\varepsilon^2)$ using Zassenhaus formula [21–24]. Equation (9) becomes

$$K(x_j, t_{j-1}+\varepsilon; x_{j-1}, t_{j-1}) = x_j|\mathrm{e}^{-\frac{\mathrm{i}}{\hbar}\varepsilon H_0}|x_{j-1}\mathrm{e}^{-\frac{\mathrm{i}}{\hbar}\varepsilon V(x_j)}$$
$$= K_0(x_j, t_{j-1}+\varepsilon; x_{j-1}, t_{j-1})\ \mathrm{e}^{-\frac{\mathrm{i}}{\hbar}\varepsilon V(x_j)} \tag{10}$$

It is important to observe the order of the various $K_0(x_j, t_{j-1}+\varepsilon; x_{j-1}, t_{j-1})$ in (10); they are noncommuting matrices and their time ordering relates to the way a given spinor evolves according to the Dirac dynamics.

The Dirae equation, being of first order in time, enables one to write a short-time free propagator $K_0(x_j, t_{j-1}+\varepsilon; x_{j-1}, t_{j-1})$ in terms of the infinitesimal generator $[I_4 - (\mathrm{i}/\hbar)\varepsilon H_0]$ as

$$K_0(x_j, t_{j-1}+\varepsilon; x_{j-1}, t_{j-1}) = \left(I_4 - \frac{\mathrm{i}}{\hbar}\varepsilon H_0\right)\delta(x_j - x_{j-1}) \tag{11}$$

The expression (11) can also be obtained by expanding the exact expression for the propagator to the first order in time.

By operating $I_4 - \frac{\mathrm{i}}{\hbar}\varepsilon H_0$ on the Fourier representations of δ-functions, the short-time free propagator becomes

$$K_0(x_j, t_{j-1}+\varepsilon; x_{j-1}, t_{j-1})$$
$$= \int \left[I_4 - \frac{\mathrm{i}}{\hbar}\varepsilon\left(c\hbar\alpha_x k_j + m_0c^2\beta\right)\right] \times \exp[\mathrm{i}k_j(x_j - x_{j-1})]\frac{\mathrm{d}k_j}{2\pi} \tag{12}$$

Here we also use the fact that H_0 does not operate on $V(x_j)$ because it is a constant potential.

Inserting (10) and (12) into (8) and making use of isomeric time partitions, *i.e.*, all ε of the Nth partition will be taken equal to ε/N, we obtain for the finite-time propagator the expression

$$K(x_b, t_b; x_a, t_a)$$
$$= \lim_{N\to\infty}\frac{1}{(2\pi)^N}\left[\int_{-a/2}^{a/2}\prod_{j=1}^{N-1}\mathrm{d}x_j\prod_{j=1}^{N}\mathrm{d}k_j\kappa_j\exp\left(-\frac{\mathrm{i}}{\hbar}\frac{\varepsilon V(x_j)}{N}\right)\right.$$
$$\left.+\int_{-\infty}^{-a/2}\prod_{j=1}^{N-1}\mathrm{d}x_j\prod_{j=1}^{N}\mathrm{d}k_j\kappa_j + \int_{a/2}^{\infty}\prod_{j=1}^{N-1}\mathrm{d}x_j\prod_{j=1}^{N}\mathrm{d}k_j\kappa_j\right]\mathrm{e}^{\mathrm{i}k_j(x_j - x_{j-1})} \tag{13}$$

where κ_j is a 4×4 matrix given by

$$\kappa_j = I_4 - \frac{\mathrm{i}}{\hbar}\frac{\varepsilon}{N}\left(c\hbar\alpha_x k_j + m_0c^2\beta\right) \tag{14}$$

Again it should be noted that as far as (13) is concerned the order of the κ_j matrices is important. Equation (13) is already a form of the path integral giving the propagator of the Dirac particle under the influence of a potential $V(x)$. The summation over all paths starting from x_a at time t_a and ending at position x_b at time t_a is attained through the infinitely multiple process of integration.

The integrations over various k_j's are essentially path summations in momentum space. However, one would like to express the summation in term of paths in configuration space. This is easily done in the following manner: the short-time propagators entering the process of multiple integration need only be taken to the first order in ε/N. If we replace $-\mathrm{i}ck_j\varepsilon/N$ in (13) by $[\exp(-\mathrm{i}ck_j\varepsilon/N)-1]$ and put the resulting κ_j in (12), the limit as $N\to\infty$ will not be affected. With the above replacement we are able to perform the integrations, and the resulting path integral in terms of configuration paths alone is given by

$$\begin{aligned} &K(x_b,t_b;x_a,t_a)\\ &=\lim_{N\to\infty}\left[\int_{-a/2}^{a/2}\prod_{j=1}^{N-1}\mathrm{d}x_j\exp\left[-\frac{\mathrm{i}}{\hbar}\frac{\varepsilon}{N}V(x_j)\right]+\int_{-\infty}^{-a/2}\prod_{j=1}^{N-1}\mathrm{d}x_j\right.\\ &\quad\left.+\int_{a/2}^{\infty}\prod_{j=1}^{N-1}\mathrm{d}x_j\right]\left\{\left[I_4-\alpha_x-\frac{\mathrm{i}}{\hbar}\frac{\varepsilon}{N}m_0c^2\beta\right]\delta\left(x_j-x_{j-1}\right)\right.\\ &\quad\left.+\alpha_x\delta\left(x_j-x_{j-1}-c\frac{\varepsilon}{N}\right)\right\} \end{aligned} \tag{15}$$

This propagator is valid for piecewise constant potential. The product of the various short-time propagators in (15) is ordered from right to left in increasing order of time.

We found that the difficulties in evaluating the integrand (15) are now obvious; the Gaussian integrals cannot be evaluated in closed form if them are restricted to a bounded domain. We repeat the integration of (8) with additional following term

$$\begin{aligned} &\int_{-a/2}^{a/2}\prod_{j=1}^{N-1}\mathrm{d}x_j\prod_{j=1}^{N}K_0(x_j,t_{j-1}+\varepsilon;x_{j-1},t_{j-1})\\ &-\int_{-a/2}^{a/2}\prod_{j=1}^{N-1}\mathrm{d}x_j\prod_{j=1}^{N}K_0(x_j,t_{j-1}+\varepsilon;x_{j-1},t_{j-1}) \end{aligned} \tag{16}$$

We can rewrite the propagator in (8) as

$$K(x_b,t_b;x_a,t_a)=K_0(x_b,t_b;x_a,t_a)+\delta K(x_b,t_b;x_a,t_a) \tag{17}$$

The first term in (17) is the free propagator (see also Ref. [14])

$$\begin{aligned} K_0(x_b,t_b;x_a,t_a)=&\int\frac{1}{2}\left(I_4+\frac{H_0(k)}{E(k)}\right)\mathrm{e}^{\left[\mathrm{i}k(x_b-x_a)-\frac{\mathrm{i}}{\hbar}E(k)\varepsilon\right]}\frac{\mathrm{d}k}{2\pi}\\ &+\int\frac{1}{2}\left(I_4-\frac{H_0(k)}{E(k)}\right)\mathrm{e}^{\left[\mathrm{i}k(x_b-x_a)+\frac{\mathrm{i}}{\hbar}E(k)\varepsilon\right]}\frac{\mathrm{d}k}{2\pi} \end{aligned} \tag{18}$$

which contains the states of positive energy, $E(k)$, in the first term and the states of negative energy, $-E(k)$, in the second term. This propagation of a given spinor both types of states enter the procedure, in general.

For the second term is the propagator due to square well potential,

called the perturbed propagator δK, reads

$$\delta K(x_b,t_b;x_a,t_a)=\lim_{N\to\infty}\frac{1}{(2\pi)^N}\int_{-a/2}^{a/2}\prod_{j=1}^{N-1}\mathrm{d}x_j\prod_{j=1}^{N}\mathrm{d}k_j\kappa_j \times \mathrm{e}^{\mathrm{i}k_j(x_j-x_{j-1})}\left[\mathrm{e}^{-\frac{\mathrm{i}}{\hbar}\frac{\varepsilon}{N}V(x_j)}-1\right] \tag{19}$$

To evaluate (19) we rearrange the exponential terms in the form $\exp \mathrm{i}(k_j-k_{j+1})x_j$, where $j=1,2,\ldots,N-1$. We can then integrate the various exponential term over x_j using the identity

$$\int_{-a/2}^{a/2}\mathrm{d}x\mathrm{e}^{ibx}=\frac{2\sin[b(a/2)]}{b} \tag{20}$$

resulting in the product of sine functions and two plane wave as

$$\frac{\sin\left[(k_{N-1}-k_N)\frac{a}{2}\right]}{(k_{N-1}-k_N)}\frac{\sin\left[(k_{N-2}-k_{N-1})\frac{a}{2}\right]}{(k_{N-2}-k_{N-1})}\cdots\frac{\sin\left[(k_2-k_3)\frac{a}{2}\right]}{(k_2-k_3)} \times\frac{\sin\left[(k_1-k_2)\frac{a}{2}\right]}{(k_1-k_2)}\exp[(\mathrm{i}k_Nx_N-\mathrm{i}k_1x_0)] \tag{21}$$

These integrations do not include the potential term becuase we set $V(x)=-V_0$ which is just a constant.

Then integrating over k_j when $j=1,...,N-1$ and setting $x_0=x_a$, $x_N=x_b$, $k_N=k$, Equation (19) becomes

$$\delta K(x_b,t_b;x_a,t_a)=\lim_{N\to\infty}\int\left[I_4-\frac{\mathrm{i}}{\hbar}\left(c\hbar\alpha_xk+m_0c^2\beta\right)\frac{\varepsilon}{N}\right]^N \times\exp[\mathrm{i}k(x_b-x_a)]\left[\exp\left(\frac{\mathrm{i}}{\hbar}\varepsilon V_0\right)-1\right]\frac{\mathrm{d}k}{2\pi} \tag{22}$$

The limit as $N\to\infty$ can now be taken and leads to

$$\delta K(x_b,t_b;x_a,t_a)=\int\exp\left[-\frac{\mathrm{i}}{\hbar}\left(c\hbar\alpha_xk+m_0c^2\beta\right)\varepsilon\right] \times\exp[\mathrm{i}k(x_b-x_a)]\left[\exp\left(\frac{\mathrm{i}}{\hbar}\varepsilon V_0\right)-1\right]\frac{\mathrm{d}k}{2\pi} \tag{23}$$

By replacing the operator $-\mathrm{i}\hbar\partial/\partial x$ in the free Dirac Hamiltonian H_0 with $\hbar k$, the free Dirac Hamiltonian in momentum vaiable is $H_0(k)=c\hbar\alpha_xk+m_0c^2\beta$. With the aid of the anticommutation relations of the matrices α_x and β, it is easy to show that $H_0^2(k)=[(c\hbar k)^2+(m_0c^2)^2]I_4=(E(k))^2$, where $E(k)$ will denote the positive root as $E(k)=+\left[(c\hbar k)^2+m_0^2c^4\right]^{1/2}$.

Next, with the aid of the first term of an exponential in (23) we are able to write

$$\exp\left(-\frac{\mathrm{i}}{\hbar}H_0\varepsilon\right)=\cos\left[\frac{1}{\hbar}E(k)\varepsilon\right]I_4-\mathrm{i}\sin\left[\frac{1}{\hbar}E(k)\varepsilon\right]\frac{H_0(k)}{E(k)} \tag{24}$$

Equation (24) inserted into (23) gives an expression for the required propagator

$$\delta K(x_b,t_b;x_a,t_a)=\int\left\{\cos\left[\frac{1}{\hbar}E(k)\varepsilon\right]I_4-\mathrm{i}\sin\left[\frac{1}{\hbar}E(k)\varepsilon\right]\frac{H_0(k)}{E(k)}\right\}\times\exp[\mathrm{i}k(x_b-x_a)]\left[\exp\left(\frac{\mathrm{i}}{\hbar}\varepsilon V_0\right)-1\right]\frac{\mathrm{d}k}{2\pi}\tag{25}$$

Clearly, (25) satisfies the bounded particles Dirac equation and at the same time as $t_b\to t_a$, it goes to $I_4\delta(x_b-x_a)$. It can therefore propagate any spinor given at $t_b=t_a$ evolving then via the Dirac equation. The matrix structure of the propagator this is in a simple form since it only depends linearly on the off-diagonal matrix $H_0(k)$.

We shall now put (25) into a more transparent form, as far as the energy spectrum is concerned. To this end we just decompose the trigonometric functions into their combinations of exponentials. We have

$$\begin{aligned}&\delta K(x_b,t_b;x_a,t_a)\\&=\left[\int\frac{1}{2}\left(I_4+\frac{H_0(k)}{E(k)}\right)\mathrm{e}^{\left[\mathrm{i}k(x_b-x_a)-\frac{\mathrm{i}}{\hbar}E(k)\varepsilon\right]}\frac{\mathrm{d}k}{2\pi}\right.\\&\quad\left.+\int\frac{1}{2}\left(I_4-\frac{H_0(k)}{E(k)}\right)\mathrm{e}^{\left[\mathrm{i}k(x_b-x_a)+\frac{\mathrm{i}}{\hbar}E(k)\varepsilon\right]}\frac{\mathrm{d}k}{2\pi}\right]\left[\mathrm{e}^{\frac{\mathrm{i}}{\hbar}\varepsilon V_0}-1\right]\end{aligned}\tag{26}$$

By substituting (14) and (26) into (17), we obtain the propagator for Dirac particles confined in an one-dimensional finite square well potential as

$$\begin{aligned}&K(x_b,t_b;x_a,t_a)\\&=\int\frac{1}{2}\left(I_4+\frac{H_0(k)}{E(k)}\right)\mathrm{e}^{\left[\mathrm{i}k(x_b-x_a)-\frac{\mathrm{i}}{\hbar}[E(k)-V_0]\varepsilon\right]}\frac{\mathrm{d}k}{2\pi}\\&\quad+\int\frac{1}{2}\left(I_4-\frac{H_0(k)}{E(k)}\right)\mathrm{e}^{\left[\mathrm{i}k(x_b-x_a)-\frac{\mathrm{i}}{\hbar}[-E(k)-V_0]\varepsilon\right]}\frac{\mathrm{d}k}{2\pi}\end{aligned}\tag{27}$$

In (27), we say that the propagator for bounded particles with potential $-V_0$ are obtained from the free propagator by the subsitution $\pm E\to\pm E-V_0$. In this case no spin-flip occurs at the border of the well. The allowed energies can take all values from $-\infty$ up to ∞, so that we can describe particles as well as antiparticles.

By performing the integrations over k and making use of the functions $\varphi(x^0,\lambda)$

$$\varphi(x^0,\lambda)=\begin{cases}\dfrac{1}{2\mathrm{i}}N_0(m\sqrt{\lambda})-\frac{1}{2}E(x^0)J_0(m\sqrt{\lambda}) & \text{for } \lambda>0\\[2ex] \dfrac{\mathrm{i}}{\pi}K_0(m\sqrt{-\lambda}) & \text{for } \lambda<0\end{cases}\tag{28}$$

with $m=m_0c/\hbar$, $x^0=c\varepsilon$, $\varepsilon=t_b-t_a$, $r=|x_b-x_a|$, $\eta=(1-V_0/E(k))$ and $\lambda=(\eta x^0)^2-r^2$, defined in Bogoliubov and Shirkov [25]. The Dirac propagator for Dirac particles confined in an one-dimensional finite square well potential is thus

$$
\begin{aligned}
&K(x_b,t_b;x_a,t_a)\\
&=\frac{1}{2}\left[I_4\frac{\partial}{\partial x^0}-\alpha_x\frac{\partial}{\partial r}-\mathrm{i}m\beta\right]\left[\frac{1}{4\pi}\frac{\partial}{\partial r}\left\{\varphi(x^0,\lambda)+\varphi^*(x^0,\lambda)\right\}\right]\\
&=\frac{1}{2}\left[I_4\frac{\partial}{\partial x^0}-\alpha_x\frac{\partial}{\partial r}-\mathrm{i}m\beta\right]\\
&\quad\left[\frac{1}{2\pi}E(x^0)\delta(\lambda)-\frac{m}{4\pi\sqrt{-\lambda}}\theta(\lambda)E(x^0)J_1(m\sqrt{\lambda})\right] \qquad (29)
\end{aligned}
$$

3. Conclusion

This paper applied the path-integral formalism to solve the Dirac equation of Dirac particles confined in a one-dimensional finite square well potential of depth $V_0 \leq 0$ and width a. The Dirac propagator which is obtained by evaluating an appropriate path integral, directly constructed from the Dirac equation, is expressed in terms of standard special functions as in Equation (29). We note that the limit of this technique for evaluating the propagator is only valid for a square well potential, which is a piecewise constant potential. For a more general potential new technique is needed. One possible direction is to write down the path integral for the special wave equation associated with the Dirac equation instead of writing down the path integral directly [14].

Acknowledgements

The work of Phonphimon Kongkhuntod and Nattapong Yongram has been supported by the Faculty of Science Funding. We would like to thank Asst. Prof. Dr. Sikarin Yoo-Kong for discussions and guidance. We would like to thank Dr.Watee Srinin for discussions, guidance and manuscript preparation. We also would like to thank Sujin Wangsuya for discussions and comments. Finally, we would like to acknowledge with thanks the Department of Physics, Naresuan University, Phitsanulok, Thailand, for its kind hospitality.

Conflicts of Interest

The authors declare no conflicts of interest regarding the publication of this paper.

References

[1] Ciftja, O. and Johnston, B. (2019) *European Journal of Physics*, **40**, Article ID: 045402. https://doi.org/10.1088/1361-6404/ab1a61

[2] Ewa, I.I., Howusu, S.X.K. and Lumbi, L.W. (2019) *Physical Science International Journal*, **22**, 1-9. https://doi.org/10.9734/psij/2019/v22i330134

[3] Al-Ani, L.A. and Abid, R.K. (2019) *Al-Nahrain Journal of Science*, **22**, 52-58. https://doi.org/10.22401/ANJS.22.4.07

[4] Ewa, I.I., Lumbi, L.W. and Howusu, S.X.K. (2018) *International Journal of Theoretical and Mathematical Physics*, **8**, 28-31.

[5] Roberts, K. and Valluri, S.R. (2017) *Canadian Journal of Physics*, **95**, 105-110. https://doi.org/10.1139/cjp-2016-0602

[6] Coulter, B.L. and Adler, C.G. (1971) *Journal of American Mathematical Society*, **39**, 305-309.

[7] Gumbs, G. and Kiang, D. (1986) *Journal of American Mathematical Society*, **54**, 462-463.

[8] Greiner, W. and Bromley, D.A. (2000) Relativistic Quantum Mechanics. 3rd Edition, Springer, Berlin. https://doi.org/10.1007/978-3-662-04275-5

[9] Nevels, R.D., Wu, Z. and Huang, C. (1993) *Physical Review A*, **48**, 3445-3451. https://doi.org/10.1103/PhysRevA.48.3445

[10] Janke, W. and Kleinert, H. (1979) *Lettere al Nuovo Cimento*, **25**, 297-300. https://doi.org/10.1007/BF02776259

[11] Goodman, M. (1981) *Journal of American Mathematical Society*, **49**, 843-847.

[12] Barut, A.O. and Duru, I.H. (1988) *Physical Review A*, **38**, 5906-5909. https://doi.org/10.1103/PhysRevA.38.5906

[13] Riazanov, G.V. (1958) *Journal of Experimental and Theoretical Physics*, **6**, 1107-1113.

[14] Papadopoulos, G.J. and Devreese, J.T. (1976) *Physical Review D*, **13**, 2227-2234. https://doi.org/10.1103/PhysRevD.13.2227

[15] Feynman, R.P. (1942) The Principle of Least Action in Quantum Mechanics. Ph.D. Thesis, Princeton University, Princeton.

[16] Feynman, R.P. Brown, L.M. and Dirac, P.A.M. (2005) Feynmans Thesis: A New Approach to Quantum Theory. World Scientific, Hackensack, NJ.

[17] Feynman, R.P. (1948) *Review Modern Physics*, **20**, 367-387. https://doi.org/10.1103/RevModPhys.20.367

[18] Feynman, R.P. and Hibbs, A.R. (1965) Quantum Mechanics and Path Integrals. McGraw-Hill College, New York.

[19] Gaveau, B. and Schulman, L.S. (2000) *Annals of Physics*, **284**, 1-9. https://doi.org/10.1006/aphy.1999.5993

[20] Rosen, G. (1983) *Physical Review A*, **28**, 1139-1140. https://doi.org/10.1103/PhysRevA.28.1139

[21] Naimark, M.A. and Stern, A.I. (1982) Theory of Group Representation. Springer, Berlin, Heidelberg.

[22] Suzuki, T. (1977) *Communications in Mathematical Physics*, **57**, 193-200. https://doi.org/10.1007/BF01614161

[23] Wilcox, R.M. (1967) *Journal of Mathematical Physics*, **8**, 962-982.

[24] Grosche, C. and Steiner, F. (1997) Handbook of Feyman Path Integrals. Springer-Verlag, Berlin.

[25] Bogoliubov, N.N. and Shirkov, D.V. (1959) Introduction to Quantized Fields. Wiley, New York, 147-150.

Journal of Modern Physics, 2020, 11, 1649-1671
https://www.scirp.org/journal/jmp
ISSN Online: 2153-120X
ISSN Print: 2153-1196

Property of Tensor Satisfying Binary Law 2

Koji Ichidayama

Okayama, Japan
Email: ichikoji@lime.ocn.ne.jp

How to cite this paper: Ichidayama, K. (2020) Property of Tensor Satisfying Binary Law 2. *Journal of Modern Physics*, **11**, 1649-1671.
https://doi.org/10.4236/jmp.2020.1110103

Received: September 13, 2020
Accepted: October 23, 2020
Published: October 26, 2020

Abstract

I have already reported "Property of Tensor Satisfying Binary Law". This article is the article that I revise the contents of "Property of Tensor Satisfying Binary Law", and increase the report about new characteristics. We may arrive at the deeper understanding in this about "Property of Tensor Satisfying Binary Law".

Keywords

Tensor Covariant Derivative

1. Introduction

I have already reported "Property of Tensor Satisfying Binary Law" [1]. This article is the article that I revise the contents of "Property of Tensor Satisfying Binary Law", and increase the report about new characteristics. I show below it about the proposition supporting each for shifts from "Property of Tensor Satisfying Binary Law" to "[Property of Tensor Satisfying Binary Law 2]".

Proposition 1 → [Proposition 2], Proposition 3 → [Proposition 6], Proposition 4 → [Proposition 7, Proposition 15], Proposition 5 → [Proposition 3].

2. Definition

Definition 1 $\overline{x^\mu} \neq x^\mu$, $\overline{x^\nu} \neq x^\nu$, $\overline{x^\mu} = x^\nu$, $\overline{x^\nu} = x^\mu$, $\left\{\overline{x_\mu} \neq x_\mu, \overline{x_\nu} \neq x_\nu, \overline{x_\mu} = x_\nu, \overline{x_\nu} = x_\mu\right\}$ is established [2]. I named $\overline{x^\mu} \neq x^\mu$, $\overline{x^\nu} \neq x^\nu$, $\overline{x^\mu} = x^\nu$, $\overline{x^\nu} = x^\mu$, $\left\{\overline{x_\mu} \neq x_\mu, \overline{x_\nu} \neq x_\nu, \overline{x_\mu} = x_\nu, \overline{x_\nu} = x_\mu\right\}$ "Binary Law" [2].

$\left\{\overline{x_\mu} \neq x_\mu, \overline{x_\nu} \neq x_\nu, \overline{x_\mu} = x_\nu, \overline{x_\nu} = x_\mu\right\}$ expresses a covariant form of Binary Law.

Definition 2 If $\overline{x^\mu} \neq x^\mu, \overline{x^\nu} \neq x^\nu, \overline{x^\mu} = x^\nu, \overline{x^\nu} = x^\mu$ is established, $x_\nu = x^\mu$ is established [2].

Definition 3 If $\overline{x^\mu} \neq x^\mu, \overline{x^\nu} \neq x^\nu, \overline{x^\mu} = x^\nu, \overline{x^\nu} = x^\mu$ is established, $x_\mu = x^\nu$ is established [2].

Definition 4 If $\overline{x^\mu} \neq x^\mu, \overline{x^\nu} \neq x^\nu, \overline{x^\mu} = x^\nu, \overline{x^\nu} = x^\mu$ is established, $x_\nu = -x_\mu$ is established [2].

Definition 5 If $\overline{x^\mu} \neq x^\mu, \overline{x^\nu} \neq x^\nu, \overline{x^\mu} = x^\nu, \overline{x^\nu} = x^\mu$ is established, $x^\nu = -x^\mu$ is established [2].

Definition 6 If all coordinate systems $x^\mu, x^\nu, x^\sigma, x^\lambda, \cdots$ satisfy $\overline{x^\mu} \neq x^\mu$, $\overline{x^\nu} \neq x^\nu$, $\overline{x^\mu} = x^\nu$, $\overline{x^\nu} = x^\mu$, all coordinate systems $x^\mu, x^\nu, x^\sigma, x^\lambda, \cdots$ shifts to only two of x^μ, x^ν [2].

Definition 7 $g^\mu_\mu = 1$, $g^\mu_\nu = 0 : (\mu \neq \nu)$ is establishment [3].

Definition 8 $\dfrac{\partial^3 x^\mu}{\partial x^\nu \partial x^\nu \partial x^\nu} = M$ is established for $\dfrac{\partial^3 x^\mu}{\partial x^\nu \partial x^\nu \partial x^\nu}$.

Definition 9 $m_{;\nu} = \dfrac{\partial m}{\partial x^\nu} = 0$ is established. "m" expresses Mass.

Hypothesis 1 $m \propto M$, $m = \epsilon M$ is established. "M" expresses $\dfrac{\partial^3 x^\mu}{\partial x^\nu \partial x^\nu \partial x^\nu} = M$, "$\epsilon$" expresses Proportional constant, and "m" expresses Mass.

Definition 10 The first-order covariant derivative of the covariant vector satisfied $x_{\mu;\nu} = \dfrac{\partial x_\mu}{\partial x^\nu} - x_\tau \Gamma^\tau_{\mu\nu} = \dfrac{\partial x_\mu}{\partial x^\nu} - x_\tau \dfrac{1}{2} g^{\epsilon\tau} \left(\dfrac{\partial g_{\mu\epsilon}}{\partial x^\nu} + \dfrac{\partial g_{\nu\epsilon}}{\partial x^\mu} - \dfrac{\partial g_{\mu\nu}}{\partial x^\epsilon} \right)$ [4].

Definition 11 The first-order covariant derivative of the contravariant vector satisfied $x^\mu_{;\nu} = \dfrac{\partial x^\mu}{\partial x^\nu} + x^\tau \Gamma^\mu_{\tau\nu} = \dfrac{\partial x^\mu}{\partial x^\nu} + x^\tau \dfrac{1}{2} g^{\epsilon\mu} \left(\dfrac{\partial g_{\tau\epsilon}}{\partial x^\nu} + \dfrac{\partial g_{\nu\epsilon}}{\partial x^\tau} - \dfrac{\partial g_{\tau\nu}}{\partial x^\epsilon} \right)$ [4].

Definition 12 The second-order covariant derivative of the contravariant vector satisfied

$$
\begin{aligned}
x^\mu_{;\nu;\sigma} &= \frac{\partial x^\mu_{;\nu}}{\partial x^\sigma} + x^\iota_{;\nu} \Gamma^\mu_{\iota\sigma} - x^\mu_{;\iota} \Gamma^\iota_{\nu\sigma} \\
&= \frac{\partial}{\partial x^\sigma} \left(\frac{\partial x^\mu}{\partial x^\nu} + x^\tau \Gamma^\mu_{\tau\nu} \right) + \left(\frac{\partial x^\iota}{\partial x^\nu} + x^\tau \Gamma^\iota_{\tau\nu} \right) \Gamma^\mu_{\iota\sigma} - \left(\frac{\partial x^\mu}{\partial x^\iota} + x^\tau \Gamma^\mu_{\tau\iota} \right) \Gamma^\iota_{\nu\sigma} \\
&= \frac{\partial^2 x^\mu}{\partial x^\nu \partial x^\sigma} + \frac{\partial}{\partial x^\sigma} \left(x^\tau \frac{1}{2} g^{\epsilon\mu} \left(\frac{\partial g_{\tau\epsilon}}{\partial x^\nu} + \frac{\partial g_{\nu\epsilon}}{\partial x^\tau} - \frac{\partial g_{\tau\nu}}{\partial x^\epsilon} \right) \right) \\
&\quad + \frac{\partial x^\iota}{\partial x^\nu} \frac{1}{2} g^{\epsilon\mu} \left(\frac{\partial g_{\iota\epsilon}}{\partial x^\sigma} + \frac{\partial g_{\sigma\epsilon}}{\partial x^\iota} - \frac{\partial g_{\iota\sigma}}{\partial x^\epsilon} \right) \\
&\quad + x^\tau \frac{1}{2} g^{\epsilon\iota} \left(\frac{\partial g_{\tau\epsilon}}{\partial x^\nu} + \frac{\partial g_{\nu\epsilon}}{\partial x^\tau} - \frac{\partial g_{\tau\nu}}{\partial x^\epsilon} \right) \frac{1}{2} g^{\epsilon\mu} \left(\frac{\partial g_{\iota\epsilon}}{\partial x^\sigma} + \frac{\partial g_{\sigma\epsilon}}{\partial x^\iota} - \frac{\partial g_{\iota\sigma}}{\partial x^\epsilon} \right) \\
&\quad - \frac{\partial x^\mu}{\partial x^\iota} \frac{1}{2} g^{\epsilon\iota} \left(\frac{\partial g_{\nu\epsilon}}{\partial x^\sigma} + \frac{\partial g_{\sigma\epsilon}}{\partial x^\nu} - \frac{\partial g_{\nu\sigma}}{\partial x^\epsilon} \right) \\
&\quad - x^\tau \frac{1}{2} g^{\epsilon\mu} \left(\frac{\partial g_{\tau\epsilon}}{\partial x^\iota} + \frac{\partial g_{\iota\epsilon}}{\partial x^\tau} - \frac{\partial g_{\tau\iota}}{\partial x^\epsilon} \right) \frac{1}{2} g^{\epsilon\iota} \left(\frac{\partial g_{\nu\epsilon}}{\partial x^\sigma} + \frac{\partial g_{\sigma\epsilon}}{\partial x^\nu} - \frac{\partial g_{\nu\sigma}}{\partial x^\epsilon} \right).
\end{aligned}
\qquad [4]
$$

Definition 13 The third-order covariant derivative of the contravariant vector satisfied

$$
\begin{aligned}
x^\mu_{;\nu;\sigma;\lambda} &= \frac{\partial x^\mu_{;\nu;\sigma}}{\partial x^\lambda} + x^\kappa_{;\nu;\sigma} \Gamma^\mu_{\kappa\lambda} - x^\mu_{;\kappa;\sigma} \Gamma^\kappa_{\nu\lambda} - x^\mu_{;\nu;\kappa} \Gamma^\kappa_{\sigma\lambda} \\
&= \frac{\partial}{\partial x^\lambda} \left\{ \frac{\partial}{\partial x^\sigma} \left(\frac{\partial x^\mu}{\partial x^\nu} + x^\tau \Gamma^\mu_{\tau\nu} \right) + \left(\frac{\partial x^\iota}{\partial x^\nu} + x^\tau \Gamma^\iota_{\tau\nu} \right) \Gamma^\mu_{\iota\sigma} - \left(\frac{\partial x^\mu}{\partial x^\iota} + x^\tau \Gamma^\mu_{\tau\iota} \right) \Gamma^\iota_{\nu\sigma} \right\}
\end{aligned}
$$

$$
\begin{aligned}
&+\left\{\frac{\partial}{\partial x^{\sigma}}\left(\frac{\partial x^{\kappa}}{\partial x^{\nu}}+x^{\tau}\Gamma^{\kappa}_{\tau\nu}\right)+\left(\frac{\partial x^{\iota}}{\partial x^{\nu}}+x^{\tau}\Gamma^{\iota}_{\tau\nu}\right)\Gamma^{\kappa}_{\iota\sigma}-\left(\frac{\partial x^{\kappa}}{\partial x^{\iota}}+x^{\tau}\Gamma^{\kappa}_{\tau\iota}\right)\Gamma^{\iota}_{\nu\sigma}\right\}\Gamma^{\mu}_{\kappa\lambda}\\
&-\left\{\frac{\partial}{\partial x^{\sigma}}\left(\frac{\partial x^{\mu}}{\partial x^{\kappa}}+x^{\tau}\Gamma^{\mu}_{\tau\kappa}\right)+\left(\frac{\partial x^{\iota}}{\partial x^{\kappa}}+x^{\tau}\Gamma^{\iota}_{\tau\kappa}\right)\Gamma^{\mu}_{\iota\sigma}-\left(\frac{\partial x^{\mu}}{\partial x^{\iota}}+x^{\tau}\Gamma^{\mu}_{\tau\iota}\right)\Gamma^{\iota}_{\kappa\sigma}\right\}\Gamma^{\kappa}_{\nu\lambda}\\
&-\left\{\frac{\partial}{\partial x^{\kappa}}\left(\frac{\partial x^{\mu}}{\partial x^{\nu}}+x^{\tau}\Gamma^{\mu}_{\tau\nu}\right)+\left(\frac{\partial x^{\iota}}{\partial x^{\nu}}+x^{\tau}\Gamma^{\iota}_{\tau\nu}\right)\Gamma^{\mu}_{\iota\kappa}-\left(\frac{\partial x^{\mu}}{\partial x^{\iota}}+x^{\tau}\Gamma^{\mu}_{\tau\iota}\right)\Gamma^{\iota}_{\nu\kappa}\right\}\Gamma^{\kappa}_{\sigma\lambda}\\
&=\frac{\partial^{3}x^{\mu}}{\partial x^{\nu}\partial x^{\sigma}\partial x^{\lambda}}+\frac{\partial^{2}}{\partial x^{\sigma}\partial x^{\lambda}}\left(x^{\tau}\frac{1}{2}g^{\epsilon\mu}\left(\frac{\partial g_{\tau\epsilon}}{\partial x^{\nu}}+\frac{\partial g_{\nu\epsilon}}{\partial x^{\tau}}-\frac{\partial g_{\tau\nu}}{\partial x^{\epsilon}}\right)\right)\\
&+\frac{\partial}{\partial x^{\lambda}}\left(\frac{\partial x^{\iota}}{\partial x^{\nu}}\frac{1}{2}g^{\epsilon\mu}\left(\frac{\partial g_{\iota\epsilon}}{\partial x^{\sigma}}+\frac{\partial g_{\sigma\epsilon}}{\partial x^{\iota}}-\frac{\partial g_{\iota\sigma}}{\partial x^{\epsilon}}\right)\right)\\
&+\frac{\partial}{\partial x^{\lambda}}\left(x^{\tau}\frac{1}{2}g^{\epsilon\iota}\left(\frac{\partial g_{\tau\epsilon}}{\partial x^{\nu}}+\frac{\partial g_{\nu\epsilon}}{\partial x^{\tau}}-\frac{\partial g_{\tau\nu}}{\partial x^{\epsilon}}\right)\frac{1}{2}g^{\epsilon\mu}\left(\frac{\partial g_{\iota\epsilon}}{\partial x^{\sigma}}+\frac{\partial g_{\sigma\epsilon}}{\partial x^{\iota}}-\frac{\partial g_{\iota\sigma}}{\partial x^{\epsilon}}\right)\right)\\
&-\frac{\partial}{\partial x^{\lambda}}\left(\frac{\partial x^{\mu}}{\partial x^{\iota}}\frac{1}{2}g^{\epsilon\iota}\left(\frac{\partial g_{\nu\epsilon}}{\partial x^{\sigma}}+\frac{\partial g_{\sigma\epsilon}}{\partial x^{\nu}}-\frac{\partial g_{\nu\sigma}}{\partial x^{\epsilon}}\right)\right)\\
&-\frac{\partial}{\partial x^{\lambda}}\left(x^{\tau}\frac{1}{2}g^{\epsilon\mu}\left(\frac{\partial g_{\tau\epsilon}}{\partial x^{\iota}}+\frac{\partial g_{\iota\epsilon}}{\partial x^{\tau}}-\frac{\partial g_{\tau\iota}}{\partial x^{\epsilon}}\right)\frac{1}{2}g^{\epsilon\iota}\left(\frac{\partial g_{\nu\epsilon}}{\partial x^{\sigma}}+\frac{\partial g_{\sigma\epsilon}}{\partial x^{\nu}}-\frac{\partial g_{\nu\sigma}}{\partial x^{\epsilon}}\right)\right)\\
&+\frac{\partial^{2}x^{\kappa}}{\partial x^{\nu}\partial x^{\sigma}}\frac{1}{2}g^{\epsilon\mu}\left(\frac{\partial g_{\kappa\epsilon}}{\partial x^{\lambda}}+\frac{\partial g_{\lambda\epsilon}}{\partial x^{\kappa}}-\frac{\partial g_{\kappa\lambda}}{\partial x^{\epsilon}}\right)\\
&+\frac{\partial}{\partial x^{\sigma}}\left(x^{\tau}\frac{1}{2}g^{\epsilon\kappa}\left(\frac{\partial g_{\tau\epsilon}}{\partial x^{\nu}}+\frac{\partial g_{\nu\epsilon}}{\partial x^{\tau}}-\frac{\partial g_{\tau\nu}}{\partial x^{\epsilon}}\right)\right)\frac{1}{2}g^{\epsilon\mu}\left(\frac{\partial g_{\kappa\epsilon}}{\partial x^{\lambda}}+\frac{\partial g_{\lambda\epsilon}}{\partial x^{\kappa}}-\frac{\partial g_{\kappa\lambda}}{\partial x^{\epsilon}}\right)\\
&+\frac{\partial x^{\iota}}{\partial x^{\nu}}\frac{1}{2}g^{\epsilon\kappa}\left(\frac{\partial g_{\iota\epsilon}}{\partial x^{\sigma}}+\frac{\partial g_{\sigma\epsilon}}{\partial x^{\iota}}-\frac{\partial g_{\iota\sigma}}{\partial x^{\epsilon}}\right)\frac{1}{2}g^{\epsilon\mu}\left(\frac{\partial g_{\kappa\epsilon}}{\partial x^{\lambda}}+\frac{\partial g_{\lambda\epsilon}}{\partial x^{\kappa}}-\frac{\partial g_{\kappa\lambda}}{\partial x^{\epsilon}}\right)\\
&+x^{\tau}\frac{1}{2}g^{\epsilon\iota}\left(\frac{\partial g_{\tau\epsilon}}{\partial x^{\nu}}+\frac{\partial g_{\nu\epsilon}}{\partial x^{\tau}}-\frac{\partial g_{\tau\nu}}{\partial x^{\epsilon}}\right)\frac{1}{2}g^{\epsilon\kappa}\left(\frac{\partial g_{\iota\epsilon}}{\partial x^{\sigma}}+\frac{\partial g_{\sigma\epsilon}}{\partial x^{\iota}}-\frac{\partial g_{\iota\sigma}}{\partial x^{\epsilon}}\right)\\
&\times\frac{1}{2}g^{\epsilon\mu}\left(\frac{\partial g_{\kappa\epsilon}}{\partial x^{\lambda}}+\frac{\partial g_{\lambda\epsilon}}{\partial x^{\kappa}}-\frac{\partial g_{\kappa\lambda}}{\partial x^{\epsilon}}\right)\\
&-\frac{\partial x^{\kappa}}{\partial x^{\iota}}\frac{1}{2}g^{\epsilon\iota}\left(\frac{\partial g_{\nu\epsilon}}{\partial x^{\sigma}}+\frac{\partial g_{\sigma\epsilon}}{\partial x^{\nu}}-\frac{\partial g_{\nu\sigma}}{\partial x^{\epsilon}}\right)\frac{1}{2}g^{\epsilon\mu}\left(\frac{\partial g_{\kappa\epsilon}}{\partial x^{\lambda}}+\frac{\partial g_{\lambda\epsilon}}{\partial x^{\kappa}}-\frac{\partial g_{\kappa\lambda}}{\partial x^{\epsilon}}\right)\\
&-x^{\tau}\frac{1}{2}g^{\epsilon\kappa}\left(\frac{\partial g_{\tau\epsilon}}{\partial x^{\iota}}+\frac{\partial g_{\iota\epsilon}}{\partial x^{\tau}}-\frac{\partial g_{\tau\iota}}{\partial x^{\epsilon}}\right)\frac{1}{2}g^{\epsilon\iota}\left(\frac{\partial g_{\nu\epsilon}}{\partial x^{\sigma}}+\frac{\partial g_{\sigma\epsilon}}{\partial x^{\nu}}-\frac{\partial g_{\nu\sigma}}{\partial x^{\epsilon}}\right)\\
&\times\frac{1}{2}g^{\epsilon\mu}\left(\frac{\partial g_{\kappa\epsilon}}{\partial x^{\lambda}}+\frac{\partial g_{\lambda\epsilon}}{\partial x^{\kappa}}-\frac{\partial g_{\kappa\lambda}}{\partial x^{\epsilon}}\right)-\frac{\partial^{2}x^{\mu}}{\partial x^{\kappa}\partial x^{\sigma}}\frac{1}{2}g^{\epsilon\kappa}\left(\frac{\partial g_{\nu\epsilon}}{\partial x^{\lambda}}+\frac{\partial g_{\lambda\epsilon}}{\partial x^{\nu}}-\frac{\partial g_{\nu\lambda}}{\partial x^{\epsilon}}\right)\\
&-\frac{\partial}{\partial x^{\sigma}}\left(x^{\tau}\frac{1}{2}g^{\epsilon\mu}\left(\frac{\partial g_{\tau\epsilon}}{\partial x^{\kappa}}+\frac{\partial g_{\kappa\epsilon}}{\partial x^{\tau}}-\frac{\partial g_{\tau\kappa}}{\partial x^{\epsilon}}\right)\right)\frac{1}{2}g^{\epsilon\kappa}\left(\frac{\partial g_{\nu\epsilon}}{\partial x^{\lambda}}+\frac{\partial g_{\lambda\epsilon}}{\partial x^{\nu}}-\frac{\partial g_{\nu\lambda}}{\partial x^{\epsilon}}\right)\\
&-\frac{\partial x^{\iota}}{\partial x^{\kappa}}\frac{1}{2}g^{\epsilon\mu}\left(\frac{\partial g_{\iota\epsilon}}{\partial x^{\sigma}}+\frac{\partial g_{\sigma\epsilon}}{\partial x^{\iota}}-\frac{\partial g_{\iota\sigma}}{\partial x^{\epsilon}}\right)\frac{1}{2}g^{\epsilon\kappa}\left(\frac{\partial g_{\nu\epsilon}}{\partial x^{\lambda}}+\frac{\partial g_{\lambda\epsilon}}{\partial x^{\nu}}-\frac{\partial g_{\nu\lambda}}{\partial x^{\epsilon}}\right)\\
&-x^{\tau}\frac{1}{2}g^{\epsilon\iota}\left(\frac{\partial g_{\tau\epsilon}}{\partial x^{\kappa}}+\frac{\partial g_{\kappa\epsilon}}{\partial x^{\tau}}-\frac{\partial g_{\tau\kappa}}{\partial x^{\epsilon}}\right)\frac{1}{2}g^{\epsilon\mu}\left(\frac{\partial g_{\iota\epsilon}}{\partial x^{\sigma}}+\frac{\partial g_{\sigma\epsilon}}{\partial x^{\iota}}-\frac{\partial g_{\iota\sigma}}{\partial x^{\epsilon}}\right)\\
&\times\frac{1}{2}g^{\epsilon\kappa}\left(\frac{\partial g_{\nu\epsilon}}{\partial x^{\lambda}}+\frac{\partial g_{\lambda\epsilon}}{\partial x^{\nu}}-\frac{\partial g_{\nu\lambda}}{\partial x^{\epsilon}}\right)
\end{aligned}
$$

$$
\begin{aligned}
&+\frac{\partial x^{\mu}}{\partial x^{\iota}}\frac{1}{2}g^{\epsilon\iota}\left(\frac{\partial g_{\kappa\epsilon}}{\partial x^{\sigma}}+\frac{\partial g_{\sigma\epsilon}}{\partial x^{\kappa}}-\frac{\partial g_{\kappa\sigma}}{\partial x^{\epsilon}}\right)\frac{1}{2}g^{\epsilon\kappa}\left(\frac{\partial g_{\nu\epsilon}}{\partial x^{\lambda}}+\frac{\partial g_{\lambda\epsilon}}{\partial x^{\nu}}-\frac{\partial g_{\nu\lambda}}{\partial x^{\epsilon}}\right)\\
&+x^{\tau}\frac{1}{2}g^{\epsilon\mu}\left(\frac{\partial g_{\tau\epsilon}}{\partial x^{\iota}}+\frac{\partial g_{\iota\epsilon}}{\partial x^{\tau}}-\frac{\partial g_{\tau\iota}}{\partial x^{\epsilon}}\right)\frac{1}{2}g^{\epsilon\iota}\left(\frac{\partial g_{\kappa\epsilon}}{\partial x^{\sigma}}+\frac{\partial g_{\sigma\epsilon}}{\partial x^{\kappa}}-\frac{\partial g_{\kappa\sigma}}{\partial x^{\epsilon}}\right)\\
&\times\frac{1}{2}g^{\epsilon\kappa}\left(\frac{\partial g_{\nu\epsilon}}{\partial x^{\lambda}}+\frac{\partial g_{\lambda\epsilon}}{\partial x^{\nu}}-\frac{\partial g_{\nu\lambda}}{\partial x^{\epsilon}}\right)-\frac{\partial^{2}x^{\mu}}{\partial x^{\nu}\partial x^{\kappa}}\frac{1}{2}g^{\epsilon\kappa}\left(\frac{\partial g_{\sigma\epsilon}}{\partial x^{\lambda}}+\frac{\partial g_{\lambda\epsilon}}{\partial x^{\sigma}}-\frac{\partial g_{\sigma\lambda}}{\partial x^{\epsilon}}\right)\\
&-\frac{\partial}{\partial x^{\kappa}}\left(x^{\tau}\frac{1}{2}g^{\epsilon\mu}\left(\frac{\partial g_{\tau\epsilon}}{\partial x^{\nu}}+\frac{\partial g_{\nu\epsilon}}{\partial x^{\tau}}-\frac{\partial g_{\tau\nu}}{\partial x^{\epsilon}}\right)\right)\frac{1}{2}g^{\epsilon\kappa}\left(\frac{\partial g_{\sigma\epsilon}}{\partial x^{\lambda}}+\frac{\partial g_{\lambda\epsilon}}{\partial x^{\sigma}}-\frac{\partial g_{\sigma\lambda}}{\partial x^{\epsilon}}\right)\\
&-\frac{\partial x^{\iota}}{\partial x^{\nu}}\frac{1}{2}g^{\epsilon\mu}\left(\frac{\partial g_{\iota\epsilon}}{\partial x^{\kappa}}+\frac{\partial g_{\kappa\epsilon}}{\partial x^{\iota}}-\frac{\partial g_{\iota\kappa}}{\partial x^{\epsilon}}\right)\frac{1}{2}g^{\epsilon\kappa}\left(\frac{\partial g_{\sigma\epsilon}}{\partial x^{\lambda}}+\frac{\partial g_{\lambda\epsilon}}{\partial x^{\sigma}}-\frac{\partial g_{\sigma\lambda}}{\partial x^{\epsilon}}\right)\\
&-x^{\tau}\frac{1}{2}g^{\epsilon\iota}\left(\frac{\partial g_{\tau\epsilon}}{\partial x^{\nu}}+\frac{\partial g_{\nu\epsilon}}{\partial x^{\tau}}-\frac{\partial g_{\tau\nu}}{\partial x^{\epsilon}}\right)\frac{1}{2}g^{\epsilon\mu}\left(\frac{\partial g_{\iota\epsilon}}{\partial x^{\kappa}}+\frac{\partial g_{\kappa\epsilon}}{\partial x^{\iota}}-\frac{\partial g_{\iota\kappa}}{\partial x^{\epsilon}}\right)\\
&\times\frac{1}{2}g^{\epsilon\kappa}\left(\frac{\partial g_{\sigma\epsilon}}{\partial x^{\lambda}}+\frac{\partial g_{\lambda\epsilon}}{\partial x^{\sigma}}-\frac{\partial g_{\sigma\lambda}}{\partial x^{\epsilon}}\right)\\
&+\frac{\partial x^{\mu}}{\partial x^{\iota}}\frac{1}{2}g^{\epsilon\iota}\left(\frac{\partial g_{\nu\epsilon}}{\partial x^{\kappa}}+\frac{\partial g_{\kappa\epsilon}}{\partial x^{\nu}}-\frac{\partial g_{\nu\kappa}}{\partial x^{\epsilon}}\right)\frac{1}{2}g^{\epsilon\kappa}\left(\frac{\partial g_{\sigma\epsilon}}{\partial x^{\lambda}}+\frac{\partial g_{\lambda\epsilon}}{\partial x^{\sigma}}-\frac{\partial g_{\sigma\lambda}}{\partial x^{\epsilon}}\right)\\
&+x^{\tau}\frac{1}{2}g^{\epsilon\mu}\left(\frac{\partial g_{\tau\epsilon}}{\partial x^{\iota}}+\frac{\partial g_{\iota\epsilon}}{\partial x^{\tau}}-\frac{\partial g_{\tau\iota}}{\partial x^{\epsilon}}\right)\frac{1}{2}g^{\epsilon\iota}\left(\frac{\partial g_{\nu\epsilon}}{\partial x^{\kappa}}+\frac{\partial g_{\kappa\epsilon}}{\partial x^{\nu}}-\frac{\partial g_{\nu\kappa}}{\partial x^{\epsilon}}\right)\\
&\times\frac{1}{2}g^{\epsilon\kappa}\left(\frac{\partial g_{\sigma\epsilon}}{\partial x^{\lambda}}+\frac{\partial g_{\lambda\epsilon}}{\partial x^{\sigma}}-\frac{\partial g_{\sigma\lambda}}{\partial x^{\epsilon}}\right).
\end{aligned}
$$

Definition 14 When the next conversion equation is established, x^{μ}_{μ} is components of a tensor of rank zero. $x^{\mu}_{\mu}=\frac{\partial x^{\mu}}{\partial x^{\nu}}\frac{\partial x^{\nu}}{\partial x^{\mu}}x^{\nu}_{\nu}$

Definition 15 When the next conversion equation is established, x^{μ} is contravariant components of a tensor of the first rank [4]. $x^{\mu}=\frac{\partial x^{\mu}}{\partial x^{\nu}}x^{\nu}$

Definition 16 When the next conversion equation is established, x_{μ} is covariant components of a tensor of the first rank [4]. $x_{\mu}=\frac{\partial x^{\nu}}{\partial x^{\mu}}x_{\nu}$

Definition 17 When the next conversion equation is established, $x^{\mu\nu}$ is contravariant components of a tensor of the second rank [4]. $x^{\mu\nu}=\frac{\partial x^{\mu}}{\partial x^{\sigma}}\frac{\partial x^{\nu}}{\partial x^{\lambda}}x^{\sigma\lambda}$

Definition 18 When the next conversion equation is established, $x_{\mu\nu}$ is covariant components of a tensor of the second rank [4]. $x_{\mu\nu}=\frac{\partial x^{\sigma}}{\partial x^{\mu}}\frac{\partial x^{\lambda}}{\partial x^{\nu}}x_{\sigma\lambda}$

Definition 19 When the next conversion equation is established, x^{μ}_{ν} is components of the mixed tensor of the second rank [4]. $x^{\mu}_{\nu}=\frac{\partial x^{\mu}}{\partial x^{\sigma}}\frac{\partial x^{\lambda}}{\partial x^{\nu}}x^{\sigma}_{\lambda}$

Definition 20 When the next conversion equation is established, $x^{\mu}_{\nu\sigma}$ is components of the mixed tensor of the third rank of the second rank covariant in the first rank contravariant [4]. $x^{\mu}_{\nu\sigma}=\frac{\partial x^{\mu}}{\partial x^{\lambda}}\frac{\partial x^{\iota}}{\partial x^{\nu}}\frac{\partial x^{\epsilon}}{\partial x^{\sigma}}x^{\lambda}_{\iota\epsilon}$

Definition 21 When the next conversion equation is established, $x^{\mu}_{\nu\sigma\lambda}$ is

components of the mixed tensor of the fourth rank of the third rank covariant in the first rank contravariant. $x^{\mu}_{\nu\sigma\lambda} = \frac{\partial x^{\mu}}{\partial x^{t}} \frac{\partial x^{\epsilon}}{\partial x^{\nu}} \frac{\partial x^{\alpha}}{\partial x^{\sigma}} \frac{\partial x^{\beta}}{\partial x^{\lambda}} x^{t}_{\epsilon\alpha\beta}$

3. About Covariant Derivative for the Scalar in Tensor Satisfying Binary Law

Proposition 1 When all coordinate systems satisfy Binary Law, $M_{;\nu} = \frac{\partial M}{\partial x^{\nu}} = 0$ is established for $\frac{\partial^3 x^{\mu}}{\partial x^{\nu} \partial x^{\nu} \partial x^{\nu}} = M$.

Proof: I get

$$M_{;\nu} = \frac{\partial M}{\partial x^{\nu}} = 0 \tag{1}$$

as $\epsilon = 1$ for Definition 9, Hypothesis 1.

-End Proof-

Proposition 2 When all coordinate systems satisfy Binary Law, $\frac{\partial^2 x_{\mu}}{\partial x^{\nu} \partial x^{\nu}} = 0$ is established.

Proof: I get

$$\frac{\partial^2 x_{\mu}}{\partial x^{\nu} \partial x^{\nu}} = 0 \tag{2}$$

from (1), (77).

-End Proof-

Proposition 3 When all coordinate systems satisfy Binary Law, $\frac{\partial^4 x^{\mu}}{\partial x^{\nu} \partial x^{\nu} \partial x^{\nu} \partial x^{\nu}} = 0$ is established.

Proof: I get

$$\frac{\partial^4 x^{\mu}}{\partial x^{\nu} \partial x^{\nu} \partial x^{\nu} \partial x^{\nu}} = 0 \tag{3}$$

from (1), Definition 8.

-End Proof-

4. About Covariant Derivative for the Vector in Tensor Satisfying Binary Law

Proposition 4 $x_{\mu;\nu} = \frac{\partial x_{\mu}}{\partial x^{\nu}}, x^{;\mu}_{\mu} = \frac{\partial x_{\mu}}{\partial x_{\mu}} - x_{\nu} \frac{1}{2} \left(\frac{\partial g^{\nu\mu}}{\partial x^{\mu}} \right)$ is established in tensor satisfying Binary Law.

Proof: If all coordinate systems satisfy Binary Law, I get

$$\begin{aligned} x_{\mu;\nu} &= \frac{\partial x_{\mu}}{\partial x^{\nu}} - x_{\nu} \frac{1}{2} g^{\nu\nu} \left(\frac{\partial g_{\mu\nu}}{\partial x^{\nu}} + \frac{\partial g_{\nu\nu}}{\partial x^{\mu}} - \frac{\partial g_{\mu\nu}}{\partial x^{\nu}} \right) \\ &= \frac{\partial x_{\mu}}{\partial x^{\nu}} - x_{\nu} \frac{1}{2} \left(\frac{\partial g^{\nu}_{\nu}}{\partial x^{\mu}} \right) \end{aligned} \tag{4}$$

from Definition 10. (4) must rewrite it in

$$x_{\mu;\nu} = \frac{\partial x_\mu}{\partial x^\nu} - x_\sigma \frac{1}{2}\left(\frac{\partial g_\nu^\sigma}{\partial x^\mu}\right) \tag{5}$$

by (4) being a tensor equation. The dummy index has an invariable property for consideration of Binary Law. In other words, the index which was dummy index in Definition 10 is dummy index in (5). I get the conclusion that (5) doesn't satisfy Binary Law from Definition 6. I get the conclusion that Definition 10 isn't an equation of the tensor satisfying Binary Law because (5) doesn't satisfy Binary Law.

I rewrite one existing index ν in each term of (5) in index μ using Definition 2 and get

$$x_\mu^{;\mu} = \frac{\partial x_\mu}{\partial x_\mu} - x_\sigma \frac{1}{2}\left(\frac{\partial g^{\sigma\mu}}{\partial x^\mu}\right),$$

$$x_\mu^{;\mu} = \frac{\partial x_\mu}{\partial x_\mu} - x_\nu \frac{1}{2}\left(\frac{\partial g^{\nu\mu}}{\partial x^\mu}\right). \tag{6}$$

I rewrite one existing index ν in each term of (5) in index μ using Definition 4 and get

$$-x_{\mu;\mu} = -\frac{\partial x_\mu}{\partial x^\mu} + x_\sigma \frac{1}{2}\left(\frac{\partial g_\mu^\sigma}{\partial x^\mu}\right). \tag{7}$$

I get

$$-x_{\mu;\mu} = -\frac{\partial x_\mu}{\partial x^\mu} \tag{8}$$

in consideration of Definition 7 for (7). Because the second term of the right side of (8) doesn't exist,

$$x_{\mu;\nu} = \frac{\partial x_\mu}{\partial x^\nu} \tag{9}$$

can rewrite (8) using Definition 4. In addition, $x_{\mu;\nu}$ can't rewrite $x_\mu^{;\mu}$ of (6) using Definition 2 because the second term of the right side exists in (6).

-End Proof-

Proposition 5 $x_{;\nu}^\mu = \frac{\partial x^\mu}{\partial x^\nu}$ is established in tensor satisfying Binary Law.

Proof: If all coordinate systems satisfy Binary Law, I get

$$x_{;\nu}^\mu = \frac{\partial x^\mu}{\partial x^\nu} + x^\nu \frac{1}{2} g^{\nu\mu}\left(\frac{\partial \widehat{g_{\nu\nu}}}{\partial x^\nu} + \frac{\partial g_{\nu\nu}}{\partial x^\nu} - \frac{\partial g_{\nu\nu}}{\partial x^\nu}\right)$$

$$= \frac{\partial x^\mu}{\partial x^\nu} + x^\nu \frac{1}{2}\left(\frac{\partial \widehat{g_\nu^\mu}}{\partial x^\nu}\right) \tag{10}$$

$$= \frac{\partial x^\mu}{\partial x^\nu} + x^\nu \frac{1}{2}\left(\frac{\partial g_\nu^\mu}{\partial x^\nu}\right) \tag{11}$$

from Definition 11. (10), (11) must rewrite it in

$$x^{\mu}_{;\nu} = \frac{\partial x^{\mu}}{\partial x^{\nu}} + x^{\sigma}\frac{1}{2}\left(\frac{\partial g^{\mu}_{\sigma}}{\partial x^{\nu}}\right) \tag{12}$$

$$= \frac{\partial x^{\mu}}{\partial x^{\nu}} + x^{\sigma}\frac{1}{2}\left(\frac{\partial g^{\mu}_{\nu}}{\partial x^{\sigma}}\right) \tag{13}$$

by (10), (11) being a tensor equation.

The dummy index has an invariable property for consideration of Binary Law. In other words, the index which was dummy index in Definition 11 is dummy index in (12), (13). I get the conclusion that (12), (13) doesn't satisfy Binary Law from Definition 6. I get the conclusion that Definition 11 isn't an equation of the tensor satisfying Binary Law because (12), (13) doesn't satisfy Binary Law.

I rewrite one existing index ν in each term of (12), (13) in index μ using Definition 4 and get

$$\begin{aligned} -x^{\mu}_{;\mu} &= -\frac{\partial x^{\mu}}{\partial x^{\mu}} - x^{\sigma}\frac{1}{2}\left(\frac{\partial g^{\mu}_{\sigma}}{\partial x^{\mu}}\right) \\ &= -\frac{\partial x^{\mu}}{\partial x^{\mu}} - x^{\sigma}\frac{1}{2}\left(\frac{\partial g^{\mu}_{\mu}}{\partial x^{\sigma}}\right). \end{aligned} \tag{14}$$

I get

$$-x^{\mu}_{;\mu} = -\frac{\partial x^{\mu}}{\partial x^{\mu}} \tag{15}$$

in consideration of Definition 7 for (14). Because the second term of the right side of (15) doesn't exist,

$$x^{\mu}_{;\nu} = \frac{\partial x^{\mu}}{\partial x^{\nu}} \tag{16}$$

can rewrite (15) using Definition 4. I rewrite one existing index ν in each term of (12), (13) in index μ using Definition 2 and get

$$\begin{aligned} x^{\mu;\mu} &= \frac{\partial x^{\mu}}{\partial x_{\mu}} + x^{\sigma}\frac{1}{2}\left(\frac{\partial g^{\mu}_{\sigma}}{\partial x_{\mu}}\right) \\ &= \frac{\partial x^{\mu}}{\partial x_{\mu}} + x^{\sigma}\frac{1}{2}\left(\frac{\partial g^{\mu\mu}}{\partial x^{\sigma}}\right). \end{aligned}$$

-End Proof-

Proposition 6 $x^{\mu}_{;\nu;\nu} = \dfrac{\partial^2 x^{\mu}}{\partial x^{\nu}\partial x^{\nu}}$ is established in tensor satisfying Binary Law.

Proof: If all coordinate systems satisfy Binary Law, I get

$$\begin{aligned} x^{\mu}_{;\nu;\nu} = \frac{\partial^2 x^{\mu}}{\partial x^{\nu}\partial x^{\nu}} &+ \frac{\partial}{\partial x^{\nu}}\left(x^{\nu}\frac{1}{2}g^{\nu\mu}\left(\frac{\partial \widehat{g_{\nu\nu}}}{\partial x^{\nu}} + \frac{\partial g_{\nu\nu}}{\partial x^{\nu}} - \frac{\partial g_{\nu\nu}}{\partial x^{\nu}}\right)\right) \\ &+ \frac{\partial x^{\nu}}{\partial x^{\nu}}\frac{1}{2}g^{\nu\mu}\left(\frac{\partial \widehat{g_{\nu\nu}}}{\partial x^{\nu}} + \frac{\partial g_{\nu\nu}}{\partial x^{\nu}} - \frac{\partial g_{\nu\nu}}{\partial x^{\nu}}\right) \end{aligned}$$

$$
\begin{aligned}
&+x^{\nu}\frac{1}{2}g^{\nu\nu}\left(\frac{\partial\widehat{g_{\nu\nu}}}{\partial x^{\nu}}+\frac{\partial g_{\nu\nu}}{\partial x^{\nu}}-\frac{\partial g_{\nu\nu}}{\partial x^{\nu}}\right)\frac{1}{2}g^{\nu\mu}\left(\frac{\partial\widehat{g_{\nu\nu}}}{\partial x^{\nu}}+\frac{\partial g_{\nu\nu}}{\partial x^{\nu}}-\frac{\partial g_{\nu\nu}}{\partial x^{\nu}}\right)\\
&-\frac{\partial x^{\mu}}{\partial x^{\nu}}\frac{1}{2}g^{\nu\nu}\left(\frac{\partial\widehat{g_{\nu\nu}}}{\partial x^{\nu}}+\frac{\partial g_{\nu\nu}}{\partial x^{\nu}}-\frac{\partial g_{\nu\nu}}{\partial x^{\nu}}\right)\\
&-x^{\nu}\frac{1}{2}g^{\nu\mu}\left(\frac{\partial\widehat{g_{\nu\nu}}}{\partial x^{\nu}}+\frac{\partial g_{\nu\nu}}{\partial x^{\nu}}-\frac{\partial g_{\nu\nu}}{\partial x^{\nu}}\right)\frac{1}{2}g^{\nu\nu}\left(\frac{\partial\widehat{g_{\nu\nu}}}{\partial x^{\nu}}+\frac{\partial g_{\nu\nu}}{\partial x^{\nu}}-\frac{\partial g_{\nu\nu}}{\partial x^{\nu}}\right)\\
&=\frac{\partial^2x^{\mu}}{\partial x^{\nu}\partial x^{\nu}}+\frac{\partial}{\partial x^{\nu}}\left(x^{\nu}\frac{1}{2}\left(\frac{\partial\widehat{g_{\nu}^{\mu}}}{\partial x^{\nu}}\right)\right)+\frac{\partial x^{\nu}}{\partial x^{\nu}}\frac{1}{2}\left(\frac{\partial\widehat{g_{\nu}^{\mu}}}{\partial x^{\nu}}\right)\\
&+x^{\nu}\frac{1}{2}\left(\frac{\partial\widehat{g_{\nu}^{\nu}}}{\partial x^{\nu}}\right)\frac{1}{2}\left(\frac{\partial\widehat{g_{\nu}^{\mu}}}{\partial x^{\nu}}\right)-\frac{\partial x^{\mu}}{\partial x^{\nu}}\frac{1}{2}\left(\frac{\partial\widehat{g_{\nu}^{\nu}}}{\partial x^{\nu}}\right)-x^{\nu}\frac{1}{2}\left(\frac{\partial\widehat{g_{\nu}^{\mu}}}{\partial x^{\nu}}\right)\frac{1}{2}\left(\frac{\partial\widehat{g_{\nu}^{\nu}}}{\partial x^{\nu}}\right)
\end{aligned}
\tag{17}
$$

$$
\begin{aligned}
&=\frac{\partial^2x^{\mu}}{\partial x^{\nu}\partial x^{\nu}}+\frac{\partial}{\partial x^{\nu}}\left(x^{\nu}\frac{1}{2}\left(\frac{\partial g_{\nu}^{\mu}}{\partial x^{\nu}}\right)\right)+\frac{\partial x^{\nu}}{\partial x^{\nu}}\frac{1}{2}\left(\frac{\partial g_{\nu}^{\mu}}{\partial x^{\nu}}\right)\\
&+x^{\nu}\frac{1}{2}\left(\frac{\partial g_{\nu}^{\nu}}{\partial x^{\nu}}\right)\frac{1}{2}\left(\frac{\partial g_{\nu}^{\mu}}{\partial x^{\nu}}\right)-\frac{\partial x^{\mu}}{\partial x^{\nu}}\frac{1}{2}\left(\frac{\partial g_{\nu}^{\nu}}{\partial x^{\nu}}\right)-x^{\nu}\frac{1}{2}\left(\frac{\partial g_{\nu}^{\mu}}{\partial x^{\nu}}\right)\frac{1}{2}\left(\frac{\partial g_{\nu}^{\nu}}{\partial x^{\nu}}\right)
\end{aligned}
\tag{18}
$$

from Definition 12. (17), (18) must rewrite it in

$$
\begin{aligned}
x^{\mu}_{;\nu;\nu}&=\frac{\partial^2x^{\mu}}{\partial x^{\nu}\partial x^{\nu}}+\frac{\partial}{\partial x^{\nu}}\left(x^{\sigma}\frac{1}{2}\left(\frac{\partial g_{\sigma}^{\mu}}{\partial x^{\nu}}\right)\right)+\frac{\partial x^{\sigma}}{\partial x^{\nu}}\frac{1}{2}\left(\frac{\partial g_{\sigma}^{\mu}}{\partial x^{\nu}}\right)\\
&+x^{\sigma}\frac{1}{2}\left(\frac{\partial g_{\sigma}^{\sigma}}{\partial x^{\nu}}\right)\frac{1}{2}\left(\frac{\partial g_{\sigma}^{\mu}}{\partial x^{\nu}}\right)-\frac{\partial x^{\mu}}{\partial x^{\sigma}}\frac{1}{2}\left(\frac{\partial g_{\nu}^{\sigma}}{\partial x^{\nu}}\right)-x^{\sigma}\frac{1}{2}\left(\frac{\partial g_{\sigma}^{\mu}}{\partial x^{\sigma}}\right)\frac{1}{2}\left(\frac{\partial g_{\nu}^{\sigma}}{\partial x^{\nu}}\right)
\end{aligned}
\tag{19}
$$

$$
\begin{aligned}
&=\frac{\partial^2x^{\mu}}{\partial x^{\nu}\partial x^{\nu}}+\frac{\partial}{\partial x^{\nu}}\left(x^{\sigma}\frac{1}{2}\left(\frac{\partial g_{\nu}^{\mu}}{\partial x^{\sigma}}\right)\right)+\frac{\partial x^{\sigma}}{\partial x^{\nu}}\frac{1}{2}\left(\frac{\partial g_{\nu}^{\mu}}{\partial x^{\sigma}}\right)\\
&+x^{\sigma}\frac{1}{2}\left(\frac{\partial g_{\nu}^{\sigma}}{\partial x^{\sigma}}\right)\frac{1}{2}\left(\frac{\partial g_{\nu}^{\mu}}{\partial x^{\sigma}}\right)-\frac{\partial x^{\mu}}{\partial x^{\sigma}}\frac{1}{2}\left(\frac{\partial g_{\nu}^{\sigma}}{\partial x^{\nu}}\right)-x^{\sigma}\frac{1}{2}\left(\frac{\partial g_{\sigma}^{\mu}}{\partial x^{\sigma}}\right)\frac{1}{2}\left(\frac{\partial g_{\nu}^{\sigma}}{\partial x^{\nu}}\right)
\end{aligned}
\tag{20}
$$

by (17), (18) being a tensor equation. The dummy index has an invariable property for consideration of Binary Law. In other words, the index which was dummy index in Definition 12 is dummy index in (19), (20). I get the conclusion that (19), (20) doesn't satisfy Binary Law from Definition 6. I get the conclusion that Definition 12 isn't an equation of the tensor satisfying Binary Law because (19), (20) doesn't satisfy Binary Law.

I rewrite two existing index ν in each term of (19), (20) in index μ using Definition 4 and get

$$
\begin{aligned}
x^{\mu}_{;\mu;\mu}&=\frac{\partial^2x^{\mu}}{\partial x^{\mu}\partial x^{\mu}}+\frac{\partial}{\partial x^{\mu}}\left(x^{\sigma}\frac{1}{2}\left(\frac{\partial g_{\sigma}^{\mu}}{\partial x^{\mu}}\right)\right)+\frac{\partial x^{\sigma}}{\partial x^{\mu}}\frac{1}{2}\left(\frac{\partial g_{\sigma}^{\mu}}{\partial x^{\mu}}\right)\\
&+x^{\sigma}\frac{1}{2}\left(\frac{\partial g_{\sigma}^{\sigma}}{\partial x^{\mu}}\right)\frac{1}{2}\left(\frac{\partial g_{\sigma}^{\mu}}{\partial x^{\mu}}\right)-\frac{\partial x^{\mu}}{\partial x^{\sigma}}\frac{1}{2}\left(\frac{\partial g_{\mu}^{\sigma}}{\partial x^{\mu}}\right)-x^{\sigma}\frac{1}{2}\left(\frac{\partial g_{\sigma}^{\mu}}{\partial x^{\sigma}}\right)\frac{1}{2}\left(\frac{\partial g_{\mu}^{\sigma}}{\partial x^{\mu}}\right)\\
&=\frac{\partial^2x^{\mu}}{\partial x^{\mu}\partial x^{\mu}}+\frac{\partial}{\partial x^{\mu}}\left(x^{\sigma}\frac{1}{2}\left(\frac{\partial g_{\mu}^{\mu}}{\partial x^{\sigma}}\right)\right)+\frac{\partial x^{\sigma}}{\partial x^{\mu}}\frac{1}{2}\left(\frac{\partial g_{\mu}^{\mu}}{\partial x^{\sigma}}\right)\\
&+x^{\sigma}\frac{1}{2}\left(\frac{\partial g_{\mu}^{\sigma}}{\partial x^{\sigma}}\right)\frac{1}{2}\left(\frac{\partial g_{\mu}^{\mu}}{\partial x^{\sigma}}\right)-\frac{\partial x^{\mu}}{\partial x^{\sigma}}\frac{1}{2}\left(\frac{\partial g_{\mu}^{\sigma}}{\partial x^{\mu}}\right)-x^{\sigma}\frac{1}{2}\left(\frac{\partial g_{\sigma}^{\mu}}{\partial x^{\sigma}}\right)\frac{1}{2}\left(\frac{\partial g_{\mu}^{\sigma}}{\partial x^{\mu}}\right).
\end{aligned}
\tag{21}
$$

I get

$$x^{\mu}_{;\mu;\mu} = \frac{\partial^2 x^{\mu}}{\partial x^{\mu}\partial x^{\mu}} \tag{22}$$

in consideration of Definition 7 for (21). Because the second term of the right side of (22) doesn't exist,

$$x^{\mu}_{;\nu;\nu} = \frac{\partial^2 x^{\mu}}{\partial x^{\nu}\partial x^{\nu}} \tag{23}$$

can rewrite (22) using Definition 4. I rewrite two existing index ν in each term of (19), (20) in index μ using Definition 2 and get

$$\begin{aligned}
x^{\mu;\mu;\mu} &= \frac{\partial^2 x^{\mu}}{\partial x_{\mu}\partial x_{\mu}} + \frac{\partial}{\partial x_{\mu}}\left(x^{\sigma}\frac{1}{2}\left(\frac{\partial g^{\mu}_{\sigma}}{\partial x_{\mu}}\right)\right) + \frac{\partial x^{\sigma}}{\partial x_{\mu}}\frac{1}{2}\left(\frac{\partial g^{\mu}_{\sigma}}{\partial x_{\mu}}\right) \\
&\quad + x^{\sigma}\frac{1}{2}\left(\frac{\partial g^{\sigma}_{\sigma}}{\partial x_{\mu}}\right)\frac{1}{2}\left(\frac{\partial g^{\mu}_{\sigma}}{\partial x_{\mu}}\right) - \frac{\partial x^{\mu}}{\partial x^{\sigma}}\frac{1}{2}\left(\frac{\partial g^{\sigma\mu}}{\partial x_{\mu}}\right) - x^{\sigma}\frac{1}{2}\left(\frac{\partial g^{\mu}_{\sigma}}{\partial x^{\sigma}}\right)\frac{1}{2}\left(\frac{\partial g^{\sigma\mu}}{\partial x_{\mu}}\right) \\
&= \frac{\partial^2 x^{\mu}}{\partial x_{\mu}\partial x_{\mu}} + \frac{\partial}{\partial x_{\mu}}\left(x^{\sigma}\frac{1}{2}\left(\frac{\partial g^{\mu\mu}}{\partial x^{\sigma}}\right)\right) + \frac{\partial x^{\sigma}}{\partial x_{\mu}}\frac{1}{2}\left(\frac{\partial g^{\mu\mu}}{\partial x^{\sigma}}\right) \\
&\quad + x^{\sigma}\frac{1}{2}\left(\frac{\partial g^{\sigma\mu}}{\partial x^{\sigma}}\right)\frac{1}{2}\left(\frac{\partial g^{\mu\mu}}{\partial x^{\sigma}}\right) - \frac{\partial x^{\mu}}{\partial x^{\sigma}}\frac{1}{2}\left(\frac{\partial g^{\sigma\mu}}{\partial x_{\mu}}\right) - x^{\sigma}\frac{1}{2}\left(\frac{\partial g^{\mu}_{\sigma}}{\partial x^{\sigma}}\right)\frac{1}{2}\left(\frac{\partial g^{\sigma\mu}}{\partial x_{\mu}}\right).
\end{aligned}$$

-End Proof-

Proposition 7 $x^{\mu}_{;\nu;\nu;\nu} = \dfrac{\partial^3 x^{\mu}}{\partial x^{\nu}\partial x^{\nu}\partial x^{\nu}}$ is established in tensor satisfying Binary Law.

Proof: If all coordinate systems satisfy Binary Law, I get

$$\begin{aligned}
x^{\mu}_{;\nu;\nu;\nu} &= \frac{\partial^3 x^{\mu}}{\partial x^{\nu}\partial x^{\nu}\partial x^{\nu}} + \frac{\partial^2}{\partial x^{\nu}\partial x^{\nu}}\left(x^{\nu}\frac{1}{2}g^{\nu\mu}\left(\frac{\partial \widehat{g_{\nu\nu}}}{\partial x^{\nu}} + \frac{\partial g_{\nu\nu}}{\partial x^{\nu}} - \frac{\partial g_{\nu\nu}}{\partial x^{\nu}}\right)\right) \\
&\quad + \frac{\partial}{\partial x^{\nu}}\left(\frac{\partial x^{\nu}}{\partial x^{\nu}}\frac{1}{2}g^{\nu\mu}\left(\frac{\partial \widehat{g_{\nu\nu}}}{\partial x^{\nu}} + \frac{\partial g_{\nu\nu}}{\partial x^{\nu}} - \frac{\partial g_{\nu\nu}}{\partial x^{\nu}}\right)\right) \\
&\quad + \frac{\partial}{\partial x^{\nu}}\left(x^{\nu}\frac{1}{2}g^{\nu\nu}\left(\frac{\partial \widehat{g_{\nu\nu}}}{\partial x^{\nu}} + \frac{\partial g_{\nu\nu}}{\partial x^{\nu}} - \frac{\partial g_{\nu\nu}}{\partial x^{\nu}}\right)\frac{1}{2}g^{\nu\mu}\left(\frac{\partial \widehat{g_{\nu\nu}}}{\partial x^{\nu}} + \frac{\partial g_{\nu\nu}}{\partial x^{\nu}} - \frac{\partial g_{\nu\nu}}{\partial x^{\nu}}\right)\right) \\
&\quad - \frac{\partial}{\partial x^{\nu}}\left(\frac{\partial x^{\mu}}{\partial x^{\nu}}\frac{1}{2}g^{\nu\nu}\left(\frac{\partial \widehat{g_{\nu\nu}}}{\partial x^{\nu}} + \frac{\partial g_{\nu\nu}}{\partial x^{\nu}} - \frac{\partial g_{\nu\nu}}{\partial x^{\nu}}\right)\right) \\
&\quad - \frac{\partial}{\partial x^{\nu}}\left(x^{\nu}\frac{1}{2}g^{\nu\mu}\left(\frac{\partial \widehat{g_{\nu\nu}}}{\partial x^{\nu}} + \frac{\partial g_{\nu\nu}}{\partial x^{\nu}} - \frac{\partial g_{\nu\nu}}{\partial x^{\nu}}\right)\frac{1}{2}g^{\nu\nu}\left(\frac{\partial \widehat{g_{\nu\nu}}}{\partial x^{\nu}} + \frac{\partial g_{\nu\nu}}{\partial x^{\nu}} - \frac{\partial g_{\nu\nu}}{\partial x^{\nu}}\right)\right) \\
&\quad + \frac{\partial^2 x^{\nu}}{\partial x^{\nu}\partial x^{\nu}}\frac{1}{2}g^{\nu\mu}\left(\frac{\partial \widehat{g_{\nu\nu}}}{\partial x^{\nu}} + \frac{\partial g_{\nu\nu}}{\partial x^{\nu}} - \frac{\partial g_{\nu\nu}}{\partial x^{\nu}}\right) \\
&\quad + \frac{\partial}{\partial x^{\nu}}\left(x^{\nu}\frac{1}{2}g^{\nu\nu}\left(\frac{\partial \widehat{g_{\nu\nu}}}{\partial x^{\nu}} + \frac{\partial g_{\nu\nu}}{\partial x^{\nu}} - \frac{\partial g_{\nu\nu}}{\partial x^{\nu}}\right)\right)\frac{1}{2}g^{\nu\mu}\left(\frac{\partial \widehat{g_{\nu\nu}}}{\partial x^{\nu}} + \frac{\partial g_{\nu\nu}}{\partial x^{\nu}} - \frac{\partial g_{\nu\nu}}{\partial x^{\nu}}\right)
\end{aligned}$$

$$+\frac{\partial x^{\nu}}{\partial x^{\nu}}\frac{1}{2}g^{\nu\nu}\left(\frac{\partial \widehat{g_{\nu\nu}}}{\partial x^{\nu}}+\frac{\partial g_{\nu\nu}}{\partial x^{\nu}}-\frac{\partial g_{\nu\nu}}{\partial x^{\nu}}\right)\frac{1}{2}g^{\nu\mu}\left(\frac{\partial \widehat{g_{\nu\nu}}}{\partial x^{\nu}}+\frac{\partial g_{\nu\nu}}{\partial x^{\nu}}-\frac{\partial g_{\nu\nu}}{\partial x^{\nu}}\right)$$

$$+x^{\nu}\frac{1}{2}g^{\nu\nu}\left(\frac{\partial \widehat{g_{\nu\nu}}}{\partial x^{\nu}}+\frac{\partial g_{\nu\nu}}{\partial x^{\nu}}-\frac{\partial g_{\nu\nu}}{\partial x^{\nu}}\right)\frac{1}{2}g^{\nu\nu}\left(\frac{\partial \widehat{g_{\nu\nu}}}{\partial x^{\nu}}+\frac{\partial g_{\nu\nu}}{\partial x^{\nu}}-\frac{\partial g_{\nu\nu}}{\partial x^{\nu}}\right)$$

$$\times\frac{1}{2}g^{\nu\mu}\left(\frac{\partial \widehat{g_{\nu\nu}}}{\partial x^{\nu}}+\frac{\partial g_{\nu\nu}}{\partial x^{\nu}}-\frac{\partial g_{\nu\nu}}{\partial x^{\nu}}\right)$$

$$-\frac{\partial x^{\nu}}{\partial x^{\nu}}\frac{1}{2}g^{\nu\nu}\left(\frac{\partial \widehat{g_{\nu\nu}}}{\partial x^{\nu}}+\frac{\partial g_{\nu\nu}}{\partial x^{\nu}}-\frac{\partial g_{\nu\nu}}{\partial x^{\nu}}\right)\frac{1}{2}g^{\nu\mu}\left(\frac{\partial \widehat{g_{\nu\nu}}}{\partial x^{\nu}}+\frac{\partial g_{\nu\nu}}{\partial x^{\nu}}-\frac{\partial g_{\nu\nu}}{\partial x^{\nu}}\right)$$

$$-x^{\nu}\frac{1}{2}g^{\nu\nu}\left(\frac{\partial \widehat{g_{\nu\nu}}}{\partial x^{\nu}}+\frac{\partial g_{\nu\nu}}{\partial x^{\nu}}-\frac{\partial g_{\nu\nu}}{\partial x^{\nu}}\right)\frac{1}{2}g^{\nu\nu}\left(\frac{\partial \widehat{g_{\nu\nu}}}{\partial x^{\nu}}+\frac{\partial g_{\nu\nu}}{\partial x^{\nu}}-\frac{\partial g_{\nu\nu}}{\partial x^{\nu}}\right)$$

$$\times\frac{1}{2}g^{\nu\mu}\left(\frac{\partial \widehat{g_{\nu\nu}}}{\partial x^{\nu}}+\frac{\partial g_{\nu\nu}}{\partial x^{\nu}}-\frac{\partial g_{\nu\nu}}{\partial x^{\nu}}\right)-\frac{\partial^2 x^{\mu}}{\partial x^{\nu}\partial x^{\nu}}\frac{1}{2}g^{\nu\nu}\left(\frac{\partial \widehat{g_{\nu\nu}}}{\partial x^{\nu}}+\frac{\partial g_{\nu\nu}}{\partial x^{\nu}}-\frac{\partial g_{\nu\nu}}{\partial x^{\nu}}\right)$$

$$-\frac{\partial}{\partial x^{\nu}}\left(x^{\nu}\frac{1}{2}g^{\nu\mu}\left(\frac{\partial \widehat{g_{\nu\nu}}}{\partial x^{\nu}}+\frac{\partial g_{\nu\nu}}{\partial x^{\nu}}-\frac{\partial g_{\nu\nu}}{\partial x^{\nu}}\right)\right)\frac{1}{2}g^{\nu\nu}\left(\frac{\partial \widehat{g_{\nu\nu}}}{\partial x^{\nu}}+\frac{\partial g_{\nu\nu}}{\partial x^{\nu}}-\frac{\partial g_{\nu\nu}}{\partial x^{\nu}}\right)$$

$$-\frac{\partial x^{\nu}}{\partial x^{\nu}}\frac{1}{2}g^{\nu\mu}\left(\frac{\partial \widehat{g_{\nu\nu}}}{\partial x^{\nu}}+\frac{\partial g_{\nu\nu}}{\partial x^{\nu}}-\frac{\partial g_{\nu\nu}}{\partial x^{\nu}}\right)\frac{1}{2}g^{\nu\nu}\left(\frac{\partial \widehat{g_{\nu\nu}}}{\partial x^{\nu}}+\frac{\partial g_{\nu\nu}}{\partial x^{\nu}}-\frac{\partial g_{\nu\nu}}{\partial x^{\nu}}\right)$$

$$-x^{\nu}\frac{1}{2}g^{\nu\nu}\left(\frac{\partial \widehat{g_{\nu\nu}}}{\partial x^{\nu}}+\frac{\partial g_{\nu\nu}}{\partial x^{\nu}}-\frac{\partial g_{\nu\nu}}{\partial x^{\nu}}\right)\frac{1}{2}g^{\nu\mu}\left(\frac{\partial \widehat{g_{\nu\nu}}}{\partial x^{\nu}}+\frac{\partial g_{\nu\nu}}{\partial x^{\nu}}-\frac{\partial g_{\nu\nu}}{\partial x^{\nu}}\right)$$

$$\times\frac{1}{2}g^{\nu\nu}\left(\frac{\partial \widehat{g_{\nu\nu}}}{\partial x^{\nu}}+\frac{\partial g_{\nu\nu}}{\partial x^{\nu}}-\frac{\partial g_{\nu\nu}}{\partial x^{\nu}}\right)$$

$$+\frac{\partial x^{\mu}}{\partial x^{\nu}}\frac{1}{2}g^{\nu\nu}\left(\frac{\partial \widehat{g_{\nu\nu}}}{\partial x^{\nu}}+\frac{\partial g_{\nu\nu}}{\partial x^{\nu}}-\frac{\partial g_{\nu\nu}}{\partial x^{\nu}}\right)\frac{1}{2}g^{\nu\nu}\left(\frac{\partial \widehat{g_{\nu\nu}}}{\partial x^{\nu}}+\frac{\partial g_{\nu\nu}}{\partial x^{\nu}}-\frac{\partial g_{\nu\nu}}{\partial x^{\nu}}\right)$$

$$+x^{\nu}\frac{1}{2}g^{\nu\mu}\left(\frac{\partial \widehat{g_{\nu\nu}}}{\partial x^{\nu}}+\frac{\partial g_{\nu\nu}}{\partial x^{\nu}}-\frac{\partial g_{\nu\nu}}{\partial x^{\nu}}\right)\frac{1}{2}g^{\nu\nu}\left(\frac{\partial \widehat{g_{\nu\nu}}}{\partial x^{\nu}}+\frac{\partial g_{\nu\nu}}{\partial x^{\nu}}-\frac{\partial g_{\nu\nu}}{\partial x^{\nu}}\right)$$

$$\times\frac{1}{2}g^{\nu\nu}\left(\frac{\partial \widehat{g_{\nu\nu}}}{\partial x^{\nu}}+\frac{\partial g_{\nu\nu}}{\partial x^{\nu}}-\frac{\partial g_{\nu\nu}}{\partial x^{\nu}}\right)-\frac{\partial^2 x^{\mu}}{\partial x^{\nu}\partial x^{\nu}}\frac{1}{2}g^{\nu\nu}\left(\frac{\partial \widehat{g_{\nu\nu}}}{\partial x^{\nu}}+\frac{\partial g_{\nu\nu}}{\partial x^{\nu}}-\frac{\partial g_{\nu\nu}}{\partial x^{\nu}}\right)$$

$$-\frac{\partial}{\partial x^{\nu}}\left(x^{\nu}\frac{1}{2}g^{\nu\mu}\left(\frac{\partial \widehat{g_{\nu\nu}}}{\partial x^{\nu}}+\frac{\partial g_{\nu\nu}}{\partial x^{\nu}}-\frac{\partial g_{\nu\nu}}{\partial x^{\nu}}\right)\right)\frac{1}{2}g^{\nu\nu}\left(\frac{\partial \widehat{g_{\nu\nu}}}{\partial x^{\nu}}+\frac{\partial g_{\nu\nu}}{\partial x^{\nu}}-\frac{\partial g_{\nu\nu}}{\partial x^{\nu}}\right)$$

$$-\frac{\partial x^{\nu}}{\partial x^{\nu}}\frac{1}{2}g^{\nu\mu}\left(\frac{\partial \widehat{g_{\nu\nu}}}{\partial x^{\nu}}+\frac{\partial g_{\nu\nu}}{\partial x^{\nu}}-\frac{\partial g_{\nu\nu}}{\partial x^{\nu}}\right)\frac{1}{2}g^{\nu\nu}\left(\frac{\partial \widehat{g_{\nu\nu}}}{\partial x^{\nu}}+\frac{\partial g_{\nu\nu}}{\partial x^{\nu}}-\frac{\partial g_{\nu\nu}}{\partial x^{\nu}}\right)$$

$$-x^{\nu}\frac{1}{2}g^{\nu\nu}\left(\frac{\partial \widehat{g_{\nu\nu}}}{\partial x^{\nu}}+\frac{\partial g_{\nu\nu}}{\partial x^{\nu}}-\frac{\partial g_{\nu\nu}}{\partial x^{\nu}}\right)\frac{1}{2}g^{\nu\mu}\left(\frac{\partial \widehat{g_{\nu\nu}}}{\partial x^{\nu}}+\frac{\partial g_{\nu\nu}}{\partial x^{\nu}}-\frac{\partial g_{\nu\nu}}{\partial x^{\nu}}\right)$$

$$\times\frac{1}{2}g^{\nu\nu}\left(\frac{\partial \widehat{g_{\nu\nu}}}{\partial x^{\nu}}+\frac{\partial g_{\nu\nu}}{\partial x^{\nu}}-\frac{\partial g_{\nu\nu}}{\partial x^{\nu}}\right)$$

$$+\frac{\partial x^{\mu}}{\partial x^{\nu}}\frac{1}{2}g^{\nu\nu}\left(\frac{\partial \widehat{g_{\nu\nu}}}{\partial x^{\nu}}+\frac{\partial g_{\nu\nu}}{\partial x^{\nu}}-\frac{\partial g_{\nu\nu}}{\partial x^{\nu}}\right)\frac{1}{2}g^{\nu\nu}\left(\frac{\partial \widehat{g_{\nu\nu}}}{\partial x^{\nu}}+\frac{\partial g_{\nu\nu}}{\partial x^{\nu}}-\frac{\partial g_{\nu\nu}}{\partial x^{\nu}}\right)$$

$$
\begin{aligned}
&+x^{\nu}\frac{1}{2}g^{\nu\mu}\left(\frac{\partial\widehat{g_{\nu\nu}}}{\partial x^{\nu}}+\frac{\partial g_{\nu\nu}}{\partial x^{\nu}}-\frac{\partial g_{\nu\nu}}{\partial x^{\nu}}\right)\frac{1}{2}g^{\nu\nu}\left(\frac{\partial\widehat{g_{\nu\nu}}}{\partial x^{\nu}}+\frac{\partial g_{\nu\nu}}{\partial x^{\nu}}-\frac{\partial g_{\nu\nu}}{\partial x^{\nu}}\right)\\
&\times\frac{1}{2}g^{\nu\nu}\left(\frac{\partial\widehat{g_{\nu\nu}}}{\partial x^{\nu}}+\frac{\partial g_{\nu\nu}}{\partial x^{\nu}}-\frac{\partial g_{\nu\nu}}{\partial x^{\nu}}\right)\\
&=\frac{\partial^3x^{\mu}}{\partial x^{\nu}\partial x^{\nu}\partial x^{\nu}}+\frac{\partial^2}{\partial x^{\nu}\partial x^{\nu}}\left(x^{\nu}\frac{1}{2}\left(\frac{\partial\widehat{g_{\nu}^{\mu}}}{\partial x^{\nu}}\right)\right)+\frac{\partial}{\partial x^{\nu}}\left(\frac{\partial x^{\nu}}{\partial x^{\nu}}\frac{1}{2}\left(\frac{\partial\widehat{g_{\nu}^{\mu}}}{\partial x^{\nu}}\right)\right)\\
&+\frac{\partial}{\partial x^{\nu}}\left(x^{\nu}\frac{1}{2}\left(\frac{\partial\widehat{g_{\nu}^{\nu}}}{\partial x^{\nu}}\right)\frac{1}{2}\left(\frac{\partial\widehat{g_{\nu}^{\mu}}}{\partial x^{\nu}}\right)\right)-\frac{\partial}{\partial x^{\nu}}\left(\frac{\partial x^{\mu}}{\partial x^{\nu}}\frac{1}{2}\left(\frac{\partial\widehat{g_{\nu}^{\nu}}}{\partial x^{\nu}}\right)\right)\\
&-\frac{\partial}{\partial x^{\nu}}\left(x^{\nu}\frac{1}{2}\left(\frac{\partial\widehat{g_{\nu}^{\mu}}}{\partial x^{\nu}}\right)\frac{1}{2}\left(\frac{\partial\widehat{g_{\nu}^{\nu}}}{\partial x^{\nu}}\right)\right)+\frac{\partial^2x^{\nu}}{\partial x^{\nu}\partial x^{\nu}}\frac{1}{2}\left(\frac{\partial\widehat{g_{\nu}^{\mu}}}{\partial x^{\nu}}\right)\\
&+\frac{\partial}{\partial x^{\nu}}\left(x^{\nu}\frac{1}{2}\left(\frac{\partial\widehat{g_{\nu}^{\nu}}}{\partial x^{\nu}}\right)\right)\frac{1}{2}\left(\frac{\partial\widehat{g_{\nu}^{\mu}}}{\partial x^{\nu}}\right)+\frac{\partial x^{\nu}}{\partial x^{\nu}}\frac{1}{2}\left(\frac{\partial\widehat{g_{\nu}^{\nu}}}{\partial x^{\nu}}\right)\frac{1}{2}\left(\frac{\partial\widehat{g_{\nu}^{\mu}}}{\partial x^{\nu}}\right)\\
&+x^{\nu}\frac{1}{2}\left(\frac{\partial\widehat{g_{\nu}^{\nu}}}{\partial x^{\nu}}\right)\frac{1}{2}\left(\frac{\partial\widehat{g_{\nu}^{\nu}}}{\partial x^{\nu}}\right)\frac{1}{2}\left(\frac{\partial\widehat{g_{\nu}^{\mu}}}{\partial x^{\nu}}\right)-\frac{\partial x^{\nu}}{\partial x^{\nu}}\frac{1}{2}\left(\frac{\partial\widehat{g_{\nu}^{\nu}}}{\partial x^{\nu}}\right)\frac{1}{2}\left(\frac{\partial\widehat{g_{\nu}^{\mu}}}{\partial x^{\nu}}\right)\\
&-x^{\nu}\frac{1}{2}\left(\frac{\partial\widehat{g_{\nu}^{\nu}}}{\partial x^{\nu}}\right)\frac{1}{2}\left(\frac{\partial\widehat{g_{\nu}^{\nu}}}{\partial x^{\nu}}\right)\frac{1}{2}\left(\frac{\partial\widehat{g_{\nu}^{\mu}}}{\partial x^{\nu}}\right)-\frac{\partial^2x^{\mu}}{\partial x^{\nu}\partial x^{\nu}}\frac{1}{2}\left(\frac{\partial\widehat{g_{\nu}^{\nu}}}{\partial x^{\nu}}\right)\\
&-\frac{\partial}{\partial x^{\nu}}\left(x^{\nu}\frac{1}{2}\left(\frac{\partial\widehat{g_{\nu}^{\mu}}}{\partial x^{\nu}}\right)\right)\frac{1}{2}\left(\frac{\partial\widehat{g_{\nu}^{\nu}}}{\partial x^{\nu}}\right)-\frac{\partial x^{\nu}}{\partial x^{\nu}}\frac{1}{2}\left(\frac{\partial\widehat{g_{\nu}^{\mu}}}{\partial x^{\nu}}\right)\frac{1}{2}\left(\frac{\partial\widehat{g_{\nu}^{\nu}}}{\partial x^{\nu}}\right)\\
&-x^{\nu}\frac{1}{2}\left(\frac{\partial\widehat{g_{\nu}^{\nu}}}{\partial x^{\nu}}\right)\frac{1}{2}\left(\frac{\partial\widehat{g_{\nu}^{\mu}}}{\partial x^{\nu}}\right)\frac{1}{2}\left(\frac{\partial\widehat{g_{\nu}^{\nu}}}{\partial x^{\nu}}\right)+\frac{\partial x^{\mu}}{\partial x^{\nu}}\frac{1}{2}\left(\frac{\partial\widehat{g_{\nu}^{\nu}}}{\partial x^{\nu}}\right)\frac{1}{2}\left(\frac{\partial\widehat{g_{\nu}^{\nu}}}{\partial x^{\nu}}\right)\\
&+x^{\nu}\frac{1}{2}\left(\frac{\partial\widehat{g_{\nu}^{\mu}}}{\partial x^{\nu}}\right)\frac{1}{2}\left(\frac{\partial\widehat{g_{\nu}^{\nu}}}{\partial x^{\nu}}\right)\frac{1}{2}\left(\frac{\partial\widehat{g_{\nu}^{\nu}}}{\partial x^{\nu}}\right)-\frac{\partial^2x^{\mu}}{\partial x^{\nu}\partial x^{\nu}}\frac{1}{2}\left(\frac{\partial\widehat{g_{\nu}^{\nu}}}{\partial x^{\nu}}\right)\\
&-\frac{\partial}{\partial x^{\nu}}\left(x^{\nu}\frac{1}{2}\left(\frac{\partial\widehat{g_{\nu}^{\mu}}}{\partial x^{\nu}}\right)\right)\frac{1}{2}\left(\frac{\partial\widehat{g_{\nu}^{\nu}}}{\partial x^{\nu}}\right)-\frac{\partial x^{\nu}}{\partial x^{\nu}}\frac{1}{2}\left(\frac{\partial\widehat{g_{\nu}^{\mu}}}{\partial x^{\nu}}\right)\frac{1}{2}\left(\frac{\partial\widehat{g_{\nu}^{\nu}}}{\partial x^{\nu}}\right)\\
&-x^{\nu}\frac{1}{2}\left(\frac{\partial\widehat{g_{\nu}^{\nu}}}{\partial x^{\nu}}\right)\frac{1}{2}\left(\frac{\partial\widehat{g_{\nu}^{\mu}}}{\partial x^{\nu}}\right)\frac{1}{2}\left(\frac{\partial\widehat{g_{\nu}^{\nu}}}{\partial x^{\nu}}\right)+\frac{\partial x^{\mu}}{\partial x^{\nu}}\frac{1}{2}\left(\frac{\partial\widehat{g_{\nu}^{\nu}}}{\partial x^{\nu}}\right)\frac{1}{2}\left(\frac{\partial\widehat{g_{\nu}^{\nu}}}{\partial x^{\nu}}\right)\\
&+x^{\nu}\frac{1}{2}\left(\frac{\partial\widehat{g_{\nu}^{\mu}}}{\partial x^{\nu}}\right)\frac{1}{2}\left(\frac{\partial\widehat{g_{\nu}^{\nu}}}{\partial x^{\nu}}\right)\frac{1}{2}\left(\frac{\partial\widehat{g_{\nu}^{\nu}}}{\partial x^{\nu}}\right)\\
&=\frac{\partial^3x^{\mu}}{\partial x^{\nu}\partial x^{\nu}\partial x^{\nu}}+\frac{\partial^2}{\partial x^{\nu}\partial x^{\nu}}\left(x^{\nu}\frac{1}{2}\left(\frac{\partial g_{\nu}^{\mu}}{\partial x^{\nu}}\right)\right)+\frac{\partial}{\partial x^{\nu}}\left(\frac{\partial x^{\nu}}{\partial x^{\nu}}\frac{1}{2}\left(\frac{\partial g_{\nu}^{\mu}}{\partial x^{\nu}}\right)\right)\\
&+\frac{\partial}{\partial x^{\nu}}\left(x^{\nu}\frac{1}{2}\left(\frac{\partial g_{\nu}^{\nu}}{\partial x^{\nu}}\right)\frac{1}{2}\left(\frac{\partial g_{\nu}^{\mu}}{\partial x^{\nu}}\right)\right)-\frac{\partial}{\partial x^{\nu}}\left(\frac{\partial x^{\mu}}{\partial x^{\nu}}\frac{1}{2}\left(\frac{\partial g_{\nu}^{\nu}}{\partial x^{\nu}}\right)\right)\\
&-\frac{\partial}{\partial x^{\nu}}\left(x^{\nu}\frac{1}{2}\left(\frac{\partial g_{\nu}^{\mu}}{\partial x^{\nu}}\right)\frac{1}{2}\left(\frac{\partial g_{\nu}^{\nu}}{\partial x^{\nu}}\right)\right)+\frac{\partial^2x^{\nu}}{\partial x^{\nu}\partial x^{\nu}}\frac{1}{2}\left(\frac{\partial g_{\nu}^{\mu}}{\partial x^{\nu}}\right)
\end{aligned}
\tag{24}
$$

$$
\begin{aligned}
&+\frac{\partial}{\partial x^{\nu}}\left(x^{\nu}\frac{1}{2}\left(\frac{\partial g_{\nu}^{\nu}}{\partial x^{\nu}}\right)\right)\frac{1}{2}\left(\frac{\partial g_{\nu}^{\mu}}{\partial x^{\nu}}\right)+\frac{\partial x^{\nu}}{\partial x^{\nu}}\frac{1}{2}\left(\frac{\partial g_{\nu}^{\nu}}{\partial x^{\nu}}\right)\frac{1}{2}\left(\frac{\partial g_{\nu}^{\mu}}{\partial x^{\nu}}\right)\\
&+x^{\nu}\frac{1}{2}\left(\frac{\partial g_{\nu}^{\nu}}{\partial x^{\nu}}\right)\frac{1}{2}\left(\frac{\partial g_{\nu}^{\nu}}{\partial x^{\nu}}\right)\frac{1}{2}\left(\frac{\partial g_{\nu}^{\mu}}{\partial x^{\nu}}\right)-\frac{\partial x^{\nu}}{\partial x^{\nu}}\frac{1}{2}\left(\frac{\partial g_{\nu}^{\nu}}{\partial x^{\nu}}\right)\frac{1}{2}\left(\frac{\partial g_{\nu}^{\mu}}{\partial x^{\nu}}\right)\\
&-x^{\nu}\frac{1}{2}\left(\frac{\partial g_{\nu}^{\nu}}{\partial x^{\nu}}\right)\frac{1}{2}\left(\frac{\partial g_{\nu}^{\nu}}{\partial x^{\nu}}\right)\frac{1}{2}\left(\frac{\partial g_{\nu}^{\mu}}{\partial x^{\nu}}\right)-\frac{\partial^{2}x^{\mu}}{\partial x^{\nu}\partial x^{\nu}}\frac{1}{2}\left(\frac{\partial g_{\nu}^{\nu}}{\partial x^{\nu}}\right)\\
&-\frac{\partial}{\partial x^{\nu}}\left(x^{\nu}\frac{1}{2}\left(\frac{\partial g_{\nu}^{\mu}}{\partial x^{\nu}}\right)\right)\frac{1}{2}\left(\frac{\partial g_{\nu}^{\nu}}{\partial x^{\nu}}\right)-\frac{\partial x^{\nu}}{\partial x^{\nu}}\frac{1}{2}\left(\frac{\partial g_{\nu}^{\mu}}{\partial x^{\nu}}\right)\frac{1}{2}\left(\frac{\partial g_{\nu}^{\nu}}{\partial x^{\nu}}\right)\\
&-x^{\nu}\frac{1}{2}\left(\frac{\partial g_{\nu}^{\nu}}{\partial x^{\nu}}\right)\frac{1}{2}\left(\frac{\partial g_{\nu}^{\mu}}{\partial x^{\nu}}\right)\frac{1}{2}\left(\frac{\partial g_{\nu}^{\nu}}{\partial x^{\nu}}\right)+\frac{\partial x^{\mu}}{\partial x^{\nu}}\frac{1}{2}\left(\frac{\partial g_{\nu}^{\nu}}{\partial x^{\nu}}\right)\frac{1}{2}\left(\frac{\partial g_{\nu}^{\nu}}{\partial x^{\nu}}\right)\\
&+x^{\nu}\frac{1}{2}\left(\frac{\partial g_{\nu}^{\mu}}{\partial x^{\nu}}\right)\frac{1}{2}\left(\frac{\partial g_{\nu}^{\nu}}{\partial x^{\nu}}\right)\frac{1}{2}\left(\frac{\partial g_{\nu}^{\nu}}{\partial x^{\nu}}\right)-\frac{\partial^{2}x^{\mu}}{\partial x^{\nu}\partial x^{\nu}}\frac{1}{2}\left(\frac{\partial g_{\nu}^{\nu}}{\partial x^{\nu}}\right)\\
&-\frac{\partial}{\partial x^{\nu}}\left(x^{\nu}\frac{1}{2}\left(\frac{\partial g_{\nu}^{\mu}}{\partial x^{\nu}}\right)\right)\frac{1}{2}\left(\frac{\partial g_{\nu}^{\nu}}{\partial x^{\nu}}\right)-\frac{\partial x^{\nu}}{\partial x^{\nu}}\frac{1}{2}\left(\frac{\partial g_{\nu}^{\mu}}{\partial x^{\nu}}\right)\frac{1}{2}\left(\frac{\partial g_{\nu}^{\nu}}{\partial x^{\nu}}\right)\\
&-x^{\nu}\frac{1}{2}\left(\frac{\partial g_{\nu}^{\nu}}{\partial x^{\nu}}\right)\frac{1}{2}\left(\frac{\partial g_{\nu}^{\mu}}{\partial x^{\nu}}\right)\frac{1}{2}\left(\frac{\partial g_{\nu}^{\nu}}{\partial x^{\nu}}\right)+\frac{\partial x^{\mu}}{\partial x^{\nu}}\frac{1}{2}\left(\frac{\partial g_{\nu}^{\nu}}{\partial x^{\nu}}\right)\frac{1}{2}\left(\frac{\partial g_{\nu}^{\nu}}{\partial x^{\nu}}\right)\\
&+x^{\nu}\frac{1}{2}\left(\frac{\partial g_{\nu}^{\mu}}{\partial x^{\nu}}\right)\frac{1}{2}\left(\frac{\partial g_{\nu}^{\nu}}{\partial x^{\nu}}\right)\frac{1}{2}\left(\frac{\partial g_{\nu}^{\nu}}{\partial x^{\nu}}\right)
\end{aligned}
\tag{25}
$$

from Definition 13. (24), (25) must rewrite it in

$$
\begin{aligned}
x^{\mu}_{;\nu;\nu;\nu}=&\frac{\partial^{3}x^{\mu}}{\partial x^{\nu}\partial x^{\nu}\partial x^{\nu}}+\frac{\partial^{2}}{\partial x^{\nu}\partial x^{\nu}}\left(x^{\sigma}\frac{1}{2}\left(\frac{\partial g_{\sigma}^{\mu}}{\partial x^{\nu}}\right)\right)+\frac{\partial}{\partial x^{\nu}}\left(\frac{\partial x^{\sigma}}{\partial x^{\nu}}\frac{1}{2}\left(\frac{\partial g_{\sigma}^{\mu}}{\partial x^{\nu}}\right)\right)\\
&+\frac{\partial}{\partial x^{\nu}}\left(x^{\sigma}\frac{1}{2}\left(\frac{\partial g_{\sigma}^{\sigma}}{\partial x^{\nu}}\right)\frac{1}{2}\left(\frac{\partial g_{\sigma}^{\mu}}{\partial x^{\nu}}\right)\right)-\frac{\partial}{\partial x^{\nu}}\left(\frac{\partial x^{\mu}}{\partial x^{\sigma}}\frac{1}{2}\left(\frac{\partial g_{\nu}^{\sigma}}{\partial x^{\nu}}\right)\right)\\
&-\frac{\partial}{\partial x^{\nu}}\left(x^{\sigma}\frac{1}{2}\left(\frac{\partial g_{\sigma}^{\mu}}{\partial x^{\sigma}}\right)\frac{1}{2}\left(\frac{\partial g_{\nu}^{\sigma}}{\partial x^{\nu}}\right)\right)+\frac{\partial^{2}x^{\sigma}}{\partial x^{\nu}\partial x^{\nu}}\frac{1}{2}\left(\frac{\partial g_{\sigma}^{\mu}}{\partial x^{\nu}}\right)\\
&+\frac{\partial}{\partial x^{\nu}}\left(x^{\sigma}\frac{1}{2}\left(\frac{\partial g_{\sigma}^{\sigma}}{\partial x^{\nu}}\right)\right)\frac{1}{2}\left(\frac{\partial g_{\sigma}^{\mu}}{\partial x^{\nu}}\right)+\frac{\partial x^{\sigma}}{\partial x^{\nu}}\frac{1}{2}\left(\frac{\partial g_{\sigma}^{\sigma}}{\partial x^{\nu}}\right)\frac{1}{2}\left(\frac{\partial g_{\sigma}^{\mu}}{\partial x^{\nu}}\right)\\
&+x^{\sigma}\frac{1}{2}\left(\frac{\partial g_{\sigma}^{\sigma}}{\partial x^{\nu}}\right)\frac{1}{2}\left(\frac{\partial g_{\sigma}^{\sigma}}{\partial x^{\nu}}\right)\frac{1}{2}\left(\frac{\partial g_{\sigma}^{\mu}}{\partial x^{\nu}}\right)-\frac{\partial x^{\sigma}}{\partial x^{\sigma}}\frac{1}{2}\left(\frac{\partial g_{\nu}^{\sigma}}{\partial x^{\nu}}\right)\frac{1}{2}\left(\frac{\partial g_{\sigma}^{\mu}}{\partial x^{\nu}}\right)\\
&-x^{\sigma}\frac{1}{2}\left(\frac{\partial g_{\sigma}^{\sigma}}{\partial x^{\sigma}}\right)\frac{1}{2}\left(\frac{\partial g_{\nu}^{\sigma}}{\partial x^{\nu}}\right)\frac{1}{2}\left(\frac{\partial g_{\sigma}^{\mu}}{\partial x^{\nu}}\right)-\frac{\partial^{2}x^{\mu}}{\partial x^{\sigma}\partial x^{\nu}}\frac{1}{2}\left(\frac{\partial g_{\nu}^{\sigma}}{\partial x^{\nu}}\right)\\
&-\frac{\partial}{\partial x^{\nu}}\left(x^{\sigma}\frac{1}{2}\left(\frac{\partial g_{\sigma}^{\mu}}{\partial x^{\sigma}}\right)\right)\frac{1}{2}\left(\frac{\partial g_{\nu}^{\sigma}}{\partial x^{\nu}}\right)-\frac{\partial x^{\sigma}}{\partial x^{\sigma}}\frac{1}{2}\left(\frac{\partial g_{\sigma}^{\mu}}{\partial x^{\nu}}\right)\frac{1}{2}\left(\frac{\partial g_{\nu}^{\sigma}}{\partial x^{\nu}}\right)\\
&-x^{\sigma}\frac{1}{2}\left(\frac{\partial g_{\sigma}^{\sigma}}{\partial x^{\sigma}}\right)\frac{1}{2}\left(\frac{\partial g_{\sigma}^{\mu}}{\partial x^{\nu}}\right)\frac{1}{2}\left(\frac{\partial g_{\nu}^{\sigma}}{\partial x^{\nu}}\right)+\frac{\partial x^{\mu}}{\partial x^{\sigma}}\frac{1}{2}\left(\frac{\partial g_{\sigma}^{\sigma}}{\partial x^{\nu}}\right)\frac{1}{2}\left(\frac{\partial g_{\nu}^{\sigma}}{\partial x^{\nu}}\right)\\
&+x^{\sigma}\frac{1}{2}\left(\frac{\partial g_{\sigma}^{\mu}}{\partial x^{\sigma}}\right)\frac{1}{2}\left(\frac{\partial g_{\sigma}^{\sigma}}{\partial x^{\nu}}\right)\frac{1}{2}\left(\frac{\partial g_{\nu}^{\sigma}}{\partial x^{\nu}}\right)-\frac{\partial^{2}x^{\mu}}{\partial x^{\nu}\partial x^{\sigma}}\frac{1}{2}\left(\frac{\partial g_{\nu}^{\sigma}}{\partial x^{\nu}}\right)
\end{aligned}
$$

$$
\begin{aligned}
&-\frac{\partial}{\partial x^{\sigma}}\left(x^{\sigma}\frac{1}{2}\left(\frac{\partial g_{\sigma}^{\mu}}{\partial x^{\nu}}\right)\right)\frac{1}{2}\left(\frac{\partial g_{\nu}^{\sigma}}{\partial x^{\nu}}\right)-\frac{\partial x^{\sigma}}{\partial x^{\nu}}\frac{1}{2}\left(\frac{\partial g_{\sigma}^{\mu}}{\partial x^{\sigma}}\right)\frac{1}{2}\left(\frac{\partial g_{\nu}^{\sigma}}{\partial x^{\nu}}\right)\\
&-x^{\sigma}\frac{1}{2}\left(\frac{\partial g_{\sigma}^{\sigma}}{\partial x^{\nu}}\right)\frac{1}{2}\left(\frac{\partial g_{\sigma}^{\mu}}{\partial x^{\sigma}}\right)\frac{1}{2}\left(\frac{\partial g_{\nu}^{\sigma}}{\partial x^{\nu}}\right)+\frac{\partial x^{\mu}}{\partial x^{\sigma}}\frac{1}{2}\left(\frac{\partial g_{\nu}^{\sigma}}{\partial x^{\sigma}}\right)\frac{1}{2}\left(\frac{\partial g_{\nu}^{\sigma}}{\partial x^{\nu}}\right)\\
&+x^{\sigma}\frac{1}{2}\left(\frac{\partial g_{\sigma}^{\mu}}{\partial x^{\sigma}}\right)\frac{1}{2}\left(\frac{\partial g_{\nu}^{\sigma}}{\partial x^{\sigma}}\right)\frac{1}{2}\left(\frac{\partial g_{\nu}^{\sigma}}{\partial x^{\nu}}\right)
\end{aligned}
\tag{26}
$$

$$
\begin{aligned}
&=\frac{\partial^{3}x^{\mu}}{\partial x^{\nu}\partial x^{\nu}\partial x^{\nu}}+\frac{\partial^{2}}{\partial x^{\nu}\partial x^{\nu}}\left(x^{\sigma}\frac{1}{2}\left(\frac{\partial g_{\nu}^{\mu}}{\partial x^{\sigma}}\right)\right)+\frac{\partial}{\partial x^{\nu}}\left(\frac{\partial x^{\sigma}}{\partial x^{\nu}}\frac{1}{2}\left(\frac{\partial g_{\nu}^{\mu}}{\partial x^{\sigma}}\right)\right)\\
&+\frac{\partial}{\partial x^{\nu}}\left(x^{\sigma}\frac{1}{2}\left(\frac{\partial g_{\nu}^{\sigma}}{\partial x^{\sigma}}\right)\frac{1}{2}\left(\frac{\partial g_{\nu}^{\mu}}{\partial x^{\sigma}}\right)\right)-\frac{\partial}{\partial x^{\nu}}\left(\frac{\partial x^{\mu}}{\partial x^{\sigma}}\frac{1}{2}\left(\frac{\partial g_{\nu}^{\sigma}}{\partial x^{\nu}}\right)\right)\\
&-\frac{\partial}{\partial x^{\nu}}\left(x^{\sigma}\frac{1}{2}\left(\frac{\partial g_{\sigma}^{\mu}}{\partial x^{\sigma}}\right)\frac{1}{2}\left(\frac{\partial g_{\nu}^{\sigma}}{\partial x^{\nu}}\right)\right)+\frac{\partial^{2}x^{\sigma}}{\partial x^{\nu}\partial x^{\nu}}\frac{1}{2}\left(\frac{\partial g_{\nu}^{\mu}}{\partial x^{\sigma}}\right)\\
&+\frac{\partial}{\partial x^{\nu}}\left(x^{\sigma}\frac{1}{2}\left(\frac{\partial g_{\nu}^{\sigma}}{\partial x^{\sigma}}\right)\right)\frac{1}{2}\left(\frac{\partial g_{\nu}^{\mu}}{\partial x^{\sigma}}\right)+\frac{\partial x^{\sigma}}{\partial x^{\nu}}\frac{1}{2}\left(\frac{\partial g_{\nu}^{\sigma}}{\partial x^{\sigma}}\right)\frac{1}{2}\left(\frac{\partial g_{\nu}^{\mu}}{\partial x^{\sigma}}\right)\\
&+x^{\sigma}\frac{1}{2}\left(\frac{\partial g_{\nu}^{\sigma}}{\partial x^{\sigma}}\right)\frac{1}{2}\left(\frac{\partial g_{\nu}^{\sigma}}{\partial x^{\sigma}}\right)\frac{1}{2}\left(\frac{\partial g_{\nu}^{\mu}}{\partial x^{\sigma}}\right)-\frac{\partial x^{\sigma}}{\partial x^{\sigma}}\frac{1}{2}\left(\frac{\partial g_{\nu}^{\sigma}}{\partial x^{\nu}}\right)\frac{1}{2}\left(\frac{\partial g_{\nu}^{\mu}}{\partial x^{\sigma}}\right)\\
&-x^{\sigma}\frac{1}{2}\left(\frac{\partial g_{\sigma}^{\sigma}}{\partial x^{\sigma}}\right)\frac{1}{2}\left(\frac{\partial g_{\nu}^{\sigma}}{\partial x^{\nu}}\right)\frac{1}{2}\left(\frac{\partial g_{\nu}^{\mu}}{\partial x^{\sigma}}\right)-\frac{\partial^{2}x^{\mu}}{\partial x^{\sigma}\partial x^{\nu}}\frac{1}{2}\left(\frac{\partial g_{\nu}^{\sigma}}{\partial x^{\nu}}\right)\\
&-\frac{\partial}{\partial x^{\nu}}\left(x^{\sigma}\frac{1}{2}\left(\frac{\partial g_{\sigma}^{\mu}}{\partial x^{\sigma}}\right)\right)\frac{1}{2}\left(\frac{\partial g_{\nu}^{\sigma}}{\partial x^{\nu}}\right)-\frac{\partial x^{\sigma}}{\partial x^{\sigma}}\frac{1}{2}\left(\frac{\partial g_{\nu}^{\mu}}{\partial x^{\sigma}}\right)\frac{1}{2}\left(\frac{\partial g_{\nu}^{\sigma}}{\partial x^{\nu}}\right)\\
&-x^{\sigma}\frac{1}{2}\left(\frac{\partial g_{\sigma}^{\sigma}}{\partial x^{\sigma}}\right)\frac{1}{2}\left(\frac{\partial g_{\nu}^{\mu}}{\partial x^{\sigma}}\right)\frac{1}{2}\left(\frac{\partial g_{\nu}^{\sigma}}{\partial x^{\nu}}\right)+\frac{\partial x^{\mu}}{\partial x^{\sigma}}\frac{1}{2}\left(\frac{\partial g_{\nu}^{\sigma}}{\partial x^{\sigma}}\right)\frac{1}{2}\left(\frac{\partial g_{\nu}^{\sigma}}{\partial x^{\nu}}\right)\\
&+x^{\sigma}\frac{1}{2}\left(\frac{\partial g_{\sigma}^{\mu}}{\partial x^{\sigma}}\right)\frac{1}{2}\left(\frac{\partial g_{\nu}^{\sigma}}{\partial x^{\sigma}}\right)\frac{1}{2}\left(\frac{\partial g_{\nu}^{\sigma}}{\partial x^{\nu}}\right)-\frac{\partial^{2}x^{\mu}}{\partial x^{\nu}\partial x^{\sigma}}\frac{1}{2}\left(\frac{\partial g_{\nu}^{\sigma}}{\partial x^{\nu}}\right)\\
&-\frac{\partial}{\partial x^{\sigma}}\left(x^{\sigma}\frac{1}{2}\left(\frac{\partial g_{\nu}^{\mu}}{\partial x^{\sigma}}\right)\right)\frac{1}{2}\left(\frac{\partial g_{\nu}^{\sigma}}{\partial x^{\nu}}\right)-\frac{\partial x^{\sigma}}{\partial x^{\nu}}\frac{1}{2}\left(\frac{\partial g_{\sigma}^{\mu}}{\partial x^{\sigma}}\right)\frac{1}{2}\left(\frac{\partial g_{\nu}^{\sigma}}{\partial x^{\nu}}\right)\\
&-x^{\sigma}\frac{1}{2}\left(\frac{\partial g_{\nu}^{\sigma}}{\partial x^{\sigma}}\right)\frac{1}{2}\left(\frac{\partial g_{\sigma}^{\mu}}{\partial x^{\sigma}}\right)\frac{1}{2}\left(\frac{\partial g_{\nu}^{\sigma}}{\partial x^{\nu}}\right)+\frac{\partial x^{\mu}}{\partial x^{\sigma}}\frac{1}{2}\left(\frac{\partial g_{\sigma}^{\sigma}}{\partial x^{\nu}}\right)\frac{1}{2}\left(\frac{\partial g_{\nu}^{\sigma}}{\partial x^{\nu}}\right)\\
&+x^{\sigma}\frac{1}{2}\left(\frac{\partial g_{\sigma}^{\mu}}{\partial x^{\sigma}}\right)\frac{1}{2}\left(\frac{\partial g_{\sigma}^{\sigma}}{\partial x^{\nu}}\right)\frac{1}{2}\left(\frac{\partial g_{\nu}^{\sigma}}{\partial x^{\nu}}\right)
\end{aligned}
\tag{27}
$$

by (24), (25) being a tensor equation. The dummy index has an invariable property for consideration of Binary Law. In other words, the index which was dummy index in Definition 13 is dummy index in (26), (27). I get the conclusion that (26), (27) doesn't satisfy Binary Law from Definition 6. I get the conclusion that Definition 13 isn't an equation of the tensor satisfying Binary Law because (26), (27) doesn't satisfy Binary Law.

I rewrite three existing index ν in each term of (26), (27) in index μ using Definition 4 and get

$$
\begin{aligned}
-x^{\mu}_{;\mu;\mu;\mu} = &-\frac{\partial^3 x^{\mu}}{\partial x^{\mu}\partial x^{\mu}\partial x^{\mu}}-\frac{\partial^2}{\partial x^{\mu}\partial x^{\mu}}\left(x^{\sigma}\frac{1}{2}\left(\frac{\partial g^{\mu}_{\sigma}}{\partial x^{\mu}}\right)\right)-\frac{\partial}{\partial x^{\mu}}\left(\frac{\partial x^{\sigma}}{\partial x^{\mu}}\frac{1}{2}\left(\frac{\partial g^{\mu}_{\sigma}}{\partial x^{\mu}}\right)\right)\\
&-\frac{\partial}{\partial x^{\mu}}\left(x^{\sigma}\frac{1}{2}\left(\frac{\partial g^{\sigma}_{\sigma}}{\partial x^{\mu}}\right)\frac{1}{2}\left(\frac{\partial g^{\mu}_{\sigma}}{\partial x^{\mu}}\right)\right)+\frac{\partial}{\partial x^{\mu}}\left(\frac{\partial x^{\mu}}{\partial x^{\sigma}}\frac{1}{2}\left(\frac{\partial g^{\sigma}_{\mu}}{\partial x^{\mu}}\right)\right)\\
&+\frac{\partial}{\partial x^{\mu}}\left(x^{\sigma}\frac{1}{2}\left(\frac{\partial g^{\mu}_{\sigma}}{\partial x^{\sigma}}\right)\frac{1}{2}\left(\frac{\partial g^{\sigma}_{\mu}}{\partial x^{\mu}}\right)\right)-\frac{\partial^2 x^{\sigma}}{\partial x^{\mu}\partial x^{\mu}}\frac{1}{2}\left(\frac{\partial g^{\mu}_{\sigma}}{\partial x^{\mu}}\right)\\
&-\frac{\partial}{\partial x^{\mu}}\left(x^{\sigma}\frac{1}{2}\left(\frac{\partial g^{\sigma}_{\sigma}}{\partial x^{\mu}}\right)\right)\frac{1}{2}\left(\frac{\partial g^{\mu}_{\sigma}}{\partial x^{\mu}}\right)-\frac{\partial x^{\sigma}}{\partial x^{\mu}}\frac{1}{2}\left(\frac{\partial g^{\sigma}_{\sigma}}{\partial x^{\mu}}\right)\frac{1}{2}\left(\frac{\partial g^{\mu}_{\sigma}}{\partial x^{\mu}}\right)\\
&-x^{\sigma}\frac{1}{2}\left(\frac{\partial g^{\sigma}_{\sigma}}{\partial x^{\mu}}\right)\frac{1}{2}\left(\frac{\partial g^{\sigma}_{\sigma}}{\partial x^{\mu}}\right)\frac{1}{2}\left(\frac{\partial g^{\mu}_{\sigma}}{\partial x^{\mu}}\right)+\frac{\partial x^{\sigma}}{\partial x^{\sigma}}\frac{1}{2}\left(\frac{\partial g^{\sigma}_{\mu}}{\partial x^{\mu}}\right)\frac{1}{2}\left(\frac{\partial g^{\mu}_{\sigma}}{\partial x^{\mu}}\right)\\
&+x^{\sigma}\frac{1}{2}\left(\frac{\partial g^{\sigma}_{\sigma}}{\partial x^{\sigma}}\right)\frac{1}{2}\left(\frac{\partial g^{\sigma}_{\mu}}{\partial x^{\mu}}\right)\frac{1}{2}\left(\frac{\partial g^{\mu}_{\sigma}}{\partial x^{\mu}}\right)+\frac{\partial^2 x^{\mu}}{\partial x^{\sigma}\partial x^{\mu}}\frac{1}{2}\left(\frac{\partial g^{\sigma}_{\mu}}{\partial x^{\mu}}\right)\\
&+\frac{\partial}{\partial x^{\mu}}\left(x^{\sigma}\frac{1}{2}\left(\frac{\partial g^{\mu}_{\sigma}}{\partial x^{\sigma}}\right)\right)\frac{1}{2}\left(\frac{\partial g^{\sigma}_{\mu}}{\partial x^{\mu}}\right)+\frac{\partial x^{\sigma}}{\partial x^{\sigma}}\frac{1}{2}\left(\frac{\partial g^{\mu}_{\sigma}}{\partial x^{\mu}}\right)\frac{1}{2}\left(\frac{\partial g^{\sigma}_{\mu}}{\partial x^{\mu}}\right)\\
&+x^{\sigma}\frac{1}{2}\left(\frac{\partial g^{\sigma}_{\sigma}}{\partial x^{\sigma}}\right)\frac{1}{2}\left(\frac{\partial g^{\mu}_{\sigma}}{\partial x^{\mu}}\right)\frac{1}{2}\left(\frac{\partial g^{\sigma}_{\mu}}{\partial x^{\mu}}\right)-\frac{\partial x^{\mu}}{\partial x^{\sigma}}\frac{1}{2}\left(\frac{\partial g^{\sigma}_{\sigma}}{\partial x^{\mu}}\right)\frac{1}{2}\left(\frac{\partial g^{\sigma}_{\mu}}{\partial x^{\mu}}\right)\\
&-x^{\sigma}\frac{1}{2}\left(\frac{\partial g^{\mu}_{\sigma}}{\partial x^{\sigma}}\right)\frac{1}{2}\left(\frac{\partial g^{\sigma}_{\sigma}}{\partial x^{\mu}}\right)\frac{1}{2}\left(\frac{\partial g^{\sigma}_{\mu}}{\partial x^{\mu}}\right)+\frac{\partial^2 x^{\mu}}{\partial x^{\mu}\partial x^{\sigma}}\frac{1}{2}\left(\frac{\partial g^{\sigma}_{\mu}}{\partial x^{\mu}}\right)\\
&+\frac{\partial}{\partial x^{\sigma}}\left(x^{\sigma}\frac{1}{2}\left(\frac{\partial g^{\mu}_{\sigma}}{\partial x^{\mu}}\right)\right)\frac{1}{2}\left(\frac{\partial g^{\sigma}_{\mu}}{\partial x^{\mu}}\right)+\frac{\partial x^{\sigma}}{\partial x^{\mu}}\frac{1}{2}\left(\frac{\partial g^{\mu}_{\sigma}}{\partial x^{\sigma}}\right)\frac{1}{2}\left(\frac{\partial g^{\sigma}_{\mu}}{\partial x^{\mu}}\right)\\
&+x^{\sigma}\frac{1}{2}\left(\frac{\partial g^{\sigma}_{\sigma}}{\partial x^{\mu}}\right)\frac{1}{2}\left(\frac{\partial g^{\mu}_{\sigma}}{\partial x^{\sigma}}\right)\frac{1}{2}\left(\frac{\partial g^{\sigma}_{\mu}}{\partial x^{\mu}}\right)-\frac{\partial x^{\mu}}{\partial x^{\sigma}}\frac{1}{2}\left(\frac{\partial g^{\mu}_{\sigma}}{\partial x^{\sigma}}\right)\frac{1}{2}\left(\frac{\partial g^{\sigma}_{\mu}}{\partial x^{\mu}}\right)\\
&-x^{\sigma}\frac{1}{2}\left(\frac{\partial g^{\mu}_{\sigma}}{\partial x^{\sigma}}\right)\frac{1}{2}\left(\frac{\partial g^{\sigma}_{\mu}}{\partial x^{\sigma}}\right)\frac{1}{2}\left(\frac{\partial g^{\sigma}_{\mu}}{\partial x^{\mu}}\right)\\
= &-\frac{\partial^3 x^{\mu}}{\partial x^{\mu}\partial x^{\mu}\partial x^{\mu}}-\frac{\partial^2}{\partial x^{\mu}\partial x^{\mu}}\left(x^{\sigma}\frac{1}{2}\left(\frac{\partial g^{\mu}_{\mu}}{\partial x^{\sigma}}\right)\right)-\frac{\partial}{\partial x^{\mu}}\left(\frac{\partial x^{\sigma}}{\partial x^{\mu}}\frac{1}{2}\left(\frac{\partial g^{\mu}_{\mu}}{\partial x^{\sigma}}\right)\right)\\
&-\frac{\partial}{\partial x^{\mu}}\left(x^{\sigma}\frac{1}{2}\left(\frac{\partial g^{\sigma}_{\mu}}{\partial x^{\sigma}}\right)\frac{1}{2}\left(\frac{\partial g^{\mu}_{\mu}}{\partial x^{\sigma}}\right)\right)+\frac{\partial}{\partial x^{\mu}}\left(\frac{\partial x^{\mu}}{\partial x^{\sigma}}\frac{1}{2}\left(\frac{\partial g^{\sigma}_{\mu}}{\partial x^{\mu}}\right)\right)\\
&+\frac{\partial}{\partial x^{\mu}}\left(x^{\sigma}\frac{1}{2}\left(\frac{\partial g^{\mu}_{\sigma}}{\partial x^{\sigma}}\right)\frac{1}{2}\left(\frac{\partial g^{\sigma}_{\mu}}{\partial x^{\mu}}\right)\right)-\frac{\partial^2 x^{\sigma}}{\partial x^{\mu}\partial x^{\mu}}\frac{1}{2}\left(\frac{\partial g^{\mu}_{\mu}}{\partial x^{\sigma}}\right)\\
&-\frac{\partial}{\partial x^{\mu}}\left(x^{\sigma}\frac{1}{2}\left(\frac{\partial g^{\sigma}_{\mu}}{\partial x^{\sigma}}\right)\right)\frac{1}{2}\left(\frac{\partial g^{\mu}_{\mu}}{\partial x^{\sigma}}\right)-\frac{\partial x^{\sigma}}{\partial x^{\mu}}\frac{1}{2}\left(\frac{\partial g^{\sigma}_{\mu}}{\partial x^{\sigma}}\right)\frac{1}{2}\left(\frac{\partial g^{\mu}_{\mu}}{\partial x^{\sigma}}\right)\\
&-x^{\sigma}\frac{1}{2}\left(\frac{\partial g^{\sigma}_{\mu}}{\partial x^{\sigma}}\right)\frac{1}{2}\left(\frac{\partial g^{\sigma}_{\mu}}{\partial x^{\sigma}}\right)\frac{1}{2}\left(\frac{\partial g^{\mu}_{\mu}}{\partial x^{\sigma}}\right)+\frac{\partial x^{\sigma}}{\partial x^{\sigma}}\frac{1}{2}\left(\frac{\partial g^{\sigma}_{\mu}}{\partial x^{\mu}}\right)\frac{1}{2}\left(\frac{\partial g^{\mu}_{\mu}}{\partial x^{\sigma}}\right)\\
&+x^{\sigma}\frac{1}{2}\left(\frac{\partial g^{\sigma}_{\sigma}}{\partial x^{\sigma}}\right)\frac{1}{2}\left(\frac{\partial g^{\sigma}_{\mu}}{\partial x^{\mu}}\right)\frac{1}{2}\left(\frac{\partial g^{\mu}_{\mu}}{\partial x^{\sigma}}\right)+\frac{\partial^2 x^{\mu}}{\partial x^{\sigma}\partial x^{\mu}}\frac{1}{2}\left(\frac{\partial g^{\sigma}_{\mu}}{\partial x^{\mu}}\right)
\end{aligned}
$$

$$
\begin{aligned}
&+\frac{\partial}{\partial x^{\mu}}\left(x^{\sigma}\frac{1}{2}\left(\frac{\partial g_{\sigma}^{\mu}}{\partial x^{\sigma}}\right)\right)\frac{1}{2}\left(\frac{\partial g_{\mu}^{\sigma}}{\partial x^{\mu}}\right)+\frac{\partial x^{\sigma}}{\partial x^{\sigma}}\frac{1}{2}\left(\frac{\partial g_{\mu}^{\mu}}{\partial x^{\sigma}}\right)\frac{1}{2}\left(\frac{\partial g_{\mu}^{\sigma}}{\partial x^{\mu}}\right)\\
&+x^{\sigma}\frac{1}{2}\left(\frac{\partial g_{\sigma}^{\sigma}}{\partial x^{\sigma}}\right)\frac{1}{2}\left(\frac{\partial g_{\mu}^{\mu}}{\partial x^{\sigma}}\right)\frac{1}{2}\left(\frac{\partial g_{\mu}^{\sigma}}{\partial x^{\mu}}\right)-\frac{\partial x^{\mu}}{\partial x^{\sigma}}\frac{1}{2}\left(\frac{\partial g_{\mu}^{\sigma}}{\partial x^{\sigma}}\right)\frac{1}{2}\left(\frac{\partial g_{\mu}^{\sigma}}{\partial x^{\mu}}\right)\\
&-x^{\sigma}\frac{1}{2}\left(\frac{\partial g_{\sigma}^{\mu}}{\partial x^{\sigma}}\right)\frac{1}{2}\left(\frac{\partial g_{\mu}^{\sigma}}{\partial x^{\sigma}}\right)\frac{1}{2}\left(\frac{\partial g_{\mu}^{\sigma}}{\partial x^{\mu}}\right)+\frac{\partial^{2}x^{\mu}}{\partial x^{\mu}\partial x^{\sigma}}\frac{1}{2}\left(\frac{\partial g_{\mu}^{\sigma}}{\partial x^{\mu}}\right)\\
&+\frac{\partial}{\partial x^{\sigma}}\left(x^{\sigma}\frac{1}{2}\left(\frac{\partial g_{\mu}^{\mu}}{\partial x^{\sigma}}\right)\right)\frac{1}{2}\left(\frac{\partial g_{\mu}^{\sigma}}{\partial x^{\mu}}\right)+\frac{\partial x^{\sigma}}{\partial x^{\mu}}\frac{1}{2}\left(\frac{\partial g_{\sigma}^{\mu}}{\partial x^{\sigma}}\right)\frac{1}{2}\left(\frac{\partial g_{\mu}^{\sigma}}{\partial x^{\mu}}\right)\\
&+x^{\sigma}\frac{1}{2}\left(\frac{\partial g_{\mu}^{\sigma}}{\partial x^{\sigma}}\right)\frac{1}{2}\left(\frac{\partial g_{\sigma}^{\mu}}{\partial x^{\sigma}}\right)\frac{1}{2}\left(\frac{\partial g_{\mu}^{\sigma}}{\partial x^{\mu}}\right)-\frac{\partial x^{\mu}}{\partial x^{\sigma}}\frac{1}{2}\left(\frac{\partial g_{\sigma}^{\sigma}}{\partial x^{\mu}}\right)\frac{1}{2}\left(\frac{\partial g_{\mu}^{\sigma}}{\partial x^{\mu}}\right)\\
&-x^{\sigma}\frac{1}{2}\left(\frac{\partial g_{\sigma}^{\mu}}{\partial x^{\sigma}}\right)\frac{1}{2}\left(\frac{\partial g_{\sigma}^{\sigma}}{\partial x^{\mu}}\right)\frac{1}{2}\left(\frac{\partial g_{\mu}^{\sigma}}{\partial x^{\mu}}\right).
\end{aligned}
\tag{28}
$$

I get

$$
-x^{\mu}_{;\mu;\mu;\mu}=-\frac{\partial^{3}x^{\mu}}{\partial x^{\mu}\partial x^{\mu}\partial x^{\mu}} \tag{29}
$$

in consideration of Definition 7 for (28). Because the second term of the right side of (29) doesn't exist,

$$
x^{\mu}_{;\nu;\nu;\nu}=\frac{\partial^{3}x^{\mu}}{\partial x^{\nu}\partial x^{\nu}\partial x^{\nu}} \tag{30}
$$

can rewrite (29) using Definition 4. I rewrite three existing index ν in each term of (26), (27) in index μ using Definition 2 and get

$$
\begin{aligned}
x^{\mu;\mu;\mu;\mu}=&\frac{\partial^{3}x^{\mu}}{\partial x_{\mu}\partial x_{\mu}\partial x_{\mu}}+\frac{\partial^{2}}{\partial x_{\mu}\partial x_{\mu}}\left(x^{\sigma}\frac{1}{2}\left(\frac{\partial g_{\sigma}^{\mu}}{\partial x_{\mu}}\right)\right)+\frac{\partial}{\partial x_{\mu}}\left(\frac{\partial x^{\sigma}}{\partial x_{\mu}}\frac{1}{2}\left(\frac{\partial g_{\sigma}^{\mu}}{\partial x_{\mu}}\right)\right)\\
&+\frac{\partial}{\partial x_{\mu}}\left(x^{\sigma}\frac{1}{2}\left(\frac{\partial g_{\sigma}^{\sigma}}{\partial x_{\mu}}\right)\frac{1}{2}\left(\frac{\partial g_{\sigma}^{\mu}}{\partial x_{\mu}}\right)\right)-\frac{\partial}{\partial x_{\mu}}\left(\frac{\partial x^{\mu}}{\partial x^{\sigma}}\frac{1}{2}\left(\frac{\partial g^{\sigma\mu}}{\partial x_{\mu}}\right)\right)\\
&-\frac{\partial}{\partial x_{\mu}}\left(x^{\sigma}\frac{1}{2}\left(\frac{\partial g_{\sigma}^{\mu}}{\partial x^{\sigma}}\right)\frac{1}{2}\left(\frac{\partial g^{\sigma\mu}}{\partial x_{\mu}}\right)\right)+\frac{\partial^{2}x^{\sigma}}{\partial x_{\mu}\partial x_{\mu}}\frac{1}{2}\left(\frac{\partial g_{\sigma}^{\mu}}{\partial x_{\mu}}\right)\\
&+\frac{\partial}{\partial x_{\mu}}\left(x^{\sigma}\frac{1}{2}\left(\frac{\partial g_{\sigma}^{\sigma}}{\partial x_{\mu}}\right)\right)\frac{1}{2}\left(\frac{\partial g_{\sigma}^{\mu}}{\partial x_{\mu}}\right)+\frac{\partial x^{\sigma}}{\partial x_{\mu}}\frac{1}{2}\left(\frac{\partial g_{\sigma}^{\sigma}}{\partial x_{\mu}}\right)\frac{1}{2}\left(\frac{\partial g_{\sigma}^{\mu}}{\partial x_{\mu}}\right)\\
&+x^{\sigma}\frac{1}{2}\left(\frac{\partial g_{\sigma}^{\sigma}}{\partial x_{\mu}}\right)\frac{1}{2}\left(\frac{\partial g_{\sigma}^{\sigma}}{\partial x_{\mu}}\right)\frac{1}{2}\left(\frac{\partial g_{\sigma}^{\mu}}{\partial x_{\mu}}\right)-\frac{\partial x^{\sigma}}{\partial x^{\sigma}}\frac{1}{2}\left(\frac{\partial g^{\sigma\mu}}{\partial x_{\mu}}\right)\frac{1}{2}\left(\frac{\partial g_{\sigma}^{\mu}}{\partial x_{\mu}}\right)\\
&-x^{\sigma}\frac{1}{2}\left(\frac{\partial g_{\sigma}^{\sigma}}{\partial x^{\sigma}}\right)\frac{1}{2}\left(\frac{\partial g^{\sigma\mu}}{\partial x_{\mu}}\right)\frac{1}{2}\left(\frac{\partial g_{\sigma}^{\mu}}{\partial x_{\mu}}\right)-\frac{\partial^{2}x^{\mu}}{\partial x^{\sigma}\partial x_{\mu}}\frac{1}{2}\left(\frac{\partial g^{\sigma\mu}}{\partial x_{\mu}}\right)\\
&-\frac{\partial}{\partial x_{\mu}}\left(x^{\sigma}\frac{1}{2}\left(\frac{\partial g_{\sigma}^{\mu}}{\partial x^{\sigma}}\right)\right)\frac{1}{2}\left(\frac{\partial g^{\sigma\mu}}{\partial x_{\mu}}\right)-\frac{\partial x^{\sigma}}{\partial x^{\sigma}}\frac{1}{2}\left(\frac{\partial g_{\sigma}^{\mu}}{\partial x_{\mu}}\right)\frac{1}{2}\left(\frac{\partial g^{\sigma\mu}}{\partial x_{\mu}}\right)\\
&-x^{\sigma}\frac{1}{2}\left(\frac{\partial g_{\sigma}^{\sigma}}{\partial x^{\sigma}}\right)\frac{1}{2}\left(\frac{\partial g_{\sigma}^{\mu}}{\partial x_{\mu}}\right)\frac{1}{2}\left(\frac{\partial g^{\sigma\mu}}{\partial x_{\mu}}\right)+\frac{\partial x^{\mu}}{\partial x^{\sigma}}\frac{1}{2}\left(\frac{\partial g_{\sigma}^{\sigma}}{\partial x_{\mu}}\right)\frac{1}{2}\left(\frac{\partial g^{\sigma\mu}}{\partial x_{\mu}}\right)
\end{aligned}
$$

$$
\begin{aligned}
&+x^{\sigma}\frac{1}{2}\left(\frac{\partial g_{\sigma}^{\mu}}{\partial x^{\sigma}}\right)\frac{1}{2}\left(\frac{\partial g_{\sigma}^{\sigma}}{\partial x_{\mu}}\right)\frac{1}{2}\left(\frac{\partial g^{\sigma\mu}}{\partial x_{\mu}}\right)-\frac{\partial^{2}x^{\mu}}{\partial x_{\mu}\partial x^{\sigma}}\frac{1}{2}\left(\frac{\partial g^{\sigma\mu}}{\partial x_{\mu}}\right)\\
&-\frac{\partial}{\partial x^{\sigma}}\left(x^{\sigma}\frac{1}{2}\left(\frac{\partial g_{\sigma}^{\mu}}{\partial x_{\mu}}\right)\right)\frac{1}{2}\left(\frac{\partial g^{\sigma\mu}}{\partial x_{\mu}}\right)-\frac{\partial x^{\sigma}}{\partial x_{\mu}}\frac{1}{2}\left(\frac{\partial g_{\sigma}^{\mu}}{\partial x^{\sigma}}\right)\frac{1}{2}\left(\frac{\partial g^{\sigma\mu}}{\partial x_{\mu}}\right)\\
&-x^{\sigma}\frac{1}{2}\left(\frac{\partial g_{\sigma}^{\sigma}}{\partial x_{\mu}}\right)\frac{1}{2}\left(\frac{\partial g_{\sigma}^{\mu}}{\partial x^{\sigma}}\right)\frac{1}{2}\left(\frac{\partial g^{\sigma\mu}}{\partial x_{\mu}}\right)+\frac{\partial x^{\mu}}{\partial x^{\sigma}}\frac{1}{2}\left(\frac{\partial g^{\sigma\mu}}{\partial x^{\sigma}}\right)\frac{1}{2}\left(\frac{\partial g^{\sigma\mu}}{\partial x_{\mu}}\right)\\
&+x^{\sigma}\frac{1}{2}\left(\frac{\partial g_{\sigma}^{\mu}}{\partial x^{\sigma}}\right)\frac{1}{2}\left(\frac{\partial g^{\sigma\mu}}{\partial x^{\sigma}}\right)\frac{1}{2}\left(\frac{\partial g^{\sigma\mu}}{\partial x_{\mu}}\right)\\
=&\frac{\partial^{3}x^{\mu}}{\partial x_{\mu}\partial x_{\mu}\partial x_{\mu}}+\frac{\partial^{2}}{\partial x_{\mu}\partial x_{\mu}}\left(x^{\sigma}\frac{1}{2}\left(\frac{\partial g^{\mu\mu}}{\partial x^{\sigma}}\right)\right)+\frac{\partial}{\partial x_{\mu}}\left(\frac{\partial x^{\sigma}}{\partial x_{\mu}}\frac{1}{2}\left(\frac{\partial g^{\mu\mu}}{\partial x^{\sigma}}\right)\right)\\
&+\frac{\partial}{\partial x_{\mu}}\left(x^{\sigma}\frac{1}{2}\left(\frac{\partial g^{\sigma\mu}}{\partial x^{\sigma}}\right)\frac{1}{2}\left(\frac{\partial g^{\mu\mu}}{\partial x^{\sigma}}\right)\right)-\frac{\partial}{\partial x_{\mu}}\left(\frac{\partial x^{\mu}}{\partial x^{\sigma}}\frac{1}{2}\left(\frac{\partial g^{\sigma\mu}}{\partial x_{\mu}}\right)\right)\\
&-\frac{\partial}{\partial x_{\mu}}\left(x^{\sigma}\frac{1}{2}\left(\frac{\partial g_{\sigma}^{\mu}}{\partial x^{\sigma}}\right)\frac{1}{2}\left(\frac{\partial g^{\sigma\mu}}{\partial x_{\mu}}\right)\right)+\frac{\partial^{2}x^{\sigma}}{\partial x_{\mu}\partial x_{\mu}}\frac{1}{2}\left(\frac{\partial g^{\mu\mu}}{\partial x^{\sigma}}\right)\\
&+\frac{\partial}{\partial x_{\mu}}\left(x^{\sigma}\frac{1}{2}\left(\frac{\partial g^{\sigma\mu}}{\partial x^{\sigma}}\right)\right)\frac{1}{2}\left(\frac{\partial g^{\mu\mu}}{\partial x^{\sigma}}\right)+\frac{\partial x^{\sigma}}{\partial x_{\mu}}\frac{1}{2}\left(\frac{\partial g^{\sigma\mu}}{\partial x^{\sigma}}\right)\frac{1}{2}\left(\frac{\partial g^{\mu\mu}}{\partial x^{\sigma}}\right)\\
&+x^{\sigma}\frac{1}{2}\left(\frac{\partial g^{\sigma\mu}}{\partial x^{\sigma}}\right)\frac{1}{2}\left(\frac{\partial g^{\sigma\mu}}{\partial x^{\sigma}}\right)\frac{1}{2}\left(\frac{\partial g^{\mu\mu}}{\partial x^{\sigma}}\right)-\frac{\partial x^{\sigma}}{\partial x^{\sigma}}\frac{1}{2}\left(\frac{\partial g^{\sigma\mu}}{\partial x_{\mu}}\right)\frac{1}{2}\left(\frac{\partial g^{\mu\mu}}{\partial x^{\sigma}}\right)\\
&-x^{\sigma}\frac{1}{2}\left(\frac{\partial g_{\sigma}^{\sigma}}{\partial x^{\sigma}}\right)\frac{1}{2}\left(\frac{\partial g^{\sigma\mu}}{\partial x_{\mu}}\right)\frac{1}{2}\left(\frac{\partial g^{\mu\mu}}{\partial x^{\sigma}}\right)-\frac{\partial^{2}x^{\mu}}{\partial x^{\sigma}\partial x_{\mu}}\frac{1}{2}\left(\frac{\partial g^{\sigma\mu}}{\partial x_{\mu}}\right)\\
&-\frac{\partial}{\partial x_{\mu}}\left(x^{\sigma}\frac{1}{2}\left(\frac{\partial g_{\sigma}^{\mu}}{\partial x^{\sigma}}\right)\right)\frac{1}{2}\left(\frac{\partial g^{\sigma\mu}}{\partial x_{\mu}}\right)-\frac{\partial x^{\sigma}}{\partial x^{\sigma}}\frac{1}{2}\left(\frac{\partial g^{\mu\mu}}{\partial x^{\sigma}}\right)\frac{1}{2}\left(\frac{\partial g^{\sigma\mu}}{\partial x_{\mu}}\right)\\
&-x^{\sigma}\frac{1}{2}\left(\frac{\partial g_{\sigma}^{\sigma}}{\partial x^{\sigma}}\right)\frac{1}{2}\left(\frac{\partial g^{\mu\mu}}{\partial x^{\sigma}}\right)\frac{1}{2}\left(\frac{\partial g^{\sigma\mu}}{\partial x_{\mu}}\right)+\frac{\partial x^{\mu}}{\partial x^{\sigma}}\frac{1}{2}\left(\frac{\partial g^{\sigma\mu}}{\partial x^{\sigma}}\right)\frac{1}{2}\left(\frac{\partial g^{\sigma\mu}}{\partial x_{\mu}}\right)\\
&+x^{\sigma}\frac{1}{2}\left(\frac{\partial g_{\sigma}^{\mu}}{\partial x^{\sigma}}\right)\frac{1}{2}\left(\frac{\partial g^{\sigma\mu}}{\partial x^{\sigma}}\right)\frac{1}{2}\left(\frac{\partial g^{\sigma\mu}}{\partial x_{\mu}}\right)-\frac{\partial^{2}x^{\mu}}{\partial x_{\mu}\partial x^{\sigma}}\frac{1}{2}\left(\frac{\partial g^{\sigma\mu}}{\partial x_{\mu}}\right)\\
&-\frac{\partial}{\partial x^{\sigma}}\left(x^{\sigma}\frac{1}{2}\left(\frac{\partial g^{\mu\mu}}{\partial x^{\sigma}}\right)\right)\frac{1}{2}\left(\frac{\partial g^{\sigma\mu}}{\partial x_{\mu}}\right)-\frac{\partial x^{\sigma}}{\partial x_{\mu}}\frac{1}{2}\left(\frac{\partial g_{\sigma}^{\mu}}{\partial x^{\sigma}}\right)\frac{1}{2}\left(\frac{\partial g^{\sigma\mu}}{\partial x_{\mu}}\right)\\
&-x^{\sigma}\frac{1}{2}\left(\frac{\partial g^{\sigma\mu}}{\partial x^{\sigma}}\right)\frac{1}{2}\left(\frac{\partial g_{\sigma}^{\mu}}{\partial x^{\sigma}}\right)\frac{1}{2}\left(\frac{\partial g^{\sigma\mu}}{\partial x_{\mu}}\right)+\frac{\partial x^{\mu}}{\partial x^{\sigma}}\frac{1}{2}\left(\frac{\partial g_{\sigma}^{\sigma}}{\partial x_{\mu}}\right)\frac{1}{2}\left(\frac{\partial g^{\sigma\mu}}{\partial x_{\mu}}\right)\\
&+x^{\sigma}\frac{1}{2}\left(\frac{\partial g_{\sigma}^{\mu}}{\partial x^{\sigma}}\right)\frac{1}{2}\left(\frac{\partial g_{\sigma}^{\sigma}}{\partial x_{\mu}}\right)\frac{1}{2}\left(\frac{\partial g^{\sigma\mu}}{\partial x_{\mu}}\right).
\end{aligned}
$$

-End Proof-

5. About a Coordinate Transformations Equation in Tensor Satisfying Binary Law

Proposition 8 When all coordinate systems satisfy Binary Law,

$x^{\mu}_{\mu} = \frac{\partial x^{\mu}}{\partial x^{\nu}} \frac{\partial x^{\nu}}{\partial x^{\mu}} x^{\nu}_{\nu} = x^{\nu}_{\nu}$ is established for x^{μ}_{μ} components of a tensor satisfying Binary law of rank zero.

Proof: When all coordinate systems satisfy Binary Law, I get

$$x^{\mu}_{\mu} = \frac{\partial x^{\mu}}{\partial x^{\nu}} \frac{\partial x^{\nu}}{\partial x^{\mu}} x^{\nu}_{\nu} = x^{\nu}_{\nu} \tag{31}$$

from Definition 14. Because (31) accords in Definition 14, the components of a tensor of rank zero are equivalent with components of a tensor satisfying Binary law of rank zero. I rewrite (31) by consideration of $x^{\mu}_{\mu} \to x^{;\mu}_{\mu}, x^{\nu}_{\nu} \to x^{;\nu}_{\nu}$, (6), $\mu - \nu$ inversion form of (6) and get

$$\begin{aligned} \left(\frac{\partial x_{\mu}}{\partial x_{\mu}} - x_{\nu} \frac{1}{2} \left(\frac{\partial g^{\nu\mu}}{\partial x^{\mu}} \right) \right) &= \frac{\partial x^{\mu}}{\partial x^{\nu}} \frac{\partial x^{\nu}}{\partial x^{\mu}} \left(\frac{\partial x_{\nu}}{\partial x_{\nu}} - x_{\mu} \frac{1}{2} \left(\frac{\partial g^{\mu\nu}}{\partial x^{\nu}} \right) \right) \\ &= \left(\frac{\partial x_{\nu}}{\partial x_{\nu}} - x_{\mu} \frac{1}{2} \left(\frac{\partial g^{\mu\nu}}{\partial x^{\nu}} \right) \right). \end{aligned} \tag{32}$$

-End Proof-

Proposition 9 When all coordinate systems satisfy Binary Law, $x^{\mu} = \frac{\partial x^{\mu}}{\partial x^{\nu}} x^{\nu}$ is established for x^{μ} contravariant components of a tensor satisfying Binary law of the first rank.

Proof: When all coordinate systems satisfy Binary Law, I get

$$x^{\mu} = \frac{\partial x^{\mu}}{\partial x^{\nu}} x^{\nu} \tag{33}$$

from Definition 15. Because (33) accords in Definition 15, the contravariant components of a tensor of the first rank are equivalent with contravariant components of a tensor satisfying Binary law of the first rank.

-End Proof-

Proposition 10 When all coordinate systems satisfy Binary Law, $x_{\mu} = \frac{\partial x^{\nu}}{\partial x^{\mu}} x_{\nu}$ is established for x_{μ} covariant components of a tensor satisfying Binary law of the first rank.

Proof: When all coordinate systems satisfy Binary Law, I get

$$x_{\mu} = \frac{\partial x^{\nu}}{\partial x^{\mu}} x_{\nu} \tag{34}$$

from Definition 16. Because (34) accords in Definition 16, the covariant components of a tensor of the first rank are equivalent with covariant components of a tensor satisfying Binary law of the first rank.

-End Proof-

Proposition 11 When all coordinate systems satisfy Binary Law, $x^{\mu\nu} = \frac{\partial x^{\mu}}{\partial x^{\nu}} \frac{\partial x^{\nu}}{\partial x^{\mu}} x^{\nu\mu} = x^{\nu\mu}$ is established for $x^{\mu\nu}$ contravariant components of a tensor satisfying Binary law of the second rank.

Proof: When all coordinate systems satisfy Binary Law, I get

$$x^{\mu\nu} = \frac{\partial x^{\mu}}{\partial x^{\nu}} \frac{\partial x^{\nu}}{\partial x^{\nu}} x^{\nu\nu} = \frac{\partial x^{\mu}}{\partial x^{\nu}} x^{\nu\nu} \tag{35}$$

from Definition 17. $x^{\mu\nu}$ isn't contravariant components of a tensor satisfying Binary law of the second rank than (35). This is a problem. The dummy index has an invariable property for consideration of Binary Law. In other words, the index which was dummy index in Definition 17 is dummy index in (35). Therefore, I rewrite dummy index ν in $\frac{\partial x^{\nu}}{\partial x^{\nu}} x^{\nu\nu}$ of (35) in μ and get

$$x^{\mu\nu} = \frac{\partial x^{\mu}}{\partial x^{\nu}} \frac{\partial x^{\nu}}{\partial x^{\mu}} x^{\nu\mu} = x^{\nu\mu}. \tag{36}$$

The kind of the optional dummy index is only two kinds of ν, μ in consideration of Definition 6 here. A problem in (35) is solved in (36). If I assume establishment of

$$x^{\mu\nu} = x^{\mu}_{\mu}, x^{\nu\mu} = x^{\nu}_{\nu} \quad (\text{False}). \tag{37}$$

I get

$$x^{\mu}_{\mu} = \frac{\partial x^{\mu}}{\partial x^{\nu}} \frac{\partial x^{\nu}}{\partial x^{\mu}} x^{\nu}_{\nu} = x^{\nu}_{\nu} \quad (\text{False}) \tag{38}$$

from (36), (37). I get

$$x^{\mu}_{\mu} = x^{\mu}_{\mu} \quad (\text{False}) \tag{39}$$

from (31), (38). Because (39) isn't established,

$$x^{\mu\nu} = x^{\mu}_{\mu}, x^{\nu\mu} = x^{\nu}_{\nu} \tag{40}$$

is established.

-End Proof-

Proposition 12 When all coordinate systems satisfy Binary Law, $x_{\mu\nu} = \frac{\partial x^{\nu}}{\partial x^{\mu}} \frac{\partial x^{\mu}}{\partial x^{\nu}} x_{\nu\mu} = x_{\nu\mu}$ is established for $x_{\mu\nu}$ covariant components of a tensor satisfying Binary law of the second rank.

Proof: When all coordinate systems satisfy Binary Law, I get

$$x_{\mu\nu} = \frac{\partial x^{\nu}}{\partial x^{\mu}} \frac{\partial x^{\nu}}{\partial x^{\nu}} x_{\nu\nu} = \frac{\partial x^{\nu}}{\partial x^{\mu}} x_{\nu\nu} \tag{41}$$

from Definition 18. $x_{\mu\nu}$ isn't covariant components of a tensor satisfying Binary law of the second rank than (41). This is a problem. The dummy index has an invariable property for consideration of Binary Law. In other words, the index which was dummy index in Definition 18 is dummy index in (41). Therefore, I rewrite dummy index ν in $\frac{\partial x^{\nu}}{\partial x^{\nu}} x_{\nu\nu}$ of (41) in μ and get

$$x_{\mu\nu} = \frac{\partial x^{\nu}}{\partial x^{\mu}} \frac{\partial x^{\mu}}{\partial x^{\nu}} x_{\nu\mu} = x_{\nu\mu}. \tag{42}$$

The kind of the optional dummy index is only two kinds of ν, μ in consideration of Definition 6 here. A problem in (41) is solved in (42). If I assume estab-

lishment of

$$x_{\mu\nu} = x_{\nu}^{\nu}, x_{\nu\mu} = x_{\mu}^{\mu} \quad (\text{False}). \tag{43}$$

I get

$$x_{\nu}^{\nu} = \frac{\partial x^{\nu}}{\partial x^{\mu}} \frac{\partial x^{\mu}}{\partial x^{\nu}} x_{\mu}^{\mu} = x_{\mu}^{\mu} \quad (\text{False}) \tag{44}$$

from (42), (43). I get

$$x_{\mu}^{\mu} = x_{\mu}^{\mu} \quad (\text{False}) \tag{45}$$

from (31), (44). Because (45) isn't established,

$$x_{\mu\nu} = x_{\nu}^{\nu}, x_{\nu\mu} = x_{\mu}^{\mu} \tag{46}$$

is established. I rewrite (42) by consideration of $x_{\mu\nu} \to x_{\mu;\nu}, x_{\nu\mu} \to x_{\nu;\mu}$, (9), $\mu - \nu$ inversion form of (9) and get

$$\left(\frac{\partial x_{\mu}}{\partial x^{\nu}}\right) = \frac{\partial x^{\nu}}{\partial x^{\mu}} \frac{\partial x^{\mu}}{\partial x^{\nu}} \left(\frac{\partial x_{\nu}}{\partial x^{\mu}}\right) = \left(\frac{\partial x_{\nu}}{\partial x^{\mu}}\right). \tag{47}$$

I rewrite (46) by consideration of $x_{\mu\nu} \to x_{\mu;\nu}, x_{\nu}^{\nu} \to x_{\nu}^{;\nu}$, (9), $\mu - \nu$ inversion form of (6) and get

$$\frac{\partial x_{\mu}}{\partial x^{\nu}} = \left(\frac{\partial x_{\nu}}{\partial x_{\nu}} - x_{\mu} \frac{1}{2}\left(\frac{\partial g^{\mu\nu}}{\partial x^{\nu}}\right)\right). \tag{48}$$

-End Proof-

Proposition 13 When all coordinate systems satisfy Binary Law, $x_{\nu}^{\mu} = \frac{\partial x^{\mu}}{\partial x^{\nu}} \frac{\partial x^{\mu}}{\partial x^{\nu}} x_{\mu}^{\nu}$ is established for x_{ν}^{μ} components of the mixed tensor satisfying Binary law of the second rank.

Proof: When all coordinate systems satisfy Binary Law, I get

$$x_{\nu}^{\mu} = \frac{\partial x^{\mu}}{\partial x^{\nu}} \frac{\partial x^{\nu}}{\partial x^{\nu}} x_{\nu}^{\nu} = \frac{\partial x^{\mu}}{\partial x^{\nu}} x_{\nu}^{\nu} \tag{49}$$

from Definition 19. x_{ν}^{μ} isn't components of the mixed tensor satisfying Binary law of the second rank than (49). This is a problem. The dummy index has an invariable property for consideration of Binary Law. In other words, the index which was dummy index in Definition 19 is dummy index in (49). Therefore, I rewrite dummy index ν in $\frac{\partial x^{\nu}}{\partial x^{\nu}} x_{\nu}^{\nu}$ of (49) in μ and get

$$x_{\nu}^{\mu} = \frac{\partial x^{\mu}}{\partial x^{\nu}} \frac{\partial x^{\mu}}{\partial x^{\nu}} x_{\mu}^{\nu}. \tag{50}$$

The kind of the optional dummy index is only two kinds of ν, μ in consideration of Definition 6 here. A problem in (49) is solved in (50). I rewrite (50) by consideration of $x_{\nu}^{\mu} \to x_{;\nu}^{\mu}, x_{\mu}^{\nu} \to x_{;\mu}^{\nu}$, (16), $\mu - \nu$ inversion form of (16) and get

$$\left(\frac{\partial x^{\mu}}{\partial x^{\nu}}\right) = \frac{\partial x^{\mu}}{\partial x^{\nu}} \frac{\partial x^{\mu}}{\partial x^{\nu}} \left(\frac{\partial x^{\nu}}{\partial x^{\mu}}\right). \tag{51}$$

-End Proof-

Proposition 14 When all coordinate systems satisfy Binary Law, $x^{\mu}_{\nu\nu}=\frac{\partial x^{\mu}}{\partial x^{\nu}}\frac{\partial x^{\nu}}{\partial x^{\mu}}\frac{\partial x^{\nu}}{\partial x^{\mu}}x^{\nu}_{\mu\mu}=\frac{\partial x^{\nu}}{\partial x^{\mu}}x^{\nu}_{\mu\mu}$ is established for $x^{\mu}_{\nu\nu}$ components of the mixed tensor satisfying Binary law of the third rank of the second rank covariant in the first rank contravariant.

Proof: When all coordinate systems satisfy Binary Law, I get

$$x^{\mu}_{\nu\nu}=\frac{\partial x^{\mu}}{\partial x^{\nu}}\frac{\partial x^{\nu}}{\partial x^{\nu}}\frac{\partial x^{\nu}}{\partial x^{\nu}}x^{\nu}_{\nu\nu}=\frac{\partial x^{\mu}}{\partial x^{\nu}}x^{\nu}_{\nu\nu} \tag{52}$$

from Definition 20. $x^{\mu}_{\nu\nu}$ isn't components of the mixed tensor satisfying Binary law of the third rank of the second rank covariant in the first rank contravariant than (52). This is a problem. The dummy index has an invariable property for consideration of Binary Law.

In other words, the index which was dummy index in Definition 20 is dummy index in (52). Therefore, I rewrite dummy index ν in $\frac{\partial x^{\nu}}{\partial x^{\nu}}\frac{\partial x^{\nu}}{\partial x^{\nu}}x^{\nu}_{\nu\nu}$ of (52) in μ and get

$$x^{\mu}_{\nu\nu}=\frac{\partial x^{\mu}}{\partial x^{\nu}}\frac{\partial x^{\mu}}{\partial x^{\nu}}\frac{\partial x^{\mu}}{\partial x^{\nu}}x^{\nu}_{\mu\mu}. \tag{53}$$

The kind of the optional dummy index is only two kinds of ν,μ in consideration of Definition 6 here. A problem in (52) is solved in (53). If I assume establishment of

$$x^{\mu}_{\nu\nu}=\frac{\partial x^{\mu}}{\partial x^{\nu}}\frac{\partial x^{\nu}}{\partial x^{\mu}}\frac{\partial x^{\nu}}{\partial x^{\mu}}x^{\nu}_{\mu\mu}=\frac{\partial x^{\nu}}{\partial x^{\mu}}x^{\nu}_{\mu\mu}\quad(\text{False}). \tag{54}$$

I get

$$\frac{\partial x^{\mu}}{\partial x^{\nu}}\frac{\partial x^{\mu}}{\partial x^{\nu}}\frac{\partial x^{\mu}}{\partial x^{\nu}}x^{\nu}_{\mu\mu}=\frac{\partial x^{\mu}}{\partial x^{\nu}}\frac{\partial x^{\nu}}{\partial x^{\mu}}\frac{\partial x^{\nu}}{\partial x^{\mu}}x^{\nu}_{\mu\mu}\quad(\text{False}) \tag{55}$$

from (53), (54). I rewrite the right side of (55) using Definition 4, Definition 5 and get

$$\begin{aligned}\frac{\partial x^{\mu}}{\partial x^{\nu}}\frac{\partial x^{\mu}}{\partial x^{\nu}}\frac{\partial x^{\mu}}{\partial x^{\nu}}x^{\nu}_{\mu\mu}&=\frac{\partial x^{\mu}}{\partial x^{\nu}}\frac{\partial\left(-x^{\mu}\right)}{\partial\left(-x^{\nu}\right)}\frac{\partial\left(-x^{\mu}\right)}{\partial\left(-x^{\nu}\right)}x^{\nu}_{\mu\mu}\\&=\frac{\partial x^{\mu}}{\partial x^{\nu}}\frac{\partial x^{\mu}}{\partial x^{\nu}}\frac{\partial x^{\mu}}{\partial x^{\nu}}x^{\nu}_{\mu\mu}\quad(\text{False}).\end{aligned} \tag{56}$$

Because (56) isn't established,

$$x^{\mu}_{\nu\nu}=\frac{\partial x^{\mu}}{\partial x^{\nu}}\frac{\partial x^{\nu}}{\partial x^{\mu}}\frac{\partial x^{\nu}}{\partial x^{\mu}}x^{\nu}_{\mu\mu}=\frac{\partial x^{\nu}}{\partial x^{\mu}}x^{\nu}_{\mu\mu} \tag{57}$$

is established. If I assume establishment of

$$x^{\mu}_{\nu\nu}=x_{\mu},x^{\nu}_{\mu\mu}=x_{\nu}\quad(\text{False}). \tag{58}$$

I get

$$x_{\mu}=\frac{\partial x^{\nu}}{\partial x^{\mu}}x_{\nu}\quad(\text{False}) \tag{59}$$

from (57), (58). I get

$$x_{\mu} = x_{\mu} \quad (\text{False}) \tag{60}$$

from (34), (59). Because (60) isn't established,

$$x^{\mu}_{\nu\nu} = x_{\mu}, x^{\nu}_{\mu\mu} = x_{\nu} \tag{61}$$

is established. I rewrite (57) by consideration of $x^{\mu}_{\nu\nu} \to x^{\mu}_{;\nu;\nu}, x^{\nu}_{\mu\mu} \to x^{\nu}_{;\mu;\mu}$, (23), $\mu - \nu$ inversion form of (23) and get

$$\frac{\partial^2 x^{\mu}}{\partial x^{\nu}\partial x^{\nu}} = \frac{\partial x^{\mu}}{\partial x^{\nu}}\frac{\partial x^{\nu}}{\partial x^{\mu}}\frac{\partial x^{\nu}}{\partial x^{\mu}}\frac{\partial^2 x^{\nu}}{\partial x^{\mu}\partial x^{\mu}} = \frac{\partial x^{\nu}}{\partial x^{\mu}}\frac{\partial^2 x^{\nu}}{\partial x^{\mu}\partial x^{\mu}}. \tag{62}$$

I rewrite (61) by consideration of $x^{\mu}_{\nu\nu} \to x^{\mu}_{;\nu;\nu}$, (23) and get

$$\frac{\partial^2 x^{\mu}}{\partial x^{\nu}\partial x^{\nu}} = x_{\mu}. \tag{63}$$

-End Proof-

Proposition 15 When all coordinate systems satisfy Binary Law, $x^{\mu}_{\nu\nu\nu} = \frac{\partial x^{\mu}}{\partial x^{\nu}}\frac{\partial x^{\mu}}{\partial x^{\nu}}\frac{\partial x^{\nu}}{\partial x^{\mu}}\frac{\partial x^{\nu}}{\partial x^{\mu}}x^{\nu}_{\mu\mu\mu} = x^{\nu}_{\mu\mu\mu}$ is established for $x^{\mu}_{\nu\nu\nu}$ components of the mixed tensor satisfying Binary law of the fourth rank of the third rank covariant in the first rank contravariant.

Proof: When all coordinate systems satisfy Binary Law, I get

$$x^{\mu}_{\nu\nu\nu} = \frac{\partial x^{\mu}}{\partial x^{\nu}}\frac{\partial x^{\nu}}{\partial x^{\nu}}\frac{\partial x^{\nu}}{\partial x^{\nu}}\frac{\partial x^{\nu}}{\partial x^{\nu}}x^{\nu}_{\nu\nu\nu} = \frac{\partial x^{\mu}}{\partial x^{\nu}}x^{\nu}_{\nu\nu\nu}. \tag{64}$$

from Definition 21. $x^{\mu}_{\nu\nu\nu}$ isn't components of the mixed tensor satisfying Binary law of the fourth rank of the third rank covariant in the first rank contravariant than (64). This is a problem. The dummy index has an invariable property for consideration of Binary Law.

In other words, the index which was dummy index in Definition 21 is dummy index in (64). Therefore, I rewrite dummy index ν in $\frac{\partial x^{\nu}}{\partial x^{\nu}}\frac{\partial x^{\nu}}{\partial x^{\nu}}\frac{\partial x^{\nu}}{\partial x^{\nu}}x^{\nu}_{\nu\nu\nu}$ of (64) in μ and get

$$x^{\mu}_{\nu\nu\nu} = \frac{\partial x^{\mu}}{\partial x^{\nu}}\frac{\partial x^{\mu}}{\partial x^{\nu}}\frac{\partial x^{\mu}}{\partial x^{\nu}}\frac{\partial x^{\mu}}{\partial x^{\nu}}x^{\nu}_{\mu\mu\mu}. \tag{65}$$

The kind of the optional dummy index is only two kinds of ν, μ in consideration of Definition 6 here. A problem in (64) is solved in (65). If I assume establishment of

$$x^{\mu}_{\nu\nu\nu} = \frac{\partial x^{\mu}}{\partial x^{\nu}}\frac{\partial x^{\mu}}{\partial x^{\nu}}\frac{\partial x^{\nu}}{\partial x^{\mu}}\frac{\partial x^{\nu}}{\partial x^{\mu}}x^{\nu}_{\mu\mu\mu} = x^{\nu}_{\mu\mu\mu} \quad (\text{False}). \tag{66}$$

I get

$$\frac{\partial x^{\mu}}{\partial x^{\nu}}\frac{\partial x^{\mu}}{\partial x^{\nu}}\frac{\partial x^{\mu}}{\partial x^{\nu}}\frac{\partial x^{\mu}}{\partial x^{\nu}}x^{\nu}_{\mu\mu\mu} = \frac{\partial x^{\mu}}{\partial x^{\nu}}\frac{\partial x^{\mu}}{\partial x^{\nu}}\frac{\partial x^{\nu}}{\partial x^{\mu}}\frac{\partial x^{\nu}}{\partial x^{\mu}}x^{\nu}_{\mu\mu\mu} \quad (\text{False}) \tag{67}$$

from (65), (66). I rewrite the right side of (67) using Definition 4, Definition 5 and get

$$\frac{\partial x^{\mu}}{\partial x^{\nu}}\frac{\partial x^{\mu}}{\partial x^{\nu}}\frac{\partial x^{\mu}}{\partial x^{\nu}}\frac{\partial x^{\mu}}{\partial x^{\nu}}x^{\nu}_{\mu\mu\mu}=\frac{\partial x^{\mu}}{\partial x^{\nu}}\frac{\partial x^{\mu}}{\partial x^{\nu}}\frac{\partial\left(-x^{\mu}\right)}{\partial\left(-x^{\nu}\right)}\frac{\partial\left(-x^{\mu}\right)}{\partial\left(-x^{\nu}\right)}x^{\nu}_{\mu\mu\mu}$$
$$=\frac{\partial x^{\mu}}{\partial x^{\nu}}\frac{\partial x^{\mu}}{\partial x^{\nu}}\frac{\partial x^{\mu}}{\partial x^{\nu}}\frac{\partial x^{\mu}}{\partial x^{\nu}}x^{\nu}_{\mu\mu\mu}\quad(\text{False}). \tag{68}$$

Because (68) isn't established,

$$x^{\mu}_{\nu\nu\nu}=\frac{\partial x^{\mu}}{\partial x^{\nu}}\frac{\partial x^{\mu}}{\partial x^{\nu}}\frac{\partial x^{\nu}}{\partial x^{\mu}}\frac{\partial x^{\nu}}{\partial x^{\mu}}x^{\nu}_{\mu\mu\mu}=x^{\nu}_{\mu\mu\mu} \tag{69}$$

is established. If I assume establishment of

$$x^{\mu}_{\nu\nu\nu}=x_{\mu\nu},x^{\nu}_{\mu\mu\mu}=x_{\nu\mu}\quad(\text{False}). \tag{70}$$

I get

$$x_{\mu\nu}=\frac{\partial x^{\mu}}{\partial x^{\nu}}\frac{\partial x^{\mu}}{\partial x^{\nu}}\frac{\partial x^{\nu}}{\partial x^{\mu}}\frac{\partial x^{\nu}}{\partial x^{\mu}}x_{\nu\mu}=x_{\nu\mu}\quad(\text{False}) \tag{71}$$

from (69), (70). I get

$$x_{\mu\nu}=x_{\mu\nu}\quad(\text{False}) \tag{72}$$

from (42), (71). Because (72) isn't established,

$$x^{\mu}_{\nu\nu\nu}=x_{\mu\nu},x^{\nu}_{\mu\mu\mu}=x_{\nu\mu} \tag{73}$$

is established. I get

$$x^{\mu}_{\nu\nu\nu}=x_{\mu\nu}=x^{\nu}_{\nu},x^{\nu}_{\mu\mu\mu}=x_{\nu\mu}=x^{\mu}_{\mu} \tag{74}$$

from (46), (73). I rewrite (69) by consideration of $x^{\mu}_{\nu\nu\nu}\to x^{\mu}_{;\nu;\nu;\nu}$, $x^{\nu}_{\mu\mu\mu}\to x^{\nu}_{;\mu;\mu;\mu}$, (30), $\mu-\nu$ inversion form of (30) and get

$$\frac{\partial^{3}x^{\mu}}{\partial x^{\nu}\partial x^{\nu}\partial x^{\nu}}=\frac{\partial x^{\mu}}{\partial x^{\nu}}\frac{\partial x^{\mu}}{\partial x^{\nu}}\frac{\partial x^{\nu}}{\partial x^{\mu}}\frac{\partial x^{\nu}}{\partial x^{\mu}}\frac{\partial^{3}x^{\nu}}{\partial x^{\mu}\partial x^{\mu}\partial x^{\mu}}=\frac{\partial^{3}x^{\nu}}{\partial x^{\mu}\partial x^{\mu}\partial x^{\mu}}. \tag{75}$$

I rewrite (74) by consideration of $x^{\mu}_{\nu\nu\nu}\to x^{\mu}_{;\nu;\nu;\nu},x_{\mu\nu}\to x_{\mu;\nu},x^{\nu}_{\nu}\to x^{;\nu}_{\nu}$, (9), (30), $\mu-\nu$ inversion form of (6) and get

$$\frac{\partial^{3}x^{\mu}}{\partial x^{\nu}\partial x^{\nu}\partial x^{\nu}}=\frac{\partial x_{\mu}}{\partial x^{\nu}}=\left(\frac{\partial x_{\nu}}{\partial x_{\nu}}-x_{\mu}\frac{1}{2}\left(\frac{\partial g^{\mu\nu}}{\partial x^{\nu}}\right)\right). \tag{76}$$

I get

$$\frac{\partial^{3}x^{\mu}}{\partial x^{\nu}\partial x^{\nu}\partial x^{\nu}}=\frac{\partial x_{\mu}}{\partial x^{\nu}}=\left(\frac{\partial x_{\nu}}{\partial x_{\nu}}-x_{\mu}\frac{1}{2}\left(\frac{\partial g^{\mu\nu}}{\partial x^{\nu}}\right)\right)=M \tag{77}$$

from (76), Definition 8.

-End Proof-

6. Discussion

About Proposition 8

Because (31) accords in Definition 14, components of a tensor of rank zero accord in components of a tensor satisfying Binary law of rank zero.

About Proposition 9

Because (33) accords in Definition 15, contravariant components of a tensor of the first rank accord in contravariant components of a tensor satisfying Binary law of the first rank.

About Proposition 10

Because (34) accords in Definision16, covariant components of a tensor of the first rank accord in covariant components of a tensor satisfying Binary law of the first rank.

About Proposition 13

I get

$$x^1_{[1]} = \frac{\partial x^1}{\partial x^{[1]}}\frac{\partial x^1}{\partial x^{[1]}}x_1^{[1]}, \quad x^1_{[2]} = \frac{\partial x^1}{\partial x^{[2]}}\frac{\partial x^1}{\partial x^{[2]}}x_1^{[2]},$$

$$x^2_{[1]} = \frac{\partial x^2}{\partial x^{[1]}}\frac{\partial x^2}{\partial x^{[1]}}x_2^{[1]}, \quad x^2_{[2]} = \frac{\partial x^2}{\partial x^{[2]}}\frac{\partial x^2}{\partial x^{[2]}}x_2^{[2]}$$

from (50) if I assume a dimensional number 2.

Conflicts of Interest

The author declares no conflicts of interest regarding the publication of this paper.

References

[1] Ichidayama, K. (2017) *Journal of Modern Physics*, **8**, 944-963. https://doi.org/10.4236/jmp.2017.86060

[2] Ichidayama, K. (2017) *Journal of Modern Physics*, **8**, 126-132. https://doi.org/10.4236/jmp.2017.81011

[3] Dirac, P.A.M. (1975) General Theory of Relativity. John Wiley and Sons, Inc., New York.

[4] Fleisch, D. (2012) A Student's Guide to Vectors and Tensors. Cambridge University Press, Cambridge.

Journal of Modern Physics, 2020, 11, 1672-1710
https://www.scirp.org/journal/jmp
ISSN Online: 2153-120X
ISSN Print: 2153-1196

A Mathematical Comparison of the Schwarzschild and Kerr Metrics

J.-F. Pommaret

CERMICS, Ecole des Ponts ParisTech, Paris, France
Email: jean-francois.pommaret@wanadoo.fr

How to cite this paper: Pommaret, J.-F. (2020) A Mathematical Comparison of the Schwarzschild and Kerr Metrics. *Journal of Modern Physics*, **11**, 1672-1710.
https://doi.org/10.4236/jmp.2020.1110104

Received: September 29, 2020
Accepted: October 23, 2020
Published: October 26, 2020

Abstract

A few physicists have recently constructed the generating compatibility conditions (CC) of the Killing operator for the Minkowski (M), Schwarzschild (S) and Kerr (K) metrics. They discovered second order CC, well known for M, but also third order CC for S and K. In a recent paper (DOI:10.4236/jmp.2018.910125) we have studied the cases of M and S, without using specific technical tools such as Teukolski scalars or Killing-Yano tensors. However, even if S(m) and K(m, a) are depending on constant parameters in such a way that S $\to$ M when $m \to 0$ and K $\to$ S when $a \to 0$, the CC of S do not provide the CC of M when $m \to 0$ while the CC of K do not provide the CC of S when $a \to 0$. In this paper, using tricky motivating examples of operators with constant or variable parameters, we explain why the CC are depending on the choice of the parameters. In particular, the only purely intrinsic objects that can be defined, namely the extension modules, may change drastically. As the algebroid bracket is compatible with the *prolongation/projection* (PP) procedure, we provide for the first time all the CC for K in an intrinsic way, showing that they only depend on the underlying Killing algebra and that the role played by the Spencer operator is crucial. We get K < S < M with 2 < 4 < 10 for the Killing algebras and explain why the formal search of the CC for M, S or K are strikingly different, even if each Spencer sequence is isomorphic to the tensor product of the Poincaré sequence for the exterior derivative by the corresponding Lie algebra.

Keywords

Formal Integrability, Involutivity, Compatibility Condition, Janet Sequence; Spencer Sequence, Minkowski Metric, Schwarzschild Metric, Kerr Metric

1. Introduction

In order to explain the type of problems we want to solve, let us start adding a

constant parameter to the example provided by Macaulay in 1916 that we have presented in a previous paper for other reasons [1]. However, before doing so, we first recall the following key definition and formal theorem before sketching the main results obtained in this paper:

DEFINITION 1.1: A *system* of order q on E is an open vector subbundle $R_q \subseteq J_q(E)$ with prolongations $\rho_r(R_q) = R_{q+r} = J_r(R_q) \cap J_{q+r}(E) \subseteq J_r(J_q(E))$ and symbols $\rho_r(g_q) = g_{q+r} = S_{q+r}T^* \otimes E \cap R_{q+r} \subseteq J_{q+r}(E)$ only depending on $g_q \subseteq S_qT^* \otimes E$. For $r,s \geq 0$, we denote by $R_{q+r}^{(s)} = \pi_{q+r}^{q+r+s}(R_{q+r+s}) \subseteq R_{q+r}$ the projection of R_{q+r+s} on R_{q+r}, which is thus defined by more equations in general. The system R_q is said to be *formally integrable* (FI) if we have $R_{q+r}^{(s)} = R_{q+r}, \forall r,s \geq 0$, that is if all the equations of order $q+r$ can be obtained by means of only r prolongations. The system R_q is said to be *involutive* if it is FI with an involutive symbol g_q. We shall simply denote by $\Theta = \{ f \in E \mid j_q(f) \in R_q \}$ the "set" of (formal) solutions. It is finally easy to prove that the Spencer operator $D: J_{q+1}(E) \to T^* \otimes J_q(E)$ restricts to $D: R_{q+1} \to T^* \otimes R_q$.

The most difficult but also the most important theorem has been discovered by M. Janet in 1920 [2] and presented by H. Goldschmidt in a modern setting in 1968 [3]. However, the first proof with examples is not intrinsic while the second, using the Spencer operator, is very technical and we have given a quite simpler different proof in 1978 ([2], also [4] [5]) that we shall use later on for studying the Killing equations for the Schwarzschild and Kerr metrics:

THEOREM 1.2: If $R_q \subset J_q(E)$ is a system of order q on E such that its first prolongation $R_{q+1} \subset J_{q+1}(E)$ is a vector bundle while its symbol g_{q+1} is also a vector bundle, then, if g_q is 2-acyclic, we have $\rho_r(R_q^{(1)}) = R_{q+r}^{(1)}$.

COROLLARY 1.3: (PP *procedure*) If a system $R_q \subset J_q(E)$ is defined over a differential field K, then one can find integers $r,s \geq 0$ such that $R_{q+r}^{(s)}$ is formally integrable or even involutive.

The paper will be organized as follows:

- First of all, starting with an arbitrary system $R_q \subset J_q(E)$, the purpose of the next motivating examples is to prove that the generating CC of the operator:

$$\mathcal{D} = \Phi_0 \circ j_q : E \overset{j_q}{\to} J_q(E) \overset{\Phi_0}{\to} J_q(E)/R_q = F_0$$

  though they are of course fully determined by the first order CC of the final involutive system $R_{q+r}^{(s)}$ produced by the *prolongation/projection* (PP) procedure, are in general of order $r+s+1$ like the Riemann or Weyl operators, but may be of strictly lower order.
- The same procedure will be applied to the two first order systems of infinitesimal Lie equations allowing to define the Killing operator for the S-metric and the K-metric while comparing the respective results obtained. We may say that the case of the S-metric has already been treated in the publication quoted in the abstract but that it took us two years just for daring to engage in dealing similarly with the K-metric as anybody can understand by looking

at the components of the Riemann tensor in the literature. It has been a surprising "*miracle*" to discover in the proof of Theorem 4.2 that there was a unique but tricky way to bring this problem to a purely mathematical and relatively simple computation on Lie equations and their prolongations.

- In the case of the S-metric, starting with the system $R_1 \subset J_1(T)$, we shall obtain $R_1^{(1)} = R_1$ but $R_1^{(2)} = R_1' \subset R_1$ with a strict inclusion both with $R_1^{(3)} = R_1'' \subset R_1'$ again with a strict inclusion but in such a way that R_1'' is FI though not involutive because only its first prolongation is involutive. From this result we shall exhibit 15 (generating) second order CC and 4 (generating) unexpected third order CC without having to refer to any specific technical relativistic tool.
- Then, the case of the K-metric seems to be similar as it is also leading to the strict inclusions $R_1'' \subset R_1' \subset R_1$ of systems but the new systems are quite different and in particular R_1'' is now involutive, a result providing 14 (generating) second order CC and 4 (generating) third order CC. As in the motivating examples, it does not seem that the total numbers $15+4=19$ or $14+4=18$ have any intrinsic mathematical meaning. In both cases, using the Spencer operator, we explain why the important object is the group of invariance of the metric but not the metric itself.
- Finally, we are able to relate these results to the computation of certain *extension modules* in *differential homological algebra*, showing why the mathematical foundations of conformal geometry in arbitrary dimension and general relativity must be entirely revisited in the light of these results.

MOTIVATING EXAMPLE 1.4: With $m=1, n=3, q=2$, let us consider the second order linear system $R_2 \subset J_2(E)$ with $\dim(R_2)=8$ and parametric jets $\{y, y_1, y_2, y_3, y_{11}, y_{12}, y_{22}, y_{23}\}$, defined by the two inhomogeneous PD equations where a is a constant parameter:

$$Py \equiv y_{33} = u, \quad Qy \equiv y_{13} + a y_2 = v$$

First of all we have to look for the symbol g_2 defined by the two linear equations $y_{33}=0, y_{13}=0$. The coordinate system is not δ-regular and exchanging x^1 with x^2, we get the Janet board:

$$\begin{cases} y_{33}=0 \\ y_{23}=0 \end{cases} \begin{array}{|ccc|} \hline 1 & 2 & 3 \\ 1 & 2 & \bullet \\ \hline \end{array}$$

g_2 is involutive, thus 2-acyclic and we obtain from the main theorem $\rho_r\left(R_2^{(1)}\right) = R_{2+r}^{(1)}$. However, $R_2^{(1)} \subset R_2$ with a strict inclusion because $R_2^{(1)}$ is now defined by adding the equations $a y_{23} = v_3 - u_1$. We may start afresh with $R_2^{(1)}$ and study its symbol $g_2^{(1)}$ with Janet tabular:

$$\begin{cases} y_{33}=0 \\ a y_{23}=0 \\ y_{13}=0 \end{cases} \begin{array}{|ccc|} \hline 1 & 2 & 3 \\ 1 & 2 & \bullet \\ 1 & \bullet & \bullet \\ \hline \end{array}$$

Since that moment, we have to consider the two possibilities:

- $a=0$: The initial system becomes $y_{33}=u$, $y_{13}=v$ and has an involutive symbol. It is thus involutive because it is trivially FI as the left members are homogeneous with only one generating first order CC, namely $u_3-v_1=0$. We have $\dim\left(g_{2+r}\right)=4+r$ and the following commutative and exact diagrams:

$$\begin{array}{ccccccccc}
 & & 0 & & 0 & & 0 & & 0 \\
 & & \downarrow & & \downarrow & & \downarrow & & \downarrow \\
0 & \to & g_3 & \to & S_3T^*\otimes E & \to & T^*\otimes F_0 & \to & F_1 & \to 0 \\
 & & \downarrow & & \downarrow & & \downarrow & & \| \\
0 & \to & R_3 & \to & J_3(E) & \to & J_1(F_0) & \to & F_1 & \to 0 \\
 & & \downarrow & & \downarrow & & \downarrow & & \downarrow \\
0 & \to & R_2 & \to & J_2(E) & \to & F_0 & \to & 0 \\
 & & \downarrow & & \downarrow & & \downarrow & & \\
 & & 0 & & 0 & & 0 & &
\end{array}$$

$$\begin{array}{ccccccccc}
 & & 0 & & 0 & & 0 & & 0 & \\
 & & \downarrow & & \downarrow & & \downarrow & & \downarrow & \\
0 & \to & 5 & \to & 10 & \to & 6 & \to & 1 & \to 0 \\
 & & \downarrow & & \downarrow & & \downarrow & & \downarrow & \\
0 & \to & 13 & \to & 20 & \to & 8 & \to & 1 & \to 0 \\
 & & \downarrow & & \downarrow & & \downarrow & & \downarrow & \\
0 & \to & 8 & \to & 10 & \to & 2 & \to & 0 & \\
 & & \downarrow & & \downarrow & & \downarrow & & & \\
 & & 0 & & 0 & & 0 & & &
\end{array}$$

We have thus the Janet sequence:

$$0\to\Theta\to E\xrightarrow[2]{\mathcal{D}}F_0\xrightarrow[1]{\mathcal{D}_1}F_1\to 0$$

or, equivalently, the exact sequence of differential modules over $D=\mathbb{Q}\left[d_1,d_2,d_3\right]=\mathbb{Q}\left[d\right]$:

$$0\to D\xrightarrow[1]{}D^2\xrightarrow[2]{}D\xrightarrow{p}M\to 0$$

where p is the canonical projection onto the residual differential module.

- $a\neq 0$: When the coefficients are in a differential field of constants, for example if $a\in\mathbb{Q}$ is invertible, we may choose $a=1$ like Macaulay [1]. It follows that $g_2^{(1)}$ is still involutive but we have the strict inclusion $g_2^{(1)}\subset g_1$ and thus the strict inclusion $R_2^{(1)}\subset R_2$ because $\dim\left(R_2^{(1)}\right)=7<8$. We may thus continue the PP procedure and obtain the new strict inclusion $R_2^{(2)}\subset R_2^{(1)}$ because $\dim\left(R_2^{(2)}\right)=6$ as $R_2^{(2)}$ is defined by the 4 equations with Janet tabular:

$$\left\{\begin{array}{l}
y_{33}=u \\
y_{23}=v_3-u_1 \\
y_{22}=v_2-v_{13}+u_{11} \\
y_{13}+y_2=v
\end{array}\right.\qquad\boxed{\begin{array}{ccc}
1 & 2 & 3 \\
1 & 2 & \bullet \\
1 & 2 & \bullet \\
1 & \bullet & \bullet
\end{array}}$$

As $R_2^{(2)}$ is easily seen to be involutive, we achieve the PP procedure, obtaining the strict intrinsic inclusions and corresponding fiber dimensions:

$$R_2^{(2)} \subset R_2^{(1)} \subset R_2 \quad \Leftrightarrow \quad 6 < 7 < 8$$

Finally, we have $\rho_r\left(R_2^{(2)}\right) = \rho_r\left(\left(R_2^{(1)}\right)^{(1)}\right) = \left(\rho_r\left(R_2^{(1)}\right)\right)^{(1)} = \left(R_{2+r}^{(1)}\right)^{(1)} = R_{2+r}^{(2)}$.

It remains to find out the CC for (u,v) in the initial inhomogeneous system. As we have used two prolongations in order to exhibit $R_2^{(2)}$, we have second order formal derivatives of u and v in the right members. Now, as we have an involutive system, we have first order CC for the new right members and could hope therefore for third order generating CC. However, we have the 4 CC:

$$\begin{cases} y_{233} = d_3\left(v_3 - u_1\right) = d_2 u \Rightarrow \boxed{v_{33} - u_{13} - u_2 = 0} \\ y_{223} = d_3\left(v_2 - v_{13} + u_{11}\right) = d_2\left(v_3 - u_1\right) \Rightarrow \boxed{v_{133} - u_{113} - u_{12} = 0} \\ y_{133} + y_{23} = d_3 v = d_1 u + \left(v_3 - u_1\right) \Rightarrow \boxed{0 = 0} \\ y_{123} + y_{22} = d_2 v = d_1\left(v_3 - u_1\right) + \left(v_2 - v_{13} + u_{11}\right) \Rightarrow \boxed{0 = 0} \end{cases}$$

It follows that we have *only* one second order and one third order CC:

$$\begin{aligned} &v_{33} - u_{13} - u_2 = 0, \\ &v_{133} - u_{113} - u_{12} = 0 \end{aligned}$$

but, *surprisingly*, we are left with the *only* generating second order CC $v_{33} - u_{13} - u_2 = 0$ which is coming from the fact that the operator P commutes with the operator Q.

We let the reader prove as an exercise (see [1] [6] for details) that $\dim\left(R_{r+2}\right) = 4r + 8$, $\forall r \geq 0$ and thus $\dim\left(R_3\right) = 12$, $\dim\left(R_4\right) = 16$ in the following commutative and exact diagrams where E is the trivial vector bundle with $\dim\left(E\right) = 1$ and $\dim\left(g_{r+2}\right) = r + 4, \forall r \geq 0$:

$$\begin{array}{ccccccccc} & & 0 & & 0 & & 0 & & \\ & & \downarrow & & \downarrow & & \downarrow & & \\ 0 & \to & g_4 & \to & S_4T^* \otimes E & \to & S_2T^* \otimes F_0 & \to & h_2 & \to 0 \\ & & \downarrow & & \downarrow & & \downarrow & & \downarrow & \\ 0 & \to & R_4 & \to & J_4\left(E\right) & \to & J_2\left(F_0\right) & \to & F_1 & \to 0 \\ & & \downarrow & & \downarrow & & \downarrow & & \downarrow & \\ 0 & \to & R_3 & \to & J_3\left(E\right) & \to & J_1\left(F_0\right) & \to & 0 & \\ & & & & \downarrow & & \downarrow & & & \\ & & & & 0 & & 0 & & & \end{array}$$

We have thus the formally exact sequence:

$$0 \to \Theta \to E \underset{2}{\overset{\mathcal{D}}{\to}} F_0 \underset{2}{\overset{\mathcal{D}_1}{\to}} F_1 \to 0$$

or, equivalently, the exact sequence of differential modules over D as before:

$$0 \to D \underset{2}{\to} D^2 \underset{2}{\to} D \overset{p}{\to} M \to 0$$

which is nevertheless *not* a Janet sequence because R_2 is *not* involutive.

MOTIVATING EXAMPLE 1.5: We now prove that the case of variable coefficients can lead to strikingly different results, even if we choose them in the differential field $K=\mathbb{Q}\left(x^1,x^2,x^3\right)$ of rational functions in the coordinates that we shall meet in the study of the S and K metrics. We denote by $D=K\left[d_1,d_2,d_3\right]=K\left[d\right]$ the ring of differential operators with coefficients in K. For this, let us consider the simplest situation met with the second order system $R_2\subset J_2\left(E\right)$:

$$\boxed{R_2\subset J_2\left(E\right)\quad \left\{y_{33}=u,\ y_{13}+x^3y_2=v\right.}$$

We may consider successively the following systems of decreasing dimensions $8>7>5>4$:

$$\boxed{R_2'=R_2^{(1)}\subset R_2\quad \left\{y_{33}=u,\ x^3y_{23}+y_2=v_3-u_1,\ y_{13}+x^3y_2=v\right.}$$

$$\boxed{R_2''=R_2^{(2)}\subset R_2'\quad \begin{cases} y_{33}=u,\ 2y_{23}=v_{33}-u_{13}-x^3u_2,\ y_{13}+x^3y_2=v, \\ \left(x^3\right)^2y_{22}-y_{12}=x^3v_2-v_{13}+u_{11} \\ 2y_2=-x^3v_{33}+x^3u_{13}+\left(x^3\right)^2u_2+2v_3-2u_1 \end{cases}}$$

$$\boxed{R_2'''=R_2^{(3)}\subset R_2''\quad \begin{cases} y_{33}=u,\ 2y_{23}=v_{33}-u_{13}-x^3u_2,\ y_{13}+x^3y_2=v, \\ 2x^3y_{22}=-v_{133}+u_{113}+x^3u_{12}+2v_2 \\ 2y_{12}=-x^3v_{133}+x^3u_{113}+\left(x^3\right)^2u_{12}+2v_{13}-2u_{11} \\ 2y_2=-x^3v_{33}+x^3u_{13}+\left(x^3\right)^2u_2+2v_3-2u_1 \end{cases}}$$

The last system is involutive with the following Janet tabular:

$$\left\{\begin{array}{l|ccc} y_{33}=0 & 1 & 2 & 3 \\ y_{23}=0 & 1 & 2 & \bullet \\ y_{22}=0 & 1 & 2 & \bullet \\ y_{13}=0 & 1 & \bullet & \bullet \\ y_{12}=0 & 1 & \bullet & \bullet \\ y_2=0 & \bullet & \bullet & \bullet \end{array}\right.$$

The generic solution is of the form $y=b\left(x^1\right)+cx^3$ and it is rather striking that such a system has constant coefficients (This will be *exactly* the case of the S and K metrics but similar examples can be found in [5]). We could hope for 9 generating CC up to order 4 but tedious computations, left to the reader as a tricky exercise, prove that we have in fact, as before, only 2 generating *third order* CC described by the following involutive system, namely:

$$\boxed{A\equiv v_{333}-u_{133}-x^3u_{23}-3u_2=0}$$

$$\boxed{B\equiv v_{133}-u_{113}-\left(x^3\right)^2v_{233}+\left(x^3\right)^2u_{123}+2x^3v_{23}+\left(x^3\right)^3u_{22}-3x^3u_{12}-2v_2=0}$$

satisfying the only first order CC: $\boxed{C\equiv d_3B-d_1A+\left(x^3\right)^2d_2A=0}$.

We obtain the sequence of D-modules:

$$0 \to D \xrightarrow[1]{} D^2 \xrightarrow[3]{} D^2 \xrightarrow[2]{} D \xrightarrow{p} M \to 0$$

where the order of an operator is written under its arrow. This example proves that even a slight modification of the parameter can change the corresponding differential resolution.

MOTIVATING EXAMPLE 1.6: We comment a tricky example first provided by M. Janet in 1920, that we have studied with details in [4] [7]. With $n=3$, $m=1$, $q=2$, $K=\mathbb{Q}\left(x^2\right)$ and using jet notations, let us consider the inhomogeneous second order system:

$$R_2 \subset J_2(E) \quad \left\{ y_{33} - x^2 y_{11} = u,\ y_{22} = v \right.$$

We let the reader prove that the space of solutions has dimension 12 over $\mathbb{Q}$ and that we have $r=0, s=5$ in such a way that $R_2^{(5)}$ is involutive and even finite type with a zero symbol. Accordingly, we have $\dim\left(R_2^{(5)}\right)=12$. Passing to the differential module point of view, it follows that $\dim_K(M)=12$ and $rk_D(M)=0$. According to the general results presented, we have thus to use 5 prolongations and could therefore wait for CC up to order … 6!!!. In fact, *and we repeat that there is no hint at all for predicting this result in any intrinsic way*, we have only two generating CC, one of order 3 and … one of order 6 indeed, namely:

$$\boxed{A \equiv v_{233} - x^2 v_{112} - u_{222} - 3v_{11} = 0}$$

$$\boxed{\begin{aligned} B \equiv\ & v_{333333} - x^2 v_{113333} - u_{223333} - 2x^2\left(v_{113333} - x^2 v_{111133} - u_{112233}\right) \\ & + \left(x^2\right)^2\left(v_{111133} - x^2 v_{111111} - u_{111122}\right) - 2u_{11233} + 2x^2 u_{11112} - 2u_{1111} \\ =\ & 0 \end{aligned}}$$

satisfying the only fourth order CC

$$\boxed{C \equiv A_{3333} - 2x^2 A_{1133} + \left(x^2\right)^2 A_{1111} - B_2 = 0}$$

It follows that we have the unexpected differential resolution:

$$0 \to D \xrightarrow[4]{} D^2 \xrightarrow[6]{} D^2 \xrightarrow[2]{} D \xrightarrow{p} M \to 0$$

with, from left to right, $D=DC$, $D^2=DA+DB$, $D^2=Du+Dv$, $D=Dy$ and Euler-Poincaré characteristic $rk_D(M)=1-2+2-1=0$ as expected. In addition, if we introduce a constant parameter a by replacing the coefficient x^2 by ax^2, we obtain $2ay_{112}=v_{33}-ax^2v_{11}-u_{22}$ and obtain the same conclusions as before. We point out the fact that, when $a=0$, the system $y_{33}=u, y_{22}=v$, which is trivially FI because it is homogeneous, has a symbol g_2 which is *neither* involutive (otherwise it should admit a first order CC), *nor even* 2-acyclic because we have the parametric jets:

$$par_2 = (y_{11}, y_{12}, y_{13}, y_{23}),\ par_3 = (y_{111}, y_{112}, y_{113}, y_{123}),$$
$$par_4 = (y_{1111}, y_{1112}, y_{1113}, y_{1123})$$

and the long δ-sequence:

$$0 \to g_4 \xrightarrow{\delta} T^* \otimes g_3 \xrightarrow{\delta} \wedge^2 T^* \otimes g_2 \xrightarrow{\delta} \wedge^3 T^* \otimes T^* \to 0$$

$$0 \to 4 \xrightarrow{\delta} 12 \xrightarrow{\delta} 12 \xrightarrow{\delta} 3 \to 0$$

in which $\dim\left(B^2(g_2)\right) = 12 - 4 = 8$, $\dim\left(Z^2(g_2)\right) = 12 - 3 = 9$
$\Rightarrow \dim\left(H^2(g_2)\right) = 9 - 8 = 1 \neq 0$.

However, g_3 is involutive with the following Janet tabular for the vertical jets $(y_{ijk}) \in S_3T^*$:

$$\begin{cases} y_{333} = 0 \\ y_{233} = 0 \\ y_{223} = 0 \\ y_{222} = 0 \\ y_{133} = 0 \\ y_{122} = 0 \end{cases} \begin{bmatrix} 1 & 2 & 3 \\ 1 & 2 & \bullet \\ 1 & 2 & \bullet \\ 1 & 2 & \bullet \\ 1 & \bullet & \bullet \\ 1 & \bullet & \bullet \end{bmatrix}$$

Accordingly, R_3 is thus involutive and the only CC $v_{33} - u_{22} = 0$ is of order 2 because we need one prolongation only to reach involution and thus 2-acyclicity.

MOTIVATING EXAMPLE 1.7: With $m = 1, n = 2, q = 2, K = \mathbb{Q}$, let us consider the inhomogeneous second order system:

$$y_{22} = u, \quad y_{12} - y = v$$

We obtain at once through crossed derivatives $y = u_{11} - v_{12} - v$ and, by substituting, two fourth order CC for (u, v), namely:

$$\boxed{A \equiv u_{1122} - v_{1222} - v_{22} - u = 0,\ B \equiv u_{1112} - u_{11} - v_{1122} = 0}$$

satisfying $\boxed{B_{12} + B - A_{11} = 0}$. However, we may also obtain a single CC for (u, v), namely $\boxed{C \equiv d_{12}u - u - d_{22}v = 0}$ and we check at once $A = d_{12}C + C$, $B = d_{11}C$ while $C = d_{22}B - d_{12}A + A$. We let the reader prove that $\dim(R_{2+r}) = 4$, $\forall r \geq 0$. Hence, if (A, B) is a section of F_1 while C is a section of F_1', the jet prolongation sequence:

$$0 \to R_6 \to J_6(E) \to J_4(F_0) \to F_1 \to 0$$

$$0 \to 4 \to 28 \to 30 \to 2 \to 0$$

is *not* formally exact because $4 - 28 + 30 - 2 = 4 \neq 0$, while the corresponding long sequence:

$$0 \to R_{r+4} \to J_{r+4}(E) \to J_{r+2}(F_0) \to J_r(F_1') \to 0$$

$$0 \to 4 \to (r+5)(r+6)/2 \to (r+3)(r+4) \to (r+1)(r+2)/2 \to 0$$

is indeed formally exact because

$$4-\frac{r^2+11r+30}{2}+\left(r^2+7r+12\right)-\frac{r^2+3r+2}{2}=0$$

but *not* strictly exact because R_2 is quite far from being FI as we have even $R_2^{(4)}=0$.

It follows from these examples and the many others presented in [6] that we cannot agree with [8] [9] [10] [11]. Indeed, it is clear that one can use successive prolongations in order to look for CC of order $1,2,3,\cdots$ and so on, selecting each time the new generating ones and knowing that Noetherian arguments will stop such a procedure … after a while!

However, as long as the numbers *r* and *s* are not known, it is not *effectively* possible to decide in advance about the maximum order that must be reached. Therefore, it becomes clear that exactly the same procedure MUST be applied when looking for the CC of the Killing operators we want to study, the problem becoming *only* a "mathematical" one but *surely not* a "physical" one.

IMPORTANT REMARK 1.8: The intrinsic properties of a system with constant coefficients may *drastically* depend on these coefficients, even if the systems do not appear to be quite different at first sight. Using jet notations, let us consider the second order system $\xi_{33}=0,\xi_{13}-a\xi_2=0$ depending on a constant parameter *a* and defining a differential module *M* by residue. When $a=0$ we have the differential sequence:

$$\xi \xrightarrow[2]{\mathcal{D}} \left(d_{33}\xi=\eta^1, d_{13}\xi=\eta^2\right) \xrightarrow[1]{\mathcal{D}_1} \left(d_3\eta^2-d_1\eta^1=\zeta\right)$$

and the adjoint sequence:

$$\left(\nu=d_{33}\mu^1+d_{13}\mu^2\right) \xleftarrow[2]{ad(\mathcal{D})} \left(\mu^1=d_1\lambda, \mu^2=-d_3\lambda\right) \xleftarrow[1]{ad(\mathcal{D}_1)} \lambda$$

though the CC sequence that must be used with $\nu=d_3\nu'$ is:

$$\left(\nu'=d_3\mu^1+d_1\mu^2\right) \xleftarrow[2]{ad(\mathcal{D})} \left(\mu^1=d_1\lambda, \mu^2=-d_3\lambda\right) \xleftarrow[1]{ad(\mathcal{D}_1)} \lambda$$

On the contrary, if $a\neq 0$ say $a=1$, we have the differential sequence:

$$\xi \xrightarrow[2]{\mathcal{D}} \left(d_{33}\xi=\eta^1, d_{13}\xi-\xi_2=\eta^2\right) \xrightarrow[2]{\mathcal{D}_1} \left(d_{33}\eta^2-\left(d_{13}-d_2\right)\eta^1=\zeta\right)$$

and the CC sequence does coincide with the adjoint sequence:

$$\left(\nu=d_{33}\mu^1+\left(d_{13}+d_2\right)\mu^2\right) \xleftarrow[2]{ad(\mathcal{D})} \left(\mu^1=-\left(d_{13}+d_2\right)\lambda, \mu^2=d_{33}\lambda\right) \xleftarrow[2]{ad(\mathcal{D}_1)} \lambda$$

It is thus essential to notice that $ad\left(\mathcal{D}\right)$ generates the CC of $ad\left(\mathcal{D}_1\right)$ when $a\neq 0$, a result leading to $ext^1\left(M\right)=0$ but this is not true when $a=0$, a result leading to $ext^1\left(M\right)\neq 0$ [5] [12] [13] [14].

Comparing the sequences obtained in the previous examples, we may state:

DEFINITION 1.9: A differential sequence is said to be *formally exact* if it is exact on the jet level composition of the prolongations involved. A formally exact sequence is said to be *strictly exact* if all the operators/systems involved are

FI (see [1] for more details). A strictly exact sequence is called *canonical* if all the operators/systems are involutive. The only known canonical sequences are the Janet and Spencer sequences that can be defined independently from each other.

With canonical projection $\Phi_0 = \Phi : J_q(E) \Rightarrow J_q(E)/R_q = F_0$, the various prolongations are described by the following commutative and exact *introductory diagram*:

$$\begin{array}{ccccccccc}
 & & 0 & & 0 & & 0 & & \\
 & & \downarrow & & \downarrow & & \downarrow & & \\
0 & \to & g_{q+r+1} & \to & S_{q+r+1}T^* \otimes E & \to & S_{r+1}T^* \otimes F_0 & \to & h_{r+1} & \to 0 \\
 & & \downarrow & & \downarrow & & \downarrow & & \downarrow & \\
0 & \to & R_{q+r+1} & \to & J_{q+r+1}(E) & \xrightarrow{\rho_{r+1}(\Phi)} & J_{r+1}(F_0) & \to & Q_{r+1} & \to 0 \\
 & & \downarrow & & \downarrow & & \downarrow & & \downarrow & \\
0 & \to & R_{q+r} & \to & J_{q+r}(E) & \xrightarrow{\rho_r(\Phi)} & J_r(F_0) & \to & Q_r & \to 0 \\
 & & & & \downarrow & & \downarrow & & \downarrow & \\
 & & & & 0 & & 0 & & 0 &
\end{array}$$

Applying the standard "*snake*" lemma, we obtain the useful *long exact connecting sequence*:

$$0 \to g_{q+1} \to R_{q+1} \to R_q \to h_1 \to Q_1 \to 0$$

which is thus connecting in a tricky way FI (*lower left*) with CC (*upper right*).

We finally recall the *Fundamental Diagram I* that we have presented in many books and papers, relating the (upper) *canonical Spencer sequence* to the (lower) *canonical Janet sequence*, that only depends on the left commutative square $\mathcal{D} = \Phi \circ j_q$ with $\Phi = \Phi_0$ when one has an involutive system $R_q \subseteq J_q(E)$ over E with $\dim(X) = n$ and $j_q : E \to J_q(E)$ is the derivative operator up to order q:

$$\begin{array}{ccccccccccccccc}
 & & & & 0 & & 0 & & 0 & & & & 0 & & \\
 & & & & \downarrow & & \downarrow & & \downarrow & & & & \downarrow & & \\
0 & \to & \Theta & \xrightarrow{j_q} & C_0 & \xrightarrow{D_1} & C_1 & \xrightarrow{D_2} & C_2 & \xrightarrow{D_3} & \cdots & \xrightarrow{D_n} & C_n & \to 0 \\
 & & & & \downarrow & & \downarrow & & \downarrow & & & & \downarrow & & \\
0 & \to & E & \xrightarrow{j_q} & C_0(E) & \xrightarrow{D_1} & C_1(E) & \xrightarrow{D_2} & C_2(E) & \xrightarrow{D_3} & \cdots & \xrightarrow{D_n} & C_n(E) & \to 0 \\
 & & \| & & \downarrow \Phi_0 & & \downarrow \Phi_1 & & \downarrow \Phi_2 & & & & \downarrow \Phi_n & & \\
0 & \to & \Theta & \to & E & \xrightarrow{\mathcal{D}} & F_0 & \xrightarrow{\mathcal{D}_1} & F_1 & \xrightarrow{\mathcal{D}_2} & F_2 & \xrightarrow{\mathcal{D}_3} \cdots \xrightarrow{D_n} & F_n & \to 0 \\
 & & & & & & \downarrow & & \downarrow & & \downarrow & & & \downarrow & \\
 & & & & & & 0 & & 0 & & 0 & & 0 &
\end{array}$$

We shall use this result, first found exactly 40 years ago [2] but never acknowledged, in order to provide a critical study of the comparison between the S and K metrics.

EXAMPLE 1.10: The Janet tabular in Example 1.4 with $a=1$ provides the fiber dimensions:

$$\begin{array}{ccccccccccccccc}
 & & & & & & 0 & & 0 & & 0 & & 0 & & \\
 & & & & & & \downarrow & & \downarrow & & \downarrow & & \downarrow & & \\
 & & & & & \overset{j_2}{\rightarrow} & & \overset{D_1}{\rightarrow} & & \overset{D_2}{\rightarrow} & & \overset{D_3}{\rightarrow} & & \\
0 & \rightarrow & \Theta & \rightarrow & & & 6 & & 16 & & 14 & & 4 & \rightarrow 0 & \\
 & & & & & & \downarrow & & \downarrow & & \downarrow & & \| & & \\
 & & & & & \overset{j_2}{\rightarrow} & & \overset{D_1}{\rightarrow} & & \overset{D_2}{\rightarrow} & & \overset{D_3}{\rightarrow} & & \\
0 & \rightarrow & 1 & \rightarrow & & & 10 & & 20 & & 15 & & 4 & \rightarrow 0 & \\
 & & \| & & & & \downarrow \Phi_0 & & \downarrow \Phi_1 & & \downarrow \Phi_2 & & \downarrow & & \\
 & & & & & \overset{\mathcal{D}}{\rightarrow} & & \overset{\mathcal{D}_1}{\rightarrow} & & \overset{\mathcal{D}_2}{\rightarrow} & & & & & \\
0 \rightarrow & \Theta & \rightarrow & 1 & \rightarrow & & 4 & & 4 & & 1 & \rightarrow & 0 & & \\
 & & & & & & \downarrow & & \downarrow & & \downarrow & & & & \\
 & & & & & & 0 & & 0 & & 0 & & & &
\end{array}$$

We notice that $6-16+14-4=0$, $1-10+20-15+4=0$ and $1-4+4-1=0$. In this diagram, the Janet sequence seems simpler than the Spencer sequence but, sometimes as we shall see, it is the contrary and there is no rule. We invite the reader to treat similarly the cases $a=0$ and $a=x^3$.

2. Schwarzschild versus Kerr

2.1. Schwarzschild Metric

In the Boyer-Lindquist (BL) coordinates $(t,r,\theta,\phi)=(x^0,x^1,x^2,x^3)$, the Schwarzschild metric is $\omega=A(r)\mathrm{d}t^2-(1/A(r))\mathrm{d}r^2-r^2\mathrm{d}\theta^2-r^2\sin^2(\theta)\mathrm{d}\phi^2$ and $\xi=\xi^i d_i\in T$, let us introduce $\xi_i=\omega_{ri}\xi^r$ with the 4 *formal derivatives* $(d_0=d_t$, $d_1=d_r, d_2=d_\theta, d_3=d_\phi)$. With speed of light $c=1$ and $A=1-\dfrac{m}{r}$ where m is a constant, the metric can be written in the diagonal form:

$$\begin{pmatrix} A & 0 & 0 & 0 \\ 0 & -1/A & 0 & 0 \\ 0 & 0 & -r^2 & 0 \\ 0 & 0 & 0 & -r^2\sin^2(\theta) \end{pmatrix}$$

with a surprisingly simple determinant $det(\omega)=-r^4\sin^2(\theta)$.

Using the notations of differential modules or jet theory, we may consider the infinitesimal Killing equations:

$$\Omega\equiv L(\xi)\omega=0 \quad\Leftrightarrow\quad \Omega_{ij}\equiv d_i\xi_j+d_j\xi_i-2\gamma_{ij}^r\xi_r=0$$
$$\Leftrightarrow\quad \Omega_{ij}\equiv\omega_{rj}\xi_i^r+\omega_{ir}\xi_j^r+\xi^r\partial_r\omega_{ij}=0$$

where we have introduced the Christoffel symbols γ through the standard Levi-Civita isomorphism $j_1(\omega)\simeq(\omega,\gamma)$ while setting $A'=\partial_r A$ in the differential field K of coefficients [15]. As in the Macaulay example just considered and in order to avoid any further confusion between sections and derivatives, we shall use the sectional point of view and rewrite the previous 10 equations in the symbolic form $\Omega\equiv L(\xi_1)\omega\in S_2T^*$ where L is the *formal Lie derivative*:

$$R_1 \subset J_1(T) \begin{cases} \Omega_{33} \equiv -2r^2\sin^2(\theta)\boxed{\xi^3_3} - 2r\sin^2(\theta)\xi^1 - 2r^2\sin(\theta)\cos(\theta)\xi^2 = 0 \\ \Omega_{23} \equiv -r^2\boxed{\xi^2_3} - r^2\sin^2(\theta)\xi^3_2 = 0 \\ \Omega_{13} \equiv -\frac{1}{A}\boxed{\xi^1_3} - r^2\sin^2(\theta)\xi^3_1 = 0 \\ \Omega_{03} \equiv A\boxed{\xi^0_3} - r^2\sin^2(\theta)\xi^3_0 = 0 \\ \Omega_{22} \equiv -2r^2\boxed{\xi^0_2} - 2r\xi^1 = 0 \\ \Omega_{12} \equiv -\frac{1}{A}\boxed{\xi^1_2} - r^2\xi^2_1 = 0 \\ \Omega_{02} \equiv A\boxed{\xi^0_2} - r^2\xi^2_0 = 0 \\ \Omega_{11} \equiv -\frac{2}{A}\boxed{\xi^1_1} + \frac{A'}{A^2}\xi^1 = 0 \\ \Omega_{01} \equiv -\frac{1}{A}\boxed{\xi^1_0} + A\xi^0_1 = 0 \\ \Omega_{00} \equiv 2A\boxed{\xi^0_0} + A'\xi^1 = 0 \end{cases}$$

Though this system $R_1 \subset J_1(T)$ has 4 equations of class 3, 3 equations of class 2, 2 equations of class 1 and 1 equation of class 0, it is far from being involutive because it is finite type with second symbol $g_2 = 0$ defined by the 40 equations $\xi^k_{ij} = 0$ in the initial coordinates. From the symmetry, it is clear that such a system has *at least* 4 solutions, namely the time translation $\partial_t \leftrightarrow \xi^0 = 1 \Leftrightarrow \xi_0 = A$ and, using cartesian coordinates (t, x, y, z), the 3 space rotations $y\partial_z - z\partial_y, z\partial_x - x\partial_z, x\partial_y - y\partial_x$.

We obtain in particular, modulo Ω:

$$\xi^0_0 = -\frac{A'}{2A}\xi^1,\ \xi^1_1 = +\frac{A'}{2A}\xi^1,\ \xi^2_2 = -\frac{1}{r}\xi^1,\ \xi^3_3 = -\frac{1}{r}\xi^1 - \cot(\theta)\xi^2$$
$$\Rightarrow \xi^0_0 + \xi^1_1 = 0,\ \xi^2_2 + \xi^3_3 = -\cot(\theta)\xi^2$$

We may also write the Schwarzschild metric in cartesian coordinates as:

$$\omega = A(r)\mathrm{d}t^2 + \left(1 - \frac{1}{A(r)}\right)\mathrm{d}r^2 - \left(\mathrm{d}x^2 + \mathrm{d}y^2 + \mathrm{d}z^2\right),$$
$$r\mathrm{d}r = x\mathrm{d}x + y\mathrm{d}y + z\mathrm{d}z$$

and notice that the 3×3 matrix of components of the three rotations has rank equal to 2, a result leading surely, before doing any computation, to the existence of *one and only one* zero order Killing equation $r\xi^r = x\xi^x + y\xi^y + z\xi^z = 0 \Rightarrow \xi^1 = \xi^r = 0$. Such a result also amounts to say that the spatial projection of any Killing vector on the radial spatial unit vector $(x/r, y/r, z/r)$ vanishes beause r must stay invariant.

However, *as we are dealing with sections*, $\xi^1 = 0$ implies $\xi^0_0 = 0$, $\xi^1_1 = 0$, $\xi^2_2 = 0$ … but *NOT* (*care*) $\xi^1_0 = 0$, these later condition being only brought by one additional prolongation and we have the strict inclusions $R_1^{(3)} \subset R_1^{(2)} \subset R_1^{(1)} = R_1$ that we rename as $R_1'' \subset R_1' \subset R_1$. Hence, it remains to determine the dimensions of these subsystems and their symbols, exactly like in

the Macaulay example. We shall prove in the next section that two prolongations bring the five new equations:

$$\xi^1=0,\ \xi_2^1=0,\ \xi_3^1=0,\ \xi_2^0=0,\ \xi_3^0=0$$

and a new prolongation *only* brings the single equation $\boxed{\xi_0^1=0}$.

Knowing that $\dim(R_1)=\dim(R_2)=10$, $\dim(R_3)=5$, $\dim(R_4)=4$, we have thus obtained the 15 equations defining $R_1'=R_1^{(2)}$ with $\dim(R_1')=20-15=5$ and let the reader draw the corresponding Janet tabular for the 4 equations of class 3, the 4 equations of class 1, the 3 equations of class 0 and the 3 equations of class 2. The symbol g_1' has the two parametric jets (ξ_2^3,ξ_0^1) and is not 2-acyclic. Adding $\xi_0^1=0\Leftrightarrow\xi_1^0=0$, we finally achieve the PP procedure with the 16 equations defining the system $R_1''=R_1^{(3)}$ with $\dim(R_1'')=20-16=4$, namely:

$$R_1''\subset R_1'\subset R_1\subset J_1(T)\begin{cases}\xi_3^3+\cot(\theta)\xi^2=0 & 2\ 0\ 1\ 3\\ \xi_3^2+\sin^2(\theta)\xi_2^3=0 & 2\ 0\ 1\ 3\\ \xi_3^1=0 & 2\ 0\ 1\ 3\\ \xi_3^0=0 & 2\ 0\ 1\ 3\\ \xi_1^3=0 & 2\ 0\ 1\ \bullet\\ \xi_1^2=0 & 2\ 0\ 1\ \bullet\\ \xi_1^1=0 & 2\ 0\ 1\ \bullet\\ \xi_1^0=0 & 2\ 0\ 1\ \bullet\\ \xi_0^3=0 & 2\ 0\ \bullet\ \bullet\\ \xi_0^2=0 & 2\ 0\ \bullet\ \bullet\\ \xi_0^1=0 & 2\ 0\ \bullet\ \bullet\\ \xi_0^0=0 & 2\ 0\ \bullet\ \bullet\\ \xi_2^2=0 & 2\ \bullet\ \bullet\ \times\\ \xi_2^1=0 & 2\ \bullet\ \bullet\ \bullet\\ \xi_2^0=0 & 2\ \bullet\ \bullet\ \bullet\\ \xi^1=0 & \bullet\ \bullet\ \bullet\ \bullet\end{cases}$$

and we have replaced by "×" the only "*dot*" (non-multiplicative variable) that cannot provide vanishing crossed derivatives and thus involution of the symbol g_1'' with the only parametric jets (v_2^3,v_0^1). It is easy to check that R_1'', having minimum dimension equal to 4, is formally integrable, though not involutive as it is finite type with $\dim(g_1'')=16-15=1\Rightarrow g_1''\neq 0$ with parametric jet v_2^3 and to exhibit 4 solutions linearly independent over the constants. We let the reader prove as an exercise that the dimension of the Spencer δ-cohomology at $\wedge^2T^*\otimes g_1''$ is $\dim(H^2(g_1''))=3\neq 0$ but we have proved in [15] that its restriction to (x^2,x^3) is of dimension 1 only. We obtain:

THIS SYSTEM IS NOT INVOLUTIVE BUT DOES NOT DEPEND ON m ANY LONGER

Denoting by $R_2''\subset R_2\subset J_2(T)$ with $\dim(R_2'')=4$ the prolongation of $R_1'\subset J_1(T)$, it is the involutive system provided by the *prolongation/projection* (PP) procedure. We are in position to construct the corresponding canoni-

cal/involutive (lower) Janet and (upper) Spencer sequences along the following *fundamental diagram I* that we recalled in the Introduction. In the present situation, the Spencer sequence is isomorphic to the tensor product of the Poincaré sequence by the underlying 4-dimensional Lie algebra G, namely:

$$\wedge^0 T^* \otimes \mathcal{G} \xrightarrow{d} \wedge^1 T^* \otimes \mathcal{G} \xrightarrow{d} \cdots \xrightarrow{d} \wedge^4 T^* \otimes \mathcal{G} \to 0$$

In this diagram, *not depending any longer on m*, we have now $C_r = \wedge^r T^* \otimes R_2''$ and $\mathcal{D}$ is of order 2 like j_2 while *all* the other operators are of order 1:

$$\begin{array}{ccccccccccccccccc}
 & & & & 0 & & 0 & & 0 & & 0 & & 0 & & \\
 & & & & \downarrow & & \downarrow & & \downarrow & & \downarrow & & \downarrow & & \\
0 & \to & \Theta & \xrightarrow{j_2} & 4 & \xrightarrow{D_1} & 16 & \xrightarrow{D_2} & 24 & \xrightarrow{D_3} & 16 & \xrightarrow{D_4} & 4 & \to 0 & \\
 & & & & \downarrow & & \downarrow & & \downarrow & & \downarrow & & \downarrow & & \\
0 & \to & 4 & \xrightarrow{j_2} & 60 & \xrightarrow{D_1} & 160 & \xrightarrow{D_2} & 180 & \xrightarrow{D_3} & 96 & \xrightarrow{D_4} & 20 & \to 0 & \\
 & & \| & & \downarrow & & \downarrow & & \downarrow & & \downarrow & & \downarrow & & \\
0 \to & \Theta & \to & 4 & \xrightarrow[2]{\mathcal{D}} & 56 & \xrightarrow{\mathcal{D}_1} & 144 & \xrightarrow{\mathcal{D}_2} & 156 & \xrightarrow{\mathcal{D}_3} & 80 & \xrightarrow{\mathcal{D}_4} & 16 & \to 0 \\
 & & & & \downarrow & & \downarrow & & \downarrow & & \downarrow & & \downarrow & & \\
 & & & & 0 & & 0 & & 0 & & 0 & & 0 & &
\end{array}$$

We notice the vanishing of the Euler-Poincaré characteristics:

$$4-16+24-16+4=0, \quad 4-60+160-180+96-20=0,$$
$$4-56+144-156+80-16=0$$

We point out that, whatever is the sequence used or the way to describe $\mathcal{D}_1$, then $ad(\mathcal{D}_1)$ is parametrizing the *Cauchy* operator $ad(\mathcal{D})$ for the S metric. However, such an approach does not tell us *explicitly* what are the second and third order CC involved in the initial situation.

In actual practice, *all the preceding computations have been finally used to reduce the Poincaré group to its subgroup made with only one time translation and three space rotations*! On the contrary, we have proved during almost fourty years that one *must* increase the Poincaré group (10 parameters), first to the Weyl group (11 parameters by adding 1 dilatation) and finally to the conformal group of space-time (15 parameters by adding 4 elations) while only dealing with he Spencer sequence in order to increase the dimensions of the Spencer bundles, thus the number $\dim(C_0)$ of *potentials* and the number $\dim(C_1)$ of *fields* (compare to [16]).

2.2. Kerr Metric

We now write the Kerr metric in Boyer-Lindquist coordinates:

$$\mathrm{d}s^2 = \frac{\rho^2 - mr}{\rho^2}\mathrm{d}t^2 - \frac{\rho^2}{\Delta}\mathrm{d}r^2 - \rho^2\mathrm{d}\theta^2 - \frac{2amr\sin^2(\theta)}{\rho^2}\mathrm{d}t\mathrm{d}\phi$$
$$-\left(r^2 + a^2 + \frac{mra^2\sin^2(\theta)}{\rho^2}\right)\sin^2(\theta)\mathrm{d}\phi^2$$

where we have set $\Delta = r^2 - mr + a^2, \rho^2 = r^2 + a^2\cos^2(\theta)$ as usual and we check that:

$$a = 0 \Rightarrow \mathrm{d}s^2 = \left(1 - \frac{m}{r}\right)\mathrm{d}t^2 - \frac{1}{1 - \frac{m}{r}}\mathrm{d}r^2 - r^2\mathrm{d}\theta^2 - r^2\sin(\theta)^2\,\mathrm{d}\phi^2$$

as a well known way to recover the Schwarschild metric. We notice that t or ϕ do not appear in the coefficients of the metric. As the maximum subgroup of invariance of the Kerr metric *must* be contained in the maximum subgroup of invariance of the Schwarzschild metric because of the above limit when $a \to 0$, we shall obtain the only two possible infinitesimal generators $\{\partial_t, \partial_\phi\}$. We shall prove that the new first order system $R_1'' = R_1^{(3)}$ is involutive, contrary to the case of the S metric. Accordingly, we have the fundamental diagram I with fiber dimensions:

$$\begin{array}{ccccccccccccccccc}
 & & & & & & 0 & & 0 & & 0 & & 0 & & 0 & & \\
 & & & & & & \downarrow & & \downarrow & & \downarrow & & \downarrow & & \downarrow & & \\
0 & \to & \Theta & \overset{j_1}{\to} & 2 & \overset{D_1}{\to} & 8 & \overset{D_2}{\to} & 12 & \overset{D_3}{\to} & 8 & \overset{D_4}{\to} & 2 & \to & 0 & & \\
 & & & & \downarrow & & \downarrow & & \downarrow & & \downarrow & & \downarrow & & & & \\
0 & \to & 4 & \overset{j_1}{\to} & 20 & \overset{D_1}{\to} & 40 & \overset{D_2}{\to} & 40 & \overset{D_3}{\to} & 20 & \overset{D_4}{\to} & 4 & \to & 0 & & \\
 & & \| & & \downarrow & & \downarrow & & \downarrow & & \downarrow & & \downarrow & & & & \\
0 & \to & \Theta & \to & 4 & \overset{\mathcal{D}}{\to} & 18 & \overset{\mathcal{D}_1}{\to} & 32 & \overset{\mathcal{D}_2}{\to} & 28 & \overset{\mathcal{D}_3}{\to} & 12 & \overset{\mathcal{D}_4}{\to} & 2 & \to & 0 \\
 & & & & & & \downarrow & & \downarrow & & \downarrow & & \downarrow & & \downarrow & & \\
 & & & & & & 0 & & 0 & & 0 & & 0 & & 0 & &
\end{array}$$

with Euler-Poincaré characteristic $4 - 18 + 32 - 28 + 12 - 2 = 0$. Comparing the *surprisingly high* dimensions of the Janet bundles with the *surprisingly low* dimensions of the Spencer bundles needs no comment on the physical usefulness of the Janet sequence, despite its purely mathematical importance. In addition, using the same notations as in the preceding section, we shall prove that we have now the additional *zero order* equations $\xi^r = 0$, $\xi^\theta = 0$ produced by the non-zero components of the Weyl tensor and thus, *at best*,
$\dim\left(R_0^{(3)}\right) = 2 \Leftrightarrow \dim\left(R_1^{(2)}\right) = 2$ as these zero order equations will be obtained after *only* two prolongations. They depend on $j_2(\Omega)$ and we should obtain therefore eventually $\dim(Q_2) = 10 + \dim(R_1'') \geq 12$ CC of order 2 without any way to know about the desired third order CC.

Using now cartesian space coordinates (x, y, z) with $\xi^z = 0$, $x\xi^x + y\xi^y = 0$, we have only to study the following first order involutive system for $\xi^x = \xi$ with coefficients no longer depending on (a, m), providing the only generator $x\partial_y - y\partial_x$:

$$\begin{cases} \Phi^3 \equiv \xi_z = 0 \\ \Phi^2 \equiv \xi_y - \dfrac{1}{y}\xi = 0 \\ \Phi^1 \equiv \xi_x = 0 \end{cases} \qquad \begin{array}{|ccc|} \hline 1 & 2 & 3 \\ 1 & 2 & \bullet \\ 1 & \bullet & \bullet \\ \hline \end{array}$$

and the fundamental diagram

$$\begin{array}{ccccccccccccccc}
 & & & & & & 0 & & 0 & & 0 & & 0 & & \\
 & & & & & & \downarrow & & \downarrow & & \downarrow & & \downarrow & & \\
0 & \to & \Theta & \xrightarrow{j_1} & 1 & \xrightarrow{D_1} & 3 & \xrightarrow{D_2} & 3 & \xrightarrow{D_3} & 1 & \to & 0 & & \\
 & & & & \downarrow & & \downarrow & & \downarrow & & \| & & & & \\
0 & \to & 1 & \xrightarrow{j_1} & 4 & \xrightarrow{D_1} & 6 & \xrightarrow{D_2} & 4 & \xrightarrow{D_3} & 1 & \to & 0 & & \\
 & & \| & & \downarrow & & \downarrow & & \downarrow & & \downarrow & & & & \\
0 \to & \Theta & \to & 1 & \xrightarrow{\mathcal{D}} & 3 & \xrightarrow{\mathcal{D}_1} & 3 & \xrightarrow{\mathcal{D}_2} & 1 & \to & 0 & & & \\
 & & & & & \downarrow & & \downarrow & & \downarrow & & & & & \\
 & & & & & 0 & & 0 & & 0 & & & & &
\end{array}$$

The involutive system produced by the PP procedure does not depend on (m,a) any longer. Accordingly, this final result definitively proves that, *as far as differential sequences are concerned*:

THE ONLY IMPORTANT OBJECT IS THE GROUP, NOT THE METRIC

2.3. Schwarzschild Metric Revisited

Let us now introduce the Riemann tensor $\left(\rho_{l,ij}^{k}\right)\in\wedge^2T^*\otimes T^*\otimes T$ and use the metric in order to raise or lower the indices in order to obtain the purely covariant tensor $\left(\rho_{kl,ij}\right)\in\wedge^2T^*\otimes T^*\otimes T^*$. Then, using r as an implicit summation index, we may consider the formal Lie derivative on sections:

$$R_{kl,ij}\equiv\rho_{rl,ij}\xi_k^r+\rho_{kr,ij}\xi_l^r+\rho_{kl,rj}\xi_i^r+\rho_{kl,ir}\xi_j^r+\xi^r\partial_r\rho_{kl,ij}=0$$

that can be considered as an infinitesimal variation. As for the Ricci tensor $\left(\rho_{ij}\right)\in S_2T^*$, we notice that $\rho_{ij}=\rho_{i,rj}^{r}=0\Rightarrow R_{ij}\equiv\rho_{rj}\xi_i^r+\rho_{ir}\xi_j^r+\xi^r\partial_r\rho_{ij}=0$ though we have only:

$$\omega^{rs}R_{ri,sj}=R_{ij}+\omega^{rs}\rho_{i,rj}^{t}\Omega_{st}\Rightarrow R_{ij}=R_{i,rj}^{r}=\omega^{rs}R_{ri,sj}\ \mathrm{mod}(\Omega)$$

The 6 non-zero components of the Riemann tensor are known to be:

$$\begin{array}{|lll|}\hline
\rho_{01,01}=+\dfrac{m}{r^3}, & \rho_{02,02}=-\dfrac{mA}{2r}, & \rho_{03,03}=-\dfrac{mA\sin^2(\theta)}{2r} \\
\rho_{12,12}=+\dfrac{m}{2rA}, & \rho_{13,13}=+\dfrac{m\sin^2(\theta)}{2rA}, & \rho_{23,23}=-mr\sin^2(\theta) \\ \hline
\end{array}$$

First of all, we notice that:

$$\xi_0^0+\frac{A'}{2A}\xi^1=0,\xi_1^1-\frac{A'}{2A}\xi^1=0\Rightarrow\xi_0^0+\xi_1^1=0$$

$$\Omega_{12}\equiv-\frac{1}{A}\xi_2^1-r^2\xi_1^2=0,\ \xi_2^2+\frac{1}{r}\xi^1=0$$

We obtain therefore:

$$R_{01,01}\equiv2\rho_{01,01}\left(\xi_0^0+\xi_1^1\right)+\xi^r\partial_r\left(\rho_{01,01}\right)=\xi^1\partial_1\rho_{01,01}=-\frac{3m}{r^4}\xi^1=0\Rightarrow\xi^1=0$$

$$R_{02,02} \equiv 2\rho_{02,02}\left(\xi_0^0+\xi_2^2\right)+\xi^r\partial_r\left(\rho_{02,02}\right)$$
$$\equiv\left(-\frac{mA}{r}\left(-\frac{A'}{2A}-\frac{1}{r}\right)-\left(\frac{mA}{2r}\right)'\right)\xi^1=\frac{3mA}{2r^2}\xi^1=0$$

Similarly, we also get:

$$\begin{cases} R_{01,02} \equiv \rho_{01,01}\xi_2^1+\rho_{02,02}\xi_1^2+\xi^r\partial_r\rho_{01,02}=0\Rightarrow\frac{m}{r^3}\xi_2^1-\frac{mA}{2r}\xi_1^2=0 & \Rightarrow \boxed{\xi_2^1=0} \\ R_{01,03} \equiv \rho_{01,01}\xi_3^1+\rho_{03,03}\xi_1^3+\xi^r\partial_r\rho_{01,03}=0\Rightarrow\frac{m}{r^3}\xi_3^1-\frac{mA\sin^2(\theta)}{2r}\xi_1^3=0 & \Rightarrow \boxed{\xi_3^1=0} \\ R_{01,12} \equiv \rho_{01,10}\xi_2^0+\rho_{21,12}\xi_0^2+\xi^r\partial_r\rho_{01,12}=0\Rightarrow-\frac{m}{r^3}\xi_2^0-\frac{m}{2rA}\xi_0^2=0 & \Rightarrow \boxed{\xi_2^0=0} \\ R_{01,13} \equiv \rho_{01,10}\xi_3^0+\rho_{31,13}\xi_0^3+\xi^r\partial_r\rho_{01,13}=0\Rightarrow-\frac{m}{r^3}\xi_3^0-\frac{m\sin^2(\theta)}{2rA}\xi_0^3=0 & \Rightarrow \boxed{\xi_3^0=0} \end{cases}$$

We also obtain for example, among the second order CC:

$$R_{01,01} \equiv -\frac{3m}{r^4}\xi^1=0,\ R_{02,02} \equiv \frac{3mA}{2r^2}\xi^1=0\Rightarrow R_{02,02}-\frac{r^2A}{2}R_{01,01}=0$$

and thus, among the first prolongations, the third order CC that cannot be obtained by prolongation of the various second order CC while taking into account the Bianchi identities [15]. Using the Spencer operator and the fact that $\xi^1\in j_2(\Omega)$, we first obtain the 3 third order CC:

$$\boxed{d_1\xi^1-\xi_1^1=d_1\xi^1-\frac{A'}{2A}\xi^1=0,\ d_2\xi^1-\xi_2^1=0,\ d_3\xi^1-\xi_3^1=0}$$

However, introducing $\xi^1\in j_2(\Omega)$ in the right member as in the motivating examples, we have 3 PD equations for $\left(\xi^2,\xi^3\right)$, namely:

$$\xi_3^3+\cot(\theta)\xi^2=-\frac{1}{r}\xi^1,\ \xi_3^2+\sin^2(\theta)\xi_2^3=0,\ \xi_2^2=-\frac{1}{r}\xi^1$$

Using two prolongations and eliminating the third order jets, we obtain successively:

$$\xi_{233}^2+\sin^2(\theta)\xi_{223}^3+2\sin(\theta)\cos(\theta)\xi_{23}^3=0$$
$$-\xi_{233}^2=\frac{1}{r}\xi_{33}^1$$
$$-\sin^2(\theta)\xi_{223}^3-\sin(\theta)\cos(\theta)\xi_{22}^2+2\xi_2^2-2\cot(\theta)\xi^2=-\frac{\sin^2(\theta)}{r}\xi_{22}^1$$
$$-2\sin(\theta)\cos(\theta)\xi_{23}^3-2\cos^2(\theta)\xi_2^2+2\cot(\theta)\xi^2=\frac{2\sin(\theta)\cos(\theta)}{r}\xi_2^1$$
$$\sin(\theta)\cos(\theta)\xi_{22}^2=-\frac{\sin(\theta)\cos(\theta)}{r}\xi_2^1$$
$$-2\sin^2(\theta)\xi_2^2=\frac{2\sin^2(\theta)}{r}\xi^1$$

Summing, we see that all terms in ξ^2 and ξ^3 disappear and that we are only

left with terms in ξ^1, including in particular the second order jets ξ^1_{22}, ξ^1_{33}, namely:

$$\xi^1_{33} - \sin^2(\theta)\xi^1_{22} - \sin(\theta)\cos(\theta)\xi^1_2 + 2\sin^2(\theta)\xi^1 = 0$$

Setting $U = \xi^1$, $V_2 = \xi^1_2$, $V_3 = \xi^1_3$, $W_2 = \xi^0_2$, $W_3 = \xi^0_3$ with $(U, V_2, V_3, W_2, W_3) \in j_2(\Omega)$, we obtain the *additional strikingly unusual* third order CC for Ω:

$$\boxed{d_3V_3 - \sin^2(\theta)d_2V_2 - \sin(\theta)\cos(\theta)V_2 + 2\sin^2(\theta)U = 0}$$

Nevertheless, *in our opinion at least*, we do not believe that such a purely "technical" relation could have any "physical" usefulness and let the reader compare it with the CC already found in ([15], Lemma 3.B.3). Finally, we have:

$$\rho_{01,23} = 0 \Rightarrow R_{01,23} \equiv \rho_{01,23}\left(\xi^0_0 + \xi^1_1 + \xi^2_2 + \xi^3_3\right) + \xi\partial\rho_{01,23} = 0$$

$$d_1R_{01,23} + d_2R_{01,31} + d_3R_{01,12} = \frac{3m}{2r^3}\left(d_2\xi^0_3 - d_3\xi^0_2\right) = 0 \bmod(\Omega, \Gamma, R)$$

a result showing that certain third order CC may be differential consequences of the Bianchi identities (see [15] for details). Finally, we notice that:

$$R_{23,23} \equiv 2\rho_{23,23}\left(\xi^2_2 + \xi^3_3\right) + \xi\partial\rho_{23,23} = 3m\sin^2(\theta)\xi^1 = 0$$

and, comparing to the previous computation for (ξ^2, ξ^3), *nothing can be said about the generating CC as long as the PP procedure has not been totally achieved with a FI or involutive system*.

2.4. Kerr Metric Revisited

Though we shall provide explicitly all the details of the computations involved, we shall change the coordinate system in order to confirm these results by only using computer algebra as less as possible. The idea is to use the so-called "*rational polynomial*" coefficients while setting anew:

$$\left(x^0 = t, x^1 = r, x^2 = c = \cos(\theta), x^3 = \phi\right)$$

$$\Rightarrow \mathrm{d}x^2 = -\sin(\theta)\mathrm{d}\theta \Rightarrow \left(\mathrm{d}x^2\right)^2 = \left(1 - c^2\right)\mathrm{d}\theta^2$$

in order to obtain over the differential field $K = \mathbb{Q}(a, m)(t, r, c, \phi) = \mathbb{Q}(a, m)(x)$:

$$\mathrm{d}s^2 = \frac{\rho^2 - mx^1}{\rho^2}\left(\mathrm{d}x^0\right)^2 - \frac{\rho^2}{\Delta}\left(\mathrm{d}x^1\right)^2 - \frac{\rho^2}{1 - \left(x^2\right)^2}\left(\mathrm{d}x^2\right)^2$$

$$- \frac{2amx^1\left(1 - \left(x^2\right)^2\right)}{\rho^2}\mathrm{d}x^0\mathrm{d}x^3$$

$$- \left(1 - \left(x^2\right)^2\right)\left(\left(x^1\right)^2 + a^2 + \frac{ma^2x^1\left(1 - \left(x^2\right)^2\right)}{\rho^2}\right)\left(\mathrm{d}x^3\right)^2$$

with now $\Delta = \left(x^1\right)^2 - mx^1 + a^2 = r^2 - mr + a^2$ and

$\rho^2=\left(x^1\right)^2+a^2\left(x^2\right)^2=r^2+a^2c^2$. For a later use, it is also possible to set $\omega_{33}=-\left(1-c^2\right)\left(\left(r^2+a^2\right)^2-a^2\left(1-c^2\right)\left(a^2-mr+r^2\right)\right)\Big/\left(r^2+a^2c^2\right)$.

As this result will be crucially used later on, we have:

LEMMA 4.1: $\det(\omega)=-\left(r^2+a^2c^2\right)^2$.

Proof: As an elementary result on matrices, we have:

$$\det(\omega)=\det\begin{pmatrix}a&0&0&e\\0&b&0&0\\0&0&c&0\\e&0&0&d\end{pmatrix}=bc\det\begin{pmatrix}a&e\\e&d\end{pmatrix}=bc\left(ad-e^2\right)$$

with $e=\omega_{03}=\dfrac{amx^1\left(1-\left(x^2\right)^2\right)}{\rho^2}$ because $\mathrm{d}s^2=\cdots+2\omega_{03}\mathrm{d}x^0\mathrm{d}x^3+\cdots$ and $\det(\omega)$ is thus equal to:

$$\frac{\rho^4}{\Delta\left(1-\left(x^2\right)^2\right)}\left[-\frac{\rho^2-mx^1}{\rho^2}\left(1-\left(x^2\right)^2\right)\left(\left(x^1\right)^2+a^2+\frac{ma^2x^1\left(1-\left(x^2\right)^2\right)}{\rho^2}\right)-\frac{\left(amx^1\left(1-\left(x^2\right)^2\right)\right)^2}{\rho^4}\right]$$

that is, after division by $\left(1-\left(x^2\right)^2\right)$ and ρ^4:

$$\frac{1}{\Delta}\left[-\left(\rho^2-mx^1\right)\left(\rho^2\left(x^1\right)^2+\rho^2a^2+ma^2x^1\left(1-\left(x^2\right)^2\right)\right)-a^2m^2\left(x^1\right)^2\left(1-\left(x^2\right)^2\right)\right]$$

Finally, after eliminating the last term, we get:

$$\frac{1}{\Delta}\left[-\rho^4\left(\left(x^1\right)^2+a^2\right)-\rho^2ma^2x^1\left(1-\left(x^2\right)^2\right)+\rho^2mx^1\left(\left(x^1\right)^2+a^2\right)\right]$$

that is (Compare to [ ] and [ ]):

$$\frac{1}{\Delta}\left[-\rho^4\left(\Delta+mx^1\right)+\rho^2ma^2x^1\left(x^2\right)^2+\rho^2m\left(x^1\right)^3\right]$$
$$=\frac{1}{\Delta}\left[-\rho^4\left(\Delta+mx^1\right)+\rho^2mx^1\left(a^2\left(x^2\right)^2+\left(x^1\right)^2\right)\right]=-\rho^4$$

in a coherent way with the result $A\left(-\dfrac{1}{A}\right)\left(-\dfrac{r^2}{1-c^2}\left(-r^2\left(1-c^2\right)\right)\right)=-r^4$ obtained for the S metric when $a\to 0$. For a later use, we have obtained $\omega_{00}\omega_{33}-\left(\omega_{03}\right)^2=-\left(1-c^2\right)\Delta$.

Q.E.D.

Contrary to the S-metric, the main "trick" for studying the K-metric is to take into account that the partition between the zero and nonzero terms will not change if we use convenient coordinates, even if the nonzero terms may change. Meanwhile, we notice that the most important property of the K-metric is the

existence of the off-diagonal term $\omega_{t\phi}=\omega_{\phi t}=-\dfrac{am\sin^2(\theta)}{\rho^2}$, that is $\dfrac{1}{2}$ the coefficient of $\mathrm{d}t\mathrm{d}\phi$ in the metric $\mathrm{d}s^2$ which is indeed $2\omega_{t\phi}\mathrm{d}t\mathrm{d}\phi$. We may obtain therefore successively the Killing equations for the Kerr type metric, using sections of jet bundles and writing simply $\xi\partial\omega=\xi^r\partial_r\omega=\xi^1\partial_1\omega+\xi^2\partial_2\omega$ while framing the principal derivative $\boxed{\xi_i^j}$ of Ω_{ij}:

$$R_1\subset J_1(T)\begin{cases}\Omega_{33}\equiv 2\left(\omega_{33}\boxed{\xi_3^3}+\omega_{03}\xi_3^0\right)+\xi\partial\omega_{33}=0\\ \Omega_{23}\equiv \omega_{33}\boxed{\xi_2^3}+\omega_{03}\xi_2^0+\omega_{22}\xi_3^2=0\\ \Omega_{22}\equiv 2\omega_{22}\boxed{\xi_2^2}+\xi\partial\omega_{22}=0\\ \Omega_{13}\equiv \omega_{33}\boxed{\xi_1^3}+\omega_{03}\xi_1^0+\omega_{11}\xi_3^1=0\\ \Omega_{12}\equiv \omega_{22}\boxed{\xi_1^2}+\omega_{11}\xi_2^1=0\\ \Omega_{11}\equiv 2\omega_{11}\boxed{\xi_1^1}+\xi\partial\omega_{11}=0\\ \Omega_{03}\equiv \omega_{33}\boxed{\xi_0^3}+\omega_{03}(\xi_0^0+\xi_3^3)+\omega_{00}\xi_3^0+\xi\partial\omega_{03}=0\\ \Omega_{02}\equiv \omega_{22}\boxed{\xi_0^2}+\omega_{00}\xi_2^0+\omega_{03}\xi_2^3=0\\ \Omega_{01}\equiv \omega_{11}\boxed{\xi_0^1}+\omega_{00}\xi_1^0+\omega_{03}\xi_1^3=0\\ \Omega_{00}\equiv 2\left(\omega_{00}\boxed{\xi_0^0}+\omega_{03}\xi_0^3\right)+\xi\partial\omega_{00}=0\end{cases}$$

With $\mathrm{mod}(\xi)=\mathrm{mod}(\xi^1,\xi^2)$, multiplying Ω_{33} by ω_{00}, Ω_{00} by ω_{33} and adding, we notice that:

$$2\omega_{00}\omega_{33}\left(\xi_0^0+\xi_3^3\right)+2\omega_{03}\left(\omega_{00}\xi_3^0+\omega_{33}\xi_0^3\right)+\xi\partial\left(\omega_{00}\omega_{33}\right)=0$$

Similarly, multiplying Ω_{03} by $2\omega_{03}$ (*care to the factor* 2), we get:

$$2\left(\omega_{03}\right)^2\left(\xi_0^0+\xi_3^3\right)+2\omega_{03}\left(\omega_{00}\xi_3^0+\omega_{33}\xi_0^3\right)+\xi\partial\left(\omega_{03}\right)^2=0$$

Substracting, we obtain therefore the *tricky* formula (see the previous Lemma):

$$2\left(\omega_{00}\omega_{33}-\left(\omega_{03}\right)^2\right)\left(\xi_0^0+\xi_3^3\right)+\xi\partial\left(\omega_{00}\omega_{33}-\left(\omega_{03}\right)^2\right)=0$$

Substituting, we obtain:

$$\omega_{33}\boxed{\xi_3^3}+\omega_{03}\xi_3^0=0\,\mathrm{mod}(\xi),\ \ \omega_{33}\boxed{\xi_0^3}+\omega_{00}\xi_3^0=0\,\mathrm{mod}(\xi),$$
$$\omega_{33}\boxed{\xi_0^0}-\omega_{03}\xi_3^0=0\,\mathrm{mod}(\xi)$$

a situation leading to modify Ω_{33}, Ω_{03} and Ω_{00}, similar to the one found in the Minkowski case with $\xi_{3,3}=0$, $\xi_{0,3}+\xi_{3,0}=0$, $\xi_{0,0}=0\,\mathrm{mod}(\xi)$ when $\omega_{03}=0$. We also obtain with Ω_{01} and Ω_{13}:

$$\boxed{\begin{aligned}&\left(\omega_{00}\omega_{33}-\left(\omega_{03}\right)^2\right)\boxed{\xi_1^0}+\omega_{11}\left(\omega_{33}\xi_0^1-\omega_{03}\xi_3^1\right)=0\,\mathrm{mod}(\xi)\\ &\left(\omega_{00}\omega_{33}-\left(\omega_{03}\right)^2\right)\boxed{\xi_1^3}-\omega_{11}\left(\omega_{03}\xi_0^1-\omega_{00}\xi_3^1\right)=0\,\mathrm{mod}(\xi)\end{aligned}}$$

and with Ω_{02} and Ω_{23}:

$$\boxed{\begin{array}{l}\left(\omega_{00}\omega_{33}-\left(\omega_{03}\right)^2\right)\boxed{\xi_2^0}+\omega_{22}\left(\omega_{33}\xi_0^2-\omega_{03}\xi_3^2\right)=0 \bmod(\xi)\\ \left(\omega_{00}\omega_{33}-\left(\omega_{03}\right)^2\right)\boxed{\xi_2^3}-\omega_{22}\left(\omega_{03}\xi_0^2-\omega_{00}\xi_3^2\right)=0 \bmod(\xi)\end{array}}$$

Finally, multiplying Ω_{22} by ω_{11}, Ω_{11} by ω_{22} and adding, we finally obtain (see the Lemma again)

$$2\left(\omega_{11}\omega_{22}\right)\left(\xi_1^1+\xi_2^2\right)+\xi\partial\left(\omega_{11}\omega_{22}\right)=0$$

Using the rational coefficients belonging to the differential field $K=\mathbb{Q}(m,a)\left(x^1,x^2\right)$, the nonzero components of the corresponding Riemann tensor can be found in textbooks.

One has the classical orthonormal decomposition:

$$\begin{aligned}\mathrm{d}s^2=&\frac{\Delta}{\rho^2}\left(\mathrm{d}t-a\sin^2(\theta)\mathrm{d}\phi\right)^2-\frac{\rho^2}{\Delta}\left(\mathrm{d}r\right)^2-\rho^2\left(\mathrm{d}\theta\right)^2\\&-\frac{\left(r^2+a^2\right)^2\sin^2(\theta)}{\rho^2}\left(\mathrm{d}\phi-\frac{a}{r^2+a^2}\mathrm{d}t\right)^2\end{aligned}$$

and defining:

$$\begin{cases}\mathrm{d}X^0=\dfrac{\sqrt{\Delta}}{\rho}\left(\mathrm{d}t-a\sin^2(\theta)\mathrm{d}\phi\right)\\ \mathrm{d}X^1=\dfrac{\rho}{\sqrt{\Delta}}\mathrm{d}r=\dfrac{\rho}{\sqrt{\Delta}}\mathrm{d}x^1\\ \mathrm{d}X^2=\rho\mathrm{d}\theta=-\dfrac{\rho}{\sin(\theta)}\mathrm{d}x^2\\ \mathrm{d}X^3=\dfrac{\left(r^2+a^2\right)\sin(\theta)}{\rho}\left(\mathrm{d}\phi-\dfrac{a}{r^2+a^2}\mathrm{d}t\right)\end{cases}$$

in which the coefficient of $\left(\mathrm{d}t\right)^2$ is $\frac{\Delta}{\rho^2}-\frac{a^2\sin^2(\theta)}{\rho^2}=1-\frac{mr}{\rho^2}$ while the coefficient of $\left(\mathrm{d}\phi\right)^2$ is $-\left(r^2+a^2+\frac{mra^2\sin^2(\theta)}{\rho^2}\right)\sin^2(\theta)$ indeed. We have $\mathrm{d}s^2=\left(\mathrm{d}X^0\right)^2-\left(\mathrm{d}X^1\right)^2-\left(\mathrm{d}X^2\right)^2-\left(\mathrm{d}X^3\right)^2$ and make thus the Minkowski metric appearing in a purely algebraic way. We now use the new coordinates $\left(x^0=t,\ x^1=r,x^2=\cos(\theta),x^3=\phi\right)$ and it follows that the conditions $\xi^1=0$, $\xi^2=0$ are invariant under such a change of basis because $\mathrm{d}X^1$ and $\mathrm{d}X^2$ are respectively proportional to $\mathrm{d}x^1$ and $\mathrm{d}x^2$. Indeed, as $\omega=\omega\left(r,\theta\right)$ and thus $\xi\partial\omega=0$, the new symbol g_1' of $R_1'=R_1^{(2)}\subset R_1\subset T^*\otimes T$ while $\rho\in\wedge^2T^*\otimes T^*\otimes T$ as mixed tensors.

We may obtain simpler formulas in the corresponding basis, in particular the 6 components with only two different indices are proportional to $\frac{mr\left(r^2-3a^2c^2\right)}{\left(r^2+a^2c^2\right)^3}$ while the 3 components with all four different indices are proportional to

$$\frac{amc\left(3r^2-a^2c^2\right)}{\left(r^2+a^2c^2\right)^3}.$$

In the original rational coordinate system, *the main nonzero components of the Riemann tensor can only be obtained by means of computer algebra*. For helping the reader to handle the literature, for example the book "Computations in Riemann Geometry" written by Kenneth R. Koehler that can be found on the net with a free access, we refer to the seventh chapter on "Black Holes". We notice that $\omega \to -\omega$, that is to say changing the sign of the metric, does not change the Christoffel symbols (γ_{ij}^{k}) and the Riemann tensor ($\rho_{l,ij}^{r}$) *but changes the sign of* ($\rho_{kl,ij}=\omega_{kr}\rho_{l,ij}^{r}$). For this reason, we have adopted the sign convention of this reference for the explicit computation of these later components as the products and quotients used in the sequel will not be changed.

We have successively:

$$\begin{cases}
\rho_{01,01}=-\dfrac{mr\left(2\left(r^2-mr+a^2\right)+a^2\left(1-c^2\right)\right)\left(r^2-3a^2c^2\right)}{2\left(r^2+a^2c^2\right)^3\left(r^2-mr+a^2\right)} \\
\rho_{02,02}=\dfrac{mr\left(r^2-mr+a^2+2a^2\left(1-c^2\right)\right)\left(r^2-3a^2c^2\right)}{2\left(1-c^2\right)\left(r^2+a^2c^2\right)^3} \\
\rho_{03,03}=\dfrac{mr\left(1-c^2\right)\left(r^2-mr+a^2\right)\left(r^2-3a^2c^2\right)}{2\left(r^2+a^2c^2\right)^3} \\
\rho_{12,12}=-\dfrac{mr\left(r^2-3a^2c^2\right)}{2\left(1-c^2\right)\left(r^2+a^2c^2\right)\left(r^2-mr+a^2\right)} \\
\rho_{13,13}=\dfrac{-\left(1-c^2\right)mr\left(r^4-2a^2c^2r^2+4a^2r^2-2a^4c^2+3a^4-2a^2mr\left(1-c^2\right)\right)\left(r^2-3a^2c^2\right)}{2\left(r^2+a^2c^2\right)^3\left(r^2-mr+a^2\right)} \\
\rho_{23,23}=\dfrac{mr\left(2r^4-a^2c^2r^2+5a^2r^2-a^4c^2+3a^4-a^2mr\left(1-c^2\right)\right)\left(r^2-3a^2c^2\right)}{2\left(r^2+a^2c^2\right)^3} \\
\rho_{01,23}=\dfrac{amc\left(2r^2-a^2c^2+3a^2\right)\left(3r^2-a^2c^2\right)}{2\left(r^2+a^2c^2\right)^3} \\
\rho_{02,31}=-\dfrac{amc\left(r^2-2a^2c^2+3a^2\right)\left(3r^2-a^2c^2\right)}{2(r^2+a^2c^2)^3} \\
\rho_{03,12}=-\dfrac{amc\left(3r^2-a^2c^2\right)}{2\left(r^2+a^2c^2\right)^2}
\end{cases}$$

It must be noticed that we have been able to factorize the six components with only two different indices by $\left(r^2-3a^2c^2\right)$ and the three components with four different indices by $\left(3r^2-a^2c^2\right)$, a result not evident at first sight but coherent with the orthogonal decomposition.

After tedious computations, we obtain:

$$-\frac{\omega^{03}}{\omega^{11}}\rho_{03,03}=-\left(-\frac{\rho^2}{\Delta}\right)\left(\frac{amr\left(1-c^2\right)}{\rho^2}\right)\left(-\frac{1}{\left(1-c^2\right)\Delta}\right)\rho_{03,03}$$
$$=-\frac{am^2r^2\left(1-c^2\right)\left(r^2-3a^2c^2\right)}{2\left(r^2+a^2c^2\right)^2\left(r^2-mr+a^2\right)}$$

which is indeed vanishing when $a=0$ for the S metric, both with:

$$\begin{cases}\rho_{02,13}+\rho_{03,12}=\dfrac{3a^3mc\left(1-c^2\right)\left(3r^2-a^2c^2\right)}{2\left(r^2+a^2c^2\right)^3}\\ \rho_{01,23}+\rho_{03,21}=\dfrac{3amc\left(r^2+a^2\right)\left(3r^2-a^2c^2\right)}{2\left(r^2+a^2c^2\right)^3}\end{cases}$$

$$\begin{cases}\rho_{02,10}=\dfrac{3a^2mc\left(3r^2-a^2c^2\right)}{2\left(r^2+a^2c^2\right)^3}\\ \rho_{02,32}=\dfrac{amr\left(3r^2-mr+3a^2\right)\left(r^2-3a^2c^2\right)}{2\left(r^2+a^2c^2\right)^3}\\ \rho_{13,23}=-\dfrac{3a^2mc\left(1-c^2\right)\left(r^2+a^2\right)\left(3r^2-a^2c^2\right)}{2\left(r^2+a^2c^2\right)^3}\\ \rho_{01,13}=\dfrac{amr\left(1-c^2\right)\left(3r^2+3a^2-2mr\right)\left(r^2-3a^2c^2\right)}{2\left(r^2+a^2c^2\right)^3\left(r^2-mr+a^2\right)}\\ \quad=\dfrac{3amr\left(1-c^2\right)\left(r^2-3a^2c^2\right)}{2\left(r^2+a^2c^2\right)^3}+\dfrac{am^2r^2\left(1-c^2\right)\left(r^2-3a^2c^2\right)}{2\left(r^2+a^2c^2\right)^3\left(r^2-mr+a^2\right)}\end{cases}$$

Introducing the *formal Lie derivative* $R=L\left(\xi_1\right)\rho$ and using the fact that $\rho\in\wedge^2T^*\otimes T^*\otimes T^*$ is a tensor, the system $R_1^{(2)}$ contains the new equations:

$$R_{kl,ij}\equiv\rho_{rl,ij}\xi_k^r+\rho_{kr,ij}\xi_l^r+\rho_{kl,rj}\xi_i^r+\rho_{kl,ir}\xi_j^r+\xi^r\partial_r\rho_{kl,ij}=0$$

Taking into account the original first order Killing equations, we obtain successively:

$$\begin{cases}R_{01,01}\equiv 2\rho_{01,01}\left(\xi_0^0+\xi_1^1\right)+2\rho_{01,31}\xi_0^3+2\rho_{01,02}\xi_1^2+\xi\partial\rho_{01,01}=0\\ R_{02,02}\equiv 2\rho_{02,02}\left(\xi_0^0+\xi_2^2\right)+2\rho_{02,32}\xi_0^3+2\rho_{01,02}\xi_2^1+\xi\partial\rho_{02,02}=0\\ R_{R_{03,03}}\equiv 2\rho_{03,03}\left(\xi_0^0+\xi_3^3\right)+\xi\partial\rho_{03,03}=0\\ R_{12,12}\equiv 2\rho_{12,12}\left(\xi_1^1+\xi_2^2\right)+\xi\partial\rho_{12,12}=0\\ R_{13,13}\equiv 2\rho_{13,13}\left(\xi_1^1+\xi_3^3\right)+2\rho_{13,23}\xi_1^2+2\rho_{13,10}\xi_3^0+\xi\partial\rho_{13,13}=0\\ R_{23,23}\equiv 2\rho_{23,23}\left(\xi_2^2+\xi_3^3\right)+2\rho_{13,23}\xi_2^1+2\rho_{20,23}\xi_3^0+\xi\partial\rho_{23,23}=0\end{cases}$$

and we must add:

$$\begin{cases} R_{01,23} \equiv \rho_{01,23}\left(\xi_0^0+\xi_1^1+\xi_2^2+\xi_3^3\right)+\xi\partial\rho_{01,23}=0 \\ R_{02,13} \equiv \rho_{02,13}\left(\xi_0^0+\xi_1^1+\xi_2^2+\xi_3^3\right)+\xi\partial\rho_{02,13}=0 \\ R_{03,12} \equiv \rho_{03,12}\left(\xi_0^0+\xi_1^1+\xi_2^2+\xi_3^3\right)+\xi\partial\rho_{03,12}=0 \end{cases}$$

These linear equations are not linearly independent because:

$$\rho_{01,23}+\rho_{02,31}+\rho_{03,12}=0 \Rightarrow R_{01,23}+R_{02,31}+R_{03,12}=0$$

Also, linearizing while using the Kronecker symbol δ, we get:

$$\omega_{ir}\omega^{kr}=\delta_i^k \Rightarrow \Omega^{kl}=-\omega^{kr}\omega^{ls}\Omega_{rs}$$

Thus, introducing the Ricci tensor and linearizing, we get:

$$\begin{aligned} &\rho_{ij}=\omega^{rs}\rho_{ri,sj}=\omega^{rs}\rho_{ir,\,js}=0 \\ &\Rightarrow R_{ij}=\omega^{rs}R_{ri,sj}+\rho_{ik,\,jl}\Omega^{kl}=\omega^{rs}R_{ir,\,js}-\rho_{ik,\,jl}\omega^{kr}\omega^{ls}\Omega_{rs} \\ &\qquad =\rho_{rj}\xi_i^r+\rho_{ir}\xi_j^r+\xi^r\partial_r\rho_{ij}=0 \end{aligned}$$

It follows that $-R_{ij}\equiv\omega^{rs}R_{ir,sj}=0\,\mathrm{mod}(\Omega)$ and we have in particular $\mathrm{mod}(\Omega)$:

$$\begin{cases} R_{00} \equiv \omega^{11}R_{01,01}+\omega^{22}R_{02,02}+\omega^{33}R_{03,03}=0 \\ R_{11} \equiv \omega^{00}R_{01,01}+2\omega^{03}R_{01,31}+\omega^{22}R_{12,12}+\omega^{33}R_{13,13}=0 \\ R_{22} \equiv \omega^{00}R_{02,02}+2\omega^{03}R_{02,32}+\omega^{11}R_{12,12}+\omega^{33}R_{23,23}=0 \\ R_{33} \equiv \omega^{00}R_{03,03}+\omega^{11}R_{13,13}+\omega^{22}R_{23,23}=0 \end{cases}$$

The first row proves that $R_{03,03}$ is a linear combination of $R_{01,01}$ and $R_{02,02}$. Then, if we want to solve the three other equations with respect to $R_{12,12}$, $R_{13,13}$ and $R_{23,23}$, the corresponding determinant is, up to sign:

$$\det\begin{pmatrix} \omega^{22} & \omega^{33} & 0 \\ \omega^{11} & 0 & \omega^{33} \\ 0 & \omega^{11} & \omega^{22} \end{pmatrix}=-2\omega^{11}\omega^{22}\omega^{33}\neq 0$$

Accordingly, we only need to take into account $R_{01,01}, R_{02,02}, R_{01,13}, R_{02,23}$.

Similarly, we also obtain $\mathrm{mod}(\Omega)$:

$$\begin{cases} R_{01} \equiv \omega^{22}R_{20,21}+\omega^{33}R_{30,31}+\omega^{03}R_{30,01}=0 \\ R_{02} \equiv \omega^{11}R_{01,21}+\omega^{33}R_{03,32}+\omega^{03}R_{30,02}=0 \\ R_{03} \equiv \boxed{\omega^{11}R_{10,13}+\omega^{22}R_{20,23}}+\omega^{03}R_{03,03}=0 \\ R_{12} \equiv \boxed{\omega^{00}R_{01,02}+\omega^{33}R_{31,32}}+\omega^{03}\left(R_{01,32}+R_{31,02}\right)=0 \\ R_{13} \equiv \omega^{00}R_{01,03}+\omega^{22}R_{21,23}+\omega^{03}R_{31,03}=0 \\ R_{23} \equiv \omega^{00}R_{02,03}+\omega^{11}R_{12,13}+\omega^{03}R_{32,03}=0 \end{cases}$$

where we have to set $R_{01,23}=0, R_{02,13}=0 \Rightarrow R_{03,12}=0$.

Hence, taking into account $R_{03}=0$, we just need to use $R_{01,01}, R_{02,02}$ and $R_{01,13}$.

However, using the previous lemma, we obtain the formal Lie derivative:

$$2\det(\omega)\left(\xi_0^0+\xi_1^1+\xi_2^2+\xi_3^3\right)+\xi\partial\det(\omega)=0$$

and thus $\xi\partial\left(\rho_{01,23}/\sqrt{\left|\det(\omega)\right|}\right)=0$ with $\sqrt{\left|\det(\omega)\right|}=r^2+a^2\cos^2(\theta)$.

In addition, we have $2(\omega_{11}\omega_{22})(\xi_1^1+\xi_2^2)+\xi\partial(\omega_{11}\omega_{22})=0$ and thus $\xi\partial\left(\rho_{12,12}/(\omega_{11}\omega_{22})\right)=0$.

We have also:

$$2(\rho_{03,03}\rho_{12,12})(\xi_0^0+\xi_1^1+\xi_2^2+\xi_3^3)+\xi\partial(\rho_{03,03}\rho_{12,12})=0$$
$$\Rightarrow \xi\partial\left(\rho_{03,03}\rho_{12,12}/\det(\omega)\right)=0$$

The following invariants are obtained successively in a coherent way:

$$\left|\rho_{03,03}\rho_{12,12}\right|=\frac{m^2r^2\left(r^2-3a^2c^2\right)^2}{4\left(r^2+a^2c^2\right)^4}\Rightarrow\left|\rho_{03,03}\rho_{12,12}\right|/\left|\det(\omega)\right|=\left(\frac{mr\left(r^2-3a^2c^2\right)}{2\left(r^2+a^2c^2\right)^3}\right)^2$$

$$\omega_{11}\omega_{22}=\frac{\left(r^2+a^2c^2\right)^2}{\left(1-c^2\right)\left(r^2-mr+a^2\right)}\Rightarrow\left|\rho_{12,12}\right|/(\omega_{11}\omega_{22})=\frac{mr\left(r^2-3a^2c^2\right)}{2\left(r^2+a^2c^2\right)^3}$$

However, as $a\in K$, then $\rho_{01,23}$ and $\rho_{02,13}$ can be both divided by a and we get the new invariant:

$$\rho_{01,23}/\rho_{03,12}=\frac{2r^2-a^2c^2+3a^2}{r^2+a^2c^2}$$

These results are leading to $\boxed{\xi^1=0}$, $\boxed{\xi^2=0}$, thus to $\boxed{\xi_1^1=0}$, $\boxed{\xi_2^2=0}$ and $\xi_0^0+\xi_3^3=0$ after substitution. In the case of the S-metric, only the first invariant can be used in order to find $\xi^1=0$.

Taking into account the previous result, we obtain the two equations:

$$\begin{cases}\rho_{01,01}\left(\xi_0^0+\xi_1^1\right)+\rho_{01,31}\xi_0^3+\rho_{01,02}\xi_1^2=0\\ \rho_{02,02}\left(\xi_0^0+\xi_2^2\right)+\rho_{02,32}\xi_0^3+\rho_{01,02}\xi_2^1=0\end{cases}$$

Using the fact that we have now:

$$\omega_{22}\xi_1^2+\omega_{11}\xi_2^1=0\Leftrightarrow\omega^{11}\xi_1^2+\omega^{22}\xi_2^1=0$$

we may multiply the first equation by ω^{11}, the second by ω^{22} and sum in order to obtain:

$$\left(\omega^{11}\rho_{01,01}+\omega^{22}\rho_{02,02}\right)\xi_0^0+\left(\omega^{11}\rho_{01,31}+\omega^{22}\rho_{02,32}\right)\xi_0^3=0$$

Using the previous identity for R_{03}, we obtain therefore:

$$\omega^{33}\rho_{03,03}\xi_0^0+\omega^{03}\rho_{03,03}\xi_0^3=0\Rightarrow\omega^{33}\xi_0^0+\omega^{03}\xi_0^3=0\Leftrightarrow\boxed{\omega_{03}\xi_0^0-\omega_{33}\xi_0^3=0}$$

Taking into account the fact that $\xi_0^0=\frac{\omega_{03}}{\omega_{33}}\xi_3^0,\xi_0^3=-\frac{\omega_{00}}{\omega_{33}}\xi_3^0$ and substituting, we finally obtain:

$$\left(\omega_{00}\omega_{33}-(\omega_{03})^2\right)\xi_3^0=0\Rightarrow\boxed{\xi_3^0=0},\boxed{\xi_2^1=0}\Leftrightarrow\boxed{\xi_0^3=0},\boxed{\xi_1^2=0},\boxed{\xi_0^0=0},\boxed{\xi_3^3=0}$$

A similar procedure could have been followed by using $R_{13,13}=0,R_{23,23}=0$ and $\rho_{33}=0$.

Now, we must distinguish among the 20 components of the Riemann tensor along with the following tabular where we have to take into account the identity $\rho_{01,23}+\rho_{02,31}+\rho_{03,12}=0$:

$$\begin{array}{cccccc}
\rho_{01,01} & \rho_{01,02} & \boxed{\rho_{01,03}} & \boxed{\rho_{01,12}} & \rho_{01,13} & \rho_{01,23} \\
\rho_{02,02} & \boxed{\rho_{02,03}} & \boxed{\rho_{02,12}} & \rho_{02,13} & & \\
\hline
\rho_{03,03} & \rho_{03,12} & \boxed{\rho_{03,13}} & \boxed{\rho_{03,23}} & \rho_{02,23} & \\
\rho_{12,12} & \boxed{\rho_{12,13}} & \boxed{\rho_{12,23}} & & & \\
\rho_{13,13} & \rho_{13,23} & & & & \\
\rho_{23,23} & & & & &
\end{array}$$

In this tabular, the vanishing components obtained by computer algebra are put in a box, the nonzero components of the left column do not vanish when $a=0$ and the other components vanish when $a=0$. Also, the 11 (*care*) lower components can be known from the 10 upper ones.

Keeping in mind the study of the S-metric and the fact that $\rho_{01,03}=0$, $\rho_{03,13}=0$, $\rho_{02,03}=0$, $\rho_{03,13}=0$ while framing the leading terms not vanishing when $a=0$, we get:

$$R_{01,03}\equiv\boxed{\rho_{01,01}\xi_3^1+\rho_{03,03}\xi_1^3}+\left(\rho_{01,23}+\rho_{03,21}\right)\xi_0^2+\rho_{01,02}\xi_3^2+\rho_{01,13}\xi_0^1=0$$

Then, taking into account the fact that $\rho_{01,12}=0,\rho_{02,12}=0,\rho_{12,13}=0$, we obtain similarly:

$$R_{01,12}\equiv\left(\rho_{01,32}+\rho_{03,12}\right)\xi_1^3+\boxed{\rho_{12,21}\xi_0^2+\rho_{01,10}\xi_2^0}+\rho_{01,13}\xi_2^3+\rho_{01,02}\xi_1^0=0$$

The leading determinant does not vanish when $a=0$ because, in this case, all terms are vanishing and we are left with the two linearly independent framed terms, a result amounting to $\xi_3^1=0\Leftrightarrow\xi_1^3=0$ and $\xi_2^0=0\Leftrightarrow\xi_0^2=0$ in the case of the S-metric in [15].

In the case of the K-metric, we may use the relations already framed in order to keep only the four parametric jets $\left(\xi_3^1,\xi_0^2,\xi_0^1,\xi_3^2\right)$ *on the right side*. We may also rewrite them as follows:

$$\boxed{\begin{cases}\omega^{11}\xi_1^0+\omega^{00}\xi_0^1+\omega^{03}\xi_3^1=0, & \omega^{11}\xi_1^3+\omega^{03}\xi_0^1+\omega^{33}\xi_3^1=0\\ \omega^{22}\xi_2^0+\omega^{00}\xi_0^2+\omega^{03}\xi_3^2=0, & \omega^{22}\xi_2^3+\omega^{03}\xi_0^2+\omega^{33}\xi_3^2=0\end{cases}}$$

if we use the fact that $\omega^{03}=-\omega_{03}\Big/\left(\omega_{00}\omega_{33}-\left(\omega_{03}\right)^2\right)$ in the inverse metric.

As a byproduct, we are now left with the *two* (complicated) equations $\xi_3^1+a(...)=0$ and $\xi_0^2+a(...)=0$ where the dots mean linear combinations of $\left(\xi_0^1,\xi_3^2\right)$ with coefficients in K and the study of the Killing operator is quite more difficult in the case of the K-metric. Of course, it becomes clear that *the use of the formal theory is absolutely necessary as an intrinsic approach could not be achieved if one uses solutions instead of sections*. Indeed the strict inclusion $R_1'=R_1^{(2)}\subset R_1$ cannot be even imagined if one does believe that $\xi^1=0$, $\xi^2=0$ brings $\xi_3^1=0$ and $\xi_0^2=0$. The computation could have been done

with $R_{12,23}=0$ and $R_{03,23}=0$ because $R_{02}=0$ and $R_{13}=0$.

The next hard step will be to prove that the other linearized components of the Riemann tensor do not produce *any new different* first order equation. The main idea will be to revisit the new linearized tabular with:

$$\begin{array}{llllll} R_{01,01} & R_{01,02} & R_{01,03} & R_{01,12} & R_{01,13} & R_{01,23} \\ R_{02,02} & R_{02,03} & R_{02,12} & R_{02,13} & & \\ \hline R_{03,03} & R_{03,12} & R_{03,13} & R_{03,23} & R_{02,23} & \\ R_{12,12} & R_{12,13} & R_{12,23} & & & \\ R_{13,13} & R_{13,23} & & & & \\ R_{23,23} & & & & & \end{array}$$

Putting the leading terms into a box, we have the identity $R_{01,23}+R_{02,31}+\boxed{R_{03,12}}=0$ that must be combined with the following formulas $\mathrm{mod}(\Omega)$:

$$\omega^{11}R_{01,13}+\boxed{\omega^{22}R_{02,23}}-\left(\omega^{03}/\omega^{33}\right)\left(\omega^{11}R_{01,01}+\omega^{22}R_{02,02}\right)=0$$

$$\omega^{11}R_{01,12}+\boxed{\omega^{33}R_{03,32}}+\omega^{03}R_{03,02}=0$$

$$\omega^{00}R_{10,01}+2\omega^{03}R_{10,31}+\omega^{22}R_{12,21}+\omega^{33}\boxed{R_{13,31}}=0$$

and so on, allowing to compute the 11 (*care*) lower terms from the 2 + 4 + 4 = 10 upper ones.

We have thus the following successive eleven logical inter-relations:

$$\left(R_{01,23},R_{02,13}\right)\to R_{03,12}$$

$$\left(R_{01,01},R_{02,02},R_{01,13}\right)\overset{(R_{00},R_{11},R_{22},R_{33},R_{03})}{\to}\left(R_{03,03},R_{12,12},R_{13,13},R_{23,23},R_{02,23}\right)$$

$$\left(R_{01,02},R_{01,23},R_{02,13}\right)\overset{R_{12}}{\to}R_{13,23}$$

$$\left(R_{01,03},R_{02,12}\right)\overset{R_{01}}{\to}R_{03,13}$$

$$\left(R_{01,12},R_{02,03}\right)\overset{R_{02}}{\to}R_{03,23}$$

$$\left(R_{01,03},R_{03,13}\right)\overset{R_{13}}{\to}R_{12,23}$$

$$\left(R_{02,03},R_{03,23}\right)\overset{R_{23}}{\to}R_{12,13}$$

Keeping in mind the four additional equations and their consequences that have been already framed, both with the vanishing components of the Riemann tensor, namely:

$$\rho_{01,03}=0,\rho_{01,12}=0,\rho_{02,03}=0,\rho_{02,12}=0,\rho_{03,13}=0,\rho_{03,23}=0,\rho_{12,13}=0,\rho_{12,23}=0$$

we get successively:

$$R_{01,01}=0,R_{02,02}=0,R_{01,02}=0,R_{01,13}=0,R_{01,23}=0,R_{02,13}=0$$

As we have already exhibited an isomorphism $\left(\xi_1^3,\xi_2^0,\xi_1^0,\xi_2^3\right)\to\left(\xi_3^1,\xi_0^2,\xi_0^1,\xi_3^2\right)$, we may use only the later right set of parametric jet components. Using the pre-

vious logical relations while framing the leading terms not vanishing *a priori* when $a=0$, *there is only one possibility to choose four components of the linearized Riemann tensor*, namely:

$$\begin{cases} R_{01,03} \equiv \boxed{\left(\rho_{01,01}\xi^1_3+\rho_{03,03}\xi^3_1\right)}+\left(\rho_{01,23}+\rho_{03,21}\right)\xi^2_0+\rho_{01,13}\xi^1_0+\rho_{01,02}\xi^2_3=0 \\ R_{03,23} \equiv \left(\rho_{01,23}+\rho_{03,21}\right)\xi^1_3+\boxed{\left(\rho_{03,03}\xi^0_2+\rho_{23,23}\xi^2_0\right)}+\rho_{13,23}\xi^1_0+\rho_{02,23}\xi^2_3=0 \\ R_{03,13} \equiv \rho_{01,13}\xi^1_3+\rho_{23,13}\xi^2_0+\boxed{\left(\rho_{03,03}\xi^0_1+\rho_{13,13}\xi^1_0\right)}+\left(\rho_{03,12}+\rho_{02,13}\right)\xi^2_3=0 \\ R_{02,03} \equiv \rho_{02,01}\xi^1_3+\rho_{02,23}\xi^2_0+\left(\rho_{03,12}+\rho_{02,13}\right)\xi^1_0+\boxed{\left(\rho_{02,02}\xi^2_3+\rho_{03,03}\xi^3_2\right)}=0 \end{cases}$$

In order to understand the difficulty of the computations involved, we propose to the reader, as an exercise, to prove "*directly*" that the two following relations:

$$R_{02,12} \equiv \boxed{\left(\rho_{12,12}\xi^1_0+\rho_{02,02}\xi^0_1\right)}+\left(\rho_{02,13}+\rho_{03,12}\right)\xi^3_2+\rho_{02,10}\xi^0_2+\rho_{02,32}\xi^3_1=0$$

$$R_{12,13} \equiv \boxed{\left(\rho_{13,13}\xi^3_2+\rho_{12,12}\xi^2_3\right)}+\left(\rho_{03,12}+\rho_{02,13}\right)\xi^0_1+\rho_{32,13}\xi^3_1+\rho_{10,13}\xi^0_2=0$$

are only linear combinations of the previous ones $\mathrm{mod}(\Omega)$.

We are facing two technical problems "spoilting", *in our opinion*, the use of the K metric:

- With ω^{-1} in place of ω, we have $\omega^{11}\xi^3_1=-\omega^{33}\xi^1_3+\cdots$ and the leading term of $R_{01,03}$ becomes proportional to $\left(\omega^{11}\rho_{01,01}-\omega^{33}\rho_{03,03}\right)\xi^1_3+\cdots$ with a *wrong sign* that cannot allow using R_{00}. A similar comment is valid for the four successive leading terms.
- We also discover the summation $\rho_{01,23}+\rho_{03,21}$ in $R_{01,03}$ with a *wrong sign* that cannot allow introducing $\rho_{02,31}$ as one could hope. A similar comment is valid for the four successive summations.

Nevertheless, we obtain the following unexpected formal linearized result that will be used in a crucial intrinsic way for finding out the generating second order and third order CC:

THEOREM 4.2: The rank of the previous system with respect to the four jet coordinates $\left(\xi^1_3,\xi^2_0,\xi^1_0,\xi^2_3\right)$ is equal to 2, for both the S and K-metrics. We obtain in particular the two striking identities:

$$\boxed{R_{03,13}+a\left(1-c^2\right)R_{01,03}=0,\ R_{02,03}+\frac{a}{\left(r^2+a^2\right)}R_{03,23}=0}$$

Proof: In the case of the S-metric with $a=0$, only the framed terms may not vanish and, denoting by "~" a linear proportionality, we have already obtained $\mathrm{mod}\left(j_2(\Omega)\right)$:

$$R_{01,03}\sim\xi^1_3, R_{03,23}\sim\xi^0_2, R_{02,03}=0, R_{03,13}=0$$

Hence, the rank of the system with respect to the 4 parametric jets $\left(\xi^1_3,\xi^2_0,\xi^1_0,\xi^2_3\right)$ just drops to 2 and this fact confirms the existence of the 5 additional first order equations obtained, as we saw, after two prolongations.

In the case of the K-metric with $a\neq 0$, the study is much more delicate.

With $a^0=1$, the coefficients of the 4×4 metric of the previous system on the basis of the above parametric jets are proportional to the symmetric matrix:

$$\begin{pmatrix} 1 & a & a & a^2 \\ a & 1 & a^2 & a \\ a & a^2 & a^2 & a^3 \\ a^2 & a & a^3 & a^2 \end{pmatrix}$$

Indeed, we have successively for the common factor $-a\left(1-c^2\right)$:

$$\begin{cases} \text{Row 1} \quad \xi_3^1 \to \rho_{01,01} - \dfrac{\omega^{33}}{\omega_{11}}\rho_{03,03} = -\dfrac{3mr\left(r^2-3a^2c^2\right)}{2\left(r^2+a^2c^2\right)^3} \\ \text{Row 3} \quad \xi_3^1 \to \rho_{01,13} = \dfrac{3amr\left(1-c^2\right)\left(r^2-3a^2c^2\right)}{2\left(r^2+a^2c^2\right)^3} \end{cases}$$

$$\begin{cases} \text{Row 1} \quad \xi_0^2 \to \rho_{01,23} + \rho_{03,21} = \dfrac{3amc\left(r^2+a^2\right)\left(3r^2-a^2c^2\right)}{2\left(r^2+a^2c^2\right)^3} \\ \text{Row 3} \quad \xi_0^2 \to \rho_{23,13} = -\dfrac{3a^2mc\left(1-c^2\right)\left(r^2+a^2\right)\left(3r^2-a^2c^2\right)}{2\left(r^2+a^2c^2\right)^3} \end{cases}$$

$$\begin{cases} \text{Row 1} \quad \xi_0^1 \to \rho_{01,13} - \dfrac{\omega^{03}}{\omega_{11}}\rho_{03,03} = \dfrac{3amr\left(1-c^2\right)\left(r^2-3a^2c^2\right)}{2\left(r^2+a^2c^2\right)^3} \\ \text{Row 3} \quad \xi_0^1 \to \rho_{13,13} - \dfrac{\omega^{03}}{\omega_{11}}\rho_{03,03} = -\dfrac{3a^2mr\left(1-c^2\right)^2\left(r^2-3a^2c^2\right)}{2\left(r^2+a^2c^2\right)^3} \end{cases}$$

$$\begin{cases} \text{Row 1} \quad \xi_3^2 \to \rho_{01,02} = -\dfrac{3a^2mc\left(3r^2-a^2c^2\right)}{2\left(r^2+a^2c^2\right)^3} \\ \text{Row 3} \quad \xi_3^2 \to \rho_{03,12} + \rho_{02,13} = \dfrac{3a^3mc\left(1-c^2\right)\left(3r^2-a^2c^2\right)}{2\left(r^2+a^2c^2\right)^3} \end{cases}$$

and similarly for the common factor $-\dfrac{a}{r^2+a^2}$:

$$\begin{cases} \text{Row 2} \quad \xi_3^1 \to \rho_{01,23} + \rho_{03,021} = -\dfrac{3amc\left(r^2+a^2\right)\left(3r^2-a^2c^2\right)}{2\left(r^2+a^2c^2\right)^3} \\ \text{Row 4} \quad \xi_3^1 \to \rho_{02,01} = -\dfrac{3a^2mc\left(3r^2-a^2c^2\right)}{2\left(r^2+a^2c^2\right)^3} \end{cases}$$

$$\begin{cases} \text{Row 2} \quad \xi_0^2 \to \rho_{23,23} - \dfrac{\omega^{00}}{\omega^{22}}\rho_{03,03} = \dfrac{3mr\left(r^2+a^2\right)^2\left(r^2-3a^2c^2\right)}{2\left(r^2+a^2c^2\right)^3} \\ \text{Row 4} \quad \xi_0^2 \to \rho_{02,23} - \dfrac{\omega^{03}}{\omega^{22}}\rho_{03,03} = -\dfrac{3amr\left(r^2+a^2\right)\left(r^2-3a^2c^2\right)}{2\left(r^2+a^2c^2\right)^3} \end{cases}$$

$$\begin{cases} \text{Row 2} \quad \xi_0^1 \to \rho_{13,23} = -\dfrac{3a^2mc\left(1-c^2\right)\left(r^2+a^2\right)\left(3r^2-a^2c^2\right)}{2\left(r^2+a^2c^2\right)^3} \\ \text{Row 4} \quad \xi_0^1 \to \rho_{03,12}+\rho_{02,13} = \dfrac{3a^3mc\left(1-c^2\right)\left(3r^2-a^2c^2\right)}{2\left(r^2+a^2c^2\right)^3} \end{cases}$$

$$\begin{cases} \text{Row 2} \quad \xi_3^2 \to \rho_{02,23} - \dfrac{\omega^{03}}{\omega^{22}}\rho_{03,03} = -\dfrac{3amr\left(r^2+a^2\right)\left(r^2-3a^2c^2\right)}{2\left(r^2+a^2c^2\right)^3} \\ \text{Row 4} \quad \xi_3^2 \to \rho_{02,02} - \dfrac{\omega^{33}}{\omega^{22}}\rho_{03,03} = \dfrac{3a^2mr\left(r^2-3a^2c^2\right)}{2\left(r^2+a^2c^2\right)^3} \end{cases}$$

We do not believe that such a purely computational mathematical result, *though striking it may look like*, could have any useful physical application and this comment will be strengthened by the next theorem provided at the end of this section.

Q.E.D.

COROLLARY 4.3: The Killing operator for the K metric has 14 generating second order CC.

Proof: According to the previous theorem, we have $\dim\left(R_1^{(2)}\right)=\dim\left(R_3\right)=4$ as we can choose the 4 parametric jets $\left(\xi^0,\xi^3,\xi_0^1,\xi_3^2\right)$ and $g_3=0$. Using the *introductory diagram* with $n=4,q=1,r=2,E=T$ and thus $\dim\left(J_2\left(F_0\right)\right)-\dim\left(J_3\left(T\right)\right)=150-140=10$, we obtain at once $\dim\left(Q_2\right)=10+\dim\left(R_1^{(2)}\right)=14$ in a purely intrinsic way. We may thus start afresh with the new first order system $R_1'=R_1^{(2)}\subset R_1\subset J_1\left(T\right)$ obtained from R_1 after 2 prolongations. This result is thus obtained *totally independently of any specific GR technical object* like the *Teukolski scalars*, the *Killing-Yano tensors* or even the *Penrose spinors* introduced in [8] [9] [10] [11] [16].

Q.E.D.

Finally, we know from [2] [4] [12] [15] [17] [18] [19] that if $R_q\subset J_q\left(T\right)$ is a system of infinitesimal Lie equations, then we have the *algebroid bracket* $\left[R_q,R_q\right]\subset R_q$ *defined on sections* by the following formula not depending on the lift $\xi_{q+1},\eta_{q+1}\in J_{q+1}\left(T\right)$ of $\xi_q,\eta_q\in R_q\subset J_q\left(T\right)$:

$$\xi_q,\eta_q\in R_q\Rightarrow\left[\xi_q,\eta_q\right]=\left\{\xi_{q+1},\eta_{q+1}\right\}+i\left(\xi\right)D\eta_{q+1}-i\left(\eta\right)D\xi_{q+1}\in R_q$$

with the *algebraic bracket* bilinearly defined by $j_q\left(\left[\xi,\eta\right]\right)=\left\{j_{q+1}\left(\xi\right),j_{q+1}\left(\eta\right)\right\}$ and such that:

$$\left[R_q,R_q\right]\subset R_q\Rightarrow\left[R_{q+r}^{(s)},R_{q+r}^{(s)}\right]\subset R_{q+r}^{(s)},\forall q,r,s\geq 0$$

It follows that $R_1'=R_1^{(2)}=\pi_1^3\left(R_3\right)$ is such that $\left[R_1',R_1'\right]\subset R_1'$ with $\dim\left(R_1'\right)=20-16=4$ because we have obtained a total of 6 *new different* first order equations. We have *on sections* (*care again*) the 16 (linear) equations of R_1' as follows:

$$R_1'=R_1^{(2)}\subset J_1(T)\begin{cases}\xi^1=0,\xi^2=0 & \Rightarrow & \boxed{\omega_{00}\xi_1^0+\omega_{03}\xi_1^3}+\omega_{11}\xi_0^1=0,\xi_1^1=0,\xi_2^2=0\\ \xi_2^1=0 & \Rightarrow & \xi_1^2=0\\ \xi_3^1+\cdots=0 & \Rightarrow & \boxed{\omega_{03}\xi_1^0+\omega_{33}\xi_1^3}+\omega_{11}\xi_3^1=0\\ \xi_0^2+\cdots=0 & \Rightarrow & \boxed{\omega_{00}\xi_2^0+\omega_{03}\xi_2^3}+\omega_{22}\xi_0^2=0,\\ & & \boxed{\omega_{03}\xi_2^0+\omega_{33}\xi_2^3}+\omega_{22}\xi_3^2=0\\ \xi_3^0=0 & \Rightarrow & \xi_0^3=0,\xi_0^0=0,\xi_3^3=0\end{cases}$$

and we may choose only the 2 parametric jets $\left(\xi_0^1,\xi_3^2\right)$ among $\left(\xi_0^1,\xi_3^1,\xi_0^2,\xi_3^2\right)$ to which we must add $\left(\xi^0,\xi^3\right)$ *in any case* as they are not appearing in the Killing equations and their prolongations.

The system is *not* involutive because it is finite type with $g_2'=0$ and g_1' cannot be thus involutive.

It remains to make one more prolongation in order to study $R_1''=R_1^{(3)}=\pi_1^4\left(R_4\right)\subset R_1'\subset R_1$ with strict inclusions in order to study the third order CC for Ω already described for the Schwarzschild metric in [15].

$$R_1''\subset R_1'\subset R_1\subset J_1(T)\begin{cases}\xi_3^3=0 & \boxed{0 & 1 & 2 & 3}\\ \xi_3^2=0 & 0 & 1 & 2 & 3\\ \xi_3^1=0 & 0 & 1 & 2 & 3\\ \xi_3^0=0 & 0 & 1 & 2 & 3\\ \xi_2^3=0 & 0 & 1 & 2 & \bullet\\ \xi_2^2=0 & 0 & 1 & 2 & \bullet\\ \xi_2^1=0 & 0 & 1 & 2 & \bullet\\ \xi_2^0=0 & 0 & 1 & 2 & \bullet\\ \xi_1^3=0 & 0 & 1 & \bullet & \bullet\\ \xi_1^2=0 & 0 & 1 & \bullet & \bullet\\ \xi_1^1=0 & 0 & 1 & \bullet & \bullet\\ \xi_1^0=0 & 0 & 1 & \bullet & \bullet\\ \xi_0^3=0 & 0 & \bullet & \bullet & \bullet\\ \xi_0^2=0 & 0 & \bullet & \bullet & \bullet\\ \xi_0^1=0 & 0 & \bullet & \bullet & \bullet\\ \xi_0^0=0 & 0 & \bullet & \bullet & \bullet\\ \xi^2=0 & \bullet & \bullet & \bullet & \bullet\\ \xi^1=0 & \bullet & \bullet & \bullet & \bullet\end{cases}$$

Surprisingly and contrary to the situation found for the S metric, we have now a trivially involutive first order system with only solutions $\left(\xi^0=cst,\ \xi^1=0,\ \xi^2=0,\ \xi^3=cst\right)$. However, the difficulty is to know what second members must be used along the procedure met for all the motivating examples. In particular, we have again identities to zero like $d_0\xi^1-\xi_0^1=0$, $d_3\xi^2-\xi_3^2=0$ or, *equivalently*, $d_3\xi^1-\xi_3^1=0$, $d_0\xi^2-\xi_0^2=0$ and thus 4 third order CC coming from the 4 following components of the Spencer operator:

$$\boxed{d_1\xi^1-\xi_1^1=0,\ d_2\xi^1-\xi_2^1=0,\ d_1\xi^2-\xi_1^2=0,\ d_2\xi^2-\xi_2^2=0}$$

a result that cannot be even imagined from [8] [9] [10] [11] [16]. Of course, proceeding like in the motivating examples, we must substitute in the right members the values obtained from $j_2(\Omega)$ and set for example $\xi_1^1 = -\frac{1}{2\omega_{11}}\xi\partial\omega_{11}$ while replacing ξ^1 and ξ^2 by the corresponding linear combinations of the Riemann tensor already obtained for the right members of the two zero order equations.

Using one more prolongation, all the *sections* (*care again*) vanish but ξ^0 and ξ^3, a result leading to $\dim(R_1'') = 2$ in a coherent way with the only nonzero Killing vectors $\{\partial_t, \partial_\phi\}$. We have indeed:

$$\boxed{\xi_0^1 = 0} \Rightarrow \xi_1^3 = 0 \Rightarrow \xi_1^0 = 0, \quad \boxed{\xi_0^2 = 0} \Rightarrow \xi_2^3 = 0 \Rightarrow \xi_3^2 = 0$$

Like in the case of the S metric, R_3 is *not* involutive but R_4 is involutive. However, contrary to the S metric with $g_1'' \neq 0$, now $g_1'' = 0$ for the K metric and R_1'' is trivially involutive with a full Janet tabular having 16 rows of first order jets and 2 rows of zero order jets.

REMARK 4.4: We have in general ([2] [5] p 339, 345):

$$R_{q+r}^{(s)} = \pi_{q+r}^{q+r+s}\left(R_{q+r+s}\right) = \pi_{q+r}^{q+r+s}\left(J_r\left(R_{q+s}\right) \cap J_{q+r+s}(E)\right)$$
$$\subseteq J_r\left(\pi_q^{q+s}\left(R_{q+s}\right)\right) \cap J_{q+r}(E) = J_r\left(R_q^{(s)}\right) \cap J_{q+r}(E) = \rho_r\left(R_q^{(s)}\right)$$

that is, in our case $R_2^{(2)} \subseteq \rho_1\left(R_1^{(2)}\right)$. However, we have indeed the equality $R_2^{(2)} = \rho_1\left(R_1^{(2)}\right)$ even if the conditions of Theorem 1.1 are not satisfied because g_1' is not 2-acyclic. Indeed, the Spencer map $\delta : \wedge^2 T^* \otimes g_1' \to \wedge^3 T^* \otimes T$ is not injective and we let the reader check as an exercise that its kernel is generated by $\{v_{1,01}^0, v_{2,23}^3\}$ and the Spencer δ-cohomology is such that $\dim\left(H_1^2(g_1')\right) = 2 \neq 0$ because the cocycles are defined by the equations $v_{i,jr}^k + v_{j,ri}^k + v_{r,ij}^k = 0$. Hence, *contrary to what could be imagined*, the major difference between the S and K-metrics is not at all the existence of off-diagonal terms but rather the fact that R_1'' *is not involutive* with $g_1'' \neq 0$ for the S-metric while R_1'' *is involutive* with $g_1'' = 0$ for the K-metric. This is the reason for which *one among the four third order CC must be added with two prolongations* for the S-metric while *the four third order CC are obtained in the same way from the Spencer operator* for the K-metric. Of course no classical approach can explain this fact which is lacking in [8] [9] [10] [11].

The following result even questions the usefulness of the whole previous approach:

THEOREM 4.5: The operator $Cauchy = ad(Killing)$ admits a minimum parametrization by the operator $Airy = ad(Riemann)$ with 1 potential when $n = 2$, found in 1863. It admits a canonical self-adjoint parametrization by the operator $Beltrami = ad(Riemann)$ with 6 potentials when $n = 3$, found in 1892 and modified to a mimimum parametrization by the operator *Maxwell* with 3 potentials, found in 1870 or *Morera* found in 1892. More generally, it admits a canonical parametrization by the operator $ad(Riemann)$ with $n^2(n^2-1)/12$

potentials that can be modified to a relative parametrization by $ad(Ricci)$ with $n(n+1)/2$ potentials which is nevertheless not minimum when $n \geq 4$, found in 2007. In all these cases, *the corresponding potentials have nothing to do with the perturbation of the metric*. Such a result is also valid for any Lie group of transformations, in particular for the conformal group in arbitrary dimension.

Proof: We provide successively the explicit corresponding parametrizations:

- $\boxed{n=2}$: Multiplying the linearized Riemann operator by a test function ϕ and integrating by parts, we obtain (*care to the factor* 2 *involved*):

$$\phi\left(d_{22}\Omega_{11}-\boxed{2}d_{12}\Omega_{12}+d_{11}\Omega_{22}\right)=\left(d_{22}\phi\Omega_{11}-\boxed{2}d_{12}\phi\Omega_{12}+d_{11}\phi\Omega_{22}\right)+div(...)$$

$$\sigma^{ij}=\sigma^{ji}\Rightarrow\sigma^{ij}\Omega_{ij}=\sigma^{11}\Omega_{11}+\boxed{2}\sigma^{12}\Omega_{12}+\sigma^{22}\Omega_{22}$$

Cauchy operator $\boxed{d_1\sigma^{11}+d_2\sigma^{12}=f^1,\ d_1\sigma^{21}+d_2\sigma^{22}=f^2}$

Airy operator $\boxed{\sigma^{11}=d_{22}\phi,\ \sigma^{12}=\sigma^{21}=-d_{12}\phi,\ \sigma^{22}=d_{11}\phi}$

$$\begin{array}{ccccccccc} & & \xi & \to & \Omega & \to & R & \to & 0 \\ & & & \overset{Killing}{} & & \overset{Riemann}{} & & & \\ & & 2 & \to & 3 & \to & 1 & \to & 0 \\ & & & & & & & & \\ & & & \overset{Cauchy}{} & & \overset{Airy}{} & & & \\ 0 & \leftarrow & 2 & \leftarrow & 3 & \leftarrow & 1 & & \\ 0 & \leftarrow & f & \leftarrow & \sigma & \leftarrow & \phi & & \end{array}$$

It is clear that *the test function ϕ has nothing to do with the metric ω* ([5], Introduction).

- $\boxed{n=3}$ We now present the original *Beltrami* parametrization:

$$\begin{Bmatrix}\sigma^{11}\\ \sigma^{12}\\ \sigma^{13}\\ \sigma^{22}\\ \sigma^{23}\\ \sigma^{33}\end{Bmatrix}=\begin{Bmatrix}0 & 0 & 0 & d_{33} & -2d_{23} & d_{22}\\ 0 & -d_{33} & d_{23} & 0 & d_{13} & -d_{12}\\ 0 & d_{23} & -d_{22} & -d_{13} & d_{12} & 0\\ d_{33} & 0 & -2d_{13} & 0 & 0 & d_{11}\\ -d_{23} & d_{13} & d_{12} & 0 & -d_{11} & 0\\ d_{22} & -2d_{12} & 0 & d_{11} & 0 & 0\end{Bmatrix}\begin{Bmatrix}\phi_{11}\\ \phi_{12}\\ \phi_{13}\\ \phi_{22}\\ \phi_{23}\\ \phi_{33}\end{Bmatrix}$$

which does not seem to be self-adjoint but is such that $d_r\sigma^{ir}=0$. Accordingly, the *Beltrami* parametrization of the *Cauchy* operator for the stress is nothing else than the formal adjoint of the *Riemann* operator. However, modifying slightly the rows, we get the new operator matrix:

$$\begin{Bmatrix}\sigma^{11}\\ 2\sigma^{12}\\ 2\sigma^{13}\\ \sigma^{22}\\ 2\sigma^{23}\\ \sigma^{33}\end{Bmatrix}=\begin{Bmatrix}0 & 0 & 0 & d_{33} & -2d_{23} & d_{22}\\ 0 & -2d_{33} & 2d_{23} & 0 & 2d_{13} & -2d_{12}\\ 0 & 2d_{23} & -2d_{22} & -2d_{13} & 2d_{12} & 0\\ d_{33} & 0 & -2d_{13} & 0 & 0 & d_{11}\\ -2d_{23} & 2d_{13} & 2d_{12} & 0 & -2d_{11} & 0\\ d_{22} & -2d_{12} & 0 & d_{11} & 0 & 0\end{Bmatrix}\begin{Bmatrix}\phi_{11}\\ \phi_{12}\\ \phi_{13}\\ \phi_{22}\\ \phi_{23}\\ \phi_{33}\end{Bmatrix}$$

which is indeed *self-adjoint*. Keeping $(\phi_{11}=A,\phi_{22}=B,\Phi_{33}=C)$ with $(\phi_{12}=0,\phi_{13}=0,\phi_{23}=0)$, we obtain the *Maxwell* parametrization:

$$\begin{Bmatrix}\sigma^{11}\\ \sigma^{12}\\ \sigma^{13}\\ \sigma^{22}\\ \sigma^{23}\\ \sigma^{33}\end{Bmatrix}=\begin{bmatrix}0 & d_{33} & d_{22}\\ 0 & 0 & -d_{12}\\ 0 & -d_{13} & 0\\ d_{33} & 0 & d_{11}\\ -d_{23} & 0 & 0\\ d_{22} & d_{11} & 0\end{bmatrix}\begin{Bmatrix}A\\ B\\ C\end{Bmatrix}$$

which is minimum because $n(n-1)/2=3$. However, the corresponding operator is FI because it is homogeneous but *it is not evident at all* to prove that it is also involutive as we must look for δ-regular coordinates (see [20] for the technical details).

- $\boxed{n\geq 4}$ This is far more complicated and *we do believe that it is not possible to avoid using differential homological algebra*, in particular *extension modules*. As we found it already in many books [4] [12] [17] [21] or papers [12] [13] [14] [15] [22], the linear Spencer sequence is (locally) isomorphic to the tensor product of the Poincaré sequence for the exterior derivative by a Lie algebra $\mathcal{G}$ with $dim(\mathcal{G})\leq n(n+1)/2$ equal to the dimension of the largest group of invariance of the metric involved. When $n=4$, this dimension is 10 for the M-metric, 4 for the S-metric and 2 for the K-metric. As a byproduct, the adjoint sequence roughly just exchanges the exterior derivatives up to sign and one has for example, when $n=3$, the relations $ad(grad)=-div$, $ad(div)=-grad$. It follows that, if D_2 generates the CC of D_1, then $ad(D_2)$ is parametrizing $ad(D_1)$, *a fact not evident at all*, even when $n=2$ for the *Cosserat couple-stress equations exactly* described by $ad(D_1)$ [18]. Passing to the differential modules point of view with the ring (even an integral domain) $D=K[d_1,\cdots,d_n]=K[d]$ of differential operators with coefficients in a differential field K, this result amounts to say that $ext_D^1(M,D)=ext^1(M)=0$. As it is known that such a result does not depend on the differential resolution used or, *equivalently*, on the differential sequence used, if $\mathcal{D}_1$ generates the CC of $\mathcal{D}$ in the Janet sequence, then $ad(\mathcal{D}_1)$ is parametrizing $ad(\mathcal{D})$ and this result is still true even if $\mathcal{D}$ is not involutive. In such a situation, which is the one considered in this paper, the *Killing* operators for the M-metric, the S-metric and the K-metric are such that, *whatever are the generating CC* $\mathcal{D}_1$ (second order for the M-metric, a mixture of second and third order for the S-metric and K-metric), then $ad(\mathcal{D}_1)$ is, *in any case*, parametrizing the Cauchy operator $ad(\mathcal{D})$ for *any* $\mathcal{D}:T\to S_2T^*:\xi\to\mathcal{L}(\xi)\omega$. Once more, *the central object is the group*, *not the metric*. The same results are also valid for any Lie group of transformations, in particular for the conformal group in arbitrary dimension, even if the operator $\mathcal{D}_1$ is of order 3 when $n=3$ as we shall see below [6] [13] [14] [23].

Q.E.D.

REMARK 4.6: Accordingly, the situation met today in GR cannot evolve as long as people will not acknowledge the fact that the components of the Weyl tensor are the torsion elements (the so-called *Lichnerowicz waves* in [22]) for

the equations $Ricci=0$ because the Einstein equations cannot be parametrized and the extension modules are torsion modules [5] [7] [13] [19]. Such a result is only depending on the group structure of the conformal group of space-time that brings the canonical splitting $Riemann=Weyl\oplus Ricci$ without any reference to a background metric as it is usually done [4] [15] [19] [22] [23]. It is an open problem to know why one may sometimes find a *self-adjoint operator*. It is such a confusion that led to introducing the so-called *Einstein* parametrizing operator [19] [22]. A minimum parametrization of the Cauchy operator when $n=4$ with 6 potentials can be found by keeping only the Lagrange multipliers λ^{ij} with $i<j$ used in [13] while setting $\lambda^{ii}=0$ like Morera when $n=3$.

EXAMPLE 4.7: (*Weyl tensor for* $n=3$ *and euclidean metric*) We proved in ([21], p 156-158) and more recently in [14] [22] [23] that, for $n=3$, the natural "geometric object" corresponding to the Weyl tensor is no longer providing a second order differential operator but by a third order *Weyl* operator $\hat{\mathcal{D}}_1$ with first order CC $\hat{\mathcal{D}}_2$ in the differential sequence:

$$0\rightarrow\hat{\Theta}\rightarrow 3\underset{1}{\overset{\hat{\mathcal{D}}}{\rightarrow}}5\underset{3}{\overset{\hat{\mathcal{D}}_1}{\rightarrow}}5\underset{1}{\overset{\hat{\mathcal{D}}_2}{\rightarrow}}3\rightarrow 0$$

corresponding to the differential sequence of D-modules where p is the canonical residual projection:

$$0\rightarrow D^3\underset{1}{\overset{\hat{\mathcal{D}}_2}{\rightarrow}}D^5\underset{3}{\overset{\hat{\mathcal{D}}_1}{\rightarrow}}D^5\underset{1}{\overset{\hat{\mathcal{D}}}{\rightarrow}}D^3\overset{p}{\rightarrow}\hat{M}\rightarrow 0$$

The true reason is that the symbol $\hat{g}_1$ of $\hat{\mathcal{D}}$ is finite type with second prolongation $\hat{g}_3=0$ while its first prolongation $\hat{g}_2$ is *not* 2-acyclic. It is important to notice that the operators are acting on the left on column vectors in the upper sequence but on the right on row vectors in the lower sequence though we have *in any case* the identities $\hat{\mathcal{D}}_1\circ\hat{\mathcal{D}}=0$ and $\hat{\mathcal{D}}_2\circ\hat{\mathcal{D}}_1=0$.

Of course, these operators can be obtained by using computer algebra like in ([21], Appendix 2) but one may check at once that $\hat{\mathcal{D}}$ and $\hat{\mathcal{D}}_2$ are completely different operators while the operator $\hat{\mathcal{D}}_1$ is far from being self-adjoint even though it is described by a 5×5 operator matrix. Our purpose is to prove that it can be nevertheless transformed in a very tricky way to a self-adjoint operator, exactly like the 3×3 *curl* operator in 3-dimensional classical geometry because $ad\left(grad\right)=-div$. It does not seem that these results are known today.

The starting point is the 3×5 first order operator matrix defining the conformal Killing operator $\hat{\mathcal{D}}$, namely:

$$\begin{pmatrix}\frac{4}{3}d_1 & -\frac{2}{3}d_2 & -\frac{2}{3}d_3\\ d_2 & d_1 & 0\\ d_3 & 0 & d_1\\ -\frac{2}{3}d_1 & \frac{4}{3}d_2 & -\frac{2}{3}d_3\\ 0 & d_3 & d_2\end{pmatrix}$$

Substracting the fourth row from the first row and multiplying the fourth row by

$\frac{3}{2}$, we obtain the operator matrix:

$$\begin{pmatrix} 2d_1 & -2d_2 & 0 \\ d_2 & d_1 & 0 \\ d_3 & 0 & d_1 \\ -d_1 & 2d_2 & -d_3 \\ 0 & d_3 & d_2 \end{pmatrix}$$

Adding the fourth row to the first, we obtain the operator matrix:

$$\begin{pmatrix} d_1 & 0 & -d_3 \\ d_2 & d_1 & 0 \\ d_3 & 0 & d_1 \\ -d_1 & 2d_2 & -d_3 \\ 0 & d_3 & d_2 \end{pmatrix}$$

Adding the first row to the fourth row and dividing by 2, we obtain the operator matrix:

$$\begin{pmatrix} d_1 & 0 & -d_3 \\ d_2 & d_1 & 0 \\ d_3 & 0 & d_1 \\ 0 & d_2 & -d_3 \\ 0 & d_3 & d_2 \end{pmatrix}$$

Multiplying the second, fourth and fifth row by −1, then multiplying the central column of the matrix thus obtained by −1, we finally obtain the operator matrix $\hat{\mathcal{D}}'$:

$$\begin{pmatrix} d_1 & 0 & -d_3 \\ -d_2 & d_1 & 0 \\ d_3 & 0 & d_1 \\ 0 & d_2 & d_3 \\ 0 & d_3 & -d_2 \end{pmatrix}$$

We now care about transforming $\hat{\mathcal{D}}_2$ given in ([21], p 158) by the 5×3 operator matrix:

$$\begin{pmatrix} -2d_3 & 0 & d_1 & -2d_3 & -d_2 \\ 2d_1 & -d_2 & d_3 & 0 & 0 \\ 0 & d_1 & 0 & -2d_2 & d_3 \end{pmatrix}$$

Dividing the first column by 2 and the fourth column by −2, then using the central row as a new top row while using the former top row as new bottom row, we obtain the operator matrix $\mathcal{D}_2'$:

$$\begin{pmatrix} d_1 & -d_2 & d_3 & 0 & 0 \\ 0 & d_1 & 0 & d_2 & d_3 \\ -d_3 & 0 & d_1 & d_3 & -d_2 \end{pmatrix}$$

and check that $ad\left(\hat{\mathcal{D}}_2'\right) = -\hat{\mathcal{D}}'$ like in the Poincaré sequence for $n=3$ where

$ad(div) = -grad$. As the new corresponding operator $\hat{\mathcal{D}}'_1$ is homogeneous and of order 3 (*care*), we obtain locally $ad(\hat{\mathcal{D}}'_1) = \hat{\mathcal{D}}'_1$, a result not evident at first sight (compare to [21], p 157).

The combination of this example with the results announced in [14] [23] brings the need to revisit almost entirely the whole conformal geometry in arbitrary dimension and we notice the essential role performed by the Spencer δ-cohomology in this new framework.

3. Conclusion

First of all, comparing the M-metric, the S-metric and the K-metric by using the corresponding systems of first order infinitesimal Lie equations, we may summarize the results previously obtained by repeating that, when $E = T$, the smaller is the background Lie group, the smaller are the dimensions of the Spencer bundles and the higher are the dimensions of the Janet bundles. As a byproduct, we claim that the only solution for escaping is to increase the dimension of the Lie group involved, adding successively 1 dilatation and 4 elations in order to deal with the conformal group of space-time while using the Spencer sequence instead of the Janet sequence. In particular, the Ricci tensor only depends on the elations of the conformal group of space-time in the Spencer sequence where the perturbation of the metric tensor does not appear any longer contrary to the Janet sequence. It finally follows that Einstein equations are not mathematically coherent with group theory and formal integrability. In other papers and books, we have also proved that they were also not coherent with differential homological algebra which is providing intrinsic properties as the extension modules, which are torsion modules, do not depend on the sequence used for their definition, a quite beautiful but difficult theorem indeed. The main problem left is thus to find the best sequence and/or the best group that must be considered. Presently, we hope to have convinced the reader that only the Spencer sequence is clearly related to the group background and must be used, on the condition to change the group. As a byproduct, we may thus finally say that the situation will not evolve in GR as long as people will not acknowledge the existence of these new *purely mathematical* tools like Lie algebroids or differential extension modules and their *purely mathematical* consequences. Summarizing this paper in a few words, we do really believe that "God used group theory rather than computer algebra when He created the World"!

Conflicts of Interest

The author declares no conflicts of interest regarding the publication of this paper.

References

[1] Pommaret, J.-F. (2015) *Multidimensional Systems and Signal Processing*, **26**, 405-437. https://doi.org/10.1007/s11045-013-0265-0

[2] Pommaret, J.-F. (1978) Systems of Partial Differential Equations and Lie Pseudogroups. Gordon and Breach, New York; Russian Translation, MIR, Moscow, 1983.

[3] Goldschmidt, H. (1968) *Annales Scientifiques de l'École Normale Supérieure*, **4**, 617-625. https://doi.org/10.24033/asens.1173

[4] Pommaret, J.-F. (1994) Partial Differential Equations and Group Theory. Kluwer, Dordrecht. https://doi.org/10.1007/978-94-017-2539-2

[5] Pommaret, J.-F. (2001) Partial Differential Control Theory. Kluwer, Dordrecht. https://worldcat.org/isbn/9780792370376

[6] Pommaret, J.-F. (2019) *Journal of Modern Physics*, **10**, 371-401. https://doi.org/10.4236/jmp.2019.103025

[7] Pommaret, J.-F. (2005) Algebraic Analysis of Control Systems Defined by Partial Differential Equations. In: *Advanced Topics in Control Systems Theory*, Lecture Notes in Control and Information Sciences 311, Springer, Berlin, Chapter 5, 155-223. https://doi.org/10.1007/11334774_5

[8] Aksteiner, S., Andersson L., Backdahl, T., Khavkine, I. and Whiting, B. (2019) Compatibility Complex for Black Hole Spacetimes. https://arxiv.org/abs/1910.08756

[9] Aksteiner, S. and Backdahl, T. (2019) *Physical Review D*, **99**, Article ID: 044043. https://arxiv.org/abs/1601.06084 https://doi.org/10.1103/PhysRevD.99.044043

[10] Aksteiner, S. and Backdahl, T. (2018) *Physical Review Letters*, **121**, Article ID: 051104. https://arxiv.org/abs/1803.05341 https://doi.org/10.1103/PhysRevLett.121.051104

[11] Andersson, L., Backdahl, T., Blue, P. and Ma, S. (2019) Stability for Linearized Gravity on the Kerr Spacetime. https://arxiv.org/abs/1903.03859

[12] Pommaret, J.-F. (2018) New Mathematical Methods for Physics, Mathematical Physics Books. Nova Science Publishers, New York, 150 p.

[13] Pommaret, J.-F. (2019) *Journal of Modern Physics*, **10**, 1454-1486. https://doi.org/10.4236/jmp.2019.1012097

[14] Pommaret, J.-F. (2020) The Conformal Group Revisited. https://arxiv.org/abs/2006.03449

[15] Pommaret, J.-F. (2018) *Journal of Modern Physics*, **9**, 1970-2007. https://doi.org/10.4236/jmp.2018.910125

[16] Khavkine, I. (2017) *Journal of Geometry and Physics*, **113**, 131-169. https://doi.org/10.1016/j.geomphys.2016.06.009

[17] Pommaret, J.-F. (1988) Lie Pseudogroups and Mechanics. Gordon and Breach, New York.

[18] Pommaret, J.-F. (2010) *Acta Mechanica*, **215**, 43-55. https://doi.org/10.1007/s00707-010-0292-y

[19] Pommaret, J.-F. (2013) *Journal of Modern Physics*, **4**, 223-239. https://doi.org/10.4236/jmp.2013.48A022

[20] Pommaret, J.-F. (2016) *Journal of Modern Physics*, **7**, 699-728. https://doi.org/10.4236/jmp.2016.77068

[21] Pommaret, J.-F. (2016) Deformation Theory of Algebraic and Geometric Structures. Lambert Academic Publisher (LAP), Saarbrucken. https://doi.org/10.1007/BFb0083506

[22] Pommaret, J.-F. (2017) *Journal of Modern Physics*, **8**, 2122-2158.

https://doi.org/10.4236/jmp.2017.813130

[23] Pommaret, J.-F. (2020) Nonlinear Conformal Electromagnetism and Gravitation. https://arxiv.org/abs/2007.01710

Scientific Research Publishing

Journal of Modern Physics, 2020, 11, 1711-1730
https://www.scirp.org/journal/jmp
ISSN Online: 2153-120X
ISSN Print: 2153-1196

On the Dynamical 4D BTZ Black Hole Solution in Conformally Invariant Gravity

Reinoud J. Slagter[1,2]

[1]Asfyon, Astronomisch Fysisch Onderzoek Nederland, Bussum, The Netherlands
[2]University of Amsterdam, Amsterdam, The Netherlands
Email: info@asfyon.com

How to cite this paper: Slagter, R.J. (2020) On the Dynamical 4D BTZ Black Hole Solution in Conformally Invariant Gravity. *Journal of Modern Physics*, **11**, 1711-1730.
https://doi.org/10.4236/jmp.2020.1110105

Received: September 11, 2020
Accepted: October 23, 2020
Published: October 26, 2020

Abstract

We review the (2 + 1)-dimensional Bañados-Teitelboim-Zanelli black hole solution in conformally invariant gravity, uplifted to (3 + 1)-dimensional spacetime. For the matter content we use a scalar-gauge field. The metric is written as $g_{\mu\nu} = \omega^2 \tilde{g}_{\mu\nu}$, where the *dilaton field* ω contains all the scale dependencies and where $\tilde{g}_{\mu\nu}$ represents the "un-physical" spacetime. A numerical solution is presented and shows how the dilaton can be treated on equal footing with the scalar field. The location of the apparent horizon and ergo-surface depends critically on the parameters and initial values of the model. It is not a hard task to find suitable initial parameters in order to obtain a regular and *singular free* $g_{\mu\nu}$ out of a BTZ-type solution for $\tilde{g}_{\mu\nu}$. In the vacuum situation, an *exact* time-dependent solution in the Eddington-Finkelstein coordinates is found, which is valid for the (2 + 1)-dimensional BTZ spacetime as well as for the uplifted (3 + 1)-dimensional BTZ spacetime. While $\tilde{g}_{\mu\nu}$ resembles the standard BTZ solution with its horizons, $g_{\mu\nu}$ is *flat*. The dilaton field becomes an infinitesimal renormalizable quantum field, which switches on and off Hawking radiation. This solution can be used to investigate the small distance scale of the model and the black hole complementarity issues. It can also be used to describe the problem of how to map the quantum states of the outgoing radiation as seen by a distant observer and the ingoing by a local observer in a one-to-one way. The two observers will use a different conformal gauge. A possible connection is made with the antipodal identification and unitarity issues. This research shows the power of conformally invariant gravity and can be applied to bridge the gap between general relativity and quantum field theory in the vicinity of the horizons of black holes.

Keywords

Scalar-Gauge Field, Bañados-Teitelboim-Zanelli Black Hole, Conformal

Invariance, Dilaton Field, Eddington-Finkelstein Coordinate, Black Hole Complementarity, Antipodal Identification

1. Introduction

Besides the well-studied Schwarzschild and Kerr solution in general relativity theory (GRT), there is another black hole solution in (2 + 1)-dimensional spacetime, *i.e.*, the Bañados-Teitelboim-Zanelli (BTZ) black hole [1] [2]. The BTZ geometry solves Einstein's equations with a negative cosmological constant in (2 + 1)-dimensions. In general, (2 + 1)-dimensional gravity has been widely recognized as a laboratory not only for studying GRT, but also *quantum-gravity* models. A nice overview of these models can be found in the book of Compère [3]. It is conjectured that this genuine solution will be of importance when one considers thermodynamic properties close to the horizon, *i.e.*, Hawking radiation. The (2 + 1)-dimensional BTZ solution is comparable with the spinning point particle solution (or "cosmon" [4]) of the dimensional reduced spinning cosmic string or Kerr solution. (2 + 1)-dimensional gravity without matter, implying that the Ricci- and Riemann tensor vanish, so matter-free regions are flat pieces of spacetime. When locally a mass at rest is present, it cuts out a wedge from the 2-dimensional space surrounding it and makes the space conical. The angle deficit is then proportional to the mass [5]. The important fact is that the spinning point particle has a physical acceptable counterpart in (3 + 1)-dimensions, *i.e.*, the spinning cosmic string. The z-coordinate is suppressed, because there is no structure in that direction altogether. It is not a surprise that these models are used in constructing quantum gravity models. In these models one uses locally Minkowski spacetime, so *planar gravity* fits in very well.

The BTZ solution is related to the Anti-deSitter/Conformal Field Theory (AdS/CFT) correspondence [6] and became a tool to understand black hole entropy [7]. For the (2 + 1)-dimensional BTZ black hole solution, one can try to follow the same procedure as used for the cosmic string, by *uplifting* the solution to (3 + 1)-dimensional spacetime. However, the cosmological constant must be taken zero, when the BTZ solution is uplifted, so it loses its connection with the asymptotic AdS_3 black hole. This opens the way to new solutions, which was done in a *conformally invariant* setting [8] [9]. Conformal invariance (CI) was originally introduced by Weyl [10]. See also the textbook of Wald [11]. The AdS/CFT correspondence renewed the interest in conformal gravity. AdS/CFT is a conjectured relationship between two kinds of physical theories. AdS spaces are used in theories of quantum gravity while CFT includes theories similar to the Yang Mills theories that describe elementary particles. It is believed that CI can help us to move a little further along the road to quantum gravity. Exact local CI at the level of the Lagrangian, will then spontaneously be broken, comparable with the Brout-Englert-Higgs (BEH) mechanism. It is an approved alterna-

tive for disclosing the small-distance structure when one tries to describe quantum-gravity problems [12] [13]. It can also be used to model scale-invariance in the cosmic microwave background radiation (CMBR) [14]. Another interesting application can be found in the work of Mannheim on conformal cosmology [15]. This model could serve as an alternative approach to explain the rotational curves of galaxies, without recourse to dark matter and dark energy (or cosmological constant). In Mannheim's model, standard Schwarzschild phenomenology can in fact be recovered in conformal gravity in the presence of a scalar-gauge field. Further, GRT will be different on different scales by virtue of the dilaton field. As regards dark matter, there is nothing in principle wrong with the existence of nonluminous material. Rather, what is disturbing is the ad hoc, after the fact, way in which dark matter is actually introduced, with its presence only being inferred after known luminous astrophysical sources are found to fail to account for any given astrophysical observation [15]. The dark energy problem is even more severe, and not simply because its composition and nature are as mysterious as that of dark matter. The introduction of a cosmological constant will not solve this problem. It is not possible to explain the huge discrepancy between the contribution from zero-point fluctuations in quantum field theory and the predicted value in GRT (some 120 orders of magnitude!). It is hoped that in future more data will become available for the rotation curves of galaxies. The validity of conformal gravity theory can also be tested with the cosmic microwave background. It is a challenge to alternate theories to fit the cosmic microwave background data. The growth of inhomogeneities in the model and the size of the fluctuation "yardstick" (determined by ω) of the conformal theory would be different from the one used in the standard theory.

Another key problem is the handling of asymptotic flatness of isolated systems in GRT, especially when they radiate and the generation of the metric $g_{\mu\nu}$ from at least Ricci-flat spacetime. In the non-vacuum case one should construct a Lagrangian where spacetime and the fields defined on it, are topological regular and physical acceptable. This can be done by considering the scale factor (or *warp factor* in higher-dimensional models [16]) as a *dilaton field* besides, for example, a conformally coupled scalar field or other fields. Conformal invariant gravity distinguishes itself by the notion that the spacetime is written as $g_{\mu\nu} = \omega^2 \tilde{g}_{\mu\nu}$, with ω a dilaton field which contains all the scale dependencies and $\tilde{g}_{\mu\nu}$ the "*un-physical*" spacetime, related to the (2 + 1)-dimensional Kerr and BTZ black hole solution. ω is just an ordinary renormalizable field, which could create the spacetime twofold: an in-falling and outside observer use different ways to fix the conformal gauge in order to overcome the *unitarity problems* encountered in standard approaches in quantum gravity models. It can be handled on equal footing with a scalar field. Renormalization and unitarity problems in general relativity at the quantum scale, have a long history [17] [18]. In first instance, it was believed that conformal invariance would not survive in quantum gravity (see, for example, the overview of Duff [19]). However, new

interest occurred, when it was realized that Weyl anomalies and unitarity problems could be overcome. In constructing an effective theory in canonical quantum gravity and to obtain quantum amplitudes, one performs a functional integration of the exponent of the entire action over, for example, all components of the metric tensor at all spacetime points. Now the integration is first performed over the dilaton function ω together with the matter fields. Integration over the ω is identical to the integration over a renormalizable scalar field. In the action the dilaton must be shifted to the complex contour, in order to obtain the same unitarity and positivity features as the scalar field. Another actual problem is the back hole *complementarity*: how to handle the in- and out-going radiation as experienced by an in-falling- and outside observer. In a dynamical setting, there will be a back-reaction on the location of the horizon(s). The in falling and outside observer will experience a different ω. They use different ways to fix the conformal gauge. Further, there is the problem of extending the Penrose diagram in a one-to-one map, in order to avoid unitarity and locality problems and to avoid the need to define the inside of the black hole (or even another universe). The *antipodal identification* could be used [20], *i.e.*, a conformal compactification of the manifold [21].

In Section 2 and 3 we describe the dynamical CI model on the original BTZ black hole spacetime, uplifted to (3 + 1) dimensions. In Section 3.2 we present a numerical solution of the complete set of coupled PDE's. In Section 4 and 5 we find an exact time-dependent solution in the vacuum situation in Eddington-Finkelstein coordinates and we explain possible ways to connect this solution with recent research on black hole complementarity, antipodal identifications and hawking radiation.

2. The BTZ Solution Revised

If one solves the Einstein equations $G_{\mu\nu} = \lambda g_{\mu\nu}$ for the spacetime

$$\mathrm{d}s^2 = -N(\rho)^2\,\mathrm{d}t^2 + \frac{1}{N(\rho)^2}\mathrm{d}\rho^2 + \rho^2\left(\mathrm{d}\varphi + N^{\varphi}(\rho)\mathrm{d}t\right)^2, \tag{1}$$

one obtains [8]

$$\begin{aligned} N(\rho)^2 &\equiv \alpha^2 - \Lambda\rho^2 + \frac{16G^2J^2}{\rho^2}, \\ N^{\varphi}(\rho) &\equiv -\frac{4GJ}{\rho^2} + S, \end{aligned} \tag{2}$$

where S, J and α are integration constants [1] [3]. The parameters α and J represent the standard ADM mass ($\alpha^2 = \pm 8GM$) and angular momentum and determine the asymptotic behavior of the solution. Λ represents the cosmological constant. There is an inner and outer horizon and an ergo-circle just as in the case of the Kerr spacetime. However, we live in a 4-dimensional spacetime, so one way or another, the BTZ solution in 3 dimensions must be up-lifted to (3 + 1) dimensions. From the Einstein equations one can then easily verify that $\Lambda = 0$. So we consider here the case $\Lambda = 0$, and we write the spacetime as

$$\begin{aligned} \mathrm{d}s^2 &= -\left[8G\left(JS-M\right)-S^2\rho^2\right]\mathrm{d}t^2+\frac{\rho^2 r_H^2}{16G^2J^2\left(\rho_H^2-r^2\right)}\mathrm{d}\rho^2 \\ &+\rho^2\mathrm{d}\varphi^2+2\rho^2\left(S-\frac{4GJ}{\rho^2}\right)\mathrm{d}t\mathrm{d}\varphi, \end{aligned} \tag{3}$$

with ρ_H the horizon $\rho_H=\sqrt{\frac{2G}{M}}J$. In the case of $S=0$, which is also done in the original BTZ solution, one can transform the spacetime to

$$\mathrm{d}s^2=-\left(\alpha\mathrm{d}t+\frac{4GJ}{\alpha}\mathrm{d}\varphi\right)^2+\mathrm{d}\left(\rho'\right)^2+\alpha^2\left(\rho'\right)^2\mathrm{d}\varphi^2, \tag{4}$$

by $\left(\rho'\right)^2=\frac{16G^2J^2+\alpha^2\rho^2}{\alpha^4}$. This is just the spinning particle spacetime [4].

In a former study [8], we investigated the revised BTZ solution in connection with the spinning cosmic strings and conformal invariance and found an up-lifted exact vacuum solution.

The spacetime Equation (1) is then replaced by

$$\mathrm{d}s^2=\omega\left(\rho\right)^2\left[-N\left(\rho\right)^2\mathrm{d}t^2+\frac{1}{N\left(\rho\right)^2}\mathrm{d}\rho^2+\rho^2\left(\mathrm{d}\varphi+N^\varphi\left(\rho\right)\mathrm{d}t\right)^2\right], \tag{5}$$

with ω the dilaton field. A typical solution is then found [8] for ω, N and N^φ, which is asymptotically regular. See Figure 1. It is remarkable that this solution resembles the standard BTZ solution. However, we don't need a cosmological constant. Further, ω plays the role here of a cosmological scale factor. So we can extend the model to small scales. This will be done, in a dynamical setting, in the next section.

3. The Dynamical BTZ Model

3.1. The Field Equations

Let us consider the time-dependent spacetime $g_{\mu\nu}\equiv\omega\left(t,\rho\right)^2\tilde{g}_{\mu\nu}$

$$\mathrm{d}s^2=\omega\left(t,\rho\right)^2\left[-N\left(t,\rho\right)^2\mathrm{d}t^2+\frac{1}{N\left(t,\rho\right)^2}\mathrm{d}\rho^2+\mathrm{d}z^2+\rho^2\left(\mathrm{d}\varphi+N^\varphi\left(t,\rho\right)\mathrm{d}t\right)^2\right], \tag{6}$$

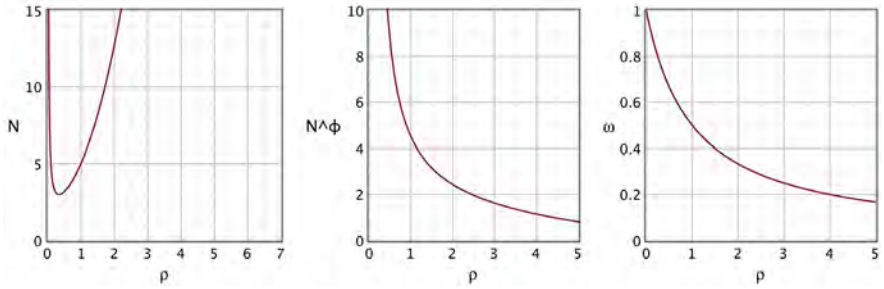

Figure 1. Example of a conformal invariant solution of the BTZ on a 3-dimensional spacetime. $N\sim\frac{\left(r+c\right)^4}{r}$. The location of the horizon is determined by the constant c.

with ω the dilaton field. The action under consideration is

$$S=\int \mathrm{d}^4x\sqrt{-\tilde{g}}\left\{-\frac{1}{12}\left(\tilde{\Phi}\tilde{\Phi}^*+\bar{\omega}^2\right)\tilde{R}-\frac{1}{2}\left(D_\alpha\tilde{\Phi}\left(D^\alpha\tilde{\Phi}\right)^*+\partial_\alpha\bar{\omega}\partial^\alpha\bar{\omega}\right)\right.$$
$$\left.-\frac{1}{4}F_{\alpha\beta}F^{\alpha\beta}-V\left(\tilde{\Phi},\bar{\omega}\right)-\frac{1}{36}\kappa^2\Lambda\bar{\omega}^4\right\}. \tag{7}$$

We parameterize the scalar and gauge field as

$$A_\mu=\left[P_0\left(t,\rho\right),0,0,\frac{1}{e}\left(P\left(t,\rho\right)-n\right)\right],\quad \tilde{\Phi}\left(t,\rho\right)=\eta X\left(t,\rho\right)\mathrm{e}^{in\varphi}. \tag{8}$$

The gauge covariant derivative is $D_\mu\Phi=\tilde{\nabla}_\mu\Phi+ieA_\mu\Phi$ and $F_{\mu\nu}$ the Abelian field strength.

In the action one redefined $\bar{\omega}^2\equiv-\frac{6\omega^2}{\kappa^2}$ (in order to ensure that the ω field has the same unitarity and positivity properties as the scalar field Φ [22]) and $\Phi=\frac{1}{\omega}\tilde{\Phi}$. This Lagrangian is local conformal invariant under the transformation $\tilde{g}_{\mu\nu}\to\Omega^2\tilde{g}_{\mu\nu},\tilde{\Phi}\to\frac{1}{\Omega}\tilde{\Phi}$ and $\bar{\omega}\to\frac{1}{\Omega}\bar{\omega}$.

Varying the Lagrangian with respect to $\tilde{g}_{\mu\nu},\tilde{\Phi},\bar{\omega}$ and A_μ, we obtain the equations

$$\tilde{G}_{\mu\nu}=\frac{1}{\bar{\omega}^2+\tilde{\Phi}\tilde{\Phi}^*}\left(\tilde{T}_{\mu\nu}^{(\bar{\omega})}+\tilde{T}_{\mu\nu}^{(\tilde{\Phi},c)}+\tilde{T}_{\mu\nu}^{(A)}+\frac{1}{6}\tilde{g}_{\mu\nu}\Lambda\kappa^2\bar{\omega}^4+\tilde{g}_{\mu\nu}V\left(\tilde{\Phi},\bar{\omega}\right)\right), \tag{9}$$

$$\tilde{\nabla}^\alpha\partial_\alpha\bar{\omega}-\frac{1}{6}\tilde{R}\bar{\omega}-\frac{\partial V}{\partial\bar{\omega}}-\frac{1}{9}\Lambda\kappa^2\bar{\omega}^3=0, \tag{10}$$

$$\tilde{D}^\alpha\tilde{D}_\alpha\tilde{\Phi}-\frac{1}{6}\tilde{R}\tilde{\Phi}-\frac{\partial V}{\partial\tilde{\Phi}^*}=0,\quad \tilde{\nabla}^\nu F_{\mu\nu}=\frac{i}{2}\varepsilon\left(\tilde{\Phi}\left(\tilde{D}_\mu\tilde{\Phi}\right)^*-\tilde{\Phi}^*\tilde{D}_\mu\tilde{\Phi}\right), \tag{11}$$

with

$$\tilde{T}_{\mu\nu}^{(A)}=F_{\mu\alpha}F_\nu^\alpha-\frac{1}{4}\tilde{g}_{\mu\nu}F_{\alpha\beta}F^{\alpha\beta}, \tag{12}$$

$$\tilde{T}_{\mu\nu}^{(\tilde{\Phi},c)}=\left(\tilde{\nabla}_\mu\partial_\nu\tilde{\Phi}\tilde{\Phi}^*-\tilde{g}_{\mu\nu}\tilde{\nabla}_\alpha\partial^\alpha\tilde{\Phi}\tilde{\Phi}^*\right)$$
$$-3\left[\tilde{D}_\mu\tilde{\Phi}\left(\tilde{D}_\nu\tilde{\Phi}\right)^*+\left(\tilde{D}_\mu\tilde{\Phi}\right)^*\tilde{D}_\nu\tilde{\Phi}-\tilde{g}_{\mu\nu}\tilde{D}_\alpha\tilde{\Phi}\left(\tilde{D}^\alpha\tilde{\Phi}\right)^*\right] \tag{13}$$

and

$$\tilde{T}_{\mu\nu}^{(\bar{\omega})}=\left(\tilde{\nabla}_\mu\partial_\nu\bar{\omega}^2-\tilde{g}_{\mu\nu}\tilde{\nabla}_\alpha\partial^\alpha\bar{\omega}^2\right)-6\left(\partial_\mu\bar{\omega}\partial_\nu\bar{\omega}-\frac{1}{2}\tilde{g}_{\mu\nu}\partial_\alpha\bar{\omega}\partial^\alpha\bar{\omega}\right). \tag{14}$$

The covariant derivatives are taken with respect to $\tilde{g}_{\mu\nu}$. Newton's constant reappears in the quadratic interaction term for the scalar field. One refers to the field $\bar{\omega}\left(t,\rho\right)$ as a dilaton field. A massive term in $V\left(\tilde{\Phi},\bar{\omega}\right)$ will break the *tracelessness* of the energy momentum tensor, a necessity for conformal invariance. The cosmological constant Λ could be ignored from the point of view of naturalness in order to avoid the inconceivable fine-tuning. Putting Λ zero increases the symmetry of the model.

Note that we cannot use in the stationary CI invariant model the *gauge* $A_t = 0$. In standard gauged vortices models, this gauge simplifies the well-known Nielsen-Olesen $n = 1$ vortex solution. The spatial rotational symmetry can then be completely compensated by a spatially uniform gauge transformation. In the stationary situation this is not the case.

For the Maxwell field A_μ, the equation for A_t is a constraint equation and in a time-dependent setting, only A_i are dynamical. Standard, one uses then the Lorentz-gauge to remove A_t completely. Gauge invariance is necessary in order to overcome breaking of locality and unitarity. In models with arbitrary vorticity n and SU(2)-Yang-Mills-Higgs theory, Gauss's law yields also a non-zero A_t for most gauges. Just as in the monopole and dyon solutions, A_t produces a back reaction on A_i perturbatively. Although the dyon fields are time-independent, there is a net kinetic energy because A_t is non-vanishing, so are steadily rotating (see for example the textbook of Weinberg [23]).

In our model we have rotation, *i.e.*, a term $N^\varphi(t,\rho)$. If we calculate the conservation equations for the Einstein equations, one easily finds that

$$P_0 = \frac{1}{e} P N^\varphi \tag{15}$$

So we obtained a kind of natural "gauge" in order to get rid of A_0 (Equation (8)). The equation for N^φ decouples from the other equations.

The field equations now become

$$\begin{aligned}\ddot{N} = &-N^4\left(N'' + 3\frac{N'}{\rho}\right) + 3\frac{\dot{N}^2}{N} - N^3 N'^2 + \frac{1}{\eta^2 X^2 + \omega^2}\left[3N\left(N^4\omega'^2 - \dot{\omega}^2\right)\right.\\ &- N^3 V - \frac{N^5}{\rho}\left(\omega\omega' + \eta^2 X X'\right) + 3\eta^2 N\left(N^4 X'^2 - \dot{X}^2\right) + 2\frac{N}{e^2\rho^2}\left(\dot{P}^2 - N^4 P'^2\right)\\ &\left. - 6\frac{N^4}{e^2\rho^3}N' - \frac{1}{6}\kappa^2\Lambda N^3\omega^4 + 6\frac{\eta^2 P^2 N^3 X^2}{\rho^2}\right] + \frac{1}{\left(\eta^2 X^2 + \omega^2\right)^2}\left[18\frac{\eta^2 P^4 X^2 N^3}{e^2\rho^4}\right.\\ &\left. + 3\frac{N P^2}{e^4\rho^4}\left(\dot{P}^2 - N^4 P'^2\right) - 6\frac{P^2 N^5}{e^2\rho^3}\left(\omega\omega' + \eta^2 X X'\right)\right],\end{aligned} \tag{16}$$

$$\begin{aligned}\ddot{\omega} = &N^4\left(\omega'' + \frac{\omega'}{\rho}\right) + 2N^3\omega' N' + 2\frac{\dot{\omega}\dot{N}}{N} + \frac{\eta X N^2}{\omega}\frac{\mathrm{d}V}{\mathrm{d}X}\\ &+ \frac{\left[\omega\left(N^4\omega'^2 - \dot{\omega}^2\right) + \eta^2\omega\left(N^4 X'^2 - \dot{X}^2\right) - 2\frac{\omega P^2 N^3}{e^2\rho^3}N'\right]}{\eta^2 X^2 + \omega^2}\\ &+ \frac{1}{\left(\eta^2 X^2 + \omega^2\right)^2}\left[-2\frac{\omega P^2 N^4}{e^2\rho^3}\left(\omega\omega' + \eta^2 X X'\right) + \frac{1}{2e^2 r^2}\omega\left(\dot{P}^2 - N^4 P'^2\right)\right.\\ &\cdot\left(\omega^2 + 2\frac{P^2}{e^2\rho^2} + \eta^2 X^2\right) + \frac{\eta^2 P^2 N^2 X^2\omega}{\rho^2}\left(\omega^2 + 6\frac{P^2}{e^2\rho^2} + \eta^2 X^2\right)\\ &\left. - \frac{N^2}{3\omega}\left(V + \frac{1}{6}\kappa^2\Lambda\omega^4\right)\left(3\omega^4 + 5\eta^2 X^2\omega^2 + 2\eta^4 X^4\right)\right],\end{aligned} \tag{17}$$

$$\ddot{X} = N^4\left(X'' + \frac{X'}{\rho}\right) + 2N^3X'N' + 2\frac{\dot{X}\dot{N}}{N} - \frac{N^2}{\eta}\frac{\mathrm{d}V}{\mathrm{d}X}$$
$$+ \frac{\left[\eta^2X\left(N^4X'^2 - \dot{X}^2\right) + X\left(N^4\omega'^2 - \dot{\omega}^2\right) - 2\frac{XP^2N^3}{e^2\rho^3}N' - \frac{XN^2}{3}\left(V + \frac{1}{6}\kappa^2\Lambda\omega^4\right)\right]}{\eta^2X^2 + \omega^2}$$
$$+ \frac{1}{\left(\eta^2X^2 + \omega^2\right)^2}\left[-2\frac{XP^2N^4}{e^2\rho^3}\left(\omega\omega' + \eta^2XX'\right) + \frac{1}{2e^2\rho^2}X\left(\dot{P}^2 - N^4P'^2\right)\right.$$
$$\left.\cdot\left(\omega^2 + 2\frac{P^2}{e^2\rho^2} + \eta^2X^2\right) - \frac{P^2N^2X}{\rho^2}\left(\omega^4 - 6\frac{\eta^2X^2P^2}{e^2\rho^2} + \eta^2X^2\omega^2\right)\right], \tag{18}$$

$$\ddot{P} = N^4\left(P'' - \frac{P'}{\rho}\right) + e^2\eta^2PX^2N^2 + N^3P'N' + 2\frac{\dot{P}\dot{N}}{N} - 4\frac{PN^3N'}{r}$$
$$+ 2\frac{P\left[\dot{P}^2 - N^4P'^2 - 2\rho e^2N^4\left(\eta^2XX' + \omega\omega'\right) + 6\eta^2e^2N^2X^2P^2\right]}{\rho^2e^2\left(\eta^2X^2 + \omega^2\right)}, \tag{19}$$

$$\left(\dot{N}^\varphi\right)' = -\left(N^\varphi\right)'\frac{\dot{P}}{P}, \quad \left(N^\varphi\right)'' = -\left(N^\varphi\right)'\left(\frac{P'}{P} + \frac{1}{\rho}\right), \tag{20}$$

$$\left(N^\varphi\right)'^2 = -4\frac{N}{\rho^3}N' + 2\frac{\left[\frac{\dot{P}^2}{N^2} - N^2P'^2 + 6e^2\eta^2X^2P^2 - 2e^2\rho N^2\left(\eta^2XX' + \omega\omega'\right)\right]}{e^2\rho^4\left(\eta^2X^2 + \omega^2\right)}. \tag{21}$$

Further, we obtain from the Maxwell equations and Einstein constraint equations

$$\dot{P} = \frac{2\eta^2X\dot{X} + \omega\dot{\omega}}{\eta^2X^2 + \omega^2 - 2\frac{P^2}{e^2\rho^2}}, \quad P' = \frac{2\eta^2XX' + \omega\omega'}{\eta^2X^2 + \omega^2 - 2\frac{P^2}{e^2\rho^2}}. \tag{22}$$

The equation for ω is obtained from the Einstein equations and the scalar equation for X. If we substitute back the equations into the dilaton equation, we obtain the relation for the potential

$$\frac{2}{3}V = \eta X\frac{\mathrm{d}V}{\mathrm{d}X} + \omega\frac{\mathrm{d}V}{\mathrm{d}\omega}, \tag{23}$$

From the conservation equations we then obtain

$$\dot{V} = 5\frac{\eta^2X^2P\dot{P}}{\rho^2} + 6\eta\dot{X}\frac{\mathrm{d}V}{\mathrm{d}X} + 6\dot{\omega}\frac{\mathrm{d}V}{\mathrm{d}\omega}, \quad V' = 5\frac{\eta^2X^2PP'}{\rho^2} + 6\eta X'\frac{\mathrm{d}V}{\mathrm{d}X} + 6\omega'\frac{\mathrm{d}V}{\mathrm{d}\omega}. \tag{24}$$

Sometimes, one chooses a unitary gauge in order to obtain a comparable relation (see for example Oda [24]).

3.2. The Numerical Solution

We can plot a numerical solution of the field equations of Section 3.1 for a set of initial and boundary values. We can choose as initial values the *vacuum solution* of Equation (16)-(21). This solution can easily be found exactly:

$$\omega = F_1(\rho)\mathrm{e}^{-\frac{1}{2}k_1t}, \quad N = \frac{1}{F_1(\rho)}G(t) - \log\left(\rho^{1/k_1}F_1(\rho)^{2/k_1}\right),$$
$$N^\varphi = H_1(t) + F_2(\rho)\mathrm{e}^{k_1t}, \quad F_2 = a_1 + a_2\int\frac{1}{\rho^3F_1^2}\mathrm{d}\rho, \tag{25}$$

where from the other PDE's a function for F_1 can be found for any k_1. We write the second order PDE system as a set of first order PDE's and used a Mathematica routine for solving the system. We checked the solution with the Cadsol-Fidisol solver.[1] In Figure 2 and Figure 3 we plotted typical solutions for different initial and boundary conditions. It turns out that the solution is insensitive for the cosmological constant (as expected), but very sensitive for the value of the potential. Further, we observe that an initial wavelike function for the scalar field, *induces a wavelike behavior in the dilaton field*. It is not a hard task to find the initial conditions and the suitable values of the several parameters in order to obtain a regular and singular free spacetime $g_{\mu\nu}$ out of a BTZ solution $\tilde{g}_{\mu\nu}$ with its horizons. We already mentioned in the introduction, that the z-coordinate don't play a role in our model. So it was possible to uplift the BTZ-spacetime. We will return to this issue in connection with *conformal compactification* in the next sections.

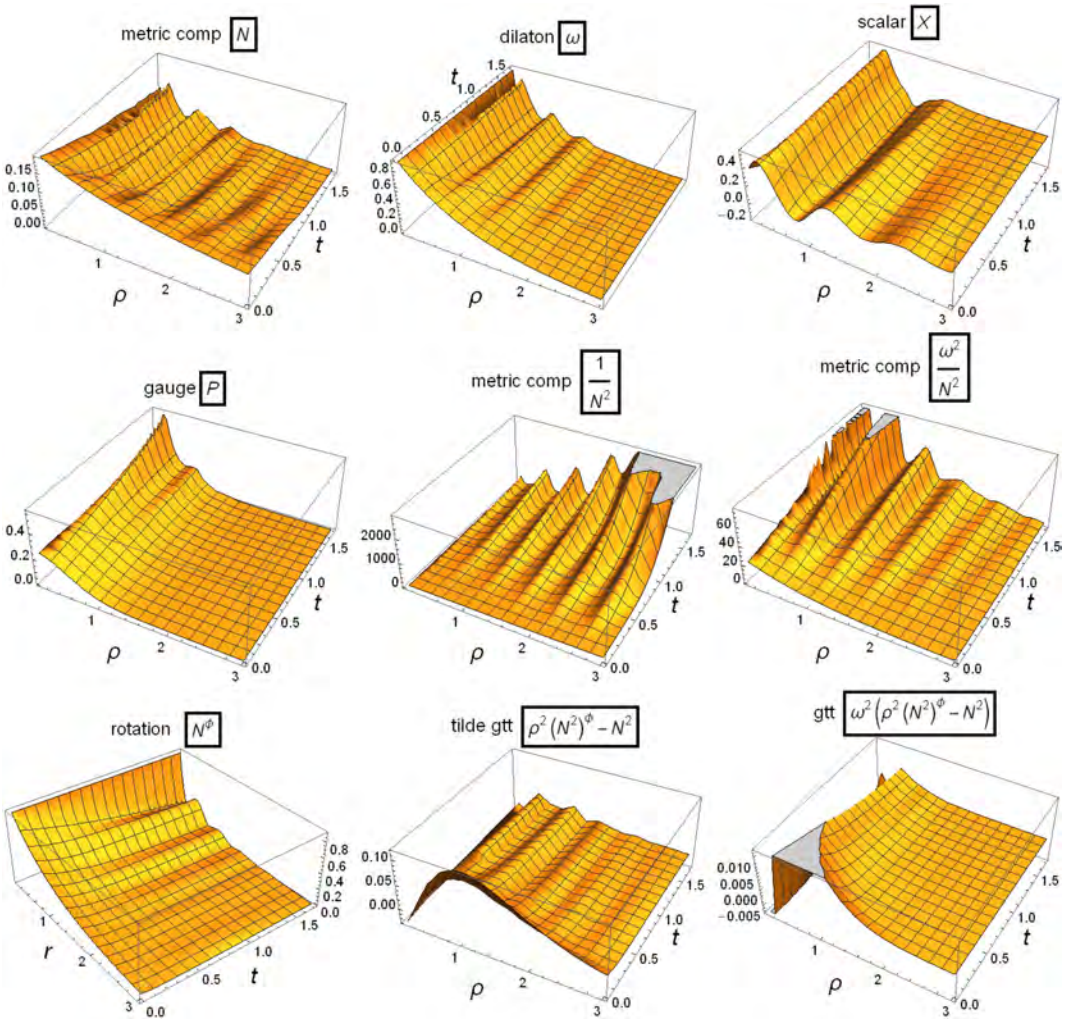

Figure 2. Example of a numerical solution of the system of Equation (16)-(21) with only for the scalar field X an outgoing wavelike initial value. We used the potential from Equation (23).

[1]See: http://www.sai.msu.su/sal/B/2/FIDISOL.html.

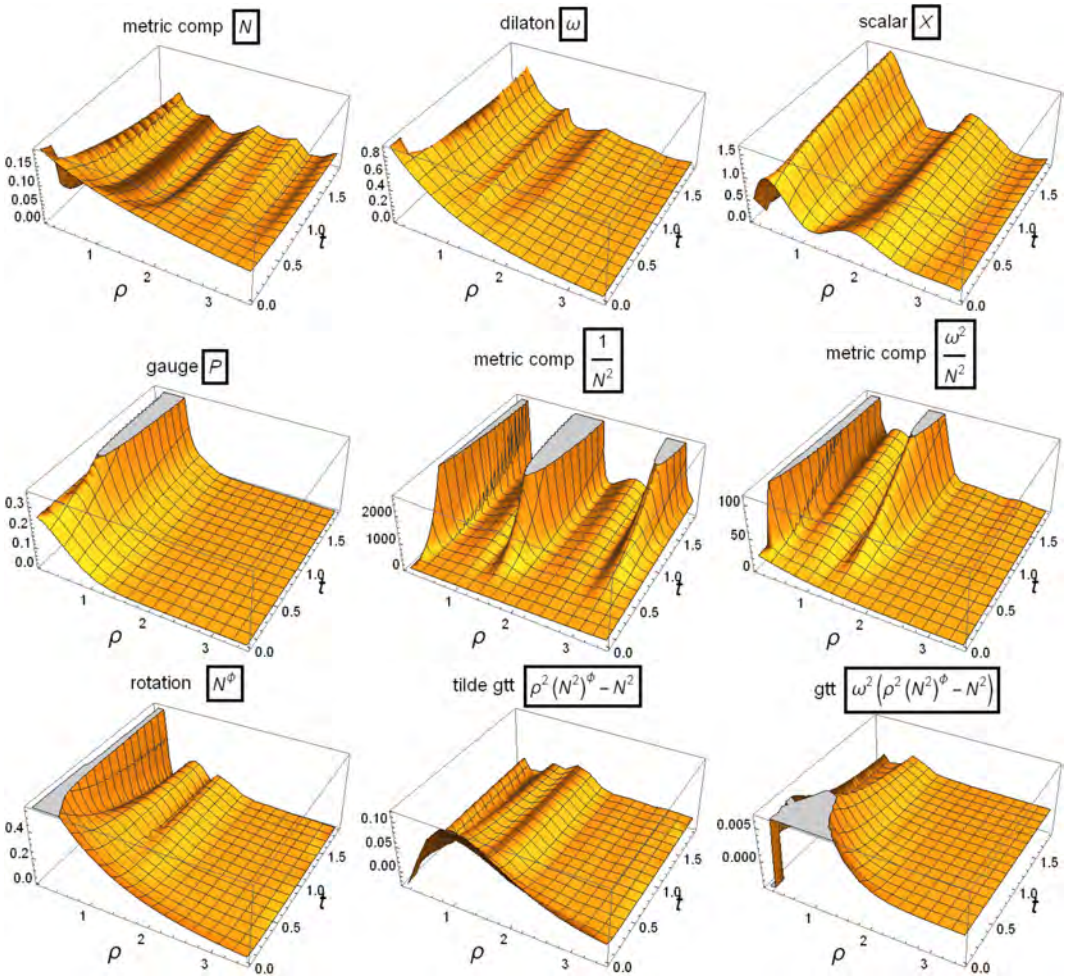

Figure 3. As **Figure 2**, but now with a different initial wave for the scalar field. We used the initial outgoing wave $X = \mathrm{e}^{-\rho}\left(\sin 4\left(\rho - t\right) + \rho\right)$. We observe that the wave turns quickly into a solitary wave and induces a wavelike behavior in ω.

4. An Exact Time-Dependent Vacuum BTZ Solution in Eddington-Finkelstein Coordinates in Conformal Invariant Gravity

Quite recently, some progress was made in understanding the physics at the horizon of black holes, where quantum effects will come into play. For a mainstream treatment on this subject we refer to Parker and Toms [25].

The fundamental question is what happens with an evaporating black hole (see for example the overview article of Page [26] and references therein). It is for sure that quantum effects will resolve the distinction between the inside and outside of the black hole and the description of the hawking radiation. It will be necessary to consider the *dynamical evolution* of the spacetime. This can be done in a tractable way in an Eddington-Finkelstein coordinate system. One of the first attempts was the Vaidya solution [27]. In fact, the Vaidya solution is one of the non-static solutions of the Einstein field equations and is a generalization of the static Schwarzschild black hole solution. This solution is characte-

rized by a dynamical mass function depending on the retarded time. A solution on the (2 + 1)-dimensional BTZ spacetime was recently found by Chan *et al.* [28] and an approximate solution by Abdolrahimi, *et al.* [29]. There are several ways to look at the "inside" of a black hole, or, differently formulated, how to extend maximally the Penrose diagram. Some authors use the existence of white holes, a parallel universe, or a wormhole to black-bounce transition [30] [31]. Another possibility was proposed by Susskind and Maldacena [32]. Two entangled particles (a so-called Einstein-Podolsky-Rosen or EPR pair) are connected by a wormhole (or Einstein Rosen bridge) and may be a basis for unifying general relativity and quantum mechanics. However, the two entangled black holes in regions I and II in the extended Penrose diagram, will interact via the ingoing and outgoing particles instantly. Another problem is, how to treat the connection between the observation of the in-falling observer and the outside observer, *i.e.*, how to map the quantum states of the in- and out-going radiation in a one-to-one way. In context of conformal invariance and black hole complementarity, there is another possibility of maximal extension of the Penrose diagram as initiated by *'t Hooft* [33], using antipodal identification as spherical harmonics (see also 't Hooft [20] and references therein). If one doesn't want to give up locality and unitarity, one needs this approach. We can ask ourselves if some of these ideas can be applied to our spacetime. It seems possible for the Kerr spacetime [3]. However, here we are dealing with the uplifted standard (2 + 1) BTZ spacetime. It is clear that one has to consider a dynamical evolution of the spacetime, as described in section 3.1. In the case of the BTZ black hole, the *evolution of the horizons* (where the inner one is the unstable Cauchy horizon) and ergo-surface outside the horizons can then be revealed.

Let us write the spacetime Equation (6) in the retarded ("outgoing") $U=t-\rho^*$ or advanced ("ingoing") $V=t+\rho^*$ Eddington-Finkelstein coordinates

$$\begin{aligned} \mathrm{d}s_r^2 &= \omega(U,\rho)^2\left[-N(U,\rho)^2\,\mathrm{d}U^2-2\mathrm{d}U\mathrm{d}\rho+\mathrm{d}z^2+\rho^2\left(\mathrm{d}\xi+N^{\xi}(U,\rho)\mathrm{d}U\right)^2\right], \\ \mathrm{d}s_a^2 &= \omega(V,\rho)^2\left[-N(V,\rho)^2\,\mathrm{d}V^2+2\mathrm{d}V\mathrm{d}\rho+\mathrm{d}z^2+\rho^2\left(\mathrm{d}\xi+N^{\xi}(V,\rho)\mathrm{d}V\right)^2\right], \end{aligned} \tag{26}$$

with

$$\begin{aligned} &\mathrm{d}U\equiv\mathrm{d}t-\frac{\mathrm{d}\rho}{N(t,\rho)^2}\equiv t-\rho^*,\ \ \mathrm{d}V\equiv\mathrm{d}t+\frac{\mathrm{d}\rho}{N(t,\rho)^2}\equiv t+\rho^*, \\ &\mathrm{d}\xi\equiv\mathrm{d}\varphi-\frac{N^{\varphi}(t,\rho)}{N(t,\rho)^2}\mathrm{d}\rho, \end{aligned} \tag{27}$$

with domains $U/V\in[-\infty,+\infty],\rho\in[-\infty,+\infty]$. We make no a priori assumptions for N and N^{ξ} (for example by writing $N=1-\frac{2M(u)}{\sqrt{\rho^2+a^2}}$ [30]). The field equations without matter terms now reduce to (an over-dot represents $\frac{\partial}{\partial U}$ and $'=\frac{\partial}{\partial\rho}$)

$$\omega'' = \frac{2\omega'}{\omega}, \tag{28}$$

$$2\omega N\omega' N' + 3N^2\omega'^2 + \frac{1}{\rho}\omega N^2\omega' + 2\omega\dot{\omega}' + 2\dot{\omega}\omega' + \frac{1}{\rho}\omega\dot{\omega}, \tag{29}$$

$$N'' = -\frac{N'^2}{N} - \frac{4\omega' N'}{\omega} - \frac{3N\omega'^2}{\omega^2} - \frac{3N'}{r} - \frac{3N\omega'}{r\omega} + 4\omega\dot{\omega}' - \frac{2\dot{\omega}\omega'}{N\omega^2} + \frac{3\dot{\omega}}{rN\omega}, \tag{30}$$

$$\begin{aligned} &4\dot{\omega}^2 - 2\omega\ddot{\omega} - \frac{\omega N^2\dot{\omega}}{r} + \frac{\dot{N}N\omega^2}{r} - 6\omega'\dot{\omega}N^2 - 2\omega\dot{\omega}NN' + 2\omega N\omega' N' \\ &+ 3\omega'^2 + 2\omega\omega' N^3 N' + \frac{\omega\omega' N^4}{r} = 0, \end{aligned} \tag{31}$$

$$\left(\dot{N}^{\xi}\right)' = -2\left(N^{\xi}\right)'\frac{\dot{\omega}}{\omega}, \quad \left(N^{\xi}\right)'' = -2\left(N^{\xi}\right)'\left(\frac{2\omega'}{\omega} + \frac{3}{r}\right), \tag{32}$$

and constraint

$$\left(N^{\xi}\right)'^2 = \frac{4}{3\rho^2}\left[NN' + N'^2 - 3N^2\frac{\omega'^2}{\omega^2} - 2N^2\frac{\omega'}{\rho\omega} + 6\frac{\omega'\dot{\omega}}{\omega} + 2\frac{\dot{\omega}}{\rho\omega}\right]. \tag{33}$$

One easily finds the non-trivial solution

$$\omega = \frac{1}{\mathrm{e}^{c_1 U}\left(c_2\rho + c_3\right)}, \quad N^2 = \pm c_1\frac{c_3^2 - c_2^2\rho^2}{c_2 c_3}, \quad N^{\xi} = F\left(U\right), \tag{34}$$

with $F\left(U\right)$ an arbitrary function of U. This solution is consistent with the dilaton equation. Further, it is remarkable that the *time dependency emerge in* ω and not N. However, $\tilde{g}_{UU}$ depends on U via N^{ξ}. So our metric $g_{\mu\nu}^{(4)}$ becomes (for the retarded case)

$$\mathrm{d}s^2 = \frac{\mathrm{e}^{-2c_1 U}}{\left(c_2\rho + c_3\right)^2}\left[\pm\frac{c_1\left(c_3^2 - c_2^2\rho^2\right)}{c_2 c_3}\mathrm{d}U^2 - 2\mathrm{d}U\mathrm{d}\rho + \mathrm{d}z^2 + \rho^2\left(\mathrm{d}\xi + F\left(U\right)\mathrm{d}U\right)^2\right], \tag{35}$$

which is *flat*, while $\tilde{R}^{(4)} = \frac{6c_1 c_2}{c_3}$. The function $F\left(U\right)$ will be fixed when matter terms are incorporated (*i.e.* for example, a scalar gauge field). The metric Equation (26) will then contain a term $b\left(U,\rho\right)^2\mathrm{d}\varphi^2$ and a relation like $\left(N^{\xi}\right)' = \frac{b}{\eta^2 X^2 + \omega^2}$ will be obtained. We can now express, for example, U in t and ρ:

$$U = t - \log\left[\frac{c_2\rho + c_3}{c_2\rho - c_3}\right]. \tag{36}$$

So we have now a complete picture of the spacetime. We must note that this solution is rather different with respect to the vacuum Vaidya spacetime. We also are dealing here with null radiation (null matter fields or gravitational radiation) as in the case of Vaidya, but we did not make any explicit assumption for the U or V dependency of ω, N and N^{ξ}. They follow from the field equations. Further, the radiation is in the $\left(\rho,z\right)$-plane instead of the $\left(r,\theta\right)$ plane in the

Vaidya case. It is interesting to compare our solution with the Vaidya-type solution of a spinning black hole in (2 + 1) dimensions found by Chan in conventional GR [28]. They also find a rotation function $N^{\xi}(U)$ which is determined by an energy-momentum tensor of null spinning dust. From Equation (35), we see that the small-scale behavior (and so the dynamical apparent Cauchy horizon) is determined by

$$\omega^2\left(\rho^2 N^{\xi 2}-N^2\right)=\frac{\rho^2 F(U)^2-\dfrac{c_1\left(c_3^2-c_2^2\rho^2\right)}{c_2 c_3}}{\mathrm{e}^{2c_1 U}\left(c_2\rho+c_3\right)^2}, \tag{37}$$

and in the advanced coordinate

$$\omega^2\left(\rho^2 N^{\xi 2}-N^2\right)=\frac{\rho^2 F(V)^2+\dfrac{c_1\left(c_3^2-c_2^2\rho^2\right)}{c_2 c_3}}{\mathrm{e}^{2c_1 V}\left(c_2\rho+c_3\right)^2}. \tag{38}$$

If we omit the dilaton factor, we obtain the expressions for $\tilde{g}_{\mu\nu}$. De apparent horizon is then determined (in V) by

$$\frac{\mathrm{d}\rho}{\mathrm{d}V}=\frac{1}{2}\left(\rho^2\left(N^{\xi}\right)^2-N^2\right)=0, \tag{39}$$

so

$$\rho_{AH}=\pm\frac{c_3}{\sqrt{c_2\left(c_2-\dfrac{c_3}{c_1}F(V)^2\right)}}, \tag{40}$$

and in U

$$\rho_{AH}=\pm\frac{c_3}{\sqrt{c_2\left(c_2+\dfrac{c_3}{c_1}F(U)^2\right)}}. \tag{41}$$

We see that the location of apparent horizon is independent of the dilaton (so also valid for $\tilde{g}_{\mu\nu}$). However, g_{VV} depends also on ω, as can be seen by inspection of Equation (35), *i.e.*, the denominator. The solution turns out to be *also valid* in the (2 + 1)-dimensional spacetime, *i.e.*, $\tilde{R}^{(3)}=\dfrac{6c_1c_2}{c_3}$ and $g^{(3)}_{\mu\nu}$ flat. So we can safely uplift the BTZ solution in Eddington-Finkelstein coordinates in vacuum to 4-dimensional spacetime. We will return to this issue in the next section. In **Figure 4** we plotted ρ^* against ρ and ρ^* against U. The asymptote is at $\dfrac{c_3}{c_2}$. In **Figure 5** we plotted the light cone structure. For the outward emitted signals, the slope is given by Equation (39) (in U) (for the inward, $\mathrm{d}U=0$). For the limiting cases, we obtain

$$\frac{\mathrm{d}\rho}{\mathrm{d}U}=\frac{1}{2}\mathrm{e}^{-2c_1U}\cdot\begin{cases}-\dfrac{c_1}{c_2c_3} & \rho\to 0\\ \dfrac{c_3F(U)^2+c_1c_2}{c_2^2c_3} & \rho\to\infty\\ 0 & \rho=\rho_{AH}\end{cases} \tag{42}$$

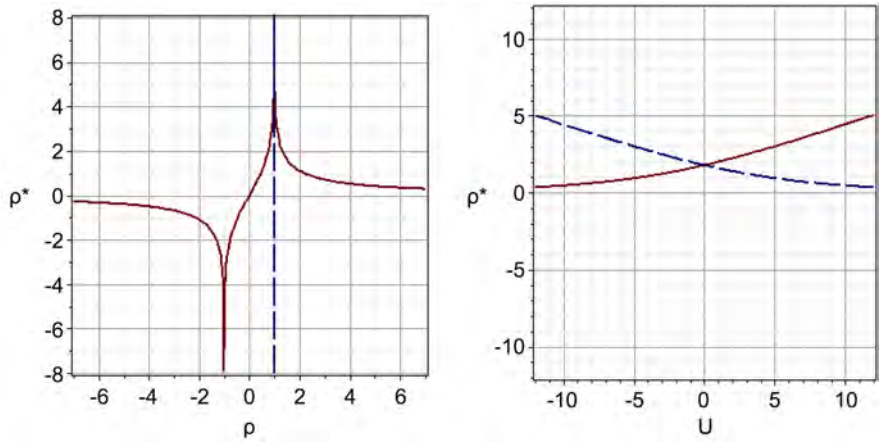

Figure 4. Left: ρ^* as function of ρ. The asymptote is at $\frac{c_3}{c_2}$. Right: ρ^* as function of U for $c_1 = c_2 = c_3 = 1$ and $c_4 = \pm 0.3$.

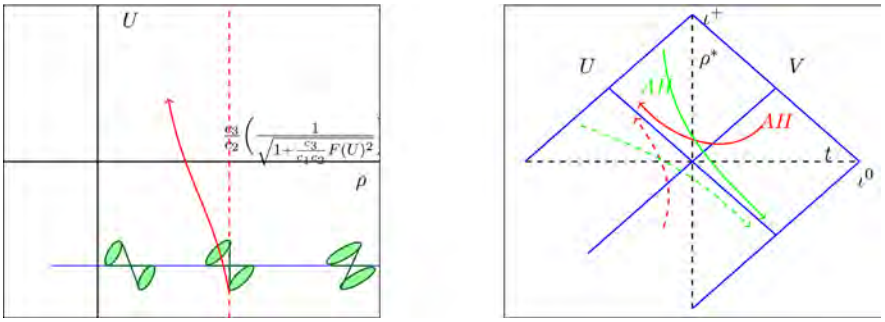

Figure 5. Left: Plot of light cone structure. The location of the apparent horizon is for small $F(U)$ at $\frac{c_3}{c_2}$. For increasing $F(U)$ it tends closer to $\rho = 0$. Right: Penrose diagram for the evaporating BTZ black hole in Eddington Finkelstein coordinates (U, ρ^*). The global location of the two pairs of the apparent horizons as function of U is indicated. Note that one pair ρ^*_{AH} enters the "future inside" region and comes from the "past inside". By the antipodal identification these regions are removed (no "inside" of the black hole) so the locations are mapped on each other. See Section 5.

For $\rho \to 0$, its value doesn't tend necessarily to $-\infty$. For increasing U it could approach zero again by suitable c_1. Note that in general the location of the apparent horizon is dependent of U (see **Figure 5**). We can express the apparent horizon also in ρ^*,

$$\rho^*_{AH} = \ln\left(\frac{1+\sqrt{1+\frac{c_3}{c_1 c_2}F(U)^2}}{1-\sqrt{1+\frac{c_3}{c_1 c_2}F(U)^2}}\right), \tag{43}$$

We can globally plot the location of the apparent horizon in a Penrose diagram, if we take for $F(U)$ for example $e^{c_4 U}$. See **Figure 5**.

Let us now describe what is the meaning of the dilaton field for an infalling

and outside observer in connection with the complementarity of the ingoing and outgoing massless particles. We will use the notion of conformal maps. The outside observed experiences a mass $\omega^2 N^2$ and an evaporating black hole (in U-coordinate) by Hawking radiation (in the case of massive particles, of course, there can also be first a growing mass; we will not consider this here). This radiation is

$$\sim \partial_U \left(\omega^2 N^2\right) = \frac{2c_1^2}{c_2 c_3} \mathrm{e}^{-2c_1 U}. \tag{44}$$

This blows up for $c_1 < 0$ and $U \to +\infty$. However, there is in g_{VV} in the denominator the factor $\mathrm{e}^{2c_1 U}$. So an infalling observer crossing the apparent horizon will need a different ω. The ingoing observer, passing the horizon, will NOT use the ω of the outside observer. In fact, it is locally unobservable. This happens at very small scales, when $g_{UU} \to 0$ and $\omega^2\left(\rho^2 N^{\xi 2} - N^2\right) \to 0$ for $U \ll -1$ in Planck units (the ergo-surface) and there is no horizon at all (note that ω^2 is an overall factor for $\tilde{g}_{\mu\nu}$). The dilaton determines the different notion of what is happening near the horizon for an infalling and outside observer. Now remember that the Ricci scalar curvature transforms under conformal transformations as $R \to \frac{1}{\Omega^2}\left(R - \frac{6}{\Omega}\nabla^\alpha \nabla_\alpha \Omega\right)$ and the additional freedom in ω, *i.e.*, $\omega \to \frac{1}{\Omega}\omega$. The dilaton equation of Equation (10) is an auxiliary equation in vacuum. It follows also from the Einstein equations. When matter is included, one obtains conditions on the potential (see, for example, Equation (23)). So it would be fine if we could impose $R = 0$ for the local observer by using $\tilde{R} - \frac{6}{\Omega}\tilde{\nabla}^\alpha \tilde{\nabla}_\alpha \Omega = 0$. One can then apply Fourier analysis of quantum mechanics and treat ω infinitesimal [34]. This is a complementarity transformation on the dilaton and *switches on and off* the effects these Hawking particles have on the metric.

5. Complementarity Transformation and Conformal Compactification

Let us first describe what is the meaning of the dilaton field for an in-falling and outside observer in connection with the complementarity of the ingoing and outgoing massless particles. We will use the notion of conformal maps. The outside observed experiences a mass $\omega^2 N^2$ and an evaporating black hole (in U-coordinate) by Hawking radiation (in the case of massive particles, of course, there can also be first a growing mass; we will not consider this here). This radiation is

$$\sim \partial_U \left(\omega^2 N^2\right) = \frac{2c_1^2}{c_2 c_3} \mathrm{e}^{-2c_1 U}. \tag{45}$$

This blows up for $c_1 < 0$ and $U \to +\infty$. However, there is in g_{VV} in the denominator the factor $\mathrm{e}^{2c_1 U}$. So an in-falling observer crossing the apparent ho-

rizon will need a different ω. The ingoing observer, passing the horizon, will NOT use the ω of the outside observer. In fact, it is locally unobservable. This happens at very small scales, when $g_{UU}\to 0$ and $\omega^2\left(\rho^2 N^{\xi 2}-N^2\right)\to 0$ for $U\ll -1$ in Planck units (the ergo-surface) and there is no horizon at all (note that ω^2 is an overall factor for $\tilde{g}_{\mu\nu}$). The dilaton determines the different notion of what is happening near the horizon for an in-falling and outside observer. Now remember that the Ricci scalar curvature transforms under conformal transformations as $R\to\frac{1}{\Omega^2}\left(R-\frac{6}{\Omega}\nabla^\alpha\nabla_\alpha\Omega\right)$ and the additional freedom in ω, *i.e.*, $\omega\to\frac{1}{\Omega}\omega$. The dilaton equation of Equation (10) is an auxiliary equation in vacuum. It follows also from the Einstein equations. When matter is included, one obtains conditions on the potential (see, for example, Equation (23)). So it would be fine if we could impose $R = 0$ for the local observer by using $\tilde{R}-\frac{6}{\Omega}\tilde{\nabla}^\alpha\tilde{\nabla}_\alpha\Omega=0$. One can then apply Fourier analysis of quantum mechanics and treat ω infinitesimal [34]. This is a complementarity transformation on the dilaton and *switches on and off* the effects these Hawking particles have on the metric.

Let us return to the *conformal mapping* in more detail. We know that in Minkowski spacetime the conformal map preserves the light-cone structure and so the null geodesics (*i.e.*, the affine parameter). The conformal group in Minkowski, however, does not act as linear transformations, so one needs a trick (see, for example Felsager [21], section 10.3).

One starts with a pseudo-Cartesian space $R^1\otimes R^1$ (for example our (x,z)). One then enlarge first the pseudo-Cartesian space by adding a "null"-cone at infinity. So one compactifies the plane in R^2. In order to apply the conformal transformation of inversion, one considers the unit sphere S^1 and map R^1 onto $S^1-\{N\}$. If we want to apply all the conformal transformations, then we must enlarge the pseudo-Cartesian space by adding two extra dimensions (t,y), (later, we replace x by $x=\rho\sin\varphi$ and $y=\rho\cos\varphi$, to get back our axially symmetric spacetime coordinates (t,ρ,z,φ)). The goal is then to embed the pseudo-Cartesian space $R^1\otimes R^1$ as a subset of $R^2\otimes R^2$. We define M as the intersection of the null cone K (in $R^2\otimes R^2$) with the hyperplane $\rho-t=1$ (or $\rho+t$) and define an isometry $F: R^1\otimes R^1\to M$. Further, one works in the particular section of M, $M\left(R^1\otimes R^1\right)$. Because F induces a coordinate system on M, one can construct characteristic lines. There are characteristic lines that are parallel to $\rho-t=1$ and are generated by null vectors where $\rho=t$. There is a one-to-one correspondence between these lines missing $M\left(R^1\otimes R^1\right)$ and points on K in $R^1\otimes R^1$. So they represent points on the null cone at infinity. One can proof [21] that local sections N_1 and N_2 on the null cone which intersect characteristic lines at most once, can be mapped onto each other by a conformal map obtained by projection along the characteristic lines. If we would now try to project $M\left(R^1\otimes R^1\right)$ onto a suitable subsection of K, then it turns out that it is

not possible to find a single section that is intersected exactly once by each characteristic line. Instead one can consider N as the product of two unit spheres in $M\left(R^2\otimes R^2\right)$, *i.e.*, N becomes a hyper-torus $S^1\otimes S^1$ and each characteristic line will then intersect K twice in antipodal points. So each point in $M\left(R^1\otimes R^1\right)$ is represented by a pair of antipodal points on $S^1\otimes S^1$. The projection is a conformal map. The procedure here described is called a conformal compactification of $M\left(R^1\otimes R^1\right)$. In our case the antipodal identification is $\left(U,V,z,\varphi\right)\to\left(-U,-V,-z,\varphi+\pi\right)$. The points are *not* physically distinct events, but identical and are different representations of one black hole. In fact, there is no inside of the black hole. The price is that the manifold is *not time-orientable* for $\rho<\rho_{AH}$. When the evaporation process speeds up, we observe from Equation (40) that the two horizons approach zero for increasing $F\left(U\right)$, which is assumable. Moreover

$$\lim_{\rho\to 0} g_{UU}\to\pm\frac{c_1}{c_2c_3\mathrm{e}^{2c_1U}} \tag{46}$$

where in the denominator appears the exponential factor from the dilaton. So ω determines the scale as function of U the local observer experiences. Note that on "*the other side*" (in the Penrose picture region II), U change sign and the righthand side of Equation (46) becomes $\frac{c_1}{c_2c_3\mathrm{e}^{-2c_1U}}$.

We found in section 4 that the solution of the BTZ spacetime in 4D in Eddington-Finkelstein coordinates in conformally invariant gravity is identical to the 3D case, where we omitted the dz^2. That is curious, because we can still apply the conformal compactification (conformal transformations) and the antipodal identifications in 4D spacetime sketched above. Further, we obtained a *flat* $g_{\mu\nu}$ out of the "un-physical" $\tilde{g}_{\mu\nu}$, which resembles the original BTZ-black hole (without the need of a cosmological constant).

Some notes can be made about the connection with the gravitational back-reaction. In the non-vacuum situation of section 3.2, the back-reaction is quite clear. In the vacuum case, there will be a shift in the location of the apparent horizon after the emission of null radiation (Equation (45)). This can be made clear in the Penrose diagram, as was also found in the time-dependent Vaidya spacetime in connection with black-bounces and traversable wormholes [30] [31]. In the conformally invariant model and the antipodal approach, however, one doesn't need such extreme escape. This shift will be related to the c_i in (Equation (45)), just as the scalar curvature of $\tilde{g}_{\mu\nu}$ was related to c_i, *i.e.*, $\tilde{R}^{(4)}=\frac{6c_1c_2}{c_3}$. A comparable effect was found in the counterpart model of the cylindrical radiating Lewis-van Stockum solution (in $\left(\rho,t\right)$ coordinates) and Einstein-Rosen pulse-wave solution [35]. This solution is obtained from the stationary $\left(z,\rho\right)$ spacetime where one replaces $t\to iz, z\to it$ and $J\to iJ$. This solution has, however, reflection symmetry, $\varphi\to-\varphi, z\to-z$. A curious feature of the solution is the fact that the Kretschmann scalar becomes zero for two dif-

ferent values of a constant in the exact solution. In some sense, the spacetime returns to his original status after the emission of the pulse wave. The relation with the antipodal symmetry is current under investigation by the author.

6. Conclusions

Using conformally invariant gravity, a new solution is found for the uplifted BTZ spacetime, without a cosmological constant. The solution shows some different features with respect to the standard BTZ solution. In the non-vacuum situation, where a scalar-gauge field is present, a numerical solution is presented on a spacetime where one writes the metric as $g_{\mu\nu}=\omega^2\tilde{g}_{\mu\nu}$, with ω a dilaton field, to be treated on equal footing with the scalar field and $\tilde{g}_{\mu\nu}$ an "un-physical" spacetime. The effect of ω on the behavior of the solution is evident. An outgoing wave-like initial value for the scalar field induces a wave-like response in the dilaton field and pushes the apparent horizon closer to $\rho=0$. The solution depends critically on the shape of the potential. The solution can be used to investigate what happens with the spacetime of an evaporating black hole through Hawking radiation. In the vacuum situation in Eddington-Finkelstein coordinates, an exact solution is found for the (2 + 1)-dimensional case *as well as* for the uplifted situation. The "un-physical" $\tilde{g}_{\mu\nu}$ (BTZ) solution has a non-zero Ricci scalar, while $g_{\mu\nu}$ *is flat*.

There is possible a link with the antipodal identification. Antipodal mapping is inevitable if one wants to maintain unitarity during quantum mechanical calculations on the Hawking particles. The antipodal identification can be represented as a conformal transformation generated from the pseudo-orthogonal matrices of $O(3,3)$, *i.e.*, the *conformal group*. Each conformal transformation in this group can be presented by a pair of antipodal matrices. This was the main reason to investigate in this manuscript the dynamics of the BTZ black hole in conformally invariant gravity. In the conformally invariant approach, the dilaton field plays a fundamental role. We find that as soon its value is fixed (by the global spacetime after choosing the coordinate frame), the local observer experiences scales. Moreover, we find that it also plays a role in the *antipodal mapping*. If we substitute the apparent horizon ρ_{AH} (Equation (41)) into ω (Equation (34)) at the horizon, we can then compare ω on both sides of the horizon by replacing U by $-U$. By imposing proper matching conditions, one could obtain restrictions on $F(U)$.

We do not pretend that our model is a new description of the physics of an evaporating BTZ black hole. We have tried to compare conformally invariant gravity solutions of the (2 + 1)-dimensional BTZ black hole solution and its uplifted counterpart model with the results of former results on black hole studies. Especially the antipodal identification seems to fit well in our model.

Conflicts of Interest

The author declares no conflicts of interest regarding the publication of this paper.

References

[1] Baňados, M., Henneaux, M., Teitelboim, C. and Zanelli, J. (1993) *Physical Review D*, **50**, 1506. https://doi.org/10.1103/PhysRevD.48.1506

[2] Carlib, S. (1995) *Classical and Quantum Gravity*, **12**, 2853. https://doi.org/10.1088/0264-9381/12/12/005

[3] Compère, G. (2019) Advanced Lectures on General Relativity (Lecture Notes in Physics 952). Springer, Heidelberg. https://doi.org/10.1007/978-3-030-04260-8

[4] Deser, S., Jackiw, R. and 't Hooft, G. (1992) *Physical Review Letters*, **68**, 267. https://doi.org/10.1103/PhysRevLett.68.267

[5] Garfinkle, D. (1985) *Physical Review D*, **32**, 1323. https://doi.org/10.1103/PhysRevD.32.1323

[6] Maldacena, J. (1999) *Advances in Theoretical and Mathematical Physics*, **2**, 231. https://doi.org/10.1088/1126-6708/1999/02/011

[7] Strominger, A. (1997) *JHEP*, **1998**, 009. https://doi.org/10.1088/1126-6708/1998/02/009

[8] Slagter, R.J. and Larosh, J. (2019) On the BTZ Black Hole and the Spinning Cosmic String. arXiv: gr-qc/191206222

[9] Slagter, R.J. and Duston, C.L. (2020) *International Journal of Modern Physics A*, **35**, Article ID: 2050024. https://doi.org/10.1142/S0217751X20500244

[10] Weyl, H. (1918) *Mathematische Zeitschrift*, **2**, 384. https://doi.org/10.1007/BF01199420

[11] Wald, R.M. (2009) General Relativity. Univ. Press, Chicago.

[12] 't Hooft, G. (2010) The Conformal Constraint in Canonical Quantum Gravity. arXiv:gr-qc/10110061

[13] 't Hooft, G. (2011) *Foundations of Physics*, **41**, 1829. https://doi.org/10.1007/s10701-011-9586-8

[14] Bars, I., Steinhardt, P. and Turok, N. (2014) *Physical Review D*, **89**, Article ID: 043515. https://doi.org/10.1103/PhysRevD.89.043515

[15] Mannheim, P.D. (2005) Alternatives to Dark Matter and Dark Energy.

[16] Slagter, R.J. and Pan, S. (2016) *Foundations of Physics*, **46**, 1075-1089. https://doi.org/10.1007/s10701-016-0002-2

[17] 't Hooft, G. and Veltman, M. (1974) *Annales de l' Institut Henri Poincaré*, **20**, 69.

[18] Stelle, K.S. (1977) *Physical Review D*, **16**, 953. https://doi.org/10.1103/PhysRevD.16.953

[19] Duff, M.J. (1993) Twenty Years of the Weyl Anomaly.

[20] 't Hooft, G. (2019) The Quantum Black Hole as a Theoretical Lab, a Pedagogical Treatment of a New Approach.

[21] Felsager, B. (1998) Geometry, Particles and Fields. Odense Univ. Press, Odense. https://doi.org/10.1007/978-1-4612-0631-6

[22] 't Hooft, G. (2015) Local Conformal Symmetry: the Missing Symmetry Component for Space and Time. arXiv: gr-qc/14106675v1.

[23] Weinberg, E.J. (2012) Classical Solutions in Quantum Field Theory. Cambridge University Press, Cambridge.

[24] Oda, I. (2015) Conformal Higgs Gravity. arXiv: gr-cq/150506760

[25] Parker, L.E. and Toms, D.J. (2009) Quantum Field Theory in Curved Spacetime.

Cambridge University Press, Cambridge.
https://doi.org/10.1017/CBO9780511813924

[26] Page, D.N. (2004) *New Journal of Physics*, **7**, 203.
https://doi.org/10.1088/1367-2630/7/1/203

[27] Vaidya, P.C. (1943) *Current Science*, **12**, 183.
https://doi.org/10.1525/as.1943.12.18.01p1268z

[28] Chan, J.S.F., Chan, K.C.H. and Mann, R.B. (1996) *Physical Review D*, **54**, 1535.
https://doi.org/10.1103/PhysRevD.54.1535

[29] Abdolrahimi, S., Page, D.N. and Tzounis, C. (2019) Ingoing Eddington-Finkelstein Metric of an Evaporating Black Hole. arXiv: hep-th/160705280V4

[30] Simpson, A., Martin-Moruna, P. and Visser, M. (2019) *Classical and Quantum Gravity*, **36**, Article ID: 145007. https://doi.org/10.1088/1361-6382/ab28a5

[31] Simpson, A. and Visser, M. (2019) Black-Bounce to Traversable Wormhole. arXiv: gr-qc/181207114v3

[32] Maldacena, J. and Susskind, L. (2013) *Fortschritte der Physik*, **61**, 781.
https://doi.org/10.1002/prop.201300020

[33] 't Hooft, G. (2016) *Foundations of Physics*, **46**, 1185.
https://doi.org/10.1007/s10701-016-0014-y

[34] 't Hooft, G. (2009) Quantum Gravity without Space-Time Singularities or Horizons. arXiv: gr-qc/09093426

[35] Islam, J.N. (1985) Rotating Fields in General Relativity. Cambridge University Press, Cambridge. https://doi.org/10.1017/CBO9780511735738

Journal of Modern Physics, 2020, 11, 1731-1742
https://www.scirp.org/journal/jmp
ISSN Online: 2153-120X
ISSN Print: 2153-1196

Charged Particle in a Flat Box with Static Electromagnetic Field and Landau's Levels

Gustavo V. López, Jorge A. Lizarraga

Departamento de Física, Universidad de Guadalajara, Guadalajara, México
Email: gulopez@cencar.udg.mx, jorge.a.lizarraga.b@gmail.com

How to cite this paper: López, G.V. and Lizarraga, J.A. (2020) Charged Particle in a Flat Box with Static Electromagnetic Field and Landau's Levels. *Journal of Modern Physics*, **11**, 1731-1742.
https://doi.org/10.4236/jmp.2020.1110106

Received: July 26, 2020
Accepted: October 25, 2020
Published: October 28, 2020

Abstract

We study the quantization of a charged particle motion without spin inside a flat box under a static electromagnetic field. Contrary to Landau's solution with constant magnetic field transverse to the box and using Fourier transformation, we found a full solution for the wave function which is different from that one given by Landau, and this fact remains when static electric field is added. However, the Landau's levels appear in all cases.

Keywords

Landau's Levels, Quantum Hall Effect, Flat Box

1. Introduction

The work of Klitzing, Dora and Pepper [1] presented a breakthrough in experimental physics due to the success in measuring the Hall voltage of a two-dimensional electron gas realized in a MOSFET. The important fact discovered in this experiment was that the Hall resistance is quantized, and Landau' eigenvalues solution [2] (Landau's levels) of a charged particle in a flat surface with magnetic field has become of great importance in trying to understand integer hall effect [1] [3] [4] [5] [6], fractional Hall effect [6] [7] [8] [9], and topological insulators [10]-[16]. These elements promise to become essential for future nanotechnology devices [17] [18] [19]. Due to this considerable application of the Landau's levels, it is worth to re-study this problem and its variations with an static electric field. In this paper, we solve the problem of a charged particle inside a flat box with lengths L_x, L_y, and L_z such that $L_z \ll L_x, L_y$ by using the Fourier transformation, for three different cases: for a transverse constant magnetic field, for a constant magnetic field orthogonal to a constant electric field, and for a constant magnetic field parallel to a constant electric field. We show that there exists

a different solution for this type of eigenvalue quantum problems than that one given by Landau, but having the same Landau's levels. We consider that this result could be relevant because Landau's solution is kept using in different works like Prange's [20], Laughling's [21], solid state and quantum transport books as well [3] [7] [22] [23].

2. Analytical Approach for the Case $B=(0,0,B)$

Let us consider a charged particle "q" with mass "m" in the box with a constant magnetic field orthogonal to the flat surface, $\boldsymbol{B}=(0,0,B)$, as shown in Figure 1.

For a nonrelativistic charged particle, the Hamiltonian of the system (units CGS) is

$$H=\frac{\left(\boldsymbol{p}-q\boldsymbol{A}/c\right)^2}{2m}, \tag{1}$$

where $\boldsymbol{p}$ is the generalized linear momentum, $\boldsymbol{A}$ is the magnetic potential such that $\boldsymbol{B}=\nabla\times\boldsymbol{A}$, and "$c$" is the speed of light. We can choose the Landau's gauge to have the vector potential of the form $\boldsymbol{A}=(-By,0,0)$. Therefore, the Hamiltonian has the following form

$$H=\frac{\left(p_x+qBy/c\right)^2}{2m}+\frac{p_y^2}{2m}+\frac{p_z^2}{2m}. \tag{2}$$

To quantize the system, we need to solve the Schrödinger's equation [24]

$$i\hbar\frac{\partial\Psi}{\partial t}=\left\{\frac{\left(\hat{p}_x+qBy/c\right)^2}{2m}+\frac{\hat{p}_y^2}{2m}+\frac{\hat{p}_z^2}{2m}\right\}\Psi. \tag{3}$$

where $\Psi=\Psi(\boldsymbol{x},t)$ is the wave function, $\hbar$ is the Plank's constant divided by 2π, $\hat{p}_i$ is the momentum operators such that $\left[x_i,\hat{p}_j\right]=i\hbar\delta_{ij}$. Now, the argument used by Landau is that due to commutation relation $\left[\hat{p}_x,\hat{H}\right]=0$, between the operators $\hat{p}_x$ and the Hamiltonian $\hat{H}$ (implying that $\hat{p}_x$ is a constant of motion), it is possible to replace this component of the momentum by $\hbar k_x$,

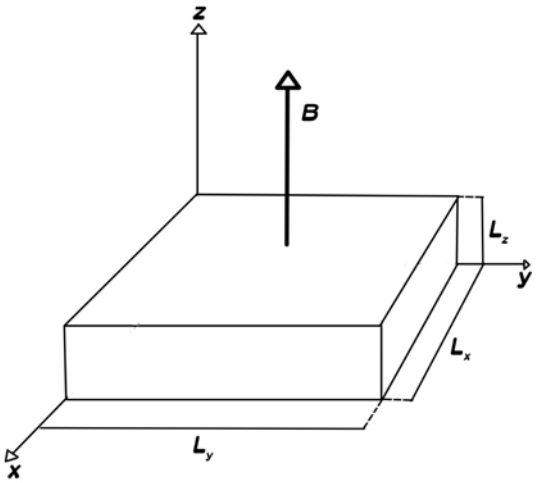

Figure 1. Electric charged in a flat box with magnetic field.

having a solution for the eigenvalue problem of separable variable type, $f_2(x) f_3(y) f_4(z)$ for the resulting eigenvalue problem, once the time variable is separated. However, this problem can be fully addressed using the Fourier transformation. First, since the Hamiltonian $\hat{H}$ does not depend explicitly on time, the proposition

$$\Psi(\boldsymbol{x},t) = \mathrm{e}^{-iEt/\hbar}\Phi(\boldsymbol{x}) \tag{4}$$

reduces the equation to an eigenvalue problem

$$\hat{H}\Phi = E\Phi. \tag{5}$$

Then, this equation is written as

$$\left\{\frac{1}{2m}\left(\hat{p}_x^2 + \frac{2qB}{c}y\hat{p}_x + \frac{q^2B^2}{c^2}y^2\right) + \frac{\hat{p}_y^2}{2m} + \frac{\hat{p}_z^2}{2m}\right\}\Phi = E\Phi. \tag{6}$$

The variable "z" is separable through the proposition

$$\Phi(\boldsymbol{x}) = \phi(x,y)\mathrm{e}^{-ik_z z}, \quad k_z \in \Re, \tag{7}$$

resulting in the following equation

$$\left\{\frac{1}{2m}\left(\hat{p}_x^2 + \frac{2qB}{c}y\hat{p}_x + \frac{q^2B^2}{c^2}y^2\right) + \frac{\hat{p}_y^2}{2m}\right\}\phi = E'\phi, \tag{8}$$

where E' is

$$E' = E - \frac{\hbar^2 k_x^2}{2m}. \tag{9}$$

That is, the resulting partial differential equation is of the form

$$\frac{1}{2m}\left\{-\hbar^2\frac{\partial^2\phi}{\partial x^2} - i\frac{2qB\hbar}{c}y\frac{\partial\phi}{\partial x} + \frac{q^2B^2}{c^2}y^2\phi\right\} - \frac{\hbar^2}{2m}\frac{\partial^2\phi}{\partial y^2} = E'\phi. \tag{10}$$

This equation will be solved using Fourier transformation [25] on the variable "x",

$$\hat{\phi}(k,y) = \mathcal{F}[\phi] = \frac{1}{\sqrt{2\pi}}\int_{\Re}\mathrm{e}^{ikx}\phi(x,y)\mathrm{d}x. \tag{11}$$

Applying Fourier transformation to this equation, knowing its property $\mathcal{F}[\partial\phi/\partial x] = (-ik)\hat{\phi}$, we get the ordinary differential equation

$$-\frac{\hbar^2}{2m}\frac{\mathrm{d}^2\hat{\phi}}{\mathrm{d}y^2} + \frac{m}{2}\omega_c^2(y-y_0)^2\hat{\phi} = E'\hat{\phi}, \tag{12}$$

where ω_c is the cyclotron frequency

$$\omega_c = \frac{qB}{mc} \tag{13a}$$

and $y_0 = y_0(k)$ is the displacement parameter

$$y_0 = \frac{\hbar c}{qB}k. \tag{13b}$$

This equation is just the quantum harmonic oscillator in the "y" direction displaced by an amount y_0. So, its solution in the Fourier' space is

$$\hat{\phi}_n(k,y)=\psi_n(\xi),\quad \xi=\sqrt{\frac{m\omega_c}{\hbar}}(y-y_0),\quad \psi_n(\xi)=A_n\mathrm{e}^{-\xi^2}H_n(\xi), \tag{14}$$

being $H_n(\xi)$ the Hermit polynomials, and A_n is a constant of normalization, $A_n=\left(m\omega_c/\pi\hbar\right)^{1/4}\Big/\sqrt{2^n n!}$. and

$$E_n'=\hbar\omega_c\left(n+1/2\right). \tag{15}$$

Now, the solution in the real space $\phi_n(x,y)$ is gotten by using the inverse Fourier transformation [25],

$$\phi_n(x,y)=\mathcal{F}^{-1}\left[\phi_n(k,y)\right]=\frac{1}{\sqrt{2\pi}}\int_{\Re}\mathrm{e}^{-ikx}\psi_n\left(\sqrt{\frac{m\omega_c}{\hbar}}\left(y-\hbar ck/qB\right)\right)\mathrm{d}k. \tag{16}$$

Making the change of variable $\sigma=\sqrt{m\omega_c/\hbar}\left(y-\hbar ck/qB\right)$, and knowing that the Fourier transform of the harmonic oscillator solution is another harmonic oscillator solution, we get

$$\phi_n(x,y)=\frac{-qB}{\sqrt{mc^2\hbar\omega_c}}\mathrm{e}^{-i\frac{qB}{\hbar c}xy}\psi_n\left(\frac{qBx}{\sqrt{mc^2\hbar\omega_c}}\right). \tag{17}$$

This last equation is indeed a nonseparable solution of (8). Therefore, the normalized eigenfunctions and the eigenvalues of the eigenvalue problem (5) are (ignoring the sign)

$$\Phi_{n,k_z}(\boldsymbol{x})=\frac{\sqrt{qB}}{\left(L_y^2L_z^2mc^2\hbar\omega_c\right)^{1/4}}\mathrm{e}^{-i\left(\frac{qB}{\hbar c}xy-k_zz\right)}\psi_n\left(\frac{qBx}{\sqrt{mc^2\hbar\omega_c}}\right). \tag{18a}$$

and

$$E_{n,k_z}=\hbar\omega_c\left(n+\frac{1}{2}\right)+\frac{\hbar^2k_z^2}{2m}. \tag{18b}$$

These eigenvalues represent just the Landau's levels, but its solution (18a) is completely different from that one given by Landau on the variables "x" and "y". One needs to point out that there is not displacement at all in the harmonic oscillation solution. Now, assuming a periodicity in the *z*-direction, $\Phi_{n,k_z}(\boldsymbol{x},t)=\Phi_{n,k_z}(x,y,z+L_z,t)$, the usual condition $k_zL_z=2\pi n',n'\in\mathcal{Z}$ makes the eigenvalues to be written as and the general solution of Schrödinger's Equation (3) can be written as

$$E_{n,n'}=\hbar\omega_c\left(n+1/2\right)+\frac{\hbar^2 2\pi^2}{mL_z^2}n'^2. \tag{19}$$

We must observe that these quantum numbers correspond to the degree of freedom in the "$y(n)$" and "$z(n')$" directions. The quantization condition of the magnetic flux appears rather naturally since $\mathrm{e}^{-iqBxy/\hbar c}=1$ for any "x" and "y" such that $qBxy/\hbar c=2\pi j$, were $j\in\mathcal{Z}$. So, in particular one can ask this to happen for $x=L_x$ and $y=L_y$. Thus, it follows from the phase term that

$$\frac{qBL_xL_y}{\hbar c}=2\pi j,\quad j\in\mathcal{Z}, \tag{20}$$

where BL_xL_y is the magnetic flux crossing the surface with area L_xL_y, and

$\hbar c/q$ is the so-called quantum flux [26]. Then, expression (18a) is written as

$$\Phi_{nn'j}(\boldsymbol{x}) = \frac{\sqrt{qB}}{\left(L_y^2 L_z^2 mc^2 \hbar\omega_c\right)^{1/4}} e^{-i\left(\frac{2\pi j}{L_x L_y}xy - \frac{2\pi n'}{L_z}z\right)} \psi_n\left(\frac{qBx}{\sqrt{mc^2\hbar\omega_c}}\right). \tag{21}$$

The degeneration of the eigenvalues (19) comes from the degree of freedom in "x" and can be obtained by making use of the following quasi-classical argument: given the energy of the harmonic oscillator $E_o = \hbar\omega_c(n+1/2)$, we know the maximum displacement of the particle (classically) is given by $x_{\max} = \pm\sqrt{2E_o/m\omega_c^2}$, and since the periodicity in the variable "y" mentioned before is valid for any "x" value, we must have that the maximum value of the quantum number "j" must be

$$\Delta j = \frac{qBL_y}{\pi\hbar c} x_{\max} = \frac{qBL_y}{\pi\hbar c}\sqrt{\frac{2\hbar(n+1/2)}{m\omega_c}}, \tag{22}$$

and this represents the degeneration, $D(n)$, we have in the system

$$D(n) = \left[\frac{qBL_y}{\pi\sqrt{mc^2\hbar\omega_c}}\sqrt{2n+1}\right]. \tag{23}$$

where $[\xi]$ means the integer part of the number ξ. Therefore, the general solution (absorbing the sign in the constants) is

$$\begin{aligned}\Psi(\boldsymbol{x},t) = \sum_{n,'n}\sum_{j=0}^{D(n)} C_{nn'j}\sqrt{\frac{2\pi j}{L_x L_y^2 L_z}}\left(\frac{\hbar}{m\omega_c}\right)^{1/4} \mathrm{e}^{-i\left(\frac{2\pi j}{L_x L_y}xy - \frac{2\pi n'}{L_z}z\right)} \mathrm{e}^{-i\frac{E_{n,n'}}{\hbar}t} \\ \times\psi_n\left(\sqrt{\frac{\hbar}{m\omega_c}}\left(\frac{2\pi j}{L_x L_y}\right)x\right),\end{aligned} \tag{24}$$

where the constants $C_{nn'j}$ must satisfy that $\sum_{n,n',j}\left|C_{nn'j}\right|^2 = 1$. The Landau's levels $E_{n,n'}$ are given by expression (19).

3. The Analytical Approach for Case $B \perp E$

This case is illustrated in Figure 2.

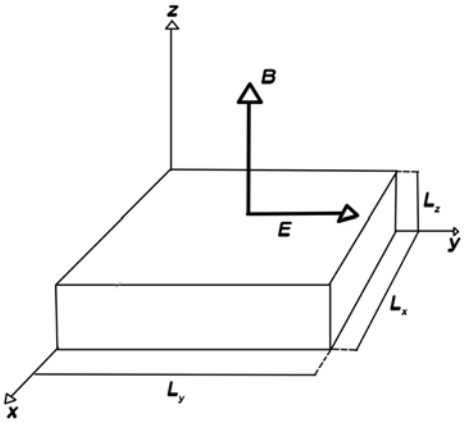

Figure 2. Electric charged in a flat box with magnetic and electric fields.

Where the magnetic and electric constant fields are given by $\boldsymbol{B}=(0,0,B)$ and $\boldsymbol{E}=(0,\mathcal{E},0)$. We select Landau's gauge for the magnetic field such that the vector and scalar potentials are $\boldsymbol{A}=(-By,0,0)$ and $\phi=-\mathcal{E}y$. Then, our Hamiltonian is [21] [22] [23]

$$\hat{H}=\frac{\left(\hat{\boldsymbol{p}}-\frac{q}{c}\boldsymbol{A}\right)^2}{2m}+q\phi(\boldsymbol{x}), \tag{25}$$

and the Schrödinger's equation,

$$i\hbar\frac{\partial\Psi}{\partial t}=\hat{H}\Psi, \tag{26}$$

is written as

$$i\hbar\frac{\partial\Psi}{\partial t}=\left\{\frac{1}{2m}\left(\hat{p}_x+\frac{qB}{c}y\right)^2+\frac{\hat{p}_y^2}{2m}+\frac{\hat{p}_z^2}{2m}\right\}\Psi-q\mathcal{E}y\Psi. \tag{27}$$

Using the definition $\hat{p}_j=-i\hbar\partial/\partial x_j$ and the commutation relation $[x_k,\hat{p}_j]=i\hbar\delta_j k$, the above expression is written as the following partial differential equation

$$i\hbar\frac{\partial\Psi}{\partial t}=-\frac{\hbar^2}{2m}\frac{\partial^2\Psi}{\partial x^2}-i\frac{qB\hbar}{mc}\frac{\partial\Psi}{\partial x}+\frac{q^2B^2}{2mc^2}y^2\Psi-\frac{\hbar^2}{2m}\frac{\partial^2\Psi}{\partial y^2}-\frac{\hbar^2}{2m}\frac{\partial^2\Psi}{\partial z^2}-q\mathcal{E}y\Psi. \tag{28}$$

Taking the Fourier transform, with respect the *x*-variable, $\hat{\Psi}(k,y,z,t)=\mathcal{F}_x\left[\Psi(\boldsymbol{x},t)\right]$, the resulting expression is

$$i\hbar\frac{\partial\hat{\Psi}}{\partial t}=\left[\frac{\hbar^2k^2}{2m}-\left(\frac{qB\hbar k}{mc}+q\mathcal{E}\right)y+\frac{q^2B^2}{2mc^2}y^2\right]\hat{\Psi}-\frac{\hbar^2}{2m}\frac{\partial^2\hat{\Psi}}{\partial y^2}-\frac{\hbar^2}{2m}\frac{\partial^2\hat{\Psi}}{\partial z^2}. \tag{29}$$

By proposing a solution of the form

$$\hat{\Psi}(k,yz,t)=\mathrm{e}^{-iEt/\hbar+ik_z z}\Phi(k,y) \tag{30}$$

and after some rearrangements, the resulting equation for Φ is

$$-\frac{\hbar^2}{2m}\frac{\mathrm{d}^2\Phi}{\mathrm{d}y^2}+\frac{1}{2}m\omega_c^2(y-y_0)^2\Phi=E'\Phi, \tag{31}$$

where ω_c is the cyclotron frequency (13a), and we have made the definitions

$$y_0=\frac{\hbar c}{qB}k+\frac{mc^2\mathcal{E}}{qB^2} \tag{32}$$

and

$$E'=E-\frac{\hbar^2k^2}{2m}-\frac{\hbar^2k_z^2}{2m}+\frac{1}{2m}\left(\hbar k+\frac{mc\mathcal{E}}{B}\right)^2. \tag{33}$$

This equation is again the quantum harmonic oscillator on the variable "*y*" with a cyclotron frequency ω_c and displaced by a quantity y_0. Therefore, the solution (14) is

$$\Phi(k,y)=\psi_n\left(\sqrt{\frac{m\omega_c}{\hbar}}(y-y_0)\right) \tag{34}$$

and

$$E_n' = \hbar\omega_c\left(n+1/2\right). \tag{35}$$

Thus, the solution in the Fourier space is

$$\hat{\Psi}\left(k,y,z,t\right) = \mathrm{e}^{-iE_{n,k_z}t/\hbar+ik_z z}\psi_n\left(\sqrt{\frac{m\omega_c}{\hbar}}\left(y-y_0\right)\right) \tag{36}$$

with the energies E_{n,k_z} given by

$$E_{n,k_z} = \hbar\omega_c\left(n+1/2\right)+\frac{\hbar^2k_z^2}{2m}-\frac{mc^2\mathcal{E}^2}{2B^2}-\frac{c\mathcal{E}\hbar}{B}k. \tag{37}$$

The solution in the space-time is obtained by applying the inverse Fourier transformation,

$$\Psi_{n,k_z}\left(\boldsymbol{x},t\right) = \mathcal{F}\left[\hat{\Psi}_{n,k_z}\left(k,y,z,t\right)\right] = \frac{1}{\sqrt{2\pi}}\int_{\Re}\mathrm{e}^{-ixk}\hat{\Psi}_{n,k_z}\left(k,y,z,t\right)\mathrm{d}k, \tag{38}$$

which after a proper change of variable and rearrangements, we get the normalized function (ignoring the sign)

$$\Psi_{n,k_z}\left(\boldsymbol{x},t\right) = \frac{\sqrt{qB}}{\left(L_y^2L_z^2mc^2\hbar\omega_c\right)^{1/4}}\mathrm{e}^{-i\phi_{n,k_z}\left(\boldsymbol{x},t\right)}\psi_n\left(\frac{qB}{\sqrt{mc^2\hbar\omega_c}}\left(x-\frac{c\mathcal{E}t}{B}\right)\right), \tag{39}$$

where the phase $\phi_{n,k_z}\left(\boldsymbol{x},t\right)$ has been defined as

$$\begin{aligned}\phi_{n,k_z}\left(\boldsymbol{x},t\right) = &\left[\hbar\omega_c\left(n+1/2\right)+\frac{\hbar^2k_z^2}{2m}-\frac{mc^2\mathcal{E}^2}{2B^2}\right]\frac{t}{\hbar}\\ &-k_z z+\frac{qB}{\hbar c}\left(x-\frac{c\mathcal{E}t}{B}\right)\left(y-\frac{mc^2\mathcal{E}}{qB^2}\right).\end{aligned} \tag{40}$$

asking for the periodicity with respect to the variable "z", $\Psi_{n,k_z}\left(x,t\right) = \Psi_{n,k_z}\left(z,y,z+L_z,t\right)$, it follows that $k_zL_z = 2\pi n'$ where n' is an integer number, and the above phase is now written as

$$\begin{aligned}\phi_{nn'}\left(\boldsymbol{x},t\right) = &\left[\hbar\omega_c\left(n+1/2\right)+\frac{\hbar^2 2\pi^2n'^2}{mL_z^2}-\frac{mc^2\mathcal{E}^2}{2B^2}\right]\frac{t}{\hbar}-\frac{2\pi n'}{L_z}z\\ &+\frac{qB}{\hbar c}\left(x-\frac{c\mathcal{E}t}{B}\right)\left(y-\frac{mc^2\mathcal{E}}{qB^2}\right).\end{aligned} \tag{41}$$

Note from this expression that the term $\mathrm{e}^{-i\phi(x,t)}$ contains the element $\mathrm{e}^{i\frac{qB}{\hbar c}xy}$, and by assuming the periodic condition $\Psi\left(\boldsymbol{x},t\right) = \Psi\left(x,y+L_y,z,t\right)$, will imply that $\Psi\left(\boldsymbol{x},t\right)$ will be periodic with respect to the variable "y", for any "x" at any time "t". In particular, this will be true for $x = L_x$. This last assumption brings about the quantization of the magnetic flux of the form

$$\frac{qBL_xL_y}{\hbar c} = 2\pi j, \quad J\in\mathcal{Z}, \tag{42}$$

obtaining the same expression as (20), and this phase is now depending on the quantum number "j"

$$\phi_{nn'j}(\boldsymbol{x},t)=e_{nn'}t/\hbar-\frac{2\pi n'}{L_z}z+\frac{2\pi j}{L_xL_y}xy-\frac{2\pi j}{L_xL_y}\left[\frac{mc^2\mathcal{E}}{qB^2}x+\frac{c\mathcal{E}}{B}ty\right]. \tag{43}$$

where $e_{nn'}$ is the energy associated with the system,

$$e_{n,n'}=\hbar\omega_c\left(n+1/2\right)+\frac{2\pi^2\hbar^2}{mL_z^2}n'^2+\frac{mc^2\mathcal{E}^2}{2B^2}. \tag{44}$$

In this way, from these relations and the expression (39) we have a family of solutions $\left\{\Psi_{nn'j}(x,t)\right\}_{n,n',j\in\mathcal{Z}}$ of the Schrödinger Equation (27),

$$\Psi_{nn'j}(\boldsymbol{x},t)=\sqrt{\frac{2\pi j}{L_xL_y^2L_z}}\left(\frac{\hbar}{m\omega_c}\right)^{1/4}\mathrm{e}^{-i\phi_{nn'j}(\boldsymbol{x},t)}\psi_n\left(\sqrt{\frac{\hbar}{m\omega_c}}\left(\frac{2\pi j}{L_xL_y}\right)\left(x-\frac{c\mathcal{E}t}{B}\right)\right), \tag{45}$$

Now, by the same arguments we did in the previous case, the degeneration of the systems would be given by (23), and the general solution would be of the form

$$\Psi(\boldsymbol{x},t)=\sum_{n,n'}\sum_{j=0}^{D(n)}\tilde{C}_{nn'j}\Psi_{nn'j}(\boldsymbol{x},t). \tag{46}$$

4. The Analytical Approach for Case $B \parallel E$

Figure 3 shows this case.

The fields are of form $\boldsymbol{B}=(0,B,0)$ and $\boldsymbol{E}=(0,\mathcal{E},0)$. The scalar and vector potentials are chosen as $\boldsymbol{A}=(Bz,0,0)$ and $\phi=-\mathcal{E}y$. The Shrödinger equation is for this case as

$$i\hbar\frac{\partial\Psi}{\partial t}=\left\{\frac{\left(\hat{p}_x-qBz/c\right)^2}{2m}+\frac{\hat{p}_y^2}{2m}+\frac{\hat{p}_z^2}{2m}-q\mathcal{E}y\right\}\Psi, \tag{47}$$

which defines the following partial differential equation

$$\begin{aligned}i\hbar\frac{\partial\Psi}{\partial t}=&-\frac{\hbar^2}{2m}\frac{\partial^2\Psi}{\partial x^2}+i\frac{qB\hbar z}{mc}\frac{\partial\Psi}{\partial x}+\frac{q^2B^2}{2mc^2}z^2\Psi\\&-\frac{\hbar^2}{2m}\frac{\partial^2\Psi}{\partial y^2}-\frac{\hbar^2}{2m}\frac{\partial^2\Psi}{\partial z^2}-q\mathcal{E}y\Psi.\end{aligned} \tag{48}$$

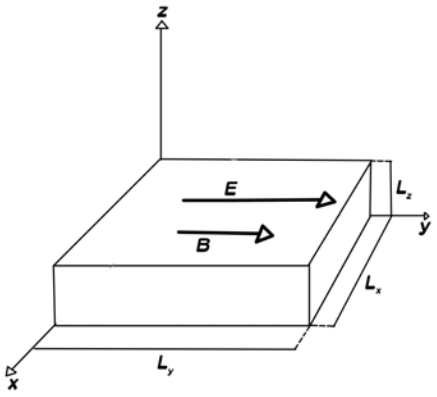

Figure 3. Electric charged in a flat box with parallel electric and magnetic fields.

Proposing a solution of the form $\Psi(\boldsymbol{x},t)=\mathrm{e}^{-iEt/\hbar}\Phi(\boldsymbol{x})$, we get the following eigenvalue problem

$$E\Phi=-\frac{\hbar^2}{2m}\frac{\partial^2\Phi}{\partial x^2}+i\frac{qB\hbar z}{mc}\frac{\partial\Phi}{\partial x}+\frac{q^2B^2}{2mc^2}z^2\Phi -\frac{\hbar^2}{2m}\frac{\partial^2\Phi}{\partial y^2}-\frac{\hbar^2}{2m}\frac{\partial^2\Phi}{\partial z^2}-q\mathcal{E}y\Phi. \tag{49}$$

Applying the Fourier transform over the *x*-variable, $\hat{\Phi}(k,y,z)=\mathcal{F}_x\left[\Phi(\boldsymbol{x})\right]$, the following equation arises after some rearrangements

$$E\hat{\Phi}=\frac{(\hbar k+qBz/c)^2}{2m}\hat{\Phi}-\frac{\hbar^2}{2m}\frac{\partial^2\hat{\phi}}{\partial z^2}-\frac{\hbar^2}{2m}\frac{\partial^2\hat{\Phi}}{\partial y^2}-q\mathcal{E}y\hat{\Phi}, \tag{50}$$

which can be written as

$$-\frac{\hbar^2}{2m}\frac{\partial^2\hat{\Phi}}{\partial z^2}+\frac{1}{2}m\omega_c(z+z_0)^2\hat{\Phi}-\frac{\hbar^2}{2m}\frac{\partial^2\hat{\Phi}}{\partial y^2}-q\mathcal{E}y\hat{\Phi}, \tag{51a}$$

where ω_c is the cyclotron frequency (13a), and $z_0=z_0(k)$ has been defined as

$$z_0=\frac{\hbar c}{qB}k. \tag{51b}$$

This equation admits a variable separable approach since by the proposition $\hat{\Phi}(k,y,z)=f(k,z)g(y)$, the following equations are bringing about

$$-\frac{\hbar^2}{2m}\frac{\mathrm{d}^2f}{\mathrm{d}z^2}+\frac{1}{2}m\omega_c^2(z+z_0)^2=E^{(1)}f \tag{52a}$$

and

$$-\frac{\hbar^2}{2m}\frac{\mathrm{d}^2g}{\mathrm{d}y^2}-g\mathcal{E}yg=E^{(2)}g, \tag{52b}$$

where $E=E^{(1)}+E^{(2)}$. The solutions of these equations are, of course, the quantum harmonic oscillator and the quantum bouncer, which are given by

$$f_n(k,z)=A_n\mathrm{e}^{-\xi^2/2}H_n(\xi),\quad \xi=\sqrt{\frac{m\omega_c}{\hbar}}(z+z_0),\quad E_n^{(1)}=\hbar\omega_c(n+1/2). \tag{53a}$$

and

$$g_{n'}(y)=\frac{Ai\left(\tilde{\xi}-\tilde{\xi}_{n'}\right)}{\left|Ai'\left(-\tilde{\xi}_{n'}\right)\right|},\quad \tilde{\xi}=y/l,\quad E_n^{(2)}=-q\mathcal{E}l\tilde{\xi}_{n'}, \tag{53b}$$

where $A_n=\left(m\omega_c/\pi\hbar\right)^{1/4}\Big/\sqrt{2^n n!}$, $l=\left(\hbar^2/(-2mq\mathcal{E})\right)^{1/3}$, $Ai\left(-\tilde{\xi}_{n'}\right)=0$, and $Ai'(\xi)$ is the differentiation of the Airy function. In this way, we have

$$\hat{\Phi}_{n,n'}(k,y,z)=a_{n'}\psi_n\left(\sqrt{\frac{m\omega_c}{\hbar}}(z+z_0)\right)Ai\left(l^{-1}(y-y_{n'})\right), \qquad E_{n,n'}=\hbar\omega_c(n+1/2)-q\mathcal{E}y_{n'}, \tag{54}$$

where we have defined $a_{n'}$ as $a_{n'}=1\Big/\left|Ai'\left(-l^{-1}y_{n'}\right)\right|$. Now, the inverse Fourier transformation will affect only the quantum harmonic oscillator function ψ_n through the *k*-dependence on the parameter z_0, and the resulting expression is

$$\Phi_{n,n'}(x)=\frac{a_{n'}\sqrt{qB}}{\left(mc^2\hbar\omega_c\right)^{1/4}}\mathrm{e}^{i\frac{qB}{\hbar c}xz}\psi_n\left(\frac{qBx}{\sqrt{mc^2\hbar\omega_c}}\right)Ai\left(l^{-1}\left(y-y_{n'}\right)\right). \tag{55}$$

Now, asking for the periodicity condition of the above solution with respect the z-variable, $\Phi_{n,n'}(\boldsymbol{x})=\Phi_{n,n'}(x,y,z+L_z)$, the periodicity must satisfy for any x-values, and in particular for $x=L_x$. Thus it follows the quantization expression for the magnetic flux

$$\frac{qBL_xL_z}{\hbar c}=2\pi j,\quad j\in\mathcal{Z}. \tag{56}$$

Using the same arguments shown above for the degeneration of the system, we have the same expression (23) for the degeneration of the system and the function (55) is given by (normalized)

$$\begin{aligned}\Phi_{nn'j}(\boldsymbol{x})=a_{n'}\sqrt{\frac{2\pi j}{L_xL_y^2L_z}}\left(\frac{\hbar}{m\omega_c}\right)^{1/4}\mathrm{e}^{i\frac{2\pi j}{L_xL_z}xz}\psi_n\left(\sqrt{\frac{\hbar}{m\omega_c}}\left(\frac{2\pi j}{L_xL_y}\right)x\right)\\ \times Ai\left(l^{-1}\left(y-y_{n'}\right)\right).\end{aligned} \tag{57}$$

Then, we have obtained a family of solution of the Schrödinger Equation (48),

$$\Psi_{n,n'}(\boldsymbol{x},t)=\mathrm{e}^{-iE_{n,n'}t/\hbar}\Phi_{nn'j}(\boldsymbol{x}), \tag{58}$$

where the energies $E_{n,n'}$ are given by the expression (54). The general solution of (48) can be written as

$$\Psi(\boldsymbol{x},t)=\sum_{n,n'}\sum_{j=0}^{D(n)}C^*_{n,n'}\mathrm{e}^{-iE_{n,n'}t/\hbar}\mathrm{e}^{i\frac{2\pi j}{L_xL_z}xz}\tilde{u}_{n,n'}(x,y), \tag{59}$$

with the condition $\sum_{n,n'}\left|C^*_{n,n'}\right|^2=1$, and where it has been defined the functions $\tilde{u}_{n,n'}$ as

$$\begin{aligned}\tilde{u}_{n,n'}(x,y)=a_{n'}\sqrt{\frac{2\pi j}{L_xL_y^2L_z}}\left(\frac{\hbar}{m\omega_c}\right)^{1/4}\psi_n\left(\sqrt{\frac{\hbar}{m\omega_c}}\left(\frac{2\pi j}{L_xL_y}\right)x\right)\\ \times Ai\left(l^{-1}\left(y-y_{n'}\right)\right).\end{aligned} \tag{60}$$

5. Conclusion and Comment

We have studied the quantization of a charged particle in a flat box and under constant magnetic and electric fields for several electromagnetic static cases using Fourier transformation to solve the linear differential equations resulting from the Shrödinger's equation, and we have shown that the full solution obtained is different from Landau's solution for the wave function, but as expected, Landau's levels appear as the solution of the eigenvalues. In all cases, a characteristic phase appears which helps us to find the quantization of the magnetic flux in a very natural way. We consider that the approach given here could be very useful to understand quantum Hall effect and related phenomena mainly because with Landau' solution a Hall's voltage appears (which is not possible with Landau' solution due to free particle solution on this direction). In addition, the

resulting degeneration in our calculations is different, and this one is used in the Fermi-Dirac distribution function to calculate the axial and transversal conductivities on the Hall's experiments.

Conflicts of Interest

The authors declare no conflicts of interest regarding the publication of this paper.

References

[1] Klitzing, K.V., Dorda, G. and Pepper, M. (1980) *Physical Review Letters*, **45**, 494. https://doi.org/10.1103/PhysRevLett.45.494

[2] Landau, L.D. and Lifshitz, E.M. (2013) Quantum Mechanics: Non-Relativistic Theory, Volume 3. Elsevier, Amsterdam.

[3] Ando, T., Matsumoto, Y. and Uemura, Y. (1975) *Journal of the Physical Society of Japan*, **39**, 279-288. https://doi.org/10.1143/JPSJ.39.279

[4] Laughlin, R.B. (1981) *Physical Review B*, **23**, 5632. https://doi.org/10.1103/PhysRevB.23.5632

[5] Halperin, B.I. (1982) *Physical Review B*, **25**, 2185. https://doi.org/10.1103/PhysRevB.25.2185

[6] Laughlin, R.B. (2000) *Uspekhi Fizicheskikh Nauk*, **170**, 292-303. https://doi.org/10.3367/UFNr.0170.200003f.0292

[7] Tsui, D.C., Stormer, H.L. and Gossard, A.C. (1982) *Physical Review Letters*, **48**, 1559. https://doi.org/10.1103/PhysRevLett.48.1559

[8] Laughlin, R.B. (1983) *Physical Review Letters*, **50**, 1395-1398. https://doi.org/10.1103/PhysRevLett.50.1395

[9] Jain, J.K. (1989) *Physical Review Letters*, **63**, 199-202. https://doi.org/10.1103/PhysRevLett.63.199

[10] Bernevig, B.A., Hughes, T.L. and Zhang, S.-C. (2006) *Science*, **314**, 1757-1761. https://doi.org/10.1126/science.1133734

[11] König, M., Wiedmann, S., Brüne, C., Roth, A., Buhmann, H., Molenkamp, L.W., Qi, X.-L. and Zhang, S.-C. (2007) *Science*, **318**, 766-770. https://doi.org/10.1126/science.1148047

[12] Li, J., Chu, R.-L., Jain, J.K. and Shen, S.-Q. (2009) *Physical Review Letters*, **102**, Article ID: 136806. https://doi.org/10.1103/PhysRevLett.102.136806

[13] Jiang, H., Wang, L., Sun, Q.-F. and Xie, X.C. (2009) *Physical Review B*, **80**, Article ID: 165316. https://doi.org/10.1103/PhysRevB.80.165316

[14] Groth, C.W., Wimmer, M., Akhmerov, A.R., Tworzydlo, J. and Beenakker, C.W.J. (2009) *Physical Review Letters*, **103**, Article ID: 196805. https://doi.org/10.1103/PhysRevLett.103.196805

[15] Mong, R.S.K., Essin, A.M. and Moore, J.E. (2010) *Physical Review B*, **81**, Article ID: 245209. https://doi.org/10.1103/PhysRevB.81.245209

[16] Pesin, D. and Balents, L. (2010) *Nature Physics*, **6**, 376-381. https://doi.org/10.1038/nphys1606

[17] Fu, L. and Kane, C.L. (2008) *Physical Review Letters*, **100**, Article ID: 096407. https://doi.org/10.1103/PhysRevLett.100.096407

[18] Freedman, M.H., Larsen, M. and Wang, Z.H. (2002) *Communications in Mathe-*

matical Physics, **227**, 605-622. https://doi.org/10.1007/s002200200645

[19] Kitaev, A. (2006) *Annals of Physics*, **321**, 2-111. https://doi.org/10.1016/j.aop.2005.10.005

[20] Prange, R.E. (1981) *Physical Review B*, **23**, 4802-4805. https://doi.org/10.1103/PhysRevB.23.4802

[21] Laughlin, R.B. (1999) *Reviews of Modern Physics*, **71**, 863-874. https://doi.org/10.1103/RevModPhys.71.863

[22] Yoshioka, D. (2013) The Quantum Hall Effect, Volume 133. Springer Science & Business Media, Berlin.

[23] Datta, S. (1997) Electronic Transport in Mesoscopic Systems. Cambridge University Press, Cambridge.

[24] Messiah, A. (1999) Quantum Mechanics. Dover, Mineola.

[25] Rudin, W. (1974) Functional Analysis. TATA McGraw-Hill Publishing Co., New Delhi.

[26] Deaver Jr., B.S. and William, F.M. (1961) *Physics Review Letters*, **7**, 43-46. https://doi.org/10.1103/PhysRevLett.7.43

Call for Papers

Journal of Modern Physics

ISSN: 2153-1196 (Print) ISSN: 2153-120X (Online)
https://www.scirp.org/journal/jmp

Journal of Modern Physics **(JMP)** is an international journal dedicated to the latest advancement of modern physics. The goal of this journal is to provide a platform for scientists and academicians all over the world to promote, share, and discuss various new issues and developments in different areas of modern physics.

Editor-in-Chief

Prof. Yang-Hui He City University, UK

Subject Coverage

Journal of Modern Physics publishes original papers including but not limited to the following fields:

Biophysics and Medical Physics
Complex Systems Physics
Computational Physics
Condensed Matter Physics
Cosmology and Early Universe
Earth and Planetary Sciences
General Relativity
High Energy Astrophysics
High Energy/Accelerator Physics
Instrumentation and Measurement
Interdisciplinary Physics
Materials Sciences and Technology
Mathematical Physics
Mechanical Response of Solids and Structures
New Materials: Micro and Nano-Mechanics and Homogeneization
Non-Equilibrium Thermodynamics and Statistical Mechanics
Nuclear Science and Engineering
Optics
Physics of Nanostructures
Plasma Physics
Quantum Mechanical Developments
Quantum Theory
Relativistic Astrophysics
String Theory
Superconducting Physics
Theoretical High Energy Physics
Thermology

We are also interested in: 1) Short Reports—2-5 page papers where an author can either present an idea with theoretical background but has not yet completed the research needed for a complete paper or preliminary data; 2) Book Reviews—Comments and critiques.

Notes for Intending Authors

Submitted papers should not have been previously published nor be currently under consideration for publication elsewhere. Paper submission will be handled electronically through the website. All papers are refereed through a peer review process. For more details about the submissions, please access the website.

Website and E-Mail

https://www.scirp.org/journal/jmp **E-mail: jmp@scirp.org**

What is SCIRP?

Scientific Research Publishing (SCIRP) is one of the largest Open Access journal publishers. It is currently publishing more than 200 open access, online, peer-reviewed journals covering a wide range of academic disciplines. SCIRP serves the worldwide academic communities and contributes to the progress and application of science with its publication.

What is Open Access?

All original research papers published by SCIRP are made freely and permanently accessible online immediately upon publication. To be able to provide open access journals, SCIRP defrays operation costs from authors and subscription charges only for its printed version. Open access publishing allows an immediate, worldwide, barrier-free, open access to the full text of research papers, which is in the best interests of the scientific community.

- High visibility for maximum global exposure with open access publishing model
- Rigorous peer review of research papers
- Prompt faster publication with less cost
- Guaranteed targeted, multidisciplinary audience

Scientific Research Publishing

Website: https://www.scirp.org

Subscription: sub@scirp.org

Advertisement: service@scirp.org